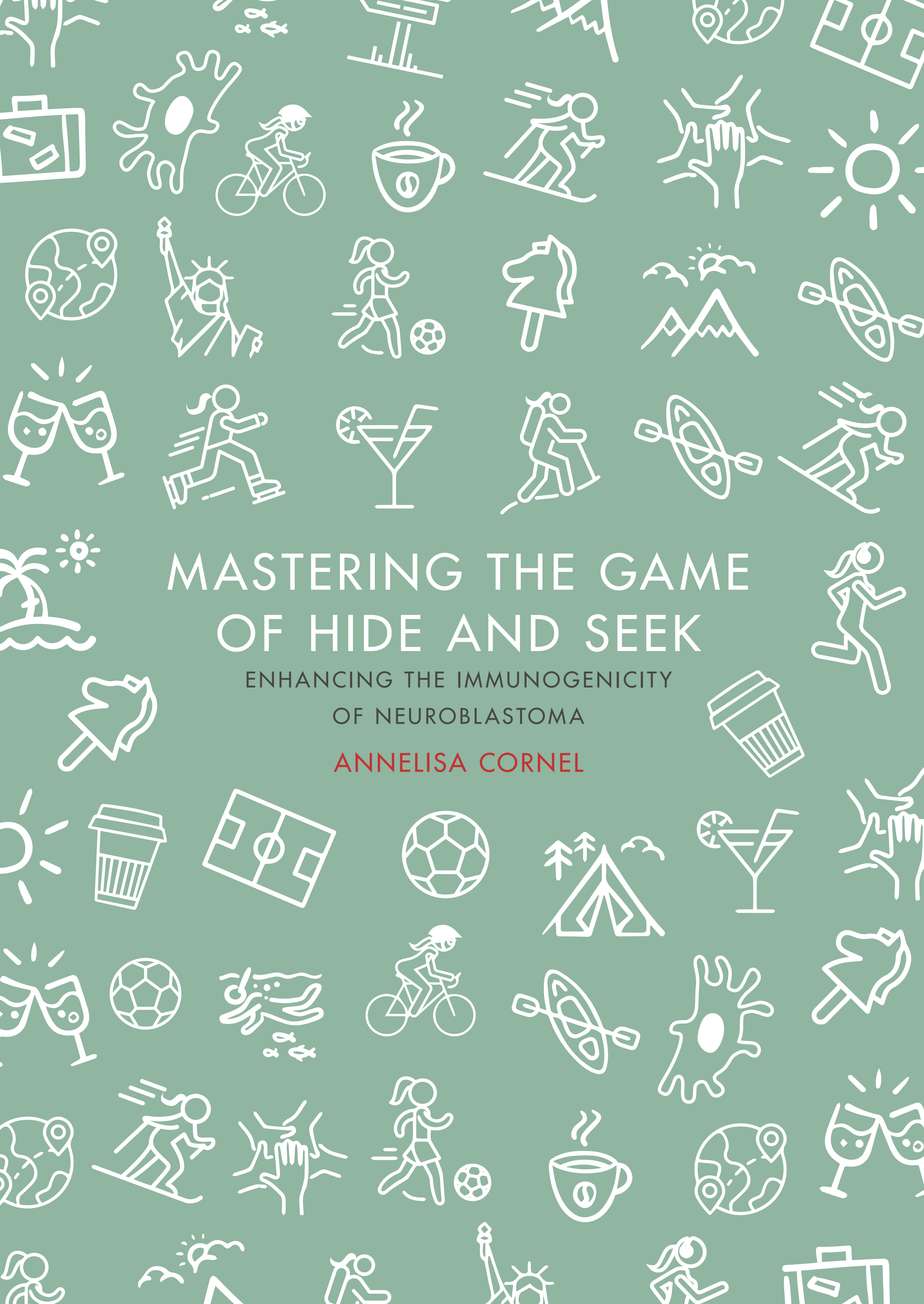

# MASTERING THE GAME OF HIDE AND SEEK

## ENHANCING THE IMMUNOGENICITY OF NEUROBLASTOMA

ANNELISA CORNEL

# Mastering the game of hide and seek

## Enhancing the Immunogenicity of Neuroblastoma

Annelisa Cornel

**Mastering the game of hide and seek**: Enhancing Immunogenicity of Neuroblastoma
Thesis with summary in Dutch, Utrecht University

ISBN: 978-94-6458-905-4
Cover Design: www.persoonlijkproefschrift.nl
Lay-out: www.persoonlijkproefschrift.nl
Printing: www.ridderprint.nl

The research in this thesis was performed at the University Medical Center Utrecht and Princess Maxima Center, Utrecht, The Netherlands. All studies were financially supported by the Villa Joep foundation (Grant Number IWOV-Actief.51381.180034). Additionally, the research in chapter 2 was supported by the Dutch Cancer Society (Grant Number 10474).

© Annelisa Cornel, 2022
The copyright of published articles have been transferred to the respective journals. All rights reserved. No part of this thesis may be reproduced, stored in a retrieval system, or transmitted in any other form or by any means, without written permission of the author.

# Mastering the game of hide and seek
## Enhancing the Immunogenicity of Neuroblastoma

# Steeds beter worden in verstoppertje
## Het Verhogen van de Immunogeniciteit van Neuroblastoom

(met een samenvatting in het Nederlands)

**Proefschrift**

ter verkrijging van de graad van doctor aan de
Universiteit Utrecht
op gezag van de
rector magnificus, prof.dr. H.R.B.M. Kummeling,
ingevolge het besluit van het college voor promoties
in het openbaar te verdedigen op

donderdag 16 februari 2023 des middags te 2.15 uur

door

**Annelisa Marjan Cornel**

geboren op 8 november 1993
te Harlingen

**Promotor:**
Dr. S. Nierkens

**Copromotor:**
Dr. M.P. Dierselhuis

**Beoordelingscommissie:**
Prof. dr. M.M. van Noesel (voorzitter)
Prof. dr. A.N. Bovenschen
Prof. dr. J.H.E. Kuball
Prof. J. Anderson
Prof. C. Rössig

**Paranimfen:**
Brigitte van den Broek
Ester Dünnebach
Vania lo Presti

**Voor jou pap, mijn grootste bron van inspiratie.**

*Dankjewel dat je me geleerd hebt*
*dat je met een ijzeren doorzettingsvermogen*
*en een flinke dosis enthousiasme*
*kan bereiken wat je wil.*

# CONTENTS

Chapter 1 General introduction, scope and outline of the thesis 9

---

**Part I** **Immune Responses during Neuroblastoma Therapy**

Chapter 2 Monitoring Immune Responses in Neuroblastoma Patients during Therapy *(Cancers 2020)* 23

Chapter 3 FACSCanto II and LSRFortessa flow cytometer instruments can be synchronized utilizing single-fluorochrome–conjugated surface-dyed beads for standardized immunophenotyping *(Cytometry A 2020 (adapted))* 53

Chapter 4 Immune Monitoring during Therapy Reveals Activatory and Regulatory Immune Responses in High-Risk Neuroblastoma (*Cancers 2021)* 67

---

**Part II** **Improving Neuroblastoma Immunogenicity via Pharmacological Upregulation of MHC-I**

Chapter 5 MHC Class I Downregulation in Cancer: Underlying Mechanisms and Potential Targets for Cancer Immunotherapy *(Cancers 2020)* 97

Chapter 6 A “No-Touch” Antibody-Staining Method of Adherent Cells for High-Throughput Flow Cytometry in 384-Well Microplate Format for Cell-Based Drug Library Screening *(Cytometry A 2019)* 141

Chapter 7 Efficient lentiviral transduction method to gene modify cord blood CD8+ T-cells for cancer therapy applications (*Molecular Therapy: Methods & Clinical Development 2021 (adapted))* 159

Chapter 8 Epigenetic modulation of neuroblastoma enhances T- and NK-cell immunogenicity by inducing a tumor cell lineage switch *(Journal for Immunotherapy of Cancer 2022, In Press)* 185

---

**Part III** **Cell Therapy Strategies to Enhance Adaptive Immune Engagement in Neuroblastoma**

Chapter 9 Best of two worlds: Engineering NKT-cells to generate an alternative adaptive cell therapy strategy against neuroblastoma 221

Chapter 10 Ex Vivo generated CD34+ stem cell-derived thymic NK-cells as a cellular therapy source in Neuroblastoma 243

Chapter 11 Immunogenicity of Neuroblastoma: Summary, Conclusion, and Perspectives 271

Chapter 12 Nederlands Samenvatting (Dutch Summary) 299

Chapter 13 Appendices 307

Curriculum Vitae 309

List of Publications 311

Dankwoord 313

# Chapter 1

## Introduction, scope and outline thesis

Neuroblastoma (NBL) is the most common extracranial tumor in children, accounting for about 15% of pediatric cancer deaths worldwide. It is a pediatric neuroendocrine tumor arising from sympathoadrenal neural crest cells of the developing sympathetic nervous system. In a healthy situation, these progenitors give rise to the adrenal medulla and sympathetic neural ganglia, hence, primary tumor masses often present at these sites. Median age at diagnosis is 18 months, of which 40% of patients are diagnosed during infancy and 90% before the age of ten. Outcome of patients largely depends on disease state. Risk classification is currently based on clinical factors, such as patients' age and International Neuroblastoma Risk Group (INRG) tumor stage, as well as on biologic factors, such as histopathologic classification, DNA ploidy, MYCN status, and copy-number of chromosome 11q. Diagnosis in patients >18 months of age, disseminated disease, and genetic aberrations, of which MYCN amplification is the most widely known aberration, all associate with higher disease risk. Low-risk patients have >90% survival chance, with tumors often regressing spontaneously, while 5-year survival of patients with high-risk (HR) disease is less than 50% [1,2]. [3–6]

HR-NBL treatment involves an intensive, multi-modal regimen, which can be subdivided into three phases: the induction, consolidation, and maintenance phase. The induction phase is composed of chemotherapy and surgical tumor removal, the consolidation phase of high-dose chemotherapy with autologous stem cell rescue and radiotherapy, and the maintenance phase of immunotherapy (IT). The Dutch IT regimen initially comprised the anti-GD2 antibody dinutuximab for tumor cell destruction, isotretinoin to trigger differentiation, and alternated cycles of interleukin-2 (IL-2) and granulocyte macrophage – colony stimulating factor (GM-CSF) for immune stimulation. Compared to isotretinoin only, IT addition resulted in a 20% 2-year and 10% 5-year increase in event-free survival [2,7]. Currently, two main changes have been made compared to the initial protocol. The immune-stimulatory cytokines have been omitted in the current Society of Pediatric Oncology Europe NBL (SIOPEN) HR-NBL2 protocol, in which the Netherlands takes part, as a recent phase III trial concluded no additive effect of IL-2 addition to the treatment regimen [8] and GM-CSF is no longer available in large parts of Europe. Besides this, short-term dinutuximab infusion is replaced by long-term infusion, as this was shown to significantly reduce toxicity and can be administered in an outpatient setting [9].

For a long time, the HR-NBL tumor environment was referred to as 'cold' or 'immune-deserted' as it was stated that very few immune cells were present in the tumor microenvironment [10,11]. This phenotype is caused by multiple immunomodulatory processes mediated by the tumor and its environment, resulting in activation of suppressive immune cells, including regulatory T-cells (Treg) and myeloid-derived suppressor cells (MDSCs), and decreased activation and cytotoxicity of immune cells capable to lyse the tumor, including T- and NK-cells (**Figure 1**). Nonetheless, in the last couple of years, multiple studies have reported the presence of tumor-infiltrating lymphocytes (TILs) in NBL tumors, including T-, NK-, (i)NKT- and γδ T-cells [11]. In addition, a correlation was observed between presence of TILs and favorable outcome [12], suggesting a role of immune interference in NBL regression. This is supported by increased serum levels of granulysin, an effector molecule of cytotoxic T-cells, in a case study of spontaneous NBL regression [13]. These findings, together with the survival benefit in IT-treated patients, show the potential of immunotherapeutic interference in HR-NBL.

Despite the benefit of IT on survival in HR-NBL patients, relapse is still observed in about half of the children. Moreover, the initial additive effect of IT seems to decline over the years. The current antibody-based IT regimen mainly engages the innate immune system, trained to hit hard and fast, but inadequately activates adaptive immunity. We hypothesize that the clue to further enhance (immuno)therapy efficacy in HR-NBL is to effectively engage T-cells, thereby enhancing anti-tumor cytotoxicity and creating immunological memory to prevent future relapse.

## SCOPE AND OUTLINE OF THIS THESIS

The research described in this thesis focusses on strategies to enhance T-cell immunogenicity of HR-NBL to improve outcome of children suffering from HR-NBL. The first part of this thesis explores the potential of monitoring immune responses along the HR-NBL therapy course to provide useful clues for (immuno)therapy improvement and biomarker development. The second part of this thesis describes the identification of pharmacological strategies to enhance T-cell immunogenicity in NBL. In the third part of this thesis, the use of cell therapy-based strategies to enhance NBL immunogenicity is explored. The final part of this thesis describes the conclusions, recommendations, and future directives of the preclinical evidence in this thesis to achieve effective T-cell engagement to maximize anti-tumor cytotoxicity and create immunological memory to prevent future relapse.

### Part I – Immune Responses during Neuroblastoma Therapy

With only 10-14 children diagnosed in the Netherlands annually [1], HR-NBL can be classified as a very rare disease. The small cohort of children makes it difficult to compare therapeutic interventions and conclude the best multimodal treatment strategy. This is underlined by the fact that dose, timing, and chosen immunotherapeutic compound combinations are currently highly empirical and do not take the immune status of patients or the effect of the individual compounds into account. Promising efforts have been made to compare outcome of patients treated with or without IL-2 [8] and with short- or long-term infusion of dinutuximab [9], however, in-depth, harmonized immunological data is largely lacking.

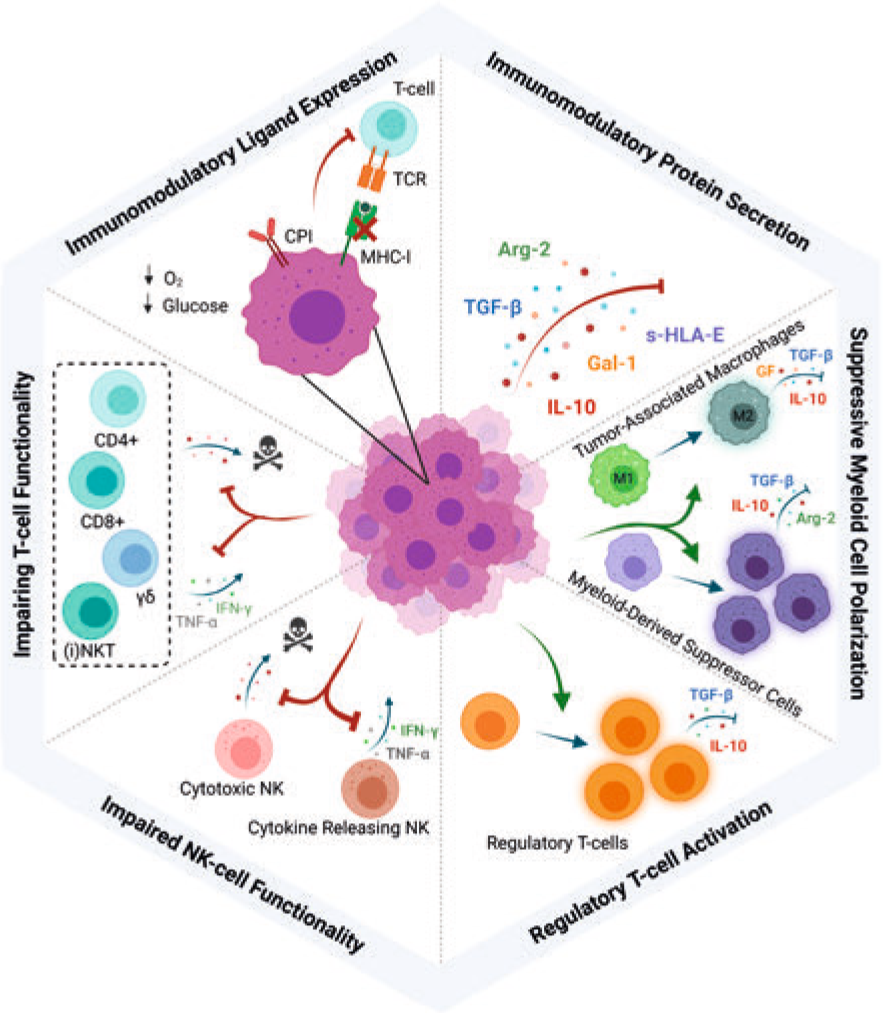
Immunomodulatory Ligand Expression
T-cell
TCR
CPI
MHC-I
↓ O₂
↓ Glucose
Immunomodulatory Protein Secretion
Arg-2
TGF-β
s-HLA-E
Gal-1
IL-10
Suppressive Myeloid Cell Polarization
Tumor-Associated Macrophages
TGF-β
GF
IL-10
M2
M1
TGF-β
IL-10
Arg-2
Myeloid-Derived Suppressor Cells
Impairing T-cell Functionality
CD4+
CD8+
γδ
(i)NKT
IFN-γ
TNF-α
Impaired NK-cell Functionality
IFN-γ
TNF-α
Cytotoxic NK
Cytokine Releasing NK
TGF-β
IL-10
Regulatory T-cells
Regulatory T-cell Activation

**Figure 1.** The immunomodulatory tumor microenvironment of Neuroblastoma.
*NBL and its microenvironment modulate activation of different branches of the immune system, thereby dampening anti-tumor immunity against NBL and favoring tumor growth and persistence. Created with BioRender.com*

**Chapter 2** describes the current literature on immune status of patients at diagnosis and along the HR-NBL treatment protocol. In addition, it provides recommendations on how to harmonize immune monitoring between centers to maximize comparability of results from different centers. Nonetheless, while harmonization of monitoring will allow comparison of abundance of clearly defined cell populations between centers, comparisons of fluorescent intensities of markers with potential clinical relevance will still be hampered due to variability between flow cytometers. **Chapter 3** describes a strategy to synchronize flow cytometers with different laser-line configurations and laser power to be able to avoid inconsistencies in interpretation of results. **Chapter 4** reports our first pilot study results in which we monitor immune subset composition and function in 25 HR-NBL patients along the therapy course.

### Part II – Improving Neuroblastoma T-cell Immunogenicity via Pharmacological MHC-I Upregulation

The low immunogenicity of NBL is likely a derivative of the embryonal tissue from which it originates [14]. One of the derivatives thought to majorly contribute to the low T-cell immunogenicity of NBL is the lack of surface display of major histocompatibility complex I (MHC-I), an important prerequisite for CD8+ T-cell activation. To understand and act upon MHC-I dysregulation, literature was reviewed in **Chapter 5** to understand underlying mechanisms and to know which strategies are described to counteract MHC-I dysregulation beyond the context of NBL.

Even though the absence of MHC-I surface expression initially limits cytotoxic T-cell engagement, we have previously shown that MHC-I expression can be readily induced by cytokine-driven immune modulation, thereby directing T-cell cytotoxicity to NBL [15,16]. MHC-I expression-enhancing cytokines (i.e. TNFα, IFNα/β/γ), however, initiate a broad range of biological activities, thereby limiting its use in therapy due to severe toxicities [17,18]. Consequently, the research described in this section of the thesis revolves around identification of pharmacological strategies to enhance MHC-I surface display in NBL (**Figure 2**).

We aimed to repurpose drugs that are already in clinical use for other purposes to allow for relatively fast and easy translation to clinical care. **Chapter 6** describes the high-throughput flow cytometry protocol we developed to screen drug repurposing libraries for their effect on MHC-I surface display. To subsequently be able to conclude whether the increased MHC-I display results in better T-cell immunogenicity, a pipeline was developed in **Chapter 7** to engineer T-cells to express a tumor-specific recombinant T-cell receptor (TCR). **Chapter 8** summarizes the results of the drug screens and elaborates on the potential of two drug classes: Inhibitor of Apoptosis Inhibitors (IAPi) and Histon Deacetylase Inhibitors (HDACi).

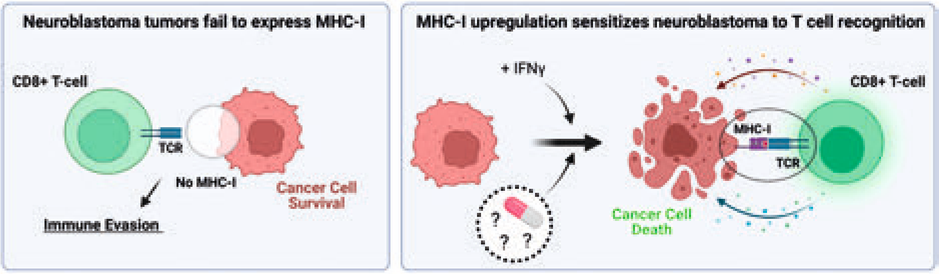
Neuroblastoma tumors fail to express MHC-I
CD8+ T-cell
TCR
No MHC-I
Cancer Cell Survival
Immune Evasion
MHC-I upregulation sensitizes neuroblastoma to T cell recognition
+ IFNγ
?
? ?
CD8+ T-cell
MHC-I
TCR
Cancer Cell Death

**Figure 2.** Triggering MHC-I surface display on Neuroblastoma enhances T-cell immunogenicity.
*Lack of MHC-I expression results in immune evasion of NBL. Nonetheless, induction of MHC-I surface display, for example by IFNγ, causes T-cells to start recognizing NBL. The research described in this thesis section aims to identify pharmacological strategies to enhance MHC-I surface display in NBL. Created with BioRender.com*

## Part III – Cell Therapy Strategies to Enhance Neuroblastoma Immunogenicity

Absence of MHC-I on cells should trigger missing-self recognition by NK-cells [19]. We have previously shown, however, that secretion of IFNγ by NK-cells upon missing-self recognition causes induction of expression of MHC-I on NBL cells, thereby resulting in evasion of missing-self mediated cytotoxicity by NK-cells [15]. This suggests that the high degree of plasticity in MHC-I expression may allow alternate evasion of both cytotoxic T- and NK-cells. We hypothesize that generation of a cell product that can both engage in NK-cell mediated cytotoxicity, for example via missing-self recognition, as well as in recognition of malignant transformation in MHC-I context will result in an effector cell that cannot be evaded by MHC-I plasticity (**Figure 3**).

This thesis section explores different immune cell sources to engineer such a cell product executing both missing-self- as well as antigen-dependent cytotoxicity. **Chapter 9** reports about the potential to use CD3+CD56+ NKT-cells. **Chapter 10** describes an OP9/DL1 co-culture system to differentiate (genetically engineered) CD34+ stem cells into TCR+ thymic NK-cells as an alternative cell source.

Finally, **Chapter 11** summarizes this thesis, presents implications of described findings, and provides recommendations for future research to achieve effective T-cell engagement to maximize anti-tumor cytotoxicity and create immunological memory to prevent relapse in children suffering from HR-NBL.

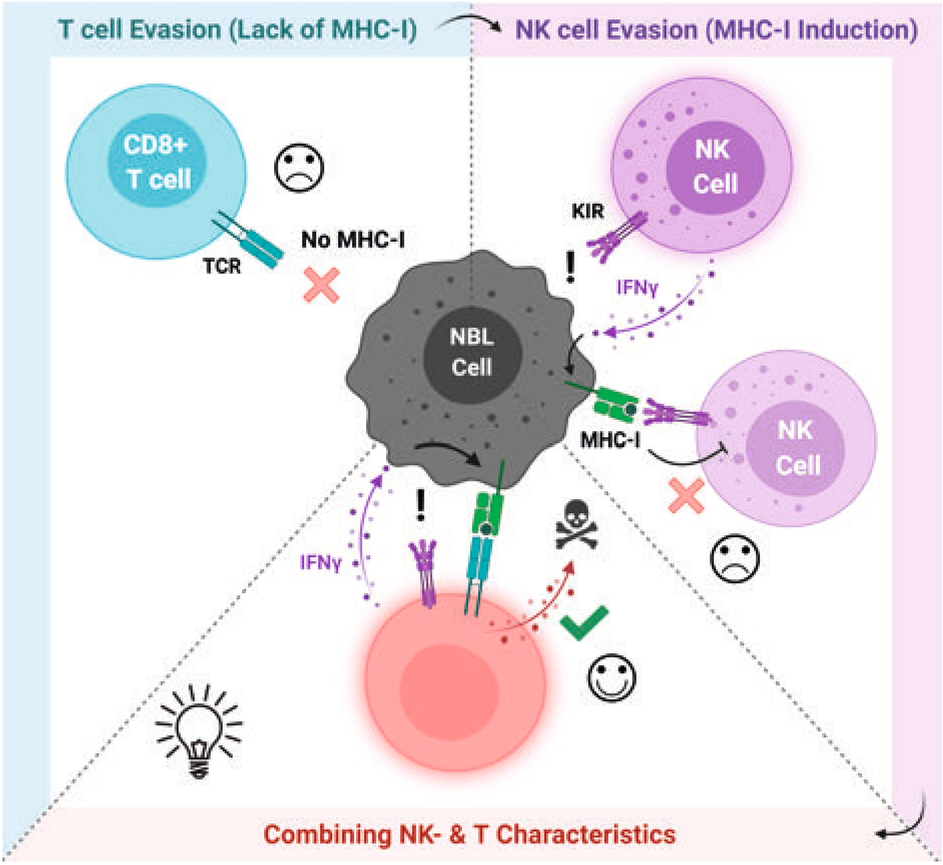
T cell Evasion (Lack of MHC-I)
NK cell Evasion (MHC-I Induction)
CD8+ T cell
TCR
No MHC-I
NBL Cell
NK Cell
KIR
IFNγ
MHC-I
NK Cell
IFNγ
Combining NK- & T Characteristics

**Figure 3.** Combining missing-self- and antigen-dependent cytotoxicity in an effector cell to circumvent MHC-I plasticity-mediated immune evasion.

*T-cell cytotoxicity is evaded by low MHC-I expression (blue), while NBL cells are subject to missing-self recognition by NK-cells. Missing-self recognition results in IFNγ secretion by NK-cells, triggering MHC-I expression on NBL cells, thereby evading missing-self mediated cytotoxicity by NK-cells (purple). This thesis section explores the generation of an effector cell both engaging in missing-self- and antigen-dependent cytotoxicity (red), thereby circumventing MHC-I plasticity-mediated immune evasion. Created with BioRender.com*

## REFERENCES

1. Tas, M.L.; Reedijk, A.M.J.; Karim-Kos, H.E.; Kremer, L.C.M.; van de Ven, C.P.; Dierselhuis, M.P.; van Eijkelenburg, N.K.A.; van Grotel, M.; Kraal, K.C.J.M.; Peek, A.M.L.; et al. Neuroblastoma between 1990 and 2014 in the Netherlands: Increased Incidence and Improved Survival of High-Risk Neuroblastoma. European Journal of Cancer **2020**, 124, 47–55, doi:10.1016/j.ejca.2019.09.025.
2. Yu, A.L.; Gilman, A.L.; Ozkaynak, M.F.; Naranjo, A.; Diccianni, M.B.; Gan, J.; Hank, J.A.; Batova, A.; London, W.B.; Tenney, S.C.; et al. Long-Term Follow-up of a Phase III Study of Ch14.18 (Dinutuximab) + Cytokine Immunotherapy in Children with High-Risk Neuroblastoma: COG Study ANBL0032. Clinical Cancer Research **2021**, 18, clincanres.3909.2020, doi:10.1158/1078-0432.ccr-20-3909.
3. Maris, J.M. Recent Advances in Neuroblastoma. New England Journal of Medicine **2010**, 362, 2202, doi:10.1056/nejmra0804577.
4. Park, J.R.; Eggert, A.; Caron, H. Neuroblastoma: Biology, Prognosis, and Treatment. Hematology/Oncology Clinics of North America **2010**, 24, 65–86, doi:10.1016/j.hoc.2009.11.011.
5. Matthay, K.K.; Maris, J.M.; Schleiermacher, G.; Nakagawara, A.; Mackall, C.L.; Diller, L.; Weiss, W.A. Neuroblastoma. Nature Reviews Disease Primers **2016**, 2, doi:10.1038/nrdp.2016.78.
6. Irwin, M.S.; Naranjo, A.; Zhang, F.F.; Cohn, S.L.; London, W.B.; Gastier-Foster, J.M.; Ramirez, N.C.; Pfau, R.; Reshmi, S.; Wagner, E.; et al. Revised Neuroblastoma Risk Classification System: A Report From the Children's Oncology Group. Journal of clinical oncology : official journal of the American Society of Clinical Oncology **2021**, 39, 3229–3241, doi:10.1200/JCO.21.00278.
7. Yu, A.L.; Gilman, A.L.; Ozkaynak, M.F.; London, W.B.; Kreissman, S.G.; Chen, H.X.; Smith, M.; Anderson, B.; Villablanca, J.G.; Matthay, K.K.; et al. Anti-GD2 Antibody with GM-CSF, Interleukin-2, and Isotretinoin for Neuroblastoma. New England Journal of Medicine **2010**, 363, 1324–1334, doi:10.1056/NEJMoa0911123.
8. Ladenstein, R.; Pötschger, U.; Valteau-Couanet, D.; Luksch, R.; Castel, V.; Yaniv, I.; Laureys, G.; Brock, P.; Michon, J.M.; Owens, C.; et al. Interleukin 2 with Anti-GD2 Antibody Ch14.18/CHO (Dinutuximab Beta) in Patients with High-Risk Neuroblastoma (HR-NBL1/SIOPEN): A Multicentre, Randomised, Phase 3 Trial. The Lancet Oncology **2018**, 19, 1617–1629, doi:10.1016/S1470-2045(18)30578-3.
9. Mueller, I.; Ehlert, K.; Endres, S.; Pill, L.; Siebert, N.; Kietz, S.; Brock, P.; Garaventa, A.; Valteau-Couanet, D.; Janzek, E.; et al. Tolerability, Response and Outcome of High-Risk Neuroblastoma Patients Treated with Long-Term Infusion of Anti-GD2 Antibody Ch14.18/CHO. mAbs **2018**, 10, 55–61, doi:10.1080/19420862.2017.1402997.
10. Park, J.A.; Cheung, N.K. V. Targets and Antibody Formats for Immunotherapy of Neuroblastoma. Journal of Clinical Oncology **2020**, 38, 1836–1848, doi:10.1200/JCO.19.01410.
11. Wienke, J.; Dierselhuis, M.P.; Tytgat, G.A.M.; Künkele, A.; Nierkens, S.; Molenaar, J.J. The Immune Landscape of Neuroblastoma: Challenges and Opportunities for Novel Therapeutic Strategies in Pediatric Oncology. European Journal of Cancer **2021**, 144, 123–150, doi:10.1016/j.ejca.2020.11.014.
12. Mina, M.; Boldrini, R.; Citti, A.; Romania, P.; D'Alicandro, V.; Ioris, M. De; Castellano, A.; Furlanello, C.; Locatelli, F.; Fruci, D. Tumor-Infiltrating T Lymphocytes Improve Clinical Outcome of Therapy-Resistant Neuroblastoma. OncoImmunology 2015, 4, 1–14, doi:10.1080/2162402X.2015.1019981.

13. Nagasawa, M.; Kawamoto, H.; Tsuji, Y.; Mizutani, S. Transient Increase of Serum Granulysin in a Stage IVs Neuroblastoma Patient during Spontaneous Regression: Case Report [1]. International Journal of Hematology **2005**, 82, 456–457, doi:10.1532/IJH97.05091.
14. Spel, L.; Schiepers, A.; Boes, M. NFκB and MHC-1 Interplay in Neuroblastoma and Immunotherapy. Trends in Cancer **2018**, 4, 715–717, doi:10.1016/j.trecan.2018.09.006
15. Spel, L.; Boelens, J.J.; Van Der Steen, D.M.; Blokland, N.J.G.; van Noesel, M.M.; Molenaar, J.J.; Heemskerk, M.H.M.; Boes, M.; Nierkens, S. Natural Killer Cells Facilitate PRAME-Specific T-Cell Reactivity against Neuroblastoma. Oncotarget **2015**, 6, 35770–35781, doi: 10.18632/oncotarget.5657.
16. Spel, L.; Nieuwenhuis, J.; Haarsma, R.; Stickel, E.; Bleijerveld, O.B.; Altelaar, M.; Boelens, J.J.; Brummelkamp, T.R.; Nierkens, S.; Boes, M. Nedd4-Binding Protein 1 and TNFAIP3-Interacting Protein 1 Control MHC-1 Display in Neuroblastoma. Cancer Research **2018**, 78, 6621–6631, doi:10.1158/0008-5472.CAN-18-0545.
17. Cai, W.; Kerner, Z.J.; Sun, J. Targeted Cancer Therapy with Tumor Necrosis Factor-Alpha. Biochem Insights **2008**, 15–21, doi:10.1038/jid.2014.371.
18. George, P.M.; Badiger, R.; Alazawi, W.; Foster, G.R.; Mitchell, J.A. Pharmacology and Therapeutic Potential of Interferons. Pharmacology and Therapeutics **2012**, 135, 44–53, doi:10.1016/j.pharmthera.2012.03.006.
19. Anfossi, N.; André, P.; Guia, S.; Falk, C.S.; Roetynck, S.; Stewart, C.A.; Breso, V.; Frassati, C.; Reviron, D.; Middleton, D.; et al. Human NK Cell Education by Inhibitory Receptors for MHC Class I. Immunity **2006**, 25, 331–342, doi:10.1016/j.immuni.2006.06.013.
20. Strijker, J.G.M.; Pscheid, R.; Drent, E.; van der Hoek, J.J.F.; Koopmans, B.; Ober, K.; van Hooff, S.R.; Kholosy, W.M.; Cornel, A.M.; Coomans, C.; et al. Aβ-T Cells Engineered to Express Γδ-T Cell Receptors Can Kill Neuroblastoma Organoids Independent of MHC-I Expression. Journal of Personalized Medicine **2021**, 11, doi:10.3390/jpm11090923.
21. Metelitsa, L.S.; Wu, H.W.; Wang, H.; Yang, Y.; Warsi, Z.; Asgharzadeh, S.; Groshen, S.; Wilson, S.B.; Seeger, R.C. Natural Killer T Cells Infiltrate Neuroblastomas Expressing the Chemokine CCL2. Journal of Experimental Medicine **2004**, 199, 1213–1221, doi:10.1084/jem.20031462.
22. Zoine, J.T.; Knight, K.A.; Fleischer, L.C.; Sutton, K.S.; Goldsmith, K.C.; Doering, C.B.; Spencer, H.T. Ex Vivo Expanded Patient-Derived Γδ T-Cell Immunotherapy Enhances Neuroblastoma Tumor Regression in a Murine Model. OncoImmunology **2019**, 8, 1–13, doi: 10.1080/2162402X.2019.1593804.
23. Heczey, A.; Courtney, A.N.; Montalbano, A.; Robinson, S.; Liu, K.; Li, M.; Ghatwai, N.; Dakhova, O.; Liu, B.; Raveh-Sadka, T.; et al. Anti-GD2 CAR-NKT Cells in Patients with Relapsed or Refractory Neuroblastoma: An Interim Analysis. Nature Medicine **2020**, 26, 1686–1690, doi:10.1038/s41591-020-1074-2.
24. Crowther, M.D.; Dolton, G.; Legut, M.; Caillaud, M.E.; Lloyd, A.; Attaf, M.; Galloway, S.A.E.; Rius, C.; Farrell, C.P.; Szomolay, B.; et al. Genome-Wide CRISPR–Cas9 Screening Reveals Ubiquitous T Cell Cancer Targeting via the Monomorphic MHC Class I-Related Protein MR1. Nature Immunology **2020**, 21, 178–185, doi:10.1038/s41590-019-0578-8.

5 4 3

# Part I

## Immune Responses during Neuroblastoma Therapy

# Chapter 2

## Monitoring Immune Responses in Neuroblastoma Patients during Therapy

Annelisa M. Cornel[1,*], Celina L. Szanto[1,*], Saskia V. Vijver[1] and Stefan Nierkens[1,2]

*[1] Center for Translational Immunology, University Medical Center Utrecht, Utrecht University, The Netherlands*
*[2] Princess Máxima Center for Pediatric Oncology, Utrecht University, 3584 CS Utrecht, The Netherlands*
*[*] These authors contributed equally to this work.*

*Cancers (Basel) 2020 Feb 24; 12(2), 519.*

## ABSTRACT

Neuroblastoma (NBL) is the most common extracranial solid tumor in childhood. Despite intense treatment, children with this high-risk disease have a poor prognosis. Immunotherapy significantly improved event-free survival in high-risk NBL patients receiving chimeric anti-GD2 in combination with cytokines and isotretinoin after myeloablative consolidation therapy. However, response to immunotherapy varies widely, and often therapy is stopped due to severe toxicities. Objective markers that help to predict which patients will respond or develop toxicity to a certain treatment are lacking. Immunotherapy guided via immune monitoring protocols will help to identify responders as early as possible, to decipher the immune response at play, and to adjust or develop new treatment strategies. In this review, we summarize recent studies investigating frequency and phenotype of immune cells in NBL patients prior and during current treatment protocols and highlight how these findings are related to clinical outcome. In addition, we discuss potential targets to improve immunogenicity and strategies that may help to improve therapy efficacy. We conclude that immune monitoring during therapy of NBL patients is essential to identify predictive biomarkers to guide patients towards effective treatment, with limited toxicities and optimal quality of life.

## 1. INTRODUCTION

Neuroblastoma (NBL) is a tumor derived from sympathoadrenal progenitor cells of the developing sympathetic nervous system. It occurs most often in the adrenal medulla or sympathetic ganglia [1,2,3]. NBL is the most commonly diagnosed solid tumor during the first year of life and is responsible for approximately 15% of pediatric cancer deaths [2,3,4]. Risk classification of patients is based on different clinical factors, such as patients' age and International Neuroblastoma Risk Group (INRG) tumor stage, as well as biologic factors, such as histopathologic classification, DNA ploidy, MYCN status, and copy-number of chromosome 11q [3]. Outcome dramatically differs between patients with different tumor stages.

The high-risk NBL tumor environment is often referred to as 'cold' or 'immune-deserted', characterized by presence of very few immune cells in the tumor microenvironment (TME) [5]. However, the probability for a cold tumor to respond to immune therapy depends on strategies to transform it to 'hot' tumors [6]. The cold phenotype is likely caused by the development of multiple immunomodulatory mechanisms by the tumor and its environment, including major histocompatibility complex I (MHC-I) downregulation, regulatory T-cell (Treg) and myeloid-derived suppressor cell (MDSC) accumulation, and decreased T-cell cytotoxicity [7]. Infiltrating immune cells are observed especially in low-risk NBL and the presence of tumor-infiltrating lymphocytes (TILs) was found to be correlated with favorable clinical outcome [8]. This suggests a role of immune infiltration in regression of NBL, which is supported by increased serum levels of granulysin, an effector molecule of cytotoxic T-cells, observed in a case study of spontaneous NBL regression [9]. Therapeutic interference to increase immune infiltration and recognition might therefore be key to increase therapy efficiency against NBL.

High-risk NBL is currently treated with surgery, radiotherapy, 5–8 cycles of intensive chemotherapy, including platinum-, alkylating-, and topoisomerase agents—which is often followed by autologous stem cell transplantation (ASCT)—and immunotherapy [1-4,10]. High expression of GD2 (a disialoganglioside) across NBLs and low expression levels in healthy tissue has led to the rationale of GD2 targeting immunotherapy [11]. Administration of the chimeric monoclonal antibody (mAb) anti-GD2 (ch14.18), combined with the cytokines IL-2 and granulocyte macrophage-colony stimulation factor (GM-CSF), and isotretinoin in patients with high-risk NBL resulted in a significant increase 2-year event-free (EFS) and overall survival (OS) [10]. The observation of this effect, despite the harsh immunomodulatory immune environment of NBL, shows the potential of immune interference in NBL. However, as about 40% relapse is still observed in these patients, there is a clear medical need to optimize (immuno)therapeutic strategies. The current immunotherapy protocol is particularly ineffective for high-burden disease. In addition, osteomedullary metastatic disease occurs in most patients with high-risk neuroblastoma [12]. Elucidating the mechanisms of effective anti-tumor responses is key to find out, and act upon, what discriminates responders from non-responders.

Several studies in multiple types of cancer report increased tumor infiltration of immune cells upon (chemo)therapy [13-15], which could potentially predict overall therapy response and prognosis in an early stage. Immune monitoring during therapy provides the opportunity to study biological mechanisms of response and resistance [16]. This enables identification of biomarkers to monitor therapy response, potentially aiding to early stratification of responders and non-responders. In the 1960s, it was reported that the correlation between prognosis and degree of lymphocyte infiltration is also observed in NBL [17-19]. It is now known that NBL tumors are intermixed with different immune cells, recently identified to include CD4+ and CD8+ T-cells, natural killer (NK) cells, and γδ T-cells [20]. Interestingly, Mina *et al.* showed that the prognostic value of TIL levels at diagnosis is even better than criteria currently used to stage NBL, such as MYCN amplification [8]. This illustrates the potential role of immune cells in influencing the clinical outcome and emphasizes the need for standardized immune monitoring during therapy in this patient group.

This review provides an overview of predictive immune biomarkers of clinical response to treatment, emphasizes the importance of immune monitoring during NBL treatment, and describes its relevance for evaluation of the immune response and patient stratification by developing new biomarkers.

## 2. IMMUNE MONITORING AT DIAGNOSIS: CORRELATES OF OUTCOME?

### 2.1. Immune Markers at the Tumor Site

Histological analysis of human tumor types, including melanoma, ovarian-, head- and neck-, breast-, urothelial-, colorectal-, lung- hepatocellular-, and esophageal cancer showed the presence of tumor infiltrating immune cells, such as macrophages, dendritic cells (DCs), polymorphonuclear cells, NK-cells, B-cells, and T-cells. Although these studies revealed a broad interpatient variability, a high density of CD3+ T-cells, CD8+ T-cells, and CD45RO+ memory T-cells was generally associated with improved EFS and OS [21,22]. In addition, for NBL, multiple studies show that increased CD3+ T-cell infiltration and proliferation is associated with favorable clinical outcome [8,23]. These data correspond with the findings that high-risk MYCN-amplified primary metastatic NBL tumors show lower levels of infiltrated lymphocytes, monocytes, and macrophages, and exhibit lower interferon pathway activity and chemokine expression [23]. T-cell proliferation is most likely impaired by high arginase activity in the TME [24], resulting in low arginine levels (an essential molecule for T-cell proliferation).

CD4+ T-cell infiltration is associated with better survival, regardless of MYCN amplification [23]. However, extensive phenotyping of these CD4+ T-cells, with markers such as CD25, CD127, and FoxP3 to distinguish regulatory T-cells (Treg), is lacking. Based on gene set enrichment analyses, gene expression of IL-4 (indicative for Th2) was elevated and associated with better prognosis in tumors with high CD4+ T-cells infiltration whereas no association was observed with interferon γ (IFNγ), IL-2, and tumor necrose factor α (TNFα) (indicative for Th1) [25]. In addition, NKT-cell infiltration has been reported to be favorable for outcome, possibly by inhibition of suppressive monocytes in the TME [26].

Presence of immune cell populations with presumed regulatory properties, including tumor associated monocytes, macrophages (TAMs), and Tregs, predict poor outcome [8,27]. Tumor infiltrating macrophages often display an immunosuppressive M2-phenotype supporting T-cell suppression, tumor cell migration, and treatment evasion [28]. High expression of TAM-associated genes CD14, CD16, IL-6, IL-6R, and transforming growth factor β1 (TGFβ1) is associated with decreased 5-year EFS [26]. Additionally, monocytes isolated from the TME are able to suppress T-cell proliferation *in vitro* [24] and excrete multiple soluble T-cell inhibitory factors, such as TGFβ and IL-10 [29,30]. Although Tregs and MDSCs are well known for their suppressive effects on the immune system, associations of these subsets with clinical outcome remain limited to studies investigating bone marrow (BM) or peripheral blood (PB). One study showed that tumor-induced overexpression of high-mobility group box 1 (HMBG1) induces a Treg phenotype [7]. Patients with overexpression of this protein were at higher risk for progression of disease, relapse, and death.

Despite these correlations in retrospective analyses, there are no prognostic markers in the TME to steer clinical decision making. Inclusion of markers of cell differentiation, function, activation, and exhaustion in multiple parameter analysis may help determine which factors have the strongest associations with, and prognostic value for patient outcome. Advanced techniques, such as tissue cytometry by time-of-flight (CyTOF), can overcome the limitations of measuring only a few markers in common practice immune histology.

## 2.2. Circulatory Immune Markers

Despite advances in immune profiling and the easy accessibility of PB, no validated circulatory immune biomarkers exist for patients with NBL. Surprisingly, studies implementing immune monitoring in NBL patients are limited.

### *2.2.1. Cytokines and Soluble Molecules in Plasma/Serum*

Cytokines and chemokines are components of a complex network promoting angiogenesis and metastasis, diminishing adaptive immunity, and changing responses to hormones and therapeutic agents. As such, cytokines involved in cancer-related inflammation are easy to monitor and relate to patient outcome and could be a target for therapeutic strategies.

Oliveira and colleagues reported an increase of IL-2, IL-4, IL-5, IL-6, IL-9, IL-10, IL-13, IL-17A, IL-17F, IL-21, IL-22, IFNγ, and TNFα in plasma of NBL patients compared to age matched controls. One of these cytokines, IL-6, is a key growth-promoting and anti-apoptotic inflammatory cytokine, which correlated with poor prognosis and high-risk disease [31]. When integrating levels of IL-6 with other candidate biomarkers (serum amyloid A (SAA), apolipoprotein (APOA1), epidermal growth factor (EGF), macrophage derived chemokine (MDC), sCD40L, and Eotaxin), the multivariate classifier predicted active disease with a sensitivity of 81% and specificity of 90% [32]. These data are encouraging and are awaiting validation in other patient cohorts.

Even though mRNA levels of IL-10 (a product of Tregs, NK-cells and macrophages) in BM and, PB; as well as IL-10 plasma concentrations were higher in metastatic NBL patients compared to healthy controls, a prognostic role of IL-10 alone could not be demonstrated [29]. Low levels of soluble proteins other than cytokines, such as human leukocyte antigens HLA-E and HLA-F, were associated with worse prognosis [33]. In contrast to this, several other studies were not able to correlate markers measured in plasma/serum to outcome.

In other cancers, the analyses of cytokine profiles rather than single markers has shown positive prediction values at diagnosis [34-37]. The studies summarized above hopefully initiate validation studies in NBL patients with multiparameter analyses in different patient cohorts.

### *2.2.2. Immune Cells in Peripheral Blood*

Leukocyte counts have been found to be significantly higher in NBL patients compared to controls [38]. Although no difference is observed in total lymphocyte count between healthy controls, localized, and metastatic patients, relative numbers of multiple lymphocyte subsets do vary [31]. Semeraro *et al*. measured a significant increase in the percentage of CD3−CD56+ NK-cells in PB of metastatic NBL patients compared to patients with localized tumors, which was associated with a minor response to induction chemotherapy. The percentage of cytotoxic (CD16+) NK-cells positively correlated with clinical response to therapy [39]. These correlations could potentially be explained by NK-cell mediated cytotoxic effects on MHC-I lacking tumor cells. Activated NK-cells may also upregulate MHC-I expression on NBL cells, thereby circumventing further NK-cell mediated cytotoxicity, while at the same time increasing their susceptibility to T-cell mediated cytotoxicity [40].

Morandi and colleagues found that Treg (CD4+CD25hiCD127−) and Tr1 (CD4+CD45R0+CD49b+LAG3+) subsets are decreased in NBL patients compared to controls, but no correlation was found with prognostic factors, such as age and stage. MYCN amplification was the only prognostic factor associated with higher levels of Treg numbers in BM and Tr1 levels in PB [41]. In addition, CD4+ and CD8+ T-cells show increased surface expression levels of the checkpoint inhibitor CTLA-4, and PD-1 on CD4+ T-cells. In contrast, Semeraro *et al.* found increased CD4+FoxP3+ T-cells in metastatic NBL patients compared to localized tumors. The differences in the markers used to identify specific cell subsets (in this case Treg) in different studies complicates a valid comparison between the data from these studies and indicates the need for harmonization of immune phenotyping protocols.

When comparing the myeloid compartment, NBL patients with localized tumors showed higher monocyte, neutrophil, and erythrocyte counts as compared to patients with metastatic disease. When zooming in on the phenotype of myeloid cells, increased levels of the checkpoint inhibitor programmed death ligand 2 (PD-L2) were observed in transitional (CD14+CD16+) and non-classical monocytes (CD14-CD16+) in patients compared to controls [31]. Furthermore, increased expression of CSF-1R, a regulator inducing MDSC expression, was observed in patients, and correlated with poor clinical outcome [42].

In summary, it is clear that NBL patients show alterations in absolute numbers and subset percentages of immune cells, as well as in immune proteins in the TME and in PB. An overview of the reviewed studies can be found in **Table 1**. However, so far, no robust prognostic marker correlating with survival has been identified and validated. Such immune signatures at diagnosis could aid in therapy decision making and prognosis prediction.

Table 1. Overview of neuroblastoma immune monitoring studies at diagnosis.

| **Flow Cytometry** | | | | |
|---|---|---|---|---|
| **Number of Unique Patient Samples Measured Including Material** | | **Tumor Characteristics** | **Markers** | **Reference** |
| 8 | Primary Tumor | I (4x) + II (1x) + III (2x) + IV (1x) | CD3, CD4, CD8, CD25, CD45RA, CCR7 | Carlson *et al.* 2013 [43] |
| | PB | | | |
| 26 | Primary Tumor | II (2x) + III (2x) + IV (21x) + IVs (1x)<br>15 MYCN amp, 11 non MYCN amp | GD2 | Mussai *et al.* 2015 [24] |
| | PB | | CD15, CD14, CD11b | |
| 20 | BM | IV (20x) | CD45, CD33, CD14, GD2, CD56 | Song *et al.* 2009 [26] |
| 41 | PB | 13 MYCN amp, 28 non MYCN amp | CD4, CD25, CD127, CD45RO, CD49b, LAG-3 | Morandi *et al.* 2015 [29] |
| 5 | PB | High-Risk Patients | HLA-DR, CD33, CD11b | Gowda *et al.* 2013 [44] |
| 21 | PB | 7 MYCN amp, 20 non MYCN amp (14 localized, 13 metastatic) | CD4, CD25, CD127, CD45RO, CD49b, LAG-3 | Morandi *et al.* 2016 [41] |
| 27 | BM | | | |
| 59 | PB<br>BM | 23 localized, 36 metastatic tumors | CD8, NKp46, CD4, CD16, CD56, NKp30, DNAM-1, CD127, CD25, CD14, CD45, CD15, GD2, CD235a, CD9, CD81, TCRgd, NKp44, NKp80, CD3e, CD158a/h, CD158b, CD158e/k, CD158i, FoxP3 | Semeraro *et al.* 2015 [39] |
| **Immunohistochemistry** | | | | |
| 24 | Primary Tumor | 7 MYCN amp, 26 non MYCN amp | CD68 | Apps *et al.* 2013 [45] |
| 21 | | | CD3 | |
| 19 | | | pSTAT3 | |
| 8 | Primary Tumor | I (4x) + II (1x) + III (2x) + IV(1x) | Ki67, CD3 | Carlson *et al.* 2013 [43] |
| 15 | Primary Tumor | 3 low risk, 6 intermediate risk, 6 high risk | CD4, CD45 | Zhang *et al.* 2017 [25] |
| 129 | Primary Tumor | IV (129x) | CD1d, Vα24-Jα18inv, TCRα6β11 | Song *et al.* 2017 [26] |
| 71 | Primary Tumor | stage I–III (n = 29), stage IV (n = 31), stage IVS (n = 11) | CD163, AIF1 | Asgharzadeh *et al.* 2012 [27] |
| 84 | Primary Tumor | I (34x) + II (19x) + III (5x) + IV (20x) + IVS (6x) | CD3, CD4, CD8, CD25, FOXP3, Ki67, β2m-free MHC1 heavy chain | Mina *et al.* 2015 [8] |

| **Number of Unique Patient Samples Measured Including Material** | | **Tumor Characteristics** | **Markers** | **Reference** |
|---|---|---|---|---|
| **ELISA** | | | | |
| 57 | Plasma | IV (49x) + non IV (8x) | IL-10, ARG-1 (57) | Morandi *et al.* 2015 [29] |
| 53 | PB | PB: I (8x) + II (8x) + III (6x) + IV (28x) + IVS (3x) | IL-6 | Egler *et al.* 2008 [46] |
| 18 | BM | BM: I (1x) + II (3x) + III (2x) + IV (11x) + IVS (1x) | | |
| 35 | PB | PB: I (5x) + II (5x) + III (3x) + IV (20x) + IVS (2x) | sIL-6R | Egler *et al.* 2008 [46] |
| 16 | BM | BM: I (1x) + II (2x) + III (2x) + IV (10x) + IVS (1x) | | |
| 84 | Primary Tumor | I (7x) + II (8x) + III (22x) + IV (42x) + 4S (5x)<br>27 MYCN amp, 57 non MYCN amp | sHLA-F, sB7H3, sHLA-E | Morandi *et al.* 2013 [33] |
| **Luminex** | | | | |
| 55 | Plasma<br>PB | 20 low-risk, 35 high-risk In addition, 28 HR blood samples from 7 patients at various timepoints during treatment | GM-CSF, G-CSF, IFNγ, IL-1a, IL-1ra, IL-1b, IL-2, IL-3, IL-4, IL-5, IL-6, IL-7, IL-8, IL-9, IL-10, IL-12p70, IL-12p40, IL-13, IL-15, IL-17, MCP-1, MCP-3, MDC, TNFα, TNFβ, TGFα, Eotaxin, IFNα2, IP-10, MIP-1a, MIP-1b, EGF, FGF-2, FLT3L, Fractalkine, GRO, VEGF, sCD40L, sIL-2Ra | Egler *et al.* 2011 [32] |

## 3. IMMUNE MONITORING DURING THERAPY

Immune monitoring during therapy is crucial to identify potentially prognostic factors that could be exploited to enhance immunogenicity of the tumor and predict treatment response. This section will start by reviewing studies which monitor the immune response upon standard therapy, including chemotherapy and monoclonal antibody therapy. Subsequently, immune monitoring in more experimental treatment regimens, including vaccination strategies, adoptive cell-, and checkpoint inhibition therapy will be discussed.

### 3.1. Chemotherapy

In general, high-risk NBL patients receive 5–8 cycles of intensive chemotherapy including platinum, alkylating, and topoisomerase agents. In North-America, induction regimens include vincristine, doxorubicin, cyclophosphamide, cisplatin, and etoposide, while the Society of pediatric oncology Europe NBL group (SIOPEN) used a rapid COJEC regimen that gives eight cycles with combinations of vincristine, carboplatin, etoposide, cyclophosphamide, and cisplatin [47].

A limited number of studies has monitored immune profiles during chemotherapy in cancer patients. Monitoring lymphocyte levels during and after chemotherapy in hematopoietic and solid tumors generally showed increased EFS in patients with higher lymphocyte counts at diagnosis as well as after induction chemotherapy [42,47–49] In addition, fast monocyte recovery after chemotherapy is predictive for EFS in patients with leukemias and lymphomas [50,51]. In line with these data, an elevated neutrophil to lymphocyte ratio after chemotherapy, but before surgical resection of the NBL tumor, was associated with decreased OS [52].

Upon chemotherapy treatment, Treg counts decreased, possibly due to nonspecific targeting of Tregs by chemotherapeutic agents. More studies are warranted to determine if the effect can be subscribed to chemotherapy-induced decrease in T-cells in general, or whether specific subsets, like Tregs, might be more susceptible to chemotherapy-induced cytotoxicity [53]. Chemotherapy generally does not affect NK-cells [54], however, the expression levels of NKp30, an NK-cell receptor involved in tumor cell killing and DC recognition, positively correlate with survival after chemotherapy [55]. Expression levels of the immunosuppressive isoform NKp30C and the activating isoforms NKp30A and NKp30B affect NK-cell function and correlate with EFS of NBL patients after chemotherapy [39].

No studies have monitored immune markers in the TME during chemotherapy in patients. An *in vivo* mouse study showed that depletion of TAMs from NBL tumors is associated with increased chemotherapeutic efficacy without requiring T-cell contribution [56]. This observation led to the author's suggestion to combine CSF-1R blockade with chemotherapy to potentially increase treatment efficacy.

To date, too few studies have monitored immune status during chemotherapy to identify markers that could predict response to therapy. It seems that patients with higher numbers or faster recovery of lymphocytes and monocytes have better EFS changes. Whether this is a reflection or a result of the development of a healthier immunological niche should be studied, but the observation could lead to the hypothesis that these patients might also be responding better to immune-related treatment options.

### 3.2. Monoclonal Antibody Therapy

A frequent immunotherapy protocol of high-risk NBL consists of anti-GD2 combined with all-trans-retinoic acid (ATRA), IL-2, and GM-CSF. Even though immunotherapy increased 2-year EFS and OS [10], relapse is still observed in 40% of patients. Elucidation of effective anti-tumor responses is key to study what discriminates responders from non-responders.

IL-2 and GM-CSF have been added to the treatment protocol as they were observed to enhance cytotoxicity of anti-GD2 *in vitro* [10,57–59]. In addition, GM-CSF also increased myeloid cell activation, another important cell type in the anti-tumor response [57,60]. The multi-component nature of the immunotherapy protocol makes that the observed immune effects cannot be ascribed to a specific component of the protocol.

A primary mechanism of action of anti-GD2 is the induction of antibody-dependent cellular cytotoxicity (ADCC), which requires recognition by effector cells (mainly NK-cells, monocytes, neutrophils, and macrophages) [11,60]. Cytotoxic activity of NK-cells is mediated by CD16, whereas cytotoxic activity of monocytes, neutrophils, and macrophages is mediated by CD32. Both receptors recognize the Fc fragment of anti-GD2 on opsonized NBL cells and induce cytotoxic effector functions. Complement-dependent cytotoxicity (CDC) is another mechanism of action of anti-GD2, however, most studies focus on its implications regarding pain toxicity rather than on-tumor toxicity.

Nassin *et al*. monitored immune reconstitution at the start of immunotherapy containing IL-2, GM-CSF, and anti-GD2 [61]. They showed that absolute lymphocyte counts (T-, B-, and NK-subsets) are lower in the vast majority of patients as compared to age-matched controls. Patients with disease progression, relapse or residual disease had significantly lower total leukocyte counts, as well as lower absolute lymphocyte-, neutrophil-, and CD16+ cell counts compared to disease-and progression-free patients observed three months after therapy. Siebert and colleagues found that presence of human anti-chimeric antibodies against chimeric anti-GD2 resulted in significant reduction in peripheral anti-GD2 levels, as well as significant abrogation in ADCC and CDC [62]. However, in this study, it is not clear whether such immune responses are a disadvantage for survival of the treated patients. In addition, the induction of a host anti-idiotype network, measured indirectly by human anti-mouse antibody responses, correlated with long term survival [63–65].

The importance of NK-cells in ADCC was illustrated by Chowdhury *et al*.; showing that *in vitro* anti-GD2 mediated lysis of the LAN1 NBL cell line upon co-culture with peripheral blood mononuclear cells (PBMCs) from a NBL patient abrogated after NK-cell depletion [66]. In addition, cell lysis correlated with NK-cell expression of CD69, an early activation marker, as well as with the degranulation marker CD107a. Furthermore, variation in ADCC between patients was found to be caused by genetic predispositions resulting in better cytotoxic activity of effector cells and correlations with better survival [59,63,64]. Siebert *et al*. studied the level of ADCC *in vitro* in combination with FCGR polymorphisms and killer cell immunoglobulin like receptor KIR/KIR ligand genotypes of 53 patients. They showed that patients with high affinity FCGRs had higher ADCC levels and better EFS compared to patients with low affinity genotypes. In addition, a correlation was found between the activating KIR 2DS2 genotype on ADCC and EFS. A combination of high-affinity FCGR2A,-3A and stimulating genotypeB/x or the presence of activating KIR 2DS2 resulted in the strongest anti-NBL cellular cytotoxicity mediated by anti-GD2 and improved EFS [67]. In addition, Tarek *et al*. found that patients treated with monoclonal antibodies lacking HLA class I ligands for their inhibitory KIRs have significantly higher survival rates [68]. Unlicensed NK-cells mediate tumor control via ADCC. These results show that FCGR polymorphisms and KIR/KIRL genotypes could function as biomarkers in response to immunotherapy.

The importance of NK-cell mediated ADCC in anti-GD2 efficacy, together with the observation of relatively fast NK-cell recovery early after ASCT was an important rationale for immunotherapy timing early after transplantation [69]. However, more detailed evaluation of NK-cell subsets showed that most of these NK-cells are immature, cytokine releasing (CD56bright, CD16+/−) rather than the cytotoxic (CD56dim, CD16+) NK-cells known to be mainly responsible for anti-GD2 dependent ADCC [61]. This is further substantiated by observed impaired immune recovery of CD16+ NK-cells in patients with disease progression or relapse at time of transplantation compared to those without. These studies may suggest suboptimal timing of anti-GD2 immunotherapy early after transplantation. Utilizing haploidentical allogeneic hematopoietic cell sources rather than autologous sources could be explored as a transplantation source regarding NK-cell recovery early after transplantation.

In addition to NK-cell subset monitoring, Nassin *et al.* showed increased CD25 expression on CD4+ T-cells as compared to CD8+ T-cells at the start of immunotherapy [61]. Even though FoxP3 expression of these cells is unknown, it is hypothesized that these cells could be classified as Tregs [70]. Ladenstein *et al.* recently concluded from a phase III clinical trial that there is no additive effect of IL-2 administration on outcome of high-risk NBL patients [71]. As (low dose) IL-2 administration to autoimmune patients resulted in preferential expression of Tregs [72], authors hypothesize that adjuvant IL-2 administration could be responsible for Treg expansion during immunotherapy, diminishing the positive effects (e.g., NK expansion) of IL-2. Indeed, we observed a rise in Treg numbers upon every round of IL-2 to NBL patients (unpublished). Furthermore, administration of IL-2 also results in development of eosinophils through stimulating growth factors derived from T-cells, such as IL-3, IL-5, and GM-CSF that help to maintain eosinophils *in vitro* [73]. In addition, an increase in IL-5 levels during immunotherapy with anti-GD2 and cytokines was observed, which could induce and maintain eosinophils [74]. Although their effect is unknown, suppressive eosinophils have been reported in murine studies and could possibly also be present in IL-2 treated NBL patients [75]. Further studies are required to confirm these effects of IL-2 on levels of Treg and eosinophils, preferably with functional testing of the different cell subsets.

To overcome limitations of the current anti-GD2 monoclonal antibody therapy, including monoclonality of the response, anti-idiotype responses, and memory induction, Kusher *et al.* reported a strategy in which patients are vaccinated with GD2 and GD3. This results in an intrinsic, polyclonal, multivalent antibody response through stimulation of B-cells to produce anti-GD2 and –GD3 [76]. As B-cell recovery is key for vaccination efficacy, immunomonitoring of B-cell recovery after ASCT is key for optimal vaccination timing.

To conclude, immune monitoring studies during immunotherapy are largely lacking and studies that are available have only monitored patients at start and end of therapy. All new phase II/III trials and standard treatment protocols should not only asses outcome but also monitor the immune system during therapy to get a better and faster understanding of treatment success.

### 3.3. Adoptive Cell Therapy

The development of adoptive cell therapy (ACT) strategies has taken flight in the last decade. These cell products should ideally possess the capacity to expand, actively migrate through the entire body (including to the solid tumor core and over the blood brain barrier), and induce systemic immune memory to prevent future relapse. ACT products are generated by harvesting, ex vivo expansion, and re-direction of immune cells to target tumor cells. Even though successes have been achieved in several hematological malignancies [77–80], translation of these successes to solid tumors is difficult. Target expression heterogeneity, localization to the tumor site, and overcoming the immunosuppressive, nutrient-, and stimuli- deprived TME are thought to be the main challenges in effective adoptive cell therapy in solid tumors [81].

To date, pre-clinical studies as well as clinical trials are exploiting T-, NK-, and NKT-cells in both autologous and allogeneic ACT strategies in NBL. Infused cells can be isolated from PB [82–85], as well as from tumor tissue (e.g., TILs) [8,20]. In addition, isolated cells can be genetically modified to improve recognition of tumor cells, for example through knock-in of a NBL-specific T-cell receptor (TCR) [40,86,87], a chimeric antigen receptor (CAR) [20,88–95], or a bispecific antibody [96,97] against tumor specific targets such as GD2, PRAME, NY-ESO-1, L1-CAM, B7-H3, and mutated ALK. Very low or even absent surface expression of major histocompatibility complex I (MHC-I) on NBL cells has led to the focus on MHC-I unrestricted ACT-strategies, mainly exploiting NK-cell- and CAR therapy (or a combination of both). Excellent overviews of clinical trials of (adoptive cell) therapy strategies in NBL are provided by Le and Thai [98] and Zage [99].

Even though multiple recent (pre-clinical) studies have demonstrated efficacy of various forms of ACT in NBL, the observed clinical benefit is limited. Persistence of ACT products in general is a widely discussed topic and is thought to be depending on balanced activation (appropriate co-stimulation, prevention of tonic/chronic receptor signaling, and of activation-induced cell death), tolerance induction (caused by native antigen expression and tumor immunosuppression), the cell phenotype of both the apheresis material and the product itself, as well as by the need of antigen availability for cell persistence [87,100,101]. The extremely immunosuppressive, nutrient- and stimuli deprived TME of solid tumors is thought to be the main factor responsible for the discrepancies in successes with hematological tumors [82,102].

Monitoring the tumor infiltrating cell population, its phenotype, and other related factors will provide the much-needed insight to predict therapy response and to understand what is driving resistance and success and where can be acted upon. Sporadic monitoring after ACT resulted in the observation that the presence of central memory and naïve T-cell phenotypes in cell products has a positive effect on persistence of the cell product in several cancer types, including NBL [8,82,103–106]. Hurtado *et al*. recently showed that the presence of central memory NBL TILs greatly decreases after non-specific ex vivo rapid expansion cycles, stressing the importance of ex vivo expansion protocol evaluation in adoptive cell strategies [20]. Moreover, lymphodepletion before T-cell infusion or early T-cell infusion after ASCT (day 2) caused significantly improved expansion and persistence of the cell product [82,89]. This indicates that the immunosuppressive status of the immune system of these patients is an important limiting factor in effective ACT and led to the rationale to combine ACT with checkpoint inhibitors [89,107]. Remarkably, combining PD-1 blockade by pembrolizumab with GD2 CAR T-cell administration upon lymphodepletion in a phase 1 clinical trial in NBL did not show any beneficial effect of PD-1 blockade on peripheral CAR T-cell expansion [89]. A limitation of this study is that the arm studying the effect of PD-1 blockade on non-lymphodepleted GD2 CAR T-cell treated patients was missing. Furthermore, T-cell expansion and persistence was solely measured in the blood and not at the tumor site. The fact that two out of three treated patients in this arm experienced stable disease that turned into complete remission after additional treatment is encouraging and warrants more research. Controversially, immune monitoring in the same phase 1 GD2 CAR study showed specific expansion of circulating immunosuppressive M2 macrophage-like myeloid cells (CD45+CD33+CD11b+CD163+) independent of lymphodepletion and PD-1 blockade [89]. Inhibitory myeloid cells are correlated with poor prognosis in several cancer types, including NBL, even though this study does not provide any data on whether these mobilized cells are attracted to the tumor site. Induction of MDSCs was also reported in GD2–CAR T-cell therapy for sarcomas in xenograft mice, which impaired CAR T-cell activity [108]. Addition of all-trans retinoic acid (ATRA) destroyed the MDSCs and thereby improved the efficacy of the GD2-CAR T-cells [108], suggesting that patients might also benefit from ATRA to eradicate the circulating M2 macrophage-like myeloid cells that are induced by GD2-CAR3. Thirdly, immune monitoring in this phase 1 study indicated a correlation between circulating IL-15 levels and GD2 CAR T-cell expansion [89]. Circulating IL-15 levels could not only potentially be used as a biomarker for CAR T-cell expansion, but a pre-clinical xenograft mouse model transduced with GD2 CAR T-cells overexpressing IL-15 also showed improved expansion, enhanced anti-tumor activity and improved survival [93].

Even though immune monitoring data during ACT in NBL is scarce, the above mentioned studies all resulted in clear rationales for research into new therapeutic strategies or biomarker development. This clearly indicates the need for more elaborate immune monitoring during ACT.

### 3.4. Checkpoint Inhibitors

Another interesting strategy would be to target the immunosuppressive environment of NBL [7]. Checkpoint inhibitors (CPis), blocking CTLA-4, PD-1, PD-L1, or PD-L2, are proven to be effective in a variety of tumors, including solid tumors [109]. The potential of these inhibitors is illustrated by the growing list of FDA-approvals, as reviewed by Hargadon *et al.* [110]. Currently, most of these approvals are in unresectable metastatic disease settings. Nevertheless, the potency of CPis to induce a more potent anti-tumor immune response, and therefore potential induction of anti-tumor immunological memory, makes checkpoint inhibition a very interesting candidate as an adjuvant therapy in curative treatment settings. The utilization of CPis as a monotherapy in NBL has been investigated in multiple pre-clinical studies [42,111–113]. These studies show no effect of CPi treatment on systemic NBL progression *in vivo*. This has been supported in a phase I clinical trial in pediatric patients with advanced solid tumors, in which one NBL patient was included [114]. More clinical trials assessing CPis as a monotherapy in refractory NBL are currently running (NCT02304458; NCT02332668; NCT02541604).

Several rationales have been proposed for the ineffectiveness of CPi therapy in high-risk NBL. First of all, evaluation of NBL tumors from patients with different tumor stages does not only, as mentioned before, show inverse correlation between tumor grade and TILs [8], but also between tumor grade and PD-L1 tumor expression [113]. Absence of TILs and PD-L1 tumor expression provides a first rationale to CPi therapy resistance. Secondly, one of the immunomodulatory mechanisms of NBL is the upregulation of PD-L1 in response to IFN-γ [111,113]. This highlights a potential resistance mechanism against CPi therapy, as persistent IFN-γ production by activated T-cells may lead to a continuous cascade causing even higher upregulation of the immune checkpoints resulting in T-cell senescence. Impaired IFN pathway activity in MYCN-amplified tumors [23] may prevent PD-L1 expression upon IFN-γ exposure and provides a third rationale for CPi therapy effectiveness in high-risk NBL.

Next to these observations, especially studies investigating CPi-including combination therapies revealed some insights in mechanisms explaining NBL resistance to CPi monotherapy [42,111–113]. Rigo and colleagues showed that combining CPi with temporary CD4 depletion by anti-CD4 monoclonal antibody treatment caused a very potent CD8+ T-cell dependent response causing significantly longer tumor-free survival, complete tumor regression, and durable anti-NBL immunity *in vivo* [111]. Combining CPi with immune enhancer IL-21, or Treg targeting agents polyoxotungstate (POM-1) and anti-CD25 antibody, revealed no significant effect. This indicates that CD4+ CD25high Tregs, as well as adenosine generation in Tregs are not responsible for CPi resistance in NBL. More specific studies into effects of CD4+ CD25−/low FOXP3+ Tregs or other CD4+ Tregs should be performed to further unravel the synergistic effect observed upon CD4 depletion [111].

Mao *et al.* reported that targeting of CSF-1Rþ+ suppressive myeloid cells in combination with CPis caused spontaneous control of NBL *in vivo* [42], a mechanism confirmed in several other types of cancers, as reviewed by Weber *et al.* [115]. A possible explanation for this is the observation that T-cells start to produce M-CSF upon PD-1 blockade, which can bind to CSF-1R on myeloid-derived suppressor cells, thereby enhancing their suppressive phenotype [116]. This causes a further reduction of IFN-regulated chemokine release (e.g., CXCL9, 10, and 11) in the TME, which are important for T-cell infiltration and could therefore potentially explain the synergistic effect of targeting CSF-1Rþ+ suppressive myeloid cells in combination with CPi.

Other combination strategies which seem promising based on preclinical studies include combinations of CPis with whole tumor cell vaccination [113], high intensity ultrasound [117], and anti-GD2 treatment [112]. All mentioned preclinical evidence of effective NBL targeting treatment combinations provides a clear rationale for clinical assessment of CPi therapy as an adjuvant therapy against NBL. Even though data obtained in these induced tumor mouse models should be interpreted with caution, the data should be used as a rationale for focusing on immune monitoring of adjuvant CPi therapy in coming clinical trials.

## 4. DISCUSSION

The present review shows the potential of standardized immune monitoring in NBL. Despite many efforts, high-risk NBL has a poor response to treatment and novel therapies are urgently required. We should therefore better understand the functional kinetics of tumor- and immune cells to guide and modulate immune therapy strategies. As such, immune monitoring may provide evidence-based directions to optimize treatment protocols, e.g. in the recent discussion whether IL-2 should be removed from the current treatment protocol [118].

Studies listed in this review use flow cytometry, CyTOF, immunohistochemistry, as well as functional assays to perform immune monitoring on tissue, PBMCs or plasma/serum from NBL patients. Monitoring PBMCs and plasma/serum cytokines is by far the easiest approach as blood is easily available during treatment. As the immune system is a multifaceted system, it is important to question if findings in the circulatory system are related to the TME. Monitoring peripheral blood subsets currently have insufficient clinical value for clinical decision making. Future studies with paired monitoring of PB, BM, and TME samples will increase our understanding of underlying mechanism and shed light on the use of biomarkers over the treatment course as predictors for efficacy and/or toxicity.

As most studies describe small patient populations, high interpatient variability, and no harmonization of monitoring protocols, it can be difficult to interpret results and relate it to recent literature [119]. The studies used in this review are sometimes limited to results of 3–5 patients. Therefore, we propose to define and implement standardized immune monitoring protocols in the trial- and study design to increase patient numbers and study interpatient variability. An example is proposed in **Figure 1**. As each patient is unique, immune monitoring can facilitate future personalized treatment in NBL.

Advances in organoid technology are promising in predicting the immunosuppressive capacities as well as the sensitivity to (immune) therapy in a personalized setting. Neuroblastoma tumor models have been developed that represent the tumor better than classical cell lines [120]. This strategy has previously shown to be effective in metastatic gastrointestinal cancers, in which patient derived organoids were instrumental in the prediction of tumor-specific responses, stimulating personalized treatment strategies [121]. Single-cell RNA sequencing of NBL tumors can, besides studying tumor heterogeneity and driving factors behind tumor heterogeneity, help to identify new leads for immunotherapeutic strategies [122].

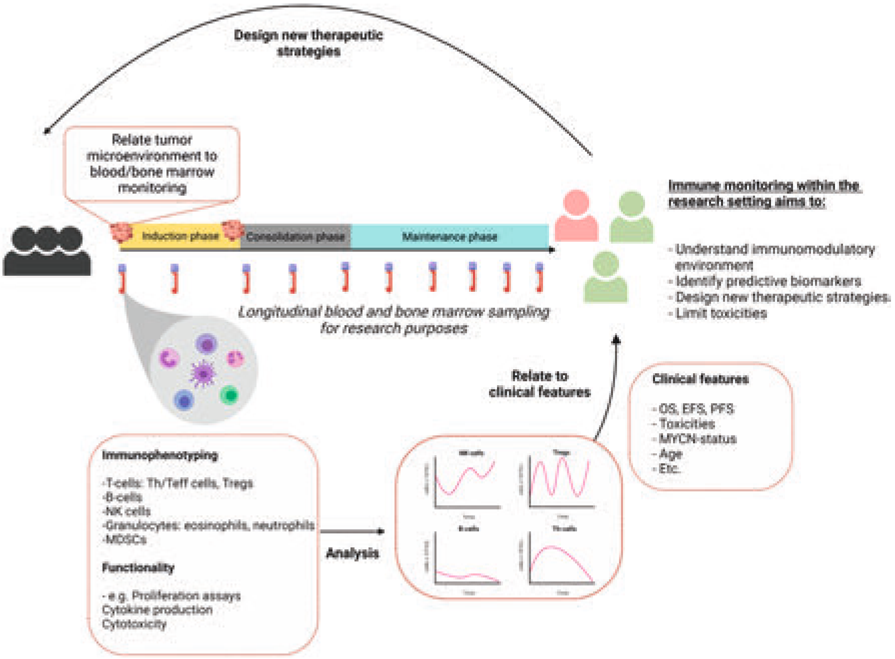
Design new therapeutic strategies
Relate tumor microenvironment to blood/bone marrow monitoring
Induction phase
Consolidation phase
Maintenance phase
Immune monitoring within the research setting aims to:
- Understand immunomodulatory environment
- Identify predictive biomarkers
- Design new therapeutic strategies
- Limit toxicities
Longitudinal blood and bone marrow sampling for research purposes
Relate to clinical features
Clinical features
- OS, EFS, PFS
- Toxicities
- MYCN-status
- Age
- Etc.
Immunophenotyping
-T-cells: Th/Teff cells, Tregs
-B-cells
-NK cells
-Granulocytes: eosinophils, neutrophils
-MDSCs
Functionality
- e.g. Proliferation assays
Cytokine production
Cytotoxicity
Analysis
Tregs

**Figure 1.** Immune monitoring for research purposes.
*Monitoring peripheral blood subsets currently have insufficient clinical value for clinical decision making. Created with BioRender.com*

## 5. CONCLUSIONS

In conclusion, immune monitoring before and during therapy of NBL patients could facilitate identification of predictive biomarkers to guide patients towards effective treatment with limited toxicities and optimal quality of life. Furthermore, understanding the immunomodulatory environment of NBL and its response to treatment in responders and non-responders is important to facilitate design of new therapeutic strategies improving outcome of high-risk NBL.

## REFERENCES

1. Matthay, K.K.; Maris, J.M.; Schleiermacher, G.; Nakagawara, A.; Mackall, C.L.; Diller, L.; Weiss, W.A. Neuroblastoma. *Nat. Rev. Dis. Prim.* **2016**, *2*, 16078, doi:10.1038/nrdp.2016.78.
2. Park, J.R.; Eggert, A.; Caron, H. Neuroblastoma: Biology, Prognosis, and Treatment. *Hematol. Oncol. Clin. N. Am.* **2010**, *24*, 65–86, doi: 10.1016/j.hoc.2009.11.011.
3. Maris, J.M. Recent Advances in Neuroblastoma. *N. Engl. J. Med.* **2010**, *362*, 2202–2211, doi:10.1056/NEJMra0804577.
4. Davidoff, A.M. Neuroblastoma. Semin. Pediatr. Surg. **2012**, 21, 2–14, doi:10.1053/j.sempedsurg.2011.10.009.
5. Chen, D.S.; Mellman, I. Elements of cancer immunity and the cancer-immune set point. *Nature* **2017**, *541*, 321–330, doi:10.1038/nature21349.
6. Bonaventura, P.; Shekarian, T.; Alcazer, V.; Valladeau-Guilemond, J.; Valsesia-Wittmann, S.; Amigorena, S.; Caux, C.; Depil, S. Cold Tumors: A Therapeutic Challenge for Immunotherapy. *Front. Immunol.* **2019**, *10*, 168, doi:10.3389/fimmu.2019.00168.
7. Vanichapol, T.; Chutipongtanate, S.; Anurathapan, U.; Hongeng, S. Immune Escape Mechanisms and Future Prospects for Immunotherapy in Neuroblastoma. *Biomed. Res. Int.* **2018**, *2018*, 1812535, doi: 10.1155/2018/1812535.
8. Mina, M.; Boldrini, R.; Citti, A.; Romania, P.; D’Alicandro, V.; Ioris, M. De; Castellano, A.; Furlanello, C.; Locatelli, F.; Fruci, D. Tumor-infiltrating T lymphocytes improve clinical outcome of therapy-resistant neuroblastoma. *Oncoimmunology* **2015**, *4*, 1–14, doi: 10.1080/2162402X.2015.1019981.
9. Nagasawa, M.; Kawamoto, H.; Tsuji, Y.; Mizutani, S. Transient increase of serum granulysin in a stage IVs neuroblastoma patient during spontaneous regression: Case report. *Int. J. Hematol.* **2005**, *82*, 456–457, doi:10.1532/IJH97.05091.
10. Yu, A.L.; Gilman, A.L.; Ozkaynak, M.F.; London, W.B.; Kreissman, S.G.; Chen, H.X.; Smith, M.; Anderson, B.; Villablanca, J.G.; Matthay, K.K.; et al. Anti-GD2 Antibody with GM-CSF, Interleukin-2, and Isotretinoin for Neuroblastoma. *N. Engl. J. Med.* **2010**, *363*, 1324–1334, doi:10.1056/NEJMoa0911123.
11. Zeng, Y.; Fest, S.; Kunert, R.; Katinger, H.; Pistoia, V.; Michon, J.; Lewis, G.; Ladenstein, R.; Lode, H.N. Anti-neuroblastoma effect of ch14.18 antibody produced in CHO cells is mediated by NK-cells in mice. *Mol. Immunol.* **2005**, *42*, 1311–1319, doi:10.1016/j.molimm.2004.12.018.
12. Modak, S.; Cheung, N.-K. V Neuroblastoma: Therapeutic strategies for a clinical enigma. *Cancer Treat. Rev.* **2010**, *36*, 307–317, doi: 10.1016/j.ctrv.2010.02.006.
13. Kim, R.; Coppola, D.; Wang, E.; Chang, Y.D.; Kim, Y.; Anaya, D.; Kim, D.W. Prognostic value of CD8CD45RO tumor infiltrating lymphocytes in patients with extrahepatic cholangiocarcinoma. *Oncotarget* **2018**, *9*, 23366–23372, doi: 10.18632/oncotarget.25163.
14. Parra, E.R.; Villalobos, P.; Behrens, C.; Jiang, M.; Pataer, A.; Swisher, S.G.; William, W.N.; Zhang, J.; Lee, J.; Cascone, T.; et al. Effect of neoadjuvant chemotherapy on the immune microenvironment in non-small cell lung carcinomas as determined by multiplex immunofluorescence and image analysis approaches. *J. Immunother. Cancer* **2018**, *6*, 48, doi:10.1186/s40425-018-0368-0.
15. Lo, C.S.; Sanii, S.; Kroeger, D.R.; Milne, K.; Talhouk, A.; Chiu, D.S.; Rahimi, K.; Shaw, P.A.; Clarke, B.A.; Nelson, B.H. Neoadjuvant chemotherapy of ovarian cancer results in three patterns of tumor-infiltrating lymphocyte response with distinct implications for immunotherapy. Clin. *Cancer Res.* **2017**, *23*, 925–934, doi:10.1158/1078-0432.CCR-16-1433.

**16.** Hegde, P.S.; Karanikas, V.; Evers, S. The where, the when, and the how of immune monitoring for cancer immunotherapies in the era of checkpoint inhibition. *Clin. Cancer Res.* **2016**, *22*, 1865–1874, doi:10.1158/1078-0432.CCR-15-1507.

**17.** Martin, R.F.; Bruce Beckwith, J. Lymphoid infiltrates in neuroblastomas: Their occurrence and prognostic significance. *J. Pediatr. Surg.* **1968**, *3*, 161–164, doi:10.1016/0022-3468(68)91005-1.

**18.** Lauder, I. The significance of lymphocytic infiltration in neuroblastoma. *Br. J. Cancer* **1972**, *26*, 321–330, doi:10.1038/bjc.1972.43.

**19.** Hellstrom, I.E.; Hellstrom, K.E.; Pierce, G.E.; Bill, A.H. Demonstration of cell-bound and humoral immunity against neuroblastoma cells. *Proc. Natl. Acad. Sci. USA* **1968**, *60*, 1231–1238, doi:10.1073/pnas.60.4.1231.

**20.** Ollé Hurtado, M.; Wolbert, J.; Fisher, J.; Flutter, B.; Stafford, S.; Barton, J.; Jain, N.; Barone, G.; Majani, Y.; Anderson, J. Tumor infiltrating lymphocytes expanded from pediatric neuroblastoma display heterogeneity of phenotype and function. *PLoS ONE* **2019**, *14*, e0216373–e0216373, doi:10.1371/journal.pone.0216373.

**21.** Fridman, W.H.; Zitvogel, L.; Sautès-Fridman, C.; Kroemer, G. The immune contexture in cancer prognosis and treatment. Nat. Rev. Clin. Oncol. **2017**, 14, 717–734, doi:10.1038/nrclinonc.2017.101.

**22.** Berghoff, A.S.; Fuchs, E.; Ricken, G.; Mlecnik, B.; Bindea, G.; Spanberger, T.; Hackl, M.; Widhalm, G.; Dieckmann, K.; Prayer, D.; et al. Density of tumor-infiltrating lymphocytes correlates with extent of brain edema and overall survival time in patients with brain metastases. *Oncoimmunology* **2016**, *5*, e1057388, doi: 10.1080/2162402X.2015.1057388.

**23.** Layer, J.P.; Kronmüller, M.T.; Quast, T.; Van Den Boorn, D.; Effern, M.; Hinze, D.; Althoff, K.; Westermann, F.; Peifer, M.; Hartmann, G.; et al. Amplification of N-Myc is associated with a T-cell-poor microenvironment in metastatic neuroblastoma restraining interferon pathway activity and chemokine expression. *Oncoimmunology* **2017**, *6*, 1–13, doi:10.1080/2162402X.2017.1320626.

**24.** Mussai, F.; Egan, S.; Hunter, S.; Webber, H.; Fisher, J.; Wheat, R.; McConville, C.; Sbirkov, Y.; Wheeler, K.; Bendle, G.; et al. Neuroblastoma arginase activity creates an immunosuppressive microenvironment that impairs autologous and engineered immunity. *Cancer Res.* **2015**, *75*, 3043–3053, doi:10.1158/0008-5472.CAN-14-3443.

**25.** Zhang, P.; Wu, X.; Basu, M.; Dong, C.; Zheng, P.; Liu, Y.; Sandler, A.D. MYCN amplification is associated with repressed cellular immunity in neuroblastoma: An in silico immunological analysis of TARGET database. *Front. Immunol.* **2017**, *8*, 1473, doi:10.3389/fimmu.2017.01473.

**26.** Song, L.; Asgharzadeh, S.; Salo, J.; Engell, K.; Wu, H.; Sposto, R.; Ara, T.; Silverman, A.M.; Declerck, Y.A.; Seeger, R.C.; et al. V α 24-invariant NKT cells mediate antitumor activity via killing of tumor-associated macrophages. *J. Clin. Invest.* **2009**, *119*, 1524–1536, doi:10.1172/JCI37869.1524.

**27.** Asgharzadeh, S.; Salo, J.A.; Ji, L.; Oberthuer, A.; Fischer, M.; Berthold, F.; Hadjidaniel, M.; Liu, C.W.Y.; Metelitsa, L.S.; Pique-Regi, R.; et al. Clinical significance of tumor-associated inflammatory cells in metastatic neuroblastoma. *J. Clin. Oncol.* **2012**, *30*, 3525–3532, doi:10.1200/JCO.2011.40.9169.

**28.** Qian, B.Z.; Pollard, J.W. Macrophage Diversity Enhances Tumor Progression and Metastasis. *Cell* **2010**, *141*, 39–51, doi: 10.1016/j.cell.2010.03.014.

**29.** Morandi, F.; Croce, M.; Cangemi, G.; Barco, S.; Rigo, V.; Carlini, B.; Amoroso, L.; Pistoia, V.; Ferrini, S.; Corrias, M.V. IL-10 and ARG-1 concentrations in bone marrow and peripheral blood of metastatic neuroblastoma patients do not associate with clinical outcome. *J. Immunol. Res.* **2015**, *2015*, 718975, doi: 10.1155/2015/718975.

**30.** Scarpa, S.; Coppa, A.; Ragano-Caracciolo, M.; Mincione, G.; Giuffrida, A.; Modesti, A.; Colletta, G. Transforming growth factor β regulates differentiation and proliferation of human neuroblastoma. *Exp. Cell Res.* **1996**, *229*, 147–154, doi:10.1006/excr.1996.0352.

**31.** Oliveira, F.B.; Magalhães, L.M.; Passos, L.S.; Neto, J.C.A.; Dutra, Á.P.; Martins, P.R.; Salles, P.G.O.; Dutra, W.O.; Gollob, K.J. Abstract 707: Circulating immune profile in childhood neuroblastoma displays an activated response with simultaneous expression of checkpoint proteins by T cells and monocytes. In Proceedings of the AACR Annual Meeting **2018**, Chicago, IL, USA, 14–18 April 2018; p. 707, doi:10.1158/1538-7445.am2018-707.

**32.** Egler, R.A.; Li, Y.; Dang, T.A.T.; Peters, T.L.; Leung, E.; Huang, S.; Russell, H.V.; Liu, H.; Man, T.K. An integrated proteomic approach to identifying circulating biomarkers in high-risk neuroblastoma and their potential in relapse monitoring. *Proteomics Clin. Appl.* **2011**, *5*, 532–541, doi:10.1002/prca.201000089.

**33.** Morandi, F.; Cangemi, G.; Barco, S.; Amoroso, L.; Giuliano, M.; Gigliotti, A.R.; Pistoia, V.; Corrias, M.V. Plasma levels of soluble HLA-E and HLA-F at diagnosis may predict overall survival of neuroblastoma patients. *Biomed Res. Int.* **2013**, *2013*, 956878, doi:10.1155/2013/956878.

**34.** Gogali, A.; Charalabopoulos, K.; Zampira, I.; Konstantinidis, A.K.; Tachmazoglou, F.; Daskalopoulos, G.; Constantopoulos, S.H.; Dalavanga, Y. Soluble Adhesion Molecules E-Cadherin, Intercellular Adhesion Molecule-1, and E-Selectin as Lung Cancer Biomarkers. *Chest* **2010**, *138*, 1173–1179, doi:10.1378/chest.10-0157.

**35.** Mirabelli, P.; Incoronato, M. Usefulness of traditional serum biomarkers for management of breast cancer patients. *Biomed. Res. Int.* **2013**, *2013*, 685641, doi:10.1155/2013/685641.

**36.** Bassani-Sternberg, M.; Barnea, E.; Beer, I.; Avivi, I.; Katz, T.; Admon, A. Soluble plasma HLA peptidome as a potential source for cancer biomarkers. *Proc. Natl. Acad. Sci. USA* **2010**, *107*, 18769, doi:10.1073/pnas.1008501107.

**37.** Baron, A.T.; Cora, E.M.; Lafky, J.M.; Boardman, C.H.; Buenafe, M.C.; Rademaker, A.; Liu, D.; Fishman, D.A.; Podratz, K.C.; Maihle, N.J. Soluble Epidermal Growth Factor Receptor (sEGFR/sErbB1) as a Potential Risk, Screening, and Diagnostic Serum Biomarker of Epithelial Ovarian Cancer. *Cancer Epidemiol. Biomarkers Prev.* **2003**, *12*, 103–113.

**38.** Morandi, F.; Barco, S.; Stigliani, S.; Croce, M.; Persico, L.; Lagazio, C.; Scuderi, F.; Belli, M.L.; Montera, M.; Cangemi, G.; et al. Altered erythropoiesis and decreased number of erythrocytes in children with neuroblastoma. *Oncotarget* **2017**, *8*, 53194–53209, doi:10.18632/oncotarget.18285

**39.** Semeraro, M.; Rusakiewicz, S.; Minard-colin, V.; Delahaye, N.F.; Enot, D.; Vély, F.; Marabelle, A.; Papoular, B.; Piperoglou, C.; Ponzoni, M.; et al. Clinical impact of the NKp30 / B7-H6 axis in high-risk neuroblastoma patients. *Sci. Transl. Med.* **2015**, *7*, 283ra55, doi:10.1126/scitranslmed.aaa2327

**40.** Spel, L.; Boelens, J.-J.; van der Steen, D.M.; Blokland, N.J.G.; van Noesel, M.M.; Molenaar, J.J.; Heemskerk, M.H.M.; Boes, M.; Nierkens, S. Natural killer cells facilitate PRAME-specific T-cell reactivity against neuroblastoma. *Oncotarget* **2015**, *6*, 35770–35781, doi:10.18632/oncotarget.5657.

**41.** Morandi, F.; Pozzi, S.; Barco, S.; Cangemi, G.; Amoroso, L.; Carlini, B.; Pistoia, V.; Corrias, M.V. CD4+CD25hiCD127– Treg and CD4+CD45R0+CD49b+LAG3+ Tr1 cells in bone marrow and peripheral blood samples from children with neuroblastoma. *Oncoimmunology* **2016**, *5*, e1249553, doi:10.1080/2162402X.2016.1249553.

**42.** Mao, Y.; Eissler, N.; Le Blanc, K.; Johnsen, J.I.; Kogner, P.; Kiessling, R. Targeting suppressive myeloid cells potentiates checkpoint inhibitors to control spontaneous neuroblastoma. *Clin. Cancer Res.* **2016**, *22*, 3849–3859, doi:10.1158/1078-0432.CCR-15-1912.

**43.** Carlson, L.-M.; De Geer, A.; Sveinbjørnsson, B.; Orrego, A.; Martinsson, T.; Kogner, P.; Levitskaya, J. The microenvironment of human neuroblastoma supports the activation of tumor-associated T lymphocytes. *Oncoimmunology* **2013**, *2*, e23618, doi:10.4161/onci.23618.

**44.** Gowda, M.; Payne, K.; Godder, K.; Manjili, M.H. HLA-DR expression on myeloid cells is a potential prognostic factor in patients with high-risk neuroblastoma. *Oncoimmunology* **2013**, *2*, e26616, doi:10.4161/onci.26616.

**45.** Apps, J.R.; Hasan, F.; Campus, O.; Behjati, S.; Jacques, T.S.; J.; Sebire, N.; Anderson, J. The immune environment of paediatric solid malignancies: Evidence from an immunohistochemical study of clinical cases. *Fetal Pediatr. Pathol.* **2013**, *32*, 298–307, doi:10.3109/15513815.2012.754527.

**46.** Egler, R.A.; Burlingame, S.M.; Nuchtern, J.G.; Russell, H.V. Interleukin-6 and soluble interleukin-6 receptor levels as markers of disease extent and prognosis in neuroblastoma. *Clin. Cancer Res.* **2008**, *14*, 7028–7034, doi:10.1158/1078-0432.CCR-07-5017.

**47.** Smith, V.; Foster, J. High-Risk Neuroblastoma Treatment Review. *Child* **2018**, *5*, 114, doi:10.3390/children5090114.

**48.** Behl, D.; Porrata, L.F.; Markovic, S.N.; Letendre, L.; Pruthi, R.K.; Hook, C.C.; Tefferi, A.; Elliot, M.A.; Kaufmann, S.H.; Mesa, R.A.; et al. Absolute lymphocyte count recovery after induction chemotherapy predicts superior survival in acute myelogenous leukemia. *Leukemia* **2006**, *20*, 29–34, doi:10.1038/sj.leu.2404032.

**49.** Siddiqui, M.; Ristow, K.; Markovic, S.N.; Witzig, T.E.; Habermann, T.M.; Colgan, J.P.; Inwards, D.J.; White, W.L.; Ansell, S.M.; Micallef, I.N.; et al. Absolute lymphocyte count predicts overall survival in follicular lymphomas. *Br. J. Haematol.* **2006**, *134*, 596–601, doi:10.1111/j.1365-2141.2006.06232.x.

**50.** Thoma, M.D.; Huneke, T.J.; DeCook, L.J.; Johnson, N.D.; Wiegand, R.A.; Litzow, M.R.; Hogan, W.J.; Porrata, L.F.; Holtan, S.G. Peripheral blood lymphocyte and monocyte recovery and survival in acute leukemia postmyeloablative allogeneic hematopoietic stem cell transplant. *Biol. Blood Marrow Transplant.* **2012**, *18*, 600–607, doi:10.1016/j.bbmt.2011.08.007.

**51.** Galvez-Silva, J.; Maher, O.M.; Park, M.; Liu, D.; Hernandez, F.; Tewari, P.; Nieto, Y. Prognostic Analysis of Absolute Lymphocyte and Monocyte Counts after Autologous Stem Cell Transplantation in Children, Adolescents, and Young Adults with Refractory or Relapsed Hodgkin Lymphoma. *Biol. Blood Marrow Transplant.* **2017**, *23*, 1276–1281, doi:10.1016/j.bbmt.2017.04.013.

**52.** Nayak, A.; McDowell, D.T.; Kellie, S.J.; Karpelowsky, J. Elevated Preoperative Neutrophil–Lymphocyte Ratio is Predictive of a Poorer Prognosis for Pediatric Patients with Solid Tumors. *Ann. Surg. Oncol.* **2017**, *23*, 1276–1281, doi:10.1245/s10434-017-6006-0.

**53.** Tilak, T.; Sherawat, S.; Agarwala, S.; Gupta, R.; Vishnubhatla, S.; Bakhshi, S. Circulating T-regulatory cells in neuroblastoma: A pilot prospective study. *Pediatr. Hematol. Oncol.* **2014**, *31*, 717–722, doi:10.3109/08880018.2014.886002.

**54.** Mackall, C.L.; Fleisher, T.A.; Brown, M.R.; Magrath, I.T.; Shad, A.T.; Horowitz, M.E.; Wexler, L.H.; Adde, M.A.; McClure, L.L.; Gress, R.E. Lymphocyte depletion during treatment with intensive chemotherapy for cancer. *Blood* **1994**, *84*, 2221–2228.

**55.** Delahaye, N.F.; Rusakiewicz, S.; Martins, I.; Ménard, C.; Roux, S.; Lyonnet, L.; Paul, P.; Sarabi, M.; Chaput, N.; Semeraro, M.; et al. Alternatively spliced NKp30 isoforms affect the prognosis of gastrointestinal stromal tumors. *Nat. Med.* **2011**, *17*, 700–707, doi:10.1038/nm.2366.

56. Webb, M.W.; Sun, J.; Sheard, M.A.; Liu, W.-Y.; Wu, H.-W.; Jackson, J.R.; Malvar, J.; Sposto, R.; Daniel, D.; Seeger, R.C. Colony stimulating factor 1 receptor blockade improves the efficacy of chemotherapy against human neuroblastoma in the absence of T lymphocytes. *Int. J. Cancer* **2018**, *143*, 1483–1493, doi:10.1002/ijc.31532.
57. Cheung, N.-K.V.; Guo, H.; Hu, J.; Tassev, D.V.; Cheung, I.Y. Humanizing murine IgG3 anti-GD2 antibody m3F8 substantially improves antibody-dependent cell-mediated cytotoxicity while retaining targeting in vivo. *Oncoimmunology* **2012**, *1*, 477–486, doi: 10.4161/onci.19864.
58. Shusterman, S.; London, W.B.; Gillies, S.D.; Hank, J.A.; Voss, S.D.; Seeger, R.C.; Reynolds, C.P.; Kimball, J.; Albertini, M.R.; Wagner, B.; et al. Antitumor activity of hu14.18-IL2 in patients with relapsed/refractory neuroblastoma: A Children's Oncology Group (COG) phase II study. *J. Clin. Oncol.* **2010**, *28*, 4969–4975, doi:10.1200/JCO.2009.27.8861.
59. Metelitsa, L.S.; Gillies, S.D.; Super, M.; Shimada, H.; Reynolds, C.P.; Seeger, R.C. Antidisialoganglioside/granulocyte macrophage-colony-stimulating factor fusion protein facilitates neutrophil antibody-dependent cellular cytotoxicity and depends on FcgammaRII (CD32) and Mac-1 (CD11b/CD18) for enhanced effector cell adhesion and azurophi. *Blood* **2002**, *99*, 4166–4173; doi:10.1182/blood.v99.11.4166.
60. Siebert, N.; Eger, C.; Seidel, D.; Jüttner, M.; Zumpe, M.; Wegner, D.; Kietz, S.; Ehlert, K.; Veal, G.J.; Siegmund, W.; et al. Pharmacokinetics and pharmacodynamics of ch14.18/CHO in relapsed/refractory high-risk neuroblastoma patients treated by long-term infusion in combination with IL-2. *MAbs* **2016**, *8*, 604–616, doi:10.1080/19420862.2015.1130196.
61. Nassin, M.L.; Nicolaou, E.; Gurbuxani, S.; Cohn, S.L.; Cunningham, J.M.; LaBelle, J.L. Immune Reconstitution Following Autologous Stem Cell Transplantation in Patients with High-Risk Neuroblastoma at the Time of Immunotherapy. *Biol. Blood Marrow Transplant.* **2017**, *24*, 452–459, doi:10.1016/j.bbmt.2017.11.012.
62. Siebert, N.; Troschke-Meurer, S.; Marx, M.; Zumpe, M.; Ehlert, K.; Gray, J.; Garaventa, A.; Manzitti, C.; Ash, S.; Klingebiel, T.; et al. Impact of HACA on Immunomodulation and Treatment Toxicity Following ch14.18/CHO Long-Term Infusion with Interleukin-2: Results from a SIOPEN Phase 2 Trial. *Cancers* **2018**, *10*, 387, doi:10.3390/cancers10100387.
63. Cheung, N.-K.V.; Guo, H.; Heller, G.; Cheung, I.Y. Induction of Ab3 and Ab3' Antibody Was Associated with Long-Term Survival after Anti-G(D2) Antibody Therapy of Stage 4 Neuroblastoma. *Clin. Cancer Res.* **2000**, *6*, 2653–2660.
64. Kushner, B.H.; Ostrovnaya, I.; Cheung, I.Y.; Kuk, D.; Kramer, K.; Modak, S.; Yataghene, K.; Cheung, N.K. Prolonged progression-free survival after consolidating second or later remissions of neuroblastoma with Anti-G(D2) immunotherapy and isotretinoin: A prospective Phase II study. *Oncoimmunology* **2015**, *4*, e1016704–e1016704, doi: 10.1080/2162402X.2015.1016704.
65. Cheung, N.K.; Kushner, B.H.; Yeh, S.D.; Larson, S.M. 3F8 monoclonal antibody treatment of patients with stage 4 neuroblastoma: A phase II study. *Int. J. Oncol.* **1998**, *12*, 1299–1306, doi:10.3892/ijo.12.6.1299
66. Chowdhury, F.; Lode, H.N.; Cragg, M.S.; Glennie, M.J.; Gray, J.C. Development of immunomonitoring of antibody-dependent cellular cytotoxicity against neuroblastoma cells using whole blood. *Cancer Immunol. Immunother.* **2014**, *63*, 559–569, doi:10.1007/s00262-014-1534-y.
67. Siebert, N.; Jensen, C.; Troschke-Meurer, S.; Zumpe, M.; Jüttner, M.; Ehlert, K.; Kietz, S.; Müller, I.; Lode, H.N. Neuroblastoma patients with high-affinity FCGR2A, -3A and stimulatory KIR 2DS2 treated by long-term infusion of anti-GD2 antibody ch14.18/CHO show higher ADCC levels and improved event-free survival. *Oncoimmunology* **2016**, *5*, e1235108, doi: 10.1080/2162402X.2016.1235108.

**68.** Tarek, N.; Le Luduec, J.-B.; Gallagher, M.M.; Zheng, J.; Venstrom, J.M.; Chamberlain, E.; Modak, S.; Heller, G.; Dupont, B.; Cheung, N.-K. V; et al. Unlicensed NK cells target neuroblastoma following anti-GD2 antibody treatment. *J. Clin. Invest.* **2012**, *122*, 3260–3270, doi:10.1172/JCI62749.

**69.** Scheid, C.; Pettengell, R.; Ghielmini, M.; Radford, J.A.; Morgenstern, G.R.; Stern, P.L.; Crowther, D. Time-course of the recovery of cellular immune function after high-dose chemotherapy and peripheral blood progenitor cell transplantation for high-grade non-Hodgkin's lymphoma. *Bone Marrow Transplant.* **1995**, *15*, 901–906.

**70.** Perez-Garcia, A.; Cabezudo, E.; Lopez-Jimenez, J.; Marugan, I.; Peralta, T.; Arnan, M.; Ramos-Oliva, P.; Benet, I.; Lopez, S.; Mestre, M.; et al. Immune Reconstitution of Regulatory T-Cells Following Autologous Hematopoietic Stem Cell Transplantation. *Biol. Blood Marrow Transplant.* **2009**, *15*, 140, doi:10.1016/j.bbmt.2008.12.426.

**71.** Ladenstein, R.; Potschger, U.; Valteau-Couanet, D.; Luksch, R.; Castel, V.; Yaniv, I.; Laureys, G.; Brock, P.; Michon, J.M.; Owens, C.; et al. Interleukin 2 with anti-GD2 antibody ch14.18/CHO (dinutuximab beta) in patients with high-risk neuroblastoma (HR-NBL1/SIOPEN): A multicentre, randomised, phase 3 trial. *Lancet. Oncol.* **2018**, *19*, 1617–1629, doi:10.1016/S1470-2045(18)30578-3.

**72.** Ye, C.; Brand, D.; Zheng, S.G. Targeting IL-2: An unexpected effect in treating immunological diseases. *Signal Transduct. Target. Ther.* **2018**, *3*, 2, doi:10.1038/s41392-017-0002-5.

**73.** Van Haelst Pisani, C.; Kovach, J.S.; Kita, H.; Leiferman, K.M.; Gleich, G.J.; Silver, J.E.; Dennin, R.; Abrams, J.S. Administration of interleukin-2 (IL-2) results in increased plasma concentrations of IL-5 and eosinophilia in patients with cancer. *Blood* **1991**, *78*, 1538–1544.

**74.** Ozkaynak, M.F.; Gilman, A.L.; London, W.B.; Naranjo, A.; Diccianni, M.B.; Tenney, S.C.; Smith, M.; Messer, K.S.; Seeger, R.; Reynolds, C.P.; et al. A Comprehensive Safety Trial of Chimeric Antibody 14.18 With GM-CSF, IL-2, and Isotretinoin in High-Risk Neuroblastoma Patients Following Myeloablative Therapy: Children's Oncology Group Study ANBL0931. *Front. Immunol.* **2018**, *9*, 1355, doi:10.3389/fimmu.2018.01355.

**75.** Goldmann, O.; Beineke, A.; Medina, E. Identifcation of a novel subset of myeloid-derived suppressor cells during chronic staphylococcal infection tat resembles immature eosinophils. *J. Infect. Dis.* **2017**, *216*, 1444–1451, doi:10.1093/infdis/jix494.

**76.** Kushner, B.H.; Cheung, I.Y.; Modak, S.; Kramer, K.; Ragupathi, G.; Cheung, N.-K. V Phase I trial of a bivalent gangliosides vaccine in combination with β-glucan for high-risk neuroblastoma in second or later remission. *Clin. Cancer Res.* **2014**, *20*, 1375–1382, doi:10.1158/1078-0432.CCR-13-1012.

**77.** Qasim, W.; Zhan, H.; Samarasinghe, S.; Adams, S.; Amrolia, P.; Stafford, S.; Butler, K.; Rivat, C.; Wright, G.; Somana, K.; et al. Molecular remission of infant B-ALL after infusion of universal TALEN gene-edited CAR T cells. *Sci. Transl. Med.* **2017**, *9*, eaaj2013, doi:10.1126/scitranslmed.aaj2013.

**78.** Park, J.H.; Rivière, I.; Gonen, M.; Wang, X.; Sénéchal, B.; Curran, K.J.; Sauter, C.; Wang, Y.; Santomasso, B.; Mead, E.; et al. Long-term follow-up of CD19 CAR therapy in acute lymphoblastic leukemia. *N. Engl. J. Med.* **2018**, *378*, 449–459, doi:10.1056/NEJMoa1709919.

**79.** Kochenderfer, J.N.; Somerville, R.P.T.; Lu, T.; Yang, J.C.; Sherry, R.M.; Feldman, S.A.; McIntyre, L.; Bot, A.; Rossi, J.; Lam, N.; et al. Long-Duration Complete Remissions of Diffuse Large B Cell Lymphoma after Anti-CD19 Chimeric Antigen Receptor T Cell Therapy. *Mol. Ther.* **2017**, *25*, 2245–2253, doi:10.1016/j.ymthe.2017.07.004.

80. Tawara, I.; Kageyama, S.; Miyahara, Y.; Fujiwara, H.; Nishida, T.; Akatsuka, Y.; Ikeda, H.; Tanimoto, K.; Terakura, S.; Murata, M.; et al. Safety and persistence of WT1-specific T-cell receptor gene2transduced lymphocytes in patients with AML and MDS. *Blood* **2017**, *130*, 1985–1994, doi:10.1182/blood-2017-06-791202.
81. Tesfaye, M.; Savoldo, B. Adoptive Cell Therapy in Treating Pediatric Solid Tumors. *Curr. Oncol. Rep.* **2018**, *20*, 73, doi:10.1007/s11912-018-0715-9.
82. Grupp, S.A.; Prak, E.L.; Boyer, J.; McDonald, K.R.; Shusterman, S.; Thompson, E.; Callahan, C.; Jawad, A.F.; Levine, B.L.; June, C.H.; et al. Adoptive transfer of autologous T cells improves T-cell repertoire diversity and long-term B-cell function in pediatric patients with neuroblastoma. *Clin. Cancer Res.* **2012**, *18*, 6732–6741, doi:10.1158/1078-0432.CCR-12-1432.
83. Kanold, J.; Paillard, C.; Tchirkov, A.; Lang, P.; Kelly, A.; Halle, P.; Isfan, F.; Merlin, E.; Marabelle, A.; Rochette, E.; et al. NK Cell immunotherapy for high-risk neuroblastoma relapse after haploidentical HSCT. *Pediatr. Blood Cancer* **2012**, *59*, 739–742, doi:10.1002/pbc.24030.
84. Federico, S.M.; McCarville, M.B.; Shulkin, B.L.; Sondel, P.M.; Hank, J.A.; Hutson, P.; Meagher, M.; Shafer, A.; Ng, C.Y.; Leung, W.; et al. A pilot trial of humanized anti-GD2 monoclonal antibody (hu14.18K322A) with chemotherapy and natural killer cells in children with recurrent/refractory neuroblastoma. *Clin. Cancer Res.* **2017**, *23*, 6441–6449, doi:10.1158/1078-0432.CCR-17-0379.
85. Modak, S.; Le Luduec, J.B.; Cheung, I.Y.; Goldman, D.A.; Ostrovnaya, I.; Doubrovina, E.; Basu, E.; Kushner, B.H.; Kramer, K.; Roberts, S.S.; et al. Adoptive immunotherapy with haploidentical natural killer cells and Anti-GD2 monoclonal antibody m3F8 for resistant neuroblastoma: Results of a phase I study. *Oncoimmunology* **2018**, *7*, e1461305, doi:10.1080/2162402X.2018.1461305.
86. Singh, N.; Kulikovskaya, I.; Barrett, D.M.; Binder-Scholl, G.; Jakobsen, B.; Martinez, D.; Pawel, B.; June, C.H.; Kalos, M.D.; Grupp, S.A. T cells targeting NY-ESO-1 demonstrate efficacy against disseminated neuroblastoma. *Oncoimmunology* **2016**, *5*, e1040216, doi:10.1080/2162402X.2015.1040216.
87. Quintarelli, C.; Orlando, D.; Boffa, I.; Guercio, M.; Polito, V.A.; Petretto, A.; Lavarello, C.; Sinibaldi, M.; Weber, G.; Del Bufalo, F.; et al. Choice of costimulatory domains and of cytokines determines CAR T-cell activity in neuroblastoma. *Oncoimmunology* **2018**, *7*, e1433518, doi:10.1080/2162402X.2018.1433518.
88. Heczey, A.; Liu, D.; Tian, G.; Courtney, A.N.; Wei, J.; Marinova, E.; Gao, X.; Guo, L.; Yvon, E.; Hicks, J.; et al. Invariant NKT cells with chimeric antigen receptor provide a novel platform for safe and effective cancer immunotherapy. *Blood* **2014**, *124*, 2824–2833, doi:10.1182/blood-2013-11-541235.
89. Heczey, A.; Louis, C.U.; Savoldo, B.; Dakhova, O.; Durett, A.; Grilley, B.; Liu, H.; Wu, M.F.; Mei, Z.; Gee, A.; et al. CAR T Cells Administered in Combination with Lymphodepletion and PD-1 Inhibition to Patients with Neuroblastoma. *Mol. Ther.* **2017**, *25*, 2214–2224, doi:10.1016/j.ymthe.2017.05.012.
90. Yang, L.; Ma, X.; Liu, Y.-C.; Zhao, W.; Yu, L.; Qin, M.; Zhu, G.; Wang, K.; Shi, X.; Zhang, Z.; et al. Chimeric Antigen Receptor 4SCAR-GD2-Modified T Cells Targeting High-Risk and Recurrent Neuroblastoma: A Phase II Multi-Center Trial in China. *Blood* **2017**, *130*, 3335, doi:10.1182/blood.V130.Suppl_1.3335.3335
91. Künkele, A.; Taraseviciute, A.; Finn, L.S.; Johnson, A.J.; Berger, C.; Finney, O.; Chang, C.A.; Rolczynski, L.S.; Brown, C.; Mgebroff, S.; et al. Preclinical assessment of CD171-directed CAR T-cell adoptive therapy for childhood neuroblastoma: CE7 epitope target safety and product manufacturing feasibility. *Clin. Cancer Res.* **2017**, *23*, 466–477, doi:10.1158/1078-0432.CCR-16-0354.

**92.** Walker, A.J.; Majzner, R.G.; Zhang, L.; Wanhainen, K.; Long, A.H.; Nguyen, S.M.; Lopomo, P.; Vigny, M.; Fry, T.J.; Orentas, R.J.; et al. Tumor Antigen and Receptor Densities Regulate Efficacy of a Chimeric Antigen Receptor Targeting Anaplastic Lymphoma Kinase. *Mol. Ther.* **2017**, *25*, 2189–2201, doi: 10.1016/j.ymthe.2017.06.008.

**93.** Chen, Y.; Sun, C.; Landoni, E.; Metelitsa, L.; Dotti, G.; Savoldo, B. Eradication of neuroblastoma by T cells redirected with an optimized GD2-specific chimeric antigen receptor and interleukin-15. *Clin. Cancer Res.* **2019**, *25*, 2915–2924, doi:10.1158/1078-0432.CCR-18-1811.

**94.** Du, H.; Hirabayashi, K.; Ahn, S.; Kren, N.P.; Montgomery, S.A.; Wang, X.; Tiruthani, K.; Mirlekar, B.; Michaud, D.; Greene, K.; et al. Antitumor Responses in the Absence of Toxicity in Solid Tumors by Targeting B7-H3 via Chimeric Antigen Receptor T Cells. *Cancer Cell* **2019**, *35*, 221–237, doi:10.1016/j.ccell.2019.01.002.

**95.** Majzner, R.G.; Theruvath, J.L.; Nellan, A.; Heitzeneder, S.; Cui, Y.; Mount, C.W.; Rietberg, S.P.; Linde, M.H.; Xu, P.; Rota, C.; et al. CAR T cells targeting B7-H3, a pan-cancer antigen, demonstrate potent preclinical activity against pediatric solid tumors and brain tumors. *Clin. Cancer Res.* **2019**, *25*, 2560–2574, doi: 10.1158/1078-0432.CCR-18-0432.

**96.** Yankelevich, M.; Kondadasula, S.V.; Thakur, A.; Buck, S.; Cheung, N.K.V.; Lum, L.G. Anti-CD3×anti-GD2 bispecific antibody redirects T-cell cytolytic activity to neuroblastoma targets. Pediatr. *Blood Cancer* **2012**, *59*, 1198–1205, doi:10.1002/pbc.24237.

**97.** Yankelevich, M.; Modak, S.; Chu, R.; Lee, D.W.; Thakur, A.; Cheung, N.-K.V.; Lum, L.G. Phase I study of OKT3 x hu3F8 bispecific antibody (GD2Bi) armed T cells (GD2BATs) in GD2-positive tumors. *J. Clin. Oncol.* **2019**, *14*, 2533, doi:10.1200/jco.2019.37.15_suppl.2533.

**98.** Le, T.P.; Thai, T.H. The state of cellular adoptive immunotherapy for neuroblastoma and other pediatric solid tumors. *Front. Immunol.* **2017**, *8*, 1640, doi:10.3389/fimmu.2017.01640.

**99.** Zage, P. Novel Therapies for Relapsed and Refractory Neuroblastoma. *Children* **2018**, *5*, 148, doi:10.3390/children5110148.

**100.** Long, A.H.; Haso, W.M.; Shern, J.F.; Wanhainen, K.M.; Murgai, M.; Ingaramo, M.; Smith, J.P.; Walker, A.J.; Kohler, M.E.; Venkateshwara, V.R.; et al. 4-1BB costimulation ameliorates T cell exhaustion induced by tonic signaling of chimeric antigen receptors. *Nat. Med.* **2015**, *21*, 581–590, doi:10.1038/nm.3838.

**101.** McLellan, A.D.; Ali Hosseini Rad, S.M. Chimeric antigen receptor T cell persistence and memory cell formation. *Immunol. Cell Biol.* **2019**, *97*, 664–674, doi:10.1111/imcb.12254.

**102.** Martinez, M.; Moon, E.K. CAR T cells for solid tumors: New strategies for finding, infiltrating, and surviving in the tumor microenvironment. Front. Immunol. **2019**, 10, 128, doi:10.3389/fimmu.2019.00128.

**103.** Gattinoni, L.; Zhong, X.S.; Palmer, D.C.; Ji, Y.; Hinrichs, C.S.; Yu, Z.; Wrzesinski, C.; Boni, A.; Cassard, L.; Garvin, L.M.; et al. Wnt signaling arrests effector T cell differentiation and generates CD8 + memory stem cells. *Nat. Med.* **2009**, *15*, 808–813, doi:10.1038/nm.1982.

**104.** Louis, C.U.; Savoldo, B.; Dotti, G.; Pule, M.; Yvon, E.; Myers, G.D.; Rossig, C.; Russell, H.V.; Diouf, O.; Liu, E.; et al. Antitumor activity and long-term fate of chimeric antigen receptor-positive T cells in patients with neuroblastoma. *Blood* **2011**, *118*, 6050–6056, doi:10.1182/blood-2011-05-354449.

**105.** Sommermeyer, D.; Hudecek, M.; Kosasih, P.L.; Gogishvili, T.; Maloney, D.G.; Turtle, C.J.; Riddell, S.R. Chimeric antigen receptor-modified T cells derived from defined CD8+ and CD4+ subsets confer superior antitumor reactivity in vivo. *Leukemia* **2016**, *30*, 492–500, doi:10.1038/leu.2015.247.

**106.** Turtle, C.J.; Hanafi, L.A.; Berger, C.; Hudecek, M.; Pender, B.; Robinson, E.; Hawkins, R.; Chaney, C.; Cherian, S.; Chen, X.; et al. Immunotherapy of non-Hodgkin's lymphoma with a defined ratio of CD8+ and CD4+ CD19-specific chimeric antigen receptor-modified T cells. *Sci. Transl. Med.* **2016**, *30*, 492–500, doi:10.1126/scitranslmed.aaf8621.

**107.** Chong, E.A.; Melenhorst, J.J.; Lacey, S.F.; Ambrose, D.E.; Gonzalez, V.; Levine, B.L.; June, C.H.; Schuster, S.J. PD-1 blockade modulates chimeric antigen receptor (CAR)-modified T cells: Refueling the CAR. *Blood* **2017**, *129*, 1039–1041, doi:10.1182/blood-2016-09-738245.

**108.** Long, A.H.; Highfill, S.L.; Cui, Y.; Smith, J.P.; Walker, A.J.; Ramakrishna, S.; El-Etriby, R.; Galli, S.; Tsokos, M.; Orentas, R.J.; et al. Reduction of MDSCs with all-trans retinoic acid improves CAR therapy efficacy for sarcomas. *Cancer Immunol. Res.* **2016**, *4*, 869–880, doi: 10.1158/2326-6066.CIR-15-0230.

**109.** Kotecki, N.; Awada, A. Checkpoints inhibitors in the (neo)adjuvant setting of solid tumors. *Curr. Opin. Oncol.* **2019**, *31*, 429–444, doi: 10.1097/cco.0000000000000565.

**110.** Hargadon, K.M.; Johnson, C.E.; Williams, C.J. Immune checkpoint blockade therapy for cancer: An overview of FDA-approved immune checkpoint inhibitors. *Int. Immunopharmacol.* **2018**, *62*, 29–39, doi: 10.1016/j.intimp.2018.06.001.

**111.** Rigo, V.; Emionite, L.; Daga, A.; Astigiano, S.; Corrias, M.V.; Quintarelli, C.; Locatelli, F.; Ferrini, S.; Croce, M. Combined immunotherapy with anti-PDL-1/PD-1 and anti-CD4 antibodies cures syngeneic disseminated neuroblastoma. *Sci. Rep.* **2017**, *25*, 14049, doi:10.1038/s41598-017-14417-6.

**112.** Siebert, N.; Zumpe, M.; Jüttner, M.; Troschke-Meurer, S.; Lode, H.N. PD-1 blockade augments anti-neuroblastoma immune response induced by anti-GD2 antibody ch14.18/CHO. *Oncoimmunology* **2017**, *6*, e1343775, doi: 10.1080/2162402X.2017.1343775.

**113.** Srinivasan, P.; Wu, X.; Basu, M.; Rossi, C.; Sandler, A.D. PD-L1 checkpoint inhibition and anti-CTLA-4 whole tumor cell vaccination counter adaptive immune resistance: A mouse neuroblastoma model that mimics human disease. *PLoS Med.* **2018**, *15*, e1002497, doi: 10.1371/journal.pmed.1002497.

**114.** Merchant, M.S.; Wright, M.; Baird, K.; Wexler, L.H.; Rodriguez-Galindo, C.; Bernstein, D.; Delbrook, C.; Lodish, M.; Bishop, R.; Wolchok, J.D.; et al. Phase i clinical trial of ipilimumab in pediatric patients with advanced solid tumors. *Clin. Cancer Res.* **2016**, *22*, 1364–1370, doi: 10.1158/1078-0432.CCR-15-0491.

**115.** Weber, R.; Fleming, V.; Hu, X.; Nagibin, V.; Groth, C.; Altevogt, P.; Utikal, J.; Umansky, V. Myeloid-derived suppressor cells hinder the anti-cancer activity of immune checkpoint inhibitors. *Front. Immunol.* **2018**, *9*, 1310, doi: 10.3389/fimmu.2018.01310.

**116.** Eissler, N.; Mao, Y.; Brodin, D.; Reuterswärd, P.; Andersson Svahn, H.; Johnsen, J.I.; Kiessling, R.; Kogner, P. Regulation of myeloid cells by activated T cells determines the efficacy of PD-1 blockade. *Oncoimmunology* **2016**, *5*, e1232222, doi: 10.1080/2162402X.2016.1232222.

**117.** Eranki, A.; Srinivasan, P.; Ries, M.; Kim, A.; Lazarski, C.A.; Rossi, C.T.; Khokhlova, T.D.; Wilson, E.; Knoblach, S.; Sharma, K. V; et al. High Intensity Focused Ultrasound (HIFU) Triggers Immune Sensitization of Refractory Murine Neuroblastoma to Checkpoint Inhibitor Therapy. *Clin. Cancer Res.* **2019**, doi:10.1158/1078-0432.CCR-19-1604.

**118.** Matthay, K.K. Interleukin 2 plus anti-GD2 immunotherapy: Helpful or harmful? *Lancet. Oncol.* **2018**, *19*, 1549–1551, doi:10.1016/S1470-2045(18)30627-2.

**119.** Nierkens, S.; Lankester, A.C.; Egeler, R.M.; Bader, P.; Locatelli, F.; Pulsipher, M.A.; Bollard, C.M.; Boelens, J.J. Challenges in the harmonization of immune monitoring studies and trial design for cell-based therapies in the context of hematopoietic cell transplantation for pediatric cancer patients. *Cytotherapy* **2015**, *17*, 1667–1674, doi:10.1016/j.jcyt.2015.09.008.

**120.** Bate-Eya, L.T.; Ebus, M.E.; Koster, J.; den Hartog, I.J.M.; Zwijnenburg, D.A.; Schild, L.; van der Ploeg, I.; Dolman, M.E.M.; Caron, H.N.; Versteeg, R.; et al. Newly-derived neuroblastoma cell lines propagated in serum-free media recapitulate the genotype and phenotype of primary neuroblastoma tumours. *Eur. J. Cancer* **2014**, *50*, 628–637, doi:10.1016/j.ejca.2013.11.015.

**121.** Vlachogiannis, G.; Hedayat, S.; Vatsiou, A.; Jamin, Y.; Fernández-Mateos, J.; Khan, K.; Lampis, A.; Eason, K.; Huntingford, I.; Burke, R.; et al. Patient-derived organoids model treatment response of metastatic gastrointestinal cancers. *Science* **2018**, *359*, 920–926, doi:10.1126/science.aao2774.

**122.** Wu, T.; Wu, X.; Wang, H.-Y.; Chen, L. Immune contexture defined by single cell technology for prognosis prediction and immunotherapy guidance in cancer. *Cancer Commun.* **2019**, *39*, 21, doi:10.1186/s40880-019-0365-9.

# Chapter 3

## FACSCanto II and LSRFortessa flow cytometer instruments can be synchronized utilizing single fluorochrome conjugated surface-dyed beads for standardized immunophenotyping

Annelisa M. Cornel[1], Christine A.J. van der Brught[1],
Stefan Nierkens[1], Jeroen F. van Velzen[1]

*[1] Center for Translational Immunology, University Medical Center Utrecht,
Utrecht University, The Netherlands*

*Adapted version*
*Cytometry A 2020 May 20; 34(9), e23361*

## ABSTRACT

### Background

Multiparameter flow cytometry is the preferred method to determine immunophenotypic features of cells present in a wide variety of sample types. Standardization is key to avoid inconsistencies and subjectivity of interpretations between clinical diagnostic laboratories. Among these standardization requirements, synchronization between different flow cytometer instruments is indispensable to obtain comparable results. This study aimed to investigate whether two widely used flow cytometers, the FACSCanto II and LSRFortessa, can be effectively synchronized utilizing calibration bead–based synchronization.

### Method

Two FACSCanto II and two LSRFortessa flow cytometers were synchronized with both multicolor hard-dyed and single-fluorochrome–conjugated surface-dyed beads according to the manufacturer's instructions. Cell staining was performed on five whole-blood samples obtained from healthy controls and were analyzed upon synchronization with the respective synchronization protocols.

### Results

Comparability criteria (defined as <15% deviation from the reference instrument) were met with both bead sets when synchronizing different FACSCanto II or LSRFortessa instruments. However, we observed that the criteria could not be met when synchronizing FACSCanto II with LSRFortessa instruments with multicolor hard-dyed beads. By utilizing single-fluorochrome–conjugated surface-dyed beads to determine and adjust PMT voltages, the accepted comparability criteria were successfully met. The protocol has been validated using five different eight-parameter stained samples.

### Conclusion

We show that FACSCanto II and LSRFortessa instruments can effectively be synchronized using single-fluorochrome–conjugated surface-dyed beads in case deviation criteria cannot be met using multicolor hard-dyed beads. Synchronization with single-fluorochrome–conjugated surface-dyed beads results in decreased deviations between instruments, allowing comparability criteria to become stricter.

## INTRODUCTION

In the past decades, precise identification and increasingly complex immunophenotyping of neoplastic cells and immune cells in a variety of tissues have become feasible by the advances in multiparameter flow cytometry technology [1,2]. Standardization of these complex panel measurements is key to avoid inconsistencies and subjectivity of interpretations between clinical diagnostic laboratories [3-18]. The recommendations and guidelines reported by experts in the field can be roughly divided into two main topics: (1) standardization of reagent use and sample preparation and (2) standardization of the acquired results on different instruments (from now on referred to as synchronization). Synchronization of flow cytometers is described in many variations, ranging from protocols synchronizing FSC/SSC characteristics [10-12] to protocols synchronizing multiple-color flow cytometry [3-6,16,18]. Even though these protocols vary in utilized standardization methods, they all agree on their main goal to achieve uniform and comparable instrument sensitivity levels, reproducible percentages, and expression patterns on different instruments.

Synchronizing instruments in different laboratories and different countries makes the use of biological samples impractical. As a result, a variety of beads have been developed which can be utilized to synchronize multiple instruments to approximately the same conditions. Available beads can be roughly divided into two categories: hard-dyed beads and surface-dyed beads. Hard-dyed beads have incorporated dyes in the polymer matrix, whereas surface-dyed beads are covalently linked with fluorochromes, thereby more closely resembling the biological situation [15]. Hard-dyed beads have a fluorochrome stability of at least two years, which is their main advantage. In contrast, surface-dyed beads are highly thermally and photolytically unstable. A clear disadvantage of hard-dyed beads over surface-dyed beads is that the dyes incorporated in hard-dyed beads merely share optical properties, but are not spectrally equivalent to the fluorochromes utilized in immunophenotyping of biological samples.

Synchronization of instruments utilizing multicolor hard-dyed beads is a widely accepted synchronization strategy, as, for instance, described in the EuroFlow standard operating procedure (SOP)3 and in the ONE study [4]. The recommendation is to first determine the mean fluorescence intensity (MFI) on a reference flow cytometer using multicolor hard-dyed beads. Subsequently, the beads are acquired on the flow cytometer to be matched and the photomultiplier tube (PMT) voltages are adjusted to meet a comparable MFI as measured on the reference flow cytometer. The acceptable comparability criteria are set on a <15% deviation from the reference instrument MFI. Synchronization was proven to be effective on the four 8-color flow cytometry instruments that were available when the EuroFlow project started in 2006 (FACSCanto

II, FACSAria, LSR II, and CyAn ADP) [3] as well as between Navios flow cytometers [4]. All four instruments have a three-laser-line configuration, with blue (488 nm), red (633 or 635 nm), and violet (405 or 407 nm) lasers.

However, as technology evolved, several new instruments have emerged which are equipped with a four (or even more)-laser-line configuration, like the LSRFortessa. Utilizing these instruments allows for measurement of more than double the number of parameters within one sample. This type of flow cytometer instruments will increasingly be used in centers to be able to keep up with the majorly increasing amount of knowledge gained about types of malignancies, immune cells, and treatment parameters. In an effort to synchronize multiple FACSCanto II and LSRFortessa instruments, we observed that acceptability criteria (<15% deviation) could not be met with multicolor hard-dyed beads. We therefore compared the level of deviation between the multicolor hard-dyed bead synchronization protocol and a method using single-fluorochrome–conjugated surface-dyed beads for synchronization of the FACSCanto II and the LSRFortessa (equipped with blue (488 nm), red (640 nm), violet (405 nm), or UV (355 nm) lasers) analyzing eight PMTs. We here report that synchronization using single-fluorochrome–conjugated surface-dyed beads results in less deviation than the use of multicolor hard-dyed beads to determine and adjust PMT voltages. The protocol has been validated using five different eight-parameter stained samples.

## MATERIALS AND METHODS

### Flow cytometer specifications

Two 3-laser FACSCanto II (BD Biosciences, Eysins, Switzerland), equipped with a 405-nm, 488-nm, and 633-nM laser, and two 4-laser LSRFortessa (BD Biosciences) cytometers, equipped with a 405, 488, 561-nm, and 633-nm laser, were used for these experiments. All instruments had matching filter configurations: a 450/50 and 510/50 BP filter for the 405-nM laser, a 660/20 and 780/60 BP filter for the 633-nM laser, and a 530/30 BP and 670 LP filter for the 488-nm laser. PE and PE-tandem labels are differently excited on the FACSCanto II (488-nm laser) and the LSRFortessa (561-nm laser). Detection was the same between instruments (585/42 and 780/60 BP filters). Furthermore, FACSCanto II laser power was 405 nM ± 25 mW, 488 nm ± 15 mW, and 633 nM ± 15 mW, whereas LSRFortessa laser power was 405 nm ± 40 mW, 488 nm ± 40 mW, 633 nm ± 40 mW, and 561 nm ± 40 mW.

CS&T beads (BD Biosciences, CE-IVD for FACSCanto instruments [catalog 662413] and research grade for LSRFortessa instruments [catalog 650622]) were used to check the performance of the flow cytometer and verify optical path and stream flow. This procedure enables controlled standardized results and allows the determination of long-term drifts and incidental changes within the flow cytometer. CS&T beads were measured before each analysis to verify optimal performance of the flow cytometer. No changes were observed which could affect the results.

### Experimental setup of synchronization

First, eight-peak Sphero™ Rainbow bead calibration particles (Spherotech [catalog RCP-30-5A]) were used to perform synchronization between flow cytometers [3]. In short, the multicolor hard-dyed calibration beads were used to determine the MFI on a reference flow cytometer. Subsequently, beads were measured on the flow cytometer to be matched and each of the eight PMT voltages was adjusted to meet a comparable MFI as measured on the reference cytometer.

Subsequently, the potential of single-fluorochrome–conjugated surface-dyed BD™ FC beads (BD Biosciences [catalog 658621]) was tested to adjust PMT voltages. Each tube contained both negative polystyrene beads and beads coupled to one specific fluorochrome. In this way, every PMT voltage adjustment is performed with a separate tube containing beads with the fluorochrome of interest. PMT voltage adjustment was performed according to the above-described procedure. The acceptable comparability criteria are set on a <15% deviation from the reference instrument MFI [3].

### Compensation

BD™ CompBeads particles (BD Biosciences) were used on all instruments to compensate for spectral overlap according to the manufacturer's instructions. A mixture of anti-mouse Ig-κ-conjugated and non-conjugated negative control CompBeads was made. Fluorochrome-conjugated mouse κ-light chain–bearing immunoglobulin will bind to the Ig-κ-conjugated beads, and the negative and positive peaks were subsequently used to determine compensation percentages. Measurement of these single-antibody–labeled beads was repeated for every fluorochrome-conjugated antibody of interest. Single-fluorochrome–conjugated surface-dyed peripheral blood mononuclear cell (PBMC) samples were measured to verify the compensation matrix.

### Sample preparation

Cell staining was performed on five EDTA-containing whole-blood samples obtained from healthy donors who gave their informed consent to participate in this study. Whole-blood samples containing 1 × $10^6$ cells were lysed by a 15-minute incubation with 1× BD Pharm Lyse™ solution at room temperature (BD Biosciences [catalog 555899]) and subsequently washed twice with PBS/HSA (0.5%) (1800 rpm, 10 minutes). Cells were incubated with titrated amounts of monoclonal antibodies directed against CD2 FITC (clone S5.2), CD3 PerCP-Cy5.5 (clone SK7), CD8 APC (clone SK1) and CD4 Pacific

Blue (PB) (clone RPA-T4) (all from BD Biosciences), CD19 APC-A750 (clone J3-119), CD7 PE (clone 8H8.1), CD14 PE-Cy7 (clone RMO52) (all from Beckman Coulter), and CD45 Pacific Orange (PO) (clone HI30; Life Technologies) in a total staining volume of 80 µL. Samples were incubated for 15 minutes at room temperature in the dark, washed (500 g, 10 minutes), resuspended in 300 µL PBS/HSA (0.5%), and analyzed on all instruments in a 30-minute time frame.

## Sample analysis

The eight-peak Sphero™ Rainbow bead calibration particles were identified based on FSC/SSC characteristics, after which the eight different bead populations can be distinguished based on emission characteristics **(Figure 1A)**. A gate was drawn which included the sixth emission peak (**Figure 1A**), after which MFIs of all PMTs were determined on one instrument. The obtained reference MFIs were subsequently used as target MFIs for all other instruments. Single-fluorochrome–conjugated surface-dyed

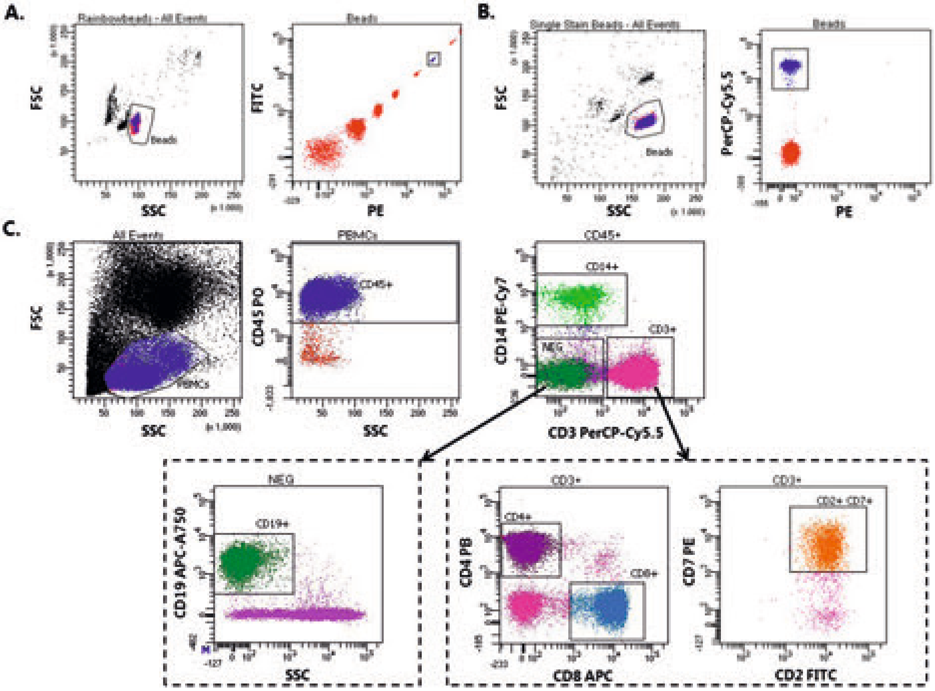

**Figure 1.** Synchronization gating strategies.
*(A)* *Multicolor hard-dyed bead calibration. Bead population is identified based on FSC/SSC characteristics, after which the sixth rainbow particle peak is identified based on emission characteristics and used to match PMT voltages.* ***(B)*** *Single-fluorochrome–conjugated surface-dyed fluorescently labeled bead calibration. Bead population is identified based on FSC/SSC and emission characteristics in the channel of interest and used to adjust PMT voltages.* ***(C)*** *Gating strategy of eight-parameter stained whole-blood samples. Lymphocytes were identified based on FSC/SSC and CD45 (PO) expression. From the CD45 + population, B cells were identified based on the absence of CD14 (PE-Cy7) and CD3 (PerCP-Cy5.5) and the presence of CD19 (APC-A750). Monocytes were identified based on CD14 expression, whereas T-cells were identified based on CD3, CD2 (FITC), and CD7 (PE), and either CD4 (PB) or CD8 (APC) expression*

BD™ FC beads were identified based on FSC/SSC characteristics, after which a negative and positive emission population can be distinguished in the channel of the single PMTs of interest (**Figure 1B**). The obtained reference MFI was subsequently used as a target for all other instruments. This was repeated for every PMT of interest.

## RESULTS

In the first part of this study, we investigated whether the multicolor hard-dyed bead synchronization protocol can be extended to include the LSRFortessa. Two FACSCanto II and two LSRFortessa flow cytometers were synchronized using the multicolor hard-dyed bead protocol (**Figure 1A**) [3]. Compensation of spectral overlap was applied as described. Subsequently, to assess synchronization efficiency, five different eight-parameter stained whole-blood samples were analyzed on all flow cytometers (gating strategy shown in **Figure 1C**), after which percentages of FACSCanto-FACSCanto, LSRFortessa-LSRFortessa, and FACSCanto-LSRFortessa deviation in MFI from the reference instrument were calculated using the provided formula (**Table 1**). The defined acceptability criterion of <15% variation in MFI was met between synchronized FACSCanto II instruments (**Figure 2A**). Variation in MFI between different LSRFortessa

**Table 1.** Deviation from reference MFI per fluorochrome after multicolor hard-dyed bead synchronization of two FACSCanto II and two LSRFortessa flow cytometers.

| | | FITC | PE | PerCP-Cy5.5 | PE-Cy7 | APC | APC-A750 | PB | PO |
|---|---|---|---|---|---|---|---|---|---|
| | Evaluated antibody conjugates | *CD2* | *CD7* | *CD3* | *CD14* | *CD8* | *CD19* | *CD4* | *CD45* |
| **FACSCanto II 1 vs FACSCanto II 2** | Mean Reference MFI | 10965 | 4471 | 8240 | 6678 | 10970 | 4546 | 3998 | 6768 |
| | Mean Matched MFI | 11591 | 4600 | 8209 | 6695 | 10154 | 3989 | 4079 | 6501 |
| | MFI difference | 627 | 129 | 30 | 17 | 816 | 557 | 81 | 268 |
| | Mean % dev. from ref. | 5.4% | 2.8% | 0.4% | 0.3% | 8.0% | 14.0% | 2.0% | 4.1% |
| | ± SD | ± 0.7% | ± 2.0% | ± 1.0% | ± 1.1% | ± 2.9% | ± 1.2% | ± 4.1% | ± 2.7% |
| **LSRFortessa 1 vs LSRFortessa 2** | Mean Reference MFI | 16915 | 10444 | 12803 | 15102 | 34846 | 5263 | 8629 | 13738 |
| | Mean Matched MFI | 15990 | 10346 | 12936 | 15101 | 33497 | 5630 | 8324 | 13429 |
| | MFI difference | 924 | 98 | 133 | 1 | 1349 | 367 | 305 | 309 |
| | Mean % dev. from ref. | 5.8% | 0.9% | 1.0% | 0.0% | 4.0% | 6.5% | 3.7% | 2.3% |
| | ± SD | ± 7.6% | ± 0.8% | ± 1.5% | ± 1.5% | ± 1.7% | ± 4.3% | ± 5.0% | ± 3.6% |

*Mean reference MFI, mean matched MFI, the observed MFI difference, and percentage of deviation from reference MFI ± SD are shown when comparing two FACSCanto II (top) and two LSRFortessa flow cytometers (bottom). Data reflect results from at least six 8-parameter stained whole-blood samples after synchronization using the multicolor hard-dyed beads. FACSCanto II vs FACSCanto II: n = 10; LSRFortessa vs LSRFortessa: n = 6.Abbreviations: dev. from ref., deviation from reference; MFI, mean fluorescence intensity; SD, standard deviation.*

instruments was also observed to be within the acceptable comparability criteria [3] (**Figure 2B**). However, when comparing synchronized FACSCanto-LSRFortessa variation in MFI, variation of five out of eight PMTs was widely out of the acceptable range (**Table 2**; **Figure 2C**).

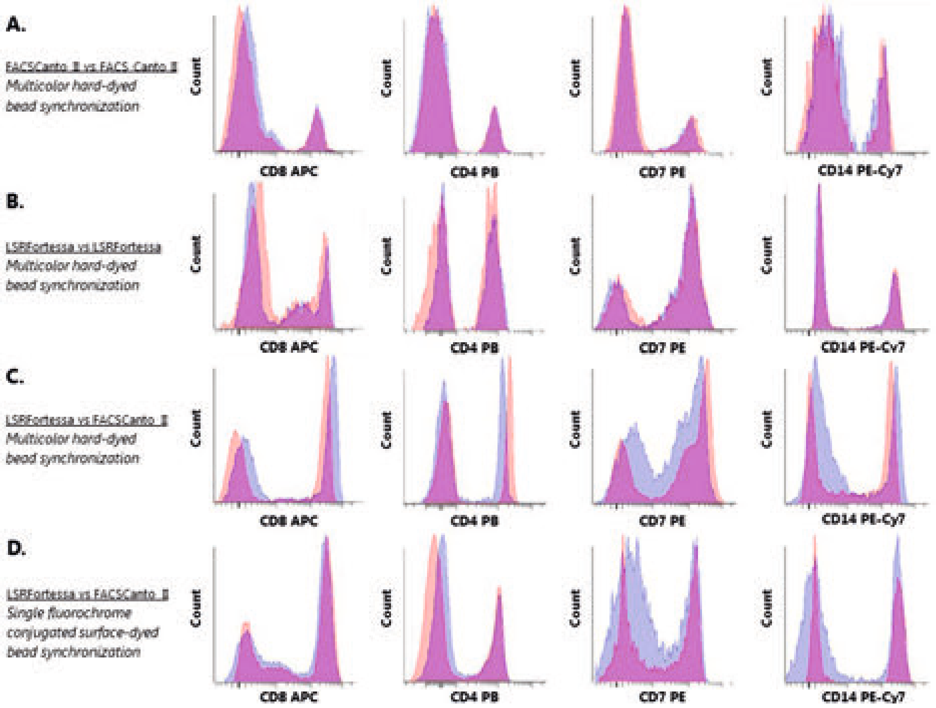

**Figure 2.** Expression patterns of four parameters between synchronized flow cytometer instruments. Representative expression patterns are shown in overlay histogram plots. Four of the eight analyzed parameters are shown (from left to right: APC—PB—PE—PE-Cy7). (**A**) FACSCanto II vs FACSCanto II using multicolor hard-dyed bead calibration. (**B**) LSRFortessa vs LSRFortessa using multicolor hard-dyed bead calibration. (**C**) FACSCanto II vs LSRFortessa using multicolor hard-dyed bead calibration. (**D**) FACSCanto II vs LSRFortessa using single-fluorochrome–conjugated surface-dyed fluorescently labeled bead calibration.

## Utilizing single-fluorochrome–conjugated surface-dyed beads for effective synchronization between the FACSCanto II and LSRFortessa

As multicolor hard-dyed bead synchronization was found to be ineffective in synchronizing FACSCanto II and LSRFortessa instruments, the above-described single-fluorochrome–conjugated surface-dyed bead synchronization protocol was subsequently tested (**Figure 1B**). Compensation of spectral overlap was applied as described. Subsequently, five different eight-parameter stained whole-blood samples were analyzed on all flow cytometers, and variation was compared between FACSCanto

II and LSRFortessa instruments (**Table 2**). Utilizing the single-fluorochrome–conjugated surface-dyed bead synchronization protocol at least halved the variations observed with the multicolor bead protocol. Variation in MFI between all parameters met the acceptable comparability criteria, indicating that the single-fluorochrome bead protocol is a good alternative for the multicolor bead protocol for synchronization between FACSCanto II and LSRFortessa instruments (**Figure 2D**).

**Table 2.** Deviation from reference MFI per fluorochrome after multicolor hard-dyed or single-fluorochrome–conjugated surface-dyed bead synchronization of a FACSCanto and a LSRFortessa flow cytometer

| | | **FITC** | **PE** | **PerCP-Cy5.5** | **PE-Cy7** | **APC** | **APC-A750** | **PB** | **PO** |
|---|---|---|---|---|---|---|---|---|---|
| | Evaluated antibody conjugates | *CD2* | *CD7* | *CD3* | *CD14* | *CD8* | *CD19* | *CD4* | *CD45* |
| **Hard-dyed beads FACSCanto II vs LSRFortessa** | Mean Reference MFI | 9490 | 23069 | 7197 | 7643 | 11532 | 2837 | 7341 | 11734 |
| | Mean Matched MFI | 8463 | 16350 | 7146 | 12810 | 19000 | 2565 | 4675 | 8955 |
| | MFI difference | 1027 | 6719 | 51 | 5167 | 7467 | 273 | 2666 | 2779 |
| | Mean % dev. from ref. | 12.1% | 41.1% | 0.7% | 40.3% | 39.3% | 10.6% | 57.0% | 31.0% |
| | ± SD | ± 9.4% | ± 8.6% | ± 2.3% | ± 1.9% | ± 3.2% | ± 3.6% | ± 7.8% | ± 1.5% |
| **Surface-dyed beads FACSCanto II vs LSRFortessa** | Mean Reference MFI | 15445 | 4437 | 4410 | 18324 | 20110 | 2587 | 5888 | 6164 |
| | Mean Matched MFI | 15014 | 4699 | 4602 | 17994 | 19448 | 2702 | 6662 | 5542 |
| | MFI difference | 432 | 262 | 192 | 331 | 662 | 116 | 774 | 622 |
| | Mean % dev. from ref. | 2.9% | 5.6% | 4.2% | 1.8% | 3.4% | 4.3% | 11.6% | 11.2% |
| | ± SD | ± 1.7% | ± 5.0% | ± 2.2% | ± 1.9% | ± 2.1% | ± 6.1% | ± 2.2% | ± 2.4% |

*Mean reference MFI, mean matched MFI, the observed MFI difference, and percentage of deviation from reference MFI ± SD are shown when utilizing the multicolor hard-dyed bead (top) and single-fluorochrome–conjugated surface-dyed bead synchronization protocol (bottom). Data reflect results from five 8-parameter stained whole-blood samples. Abbreviations: dev. from ref., deviation from reference; MFI, mean fluorescence intensity; SD, standard deviation.*

## DISCUSSION AND CONCLUSION

Standardization of immunophenotyping to provide information for diagnosis and treatment of malignancies is crucial to avoid inconsistencies between clinical diagnostic laboratories. **Chapter 2** of this thesis underlines the necessity of harmonization of immune monitoring in neuroblastoma. The small patient population, high interpatient variability, and inconsistency of included markers in studies make it difficult to interpret results and relate them to each other. Synchronization of flow cytometers, on top of harmonization of monitoring protocols, would make it possible to not only compare populations of cells, but also enables monitoring of MFIs of markers with potential clinical relevance between centers.

Excellent recommendations and guidelines have been reported to deal with standardization of sample preparations and synchronization of flow cytometer instruments [3-8,13,14]. However, as technology evolved, several new instruments have emerged which are equipped with a four (or even more)-laser-line configuration. In this study, we show that the defined acceptable comparability criteria (<15% variation in MFIs from the reference instrument) could be met when utilizing single-fluorochrome–conjugated surface-dyed beads to determine and adjust PMT voltages to synchronize our FACSCanto and LSRFortessa instruments. In contrast, defined comparability criteria could not be met when utilizing multicolor hard-dyed beads for instrument synchronization.

In principle, all instruments containing a 405-nm, 488-nm, and 633- to 640-nm excitation laser and at least two, four, and two detectors for each excitation line, respectively, fulfill the technical requirements for acquisition of the eight-color panel of fluorochromes [16]. Differences in laser power between instruments should be taken into account, as this causes differences in spread of the negative peaks and is independent of the utilized synchronization protocol.

Solly *et al*. reported that multicolor hard-dyed bead synchronization between FACSCanto II and Navios is feasible, but less effective compared to synchronization of instruments from the same manufacturer [9]. Nováková *et al.* shed light on the fact that synchronization of instruments from different manufacturers is hampered by adjusted emission filters for optimal detection of the manufacturers' proprietary fluorochromes [16]. They report that extension of the EuroFlow SOP with single-fluorochrome–conjugated surface-dyed BD™ CompBeads to further synchronize PMT voltages between Navios, MACSQuant, and FACSCanto is necessary to meet the acceptable comparability criteria between these instruments. Blanco *et al.* reported in the same issue that these settings can also be utilized to synchronize FACSCanto II and LSRFortessa instruments [17], even though hampered multicolor hard-dyed bead synchronization cannot be explained by emission filter differences and is most probably due to the higher laser power of the LSRFortessa.

Hard-dyed beads have incorporated surrogate dyes in their polymer matrix, causing them to merely share optical properties, but no spectral equivalence to the fluorochromes utilized in immunophenotyping of biological samples. Furthermore, incorporation of the dyes in the polymer matrix does not resemble fluorochrome-stained biological samples.

This is a major drawback of hard-dyed bead–based synchronization, as synchronization of these internal surrogate dyes does not necessarily mean synchronization of the actual fluorochromes of interest. [15] We therefore hypothesize that the differences in laser-line configurations and laser power between FACSCanto II and LSRFortessa may result in different proportions between the surrogate dyes and the actual fluorochromes to be synchronized, causing differences in MFIs to occur when surrogate dye MFIs are matched. This is further substantiated by the fact that we are able to effectively synchronize FACSCanto II and LSRFortessa instruments when utilizing single-fluorochrome–conjugated surface-dyed beads.

## REFERENCES

1. Swerdlow SH, Campo E, Pileri SA, et al. The 2016 revision of the World Health Organization classification of lymphoid neoplasms. Blood. **2016**;127:2375-2390, doi:10.1182/blood-2016-01-643569
2. Arber DA, Orazi A, Hasserjian R, et al. The 2016 revision to the World Health Organization classification of myeloid neoplasms andacute leukemia. Blood. **2016**;127:2391-2405, doi: 10.1182/blood-2016-03-643544
3. Kalina T, Flores-Montero J, van der Velden VHJ, et al. EuroFlow standardization of flow cytometer instrument settings and immunophenotyping protocols. Leukemia. **2012**;26:1986-2010, doi:10.1038/leu.2012.122
4. Streitz M, Miloud T, Kapinsky M, et al. Standardization of whole blood immune phenotype monitoring for clinical trials: panels and methods from the ONE study. Transplant Res. **2013**;2(1):17, doi:10.1186/2047-1440-2-17.
5. Gratama JW, Kraan J, Adriaansen H, et al. Reduction of interlaboratory variability in flow cytometric immunophenotyping by standardization of instrument set-up and calibration, and standard list mode data analysis. Cytometry. **1997**;30:10-22
6. Feller N, van der Velden VH, Brooimans RA, et al. Defining consensus leukemia-associated immunophenotypes for detection of minimal residual disease in acute myeloid leukemia in a multicenter setting. Blood Cancer J. **2013**; 3:e129, doi:10.1038/bcj.2013.27
7. Arnoulet C, Béné MC, Durrieu F, et al. Four- and five-color flow cytometry analysis of leukocyte differentiation pathways in normal bone marrow: a reference document based on a systematic approach by the GTLLF and GEIL. Cytometry B Clin Cytom. **2010**;78:4-10, doi:10.1002/cyto.b.20484
8. Béné MC, Nebe T, Bettelheim P, et al. Immunophenotyping of acute leukemia and lymphoproliferative disorders: a consensus proposal of the European LeukemiaNet Work Package 10. Leukemia. **2011**;25:567-574, doi: 10.1038/leu.2010.312
9. Solly F, Rigollet L, Baseggio L, et al. Comparable flow cytometry data can be obtained with two types of instruments, Canto II, and Navios. A GEIL study. Cytometry A. **2013**;83:1066-1072, doi:10.1002/cyto.a.22404.
10. Robert S, Poncelet P, Lacroix R, et al. Standardization of platelet-derived microparticle counting using calibrated beads and a Cytomics FC500 routine flow cytometer: a first step towards multicenter studies? J Thromb Haemost. **2009**;7:190-197, doi:10.1111/j.1538-7836.2008.03200.x
11. Cointe S, Judicone C, Robert S, et al. Standardization of microparticle enumeration across different flow cytometry platforms: results of a multicenter collaborative workshop. J Thromb Haemost. **2017**;15:187-193, doi:10.1111/jth.13514.
12. Lacroix R, Robert S, Poncelet P, Kasthuri RS, Key NS, Dignat-George F. Standardization of platelet-derived microparticle enumeration by flow cytometry with calibrated beads: results of the International Society on Thrombosis and Haemostasis SSC Collaborative workshop. J Thromb Haemost. **2010**;8:2571-2574, doi: 10.1111/j.1538-7836.2010.04047.x.
13. Finak G, Frelinger J, Jiang W, et al. OpenCyto: an open source infrastructure for scalable, robust, reproducible, and automated, end-to-end flow cytometry data analysis. PLoS Comput Biol. **2014**;10:e1003806, doi:10.1371/journal.pcbi.1003806
14. Perfetto SP, Ambrozak D, Nguyen R, Chattopadhyay PK, Roederer M. Quality assurance for polychromatic flow cytometry using a suite of calibration beads. Nat Protoc. **2012**;7:2067-2079, doi:10.1038/nprot.2012.126.
15. Hoffman RA, Wang L, Bigos M, Nolan JP. NIST/ISAC standardization study: variability in assignment of intensity values to fluorescence standard beads and in cross calibration of standard beads to hard dyed beads. Cytometry A. **2012**;81:785-796, doi:10.1002/cyto.a.22086

**16.** Nováková M, Glier H, Brdičková N, et al. How to make usage of the standardized EuroFlow 8-color protocols possible for instruments of different manufacturers. J Immunol Methods. **2017**;S0022–1759(17):30139-30144, doi: 10.1016/j.jim.2017.11.007

**17.** Blanco E, Perez-Andres M, Sanoja-Flores L, et al. Selection and validation of antibody clones against IgG and IgA subclasses in switched memory B-cell and plasma cells. J Immunol Methods. **2017**;S0022–1759(17):30079, doi: 10.1016/j.jim.2017.09.008

**18.** Giagalas AK, Li L, Henderson O, et al. The development of fluorescence intensity standards. J Res Natl Inst Stand Technol. **2001**; 106(2):381-389, doi:10.6028/jres.106.015.

# Chapter 4

## Immune Monitoring during Therapy Reveals Activitory and Regulatory Immune Responses in High-Risk Neuroblastoma

Annelisa M. Cornel[1,2,*], Celina L. Szanto[1,2,*], Sara M. Tamminga[2], Eveline M. Delemarre[2], Coco C.H. de Koning[1,2], Denise A.M.H. van den Beemt[1,2], Ester Dunnebach[1,2], Michelle L. Tas[1], Miranda P. Dierselhuis[1], Lieve G.A.M. Tytgat[1], Max M. van Noesel[1,3], Kathelijne C.J.M. Kraal[1], Jaap-Jan Boelens[4], Alwin D. R. Huitema[1,5,6], Stefan Nierkens[1,2]

*[1] Princess Máxima Center for Pediatric Oncology, Utrecht University, Utrecht, The Netherlands*
*[2] Center for Translational Immunology, University Medical Center Utrecht, Utrecht University, Utrecht, The Netherlands*
*[3] Division Imaging& Cancer, University Medical Center Utrecht, Utrecht University, Utrecht, The Netherlands*
*[4] Stem Cell Transplantation and Cellular Therapies Program, Department of Pediatrics, Memorial Sloan Kettering Cancer Center, New York, USA*
*[5] Department of Pharmacy & Pharmacology, Netherlands Cancer Institute, Amsterdam, The Netherlands*
*[6] Dept. Clinical Pharmacy, University Medical Center Utrecht, Utrecht University, Utrecht, The Netherlands.*
*[*] These authors contributed equally to this work.*

*Cancers (Basel) 2021 Apr 26; 13(9), 2096.*

## ABSTRACT

Despite intensive treatment, including consolidation immunotherapy (IT), prognosis of high-risk neuroblastoma (HR-NBL) is poor. Immune status of patients over the course of treatment, and thus immunological features potentially explaining therapy efficacy, are largely unknown. In this study, the dynamics of immune cell subsets and their function were explored in 25 HR-NBL patients at diagnosis, during induction chemotherapy, before high-dose chemotherapy, and during IT. The dynamics of immune cells varied largely between patients. IL-2- and GM-CSF-containing IT cycles resulted in significant expansion of effector cells (NK-cells in IL-2 cycles, neutrophils and monocytes in GM-CSF cycles). Nonetheless, the cytotoxic phenotype of NK-cells was majorly disturbed at the start of IT, and both IL-2 and GM-CSF IT cycles induced preferential expansion of suppressive regulatory T-cells. Interestingly, proliferative capacity of purified patient T-cells was impaired at diagnosis as well as during therapy. This study indicates the presence of both immune-enhancing as well as regulatory responses in HR-NBL patients during (immuno)therapy. Especially the double-edged effects observed in IL-2-containing IT cycles are interesting, as this potentially explains the absence of clinical benefit of IL-2 addition to IT cycles. This suggests that there is a need to combine anti-GD2 with more specific immune-enhancing strategies to improve IT outcome in HR-NBL.

### Visual Abstract

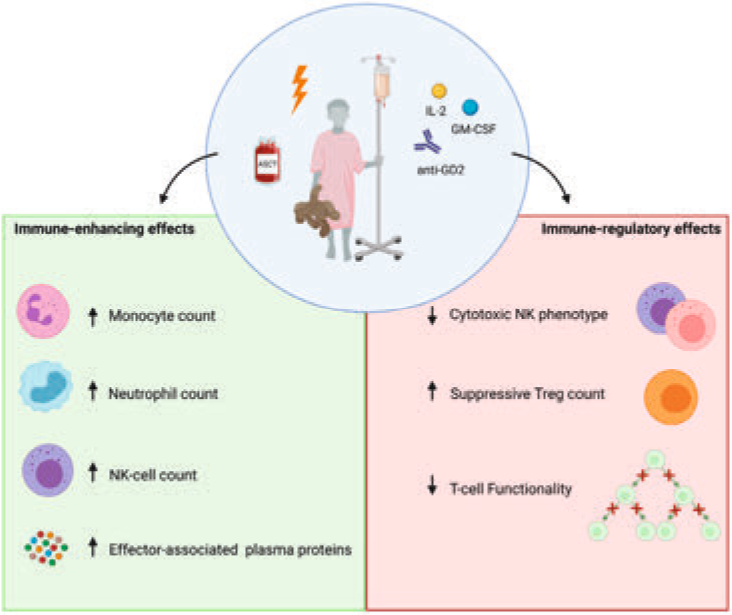
IL-2
GM-CSF
anti-GD2
ASCT
Immune-enhancing effects
↑ Monocyte count
↑ Neutrophil count
↑ NK-cell count
↑ Effector-associated plasma proteins
Immune-regulatory effects
↓ Cytotoxic NK phenotype
↑ Suppressive Treg count
↓ T-cell Functionality

*Created with BioRender.com*

## INTRODUCTION

Neuroblastoma (NBL) is the most common extracranial solid tumor in children, accounting for approximately 15% of all pediatric oncology deaths [1]. Patients are stratified as low, intermediate or high risk (HR), depending on various factors (e.g., age, tumor stage, and several genetic components, such as MYCN amplification) [2]. HR-NBL patients are treated with multimodal therapy consisting of chemotherapy, high-dose chemotherapy followed by autologous stem cell transplantation (ASCT), resection of the tumor, local radiation, and maintenance immunotherapy (IT) consisting of the anti-GD2 monoclonal antibody, often combined with the cytokines IL-2 and GM-CSF, and isotretinoin acid [3-5]. Despite intensive treatment, 5 year event-free survival (EFS) is <50% [6,7].

Dinutuximab, the monoclonal antibody used in NBL IT, targets GD2 on the surface of NBL cells and signals antibody-dependent cell-mediated cytotoxicity (ADCC) and complement-dependent cytotoxicity (CDC) [3]. The rationale to alternately add GM-CSF and IL-2 to the IT cycles was to increase expansion and functional activity of natural killer (NK) cells, lymphocytes, monocytes/macrophages, and neutrophils. This was mainly supported by *in vitro* data indicating superior cytotoxic effects when combining dinutuximab with these cytokines [8,9]. Even though IT increased 2 year EFS and overall survival (OS) [3], relapses are still observed in the majority of patients.

The dose, timing, and chosen immunotherapeutic compound combinations are currently highly empirical and do not take patients' immune status into account. Fast immune reconstitution during chemotherapy and higher absolute lymphocyte and monocyte counts have been associated with improved overall outcome in multiple cancers [10-12]. Nassin *et al*. showed that most patients with HR-NBL do not have full immune reconstitution at the start of IT (based on total white blood cell count (WBC), hemoglobin, and platelet, absolute neutrophil, lymphocyte and monocyte counts) and that immune recovery may correlate with disease-related outcomes [13]. Relatively fast NK-cell recovery early after ASCT was an important rationale for timing of IT early after transplantation [14]. Nonetheless, more detailed evaluation of NK-cell subsets showed that most cells are immature, cytokine-releasing (CD56bright, CD16+/−) rather than cytotoxic (CD56dim, CD16+). This may suggest suboptimal timing of dinutuximab IT early after transplantation, as cytotoxic NK-cells are mainly responsible for anti-GD2-dependent ADCC [13]. Nonetheless, to date, the potential effect of the IT regimen on shifting to the mature NK-cell phenotype has not been addressed.

Another important observation came from a phase III clinical trial where no additive effect of IL-2 administration on outcome of high-risk NBL patients was observed [4].

It is hypothesized that this may be the result of masking of the positive effects of IL-2 (e.g., on NK-cell expansion and functionality) by preferential regulatory T-cell (Treg) expansion [4,13], an effect known when administering (low dose) IL-2 to patients with autoimmune diseases [15]. Nevertheless, studies addressing this observation during NBL IT are lacking.

It may be hypothesized that post-ASCT immune reconstitution occurs with disparate kinetics in different patients, which may affect treatment efficacy of immune-targeting therapy. Comprehensive understanding of the status of the immune system in these patients may be instrumental for further development of immunotherapeutic interventions after ASCT. However, no studies have monitored the immune status in NBL patients during chemotherapy and IT and included functional analysis. Therefore, we monitored the immune status in NBL patients during chemo- and immunotherapy. In addition, the effect of IL-2 and GM-CSF on leukocyte and lymphocyte subpopulations and their (effector) cell functions during IT were studied.

## MATERIALS AND METHODS

### Patients and Treatment

HR-NBL patients diagnosed between January 2015 and January 2018 treated in the Princess Máxima Center for Pediatric Oncology (Utrecht, The Netherlands) or Uniklinik Köln (Cologne, Germany) were included in this study. Patients were treated following the same treatment protocol based on N5/N6 chemotherapy (Dutch NBL2009 trial [16] and NB2013-HR pilot GPOH/DCOG trial; N5 = cisplatin, etoposide, vindesine, N6 = vincristine, dacarbacin, ifosfamide, doxorubicin). Staging was performed according to the International NBL Staging System (INSS) [17]. MYCN and ALK amplification status was determined with FISH, SNP-array was used for the determination of copy number variants in 1p and 17q. The study was approved by the Medical Ethical Committees (Academic Medical Center, Amsterdam, the Netherlands; NL50762.018.14 and the University of Cologne, German trial 2013-004481-34). Written informed consent was obtained from the parents or guardians before enrollment in accordance with the Declaration of Helsinki.

### Sample Collection

Peripheral blood samples (EDTA) were transported to the laboratory at room temperature (RT), and a Trucount cell subset enumeration tube was analyzed using flow cytometry within 24 h after blood withdrawal. Plasma was isolated after centrifugation and stored at −80 °C until analysis. Peripheral blood mononuclear cells (PBMCs) were isolated using Ficoll density gradient centrifugation, frozen in fetal calf serum (Bodinco, Alkmaar, The Netherlands) containing 10% dimethyl sulphoxide (Sigma-Aldrich, St. Louis, MO, USA), and stored in liquid nitrogen in the UMCU biobank until use in experiments. Frozen control donor PBMCs, taken from healthy adult volunteers, served as control group.

In Utrecht, peripheral blood samples were taken at diagnosis (1 sample from 7 patients), after each N5/N6 cycle (1–3 samples from 18 patients), before the high-dose (HD) chemotherapy regimen (1 sample from 7 patients), at start of IT (1 sample from 7 patients) and after 3 and 6 cycles of IT (1–2 samples from 8 patients) as depicted in Figure S1. In Cologne, peripheral blood samples were taken at start of IT and every 2 weeks during IT cycle 1–5. Samples were shipped at RT to the laboratory in Utrecht and processed within 24 h as described above.

### Treg and NK-Cell Phenotyping

PBMCs were thawed and stained with either Treg or NK-cell discriminating antibodies. The Treg panel was comprised of the following extracellular antibodies: CD3-AF700, CD4-eFluor780, CD8-PE-Cy7, CD25-PE, CD127-BV421, CD45RO-BV711 (Biolegend, Koblenz; Germany). For intracellular staining, cells were permeabilized after extracellular staining, using the eBioscience kit (Thermo Fisher Scientific, Darmstadt, Germany) and stained for FOXP3 expression. The NK-cell panel comprised of CD3-AF700, CD19-eFluor780, CD56-PE-Cy7, CD16-BV510, CD45RO-BV711, TCRVα24-PE, TCRVβ11-FITC (Biolegend). All samples were measured within 24 h after staining on a BD LSR Fortessa (BD Biosciences, Heidelberg, Germany). All flow cytometry data were analyzed with FlowJo software version 10.6.0 (Tree Star, Ashland, OR, USA). Output CSV documents were further analyzed using RStudio (version 1.2.1335).

### Proliferation Assay

To assess proliferation of T-cells, PBMCs were thawed, labelled with Celltrace Violet (CTV) (ThermoFisher Scientific)) and cultured in a round-bottom 96-well plate for 3 days at 37 °C and 5% CO2. 25,000 PBMCs were cultured in duplicates in the presence of anti-CD3 (0.5 μg/mL, 16-0037-81; ThermoFisher Scientific), or without stimuli. On day 3, supernatants were collected (pooled from duplos) and stored (as described in Section 2.6). Proliferation of PBMCs was analyzed using flow cytometry.

### Suppression Assay

Patient and healthy-donor (HD) CD4+CD25highCD127low Tregs were sorted using BD FACSAriaTM. Tregs were added to CTV-labelled effector cells at an effector-to-target ratio (E:T) of 2:1 in a crossover manner: (1) Tregs patient + effector cells patient;

(2) Tregs patient + effector cells HD; (3) Tregs HD + effector cells patient; (4) Tregs HD + effector cells HD. Then, 96-well plates were coated with anti-CD3 (16-0037-81; ThermoFisher) to provide a proliferation stimulus. At day 3, the proliferation of effector cells was analyzed with flow cytometry.

### Protein Profiling

Supernatant from the proliferation assays was collected after 3 days of culture, and stored at −80 °C until cytokine measurement. Interferon-γ (IFN-γ), tumor necrosis factor α (TNF-α), soluble IL-2R, IL-2, IL-10, IL-13, and IL-17 were measured using multiplex immunoassays (Luminex Technology, Austin, TX, USA). The multiplex immunoassay was performed as described previously by the MultiPlex Core Facility (MPCF) of the UMCU [18]. Out-of-range (OOR</OOR>) and extrapolated values were systematically replaced using the following procedure. The LLOQ (lower limit of quantification) and ULOQ (upper limit of quantification) were retrieved for the measured analytes of the experiment. The LLOQ and ULOQ values were retrieved per analyte by the MPCF. The lowest measurement was compared with LLOQ for each marker, to retrieve the lowest values for all measured markers. The same was performed for the highest value. OOR< data were replaced by the lowest value divided by 2. OOR> data were replaced by highest value times 2. The same procedure was performed for extrapolated data. For some markers, there are no LLOQ and ULOQ obtained yet. In that case, the lowest and highest measurements within the experiment were used for the replacement of OOR and extrapolated data.

Plasma samples were analyzed using the Proseek Multiplex Immuno-oncology immunoassay panel (Olink Biosciences, Uppsala, Sweden). Proseek is a high-throughput multiplex immunoassay based on proximity extension assay (PEA) technology that enables the analysis of 92 immuno-oncology-related biomarkers simultaneously. In short, PEA technology makes use of antibody pairs linked with matching DNA-oligonucleotides per protein of interest. These oligonucleotides hybridize when brought into proximity after binding the protein and are extended by DNA polymerase, thereby forming PCR targets. These targets are quantified by real-time PCR. Obtained results are expressed in normalized protein expression (NPX) values, which are in a log2 scale.

### Statistics

Statistical analysis of absolute cell numbers and Treg expansion during IT was performed using the Mann–Whitney U test, comparing differences between groups before and after administration of IL-2 and GM-CSF. Hierarchical clustering analyses, presented as heatmaps, were based on Ward’s method and pairwise correlation distance. Heatmaps were generated using the heatmap.2 function from the gplots package [19]. To identify significant differences between protein levels before and after IL-2 and GM-CSF IT cycles, the Wilcoxon signed rank test was performed with correction for multiple testing according to Benjamini and Hochberg [20] for IL-2 cycles and the Mann–Whitney test with correction for multiple testing [20] for GM-CSF cycles. RStudio Project Software (version 1.2.1335) [21] was used for statistical analyses. Adjusted p-values of < 0.05 were considered statistically significant.

## RESULTS

### Patient Characteristics

Twenty-five patients were included in this study (**Table 1**) with a median age at diagnosis of 3.9 years (range 0.3–10.8). A slight majority (56%, n = 14) had at least a partial response after induction chemotherapy. These patients continued therapy following the HR treatment protocol. Nonresponders (44%, n = 11) received additional chemotherapy (2–4 N8 cycles (etoposide, topotecan, cyclophosphamide)), and 14% (n = 4) received 131I-metaiodobenzylguanidine (131I-MIBG) therapy. Twenty out of 25 patients received high-dose (HD) chemotherapy followed by ASCT, seventy percent (n = 14/20) of patients received HD busulfan and melphalan (Bu-Mel) and 30% (n = 7/20) received HD carboplatin, etoposide, and melphalan. Following ASCT, 80% (n = 6/20) received dinutuximab IT in combination with cytokines. The four patients who did not receive IT had progressive disease. The mean time from ASCT to start IT was 137 days (range 108–193 days). The median time of follow-up for surviving patients was 2.14 years (range 0.65–3.67). The median event-free survival (EFS) was 1.65 years (range 0.11–3.67).

### Immune Profiles at Diagnosis, during Induction Chemotherapy, and before High-Dose Chemotherapy Show Broad Variation between Patients

In the period before ASCT, large variations were observed between patients and between treatment cycles within individual patients in absolute leukocyte, lymphocyte, monocyte, neutrophil, eosinophil and specific lymphocyte subsets (B-cells, NK-cells, and T-cells) (**Figure 1**). Absolute neutrophil counts fluctuated most, peaking after the first N5/N6 chemotherapy cycle. B-cells decreased after the first round of N5/N6 chemotherapy and remained low during chemotherapy. Absolute lymphocyte counts remained similar between patients, while NK-cells and T-cells showed a large variation between patients. No correlation was found between absolute lymphocyte counts and occurrence of an event or MYCN status.

**Table 1.** Patient Characteristics and time of sampling

| | **Total (n=25)** |
|---|---|
| **Gender** | |
| male | 14 (56%) |
| female | 11 (44%) |
| **Median age at diagnosis**, yr, (range) | 3.9 (0.3-10.8) |
| Stage 3 disease | 1 (4%) |
| Stage 4 disease | 24 (96%) |
| ***Genetics*** | |
| **MYCN** | |
| Neg | 18 (72%) |
| Gain | 2 (8%) |
| Amp | 5 (20%) |
| **1p** | |
| normal | 14 (56%) |
| partial loss | 9 (36%) |
| loss | 1 (4%) |
| gain | 1 (4%) |
| **17q** | |
| normal | 1 (4%) |
| partial gain | 10 (40%) |
| gain | 11 (44%) |
| unknown | 3 (12%) |
| **ALK mutation** | |
| Yes | 5 (20%) |
| no | 16 (64%) |
| gain | 1 (4%) |
| unknown | 3 (12%) |
| **CR or PR after induction chemotherapy** (3x N5/N6) | 14 (56%) |
| **HD + ASCT** | 20 (80%) |
| ***Therapy & outcome*** | |
| **Conditioning Regimen** | |
| Busulfan/melphalan | 14/20 (70%) |
| Carboplatin/etoposide/melphalan | 6/20 (30%) |
| **CD34+ cell dose x 10^6/kg**, (range) | 2.47 (0.59-21.73) |
| **Immunotherapy** | 16 (64%) |
| **Time to immunotherapy**, d, (range) | 137 (108-193) |
| **Event: progression or relapse** | 7 (31%) |
| **Event: Refractory Disease** | 3 (14%) |
| **Event: Toxicity** | 1 (5%) |
| **Alive at last FU** | 14 (56%) |
| **Median EFS**, yr (range) | 1.65 (0.11-3.67) |
| **Median follow up OS**, yr, (range) | 2.14 (0.65-3.67) |

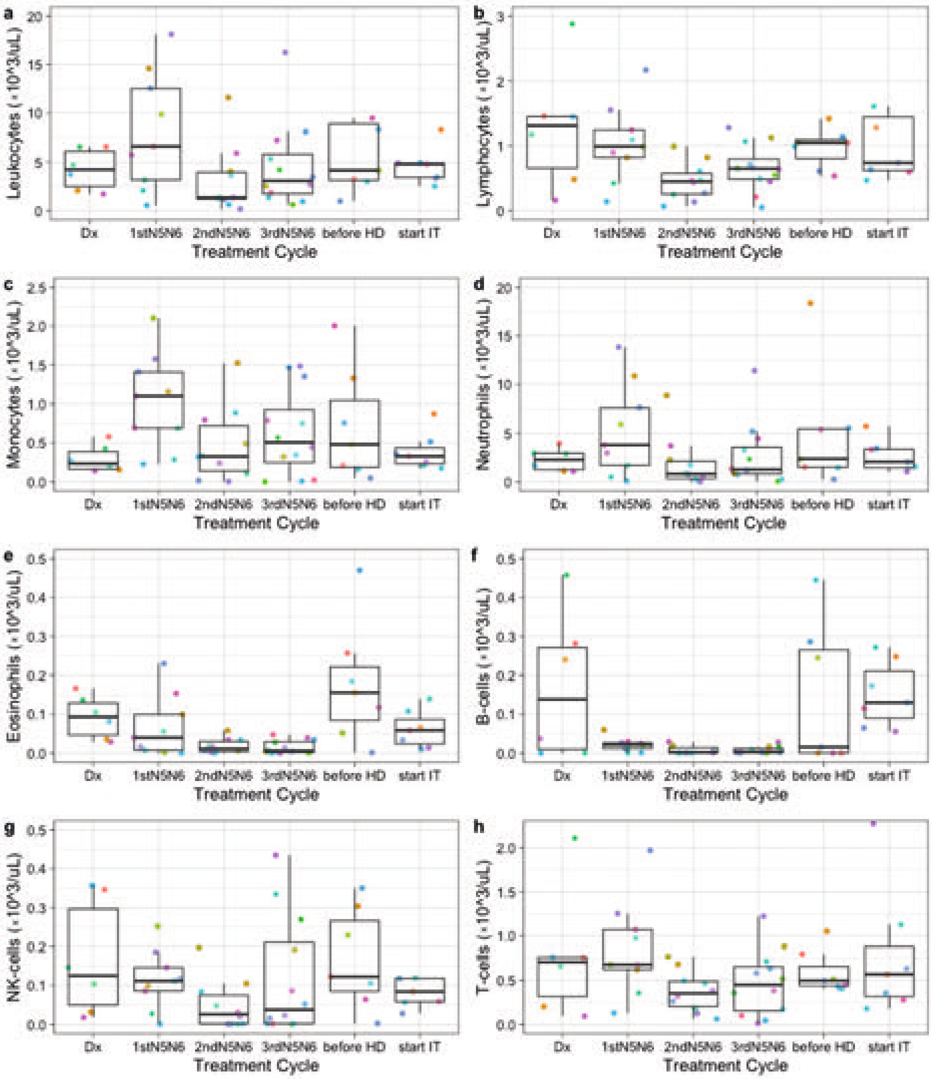

**Figure 1.** Immune profiles at diagnosis, during induction chemotherapy, and before high-dose conditioning.

*Each colored dot indicates absolute counts from one patient (×10$^3$/uL). Absolute leukocyte (**A**), lymphocyte (**B**), monocyte (**C**), neutrophil (**D**), eosinophil (**E**), B-cell (**F**), NK-cell (**G**), and T-cell (**H**) numbers are shown at diagnosis (Dx), after the 1st, 2nd, and 3rd round of N5/N6 induction chemotherapy, before high-dose chemotherapy (before HD), and at start of immunotherapy (start IT) from 6, 9, 10, 12, 7, and 4 patients respectively.*

### Immune Profiles during Immunotherapy Show Effect of IL-2 and GM-CSF on Leukocyte and Lymphocyte Subsets

To determine whether the *in vitro* effects of IL-2 and GM-CSF are also observed *in vivo*, immune profiles were generated during IT. In concordance with the rationale, total lymphocyte counts increased significantly after IL-2-containing IT cycles (p = 0.01), due to an increase of NK-cells (p < 0.01) (**Figure 2 and Figure S2**). IL-2 had no effect on total CD3+ T-cells (p = 0.67), CD19+ B cells (p = 0.70), and monocytes (p = 0.57). Neutrophils decreased significantly after IL-2 administration (p = 0.01), while eosinophils showed a trend towards increased numbers in peripheral blood after IL-2 (p = 0.19).

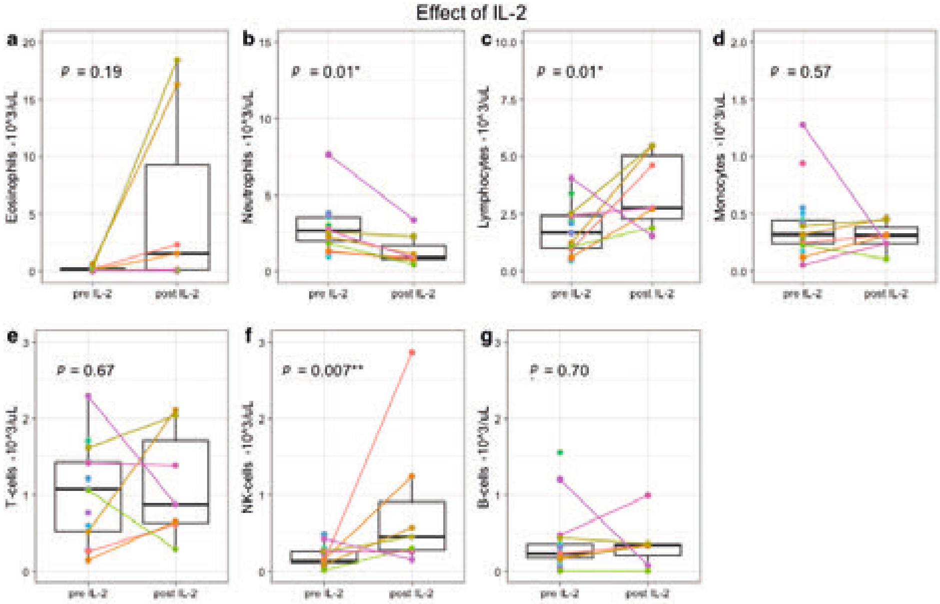

**Figure 2.** Immune profiles before and after IL-2-containing immunotherapy cycles.
*Each colored dot indicates absolute counts from one patient (×$10^3$ cells/uL). From 5 patients, samples were paired before IL-2 (day 1 IT cycle 2 or 4) and after IL-2 (day 15 IT cycle 2 or 4). In total, 7 paired samples are depicted (colored lines), because two patients were monitored in both IL-2 cycles. Nine single measurements from 9 other patients were included, resulting in a total of 14 patients (11 in study, 3 leftover material during IT). Absolute eosinophil (**A**), neutrophil (**B**), lymphocyte (**C**), monocyte (**D**), T-cell (**E**), NK-cell (**F**), and B-cell numbers (**G**) are shown. * p < 0.05, ** p < 0.001.*

GM-CSF-containing IT cycles increased total lymphocytes (p = 0.05) and monocytes (p = 0.03), and a trend towards increased neutrophils (p = 0.07). GM-CSF had no effect on total CD3+ T-cells (p = 0.28), NK-cells (p = 0.12), and CD19+ B-cells (p = 0.19) (**Figure 3** and **Figure S3**). In addition, administration of GM-CSF resulted in a notable increase of eosinophils (p < 0.001).

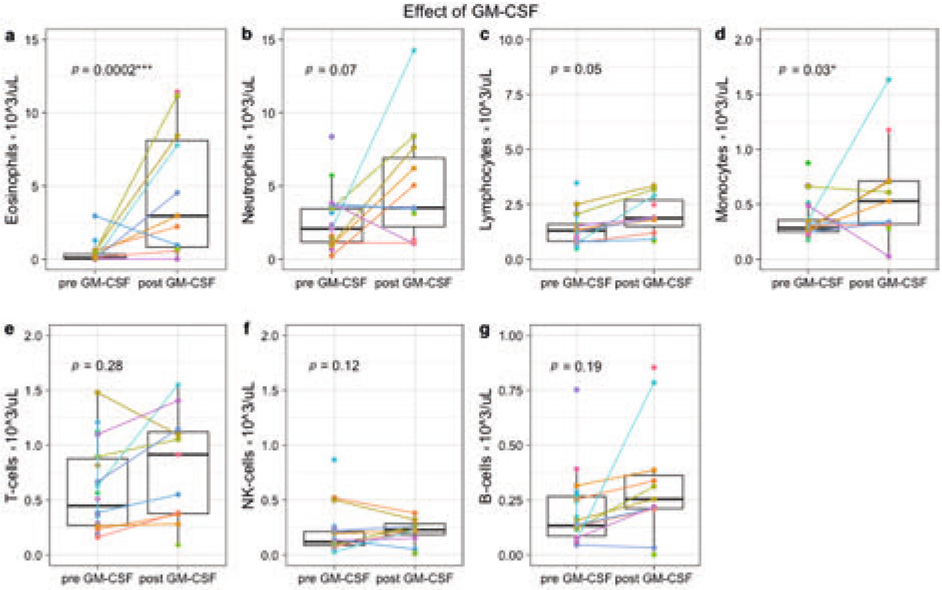

**Figure 3.** Immune profiles before and after GM-CSF-containing immunotherapy cycle.
*Each colored dot indicates absolute counts from one patient (×$10^3$ cells/uL). From 5 patients, samples were paired before GM-CSF (day 1 IT cycle 1, 3 or 5) and after GM-CSF (day 15 IT cycle 1, 3 or 5). In total, 9 paired samples are depicted (colored lines), because two patients were monitored during all 3 GM-CSF cycles. Twelve single measurements from 12 other patients were included, resulting in a total of 17 patients (11 in study, 6 left over material during IT). Absolute eosinophil (**A**), neutrophil (**B**), lymphocyte (**C**), monocyte (**D**), T-cell (**E**), NK-cell (**F**), and B-cell numbers (**G**) are shown. * p < 0.05, *** p < 0.0001*

## Plasma Protein Profiling Further Supports IL-2 and GM-CSF Mediated Immune Engagement during Immunotherapy

Olink protein analysis was subsequently performed in plasma samples of 6 patients to determine protein profiles along the IT course. Protein profiling showed distinct patterns between pre- and post-IL-2 and pre- and post-GM-CSF-containing IT cycles. Unsupervised clustering resulted in complete separation of protein profiles pre- and post-IL-2-containing IT cycles (**Figure S4A**) and partial separation of protein profiles pre- and post-GM-CSF-containing IT cycles (**Figure S4B**).

Even though the sample sizes are too small to observe statistically significant differences upon IL-2-containing IT, increases can be observed in many NK-cell activation-associated markers, including GZMA/B/H, KIR3DL1, and NCR1 (all p = 0.18), IFN-γ (p = 0.34), CASP-8 (p = 0.17), and KLRD1 (p = 0.32) (**Figure 4**). Upon GM-CSF-containing IT cycles, significant increases in several neutrophil-, monocyte-, and eosinophil-associated factors, including CCL23 (p = 0.046), CCL17 (p = 0.015), CXCL11 (p = 0.037), and MCP-4 (p = 0.015) are observed (**Figure 5**).

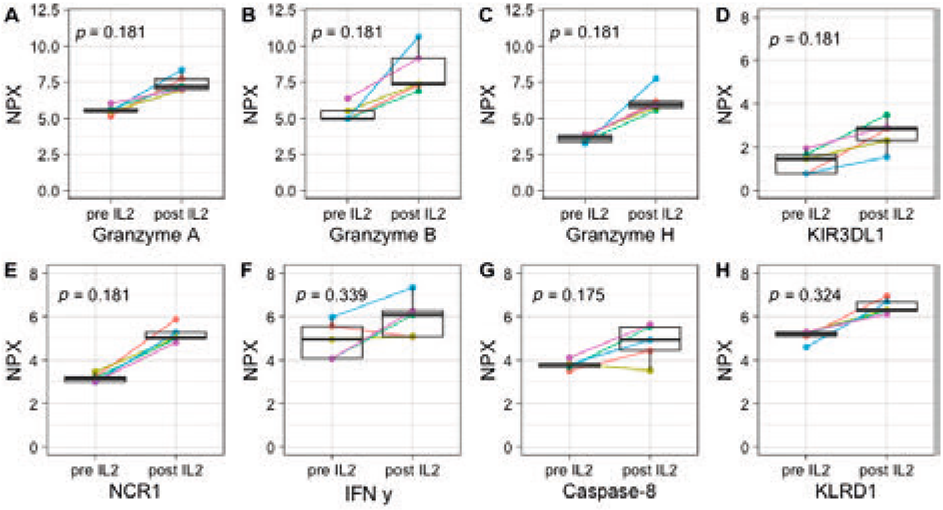

**Figure 4.** Upregulation of NK-cell activation-associated protein markers upon IL-2-containing immunotherapy cycles.
*Plasma protein concentration of GZMA/B/H (p = 0.181) (**A–C**), and KIR3DL1 (p = 0.181) (**D**), NCR1 (p = 0.181) (**E**), IFN-y (p = 0.339) (**F**), CASP-8 (p = 0.175) (**G**), and KLRD1 (p = 0.324) **(H)** pre- and post-IL-2-containing IT cycles. Protein expression is shown as normalized protein expression (NPX). In total, 5 paired samples are shown, as two patients were monitored during both IT cycles.*

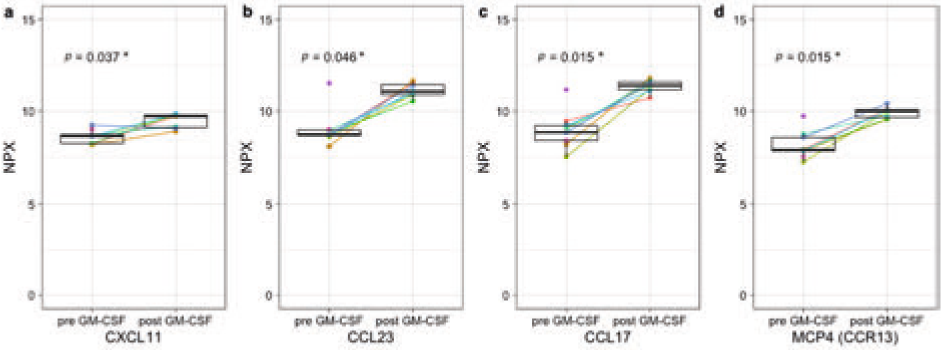

**Figure 5.** Upregulation of neutrophil-, monocyte-, and eosinophil-associated factors upon GM-CSF-containing immunotherapy cycles.
*Plasma protein concentration of CXCL11 (p = 0.037) (**A**), CCL23 (p = 0.046) (**B**), CCL17 (p = 0.015) (**C**), and MCP-4 (p = 0.015) (**D**) pre- and post-GM-CSF-containing IT cycles. Protein expression is shown as normalized protein expression (NPX). In total, 7 paired samples are shown, as two patients were monitored during all three IT cycles. Two single measurements from patients pre-GM-CSF were included, resulting in a total of 9 patients pre- and 7 post-GM-CSF. * p < 0.05.*

## NK-Cell Phenotype Varies Widely between Patients and Is Suboptimal for Efficient Dinutuximab-Mediated Cytotoxicity

As mentioned, the timing of IT in the NBL treatment protocol is established based on the observation of relatively fast NK-cell recovery early after ASCT [14]. Fast NK-cell recovery was observed based on absolute cell numbers (**Figure 1G**). However, even though variation is large, the balance between absolute numbers of mature, cytotoxic NK-cells (CD56dimCD16+) known to be mainly responsible for anti-GD2-dependent ADCC [13] and immature, cytokine-releasing NK-cells (CD56brightCD16−) was majorly disturbed at diagnosis and during all phases of the treatment protocol [22] (**Figure 6A**).

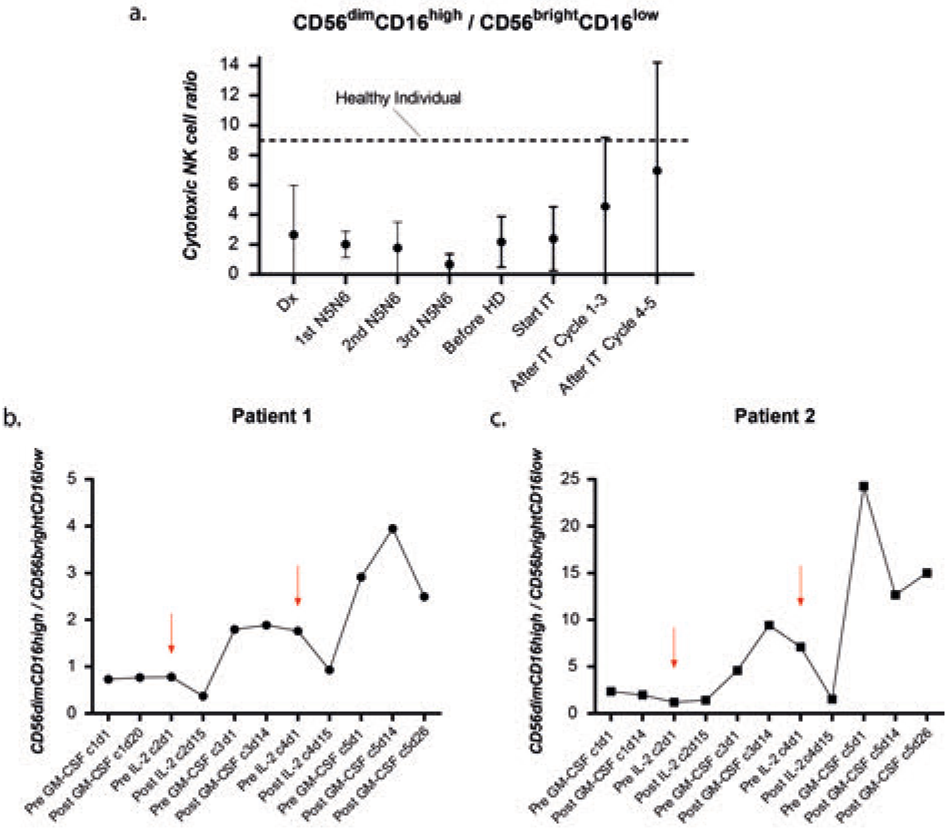

**Figure 6.** The cytotoxic CD56dimCD16+/CD56brightCD16− NK-cell ratio during HR-NBL therapy.
*(**A**) The ratio of absolute CD56dimCD16+ and CD56brightCD16− Trucount cell numbers is highly variable between patients and is decreased at diagnosis and during therapy of HR-NBL patients. Dx: n = 7, 1st N5/N6: n = 11, 2nd N5/N6: n = 10; 3rd N5/N6: n = 11, before HD: n = 7, start IT: n = 7, After IT Cycle 1–3: n = 10, After IT cycle 4–5: n = 8. The dotted line reflects the reference value of the cytotoxic NK-cell ratio of healthy individuals [22]. (**B,C**) In-depth monitoring of the fraction of CD56dimCD16+ and CD56brightCD16− in two patients during the IT course shows an increase in cytotoxic (CD56dimCD16+) NK-cell phenotype after IL-2-containing IT cycles. In patient 1, the ratio remains below the normal cytotoxic NK-cell ratio of 9, whereas the ratio of patient 1 reaches normal values after the first IL-2-containing IT cycle and is increased after the second IL-2-containing IT cycle. Red arrows indicate start of IL-2-containing therapy cycles.*

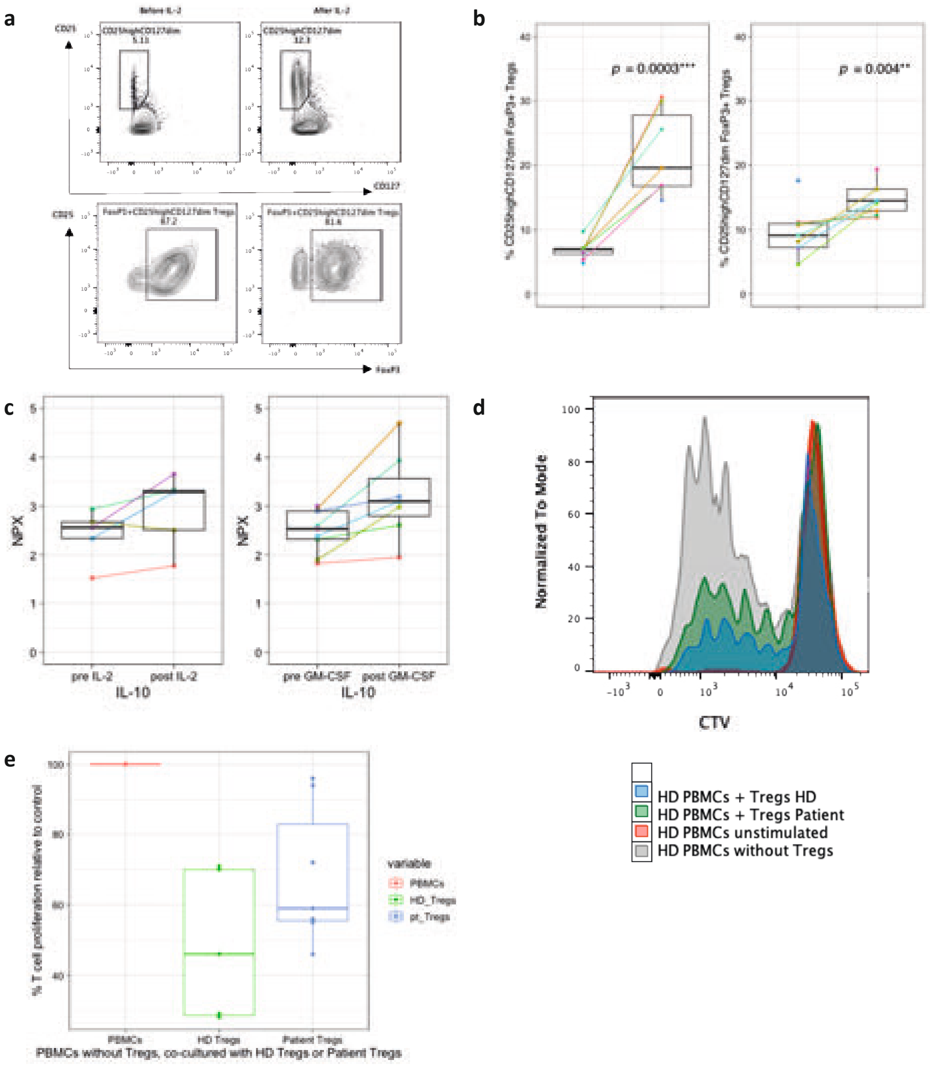

**Figure 7.** Regulatory T-cell profiles and their suppressive capacity during immunotherapy.
*(**A**) Example of gating of CD25$^{high}$CD127$^{dim}$ cells within the CD3+CD4+ T-cell population (upper panels) and gating of FoxP3 within the CD25$^{high}$CD127$^{dim}$ cell population before and after IL-2 administration (lower panels). (**B**) Percentages of Tregs (within CD3+CD4+ T-cell population) increase 4–5-fold after IL-2 administration (left) and increase 1–2-fold after GM-CSF administration (right). (**C**) Plasma IL-10 levels pre- and post-IL-2 (p = 0.339) (left) and GM-CSF (p = 0.144) (right). Protein expression is shown as normalized protein expression (NPX). IL-2: In total, 5 paired samples are shown, as two patients were monitored during both IT cycles. GM-CSF: In total, 7 paired samples are shown, as two patients were monitored during all three IT cycles. Two single measurements from patients pre-GM-CSF were included, resulting in a total of 9 patients pre- and 7 post-GM-CSF. (**D**) CTV staining of PBMCs of a healthy donor co-cultured without Tregs (grey), with patient Tregs (green), or healthy-donor Tregs (blue), or unstimulated (red) at an effector-to-target ratio of 2:1. (**E**) Relative percentages of proliferation of HD CD3+ T-cells co-cultured with patient Tregs (blue) or HD Tregs (green) compared to proliferation without Tregs (red). CD3+ T-cell proliferation was measured in patient 1 (during cycle 2 and 4), patient 2 (during cycles 1, 2 and 5) and patient 3 (during cycle 1 and 2). HD = healthy donor, PT = patient. ** p < 0.001, *** p < 0.0001.*

As plasma levels of NK-cell activation-associated markers increased upon IL-2-containing IT cycles, the NK-cell phenotype of two patients was subsequently assessed along the IT course. In both patients, we observed a major shift towards the mature, cytotoxic CD56dimCD16+ phenotype after both IL-2-containing IT cycles (**Figure 6B,C**). The CD56dimCD16+/CD56brightCD16– ratio of patient 1 remained lower than the ratio of 9–9.5 in healthy controls [23], whereas the ratio of patient 2 reached a normal (IL-2 cycle 1) or superior (IL-2 cycle 2) NK-cell ratio.

### Preferential Treg Expansion and Impaired T-Cell Proliferation during Therapy

Even though no significant changes were observed in absolute CD3+ T-cell levels after IL-2- or GM-CSF-containing IT cycles, it is suggested that cytokine therapy can shift the phenotype of CD3+ T-cells. To explore this effect during IT, extensive phenotyping of the CD3+ T-cell fraction was performed. Administration of IL-2 in this study massively increased the frequency of circulating CD4+CD25highCD127dim FOXP3+ Tregs (**Figure 7A,B**). In addition, GM-CSF also increased the frequency of Tregs, although to a lower extent than IL-2 (**Figure 7B**). These data were supported by an increased trend in plasma levels of IL-10 (GM-CSF: $p = 0.144$, IL-2: $p = 0.339$) (**Figure 7C**).

To subsequently determine whether patient Tregs are functional, a Treg crossover suppression assay was performed in which patient Tregs from different IT time points were co-cultured with healthy-donor PBMCs. Healthy-donor PBMC proliferation was decreased upon co-culture with patient Tregs, indicating their suppressive capacity, even though suppressive capacity seems to be decreased when compared with healthy-donor Tregs (**Figure 7D,E**). In 2 of the 7 measurements (patient 1 cycle 2 and patient 3 cycle 1), no T-cell suppression was noticed.

To assess functionality of the CD3+ T-cell fraction in terms of proliferative capacity during IT, PBMCs were stimulated for three days with anti-CD3. Interestingly, anti-CD3-mediated T-cell proliferation was impaired in the majority of patients at different IT time points (**Figure 8A**). This was supported by decreased levels of secreted cytokines in stimulated patient PBMCs as compared to healthy-donor PBMCs (**Figure 8B**). Possible interference of CD25+CD127low Tregs or low-density eosinophils on T-cell proliferation was ruled out by performing additional T-cell proliferation assays without these cell populations.

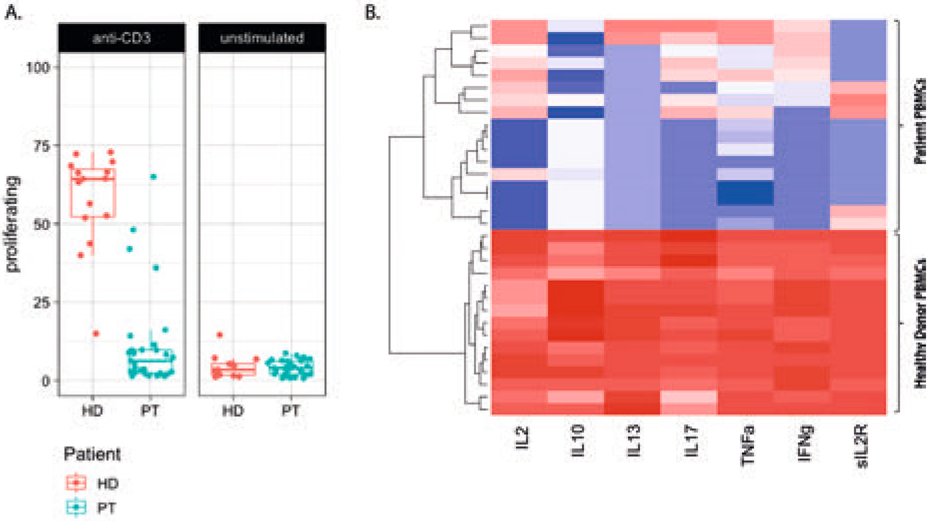

**Figure 8.** T-cell proliferation is impaired at diagnosis as well as during therapy in HR-NBL.
*(**A**) PBMCs of healthy donors (HD) (red) and patients (PT) (blue) were stimulated with anti-CD3 (0.5 µg/mL). T-cell proliferation of each individual sample is shown (duplos were pooled); PBMCs HD (n = 8), PBMCs patients (n = 12). (**B**) Supernatants (HD n = 15, patients n = 17) were analyzed using Luminex-based multiplex immunoassays. The heatmap shows the log concentration of IL-2, IL-10, IL-13, IL-7, TNF-α, IFN-γ and soluble IL-2R, with low levels indicated in blue and high levels indicated in red.*

## DISCUSSION

Absolute lymphocyte counts, relative presence of subsets, and their phenotypical characteristics are rarely monitored in NBL patients and not used as prognostic criteria or treatment guidance, largely due to a lack of knowledge on clinical significance. In the present study, we show that immune profiles of HR-NBL patients are already disturbed (reduced levels of CD3+, CD56+, and CD19+ lymphocyte subsets) at diagnosis when compared to age-matched controls [24]. This is in line with Tamura *et al.* [25], who also reported that lower levels of immune cells at diagnosis may predict poor prognosis in patients with NBL. As HR-NBL often disseminates to the bone marrow, it is hypothesized that the decreased immune cell levels are most likely caused by tumor replacement and/or by tumor-related suppressive factors present in the bone marrow niche [25,26]. This is supported by studies observing lower leukocyte [26] or monocyte and lymphocyte [25] levels in patients with bone marrow metastases.

Moreover, we confirm data from Chung *et al.* [26] showing that the decrease in total leukocytes and lymphocytes in children with HR-NBL is even more pronounced after chemotherapy. We however observed a large interpatient variability between chemotherapy cycles; while B cells are completely depressed during all stages of N5/N6 chemotherapy, the numbers of monocytes, NK and T lymphocytes differed enormously. Whether these variations correlate to clinical outcome will be subject of follow-up studies with larger cohorts.

The effect of chemotherapeutic agents on the immune compartment should be kept in mind when combining IT with re-induction chemotherapy in relapsed/refractory patients. The effect of chemotherapy on IT efficacy is paradoxal, as levels of effector cells are often affected. On the other hand, targeting of immunosuppressive immune subsets and increased immunogenicity of tumor cells are described as processes to enhance IT efficacy [27,28,29]. Timing and chemotherapeutic compound selection are key to maximize the effect of IT in refractory/relapsed patients.

When subsequently looking into the functionality of T-cells at diagnosis and during the therapy regimen, we noticed hampered proliferation and cytokine secretion upon anti-CD3-mediated T-cell stimulation. In line with this, impaired PHA mitogenesis at diagnosis and during NBL therapy has been observed in several studies [30,31]. Helson *et al.* [31] and Pelizzo *et al.* [32] showed hampered PHA-mediated T-cell mitogenesis when cultures were supplemented with serum of NBL-patients, or mesenchymal stromal cells (MSCs) from HR-NBL patients, respectively. This indicates the presence of both local and systemic immune modulation by the NBL tumor. Several factors have been described that are able to modulate T-cell functionality, including TGF-β, Indoleamine-pyrrole 2,3-dioxygenase (IDO), and arginase [33,34]. The depletion of arginine by arginase [33] leads to T-cell cycle arrest, impaired proliferation, and reduced activation [35,36]. Although impaired T-cell proliferation is already noticed at diagnosis, it should be noted that immune function may be further inhibited by intensive treatment. In-depth phenotyping, proteomics, and pathway-analysis of T-cells during HR-NBL treatment is necessary to unravel mechanisms responsible for T-cell dysfunctionality as a first step to develop strategies to counteract this effect.

The effect of the IT regimen on NK-cell phenotype is largely unknown. Even though variation between patients is considerable, our data indicate that the cytotoxic NK-cell ratio increased during IT. We observed a delayed increase of the cytotoxic ratio in two patients upon IL-2-containing IT cycles. However, the NK-cell phenotype ratio of the majority of patients is still decreased at the end of IT, which suggests suboptimal IT timing. The observed differential effect of GM-CSF- and IL-2-containing IT cycles on the cytotoxic NK-cell ratio indicates that this is an effect induced by IL-2 rather than dinutuximab itself.

To our knowledge, this is the first study to show beneficial effects of GM-CSF and IL-2 addition to IT cycles in HR-NBL patients on both NK-cells (increased cytotoxic NK-cell ratio and plasma levels of NK-cell-associated factors (e.g., granzymes, KLRD1, NCR1, IFN-γ, CASP-8, KLRD1)), as well as on myeloid cells (based on plasma levels of neutrophil/monocyte-associated factors (e.g., CXCL11, CCL17, CCL23, and MCP4)). Nonetheless, Ladenstein and colleagues [4] recently concluded from a phase III clinical trial that there is no additive effect of IL-2 administration on outcome of HR-NBL patients. We noticed a strong increase of CD127dimCD25highFOXP3+ Tregs after IL-2, and to a lesser extent, also GM-CSF administration. This increase has been described before [37]; however, in many cases without confirming FOXP3 positivity, this may be expected based on results from autoimmune patients [15] where (low dose) IL-2 is administered to induce Tregs. Previously, preclinical data showed that Tregs inhibit anti-NBL immune responses before and after ASCT [38-40]. Using functional suppression assays in a crossover format, we showed that these Tregs also maintain their suppressive capacity at multiple time points during IT. Together, these data suggest that the beneficial effects of IL-2 may be masked by preferential Treg expansion.

The observation of increased NK-cell cytotoxicity during IL-2-containing IT cycles in our opinion substantiates the need to replace IL-2 during dinutuximab IT with other non-Treg engaging (immuno)therapeutic compounds/strategies to maximize IT efficacy. First of all, the start of IT can be delayed to allow further recovery of the NK-cell fraction. However, the observation that the NK-cell phenotype is already disturbed at diagnosis, together with the risk of the tumor to expand before the start of IT, are arguments against postponement of IT. A second strategy would be to combine dinutuximab with soluble factors more specifically activating NK-cells, for example, Lirilumab, an anti-KIR antibody currently tested in the ESMART trial from the ITCC (ClinicalTrials.gov Identifier: NCT02813135). In addition, NKTR-214, a CD122-biased cytokine agonist designed to preferentially activate and expand effector CD8+ T- and NK-cells over Tregs via the heterodimeric IL-2 receptor pathway (IL-2R-βɣ) [41], is an interesting candidate to replace IL-2 [42]. Combining dinutuximab with IL-15 is also of interest, as this cytokine is known to specifically expand and mature NK-cells, without affecting Treg expansion [43,44]. The delayed effect of IL-2 on the cytotoxic NK-cell ratio observed in this study may substantiate an approach in which NK-cell engaging therapy is provided prior to dinituximab-based IT. A third strategy would be to combine IT with an adoptive NK-cell therapy at the start of IT to maximize effector cell function, either via an autologous (ClinicalTrials.gov Identifiers: NCT02573896, NCT04211675) or allogeneic (haploidentical) [45] strategy (ClinicalTrials.gov Identifier: NCT03242603). The advantage of using allogeneic cells is the potential to select a mismatched donor to maximize anti-tumor effect. On the other hand, the risk of graft rejection and mismatch-related adverse events in allogeneic settings is a clear disadvantage compared to the use of an autologous, ex vivo-expanded, cell product.

Immune monitoring of HR-NBL patients comes with some limitations. The availability of patient samples was limited by dropout of patients from the study after relapse/progression of disease, transfer to other trials, failure of blood sampling, and logistical issues. In this study, immune status was monitored in peripheral blood only, which provides markers that would be easily translatable to monitoring protocols in the clinic. Nevertheless, information on tumor-infiltrating lymphocytes (TILs), and monitoring lymphocytes in tissues, would help to elucidate the mechanisms of (resistance to) therapy, and indicate whether markers at the tumor site are systemically reflected in the blood. Multinational collaborations in NBL cohorts are needed to allow for a larger sample size to confirm the findings from this study and relate them to clinical parameters and outcome.

## CONCLUSIONS

(Functional) immune monitoring in HR-NBL patients revealed the presence of both immune-enhancing and immune regulatory effects during the therapy course. The immune-enhancing effects observed upon IL-2-containing IT cycles, despite simultaneous Treg expansion, clearly demonstrate the potential of combining dinutuximab with other NK-cell engaging strategies. In addition, the observed systemic T-cell dysfunction at diagnosis as well as during HR-NBL therapy highlights another mechanism, besides lack of MHC-I expression and immune checkpoint expression, that should be unraveled to generate long-term anti-NBL immune responses and immunological memory needed to prevent relapse.

## REFERENCES

1. Howlader, N.; Noone, A.M.; Krapcho, M.; Miller, D.; Brest, A.; Yu, M.; Ruhl, J.; Tatalovich, Z.; Mariotto, A.; Lewis, D.R.; et al. (Eds.) *SEER Cancer Statistics Review, 1975–2016*; National Cancer Institute: Bethesda, MD, USA, **2016**.
2. Cohn, S.L.; Pearson, A.D.J.; London, W.B.; Monclair, T.; Ambros, P.F.; Brodeur, G.M.; Faldum, A.; Hero, B.; Iehara, T.; Machin, D.; et al. The International Neuroblastoma Risk Group (INRG) classification system: An INRG task force report. *J. Clin. Oncol.* **2009**, *27*, 289–297, doi:10.1200/JCO.2008.16.6785.
3. Yu, A.L.; Gilman, A.L.; Ozkaynak, M.F.; London, W.B.; Kreissman, S.G.; Chen, H.X.; Smith, M.; Anderson, B.; Villablanca, J.G.; Matthay, K.K.; et al. Anti-GD2 Antibody with GM-CSF, Interleukin-2, and Isotretinoin for Neuroblastoma. *N. Engl. J. Med.* **2010**, *363*, 1324–1334, doi:10.1056/NEJMoa0911123.
4. Ladenstein, R.; Pötschger, U.; Valteau-Couanet, D.; Luksch, R.; Castel, V.; Yaniv, I.; Laureys, G.; Brock, P.; Michon, J.M.; Owens, C.; et al. Interleukin 2 with anti-GD2 antibody ch14.18/CHO (dinutuximab beta) in patients with high-risk neuroblastoma (HR-NBL1/SIOPEN): A multicentre, randomised, phase 3 trial. *Lancet Oncol.* **2018**, *19*, 1617–1629, doi:10.1016/S1470-2045(18)30578-3.
5. Yu, A.L.; Gilman, A.L.; Ozkaynak, M.F.; Naranjo, A.; Diccianni, M.B.; Gan, J.; Hank, J.A.; Batova, A.; London, W.B.; Tenney, S.C.; et al. Long-term follow-up of a Phase III Study of ch14.18 (Dinutuximab) + Cytokine Immunotherapy in Children with High-risk Neuroblastoma: COG Study ANBL0032. *Clin. Cancer Res.* **2021**, *18*, doi:10.1158/1078-0432.ccr-20-3909.
6. Park, J.R.; Bagatell, R.; London, W.B.; Maris, J.M.; Cohn, S.L.; Mattay, K.M.; Hogarty, M. Children's Oncology Group's 2013 blueprint for research: Neuroblastoma. *Pediatr. Blood Cancer* **2013**, *60*, 985–993, doi:10.1002/pbc.24433.
7. Pinto, N.R.; Applebaum, M.A.; Volchenboum, S.L.; Matthay, K.K.; London, W.B.; Ambros, P.F.; Nakagawara, A.; Berthold, F.; Schleiermacher, G.; Park, J.R.; et al. Advances in risk classification and treatment strategies for neuroblastoma. *J. Clin. Oncol.* **2015**, *33*, 3008–3017, doi:10.1200/JCO.2014.59.4648.
8. Masucci, G.; Ragnhammar, P.; Wersäll, P.; Mellstedt, H. Granulocyte-monocyte colony-stimulating-factor augments the interleukin-2-induced cytotoxic activity of human lymphocytes in the absence and presence of mouse or chimeric monoclonal antibodies (mAb 17-1A). *Cancer Immunol. Immunother.* **1990**, *31*, 231–235.
9. Hank, J.A.; Surfus, J.; Sondel, P.M.; Robinson, R.R.; Mueller, B.M.; Reisfeld, R.A.; Cheung, N.K. Augmentation of Antibody Dependent Cell Mediated Cytotoxicity following in Vivo Therapy with Recombinant Interleukin 2. *Cancer Res.* **1990**, *50*, 5234–5239.
10. Thoma, M.D.; Huneke, T.J.; DeCook, L.J.; Johnson, N.D.; Wiegand, R.A.; Litzow, M.R.; Hogan, W.J.; Porrata, L.F.; Holtan, S.G. Peripheral blood lymphocyte and monocyte recovery and survival in acute leukemia postmyeloablative allogeneic hematopoietic stem cell transplant. *Biol. Blood Marrow Transplant.* **2012**, *18*, 600–607, doi:10.1016/j.bbmt.2011.08.007.
11. Galvez-Silva, J.; Maher, O.M.; Park, M.; Liu, D.; Hernandez, F.; Tewari, P.; Nieto, Y. Prognostic Analysis of Absolute Lymphocyte and Monocyte Counts after Autologous Stem Cell Transplantation in Children, Adolescents, and Young Adults with Refractory or Relapsed Hodgkin Lymphoma. *Biol. Blood Marrow Transplant.* **2017**, *23*, 1276–1281, doi:10.1016/j.bbmt.2017.04.013.
12. Kim, H.T.; Armand, P.; Frederick, D.; Andler, E.; Cutler, C.; Koreth, J.; Alyea, E.P.; Antin, J.H.; Soiffer, R.J.; Ritz, J.; et al. Absolute lymphocyte count recovery after allogeneic hematopoietic stem cell transplantation predicts clinical outcome. *Biol. Blood Marrow Transplant.* **2015**, *21*, 873–880, doi:10.1016/j.bbmt.2015.01.019.

**13.** Nassin, M.L.; Nicolaou, E.; Gurbuxani, S.; Cohn, S.L.; Cunningham, J.M.; LaBelle, J.L. Immune Reconstitution Following Autologous Stem Cell Transplantation in Patients with High-Risk Neuroblastoma at the Time of Immunotherapy. *Biol. Blood Marrow Transplant.* **2018**, *24*, 452–459, doi:10.1016/j.bbmt.2017.11.012.

**14.** Scheid, C.; Pettengell, R.; Ghielmini, M.; Radford, J.A.; Morgenstern, G.R.; Stern, P.L.; Crowther, D. Time-course of the recovery of cellular immune function after high-dose chemotherapy and peripheral blood progenitor cell transplantation for high-grade non-Hodgkin's lymphoma. *Bone Marrow Transplant.* **1995**, *15*, 901–906.

**15.** Ye, C.; Brand, D.; Zheng, S.G. Targeting IL-2: An unexpected effect in treating immunological diseases. *Signal Transduct. Target. Ther.* **2018**, *3*, 1–10, doi:10.1038/s41392-017-0002-5.

**16.** Dutch Childhood Oncology Group (DCOG). *DCOG NBL 2009 Treatment Protocol for Risk Adapted Treatment of Children with Neuroblastoma Admendment 1*; **2012**.

**17.** Brodeur, G.M.; Pritchard, J.; Berthold, F.; Carlsen, N.L.; Castel, V.; Castelberry, R.P.; De Bernardi, B.; Evans, A.E.; Favrot, M.; Hedborg, F. Revisions of the international criteria for neuroblastoma diagnosis, staging and response to treatment. *Prog. Clin. Biol. Res.* **1994**, *385*, 363–369, doi:10.1080/16501960410016046.

**18.** De Jager, W.; Prakken, B.J.; Bijlsma, J.W.J.; Kuis, W.; Rijkers, G.T. Improved multiplex immunoassay performance in human plasma and synovial fluid following removal of interfering heterophilic antibodies. *J. Immunol. Methods* **2005**, *300*, 124–135, doi:10.1016/j.jim.2005.03.009.

**19.** Warnes, G.J.; Bolker, B.; Bonebakker, L.; Gentleman, G.; Liaw, W.H.A.; Lumley, T.; Maechler, M.; Magnusson, A.; Moeller, S.; Schwartz, M.; et al. gplots: Various R Programming Tools for Plotting Data. *R Package Version* **2019**, *2*, 1.

**20.** Url, S.; Society, R.S.; Society, R.S. Controlling the False Discovery Rate : A Practical and Powerful Approach to Multiple Testing. *J. R. Stat. Soc. Ser. B* **1995**, *57*, 289–300.

**21.** R Core Team. *R: A Language and Environment for Statistical Computing*; R Foundation for Statistical Computing: Vienna, Austria, **2018**.

**22.** Angelo, L.S.; Banerjee, P.P.; Monaco-Shawver, L.; Rosen, J.B.; Makedonas, G.; Forbes, L.R.; Mace, E.M.; Orange, J.S. Practical NK cell phenotyping and variability in healthy adults. *Immunol. Res.* **2015**, *62*, 341–356, doi:10.1007/s12026-015-8664-y.

**23.** Cooper, M.A.; Fehniger, T.A.; Caligiuri, M.A. The biology of human natural killer-cell subsets. *Trends Immunol.* **2001**, *22*, 633–640, doi:10.1016/S1471-4906(01)02060-9.

**24.** Tosato, F.; Bucciol, G.; Pantano, G.; Putti, M.C.; Sanzari, M.C.; Basso, G.; Plebani, M. Lymphocytes subsets reference values in childhood. *Cytom. Part A* **2015**, *87*, 81–85, doi:10.1002/cyto.a.22520.

**25.** Tamura, A.; Inoue, S.; Mori, T.; Noguchi, J.; Nakamura, S.; Saito, A.; Kozaki, A.; Ishida, T.; Sadaoka, K.; Hasegawa, D.; et al. Low Multiplication Value of Absolute Monocyte Count and Absolute Lymphocyte Count at Diagnosis May Predict Poor Prognosis in Neuroblastoma. *Front. Oncol.* **2020**, *10*, 1–9, doi:10.3389/fonc.2020.572413.

**26.** Chung, H.S.; Higgins, G.R.; Siegel, S.E.; Seeger, R.C. Abnormalities of the immune system in children with neuroblastoma related to the neoplasm and chemotherapy. *J. Pediatr.* **1977**, *90*, 548–554, doi:10.1016/S0022-3476(77)80364-8.

**27.** Cornel, A.M.; Mimpen, I.L.; Nierkens, S. MHC class I downregulation in cancer: Underlying mechanisms and potential targets for cancer immunotherapy. *Cancers* **2020**, *12*, 1760, doi:10.3390/cancers12071760.

**28.** Domingos-pereira, S.; Galliverti, G.; Hanahan, D.; Nardelli-haefliger, D. Intravaginal CpG as tri-therapy towards efficient regression of genital HPV16 tumors. *J. Immunol. Ther. Cancer* **2019**, *1*, 1–7, doi:10.1186/s40425-019-0593-1.

**29.** Chitadze, G.; Lettau, M.; Luecke, S.; Wang, T.; Janssen, O.; Fürst, D.; Mytilineos, J.; Wesch, D.; Oberg, H.H.; Held-Feindt, J.; et al. NKG2D- and T-cell receptor-dependent lysis of malignant glioma cell lines by human γδ T cells: Modulation by temozolomide and A disintegrin and metalloproteases 10 and 17 inhibitors. *Oncoimmunology* **2016**, *5*, 1–13, doi:10.1080/2162402X.2015.1093276.

**30.** Rosanda, C.; De Bernardi, B.; Pasino, M.; Bisogni, M.C.; Maggio, A.; Haupt, R.; Tonini, G.P.; Ponzoni, M. Immune Evaluation of 50 Children With Neuroblastoma at Onset. *Med. Pediatr. Oncol.* **1982**, doi:10.1002/mpo.2950100402.

**31.** Helson, L.; Shou, L.; Tauber, J. Lymphocyte transformation in children with neuroblastoma. *J. Natl. Cancer Inst.* **1976**, *57*, 721–722, doi:10.1093/jnci/57.3.721.

**32.** Pelizzo, G.; Veschi, V.; Mantelli, M.; Croce, S.; Di Benedetto, V.; D'Angelo, P.; Maltese, A.; Catenacci, L.; Apuzzo, T.; Scavo, E.; et al. Microenvironment in neuroblastoma: Isolation and characterization of tumor-derived mesenchymal stromal cells. *BMC Cancer* **2018**, *18*, 1176, doi:10.1186/s12885-018-5082-2.

**33.** Mussai, F.; Egan, S.; Hunter, S.; Webber, H.; Fisher, J.; Wheat, R.; McConville, C.; Sbirkov, Y.; Wheeler, K.; Bendle, G.; et al. Neuroblastoma arginase activity creates an immunosuppressive microenvironment that impairs autologous and engineered immunity. *Cancer Res.* **2015**, *75*, 3043–3053, doi:10.1158/0008-5472.CAN-14-3443.

**34.** Wang, Q.; Ding, G.; Xu, X. Immunomodulatory functions of mesenchymal stem cells and possible mechanisms. *Histol. Histopathol.* **2016**, *31*, 949–959, doi:10.14670/HH-11-750.

**35.** Rodriguez, P.C.; Quiceno, D.G.; Ochoa, A.C. L-arginine availability regulates T-lymphocyte cell-cycle progression. *Blood* **2007**, *109*, 1568–1573, doi:10.1182/blood-2006-06-031856.

**36.** Zea, A.H.; Rodriguez, P.C.; Culotta, K.S.; Hernandez, C.P.; DeSalvo, J.; Ochoa, J.B.; Park, H.J.; Zabaleta, J.; Ochoa, A.C. L-Arginine modulates CD3ζ expression and T cell function in activated human T lymphocytes. *Cell. Immunol.* **2004**, *232*, 21–31, doi:10.1016/j.cellimm.2005.01.004.

**37.** Troschke-Meurer, S.; Siebert, N.; Marx, M.; Zumpe, M.; Ehlert, K.; Mutschlechner, O.; Loibner, H.; Ladenstein, R.; Lode, H.N. Low $CD4^+/CD25^+/CD127^-$ regulatory T cell- and high INF-γ levels are associated with improved survival of neuroblastoma patients treated with long-term infusion of ch14.18/CHO combined with interleukin-2. *Oncoimmunology* **2019**, *8*, doi:10.1080/2162402X.2019.1661194.

**38.** Jing, W.; Gershan, J.A.; Johnson, B.D. Depletion of CD4 T cells enhances immunotherapy for neuroblastoma after syngeneic HSCT but compromises development of antitumor immune memory. *Blood* **2009**, *113*, 4449–4457, doi:10.1182/blood-2008-11-190827.

**39.** Jing, W.; Yan, X.; Hallett, W.H.D.; Gershan, J.A.; Johnson, B.D. Depletion of CD25+ T cells from hematopoietic stem cell grafts increases posttransplantation vaccine-induced immunity to neuroblastoma. *Blood* **2011**, doi:10.1182/blood-2010-12-326108.

**40.** Johnson, B.D.; Jing, W.; Orentas, R.J. CD25+ regulatory T cell inhibition enhances vaccine-induced immunity to neuroblastoma. *J. Immunother.* **2007**, *30*, 203–214, doi:10.1097/01.cji.0000211336.91513.dd.

**41.** Charych, D.H.; Hoch, U.; Langowski, J.L.; Lee, S.R.; Addepalli, M.K.; Kirk, P.B.; Sheng, D.; Liu, X.; Sims, P.W.; VanderVeen, L.A.; et al. NKTR-214, an Engineered Cytokine with Biased IL2 Receptor Binding, Increased Tumor Exposure, and Marked Efficacy in Mouse Tumor Models. *Clin. Cancer Res.* **2016**, *22*, 680–690, doi:10.1158/1078-0432.CCR-15-1631.

**42.** Diab, A.; Tannir, N.M.; Bentebibel, S.E.; Hwu, P.; Papadimitrakopoulou, V.; Haymaker, C.; Kluger, H.M.; Gettinger, S.N.; Sznol, M.; Tykodi, S.S.; et al. Bempegaldesleukin (NKTR-214) plus Nivolumab in Patients with Advanced Solid Tumors: Phase I Dose-Escalation Study of Safety, Efficacy, and Immune Activation (PIVOT-02). *Cancer Discov.* **2020**, *10*, 1158–1173, doi:10.1158/2159-8290.CD-19-1510.

**43.** Waldmann, T.A. The biology of interleukin-2 and interleukin-15: Implications for cancer therapy and vaccine design. *Nat. Rev. Immunol.* **2006**, *6*, 595–601, doi:10.1038/nri1901.

**44.** Heinze, A.; Grebe, B.; Bremm, M.; Huenecke, S.; Munir, T.A.; Graafen, L.; Frueh, J.T.; Merker, M.; Rettinger, E.; Soerensen, J.; et al. The Synergistic Use of IL-15 and IL-21 for the Generation of NK Cells From CD3/CD19-Depleted Grafts Improves Their ex vivo Expansion and Cytotoxic Potential against Neuroblastoma: Perspective for Optimized Immunotherapy Post Haploidentical Stem Cell Trans. *Front. Immunol.* **2019**, *10*, 1–20, doi:10.3389/fimmu.2019.02816.

**45.** Modak, S.; Le Luduec, J.B.; Cheung, I.Y.; Goldman, D.A.; Ostrovnaya, I.; Doubrovina, E.; Basu, E.; Kushner, B.H.; Kramer, K.; Roberts, S.S.; et al. Adoptive immunotherapy with haploidentical natural killer cells and Anti-GD2 monoclonal antibody m3F8 for resistant neuroblastoma: Results of a phase I study. *Oncoimmunology* **2018**, *7*, 1–10, doi: 10.1080/2162402X.2018.1461305.

## SUPPLEMENTARY MATERIAL

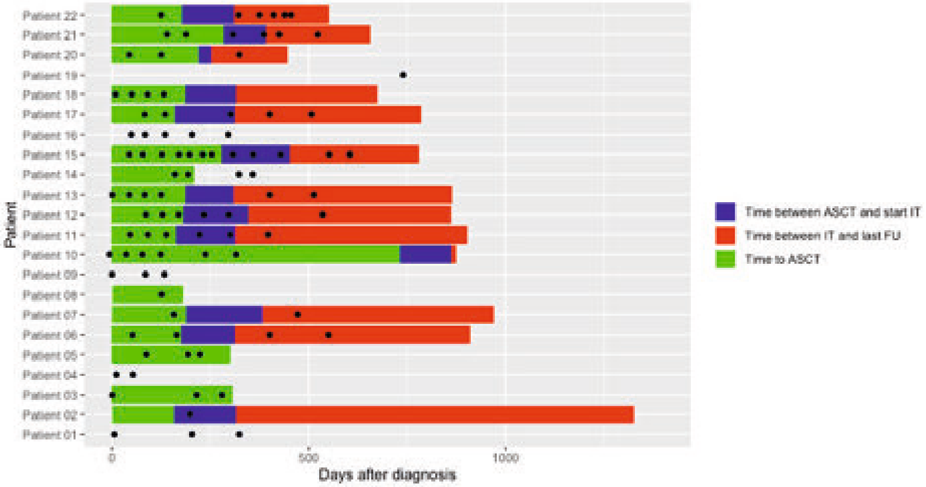

**Figure S1.** Schematic overview of sampling time points during the HR-NBL treatment course. *Patient 4, 9, 16, and 19 did not receive ASCT as a result of disease progression and mortality.*

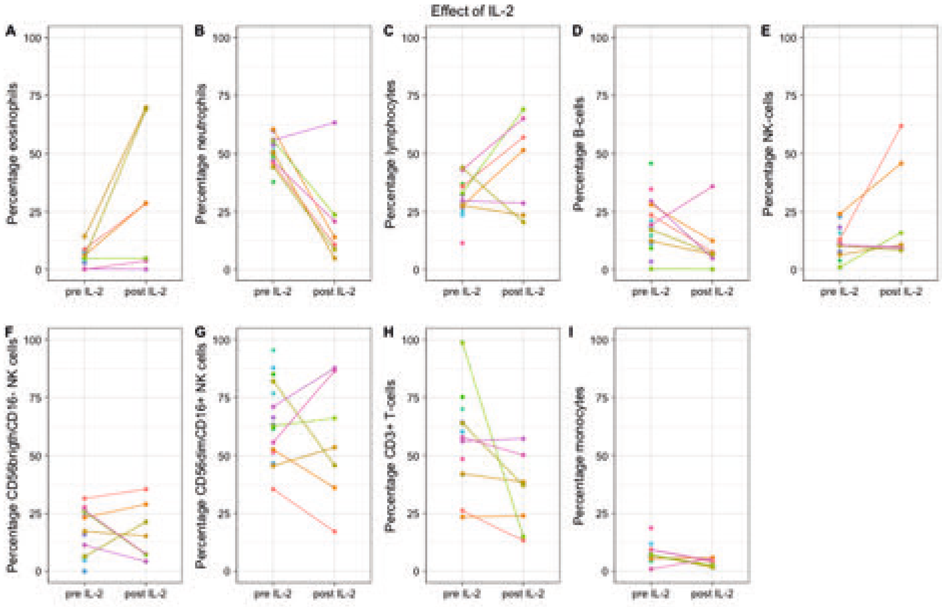

**Figure S2.** Percentages of cell types based on trucount data before and after IL-2 containing immunotherapy cycles.

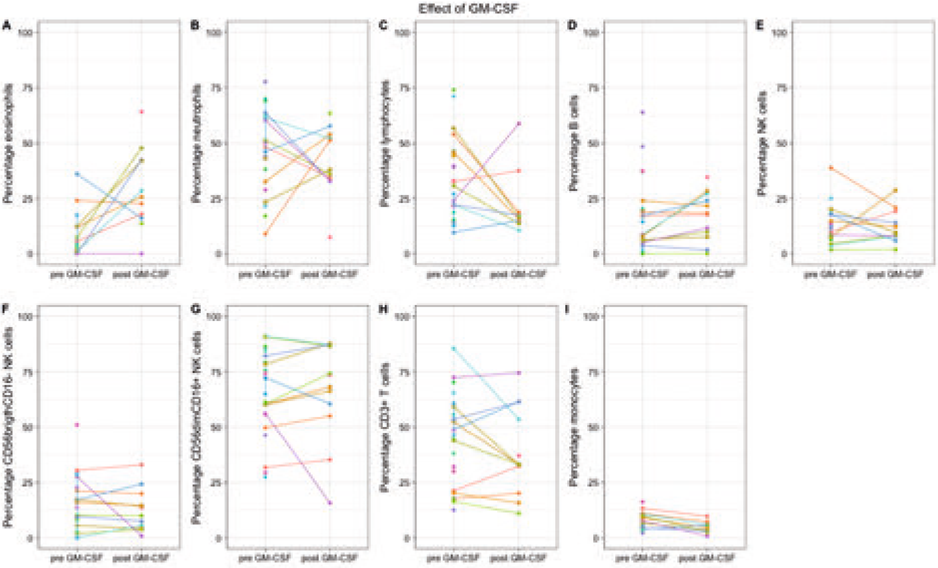

**Figure S3.** Percentages of cell types based on trucount data before and after GM-CSF containing immunotherapy cycle.

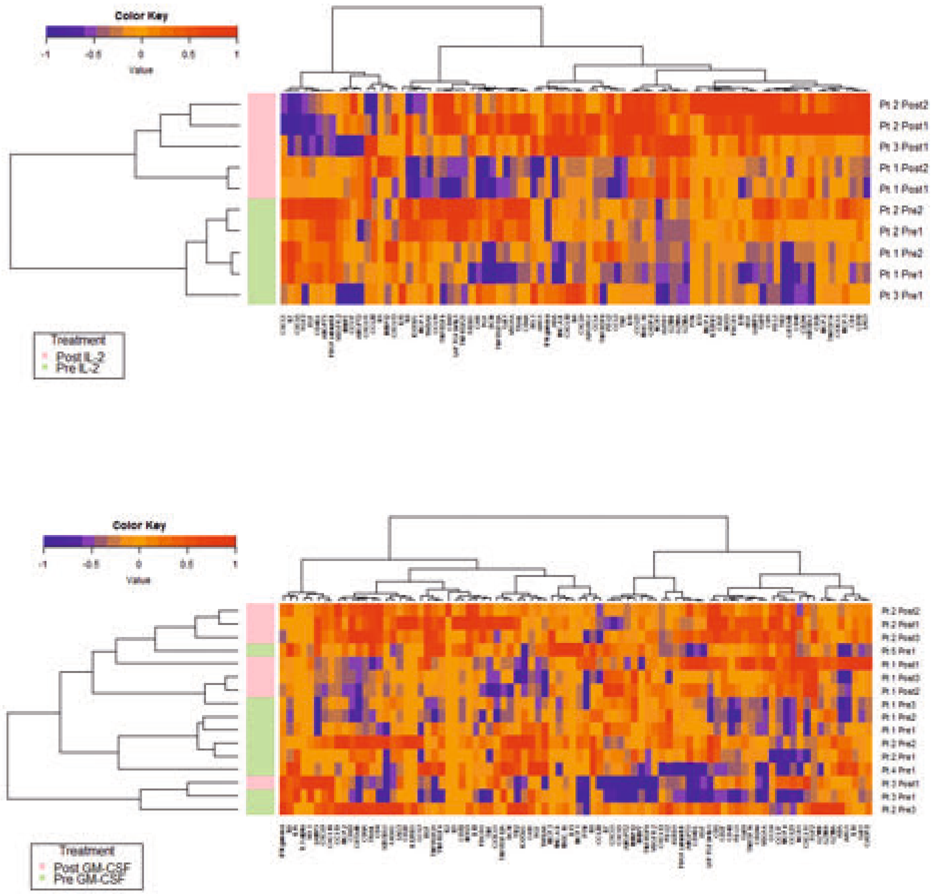

**Figure S4.** Clustering of immune-oncology related plasma protein concentrations of patients pre- and post-IL2 and GM-CSF containing immunotherapy cycles.

*Unsupervised clustering of 92 immuno-oncology related biomarkers. Top heatmap: Complete separation of protein profiles pre- and post IL-2 containing IT-cycles. From three patients, samples were paired before (day 1 IT-cycle 2 or 4) and after (day 15 IT-cycle 2 or 4) IL-2 containing IT. In total, 5 paired samples are shown, as two patients were monitored during both IT-cycles. Bottom heatmap: Partial separation of protein profiles pre- and post GM-CSF containing IT-cycles. From three patients, samples were paired before (day 1 IT-cycle 1,3 or 5) and after (day 15 IT-cycle 1,3 or 5) GM-CSF containing IT. In total, 7 paired samples are shown, as two patients were monitored during all three IT-cycles. 2 single measurements from patients pre GM-CSF were included, resulting in a total of 9 patients pre- and 7 post GM-CSF. Protein profiles of patient 3 (GM-CSF cycle 1) cluster together, indicating the absence of major differences in protein profiles in this patient upon GM-CSF containing IT. In addition, Protein profiles of patient 5 (unpaired, pre-GM-CSF) did cluster together with protein profiles of other patients post-GM-CSF.*

# Part II

## Improving Neuroblastoma Immunogenicity via Pharmacological Upregulation of MHC-I

# Chapter 5

## MHC Class I Downregulation in Cancer: Underlying Mechanisms and Potential Targets for Cancer Immunotherapy

Annelisa M. Cornel[1,*], Iris L Mimpen[1,*], Stefan Nierkens[1,2]

[1] *Center for Translational Immunology, University Medical Center Utrecht, Utrecht University, The Netherlands*
[2] *Princess Máxima Center for Pediatric Oncology, Utrecht University, 3584 CS Utrecht, The Netherlands*

[*] *These authors contributed equally to this work.*

*Cancers (Basel) 2020 Jul 2; 12(7), 1760*

## ABSTRACT

In recent years, major advances have been made in cancer immunotherapy. This has led to significant improvement in prognosis of cancer patients, especially in the hematological setting. Nonetheless, translation of these successes to solid tumors was found difficult. One major mechanism through which solid tumors can avoid anti-tumor immunity is the downregulation of major histocompatibility complex class I (MHC-I), which causes reduced recognition by- and cytotoxicity of CD8+ T-cells. Downregulation of MHC-I has been described in 40–90% of human tumors, often correlating with worse prognosis. Epigenetic and (post-)transcriptional dysregulations relevant in the stabilization of NFκB, Interferon Regulatory Factors (IRFs), and NLRC5 are often responsible for MHC-I downregulation in cancer. The intrinsic reversible nature of these dysregulations provides an opportunity to restore MHC-I expression and facilitate adaptive anti-tumor immunity. In this review, we provide an overview of the mechanisms underlying reversible MHC-I downregulation and describe potential strategies to counteract this reduction in MHC-I antigen presentation in cancer.

## 1. INTRODUCTION

In recent years, major advances have been made in cancer immunotherapy, thereby drastically improving the prognosis of cancer patients. Several types of Food and Drug Administration (FDA)-approved immunotherapies, such as checkpoint inhibitors (CPI), chimeric antigen receptor (CAR) T-cells, and dendritic cell vaccines, aim to boost T-cell-mediated cytotoxicity to combat cancer. These treatments led to increased survival chances, particularly for patients suffering from hematological cancers, but translation to the solid tumor setting was found difficult. Additional immune escape mechanisms, including immune checkpoint expression, induction of immunosuppressive immune subsets (e.g., regulatory T-cells and myeloid-derived suppressor cells (MDSCs)), loss of immunogenic antigens, and decreased antigen presentation allow these tumors to evade anti-tumor immunity (reviewed by Sharma *et al.* [1]), posing serious challenges to overcome in order to improve therapy response.

One way in which tumors can avoid tumor-associated antigen presentation, and therewith T-cell-mediated cytotoxicity, is the downregulation of surface display of major histocompatibility complex (MHC) class I, a crucial factor in the initiation of an adaptive immune response. The importance of MHC-I downregulation in immune evasion is substantiated by the observed correlations between MHC-I expression on tumor cells and the amount of tumor infiltrating lymphocytes (TILs) in several cancers [2,3]. Furthermore, several groups have reported impaired MHC-I antigen processing and presentation as a predictor of (acquired) resistance to CPI therapy [4-8] and adoptive cell therapy [9-11].

Downregulation of MHC-I has been described in 40–90% of human tumors [9,12-20], often correlating with worse prognosis [18,21-29]. Both adult and pediatric tumors are able to reduce MHC-I surface display by the use of different regulatory mechanisms. Where adult tumors downregulate MHC-I expression in order to escape from the immune system, pediatric cancers, such as neuroblastoma, often arise from embryonic tissues that intrinsically lack immunological features, potentially explaining the low expression of MHC-I in these cancer types [30].

The intrinsic reversible nature of most MHC-I dysregulations provides an opportunity to restore MHC-I antigen presentation and facilitate adaptive anti-tumor immunity. This review aims to provide an overview of the mechanisms underlying reversible MHC-I downregulation and demonstrate potential therapeutic targets to induce MHC-I expression and improve T-cell-mediated cytotoxicity in cancer.

## 2. DYSREGULATION OF MHC-I EXPRESSION IN CANCER

T-cell receptors (TCRs) of CD8+ T-cells can only bind to their targets in the context of MHC-I, which is expressed on all nucleated cells. MHC-I presents endogenous antigens, a process important for reporting intracellular changes, for example caused by viral infections or malignant transformation, to the immune system in order to initiate a CD8+ T-cell response. The heterodimer MHC-I consists of a heavy chain, encoded by the human leukocyte antigen (HLA)-A, HLA-B, and HLA-C genes, and an invariant light chain called β2-microglobulin (β2M). The heterodimer requires stabilization by a peptide, which is loaded into the MHC-I peptide-binding groove by the antigen processing machinery (APM).

Antigen presentation in MHC-I context is a complex, multi-step process which can be dysregulated at many levels. MHC-I and β2M are synthesized in the endoplasmic reticulum (ER) and require stabilization by chaperone proteins (e.g., calreticulin, ERp57, and tapasin). Designated intracellular proteins are targeted for degradation by ubiquitination, after which they undergo proteasomal degradation into peptides. These peptides are subsequently translocated into the ER by the transporter associated with antigen processing (TAP) and bind to MHC-I directly or after further processing by ER aminopeptidases (ERAP1 and ERAP2). Interaction between tapasin and TAP allows translocation of peptides into the MHC-I binding groove, release of chaperone proteins, and stabilization of the MHC-I complex. Finally, the MHC-I-antigen complex travels via the Golgi apparatus to the cell surface, where antigen presentation to CD8+ T-cells can start. In cancer, one or several proteins in this complex pathway can be dysregulated, which may have major consequences on cell surface display of MHC-I (**Figure 1**).

Although downregulation of surface expression of MHC-I allows evasion from T-cell-mediated anti-tumor immunity, low MHC-I expression sensitizes cells to Natural Killer (NK) cell-mediated cytotoxicity. MHC-I functions as an inhibitory ligand for NK-cells by binding to inhibitory receptors, such as killer cell immunoglobulin-like receptors (KIRs), thereby dampening NK-cell activation. Accordingly, when MHC-I is downregulated, the inhibitory signals initiated by MHC-I are no longer present, leading to enhanced NK-cell activation and cytotoxicity [31]. Nonetheless, tumors have developed several mechanisms to escape NK-cell-mediated cytotoxicity. For example, tumors often produce factors, such as transforming growth factor β (TGF-β) and prostaglandin, that impair NK-cell function and block their infiltration into the tumor site [32]. Additionally, tumors may temporarily upregulate MHC-I expression in response to NK-cells, which allows them to avoid recognition by these cells [19,22,33]. As a result, tumors show plasticity in evading both NK- and T-cell-mediated cytotoxicity, thereby facilitating tumor immune escape. The importance of this plasticity is substantiated by the observation that colorectal cancer patients with reversible MHC-I downregulations have a worse prognosis compared to patients with irreversible MHC-I downregulations [22].

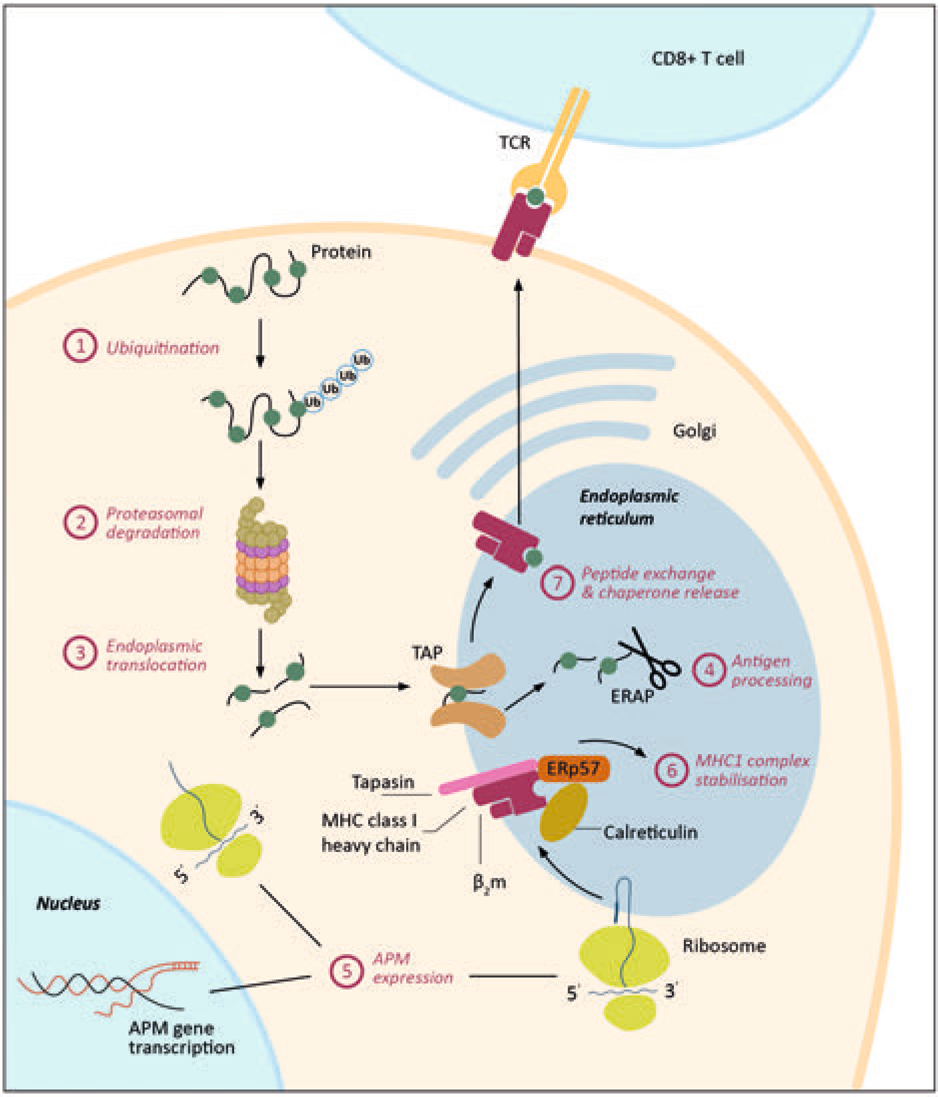
CD8+ T cell
TCR
Protein
① Ubiquitination
Ub
Ub
Ub
Ub
Golgi
② Proteasomal degradation
Endoplasmic reticulum
⑦ Peptide exchange & chaperone release
③ Endoplasmic translocation
TAP
ERAP
④ Antigen processing
ERp57
⑥ MHCI complex stabilisation
Tapasin
MHC class I heavy chain
Calreticulin
3'
5'
β2m
Nucleus
Ribosome
⑤ APM expression
5'
3'
APM gene transcription

**Figure 1.** Major histocompatibility complex class I (MHC-I) antigen processing and presentation is a complex, multi-step process and can be dysregulated in cancer at multiple levels.
*APM = antigen processing machinery; ERAP = ER aminopeptidases; MHC-I = major histocompatibility complex I; TCR = T-cell receptor*

Dysregulated cell surface display of MHC-I complexes may be caused by genetic, epigenetic, transcriptional, and post-transcriptional alterations, which leads either to irreversible or reversible changes in MHC-I expression. Irreversible MHC-I defects are described in multiple types of cancer, including melanoma, head and neck squamous cell carcinoma (HNSCC), and lung, colorectal, bladder, laryngeal, and breast cancer [9,12-17] and arise due to structural genetic alterations, for example, in the class I heavy chain genes [12-14], β2M [9,15,16], and the TAP-encoding genes [17]. As MHC-I expression cannot be upregulated in tumors harboring this type of mutations, these irreversible defects will not be the main focus of this review. Reversible MHC-I dysregulations are characterized by the coordinated (post-)transcriptional downregulation of the HLA class I heavy chain, components of the APM, or β2M and have been observed in several types of tumors, including HNSCC, bladder cancer, and neuroblastoma [18-20]. The reversible nature of these pathway dysregulations makes them interesting targets in cancer immunotherapy.

## 3. MHC-I EXPRESSION REGULATION

Three major transcription binding sites responsible for MHC-I heavy chain expression can be distinguished: an Enhancer A region, which can be recognized by NFκB; an interferon-stimulated response element (ISRE), which can be bound by interferon regulatory factor (IRF) 1; an SXY-module, which is recognized by NOD-like receptor family CARD domain containing 5 (NLRC5) [34]. Other APM genes are induced by the same set of transcription factors, resulting in the observation that the downregulation of APM players often coincides [35]. Accordingly, different pathways can lead to transcriptional activation of the MHC-I heavy chain-encoding genes as well as other genes responsible for the APM. In addition, these pathways can also act synergistically, magnifying the effect on MHC-I expression. By studying how MHC-I expression is normally regulated, we may be able to better understand the underlying mechanisms of MHC-I downregulation in tumors and find potential targets for cancer immunotherapy in order to reverse this downregulation.

## 4. INDUCING MHC-I EXPRESSION IN CANCER VIA NFKB STABILIZATION

The NFκB family consists of many inducible transcription factors, including NFκB1 (p50), NFκB2 (p52), RelA, RelB, and c-REL. During homeostasis, these proteins are sequestered in inactive cytosolic complexes by interaction with inhibitor of kB (IkB) family members (e.g., IkBα and p105). Upon pathway activation, IkB proteins are degraded, causing the release of NFκB transcription factors, allowing them to migrate to the nucleus to affect expression of target genes. Two major NFκB-inducing pathways can be distinguished: the canonical and the non-canonical NFκB pathway (Figure 2A,B) [36]. An elaborate description of pathway players important in this review can be found in Box 1. Although NFκB is constitutively active in most cancers [37], some tumors are able to downregulate NFκB signaling, which has been shown to impair MHC-I expression [35]. NFκB expression was found to be associated with favorable response to CPI therapy in patients with melanoma, indicating the potential of upregulating its expression to increase anti-tumor immunity [4,38]. To date, several regulators of the NFκB pathways have been described, revealing potential targets to enforce upregulation of MHC-I expression in cancer.

**Box 1.** NFκB -mediated upregulation of MHC-I.

The canonical NFκB pathway can be activated by stimulation of several immune receptors, including the TNFα Receptor (TNFR), Toll-like receptors (TLR), and cytokines receptors, by their ligands (e.g., TNFα, IL-1, or LPS). Upon receptor stimulation, TRAF2/6 and receptor-interacting protein 1 (RIP-1) are recruited, after which TRAF2/6 polyubiquitinates itself and RIP-1. In addition, TGF-β-activated kinase 1 (TAK1) is ubiquitinated and activated. TAK1 in turn is able to phosphorylate and activate the IkB kinase (IKK) complex (consisting of IKKα, IKKβ, and NF-kappa-B essential modulator (NEMO) (also known as IKKγ)). IKK needs to be recruited to the stimulated receptor before it can become phosphorylated, which is triggered by NEMO-mediated interaction of IKK with polyubiquitinated RIP-1 [39]. Subsequently, IKK phosphorylates IkB proteins, thereby targeting it for ubiquitination and degradation. Consequently, RelA-p50 and c-REL-p50 are released from their inactivating complexes, which results in translocation to the nucleus. Here they can activate transcription of their target genes, including MHC-I heavy chain- and other APM-encoding genes, by binding to kB enhancers in their promotors. A schematic overview of the canonical NFκB pathway can be found in Figure 2A [36].

Activation of the non-canonical NFκB pathway is initiated by the binding of a ligand (e.g., TNFα, CD40L, or B-cell activating factor (BAFF)) to one of the TNFR superfamily members. NFκB-inducing kinase (NIK) becomes activated, which in turn is able to phosphorylate and activate IKKα, one of the subunits of the IKK complex. IKKα subsequently phosphorylates the carboxy-terminal serine residues of p100, which is an IkB-like molecule that sequesters the NFκB transcription factor RelB in the cytosol, resulting in ubiquitination and degradation of the C-terminus of p100. As a result, p52 is generated, which forms a heterodimer with RelB, thereby allowing migration to the nucleus, resulting in induction of transcription of target genes. A schematic overview of the non-canonical NFκB pathway can be found in Figure 2B [36].

## 4.1. Positive Regulators of NFκB Expression

TNFα forcefully stimulates NFκB signaling and subsequent MHC-I expression. However, its use in cancer therapy is limited due to severe toxicities [40]. Alternatively, retinoids have been described to induce MHC-I upregulation in cancer, which is suggested to be the result of stimulation of NFκB signaling, even though the exact mechanism is still under debate. Studies in neuroblastoma and embryonic carcinoma cells revealed that retinoids increase MHC-I expression via increased expression of NFκB p50 and RelA [41,42]. In addition, Vertuani *et al.* [43] reported that upregulation of proteasome subunits (Latent Membrane Protein (LMP)-2, -7, and -10) and increased half-life of MHC-I complexes are responsible for increased MHC-I expression in neuroblastoma cell lines. Retinoids are currently being used to treat several types of cancer, including neuroblastoma and promyelocytic leukemia, and are known to induce differentiation, apoptosis, and inhibition of proliferation of tumor cells [44].

Other compounds reported to positively affect NFκB signaling of which to date the effect on MHC-I expression has not been assessed, are betulinic acid, and calcium/calcineurin combined with protein kinase C (PKC) antagonists. Betulinic acid upregulates canonical pathway activity via boosting the activity of IKK as well as phosphorylation and degradation of IkBα in multiple cancer cell lines, including neuroblastoma, glioblastoma,

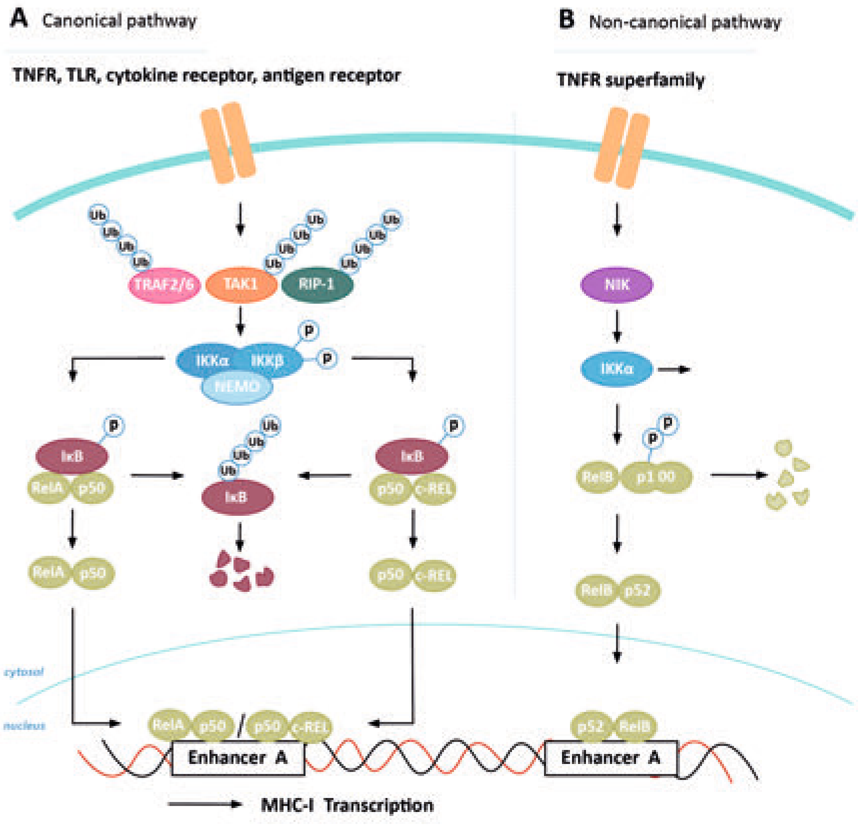
A Canonical pathway
TNFR, TLR, cytokine receptor, antigen receptor
B Non-canonical pathway
TNFR superfamily
Ub
TRAF2/6
TAK1
RIP-1
IKKα
IKKβ
NEMO
P
IκB
RelA
p50
c-REL
NIK
IKKα
RelB
p1 00
p52
cytosol
nucleus
Enhancer A
Enhancer A
MHC-I Transcription

**Figure 2.** NFκB-induced expression of MHC-I.

*Transcriptional activation of MHC-I heavy chain, but also other genes encoding for antigen processing machinery (APM) proteins, can be initiated by both the canonical **(A)** and non-canonical **(B)** NFκB pathway. IkB = inhibitors of kB; IKK = IkB kinase; NEMO = NF-kappa-B essential modulator; NIK = NFκB-inducing kinase; RIP-1 = receptor-interacting protein 1; TAK1 = TGF-β-activated kinase 1; TLR = toll-like receptor; TNFR = TNFα receptor; TRAF = TNF receptor-associated factor.*

and melanoma [45]. In addition, it induces apoptosis, inhibits topoisomerase I activity, and suppresses angiogenesis in cancer [46,47,48,49,50]. Secondly, a study into latent HIV infections in CD4+ T-cells revealed that combining calcium/calcineurin and the protein kinase C (PKC) antagonist prostatin causes synergistic activation of NFκB through a similar mechanism as betulinic acid [51]. A third strategy would be to increase expression of the E3 ubiquitin ligase Nedd4 [52], which triggers polyubiquitination and proteasomal degradation of N4BP1 [53], a suppressor of NFκB. In addition, in B-cells, Nedd4 has been reported to induce ubiquitination and degradation of TNF receptor-associated factor (TRAF) 3 via the TNFR CD40, thereby inducing activation of both the canonical and non-canonical NFκB pathway [52]. However, to date, no Nedd4 stimulatory compounds have been described.

Nonetheless, dysregulation of factors affecting downstream signaling of NFκB-inducing pathways makes it questionable whether NFκB activity, and thus MHC-I expression, can be restored by upstream pathway activation. As a result, therapeutic intervention to inhibit negative regulators of NFκB may be a more effective strategy to explore.

### 4.2. Negative Regulators of NFκB Expression

The pediatric tumor neuroblastoma is well known for its low MHC-I expression. We have previously identified two major negative regulators of MHC-I via NFκB signaling in neuroblastoma: Nedd4 Binding Protein 1 (N4BP1) and TNFα-induced protein 3 interacting protein 1 (TNIP1) [54]. TNIP1 affects canonical NFκB activation, whereas N4BP1 exerts an effect on both canonical and non-canonical pathway activation.

N4BP1 interacts with several proteins involved in (de)ubiquitination, including NEDD4, Cezanne-1, A20, and Itch [53,54] and potentially also binds to polyubiquitin itself [55,56]. Polyubiquitin binding proteins, like N4BP1, can compete with NEMO for polyubiquitin binding, thereby directly antagonizing activation of canonical NFκB [56]. Besides this, N4BP1 interacts with the deubiquitinase (DUB) Cezanne-1, which functions in the deubiquitination and stabilization of TRAF3 [54] and subsequently modulates the activation of both the canonical [54] and non-canonical NFκB [57] by affecting the degradation of NIK and IkB, and the induction of c-REL ubiquitination and proteasome-mediated degradation [58].

TNIP1 (also known as A20-binding inhibitor of NF-kB (ABIN)-1) is known for its stimulatory effect on the NFκB inhibiting DUB A20 and inhibition of TNF-induced apoptosis and is upregulated in several types of cancer [59]. Similar to N4BP1, TNIP1 inhibits NFκB by impairing NEMO-mediated translocation of IKK to the receptor site. The exact mechanism remains unclear, but it is suggested to be via competing with NEMO binding to RIP-1 as well as via binding to a polyubiquitin group on NEMO itself [60]. TNIP1 is also able to prevent processing the IkB p105 into p50 [61] and to interact with the NFκB inhibiting DUB A20, stimulating deubiquitination of NEMO, thereby impairing IKK activation and thus canonical NFκB activation [62]. IL-17 treatment has been shown to induce proteasome-dependent downregulation of TNIP1 [63]. This resulted in NFκB activation, thereby suggesting its potential to upregulate MHC-I expression. However, IL-17 has been shown to play a key role in the promotion of tumor progression by inducing chronic inflammation, tumor cell proliferation, angiogenesis, and metastasis, which may majorly limit the use of this cytokine to induce MHC-I expression in cancer [64].

Hence, targeting N4BP1 or TNIP1 will result in strong activation of NFκB signaling, which in turn boosts MHC-I expression. Indeed microRNA (miR) 28-5p is an inhibitor of N4BP1 and has been demonstrated to act as a tumor suppressor in many cancer types, including colorectal cancer, renal cell carcinoma, and hepatocellular carcinoma [65-67]. In addition, MiR-1180 and miR-486 have also been demonstrated to induce NFκB activation via targeting of several inhibiting players of the NFκB pathway, including Cezanne, A20, and TNIP1-3 [68,69]. Nevertheless, it should be taken into account that these miRs have also been associated with cancer cell growth, survival, migration, and progression, emphasizing the need to further investigate the effect of these miRs in cancer [70,71].

The NFκB inhibiting DUB A20 is also involved in TNIP-independent regulation of NFκB signaling [72]. A20 can form a ubiquitin-editing complex together with the ubiquitin binding protein TAX1 Binding Protein 1 (TAX1BP1) and the E3 ubiquitin-protein ligase Itch. This complex can deubiquitinate RIP-1 and TRAF6, thereby inhibiting TAK1 activation as well as NEMO-mediated recruitment and activation of IKK. In addition, A20 can induce K48-polyubiquitination of RIP-1, thereby targeting it for proteasomal degradation [73]. TAX1BP1 is responsible for Itch recruitment to A20, whereas Itch controls the interaction between A20 and its substrates RIP-1 and TRAF6, enabling inactivation of these substrates. Knockout of either of these proteins results in inadequate NFκB inhibition, indicating that all three proteins are indispensable in the functioning of this ubiquitin-editing complex [74]. Itch has been shown to be upregulated in several types of cancer, such as breast cancer and neuroblastoma, in which it was shown to play a major role in cancer progression [75-79]. The antidepressant clomipramine, its structural homologue norclomipramine, and 1,4-naphthoquinone 10E have been shown to reduce tumor growth and enhance chemotherapy in multiple cancer cell lines, including breast, prostate, and bladder cancer lines, as well as in a multiple myeloma xenograft model [80,81]. In addition, clomipramine has been shown to induce MHC-I expression in a rat model of experimental allergic neuritis [82]. Controversially, N4BP1 has also been described to negatively regulate Itch by blocking the binding of Itch to its substrates [53]. However, as both N4BP1 and Itch play an important role in suppressing NFκB signaling, the potential for therapeutic inhibition of Itch remains elusive.

Another DUB enzyme, cylindromatosis (CYLD) plays a role in the inhibition of NFκB signaling through the removal of polyubiquitin motifs from NEMO and another important upstream protein in the NFκB signaling pathway called TRAF2 [83]. Several miRs have been reported to target CYLD, including miR-1288, -196, and -372-5p [84-86]. Recently, as reviewed by Farshi and colleagues, several DUB inhibitors have been developed for the treatment of cancer, all targeting different DUB enzymes that play distinct roles in the promotion of cancer [87]. To date, no specific DUB inhibitors have been described to specifically target Cezanne-1, A20, or CYLD. Nonetheless, aspecific DUB small molecule inhibitors, such as ubiquitin aldehyde (Ubal) have been described, which may suppress the activity of these NFκB targeting DUBs [87]. However, the use of aspecific inhibitors is limited due to the severe toxicity and simultaneous targeting of beneficial DUBs. Therefore, additional research should be conducted to develop specific DUB inhibitors. A patent (WO2017109488) describes cyanopyrrolidine derivates as specific inhibitors of Cezanne-1. In addition, as Cezanne-1 and A20 show sequence homology, it might potentially be possible to find cross-reactive DUB inhibitors to boost NFκB activity. However, in line with the above described miRs, Cezanne-1, A20, and CYLD are described in tumor suppressive as well as tumor progressive processes, which may be a counterindication for the use of inhibitors of these proteins in cancer [88,89].

Altogether, these studies show that there are multiple proteins that play a role in suppressing NFκB signaling, which may subsequently lead to hampered MHC-I expression. Several therapeutic interventions have been described, which could potentially trigger NFκB expression in cancer. A major contradiction we should be aware of is that the NFκB pathway is constitutionally active in a variety of tumors, playing an important role in many tumor-promoting processes, including inflammation, invasion, proliferation, angiogenesis, and metastasis [37]. This is further substantiated by the dual effect of most described proteins [53], miRs [68-71], and therapeutic interventions [53,64,75-78,88,89] affecting NFκB pathway induction on tumor-suppressing and tumor-promoting processes. It has been hypothesized that NF-kB inhibits tumor growth in cancers with a low mutational burden (early stages of cancer and potentially pediatric tumors), but that accumulation of mutations may lead to a loss of tumor suppressive function and the oncogenic features of NF-kB can become more dominant [90]. Therefore, we should carefully study the effects of NFκB pathway induction in NFκB-downregulated tumors as this could shift the balance from immune evasion towards tumor progression, thereby potentially even hampering the efficacy of cancer immunotherapy.

## 5. INDUCING MHC-I EXPRESSION IN CANCER VIA RESTORED IFN SIGNALING

In addition to NFκB, Interferons (IFNs) play a significant role in the induction of MHC-I expression. During homeostasis, the signal transducer and activator of transcription (STAT) proteins are present in the cytosol in their inactive form. Upon pathway activation, STATs become phosphorylated and dimerize, allowing them to migrate to the nucleus to affect expression of target genes. Both type I and type II interferon pathways are able to induce dimerization of STATs, thereby upregulating MHC-I expression using different signaling pathways (**Figure 3A,B**). An elaborate description of pathway players important in this review can be found in Box 2. IFNs play an important role in the regulation of antigen processing and presentation and are described to exert pro- and anti-tumorigenic effects in various types of cancer as extensively reviewed by Musella *et al.* and Castro *et al.* [91,92]. Downregulation of both type I and II IFN-mediated pathways have been described as mechanisms involved in resistance to CPI- and adoptive cell therapy in melanoma and lung cancer, indicating the potential of interference in these pathways to increase anti-tumor immunity [4,5,6,10,93-96]. Several factors affecting IFN pathway expression have been described, revealing potential targets to modulate MHC-I expression in cancer.

**Box 2.** Interferon-mediated upregulation of MHC-I.

The type II IFN pathway can be activated by stimulation of the IFNG receptor (consisting of IFNGR1 and IFNGR2) by IFNγ, allowing binding, phosphorylation, and activation of Janus Activated Kinase (JAK) 1 and JAK2. The intracellular domain of IFNGR1 is phosphorylated, creating a docking site for signal transducer and activator of transcription (STAT)1, which is phosphorylated by JAK1/2, forms homodimers, and translocates to the nucleus to activate target gene expression via binding to gamma-activated site (GAS) elements in the promotor regions of IFN-stimulated genes (ISG). One of the genes induced by STAT1 signaling is the transcription factor IRF1, which in turn is able to bind to the ISRE site present in the MHC-I promoter [34]. A schematic overview of the type II IFN pathway can be found in Figure 3A [97].

Activation of the type I IFN pathway is initiated by binding of type I IFNs (e.g., IFNα and IFNβ) to the IFNA receptor (consisting of IFNAR1 and IFNAR2), allowing binding, phosphorylation, and activation of JAK1 and tyrosine kinase 2 (TYK2). The cytoplasmic tail of IFNAR is phosphorylated, creating a docking site for STAT1-3, which are again phosphorylated by JAK1 to form homo and heterodimers. STAT1 homodimers can activate IRF1 expression as described for the type II IFN pathway. Additionally, STAT1/STAT2 forms a complex with IRF9 (called IFN-stimulated gene factor 3 (ISGF3), which is able to bind to the ISRE element in the MHC-I promotor. STAT3 homodimerization also occurs, however, this does not lead to MHC-I upregulation, but rather functions as a negative feedback loop to inhibit expression of pro-inflammatory genes. A schematic overview of the type I IFN pathway can be found in Figure 3B [98].

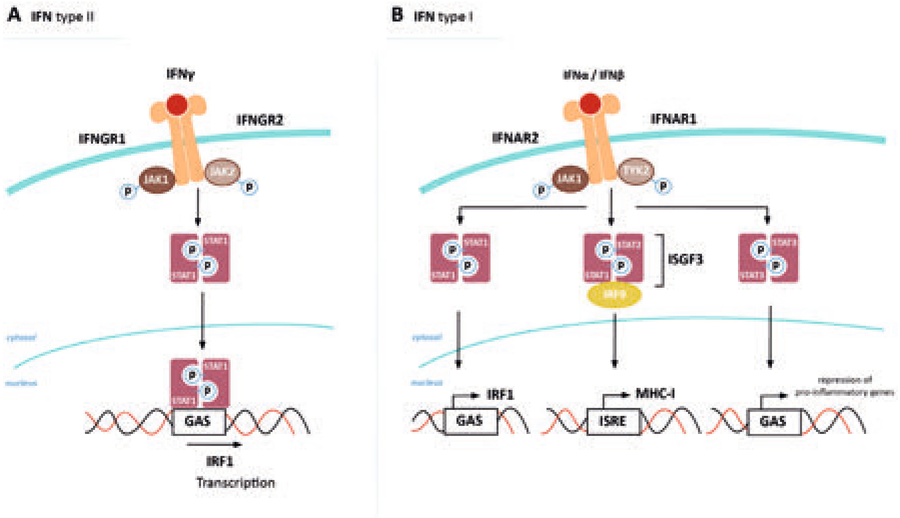
A IFN type II
IFNγ
IFNGR1
IFNGR2
JAK1
JAK2
P
STAT1
cytosol
nucleus
GAS
IRF1
Transcription
B IFN type I
IFNα / IFNβ
IFNAR2
IFNAR1
JAK1
TYK2
STAT1
STAT2
STAT3
ISGF3
IRF9
IRF1
MHC-I
repression of pro-inflammatory genes
GAS
ISRE
GAS

**Figure 3.** Interferon (IFN)-induced expression of MHC-I.
*Transcriptional activation of MHC-I heavy chain, but also other genes encoding for antigen processing machinery (APM) proteins, can be initiated by both the type II (A) and I (B) IFN pathway. GAS = gamma-activated site; IFNAR = IFNα receptor; IFNGR = IFNγ receptor; ISGF3 = IFN-stimulated gene factor 3; IRF = interferon regulatory factor; ISRE = interferon-stimulated response element; JAK = Janus Activated Kinase; STAT = signal transducer and activator of transcription; TYK2 = tyrosine kinase 2.*

## 5.1. Positive Regulators of IFN Signalling

IFN signaling can be induced via treatment with IFN-inducing ligands, such as IFNα, IFNβ, and IFNγ. In addition, stimulation of several PRRs may result in downstream type I IFN production, thereby indirectly promoting MHC-I expression. IFNγ has been suggested to have the most potent effect on the expression levels of APM genes, including MHC-I, TAP, and ERAP, which may imply its beneficial effect in cancer immunotherapy [35,99,100]. However, in line with NFκB-inducing ligands, IFNs and PRR stimulation initiates a broad range of biological activities, thereby limiting its use in cancer therapy due to severe toxicities [101]. To avoid toxicities, targeted delivery of IFNγ to the tumor site may be of interest, for example by fusing it to an antibody specific for a tumor-associated antigen [102].

Another targeted approach would be a cellular NK-cell therapy strategy, as NK-cells are capable of either killing or upregulating MHC-I expression on MHC-I-lacking cells (via IFNγ secretion) [19,33,103]. The potential of NK-cell therapy is substantiated by observed correlations between the abundance of functional NK-cells and checkpoint inhibition efficacy in non-small cell lung cancer (NSCLC) [104,105]. However, several challenges remain, including anti-inflammatory responses within the tumor microenvironment (TME), which cause impaired NK-cell function and TME infiltration

[19,33,106,107], as well as ex vivo expansion to generate sufficient NK-cell numbers, and *in vivo* persistence [108]. The suggested ability of tumors to both evade NK- and T-cell mediated cytotoxicity via plasticity in MHC-I expression is one of the anti-inflammatory mechanisms potentially decreasing efficacy of NK-cell therapy. Interestingly, several studies have observed a beneficial outcome for individuals with an inhibitory KIR genotype with lacking HLA-ligands (the ‘missing ligand’ genotype) undergoing cancer immunotherapy, as inhibitory KIRs without matching HLA-ligands cannot inhibit NK-cell cytotoxicity [109,110]. This led to the rationale of allogeneic, KIR genotype-mismatched NK-cell therapy strategies to optimize NK-cell cytotoxicity by decreasing HLA-dependent inhibition of NK-cells [111]. Besides this, it should be considered that the immune checkpoint programmed cell death-ligand 1 (PD-L1) is also shown to be upregulated by IFNγ [112,113]. As a result, IFNγ simultaneously induces MHC-I upregulation and T-cell suppression, thereby potentially creating a vicious circle of T-cell activation and inhibition.

### 5.2. Negative Regulators of IFN Signaling

The embryonic transcription factor double homeobox 4 (DUX4) has been shown to be upregulated in many cancer types, in which it causes downregulation of JAK1/2 and STAT1, thereby suppressing IFN target gene transcription, including MHC-I and other APM genes [114]. In line with this, DUX4 has been demonstrated to be significantly upregulated in non-responders to CPI, indicating that the DUX4-induced reduction in MHC-I expression results in decreased T-cell cytotoxicity in patients [114]. The exact mechanism in which DUX4 downregulates JAK1/2 and STAT1 remains to be elucidated. As DUX4 is studied in more detail in a disease called facioscapulohumeral dystrophy (FSHD), knowledge on treatment strategies could be gained from this disease. Bosnakovski *et al.* [115] reported that inhibition of p300, a histone acetyltransferase recruited by DUX4 to affect target gene expression, by a specific inhibitor, counteracted the effect DUX-4 overexpression *in vitro* and *in vivo*. Others reported before that p300 inhibition in multiple types of cancer led to suppressed proliferation [116]. However, whether p300 inhibition also restores IFN signaling remains to be elucidated. DUX4 downregulation was also observed when treated with p38 inhibitors *in vitro* and *in vivo* in FSHD models [117]. P38 inhibition has a favorable effect in cancer treatment, however, the wide variety of processes in which p38 is involved, including tumor suppressive processes, is a clear disadvantage of this inhibitor [118].

Lymphocyte adapter protein (LNK) has been reported to be able to negatively regulate IFN signaling via the induction of dephosphorylation of STAT1 [119,120]. LNK has been shown to be overexpressed in several solid tumors, including melanoma and ovarian cancer, and was found to be significantly increased in patients who did not respond to

CPI therapy [120]. LNK has been reported to be targeted by miR-29b, miR-30-5p, miR-98, miR-181a-5p [121,122]. To date, no other therapeutic LNK inhibitors have been reported.

The peptidyl-prolyl isomerase Pin1 has been reported to induce ubiquitination and degradation of the type I IFN inducing transcription factor IRF3, which normally triggers a positive feedback loop upon type I IFN pathway stimulation [123]. Pin1 has been demonstrated to be elevated in multiple types of cancer, playing a role in stimulating several cancer-driving processes [124]. As Pin1 is involved in downregulating type I IFN signaling, its suppression may lead to enhanced MHC-I expression, thereby advancing T-cell-mediated cytotoxicity. Presently, several Pin1 inhibitors have been developed, such as miR-200b, miR-200c, and miR296-5p, the small molecules all-trans retinoic acid (ATRA) and KPT-6566, and the natural compound Juglone, which all showed anti-cancer activity in different types of cancer [125-130].

Several protein tyrosine phosphatases (PTPs) have been described to downregulate tyrosine phosphorylation in the JAK/STAT pathway, thereby interfering with induction of both type I and II IFN signaling. For example, PTPN1 dephosphorylates TYK2 and JAK2 [131], PTPN2 dephosphorylates JAK1, and PTPN11 (SHP2) has been demonstrated to inhibit phosphorylation of JAK1, STAT1, and STAT2 [132]. Tyrosine phosphatases have been shown to be elevated in multiple types of cancer, including breast, ovarian, gastric cancer, and glioma, in which they promote tumor growth, survival, and metastases [133]. To date, several efforts have been attempted in the development of tyrosine phosphatase inhibitors, including the PTPN11 inhibitor sodium stibogluconate, and the PTP1B inhibitor MSI-1436C, which are now being tested in clinical trials for various cancer types [133-135]. In addition, miR-155 has been reported to target several negative regulators of IFN signaling, including PTPN2, which has been shown to result in increased IFNγ production by T-cells within the TME, thereby promoting MHC-I expression [136]. In contrast, miRNA-155 has been demonstrated to be overexpressed in multiple types of cancer, playing a pivotal role in oncogenesis, which may limit its use in cancer [137].

The ubiquitin ligases RING finger protein 2 (RNF2) and Smad ubiquitination regulatory factor-1 (Smurf1) and the protein inhibitor of activated STAT (PIAS) all function via inhibiting transcription activation of STAT1 [138-140]. These proteins have been shown to be overexpressed in several types of cancer, including melanoma, gastrointestinal tumors, lymphoma, and pancreatic cancer, thereby playing an active role in cancer promotion [141-146]. Likewise, the ubiquitin ligase DCST1 is able to induce ubiquitination and degradation of STAT2, which results in hampered type I IFN signaling and has also been shown to be elevated in various cancers [147]. The small molecule inhibitors PRT4165 and A01 successfully inhibit, respectively, RNF2 and Smurf1 *in vitro* [148,149].

In addition, indirect inhibition of RNF2 was reported via inhibition of MEK-induced activation by the MEK-inhibitor trametinib [143]. To date, no DCST1 inhibitors have been described.

Finally, the protein kinase D2 (PKD2) has been shown to dampen type I IFN signaling via stimulating ubiquitination and endocytosis of IFNAR1, thereby causing rapid turnover of the type I IFN receptor [150]. PKD2 has been associated with multiple types of cancer, functioning by promoting tumor progression and blocking type I IFN signaling [151]. To date, several inhibitors of PKD2 have been developed, for example the small molecule inhibitor CRT0066101 and the pyrazolopyrimidine pan-PKD inhibitor SD-208, which both show anti-tumor activity in xenograft mouse models of various cancers [152,153].

Taken together, several proteins have been implicated in impaired IFN signaling in cancer. Accordingly, therapeutic intervention of these dysregulations may be beneficial when combined with immunotherapy to increase MHC-I expression and enhance T-cell-mediated cytotoxicity. However, many of these proteins have not been associated with MHC-I downregulation before, highlighting the need to investigate their effect on MHC-I expression. In addition, as stated for NFκB, IFNs are also reported to exert both pro- and anti-tumorigenic effects in various types of cancer [91,92], indicating the need to closely study these effects.

## 6. NLRC5-MEDIATED UPREGULATION OF MHC-I

Only recently, NLRC5 was discovered as a third key regulator of MHC-I transcription [154]. NLRC5 is expressed in response to IFN-mediated signaling, in particular via IFNγ, by binding of a STAT1 homodimer to GAS in the NLRC5 promoter [154,155]. Interestingly, this STAT1 binding site in the NLRC5 promoter was shown to partially overlap with an NFκB binding site, suggesting that NLRC5 expression may be induced by NFκB as well [156]. Moreover, it has been suggested that the NLRC5 promoter contains an ISRE site, which may allow transcriptional activation by IRF1. Upon its expression, NLRC5 migrates to the nucleus, where it assembles with several proteins, including RFX, ATF1/CREB, and the NFY complex, resulting in the formation of the MHC enhanceosome. This complex is able to bind the SXY module in the MHC-I promoter, causing the induction of MHC-I expression. Additionally, NLRC5 is able to recruit transcriptional initiation and elongation factors, and histon-modifying enzymes, for example histon acetyltransferases and methyltransferases, which may further enhance transcriptional activation of MHC-I [82,157]. (Epigenetic) downregulation of NLRC5 expression has been observed as a mechanism of immune evasion in several types of cancer, including colorectal, ovarian, breast and uterine cancers [158,159]. NLRC5 has been reported to elicit anti-tumor immunity by enhancing antigen processing and presentation in melanoma [160]. In addition, NLRC5 expression correlates with response to CPI in melanoma (US20170321285A1). Controversially, as also observed for NFκB- and IFN-mediated signaling pathways, NLRC5 has been reported to exert both pro- and anti-tumorigenic effects in various types of cancer (reviewed by Tang *et al.* [161]), indicating the need of careful evaluation of upregulation of NLRC5 in cancer. To date, no specific NLRC5 targeting compounds have been described. Nonetheless, as NLRC5 activation pathways largely overlap with the above described pathways, compounds inducing these pathways may also result in NLRC5 activation.

## 7. INDUCING MHC-I EXPRESSION IN CANCER VIA STAT3 INHIBITION

As briefly touched upon in the section above, STAT3 becomes activated upon type I IFN signaling to function as a negative feedback loop to inhibit expression of pro-inflammatory genes, thereby contributing to balanced immune responses [98]. STAT3 is implicated in dampening a variety of immune responses, including inhibition of both NFκB- and IFN-mediated pathways. STAT3 is able to inhibit activation of the IKK-complex, thereby preventing phosphorylation and degradation of IkB, which results in sequestering of NFκB transcription factors in the cytosol.

STAT3 has been shown to play a key role in the promotion of cancer by mediating proliferation, survival, invasion, and metastasis [162]. STAT3 inhibition resulted in increased anti-tumor activity and superior responses to immunotherapy and immunogenic chemotherapy in several pre-clinical studies and trials [163-172]. Combinations of CPI and STAT3 inhibitors are currently tested in clinical trials [173]. STAT3 can be inhibited via upstream JAK inhibition as well as by direct inhibition of STAT3. Several specific STAT3 inhibitors have been described, including JSI-124 (cucurbitacin I) [163], static [166], indirubin [164], resveratrol [165], and the antibiotic nifuroxazide [170]. In addition, the multitarget tyrosine kinase inhibitors sorafenib and sunitinib are also reported to specifically target STAT3 phosphorylation and activation [167,168].

As STAT3 overexpression inhibits both NFκB- and IFN-signaling pathways, specific inhibition of STAT3 may be an interesting strategy to target downregulation of these pathways and potentially induce MHC-I upregulation. However, as is the case for other NFκB- and IFN-signaling pathway inhibitors, these pathway inhibitors also exhibit favorable effects, as for example indicated by the fact that STAT3 also elicits tumor-suppressive functions [174].

## 8. INDUCING MHC-I EXPRESSION IN CANCER VIA STING INDUCTION

Stimulator of Interferon Genes (STING) is a DNA-sensing molecule which activates upon encountering foreign DNA by cyclic dinucleotide recognition [175]. Upon cyclic dinucleotide recognition, STING becomes activated and forms a complex with TANK-binding kinase 1 (TBK1), which in turn is able to phosphorylate and activate both RelA and IRF3, thereby stimulating both NFκB- and type I IFN-activation [176]. To date, several STING agonists have been developed to exploit this response in cancer. One example is the STING agonist SB 11285, which is currently tested in clinical trials in several solid tumors, including HNSCC and melanoma (ClinicalTrials.gov Identifier: NCT04096638), and previously showed strong anti-tumor immunity induction in mouse models [177].

As STING induced both NFκB- and IFN-pathway activation, agonizing its activity may be an interesting strategy to upregulate these pathways to potentially induce MHC-I upregulation. This is further substantiated by the correlation between STING expression and HLA-associated genes in neuroblastoma [178]. In addition, preclinical studies have reported superior effects of CPI therapy in combination with STING agonists [179,180]. Combining CPI with STING agonists is currently being tested in clinical trials [181]. The multi-facet involvement of STING in immune activation, however, underlines the need to study its effect to improve therapy outcomes while not compromising treatment safety.

## 9. WELL-KNOWN ONCOGENIC PATHWAYS AFFECT MHC-I EXPRESSION

Various oncogenic pathways have been reported to affect expression of MHC-I, β2M, and other APM components in cancer, including the MAPK-, epidermal growth factor receptor (EGFR), HER2, c-MYC, and n-MYC pathway [182-187]. MAPK pathway activation is suggested to negatively influence MHC-I expression via decreased IRF1 activity and STAT1 expression [188]. The MEK inhibitors trametinib and cobimetinib have been demonstrated to enhance IRF1 expression and increased STAT1 phosphorylation in human keratinocytes [188]. Watanabe *et al.* [189] reported that treatment of a NSCLC cell line with trametinib also increased MHC-I expression *in vitro*. Another MEK inhibitor, selumetinib, increased MHC-I expression in papillary thyroid cancer cell lines [2]. In addition, upstream inhibition of BRAF by vemurafenib and dabrafenib also induced MHC-I and β2M upregulation in multiple melanoma cell lines [190].

Overexpression of the EGFR family member HER2/neu was shown to be inversely correlated with MHC-I expression in different types of cancer, including breast cancer, esophageal squamous cell carcinoma, and melanoma [191,192]. Additionally, overexpression of EGFR was associated with less potent responses to cancer immunotherapy in NSCLC and neuroblastoma [193,194]. EGFR activates PTNP11, which was mentioned above as a STAT1 inactivator [195]. PTNP11 also inhibits RAS GTPase-activating protein, which normally functions in downregulating MAPK signaling, thereby also contributing to impaired IFN signaling via the MAPK pathway [196]. A third mechanism in which EGFR signaling impairs MHC-I expression is the promotion of STAT3 activation [197]. HER2 in turn also induces proteasomal degradation of the tumor suppressor Fhit, which normally upregulates expression of MHC-I, APM components, and β2M via an as-yet unclear mechanism [142]. Hence, targeting tyrosine kinase receptors, for example by the anti-EGFR antibodies nimotuzumab and cetuximab, and the EGFR inhibitors afatinib, erlotinib, and gefitinib, results in enhanced expression of MHC-I and APM components in different cancer cell lines as well as in cancer patients [185,198-202].

Finally, oncogenes c- and n-MYC have both been associated with MHC-I downregulation [186,187,203]. N-MYC has been shown to decrease MHC-I expression in rat neuroblastoma cell lines through the inhibition of the NFκB transcription factor p50 [203]. On the contrary, Forloni *et al*. [204] showed that that the downregulation of MHC-I in human neuroblastoma cells was not caused by n-MYC. In line with this, we did not identify n-MYC as a negative regulator of NFκB [54]. However, one limitation of our study was the use of an early phase CRISPR/Cas 9 library, which impairs the ability to fully confirm the results found in previous studies. Recently, Yang and colleagues showed that c-MYC expression induction by the Wnt/B-catenin pathway is responsible for MHC-I downregulation in glioma [187]. This again hints towards involvement of MYC-family members in MHC-I expression regulation in cancer.

Altogether, by targeting these oncogenic pathways, we potentially will not only be able to impair tumor growth and proliferation, but also exhibit anti-tumor responses via increasing the immunogenicity of the tumor.

## 10. CHEMOTHERAPY- AND RADIATION-INDUCED MHC-I EXPRESSION

Certain chemotherapeutic therapy regimens are known to induce anti-tumor immune responses without inducing classical immunogenic cell death (ICD). Hodge and colleagues showed that both docetaxel-induced ICD-sensitive and resistant tumor cells expressed increased levels of APM components, including TAP2, calnexin and calreticulin [205]. In addition, immunochemotherapy combining IFNα and 5-fluorouracil treatment resulted in increased MHC-I expression via STAT1/2 activation in murine pancreatic cancer models [206]. Besides this, several topoisomerase inhibitors (e.g., topotecan, irinotecan, and etoposide), microtubule stabilizers (e.g., paclitaxel and vinblastine), cisplatin, and ionizing radiation elevate MHC-I surface expression, which is thought to be induced via NFκB stabilization and IFNβ secretion [207-209]. These studies indicate that cytostatic drugs may, besides direct induction of cell death, also be involved in decreasing tumor immune escape via upregulation of antigen presentation, thereby making these drugs interesting candidates for combination therapy to improve immunotherapeutic strategies in cancer.

## 11. EPIGENETIC SILENCING AFFECTING MHC-I EXPRESSION

Another common reversible defect in MHC-I antigen presentation is the occurrence of epigenetic modulation, which may impair the transcription of MHC-I, APM components, β2M, or MHC-I regulatory proteins. Histon deacetylation (HDAC) has been reported to reduce expression of MHC-I and key components of the APM, such as the proteasome subunits LMP-2 and LMP-7, and TAP in multiple types of cancer, including neuroblastoma, glioma, Merkel cell carcinoma, cervical cancer, and melanoma [187,210-212]. HDAC inhibitors, of which several already are FDA approved (e.g., Romidepsin, Vorinostat and Panobinostat), show increased expression of MHC-I and APM components both *in vitro* and *in vivo* [187,210,211,213]. Multiple other HDAC inhibitors are currently tested in clinical trials either alone or in combination with other drugs in various types of cancer, including melanoma, breast cancer, and lung cancer [214].

Epigenetic modulation by DNA hypermethylation has also been reported to cause reduced expression of MHC-I and related genes, which may be reversed by treatment with DNA methyltransferase inhibitors (DNMTi). The DNMTis guadecitabine, 5-azacytidine, and decitabine increased MHC-I expression in breast cancer, melanoma, and neuroblastoma cell lines [54,215-217]. Interestingly, combinatory treatment with TNFα, IFNγ, or knockout of known inhibitors of NFκB signaling (TNIP and N4BP1) further exaggerated the effect of these epigenetic modulators [54,215,217]. Additionally, increased MHC-I expression was observed in breast cancer patients treated with a combination of DNMT and HDAC inhibitors [216], indicating the potential of epigenetic modification to reintroduce MHC-I expression in tumors.

## 12. DISCUSSION

MHC-I-mediated antigen presentation is crucial for CD8+ T-cell cytotoxicity and is one of the key factors in endogenous adaptive immune response development as well as T-cell mediated immunotherapy efficacy in cancer. The often intrinsically reversible nature of these dysregulations provides an opportunity to restore MHC-I expression and therewith adaptive anti-tumor immunity. In this review, we highlight that MHC-I-mediated antigen presentation is a complex, multi-faceted process, which can be dysregulated at many levels. As APM players are often induced by the same set of transcription factors, downregulation of APM players often coincides. To identify therapeutic targets to increase immunotherapy efficiency in cancer, a better understanding of the underlying mechanisms of MHC-I downregulation in tumors is required. A summary of regulators of MHC-I expression and potential therapeutic strategies described in this review can be found in **Table 1** and **Figure 4**.

Dysregulation of factors affecting the downstream signaling of MHC-I-inducing pathways makes it questionable whether pathway activity can be restored by upstream pathway activation. As a result, therapeutic intervention to inhibit negative regulators of these pathways, possibly combined with stimulation of positive regulators of these pathways, may be the most promising strategy to explore.

Downregulation of MHC-I is an important factor contributing to the immune evasion of tumors. However, as underlined by the observed resistance of solid tumors to CAR-therapy as well as by IFNγ-mediated upregulation of PD-L1 [112,113], immune evasion of tumors is a multifaced process. As a result, the authors hypothesize that combination therapy targeting several tumor-immunomodulatory processes simultaneously will be necessary to avoid immune evasion of tumors. Several combinations of immunomodulatory drugs, including combining CPI with STAT3 inhibitors or STING agonists, show promising results in (pre-)clinical studies [171-173,179-181].

An important contradiction in enhancing NFκB-, IFN-, and NLRC5-mediated MHC-I expression is the dual role of these pathways in cancer [37,91,92,161]. They have been described in both tumor-promoting as well as tumor-suppressive mechanisms in several types of cancer. The authors hypothesize that, depending on the activation status of these pathways, its function will either be to promote or suppress tumor progression. Hence, it is important to study the effect of (pharmacological) enhancement of these pathways in MHC-I lacking tumors, as overactivation might shift the balance from immune evasion towards tumor progression. However, the observation that several NFκB/IFN upregulatory drugs do show beneficial effects in the treatment of several types of cancer highlights the potential of these drugs in improving immunotherapy outcomes in cancer.

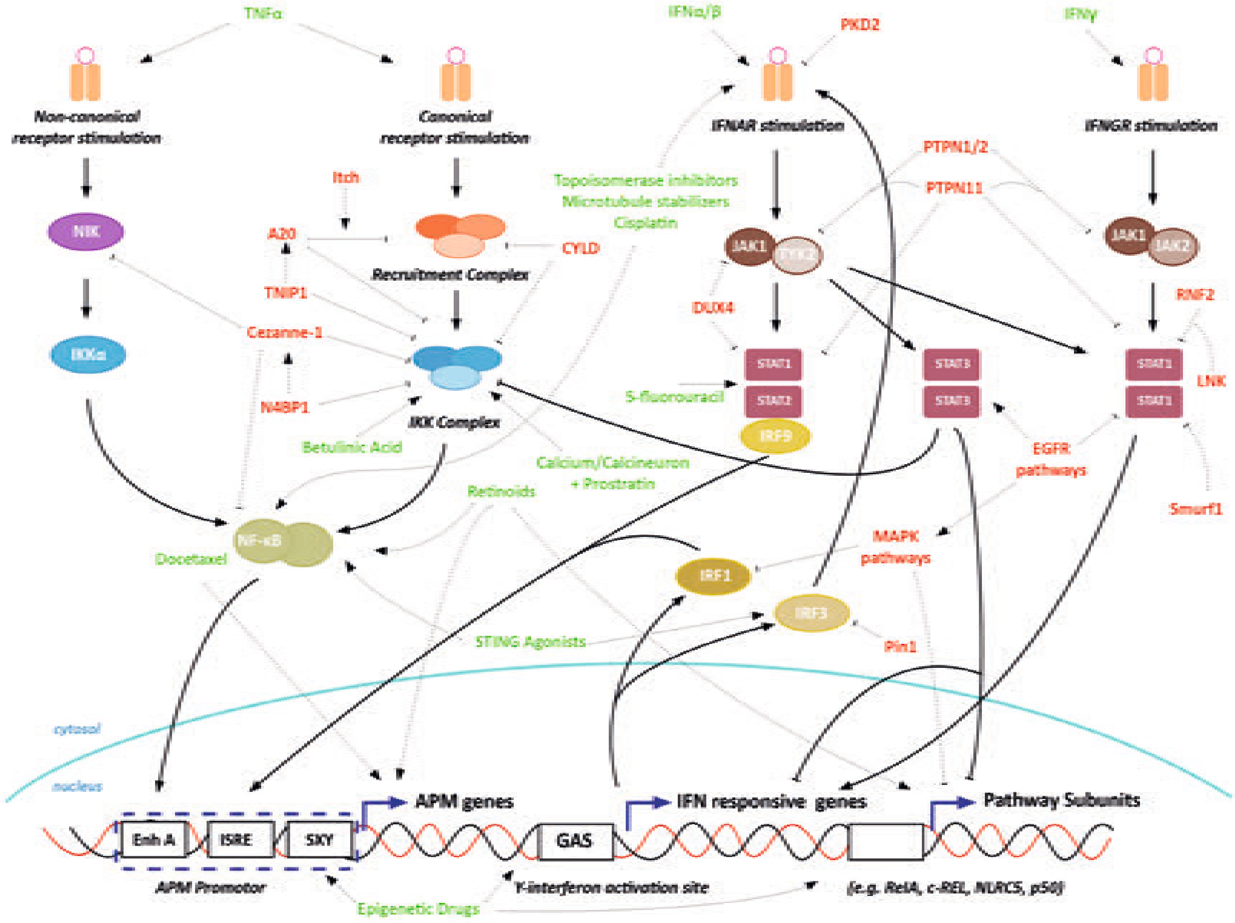
TNFα
IFNα/β
PKD2
IFNγ
Non-canonical receptor stimulation
Canonical receptor stimulation
IFNAR stimulation
IFNGR stimulation
Itch
A20
CYLD
Recruitment Complex
TNIP1
Cezanne-1
N4BP1
NIK
IKKα
IKK Complex
Betulinic Acid
Topoisomerase inhibitors
Microtubule stabilizers
Cisplatin
PTPN1/2
PTPN11
JAK1
TYK2
JAK1
JAK2
DUX4
RNF2
LNK
STAT1
STAT2
IRF9
STAT3
STAT3
STAT1
STAT1
5-fluorouracil
EGFR pathways
Smurf1
Calcium/Calcineuron + Prostratin
Retinoids
NF-κB
Docetaxel
MAPK pathways
IRF1
IRF3
Pin1
STING Agonists
cytosol
nucleus
APM genes
IFN responsive genes
Pathway Subunits
Enh A
ISRE
SXY
GAS
APM Promotor
Epigenetic Drugs
Γ-interferon activation site
(e.g. RelA, c-REL, NLRC5, p50)

**Figure 4.** Potential therapeutic interference to boost MHC-I antigen presentation of tumors.
*Targetable negative pathway regulators are shown in red, (general groups of) compounds positively affecting pathway activation are shown in green.*

**Table 1.** Overview of described pathways and potential therapeutic strategies to boost MHC-I antigen presentation

| **Regulation** | **Pathway** | **Effector** | **Described Mechanism(s)** | **Potential Therapeutic Strategy** | **Clinical Status** |
|---|---|---|---|---|---|
| Negative Regulators | NFκB pathway | N4BP1 | 1. Cezanne-1 stabilization;<br>2. Preventing recruitment of NEMO to RIP1. | - miRNA-28-5p [65-67,70,71]]. | Pre-clinical. |
| | | Cezanne-1 | 1. Deubiquitination and stabilization of TRAF3. | - Aspecific DUB inhibitors (e.g. Ubal) [87];<br>- miR-1180 [69], miR-486 [68];<br>- Cyanopyrrolidine derivates (WO2017109488). | Pre-clinical. |
| | | TNIP1 | 1. Preventing recruitment of NEMO to RIP1;<br>2. Preventing degradation of the IkB p105 into p50;<br>3. A20 stabilization. | - IL-17 [63];<br>- miR-1180 [69], miR-486 [68]. | Pre-clinical. |
| | | A20 | 1. Deubiquitination of NEMO;<br>2. Deubiquitination of RIP-1 & TRAF6;<br>3. Degradation of RIP-1. | - Aspecific DUB inhibitors (e.g. Ubal) [87];<br>- miR-1180 [69], miR-486 [68]. | Pre-clinical. |
| | | TAX1BP1 | 1. Itch recruitment to A20. | | |
| | | Itch | 1. Controlling interaction between A20 and RIP1/TRAF6. | - Clomipramine & norclomipramine [80];<br>- 1,4-naphthoquinone 10e [81]. | - FDA-approved antidepressants;<br>- Pre-clinical. |
| | | CYLD | 1. Deubiquitination of NEMO;<br>2. Deubiquitination of TRAF2. | - miR-1288 [84], miR-186 [85], miR-362-5p [86]. | Pre-clinical. |
| | Type I/II IFN pathway | DUX4 | 1. JAK 1/2 downregulation;<br>2. STAT2 downregulation. | - p300 inhibitors [115];<br>- p38 inhibitors [117]. | - Pre-clinical;<br>- Several Phase II Trials (Rheumatoid Arthritis, Asthma, LMNA-related cardiomyopathy). |
| | | LNK (SH2B3) | 1. Dephosphorylation of STAT1 | - miR-29b [122], miR-30-5p [121], miR-98 [121],<br>miR181a-5p [121]. | |
| | | PTPN1 (PTP1B) | 1. Dephosphorylation of TYK2;<br>2. Dephosphorylation of JAK2. | - MSI-1436C [135]. | Phase I Trial, metastatic breast cancer. |
| | | PTPN2 (TC-PTP) | 1. Dephosphorylation of JAK1. | - miRNA-155 [136]. | Pre-clinical. |
| | | PTPN11 (SHP2) | 1. Dephosphorylation of JAK1;<br>2. Dephosphorylation of STAT1;<br>3. Dephosphorylation of STAT2. | - Sodium stibogluconate [134]. | Phase II Trial, Leishmaniasis, stage IV melanoma, advanced solid tumor. |

**Table 1.** Overview of described pathways and potential therapeutic strategies to boost MHC-I antigen presentation (continued)

| Regulation | Pathway | Effector | Described Mechanism(s) | Potential Therapeutic Strategy | Clinical Status |
|---|---|---|---|---|---|
| Negative Regulators | Type I/II IFN pathway | RNF2 | 1. Polyubiquitination of STAT1, resulting in release from DNA. | - Trametinib [143];<br>- PRT4165 [148]. | - FDA-approved in several advanced-stage cancers;<br>- Pre-clinical. |
| | | Smurf1 | 1. Degradation of STAT1. | - A01 [149]. | - Pre-clinical. |
| | | PIAS | 1. Inhibiting STAT1 promotor recruitment. | | |
| | Type I IFN pathway | DCST1 | 1. Ubiquitination and degradation of STAT2. | | |
| | | PKD2 | 1. Stimulating ubiquitination and endocytosis of IFNAR1. | - CRT0066101 [152];<br>- SD-208 [153]. | Pre-clinical. |
| | | Pin1 | 1. Ubiquitination and degradation of IRF3. | - miR-200b [126], miR-200c [127], miR-296-5p [128];<br>- ATRA [129];<br>- KPT-6566 [130];<br>- Juglone [125]. | - Pre-clinical;<br>- FDA-approved in cancer;<br>- Pre-clinical;<br>- Pre-clinical. |
| | NFκB and type I/II IFN pathway | STAT3 | 1. Negative feedback loop of pro-inflammatory type I signaling;<br>2. Inhibition of IKK activation | STAT3 inhibitors:<br>- JSI-124 [169];<br>- Indirubin [164];<br>- Resveratrol [165];<br>- Nifuroxazide [170];<br>- Static [166];<br>- Sorafenib [167];<br>- Sunitinib [168]. | - Pre-clinical;<br>- Phase 3/4 trials in acute promyelocytic leukemia, phase 2/3 in dermatitis and psoriasis;<br>- Phase 2/3 in congestive heart failure, Friedreich Ataxia, Gulf War Illness, Lymphangioleiomyomatosis, and infertility;<br>- FDA-approved antibiotic;<br>- Pre-clinical;<br>- Pre-clinical;<br>- Pre-clinical. |
| Positive Regulators | | EGFR receptor family (including HER2/neu) | 1. STAT1 inactivation;<br>2. Stimulation of MAPK pathway;<br>3. STAT3 activation;<br>4. Fhit degradation. | Tyrosine Kinase inhibitors:<br>- EGFR inhibitors (e.g. nimotuzumab [198], cetuximab [199] , afatinib [185], erlotinib [185], gefitinib[202]). | - FDA-approved in cancer. |
| | | NMYC | 1. Inhibition of p50 (although inconsistent) | | |
| | | MAPK pathway | 1. Decreases IRF1 activity;<br>2. Decreases STAT1 expression. | Tyrosine Kinase inhibitors:<br>- MEK-inhibitors (e.g. trametinib [188,189], cobimetinib [188], selumetinib [2]);<br>- BRAF inhibitors (e.g. vemurafenib 184,190], dabrafenib [41]). | - FDA-approved in cancer, selumetinib in phase 3;<br>- FDA-approved in cancer. |

**Table 1.** Overview of described pathways and potential therapeutic strategies to boost MHC-I antigen presentation (continued)

| Regulation | Pathway | Effector | Described Mechanism(s) | Potential Therapeutic Strategy | Clinical Status |
|---|---|---|---|---|---|
| Positive Regulators | NFκB pathway | NFκB-inducing receptor stimulation | 1. TNFR superfamily stimulation;<br>2. PRR Receptor stimulation;<br>3. IL-1 receptor stimulation. | - TNFα [40]. | Phase I-III trials in cancer, all localized infusions. |
| | | IKK/IkBα | 1. Boosting IKK-activity;<br>2. Degradation of IkBα. | - Betulinic acid [45]. | Phase I trial, Anxiety. |
| | | IKK | 1. Boosting IKK-activity. | - Calcium/calcineurin + prostratin [51]. | Pre-clinical. |
| | | Nedd4 | 1. Degradation of N4BP1;<br>2. Degradation of TRAF3. | | |
| | | p50, RelA, and LMP-2/-7/-10 | 1. Enhanced expression of p50;<br>2. Enhanced expression of RelA;<br>3. Enhances expression of LMP-2/-7/-10. | - Retinoids [41,218]. | FDA-approved in several diseases, including cancers. |
| | Type I IFN pathway | IFN-inducing receptor stimulation | 1. PRR Receptors stimulation (e.g. RNF135, TRIM25, ISG15, NAB2);<br>2. IFNA Receptor stimulation. | - IFNα [100,101];<br>- IFNβ therapy [101]. | - FDA-approved in hepatitis B & high-risk melanoma;<br>- Phase III trial in relapsing multiple sclerosis, Phase I in refractory solid tumors. |
| | Type II IFN pathway | IFN-inducing receptor stimulation | 1. IFNG Receptor stimulation. | - IFNγ-1b;<br>- NK cell therapy [19,33,103,106,107,219]. | - FDA approved as localized injection in chronic granulomatous disease (CGD) & severe, malignant ostepetrosis (SMO), phase I-III in cancers;<br>- Phase I/II Trial in several cancer types. |
| | NFκB- and type I IFN pathway | STING | 1. Phosphorylation and activation of RelA;<br>2. Phosphorylation and activation of IRF3. | - STING agonists (e.g. SB 11285 [177]). | Phase I Trial in patients with advanced solid tumors. |
| | NFκB- and type I IFN pathway | | 1. Increasing APM expression (Calreticulin, TAP2, calnexin).<br>2. Enhancing type I IFN signaling<br>3. NFκB stabilization<br>4. IFNβ secretion | - Docetaxel [205];<br>- 5-Fluorouracil [206];<br>- Topoisomerase inhibitors (e.g. topotecan [207,209], irinotecan [208], and etoposide [207];<br>- Microtubule stabilizers (e.g. paclitaxel [207,209] and vinblastine [207]);<br>- Cisplatin [207] | All FDA-approved in cancer. |

**Table 1.** Overview of described pathways and potential therapeutic strategies to boost MHC-I antigen presentation (continued)

| Regulation | Pathway | Effector | Described Mechanism(s) | Potential Therapeutic Strategy | Clinical Status |
|---|---|---|---|---|---|
| Epigenetic modification | NFκB and type I/II IFN pathway | | 1. Histon acetylation to decrease genome accessibility;<br>2. DNA methylation to decrease genome accessibility. | - HDAC inhibitors: (e.g. Romidepsin, Vorinostat [212] and Panobinostat) [1,211-214];<br>- DNMTis (e.g. 5'azacytidine [212], Decitabine [54], and Guadecitabine [216]). | - All FDA-approved in cancer;<br>- FDA approved, Guadecitabine phase II trials in cancer). |

## 13. CONCLUSIONS

In conclusion, MHC-I antigen presentation is a complex process regulated by multiple pathways that can be pharmacologically targeted on multiple levels to increase pathway activation and trigger MHC-I expression in cancer. Increasing antigen presentation in MHC-I-downregulated tumors is key to increase adaptive anti-tumor immunity and improve (immuno)therapy efficacy.

## ACKNOWLEDGMENTS

The authors thank Yvonne van de Grint for designing the figures.

## REFERENCES

1. Sharma P., Hu-Lieskovan S., Wargo J.A., Ribas A. Primary, adaptive, and acquired resistance to cancer immunotherapy. *Cell*. **2017**;168: 707–723. doi:10.1016/j.cell.2017.01.017.
2. Angell T.E., Lechner M.G., Jang J.K., LoPresti J.S., Epstein A.L. MHC class I loss is a frequent mechanism of immune escape in papillary thyroid cancer that is reversed by interferon and selumetinib treatment in Vitro. *Clin. Cancer Res*. **2014**;20:6034–6044. doi:10.1158/1078-0432.CCR-14-0879.
3. Mina M., Boldrini R., Citti A., Romania P., D'Alicandro V., De Ioris M., Castellano A., Furlanello C., Locatelli F., Fruci D. Tumor-infiltrating T lymphocytes improve clinical outcome of therapy-resistant neuroblastoma. *Oncoimmunology*. **2015**;4: 1–14. doi:10.1080/2162402X.2015.1019981.
4. Shi A.H., Ho L.-L., Levine S., Yadav V., Cheah J., Soule C., Frederick D.T., Liu D., Boland G., Kellis M. Epigenomic correlates of checkpoint blockade immunotherapy resistance. *Proc. Am. Assoc. Cancer Res. Annu. Meet*. **2019**; 79 doi:10.1158/1538-7445.AM2019-948.
5. Gettinger S., Choi J., Hastings K., Truini A., Datar I., Sowell R., Wurtz A., Dong W., Cai G., Melnick M.A., et al. Impaired HLA class I antigen processing and presentation as a mechanism of acquired resistance to immune checkpoint inhibitors in lung cancer. *Cancer Discov*. **2017**;7:1420–1435. doi:10.1158/2159-8290.CD-17-0593.
6. Sade-Feldman M., Jiao Y.J., Chen J.H., Rooney M.S., Barzily-Rokni M., Eliane J.P., Bjorgaard S.L., Hammond M.R., Vitzthum H., Blackmon S.M., et al. Resistance to checkpoint blockade therapy through inactivation of antigen presentation. *Nat. Commun*. **2017**; 8 doi:10.1038/s41467-017-01062-w.
7. Chowell D., Morris L.G.T., Grigg C.M., Weber J.K., Samstein R.M., Makarov V., Kuo F., Kendall S.M., Requena D., Riaz N., et al. Patient HLA class I genotype influences cancer response to checkpoint blockade immunotherapy. *Science*. **2018**;359:582–587. doi:10.1126/science.aao4572.
8. Lee J.H., Shklovskaya E., Lim S.Y., Carlino M.S., Menzies A.M., Stewart A., Pedersen B., Irvine M., Alavi S., Yang J.Y.H., et al. Transcriptional downregulation of MHC class I and melanoma de- differentiation in resistance to PD-1 inhibition. *Nat. Commun*. **2020**;11: 1–12. doi:10.1038/s41467-020-15726-7.
9. Benitez R., Godelaine D., Lopez-Nevot M.A., Brasseur F., Jiménez P., Marchand M., Oliva M.R., Van Baren N., Cabrera T., Andry G., et al. Mutations of the β2-microglobulin gene result in a lack of HLA class I molecules on melanoma cells of two patients immunized with MAGE peptides. *Tissue Antigens*. **1998**; 52:520–529. doi:10.1111/j.1399-0039.1998.tb03082.x.
10. Lauss M., Donia M., Harbst K., Andersen R., Mitra S., Rosengren F., Salim M., Vallon-Christersson J., Törngren T., Kvist A., et al. Mutational and putative neoantigen load predict clinical benefit of adoptive T cell therapy in melanoma. *Nat. Commun*. **2017**; 8:1–11. doi:10.1038/s41467-017-01460-0.
11. Khong H.T., Wang Q.J., Rosenberg S.A. Identification of multiple antigens recognized by tumor-infiltrating lymphocytes from a single patient: Tumor escape by antigen loss and loss of MHC expression. *J. Immunother*. **2004**;27: 184–190. doi:10.1097/00002371-200405000-00002.
12. Maleno I., López-Nevot M., Cabrera T., Salinero J., Garrido F. Multiple mechanisms generate HLA class I altered phenotypes in laryngeal carcinomas: High frequency of HLA haplotype loss associated with loss of heterozygosity in chromosome region 6p21. *Cancer Immunol. Immunother*. **2002**;51:389–396. doi:10.1007/s00262-002-0296-0.
13. Maleno I., Cabrera C.M., Cabrera T., Paco L., López-Nevot M.A., Collado A., Ferrón A., Garrido F. Distribution of HLA class I altered phenotypes in colorectal carcinomas: High frequency of HLA haplotype loss associated with loss of heterozygosity in chromosome region 6p21. *Immunogenetics*. **2004**;56: 244–253. doi:10.1007/s00251-004-0692-z.

**14.** Maleno I., Romero J.M., Cabrera T., Paco L., Aptsiauri N., Cozar J.M., Tallada M., López-Nevot M.A., Garrido F. LOH at 6p21.3 region and HLA class altered phenotypes in bladder carcinomas. *Immunogenetics*. **2006**;58:503–510. doi:10.1007/s00251-006-0111-8.

**15.** Feenstra M., Veltkamp M., Van Kuik J., Wiertsema S., Slootweg P., Van den Tweel J., De Weger R., Tilanus M. HLA class 1 expression and chromosomal deletions at 6p and 15q in head and neck squamous cell carcinomas. *Tissue Antigens*. **1999**;54:235–245. doi:10.1034/j.1399-0039.1999.540304.x.

**16.** Garrido M.A., Rodriguez T., Zinchenko S., Maleno I., Ruiz-Cabello F., Concha Á., Olea N., Garrido F., Aptsiauri N. HLA class I alterations in breast carcinoma are associated with a high frequency of the loss of heterozygosity at chromosomes 6 and 15. *Immunogenetics*. **2018**;70:647–659. doi:10.1007/s00251-018-1074-2.

**17.** Seliger B., Ritz U., Bock M., Huber C., Abele R., Tampé R., Sutter G., Sutter G., Drexler I., Ferrone S. Immune escape of melanoma: First evidence of structural alterations in two distinct components of the MHC class I antigen processing pathway. *Cancer Res.* **2001**; 61:8647–8650.

**18.** Meissner M., Reichert T.E., Kunkel M., Gooding W., Whiteside T.L., Ferrone S., Seliger B. Defects in the human leukocyte antigen class I antigen-processing machinery in head and neck squamous cell carcinoma: Association with clinical outcome. *Clin. Cancer Res.* **2005**; 11:2552–2560. doi:10.1158/1078-0432.CCR-04-2146.

**19.** Spel L., Boelens J.J., Van Der Steen D.M., Blokland N.J.G., van Noesel M.M., Molenaar J.J., Heemskerk M.H.M., Boes M., Nierkens S. Natural killer cells facilitate PRAME-specific T-cell reactivity against neuroblastoma. *Oncotarget.* **2015**;6:35770–35781. doi:10.18632/oncotarget.5657.

**20.** Romero J.M., Jiménez P., Cabrera T., Cózar J.M., Pedrinaci S., Tallada M., Garrido F., Ruiz-Cabello F. Coordinated downregulation of the antigen presentation machinery and HLA class I/β2-microglobulin complex is responsible for HLA-ABC loss in bladder cancer. *Int. J. Cancer.* **2005**;113:605–610. doi:10.1002/ijc.20499.

**21.** Squire R., Fowler C.L., Brooks S.P., Rich G.A., Cooney D.R. The relationship of class I MHC antigen expression to stage IV-S disease and survival in neuroblastoma. *J. Pediatr. Surg.* **1990**;25:381–386. doi:10.1016/0022-3468(90)90375-J.

**22.** Watson N.F.S., Ramage J.M., Madjd Z., Spendlove I., Ellis I.O., Scholefield J.H., Durrant L.G. Immunosurveillance is active in colorectal cancer as downregulation but not complete loss of MHC class I expression correlates with a poor prognosis. *Int. J. Cancer.* **2006**; 118:6–10. doi:10.1002/ijc.21303.

**23.** Turcotte S., Katz S.C., Shia J., Jarnagin W.R., Kingham T.P., Allen P.J., Fong Y., D'Angelica M.I., DeMatteo R.P. Tumor MHC class I expression improves the prognostic value of T-cell density in resected colorectal liver metastases. *Cancer Immunol. Res.* **2014**;2: 530–537. doi:10.1158/2326-6066.CIR-13-0180.

**24.** Andersson E., Villabona L., Bergfeldt K., Carlson J.W., Ferrone S., Kiessling R., Seliger B., Masucci G.V. Correlation of HLA-A02* genotype and HLA class I antigen down-regulation with the prognosis of epithelial ovarian cancer. *Cancer Immunol. Immunother.* **2012**;61:1243–1253. doi:10.1007/s00262-012-1201-0.

**25.** Roemer M.G.M., Advani R.H., Redd R.A., Pinkus G.S., Natkunam Y., Ligon A.H., Connelly C.F., Pak C.J., Carey C.D., Daadi S.E., et al. Classical Hodgkin lymphoma with reduced β2M/MHC class i expression is associated with inferior outcome independent of 9p24.1 status. *Cancer Immunol. Res.* **2016**;4:910–916. doi:10.1158/2326-6066.CIR-16-0201.

**26.** Van Houdt I.S., Sluijter B.J.R., Moesbergen L.M., Vos W.M., De Gruijl T.D., Molenkamp B.G., Van Den Eertwegh A.J.M., Hooijberg E., Van Leeuwen P.A.M., Meijer C.J.L.M., et al. Favorable outcome in clinically stage II melanoma patients is associated with the presence of activated tumor infiltrating T-lymphocytes and preserved MHC class I antigen expression. *Int. J. Cancer.* **2008**;123: 609–615. doi:10.1002/ijc.23543.

**27.** Simpson J.A.D., Al-Attar A., Watson N.F.S., Scholefield J.H., Ilyas M., Durrant L.G. Intratumoral T cell infiltration, MHC class I and STAT1 as biomarkers of good prognosis in colorectal cancer. *Gut.* **2010**;59:926–933. doi:10.1136/gut.2009.194472.

**28.** Inoue M., Mimura K., Izawa S., Shiraishi K., Inoue A., Shiba S., Watanabe M., Maruyama T., Kawaguchi Y., Inoue S., et al. Expression of mhc class i on breast cancer cells correlates inversely with her2 expression. *Oncoimmunology.* **2012**;1:1104–1110. doi:10.4161/onci.21056.

**29.** Hanagiri T., Shigematsu Y., Kuroda K., Baba T., Shiota H., Ichiki Y., Nagata Y., Yasuda M., Uramoto H., So T., et al. Prognostic implications of human leukocyte antigen class i expression in patients who underwent surgical resection for non-small-cell lung cancer. *J. Surg. Res.* **2013**;181:e57–e63. doi:10.1016/j.jss.2012.07.029.

**30.** Spel L., Schiepers A., Boes M. NFκB and MHC-1 interplay in neuroblastoma and immunotherapy. *Trends Cancer.* **2018**;4: 715–717. doi:10.1016/j.trecan.2018.09.006.

**31.** Anfossi N., André P., Guia S., Falk C.S., Roetynck S., Stewart C.A., Breso V., Frassati C., Reviron D., Middleton D., et al. Human NK Cell Education by Inhibitory Receptors for MHC Class, I. *Immunity.* **2006**;25:331–342. doi:10.1016/j.immuni.2006.06.013.

**32.** Lee J.-C., Lee K.-M., Kim D.-W., Heo D.S. Elevated TGF-β1 Secretion and Down-Modulation of NKG2D Underlies Impaired NK Cytotoxicity in Cancer Patients. *J. Immunol.* **2004**;172:7335–7340. doi:10.4049/jimmunol.172.12.7335.

**33.** Jonges L.E., Giezeman-Smits K.M., Van Vlierberghe R.L.E., Ensink N.G., Hagenaars M., Joly É., Eggermont A.M.M., Van de Velde C.J.H., Fleuren G.J., Kuppen P.J.K. NK cells modulate MHC class I expression on tumor cells and their susceptibility to lysis. *Immunobiology.* **2000**;202:326–338. doi:10.1016/S0171-2985(00)80037-6.

**34.** Jongsma M.L.M., Guarda G., Spaapen R.M. The regulatory network behind MHC class I expression. *Mol. Immunol.* **2019**;113:16–21. doi:10.1016/j.molimm.2017.12.005.

**35.** Lorenzi S., Forloni M., Cifaldi L., Antonucci C., Citti A., Boldrini R., Pezzullo M., Castellano A., Russo V., van der Bruggen P., et al. IRF1 and NF-kB Restore MHC Class I-Restricted Tumor Antigen Processing and Presentation to Cytotoxic T Cells in Aggressive Neuroblastoma. *PLoS ONE.* **2012**;7:1–8. doi:10.1371/journal.pone.0046928.

**36.** Sun S.C. The non-canonical NF-κB pathway in immunity and inflammation. *Nat. Rev. Immunol.* **2017**;17:545–558. doi:10.1038/nri.2017.52.

**37.** Chaturvedi M.M., Sung B., Yadav V.R., Kannappan R., Aggarwal B.B. NF-κB addiction and its role in cancer: One size does not fit all. *Oncogene.* **2011**;30:1615–1630. doi:10.1038/onc.2010.566.

**38.** Wells K., Hintzsche J., Amato C.M., Tobin R., Vorwald V., McCarter M., Shellman Y., Tan A.C., Robinson W. Investigating the role of NF- κB signaling and immune checkpoint blockade therapy in melanoma. *Clin. Res.* **2019**;90: abstract 5002.

**39.** Ea C.K., Deng L., Xia Z.P., Pineda G., Chen Z.J. Activation of IKK by TNFα Requires Site-Specific Ubiquitination of RIP1 and Polyubiquitin Binding by NEMO. *Mol. Cell.* **2006**;22:245–257. doi:10.1016/j.molcel.2006.03.026.

**40.** Cai W., Kerner Z.J., Sun J. Targeted Cancer Therapy with Tumor Necrosis Factor-Alpha. *Biochem. Insights.* **2008**:15–21. doi:10.4137/BCI.S901.

**41.** Segars J.H., Nagata T., Bours V., Medin J.A., Franzoso G., Blanco J.C., Drew P.D., Becker K.G., An J., Tang T. Retinoic acid induction of major histocompatibility complex class I genes in NTera-2 embryonal carcinoma cells involves induction of NF-kappa B (p50-p65) and retinoic acid receptor beta-retinoid X receptor beta heterodimers. *Mol. Cell. Biol.* **1993**;13:6157–6169. doi:10.1128/MCB.13.10.6157.

**42.** Farina A.R., Masciulli M.P., Tacconelli A., Cappabianca L., De Santis G., Gulino A., Mackay A.R. All-trans-retinoic acid induces nuclear factor κB activation and matrix metalloproteinase-9 expression and enhances basement membrane invasivity of differentiation-resistant human SK-N-BE 9N neuroblastoma cells. *Cell Growth Differ.* **2002**; 13:343–354.

**43.** Vertuani S., De Geer A., Levitsky V., Kogner P., Kiessling R., Levitskaya J. Retinoids Act as Multistep Modulators of the Major Histocompatibility Class I Presentation Pathway and Sensitize Neuroblastomas to Cytotoxic Lymphocytes. *Cancer Res.* **2003**; 63:8006–8013.

**44.** Matthay K.K., Reynolds C.P., Seeger R.C., Shimada H., Adkins E.S., Haas-Kogan D., Gerbing R.B., London W.B., Villablanca J.G. Long-term results for children with high-risk neuroblastoma treated on a randomized trial of myeloablative therapy followed by 13-cis-retinoic acid: A children's oncology group study. *J. Clin. Oncol.* **2009**;27:1007–1013. doi:10.1200/JCO.2007.13.8925.

**45.** Kasperczyk H., La Ferla-Brühl K., Westhoff M.A., Behrend L., Zwacka R.M., Debatin K.M., Fulda S. Betulinic acid as new activator of NF-κB: Molecular mechanisms and implications for cancer therapy. *Oncogene.* **2005**;24:6945–6956. doi:10.1038/sj.onc.1208842.

**46.** Selzer E., Pimentel E., Wacheck V., Schlegel W., Pehamberger H., Jansen B., Kodym R. Effects of betulinic acid alone and in combination with irradiation in human melanoma cells. *J. Invest. Dermatol.* **2000**;114:935–940. doi:10.1046/j.1523-1747.2000.00972.x.

**47.** Wick W., Grimmel C., Wagenknecht B., Dichgans J., Weller M. Betulinic acid-induced apoptosis in glioma cells: A sequential requirement for new protein synthesis, formation of reactive oxygen species, and caspase processing. *J. Pharmacol. Exp. Ther.* **1999**;289:1306–1312.

**48.** Fulda S., Friesen C., Los M., Scaffidi C., Mier W., Benedict M., Nuñez G., Krammer P.H., Peter M.E., Debatin K.M. Betulinic acid triggers CD95 (APO-1/Fas)- and p53-independent apoptosis via activation of caspases in neuroectodermal tumors. *Cancer Res.* **1997**;57:4956–4964.

**49.** Chowdhury A.R., Suparna M., Mittra B., Sharma S., Mukhopadhyay S., Majumder H.K. Betulinic acid, a potent inhibitor of eukaryotic topoisomerase I: Identification of the inhibitory step, the major functional group responsible and development of more potent derivatives. *Med. Sci. Monit.* **2002**;8: 254–261.

**50.** Kwon H.J., Shim J.S., Kim J.H., Cho H.Y., Yum Y.N., Kim S.H., Yu J. Betulinic acid inhibits growth factor-induced in vitro angiogenesis via the modulation of mitochondrial function in endothelial cells. *Japanese J. Cancer Res.* **2002**;93:417–425. doi:10.1111/j.1349-7006.2002.tb01273.x.

**51.** Chan J.K., Bhattacharyya D., Lassen K.G., Ruelas D., Greene W.C. Calcium/calcineurin synergizes with prostratin to promote NF-κB dependent activation of latent HIV. *PLoS ONE.* **2013**;8:e77749. doi:10.1371/journal.pone.0077749.

**52.** Fang D.F., He K., Wang N., Sang Z.H., Qiu X., Xu G., Jian Z., Liang B., Li T., Li H.Y., et al. NEDD4 ubiquitinates TRAF3 to promote CD40-mediated AKT activation. *Nat. Commun.* **2014**; 5:1–11. doi:10.1038/ncomms5513.

**53.** Oberst A., Malatesta M., Aqeilan R.I., Rossi M., Salomoni P., Murillas R., Sharma P., Kuehn M.R., Oren M., Croce C.M., et al. The Nedd4-binding partner 1 (N4BP1) protein is an inhibitor of the E3 ligase Itch. *Proc. Natl. Acad. Sci. USA.* **2007**;104:11280–11285. doi:10.1073/pnas.0701773104.

**54.** Spel L., Nieuwenhuis J., Haarsma R., Stickel E., Bleijerveld O.B., Altelaar M., Boelens J.J., Brummelkamp T.R., Nierkens S., Boes M. Nedd4-binding protein 1 and TNFAIP3-interacting protein 1 control MHC-1 display in neuroblastoma. *Cancer Res.* **2018**;78:6621–6631. doi:10.1158/0008-5472.CAN-18-0545.

**55.** Fenner B.J., Scannell M., Prehn J.H.M. Identification of polyubiquitin binding proteins involved in NF-κB signaling using protein arrays. *Biochim. Biophys. Acta Proteins Proteomics.* **2009**;1794:1010–1016. doi:10.1016/j.bbapap.2009.02.013.

**56.** Nepravishta R., Ferrentino F., Mandaliti W., Mattioni A., Weber J., Polo S., Castagnoli L., Cesareni G., Paci M., Santonico E. CoCUN, a novel ubiquitin binding domain identified in N4BP1. *Biomolecules.* **2019**;9:284. doi:10.3390/biom9070284.

**57.** Hu H., Brittain G.C., Chang J.H., Puebla-Osorio N., Jin J., Zal A., Xiao Y., Cheng X., Chang M., Fu Y.X., et al. OTUD7B controls non-canonical NF-κB activation through deubiquitination of TRAF3. *Nature.* **2013**;494:371–374. doi:10.1038/nature11831.

**58.** Yang X.D., Sun S.C. Targeting signaling factors for degradation, an emerging mechanism for TRAF functions. *Immunol. Rev.* **2015**;266:56–71. doi:10.1111/imr.12311.

**59.** G'Sell R.T., Gaffney P.M., Powell D.W. A20-binding inhibitor of NF-κB activation 1 is a physiologic inhibitor of NF-κB: A molecular switch for inflammation and autoimmunity. *Arthritis Rheumatol.* **2015**;67:2292–2302. doi:10.1002/art.39245.

**60.** Wagner S., Carpentier I., Rogov V., Kreike M., Ikeda F., Löhr F., Wu C.J., Ashwell J.D., Dötsch V., Dikic I., et al. Ubiquitin binding mediates the NF-κB inhibitory potential of ABIN proteins. *Oncogene.* **2008**;27:3739–3745. doi:10.1038/sj.onc.1211042.

**61.** Cohen S., Ciechanover A., Kravtsova-Ivantsiv Y., Lapid D., Lahav-Baratz S. ABIN-1 negatively regulates NF-κB by inhibiting processing of the p105 precursor. *Biochem. Biophys. Res. Commun.* **2009**;389:205–210. doi:10.1016/j.bbrc.2009.08.074.

**62.** Mauro C., Pacifico F., Lavorgna A., Mellone S., Iannetti A., Acquaviva R., Formisano S., Vito P., Leonardi A. ABIN-1 binds to NEMO/IKKγ and co-operates with A20 in inhibiting NF-κB. *J. Biol. Chem.* **2006**;281:18482–18488. doi:10.1074/jbc.M601502200.

**63.** Cruz J.A., Childs E.E., Amatya N., Garg A.V., Beyaert R., Kane L.P., Aneskievich B.J., Ma A., Gaffen S.L. IL-17 Signaling Triggers Degradation of the Constitutive NF-κB Inhibitor ABIN-1. *ImmunoHorizons.* **2017**;1:133–141. doi:10.4049/immunohorizons.1700035.

**64.** Yang B., Kang H., Fung A., Zhao H., Wang T., Ma D. The role of interleukin 17 in tumour proliferation, angiogenesis, and metastasis. *Mediators Inflamm.* **2014**;2014 doi:10.1155/2014/623759.

**65.** Wu W., He K., Guo Q., Chen J., Zhang M., Huang K., Yang D., Wu L., Deng Y., Luo X., et al. SSRP1 promotes colorectal cancer progression and is negatively regulated by miR-28-5p. *J. Cell. Mol. Med.* **2019**;23:3118–3129. doi:10.1111/jcmm.14134.

**66.** Wang C., Wu C., Yang Q., Ding M., Zhong J., Zhang C.Y., Ge J., Wang J., Zhang C. miR-28-5p acts as a tumor suppressor in renal cell carcinoma for multiple antitumor effects by targeting RAP1B. *Oncotarget.* **2016**;7:73888–73902. doi:10.18632/oncotarget.12516.

**67.** Shi X., Teng F. Down-regulated miR-28-5p in human hepatocellular carcinoma correlated with tumor proliferation and migration by targeting insulin-like growth factor-1 (IGF-1) *Mol. Cell. Biochem.* **2015**;408:283–293. doi:10.1007/s11010-015-2506-z.

**68.** Song L., Lin C., Gong H., Wang C., Liu L., Wu J., Tao S., Hu B., Cheng S.Y., Li M., et al. MiR-486 sustains NF-κB activity by disrupting multiple NF-κB-negative feedback loops. *Cell Res.* **2013**;23:274–289. doi:10.1038/cr.2012.174.

**69.** Tan G., Wu L., Tan J., Zhang B., Tai W.C.S., Xiong S., Chen W., Yang J., Li H. MIR-1180 promotes apoptotic resistance to human hepatocellular carcinoma via activation of NF-κB signaling pathway. *Sci. Rep.* **2016**;6:1–11. doi:10.1038/srep22328.

**70.** Xu J., Jiang N., Shi H., Zhao S., Yao S., Shen H. MiR-28-5p promotes the development and progression of ovarian cancer through inhibition of N4BP1. *Int. J. Oncol.* **2017**;50: 1383–1391. doi:10.3892/ijo.2017.3915.

**71.** Zhu G., Wang Z., Mijiti M., Du G., Li Y., Dangmurenjiafu G. MiR-28-5p promotes human glioblastoma cell growth through inactivation of FOXO1. *Int. J. Clin. Exp. Pathol.* **2019**;12:2972–2980.

**72.** Shembade N., Harhaj E.W. Regulation of NF-κB signaling by the A20 deubiquitinase. *Cell. Mol. Immunol.* **2012**;9:123–130. doi:10.1038/cmi.2011.59.

**73.** Wertz I.E., Rourke K.M.O., Zhou H., Eby M., Aravind L., Seshagiri S., Wu P., Wiesmann C., Dixit V.M. ligase domains of A20 downregulate NF-kB signalling. *Nature.* **2004**;430:1–6. doi:10.1038/nature02794.

**74.** Shembade N., Harhaj N.S., Parvatiyar K., Copeland N.G., Jenkins N.A., Matesic L.E., Harhaj E.W. The E3 ligase Itch negatively regulates inflammatory signaling pathways by controlling the function of the ubiquitin-editing enzyme A20. *Nat. Immunol.* **2008**;9: 254–262. doi:10.1038/ni1563.

**75.** Ishihara T., Tsuda H., Hotta A., Kozaki K.I., Yoshida A., Noh J.Y., Ito K., Imoto I., Inazawa J. ITCH is a putative target for a novel 20q11.22 amplification detected in anaplastic thyroid carcinoma cells by array-based comparative genomic hybridization. *Cancer Sci.* **2008**;99:1940–1949. doi:10.1111/j.1349-7006.2008.00900.x.

**76.** Ho K.C., Zhou Z., She Y.M., Chun A., Cyr T.D., Yang X. Itch E3 ubiquitin ligase regulates large tumor suppressor 1 tumor-suppressor stability. *Proc. Natl. Acad. Sci. USA.* **2011**;108: 4870–4875. doi:10.1073/pnas.1101273108.

**77.** Salah Z., Melino G., Aqeilan R.I. Negative regulation of the Hippo pathway by E3 ubiquitin ligase ITCH is sufficient to promote tumorigenicity. *Cancer Res.* **2011**;71:2010–2020. doi:10.1158/0008-5472.CAN-10-3516.

**78.** Salah Z., Itzhaki E., Aqeilan R.I. The ubiquitin E3 ligase ITCH enhances breast tumor progression by inhibiting the Hippo tumor suppressor pathway. *Oncotarget.* **2014**;5: 10886–10900. doi:10.18632/oncotarget.2540.

**79.** Meng J., Tagalakis A.D., Hart S.L. Silencing E3 Ubiqutin ligase ITCH as a potential therapy to enhance chemotherapy efficacy in p53 mutant neuroblastoma cells. *Sci. Rep.* **2020**;10:1–12. doi:10.1038/s41598-020-57854-6.

**80.** Rossi M., Rotblat B., Ansell K., Amelio I., Caraglia M., Misso G., Bernassola F., Cavasotto C.N., Knight R.A., Ciechanover A., et al. High throughput screening for inhibitors of the HECT ubiquitin E3 ligase ITCH identifies antidepressant drugs as regulators of autophagy. *Cell Death Dis.* **2014**;5:1–12. doi:10.1038/cddis.2014.113.

**81.** Liu Y.M., HuangFu W.C., Huang H.L., Wu W.C., Chen Y.L., Yen Y., Huang H.L., Nien C.Y., Lai M.J., Pan S.L., et al. 1,4-Naphthoquinones as inhibitors of Itch, a HECT domain-E3 ligase, and tumor growth suppressors in multiple myeloma. *Eur. J. Med. Chem.* **2017**;140:84–91. doi:10.1016/j.ejmech.2017.09.011.

**82.** Zhu J., Bengtsson B.O., Mix E., Thorell L.H., Olsson T., Link H. Effect of monoamine reuptake inhibiting antidepressants on major histocompatibility complex expression on macrophages in normal rats and rats with experimental allergic neuritis (EAN) *Immunopharmacology.* **1994**;27:225–244. doi:10.1016/0162-3109(94)90019-1.

**83.** Kovalenko A., Chable-Bessia C., Cantarella G., Israël A., Wallach D., Courtois G. The tumour suppressor CYLD negatively regulates NF-κB signalling by deubiquitination. *Nature.* **2003**; 424:801–805. doi:10.1038/nature01802.

**84.** Yin J., Weng C., Ma J., Chen F., Huang Y., Feng M. MicroRNA-1288 promotes cell proliferation of human glioblastoma cells by repressing ubiquitin carboxyl-terminal hydrolase CYLD expression. *Mol. Med. Rep.* **2017**;16:6764–6770. doi:10.3892/mmr.2017.7481.

**85.** Qiu H., Yuan S., Lu X. miR-186 suppressed CYLD expression and promoted cell proliferation in human melanoma. *Oncol. Lett.* **2016**;12: 2301–2306. doi:10.3892/ol.2016.5002.

**86.** Ni F., Zhao H., Cui H., Wu Z., Chen L., Hu Z., Guo C., Liu Y., Chen Z., Wang X., et al. MicroRNA-362-5p promotes tumor growth and metastasis by targeting CYLD in hepatocellular carcinoma. *Cancer Lett.* **2015**;356:809–818. doi:10.1016/j.canlet.2014.10.041.

**87.** Farshi P., Deshmukh R.R., Nwankwo J.O., Arkwright R.T., Cvek B., Liu J., Dou Q.P. Deubiquitinases (DUBs) and DUB inhibitors: A patent review. *Expert Opin. Ther. Pat.* **2015**; 25:1191–1208. doi:10.1517/13543776.2015.1056737.

**88.** Sun S.C. CYLD: A tumor suppressor deubiquitinase regulating NF-B activation and diverse biological processes. *Cell Death Differ.* **2010**;17:25–34. doi:10.1038/cdd.2009.43.

**89.** Wang J.H., Wei W., Guo Z.X., Shi M., Guo R. Decreased Cezanne expression is associated with the progression and poor prognosis in hepatocellular carcinoma. *J. Transl. Med.* **2015**;13:1–10. doi:10.1186/s12967-015-0396-1.

**90.** Tilborghs S., Corthouts J., Verhoeven Y., Arias D., Rolfo C., Trinh X.B., van Dam P.A. The role of Nuclear Factor-kappa B signaling in human cervical cancer. *Crit. Rev. Oncol. Hematol.* **2017**;120:141–150. doi:10.1016/j.critrevonc.2017.11.001.

**91.** Musella M., Manic G., De Maria R., Vitale I., Sistigu A. Type-I-interferons in infection and cancer: Unanticipated dynamics with therapeutic implications. *Oncoimmunology.* **2017**;6:1–12. doi:10.1080/2162402X.2017.1314424.

**92.** Castro F., Cardoso A.P., Gonçalves R.M., Serre K., Oliveira M.J. Interferon-gamma at the crossroads of tumor immune surveillance or evasion. *Front. Immunol.* **2018**;9:1–19. doi:10.3389/fimmu.2018.00847.

**93.** Zaretsky J.M., Garcia-Diaz A., Shin D.S., Escuin-Ordinas H., Hugo W., Hu-Lieskovan S., Torrejon D.Y., Abril-Rodriguez G., Sandoval S., Barthly L., et al. Mutations associated with acquired resistance to PD-1 blockade in melanoma. *N. Engl. J. Med.* **2016;**375:819–829. doi:10.1056/NEJMoa1604958.

**94.** Gao J., Shi L.Z., Zhao H., Chen J., Xiong L., He Q., Chen T., Roszik J., Bernatchez C., Woodman S.E., et al. Loss of IFN-γ Pathway Genes in Tumor Cells as a Mechanism of Resistance to Anti-CTLA-4 Therapy. *Cell.* **2016**;167:397–404.e9. doi:10.1016/j.cell.2016.08.069.

**95.** Stelloo E., Versluis M.A., Nijman H.W., De Bruyn M., Plat A., Osse E.M., Van Dijk R.H., Nout R.A., Creutzberg C.L., De Bock G.H., et al. Microsatellite instability derived JAK1 frameshift mutations are associated with tumor immune evasion in endometrioid endometrial cancer. *Oncotarget.* **2016**;7: 39885–39893. doi:10.18632/oncotarget.9414.

**96.** Smithy J.W., Moore L.M., Pelekanou V., Rehman J., Gaule P., Wong P.F., Neumeister V.M., Sznol M., Kluger H.M., Rimm D.L. Nuclear IRF-1 expression as a mechanism to assess "Capability" to express PD-L1 and response to PD-1 therapy in metastatic melanoma. *J. Immunother. Cancer.* **2017**;5:1–9. doi:10.1186/s40425-017-0229-2.

**97.** Bhat M.Y., Solanki H.S., Advani J., Khan A.A., Keshava Prasad T.S., Gowda H., Thiyagarajan S., Chatterjee A. Comprehensive network map of interferon gamma signaling. *J. Cell Commun. Signal.* **2018**;12:745–751. doi:10.1007/s12079-018-0486-y.

**98.** Ivashkiv L.B., Donlin L.T. Regulation of type i interferon responses. *Nat. Rev. Immunol.* **2014**; 14:36–49. doi:10.1038/nri3581.

**99.** Propper D.J., Chao D., Braybrooke J.P., Bahl P., Thavasu P., Balkwill F., Turley H., Dobbs N., Gatter K., Talbot D.C., et al. Low-Dose IFN-γ Induces Tumor MHC Expression in Metastatic Malignant Melanoma. *Clin. Cancer Res.* **2003**; 9:84–92.

**100.** Yang I., Kremen T.J., Giovannone A.J., Paik E., Odesa S.K., Prins R.M., Liau L.M. Modulation of major histocompatibility complex Class I molecules and major histocompatibility complex-bound immunogenic peptides induced by interferon-α and interferon-γ treatment of human glioblastoma multiforme. *J. Neurosurg.* **2004**;100:310–319. doi:10.3171/jns.2004.100.2.0310.

**101.** George P.M., Badiger R., Alazawi W., Foster G.R., Mitchell J.A. Pharmacology and therapeutic potential of interferons. *Pharmacol. Ther.* **2012**;135:44–53. doi:10.1016/j.pharmthera.2012.03.006.

**102.** Hemmerle T., Neri D. The dose-dependent tumor targeting of antibody-IFNγ fusion proteins reveals an unexpected receptor-trapping mechanism in vivo. *Cancer Immunol. Res.* **2014**;2:559–567. doi:10.1158/2326-6066.CIR-13-0182.

**103.** Yang Y., Lim O., Kim T.M., Ahn Y.O., Choi H., Chung H., Min B., Her J.H., Cho S.Y., Keam B., et al. Phase I study of random healthy donor-derived allogeneic natural killer cell therapy in patients with malignant lymphoma or advanced solid tumors. *Cancer Immunol. Res.* **2016**;4:215–224. doi:10.1158/2326-6066.CIR-15-0118.

**104.** Cho Y.-H., Choi M.G., Kim D.H., Choi Y.J., Kim S.Y., Sung K.J., Lee J.C., Kim S.-Y., Rho J.K., Choi C.M. Natural Killer Cells as a Potential Biomarker for Predicting Immunotherapy Efficacy in Patients with Non-Small Cell Lung Cancer. *Target. Oncol.* **2020**;15:241–247. doi:10.1007/s11523-020-00712-2.

**105.** Mazzaschi G., Facchinetti F., Missale G., Canetti D., Madeddu D., Zecca A., Veneziani M., Gelsomino F., Goldoni M., Buti S., et al. The circulating pool of functionally competent NK and CD8+ cells predicts the outcome of anti-PD1 treatment in advanced NSCLC. *Lung Cancer.* **2019**;127:153–163. doi:10.1016/j.lungcan.2018.11.038.

**106.** Castriconi R., Dondero A., Augugliaro R., Cantoni C., Carnemolla B., Sementa A.R., Negri F., Conte R., Corrias M.V., Moretta L., et al. Identification of 4Ig-B7-H3 as a neuroblastoma-associated molecule that exerts a protective role from an NK cell-mediated lysis. *Proc. Natl. Acad. Sci. USA.* **2004**;101:12640–12645. doi:10.1073/pnas.0405025101.

**107.** Lee Y.H., Martin-Orozco N., Zheng P., Li J., Zhang P., Tan H., Park H.J., Jeong M., Chang S.H., Kim B.S., et al. Inhibition of the B7-H3 immune checkpoint limits tumor growth by enhancing cytotoxic lymphocyte function. *Cell Res.* **2017**;27:1034–1045. doi:10.1038/cr.2017.90.

**108.** Hu Y., Tian Z., Zhang C. Natural Killer Cell-Based Immunotherapy for Cancer: Advances and Prospects. *Engineering.* **2019**;5:106–114. doi:10.1016/j.eng.2018.11.015.

**109.** Bernson E., Hallner A., E Sander F., Wilsson O., Werlenius O., Rydström A., Kiffin R., Brune M., Foà R., Aurelius J., et al. Impact of killer-immunoglobulin-like receptor and human leukocyte antigen genotypes on the efficacy of immunotherapy in acute myeloid leukemia. *Leuk.* **2017**;31:2552–2559. doi:10.1038/leu.2017.151.

**110.** Boudreau J.E., Giglio F., Gooley T.A., Stevenson P.A., Le Luduec J.-B., Shaffer B.C., Rajalingam R., Hou L., Hurley C.K., Noreen H., et al. KIR3DL1/HLA-B Subtypes Govern Acute Myelogenous Leukemia Relapse After Hematopoietic Cell Transplantation. *J. Clin. Oncol.* **2017**;35:2268–2278. doi:10.1200/JCO.2016.70.7059.

**111.** Lupo K.B., Matosevic S. Natural Killer Cells as Allogeneic Effectors in Adoptive Cancer Immunotherapy. *Cancers.* **2019**;11:769. doi:10.3390/cancers11060769.

**112.** Dondero A., Pastorino F., Della Chiesa M., Corrias M.V., Morandi F., Pistoia V., Olive D., Bellora F., Locatelli F., Castellano A., et al. PD-L1 expression in metastatic neuroblastoma as an additional mechanism for limiting immune surveillance. *Oncoimmunology.* **2016**;5:1–9. doi:10.1080/2162402X.2015.1064578.

**113.** Chen S., Crabill G.A., Pritchard T.S., McMiller T.L., Wei P., Pardoll D.M., Pan F., Topalian S.L. Mechanisms regulating PD-L1 expression on tumor and immune cells. *J. Immunother. Cancer.* **2019**;7:1–12. doi:10.1186/s40425-019-0770-2.

**114.** Chew G.-L., Campbell A.E., De Neef E., Sutliff N.A., Shadle S.C., Tapscott S.J., Bradley R.K. DUX4 Suppresses MHC Class I to Promote Cancer Immune Evasion and Resistance to Checkpoint Blockade. *Dev. Cell.* **2019**;50: 658–671.e7. doi:10.1016/j.devcel.2019.06.011.

**115.** Bosnakovski D., da Silva M.T., Sunny S.T., Ener E.T., Toso E.A., Yuan C., Cui Z., Walters M.A., Jadhav A., Kyba M. A novel P300 inhibitor reverses DUX4-mediated global histone H3 hyperacetylation, target gene expression, and cell death. *Sci. Adv.* **2019**;5:eaaw7781. doi:10.1126/sciadv.aaw7781.

**116.** Lasko L.M., Jakob C.G., Edalji R.P., Qiu W., Montgomery D., Digiammarino E.L., Hansen T.M., Risi R.M., Frey R., Manaves V., et al. Discovery of a selective catalytic p300/CBP inhibitor that targets lineage-specific tumours. *Nature.* **2017**;550:128–132. doi:10.1038/nature24028.

**117.** Oliva J., Galasinski S., Richey A., Campbell A.E., Meyers M.J., Modi N., Zhong J.W., Tawil R., Tapscott S.J., Sverdrup F.M. Clinically advanced p38 inhibitors suppress DUX4 expression in cellular and animal models of facioscapulohumeral muscular dystrophys. *J. Pharmacol. Exp. Ther.* **2019**;370:219–230. doi:10.1124/jpet.119.259663.

**118.** Yong H.Y., Koh M.S., Moon A. The p38 MAPK inhibitors for the treatment of inflammatory diseases and cancer. *Expert Opin. Investig. Drugs.* **2009**;18:1893–1905. doi:10.1517/13543780903321490.

**119.** Ding L.W., Sun Q.Y., Lin D.C., Chien W., Hattori N., Dong X.M., Gery S., Garg M., Doan N.B., Said J.W., et al. LNK (SH2B3): Paradoxical effects in ovarian cancer. *Oncogene.* **2015**; 34:1463–1474. doi:10.1038/onc.2014.34.

**120.** Ding L.W., Sun Q.Y., Edwards J.J., Fernández L.T., Ran X.B., Zhou S.Q., Scolyer R.A., Wilmott J.S., Thompson J.F., Doan N., et al. LNK suppresses interferon signaling in melanoma. *Nat. Commun.* **2019**; 10 doi:10.1038/s41467-019-09711-y.

**121.** Kriegel A.J., Baker M.A., Liu Y., Liu P., Cowley A.W., Liang M. Endogenous MicroRNAs in human microvascular endothelial cells regulate mRNAs encoded by hypertension-related genes. *Hypertension.* **2015**;66:793–799. doi:10.1161/HYPERTENSIONAHA.115.05645.

**122.** Wang Y., Jin B.J., Chen Q., Yan B.J., Liu Z.L. MicroRNA-29b upregulation improves myocardial fibrosis and cardiac function in myocardial infarction rats through targeting SH2B3. *Eur. Rev. Med. Pharmacol. Sci.* **2019**;23:10115–10122. doi:10.26355/eurrev_201911_19581.

**123.** Saitoh T., Tun-Kyi A., Ryo A., Yamamoto M., Finn G., Fujita T., Akira S., Yamamoto N., Lu K.P., Yamaoka S. Negative regulation of interferon-regulatory factor 3-dependent innate antiviral response by the prolyl isomerase Pin1. *Nat. Immunol.* **2006**;7:598–605. doi:10.1038/ni1347.

**124.** Chen Y., Wu Y., Yang H., Li X., Jie M., Hu C., Wu Y., Yang S., Yang Y. Prolyl isomerase Pin1: A promoter of cancer and a target for therapy. *Cell Death Dis.* **2018**;9 doi:10.1038/s41419-018-0844-y.

**125.** Hennig L., Christner C., Kipping M., Schelbert B., Rücknagel K.P., Grabley S., Küllertz G., Fischer G. Selective inactivation of parvulin-like peptidyl-prolyl cis/trans isomerases by juglone. *Biochemistry.* **1998**;37:5953–5960. doi:10.1021/bi973162p.

**126.** Zhang X., Zhang B., Gao J., Wang X., Liu Z. Regulation of the MicroRNA 200b (miRNA-200b) by transcriptional regulators PEA3 and ELK-1 protein affects expression of Pin1 protein to control anoikis. *J. Biol. Chem.* **2013**;288:32742–32752. doi:10.1074/jbc.M113.478016.

**127.** Luo M.L., Gong C., Chen C.H., Lee D.Y., Hu H., Huang P., Yao Y., Guo W., Reinhardt F., Wulf G., et al. Prolyl isomerase pin1 acts downstream of mir200c to promote cancer stem-like cell traits in breast cancer. *Cancer Res.* **2014**;74: 3603–3616. doi:10.1158/0008-5472.CAN-13-2785.

**128.** Lee K.H., Lin F.C., Hsu T.I., Lin J.T., Guo J.H., Tsai C.H., Lee Y.C., Lee Y.C., Chen C.L., Hsiao M., et al. MicroRNA-296-5p (miR-296-5p) functions as a tumor suppressor in prostate cancer by directly targeting Pin1. *Biochim. Biophys. Acta Mol. Cell Res.* **2014**;1843:2055–2066. doi:10.1016/j.bbamcr.2014.06.001.

**129.** Wei S., Kozono S., Kats L., Nechama M., Li W., Guarnerio J., Luo M., You M.H., Yao Y., Kondo A., et al. Active Pin1 is a key target of all-trans retinoic acid in acute promyelocytic leukemia and breast cancer. *Nat. Med.* **2015**; 21:457–466. doi:10.1038/nm.3839.

**130.** Campaner E., Rustighi A., Zannini A., Cristiani A., Piazza S., Ciani Y., Kalid O., Golan G., Baloglu E., Shacham S., et al. A covalent PIN1 inhibitor selectively targets cancer cells by a dual mechanism of action. *Nat. Commun.* **2017**; 8 doi:10.1038/ncomms15772.

**131.** Myers M.P., Andersen J.N., Cheng A., Tremblay M.L., Horvath C.M., Parisien J.P., Salmeen A., Barford D., Tonks N.K. TYK2 and JAK2 Are Substrates of Protein-tyrosine Phosphatase 1B. *J. Biol. Chem.* **2001**;276:47771–47774. doi:10.1074/jbc.C100583200.

**132.** You M., Yu D.-H., Feng G.-S. Shp-2 Tyrosine Phosphatase Functions as a Negative Regulator of the Interferon-Stimulated Jak/STAT Pathway. *Mol. Cell. Biol.* **1999**;19:2416–2424. doi:10.1128/MCB.19.3.2416.

**133.** Bollu L.R., Mazumdar A., Savage M.I., Brown P.H. Molecular pathways: Targeting protein tyrosine phosphatases in cancer. *Clin. Cancer Res.* **2017**;23:2136–2142. doi:10.1158/1078-0432.CCR-16-0934.

**134.** Yi T., Pathak M.K., Lindner D.J., Ketterer M.E., Farver C., Borden E.C. Anticancer Activity of Sodium Stibogluconate in Synergy with IFNs. *J. Immunol.* **2002**;169:5978–5985. doi:10.4049/jimmunol.169.10.5978.

**135.** Lantz K.A., Hart S.G.E., Planey S.L., Roitman M.F., Ruiz-White I.A., Wolfe H.R., McLane M.P. Inhibition of PTP1B by trodusquemine (MSI-1436) causes fat-specific weight loss in diet-induced obese mice. *Obesity.* **2010**; 18:1516–1523. doi:10.1038/oby.2009.444.

**136.** Huffaker T.B., Lee S.H., Tang W.W., Wallace J.A., Alexander M., Runtsch M.C., Larsen D.K., Thompson J., Ramstead A.G., Voth W.P., et al. Antitumor immunity is defective in T cell–specific microRNA-155– deficient mice and is rescued by immune checkpoint blockade. *J. Biol. Chem.* **2017**;292:18530–18541. doi:10.1074/jbc.M117.808121.

**137.** Higgs G., Slack F. The multiple roles of microRNA-155 in oncogenesis. *J. Clin. Bioinforma.* **2013**;3:1–8. doi:10.1186/2043-9113-3-17.

**138.** Liu B., Mink S., Wong K.A., Stein N., Getman C., Dempsey P.W., Wu H., Shuai K. PIAS1 selectively inhibits interferon-inducible genes and is important in innate immunity. *Nat. Immunol.* **2004**;5:891–898. doi:10.1038/ni1104.

**139.** Yuan C., Qi J., Zhao X., Gao C. Smurf1 protein negatively regulates interferon-γ signaling through promoting STAT1 protein ubiquitination and degradation. *J. Biol. Chem.* **2012**;287:17006–17015. doi:10.1074/jbc.M112.341198.

**140.** Liu S., Jiang M., Wang W., Liu W., Song X., Ma Z., Zhang S., Liu L., Liu Y., Cao X. Nuclear RNF2 inhibits interferon function by promoting K33-linked STAT1 disassociation from DNA article. *Nat. Immunol.* **2018**;19:41–50. doi:10.1038/s41590-017-0003-0.

**141.** Sánchez-Beato M., Sánchez E., González-Carreró J., Morente M., Díez A., Sánchez-Verde L., Martín M.C., Cigudosa J.C., Vidal M., Piris M.A. Variability in the expression of polycomb proteins in different normal and tumoral tissues. A pilot study using tissue microarrays. *Mod. Pathol.* **2006;**19:684–694. doi:10.1038/modpathol.3800577.

**142.** Romero I., Martinez M., Garrido C., Collado A., Algarra I., Garrido F., Garcia-Lora A.M. The tumour suppressor Fhit positively regulates MHC class I expression on cancer cells. *J. Pathol.* **2012**;227:367–379. doi:10.1002/path.4029.

**143.** Rai K., Akdemir K.C., Kwong L.N., Fiziev P., Wu C.J., Keung E.Z., Sharma S., Samant N.S., Williams M., Axelrad J.B., et al. Dual roles of RNF2 in melanoma progression. *Cancer Discov.* **2015;**5:1314–1327. doi:10.1158/2159-8290.CD-15-0493.

**144.** Rabellino A., Andreani C., Scaglioni P.P. The Role of PIAS SUMO E3-Ligases in Cancer. *Cancer Res.* **2017**;77:1542–1547. doi:10.1158/0008-5472.CAN-16-2958.

**145.** Yang H., Yu N., Xu J., Ding X., Deng W., Wu G., Li X., Hou Y., Liu Z., Zhao Y., et al. SMURF1 facilitates estrogen receptor a signaling in breast cancer cells. *J. Exp. Clin. Cancer Res.* **2018**;37:1–12. doi:10.1186/s13046-017-0664-4.

**146.** Chen X., Chen S., Li Y., Gao Y., Huang S., Li H., Zhu Y. SMURF1-mediated ubiquitination of ARHGAP26 promotes ovarian cancer cell invasion and migration. *Exp. Mol. Med.* **2019**; 51 doi:10.1038/s12276-019-0236-0.

**147.** Nair S., Bist P., Dikshit N., Krishnan M.N. Global functional profiling of human ubiquitome identifies E3 ubiquitin ligase DCST1 as a novel negative regulator of Type-I interferon signaling. *Sci. Rep.* **2016**;6:1–13. doi:10.1038/srep36179.

**148.** Ismail I.H., McDonald D., Strickfaden H., Xu Z., Hendzel M.J. A small molecule inhibitor of polycomb repressive complex 1 inhibits ubiquitin signaling at DNA double-strand breaks. *J. Biol. Chem.* **2013**;288:26944–26954. doi:10.1074/jbc.M113.461699.

**149.** Cao Y., Wang C., Zhang X., Xing G., Lu K., Gu Y., He F., Zhang L. Selective small molecule compounds increase BMP-2 responsiveness by inhibiting Smurf1-mediated Smad1/5 degradation. *Sci. Rep.* **2014**;4:1–11. doi:10.1038/srep04965.

**150.** Zheng H., Qian J., Varghese B., Baker D.P., Fuchs S. Ligand-Stimulated Downregulation of the Alpha Interferon Receptor: Role of Protein Kinase D2. *Mol. Cell. Biol.* **2011**;31:710–720. doi:10.1128/MCB.01154-10.

**151.** Azoitei N., Cobbaut M., Becher A., Van Lint J., Seufferlein T. Protein kinase D2: A versatile player in cancer biology. *Oncogene.* **2018**;37: 1263–1278. doi:10.1038/s41388-017-0052-8.

**152.** Wei N., Chu E., Wipf P., Schmitz J.C. Protein kinase D as a potential chemotherapeutic target for colorectal cancer. *Mol. Cancer Ther.* **2014**;13:1130–1141. doi:10.1158/1535-7163.MCT-13-0880.

**153.** Tandon M., Salamoun J.M., Carder E.J., Farber E., Xu S., Deng F., Tang H., Wipf P., Wang Q.J. SD-208, a novel protein kinase D inhibitor, blocks prostate cancer cell proliferation and tumor Growth in Vivo by inducing G2/M cell cycle arrest. *PLoS ONE.* **2015**;10:1–19. doi:10.1371/journal.pone.0119346.

**154.** Meissner T.B., Li A., Biswas A., Lee K.H., Liu Y.J., Bayir E., Iliopoulos D., Van Den Elsen P.J., Kobayashi K.S. NLR family member NLRC5 is a transcriptional regulator of MHC class I genes. *Proc. Natl. Acad. Sci. USA.* **2010**;107: 13794–13799. doi:10.1073/pnas.1008684107.

**155.** Staehli F., Ludigs K., Heinz L.X., Seguín-Estévez Q., Ferrero I., Braun M., Schroder K., Rebsamen M., Tardivel A., Mattmann C., et al. NLRC5 Deficiency Selectively Impairs MHC Class I- Dependent Lymphocyte Killing by Cytotoxic T Cells. *J. Immunol.* **2012**;188: 3820–3828. doi:10.4049/jimmunol.1102671.

**156.** Kuenzel S., Till A., Winkler M., Häsler R., Lipinski S., Jung S., Grötzinger J., Fickenscher H., Schreiber S., Rosenstiel P. The Nucleotide-Binding Oligomerization Domain-Like Receptor NLRC5 Is Involved in IFN-Dependent Antiviral Immune Responses. *J. Immunol.* **2010**;184: 1990–2000. doi:10.4049/jimmunol.0900557.

**157.** Kobayashi K.S., Van Den Elsen P.J. NLRC5: A key regulator of MHC class I-dependent immune responses. *Nat. Rev. Immunol.* **2012**; 12:813–820. doi:10.1038/nri3339.

**158.** Ozcan M., Janikovits J., von Knebel Doeberitz M., Kloor M. Complex pattern of immune evasion in MSI colorectal cancer. *Oncoimmunology.* **2018**;7:1–10. doi :10.1080/2162402X.2018.1445453.

**159.** Yoshihama S., Roszik J., Downs I., Meissner T.B., Vijayan S., Chapuy B., Sidiq T., Shipp M.A., Lizee G.A., Kobayashi K.S. NLRC5/MHC class I transactivator is a target for immune evasion in cancer. *Proc. Natl. Acad. Sci. USA.* **2016**;113: 5999–6004. doi:10.1073/pnas.1602069113.

**160.** Rodriguez G.M., Bobbala D., Serrano D., Mayhue M., Champagne A., Saucier C., Steimle V., Kufer T.A., Menendez A., Ramanathan S., et al. NLRC5 elicits antitumor immunity by enhancing processing and presentation of tumor antigens to CD8+ T lymphocytes. *Oncoimmunology.* **2016**;5:1–12. doi:10.1080/2162402X.2016.1151593.

**161.** Tang F., Xu Y., Zhao B. NLRC5: New cancer buster? *Mol. Biol. Rep.* **2020**;47:2265–2277. doi:10.1007/s11033-020-05253-5.

**162.** Huynh J., Chand A., Gough D., Ernst M. Therapeutically exploiting STAT3 activity in cancer—using tissue repair as a road map. *Nat. Rev. Cancer.* **2019**;19:82–96. doi:10.1038/s41568-018-0090-8.

**163.** Blaskovich M.A., Sun J., Cantor A., Turkson J., Jove R., Sebti S.M. Discovery of JSI-124 (cucurbitacin I), a selective Janus kinase/signal transducer and activator of transcription 3 signaling pathway inhibitor with potent antitumor activity against human and murine cancer cells in mice. *Cancer Res.* **2003**;63: 1270–1279.

**164.** Nam S., Buettner R., Turkson J., Kim D., Cheng J.Q., Muehlbeyer S., Hippe F., Vatter S., Merz K.H., Eisenbrand G., et al. Indirubin derivatives inhibit Stat3 signaling and induce apoptosis in human cancer cells. *Proc. Natl. Acad. Sci. USA.* **2005**;102:5998–6003. doi:10.1073/pnas.0409467102.

**165.** Kotha A., Sekharam M., Cilenti L., Siddiquee K., Khaled A., Zervos A.S., Carter B., Turkson J., Jove R. Resveratrol inhibits Src and Stat3 signaling and induces the apoptosis of malignant cells containing activated Stat3 protein. *Mol. Cancer Ther.* **2006**;5:621–629. doi:10.1158/1535-7163.MCT-05-0268.

**166.** Schust J., Sperl B., Hollis A., Mayer T.U., Berg T. Stattic: A Small-Molecule Inhibitor of STAT3 Activation and Dimerization. *Chem. Biol.* **2006**;13:1235–1242. doi:10.1016/j.chembiol.2006.09.018.

**167.** Yang F., Van Meter T.E., Buettner R., Hedvat M., Liang W., Kowolik C.M., Mepani N., Mirosevich J., Nam S., Chen M.Y., et al. Sorafenib inhibits signal transducer and activator of transcription 3 signaling associated with growth arrest and apoptosis of medulloblastomas. *Mol. Cancer Ther.* **2008**;7:3519–3526. doi:10.1158/1535-7163.MCT-08-0138.

**168.** Xin H., Zhang C., Herrmann A., Du Y., Figlin R., Yu H. Sunitinib inhibition of Stat3 induces renal cell carcinoma tumor cell apoptosis and reduces immunosuppressive cells. *Cancer Res.* **2009**;69:2506–2513. doi:10.1158/0008-5472.CAN-08-4323.

**169.** McFarland B.C., Gray G.K., Nozell S.E., Hong S.W., Benveniste E.N. Activation of the NF-κB pathway by the STAT3 inhibitor JSI-124 in human glioblastoma cells. *Mol. Cancer Res.* **2013**;11:494–505. doi:10.1158/1541-7786.MCR-12-0528.

**170.** Zhu Y., Ye T., Yu X., Lei Q., Yang F., Xia Y., Song X., Liu L., Deng H., Gao T., et al. Nifuroxazide exerts potent anti-tumor and anti-metastasis activity in melanoma. *Sci. Rep.* **2016**;6:1–13. doi:10.1038/srep20253.

**171.** Yang H., Yamazaki T., Pietrocola F., Zhou H., Zitvogel L., Ma Y., Kroemer G. STAT3 inhibition enhances the therapeutic efficacy of immunogenic chemotherapy by stimulating type 1 interferon production by cancer cells. *Cancer Res.* **2015**;75:3812–3822. doi:10.1158/0008-5472.CAN-15-1122.

**172.** Lu C., Talukder A., Savage N.M., Singh N., Liu K. JAK-STAT-mediated chronic inflammation impairs cytotoxic T lymphocyte activation to decrease anti-PD-1 immunotherapy efficacy in pancreatic cancer. *Oncoimmunology.* **2017**;6:1–15. doi:10.1080/2162402X.2017.1291106.

**173.** Cohen E.E.W., Harrington K.J., Hong D.S., Mesia R., Brana I., Perez Segura P., Wise-Draper T., Scott M.L., Mitchell P.D., Mugundu G.M., et al. A phase Ib/II study (SCORES) of durvalumab (D) plus danvatirsen (DAN.; AZD9150) or AZD5069 (CX2i) in advanced solid malignancies and recurrent/metastatic head and neck squamous cell carcinoma (RM-HNSCC): Updated results. *Ann. Oncol. Off. J. Eur. Soc. Med. Oncol.* **2018**;29:viii372. doi:10.1093/annonc/mdy287.

**174.** D'amico S., Shi J., Martin B.L., Crawford H.C., Petrenko O., Reich N.C. STAT3 is a master regulator of epithelial identity and KRAS-driven tumorigenesis. *Genes Dev.* **2018**;32: 1175–1187. doi:10.1101/gad.311852.118.

**175.** Barber G.N. STING: Infection, inflammation and cancer. *Nat. Rev. Immunol.* **2015**;15:760–770. doi:10.1038/nri3921.

**176.** Abe T., Barber G.N. Cytosolic-DNA-Mediated, STING-Dependent Proinflammatory Gene Induction Necessitates Canonical NF- B Activation through TBK1. *J. Virol.* **2014**;88: 5328–5341. doi:10.1128/JVI.00037-14.

**177.** Challa S.V., Zhou S., Sheri A., Padmanabhan S., Meher G., Gimi R., Schmidt D., Cleary D., Afdhal N., Iyer R. Preclinical studies of SB 11285, a novel STING agonist for immuno-oncology. *J. Clin. Oncol.* **2017**;35:e14616. doi:10.1200/JCO.2017.35.15_suppl.e14616.

**178.** Wang-Bishop L., Wehbe M., Shae D., James J., Hacker B.C., Garland K., Chistov P.P., Rafat M., Balko J.M., Wilson J.T. Potent STING activation stimulates immunogenic cell death to enhance antitumor immunity in neuroblastoma. *J. Immunother. Cancer.* **2020**;8:1–17. doi:10.1136/jitc-2019-000282.

**179.** Ager C.R., Reilley M.J., Nicholas C., Bartkowiak T., Jaiswal A.R., Curran M.A. Intratumoral STING activation with T-cell checkpoint modulation generates systemic antitumor immunity. *Cancer Immunol. Res.* **2017**;5: 676–684. doi:10.1158/2326-6066.CIR-17-0049.

**180.** Ghaffari A., Peterson N., Khalaj K., Vitkin N., Robinson A., Francis J.A., Koti M. Sting agonist therapy in combination with pd-1 immune checkpoint blockade enhances response to carboplatin chemotherapy in high-grade serous ovarian cancer. *Br. J. Cancer.* **2018**; 119:440–449. doi:10.1038/s41416-018-0188-5.

**181.** Meric-Bernstam F., Sandhu S.K., Hamid O., Spreafico A., Kasper S., Dummer R., Shimizu T., Steeghs N., Lewis N., Talluto C.C., et al. Phase Ib study of MIW815 (ADU-S100) in combination with spartalizumab (PDR001) in patients (pts) with advanced/metastatic solid tumors or lymphomas. *J. Clin. Oncol.* **2019**; 37 doi:10.1200/JCO.2019.37.15_suppl.2507.

**182.** Seliger B., Harders C., Lohmann S., Momburg F., Urlinger S., Tampé R., Huber C. Down-regulation of the MHC class I antigen-processing machinery after oncogenic transformation of murine fibroblasts. *Eur. J. Immunol.* **1998**;28:122–133. doi:10.1002/(SICI)1521-4141(199801)28:01<122::AID-IMMU122>3.0.CO;2-F.

**183.** Herrmann F., Lehr H.A., Drexler I., Sutter G., Hengstler J., Wollscheid U., Seliger B. HER-2/neu-Mediated Regulation of Components of the MHC Class I Antigen-Processing Pathway. *Cancer Res.* **2004**;64:215–220. doi:10.1158/0008-5472.CAN-2522-2.

**184.** Bradley S.D., Chen Z., Melendez B., Talukder A., Khalili J.S., Rodriguez-Cruz T., Liu S., Whittington M., Deng W., Li F., et al. BRAFV600E co-opts a conserved MHC class I internalization pathway to diminish antigen presentation and CD8+ T-cell recognition of melanoma. *Cancer Immunol. Res.* **2015**;3: 602–609. doi:10.1158/2326-6066.CIR-15-0030.

**185.** Brea E.J., Oh C.Y., Manchado E., Budhu S., Gejman R.S., Mo G., Mondello P., Han J.E., Jarvis C.A., Ulmert D., et al. Kinase regulation of human MHC class i molecule expression on cancer cells. *Cancer Immunol. Res.* **2016**; 4:936–947. doi:10.1158/2326-6066.CIR-16-0177.

**186.** Versteeg R., Noordermeer I.A., Krüse-Wolters M., Ruiter D.J., Schrier P.I. c-myc down-regulates class I HLA expression in human melanomas. *EMBO J.* **1988**;7:1023–1029. doi:10.1002/j.1460-2075.1988.tb02909.x.

**187.** Yang W., Li Y., Gao R., Xiu Z., Sun T. MHC class I dysfunction of glioma stem cells escapes from CTL-mediated immune response via activation of Wnt/β-catenin signaling pathway. *Oncogene.* **2020**;39:1098–1111. doi:10.1038/s41388-019-1045-6.

**188.** Lulli D., Carbone M.L., Pastore S. The MEK inhibitors trametinib and cobimetinib induce a type I interferon response in human keratinocytes. *Int. J. Mol. Sci.* **2017**;18:2227. doi:10.3390/ijms18102227.

**189.** Watanabe S., Hayashi H., Haratani K., Shimizu S., Tanizaki J., Sakai K., Kawakami H., Yonesaka K., Tsurutani J., Togashi Y., et al. Mutational activation of the epidermal growth factor receptor down-regulates major histocompatibility complex class I expression via the extracellular signal-regulated kinase in non–small cell lung cancer. *Cancer Sci.* **2019**; 110:52–60. doi:10.1111/cas.13860.

**190.** Sapkota B., Hill C.E., Pollack B.P. Vemurafenib enhances MHC induction in BRAFV600E homozygous melanoma cells. *Oncoimmunology*. **2013**;2:e22890. doi:10.4161/onci.22890.

**191.** Mimura K., Ando T., Poschke I., Mougiakakos D., Johansson C.C., Ichikawa J., Okita R., Nishimura M.I., Handke D., Krug N., et al. T cell recognition of HLA-A2 restricted tumor antigens is impaired by the oncogene HER2. *Int. J. Cancer*. **2011**;128:390–401. doi:10.1002/ijc.25613.

**192.** Maruyama T., Mimura K., Sato E., Watanabe M., Mizukami Y., Kawaguchi Y., Ando T., Kinouchi H., Fujii H., Kono K. Inverse correlation of HER2 with MHC class i expression on oesophageal squamous cell carcinoma. *Br. J. Cancer*. **2010**; 103:552–559. doi:10.1038/sj.bjc.6605772.

**193.** Hastings K., Yu H.A., Wei W., Sanchez-Vega F., Deveaux M., Choi J., Rizvi H., Lisberg A., Truini A., Lydon C.A., et al. EGFR mutation subtypes and response to immune checkpoint blockade treatment in non-small-cell lung cancer. *Ann. Oncol*. **2019**;30:1311–1320. doi:10.1093/annonc/mdz141.

**194.** Zage P.E., Sirisaengtaksin N., Liu Y., Gireud M., Brown B.S., Palla S., Richards K.N., Hughes D.P.M., Bean A.J. UBE4B levels are correlated with clinical outcomes in neuroblastoma patients and with altered neuroblastoma cell proliferation and sensitivity to epidermal growth factor receptor inhibitors. *Cancer*. **2013**; 119:915–923. doi:10.1002/cncr.27785.

**195.** Leibowitz M.S., Srivastava R.M., Filho P.A.A., Egloff A.M., Wang L., Seethala R.R., Ferrone S., Ferris R.L. SHP2 is overexpressed and inhibits pSTAT1-mediated APM component expression, T cell attracting chemokine secretion, and CTL recognition in head and neck cancer cells. *Clin. Cancer Res*. **2013**;19: 798–808. doi:10.1158/1078-0432.CCR-12-1517.

**196.** Agazie Y.M., Hayman M.J. Molecular Mechanism for a Role of SHP2 in Epidermal Growth Factor Receptor Signaling. *Mol. Cell. Biol*. **2003**;23:7875–7886. doi:10.1128/MCB.23.21.7875-7886.2003.

**197.** Grandis J.R., Drenning S.D., Zeng Q., Watkins S.C., Melhem M.F., Endo S., Johnson D.E., Huang L., He Y., Kim J.D. Constitutive activation of stat3 signaling abrogates apoptosis in squamous cell carcinogenesis in vivo. *Proc. Natl. Acad. Sci. USA*. **2000**;97: 4227–4232. doi:10.1073/pnas.97.8.4227.

**198.** Garrido G., Rabasa A., Garrido C., Chao L., Garrido F., García-Lora Á.M., Sánchez-Ramírez B. Upregulation of HLA Class I Expression on Tumor Cells by the Anti-EGFR Antibody Nimotuzumab. *Front. Pharmacol*. **2017**;8: 1–11. doi:10.3389/fphar.2017.00595.

**199.** Srivastava R.M., Trivedi S., Concha-Benavente F., Hyun-Bae J., Wang L., Seethala R.R., Branstetter IV B.F., Ferrone S., Ferris R.L. Stat1-induced HLA class i upregulation enhances immunogenicity and clinical response to anti-EGFR mab cetuximab therapy in HNC patients. *Cancer Immunol. Res*. **2015**;3:936–945. doi:10.1158/2326-6066.CIR-15-0053.

**200.** Pollack B.P., Sapkota B., Cartee T.V. Epidermal growth factor receptor inhibition augments the expression of MHC class I and II genes. *Clin. Cancer Res*. **2011**;17:4400–4413. doi:10.1158/1078-0432.CCR-10-3283.

**201.** Freeman A.J., Vervoort S.J., Ramsbottom K.M., Kelly M.J., Michie J., Pijpers L., Johnstone R.W., Kearney C.J., Oliaro J. Natural Killer Cells Suppress T Cell-Associated Tumor Immune Evasion. *Cell Rep*. **2019**;28:2784–2794.e5. doi:10.1016/j.celrep.2019.08.017.

**202.** He S., Yin T., Li D., Gao X., Wan Y., Ma X., Ye T., Guo F., Sun J., Lin Z., et al. Enhanced interaction between natural killer cells and lung cancer cells: Involvement in gefitinib-mediated immunoregulation. *J. Transl. Med.* **2013**;11:1. doi:10.1186/1479-5876-11-186.

**203.** Van't Veer L.J., Beijersbergen R.L., Bernards R. N-myc suppresses major histocompatibility complex class I gene expression through down-regulation of the p50 subunit of NF-kappa B. *EMBO J.* **1993**;12:195–200. doi:10.1002/j.1460-2075.1993.tb05645.x.

**204.** Forloni M., Albini S., Limongi M.Z., Cifaldi L., Boldrini R., Nicotra M.R., Giannini G., Natali P.G., Giacomini P., Fruci D. NF-κB, and not MYCN, regulates MHC class I and endoplasmic reticulum aminopeptidases in human neuroblastoma cells. *Cancer Res.* **2010**; 70:916–924. doi:10.1158/0008-5472.CAN-09-2582.

**205.** Hodge J.W., Garnett C.T., Farsaci B., Palena C., Tsang K.Y., Ferrone S., Gameiro S.R. Chemotherapy-induced immunogenic modulation of tumor cells enhances killing by cytotoxic T lymphocytes and is distinct from immunogenic cell death. *Int. J. Cancer.* **2013**; 133:624–636. doi:10.1002/ijc.28070.

**206.** Khallouf H., Märten A., Serba S., Teichgräber V., Büchler M.W., Jäger D., Schmidt J. 5-fluorouracil and interferon-α immunochemotherapy enhances immunogenicity of murine pancreatic cancer through upregulation of NKG2D ligands and MHC class i. *J. Immunother.* **2012**;35:245–253. doi:10.1097/CJI.0b013e31824b3a76.

**207.** Wan S., Pestka S., Jubin R.G., Lyu Y.L., Tsai Y.C., Liu L.F. Chemotherapeutics and radiation stimulate MHC class i expression through elevated interferon-beta signaling in breast cancer cells. *PLoS ONE.* **2012**;7:e32542. doi:10.1371/journal.pone.0032542.

**208.** Iwai T., Sugimoto M., Wakita D., Yorozu K., Kurasawa M., Yamamoto K. Topoisomerase I inhibitor, irinotecan, depletes regulatory T cells and up-regulates MHC class I and PD-L1 expression, resulting in a supra-additive antitumor effect when combined with anti-PD-L1 antibodies. *Oncotarget.* **2018**;9:31411–31421. doi:10.18632/oncotarget.25830.

**209.** Alagkiozidis I., Facciabene A., Tsiatas M., Carpenito C., Benencia F., Adams S., Jonak Z., June C.H., Powell D.J., Coukos G. Time-dependent cytotoxic drugs selectively cooperate with IL-18 for cancer chemo-immunotherapy. *J. Transl. Med.* **2011**;9:77. doi:10.1186/1479-5876-9-77.

**210.** De Mora-García M.L., Duenas-González A., Hernández-Montes J., De la Cruz-Hernández E., Pérez-Cárdenas E., Weiss-Steider B., Santiago-Osorio E., Ortíz-Navarrete V.F., Rosales V.H., Cantú D., et al. Up-regulation of HLA class-I antigen expression and antigen-specific CTL response in cervical cancer cells by the demethylating agent hydralazine and the histone deacetylase inhibitor valproic acid. *J. Transl. Med.* **2006**;4:1–14. doi:10.1186/1471-2407-7-S1-A12.

**211.** Khan A.N.H., Gregorie C.J., Tomasi T.B. Histone deacetylase inhibitors induce TAP, LMP, Tapasin genes and MHC class I antigen presentation by melanoma cells. *Cancer Immunol. Immunother.* **2008**;57:647–654. doi:10.1007/s00262-007-0402-4.

**212.** Ritter C., Fan K., Paschen A., Reker Hardrup S., Ferrone S., Nghiem P., Ugurel S., Schrama D., Becker J.C. Epigenetic priming restores the HLA class-I antigen processing machinery expression in Merkel cell carcinoma. *Sci. Rep.* **2017**;7:1–11. doi:10.1038/s41598-017-02608-0.

**213.** Setiadi A.F., Omilusik K., David M.D., Seipp R.P., Hartikainen J., Gopaul R., Choi K.B., Jefferies W.A. Epigenetic enhancement of antigen processing and presentation promotes immune recognition of tumors. *Cancer Res.* **2008**;68:9601–9607. doi:10.1158/0008-5472.CAN-07-5270.

**214.** Suraweera A., O'Byrne K.J., Richard D.J. Combination therapy with histone deacetylase inhibitors (HDACi) for the treatment of cancer: Achieving the full therapeutic potential of HDACi. *Front. Oncol.* **2018**;8:1–15. doi:10.3389/fonc.2018.00092.

**215.** Serrano A., Tanzarella S., Lionello I., Mendez R., Traversari C., Ruiz-Cabello F., Garrido F. Expression of HLA class I antigens and restoration of antigen-specific CTL response in melanoma cells following 5-aza-2'-deoxycytidine treatment. *Int. J. Cancer.* **2001**; 94:243–251. doi:10.1002/ijc.1452.

**216.** Luo N., Nixon M.J., Gonzalez-Ericsson P.I., Sanchez V., Opalenik S.R., Li H., Zahnow C.A., Nickels M.L., Liu F., Tantawy M.N., et al. DNA methyltransferase inhibition upregulates MHC-I to potentiate cytotoxic T lymphocyte responses in breast cancer. *Nat. Commun.* **2018**;9:248. doi:10.1038/s41467-017-02630-w.

**217.** Fonsatti E., Nicolay H.J.M., Sigalotti L., Calabrò L., Pezzani L., Colizzi F., Altomonte M., Guidoboni M., Marincola F.M., Maio M. Functional up-regulation of human leukocyte antigen class I antigens expression by 5-aza-2'-deoxycytidine in cutaneous melanoma: Immunotherapeutic implications. *Clin. Cancer Res.* **2007**;13:3333–3338. doi:10.1158/1078-0432.CCR-06-3091.

**218.** Santin A.D., Hermonat P.L., Ravaggi A., Chiriva-Internati M., Pecorelli S., Parham G.P., Retinoic acid up-regulates the expression of major histocompatibility complex molecules and adhesion/costimulation molecules (specifically, intercellular adhesion molecule ICAM-1) in human cervical cancer. *Am. J. Obstet. Gynecol.* **1998**;179:1020-1025. doi:10.1016/s0002-9378(98)70209-1

**219.** Castriconi R., Dondero A., Cilli M., Ognio E., Pezzolo A., De Giovanni B., Gambini C., Pistoia V., Moretta L., Moretta A., et al. Human NK cell infusions prolong survival of metastatic human neuroblastoma-bearing NOD/scid mice. *Cancer Immunol. Immunother.* **2007**;56: 1733–1742. doi:10.1007/s00262-007-0317-0.

# Chapter 6

## A “No-Touch” Antibody-Staining Method of Adherent Cells for High-Throughput Flow Cytometry in 384-Well Microplate Format for Cell-Based Drug Library Screening

Annelisa M. Cornel[1], Celina L. Szanto[1], Niek P. van Til[1],
Jeroen F. van Velzen[1], Jaap J. Boelens[2], Stefan Nierkens[1,3]

*[1] Center for Translational Immunology, University Medical Center Utrecht, Utrecht University, The Netherlands*
*[2] Stem Cell transplantation and Cellular Therapies Program, Department Pediatrics, Memorial Sloan Kettering Cancer Center, New York, USA*
*[3] Princess Máxima Center for Pediatric Oncology, Utrecht University, 3584 CS Utrecht, The Netherlands*

*Cytometry A 2019 Dec 26;97(8), 845-851*

## ABSTRACT

In the last decade, screening compound libraries on live cells has become an important step in drug discovery. The abundance of compounds in these libraries requires effective high-throughput (HT) analyzing methods. Although current cell-based assay protocols are suitable for HT analyses, the analysis itself is often restrained to simple, singular outcomes. Incorporation of HT samplers on flow cytometers has provided an interesting approach to increase the number of measurable parameters and increase the sensitivity and specificity of analyses. Nonetheless, to date, the labor intensive and time-consuming strategies to detach and stain adherent cells before flow cytometric analysis has restricted use of HT flow cytometry (HTFC) to suspension cells. We have developed a universal “no-touch” HTFC antibody staining protocol in 384-well microplates to bypass washing and centrifuging steps of conventional flow cytometry protocols. Optimizing culture conditions, cell-detachment and staining strategies in 384-well microplates resulted in an HTFC protocol with an optimal stain index with minimal background staining. The method has been validated using six adherent cell lines and simultaneous staining of four parameters. This HT screening protocol allows for effective monitoring of multiple cellular markers simultaneously, thereby increasing informativity and cost-effectiveness of drug screening.

## INTRODUCTION

The new era of biologicals used in anticancer therapy shifts the focus of therapeutic intervention from achieving cell death to (immune) cell modulation, thereby making cells more susceptible to other compounds or immune clearance. Cell-based screening of drug libraries has become an important approach in discovering new drugs against these targets of interest. Biochemical assays are more and more replaced by cell-based assays, as they enable studying underlying cellular mechanisms [1]. Many cell-based assays have been developed in recent years, including functional, reporter, and phenotypic assays. Nonetheless, high-throughput (HT) cell-based screening is still limited by labor-intensive, expensive, and throughput limiting analyzing methods.

Equipment of flow cytometers with HT samplers (both 96- and 384-well format) has made otherwise low-throughput flow cytometry more suitable as a HT analyzing strategy [2]. In this way, whole 96-well microplates can be analyzed in as little as 15 min. One of the most favorable aspects of flow cytometry is the opportunity to multiplex the measurement of protein expression on the surface or in the cytosol of individual cells. In this way, multiple effects or the underlying mechanisms of drugs can be studied in more detail, contributing to the informativity of drug screens.

The application of HT flow cytometry (HTFC) multiparameter analysis may, however, still be compromised due to labor intensive and time-consuming staining protocols, especially when analyzing adherent cell types. As a result, HT microscopy (HTM) is currently recommended as the method of choice when analyzing adherent cells [3]. It is important to note that different research questions can be answered with HTM compared to HTFC. A major advantage of HTM analysis is that cells can be analyzed in their natural shape and effects of compounds on morphology can be assessed. Disadvantages of HTM are the requisite of multiple wash steps, causing cell loss, the fact that HTM output files are typically 10–100 times bigger and less straightforward to analyze, as well as the restricted potential to multiplex protein expression measurements when compared to HTFC [3]. This clearly indicates the potential of a "no-touch" antibody staining protocol to efficiently use HTFC to analyze protein expression on adherent cells.

A limited number of studies reports the preparation of adherent cells for HTFC [4-10]. The published protocols either involve one or more washing steps or use trypsin/EDTA to generate single-cell suspensions [4-7]. Washing steps may cause loss of cells, thereby hampering HT screening protocols, whereas trypsin is reported to potentially cause loss of surface antigen expression [8,9]. A recent article by Kaur and Esau describes a two-step protocol to prepare adherent cells for HTFC [10]. They show that the use of EDTA as a cell detachment reagent bypasses the need of washing, enzymatic inactivation, centrifugation, and transfer between plates, reducing cell loss and labor-intensity of the protocol [10]. Even though the report shows the 384-well protocol is compatible with several commercially available dyes to measure, for instance, apoptosis and production of reactive oxygen species, there is no data on the use of antibody staining to detect the dynamics of protein expression within or on the surface of the 384-well microplate seeded cells. The described universal protocol allows for antibody staining in 384-well format and is validated with six adherent cell lines, including neuroblastoma, cervical-, hepatocellular-, and breast cancer lines. We demonstrate that there is no difference in staining effectiveness between single and multiple stained samples, showing the potential of adherent-cell HTFC to increase the informativity of HT screening protocols.

## MATERIALS AND METHODS

### Cell Lines and Reagents

MCF-7 (human breast adenocarcinoma; ATCC HTB-22), SKBR3 (human breast adenocarcinoma; ATCC HTB30), HepG2 (human hepatocellular carcinoma; ATCC HB-8065), HeLa (human cervical adenocarcinoma; ATCC CCL-2), and HEK-293 T (human embryonic kidney; ATCC CRL-3216) cells were obtained from ATCC (Manassas, VA). The GIMEN neuroblastoma cell line was obtained from the Academic Medical Center of Amsterdam. GIMEN NFκB reporter cells were generated as previously described [11]. SKBR3 cells were maintained in RPMI 1640 GlutaMAX supplement medium (Life Technologies, Carlsbad, CA), supplemented with 10% FCS (Sigma-Aldrich, Steinheim, Germany) and 1% penicillin/streptomycin (50 U/ml, Life Technologies). GIMEN, HeLa, and HEK-293 T were maintained in Dulbecco's Modified eagle medium (DMEM) GlutaMAX supplement medium (Life Technologies), supplemented with 10% FCS (Sigma-Aldrich) and 1% penicillin/streptomycin (50 U/ml, Life Technologies).

### Cell Plating and Compound Addition

Cells were cultured in T75 flasks until 80% confluency, detached with 0.05% Trypsin/EDTA (Life Technologies), and counted using the Countess automated cell counter (Life Technologies). Optimal seeding density was determined. Cells were plated in a culture volume of 15 µl in a low flange, polystyrene, tissue culture treated, flat bottom 384-well tissue-culture treated microplate (stock number: 3764, lot: 22017037, Corning, NY) using a multidrop combi reagent dispenser (Life Technologies). Cells were cultured for 16–24 h under standard culturing conditions (5% CO2, 37°C), after which 5 µl of compound library would normally have been added to the cells using a liquid handling system, for example, the Sciclone G3 liquid handling system (PerkinElmer, Waltham, MA). As a proof of principle for this article, we added TNF-α and IFN-γ as a positive control for upregulation of the markers of interest [11]. TNF-α was added at a final concentration of 50 ng/µL (Miltenyi Biotec, Bergisch Gladbach, Germany), IFN-γ at a final concentration of 1,000 U/ml (R&D, Abingdon, UK). Cells were incubated in the presence of compounds for 16–24 h (5% CO2, 37°C) after which the effect on the protein(s) of interest was measured with HTFC.

## Sample Preparation for HTFC

EDTA (Life Technologies) was diluted with deionized $H_2O$ (pH = 6.14), after which the optimal EDTA concentration was determined. Addition of 5 µl 15 mM EDTA per well resulted in an optimal EDTA concentration of 3 mM per well. EDTA was added to the plate and after shaking at 1000 RPM with an orbital shaker (Heidolph Titramax 1,000; Schabwach, Germany) for 30 s, incubated at 37°C for 45 min to allow detachment of the cells. Plates were shaken again at 1000 RPM for 30 s, after which 5 µl antibody, diluted in serum-free medium, was added in the concentration established with titration. The following monoclonal antibodies have been used: AlexaFluor-647-labeled mouse-anti-human HLA-ABC (W6/32; Biolegend, London, UK), FITC-labeled mouse-anti-human HLA-ABC (W6/32, Sony Biotechnology, Weybridge, UK), APC-labeled mouse-anti-human CD274 (PD-L1) (Clone MIH1, Life Technologies), and PE-labeled mouse-anti-human CD54 (ICAM-1) (MEM-111, Exbio, London, UK). The nucleic acid dye 7-AAD (BD Biosciences, Eysins, Switzerland) was used for exclusion of nonviable cells. Gating was based on unstained samples and verified using conventional flow cytometry. Cell viability has been validated with the mitochondrial membrane potential dye tetramethylrhodamine (TMRM) at a concentration of 50 nM (Sigma-Aldrich). Addition of 50 uM carbonyl cyanide-4-(trifluoromethoxy)phenylhydrazone (FCCP), a mitochondrial oxidative phosphorylation uncoupler (Sigma-Aldrich), was used as a negative control for TMRM staining. Cells were incubated for 20 min on an orbital shaker at 4°C to allow for antibody staining (300 RPM). Subsequently, 50 µl of PBS supplemented with 2% FCS and 2 µM EDTA was added per well using the multidrop combi reagent dispenser to dilute the samples. Plates were kept on ice until analysis.

## Flow Cytometry and Analysis

Cells were acquired on the FACSCanto II HT sampler (BD Biosciences), by measuring a fixed volume of 50 µl sample per well at a flow rate of 3 µl/s. Analysis of a full 384-well plate will take about 100 min. Fluorescent-labeled beads (CS&T beads, Becton Dickinson) were used to check the performance and verify the optical path and stream flow of the flow cytometer. This procedure enables controlled standardized results and allows the determination of long-term drifts and incidental changes within the flow cytometer. No changes were observed which could affect the results. The data shown is a representation of at least six independent experiments. The Stain Index (SI) was used to reflect the ratio of separation between the positive and the negative population divided by two times the standard deviation (SD) of the negative population [12]. Data were analyzed using FACS Diva Version 8.0.1 (BD Bioscience), FlowJo version 10.1, and Graphpad Prism version 7.

### Statistical Analysis

The nonparametric Mann–Whitney U-test was performed for statistical testing between single-cell counts before and after optimization. P-values <0.05 are considered significant. A Z-score was calculated to define the difference in fluorescent intensity between medium- and cytokine-treated samples (n = 8 per group) using the following equation:

$$Z = \frac{\mathrm{X} - \mu}{\sigma}$$

In which X is the mean fluorescent intensity (MFI) of the cytokine treated group, μ is the mean MFI of the medium control group, and σ is the standard deviation of the medium control group. All data are shown ±SD.

## RESULTS

### Optimization of Cell Seeding Density, EDTA Concentration, and Cell Density during Analysis Results in a 12-Fold Increase in Single-Cell Retrieval

The first goal in the development of this HTFC protocol was to find a strategy to optimize reproducible cell retrieval, using the adherent edGIMEN neuroblastoma cell line. Initially, we adapted the cell detachment protocol of Kaur and Esau [10] to a 384-well format but were unable to achieve sufficient and reproducible cell retrieval (**Figure 1A**, before optimization).

First, cell seeding density was evaluated by seeding increasing numbers of cells per well. As expected, cell retrieval markedly improved when more cells were plated (**Figure 1B**). However, reproducibility of cell retrieval decreased when seeding density exceeded 5,000 cells/well, as observed by an increase in SD. Based on these data, it was concluded that a cell seeding density of 4,500 cells/well was optimal. Second, microscopic evaluation of the cell suspensions after different lengths of incubation periods with increasing EDTA concentrations revealed a minimum incubation time of 45 min and a minimum EDTA concentration of 3 mM (data not shown). Further increase

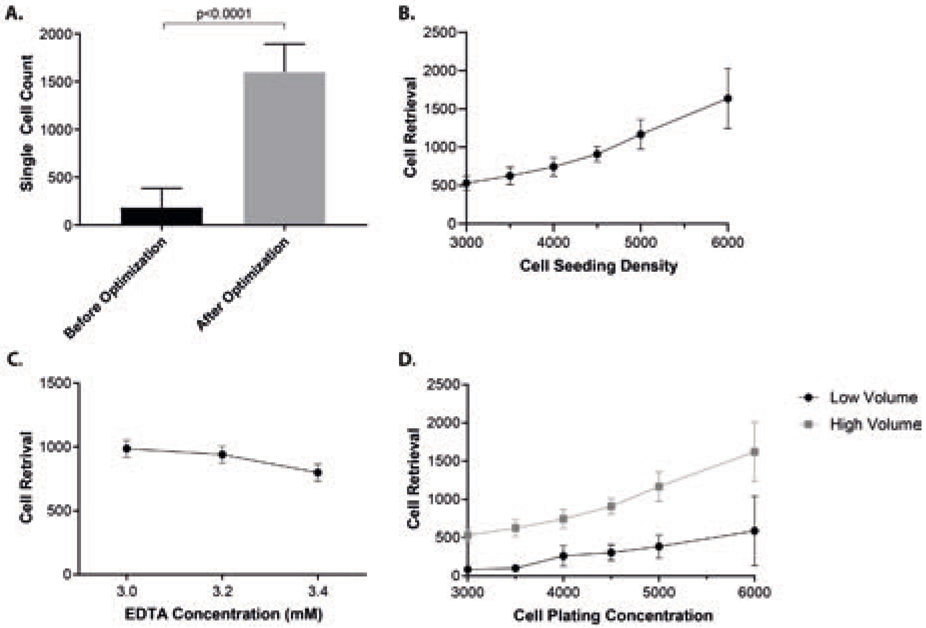

**Figure 1.** Optimization of flow cytometric cell retrieval using GIMEN cells.
*An over 12-fold increase in single-cell retrieval is observed upon sample preparation optimization.* ***(A)*** *Bar graph representing average single-cell retrieval prior to and after optimization. Before optimization: n = 60, after optimization: n = 7,153.* ***(B)*** *Graphical display of flow cytometric cell retrieval when increasing cell-seeding density.* ***(C)*** *Graphical display of cell retrieval after incubation with increasing EDTA concentrations at a seeding density of 4,500 cells/well, n = 2 per group.* ***(D)*** *Cell retrieval when well volume is 30 µL (low volume) or 80 µl (high volume). Graphs: Dots reflect mean, error bars reflect SD between samples, n = 6 per group unless otherwise indicated. Mann–Whitney U-test was performed, $p < 0.05$ was considered significant. SD = standard deviation.*

in the EDTA concentration to 3.2 and 3.4 mM did not result in further improvement of cell retrieval (**Figure 1C**). Finally, we assessed the effect of sample dilution prior to flow cytometric analysis. Dilution of the samples with 50 µL PBS supplemented with 2% FCS + 2 µM EDTA resulted in a 3.8-fold increase in cell retrieval (**Figure 1D**). Optimal cell seeding density, EDTA cell detachment concentration and incubation times, and final cell suspension density of the flow cytometry sample per well resulted in an over 12-fold increase in single-cell retrieval (**Figure 1A**). More than 90% of the nondebris cell population were single cells and flow rate was constant. 7-AAD and TMRM staining confirmed the cells were alive (**Figure S1**).

The reproducibility of the cell numbers retrieved with the protocol can be concluded from a HTFC compound screen we have performed utilizing this protocol, in which over 10,000 wells were analyzed with an average retrieval of 1,600 (±SD 294) alive single cells/well. This corresponds to 74% alive single cell retrieval when corrected for sampled volume.

### Optimized Antibody Staining Allows for (Multiplexed) Staining with Minimal Nonspecific Background Signal

Elimination of all washing steps from the HTFC protocol contributes to the HT nature of the protocol by decreasing the labor intensity, while minimizing cell loss inherent to washing. On the other hand, elimination of these steps also clearly indicates the need for antibody concentration titration. TNF-α and IFN-γ are involved in the upregulation of cell surface protein expression of MHC-I [11], CD54 (ICAM-1) [13, 14], and CD274 (PD-L1) [15] in several tumor cell types. Effects of these cytokines on protein expression have been validated for all utilized cell lines using conventional flow cytometry (shown for GIMEN; **Figure 2A** and **Figure S2**).

Decreasing the antibody concentration caused a clear decrease in background staining in medium-treated HLA-ABC stained MHC-I lacking GIMEN cells (**Figure 2B**). However, a marked decrease in the stain index between untreated and TNF-α + IFN-γ treated samples was observed when decreasing the antibody concentration (**Figure 2C**). This indicated a delicate balance between nonspecific background staining and discriminative ability of the antibody staining. Titration showed that HLA-ABC antibody concentration was optimal at a concentration of 8 ng/well (final concentration of 0.27 ng/µL). The HTFC staining protocol allows for distinct discrimination between HLA-ABC expression in untreated versus TNF-α-treated ($Z = 49$) and versus TNF-α + IFN-γ treated cells ($Z = 94$) ($n = 8$ per group), comparable with results from a typical conventional staining protocol (**Figure 2A**). The same effect is observed for the other utilized antibodies (**Figure S2**).

A unique aspect of flow cytometry is the opportunity to multiplex expression analysis of proteins on/in the same cell. Combining this aspect with HTS allows for an opportunity to increase the possibilities and informativity of HTS analysis. Combining antibody staining of HLA-ABC with the nucleic acid dye 7-AAD and antibody staining against PD-L1 and ICAM-1 revealed no noticeable differences in individual staining efficacy of the HTFC protocol, as shown for HLA-ABC antibody staining (**Figure 3A**).

We previously generated a GIMEN NFκB reporter cell line and found that TNF-α upregulates MHC-I expression in an NFκB-dependent manner, whereas IFN-γ-induced MHC-I upregulation is independent of NFκB [11]. Utilizing our HTFC protocol combining HLA-ABC antibody staining with evaluation of the intrinsic NFκB reporter expression confirmed NFκB (in)dependency of the observed MHC-I upregulations (**Figure 3B**). This shows that the protocol is also suitable to study the effects of compounds on intracellular transcription factors using reporter cell lines.

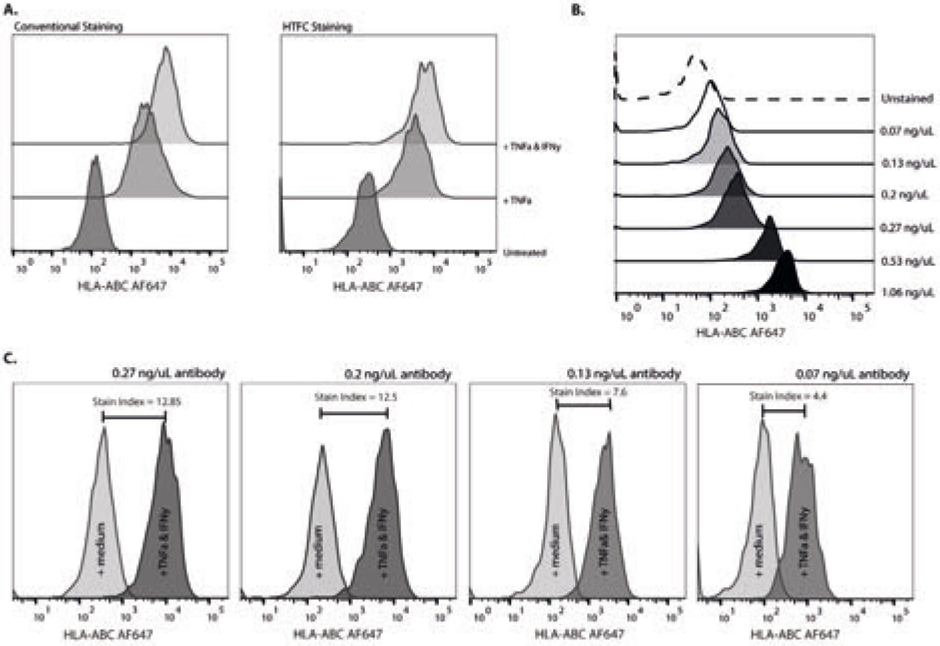

**Figure 2.** Antibody staining optimization in GIMEN cells.
***(A)*** *The optimized HTFC staining protocol (right) shows similar expression patterns to a typical conventional staining protocol (left). Z-score of expression in untreated versus TNF-α-treated cells is 49 (X = 1911, μ = 217, σ = 35), and 94 (X = 3,466, μ = 217, σ = 35) in TNF-α + IFN-γ treated cells (n = 8 per group).* ***(B)*** *HLA-ABC background staining decreases when antibody concentration (ng/μL) decreases. The dashed line represents the unstained control. (****C****) Histograms depicting HLA-ABC MFIs of untreated and TNF-α + IFN-γ-treated samples with diluting antibody concentrations. The stain index decreases when antibody concentration is reduced. Data shown are from a representative experiment using the HTFC protocol on GIMEN neuroblastoma cells. MFI = mean fluorescent intensity.*

## The Staining Protocol is Translatable to Multiple Cell Lines without any Modifications

The optimized HTFC protocol was subsequently performed using five additional cell lines, including breast cancer, cervical cancer, hepatocellular cancer, and human embryonal kidney cells. Retrieved single cell counts were lower (HepG2), comparable (MCF-7, SKBR3), or superior (HeLa, HEK293T) to the counts obtained in GIMEN neuroblastoma cells (**Figure S3**). Individual and multiplex HTFC staining was performed and validated with conventional flow cytometry staining (data not shown). The HepG2 and MCF-7 cell lines were selected based on their trypsinization resistant nature. The MCF-7 line shows sufficiently high and reproducible cell retrieval, even though we do observe more doublets, which were excluded from analysis (**Figure S3A**). In contrast, the slower growing, clumping HepG2 cells showed decreased cell counts, with an average single cell retrieval of 814 (n = 44, two individual experiments), but the counts were still sufficiently high and reproducible for reliable results (**Figure S3E**). This indicates the potential to translate the HTFC protocol universally to other adherent cell lines of interest, contributing to the versatility of the protocol.

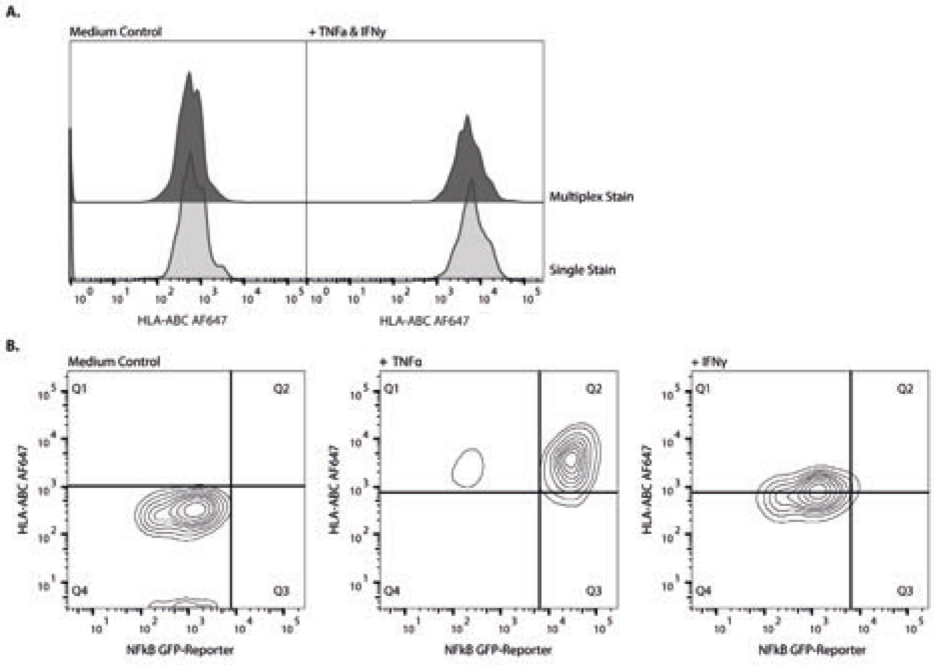

**Figure 3.** Multiplexed antibody staining in GIMEN cells.
*Multiplexing antibody staining using the HTFC protocol is technically feasible and as effective as singular staining.* ***(A)*** *HLA-ABC MFI in untreated controls (left) and TNF-α + IFN-γ-treated cells (right). Top graphs show the MFI in multiplexed stained samples, lower graphs show MFIs in single stained samples.* ***(B)*** *NFκB-GFP-reporter × HLA-ABC. Treatment of GIMEN NFκB GFP reporter cells with TNF-α or IFN-γ shows dependence of TNF-α induced upregulation of MHC-I, and independence of IFN-γ induced upregulation. Left graph: untreated control, middle graph: TNF-α-treated cells, right graph: IFN-γ-treated cells. Data shown are from a representative experiment using the HTFC protocol on GIMEN neuroblastoma cells. MFI = mean fluorescent intensity.*

## DISCUSSION AND CONCLUSION

HT cell-based screening of drug libraries is currently still limited by labor-intensive, time-consuming, expensive, and throughput limiting analyzing methods. The new era of biologicals used in anticancer therapy, including (immune) cell modulating biologicals, asks for novel, more delicate HT analyzing protocols to screen for effects beyond cell death. Cell surface expression of proteins is often key in treatment response to (immuno)therapies in cancer [11,16-21]. Screening for compounds affecting expression of these proteins may contribute to therapy efficacy in the future. For example, neuroblastoma immunotherapy efficacy is hampered by low MHC-I expression and requires upregulation [11], for which potential compounds can be selected by a compound screen. Similarly, novel compounds may affect immune checkpoint regulator expression as expression is correlated with poor survival in multiple cancers [16-21]. Here, we report the development of a universal "no-touch" HTFC antibody staining protocol in 384-well microplate format for adherent cells in which we are able to bypass washing and centrifuging steps of conventional flow cytometry protocols.

We have adapted a protocol from Kaur and Esau, in which the potential of EDTA as a nonenzymatic cell detachment agent in "no-touch" HTFC was demonstrated [10]. Using EDTA instead of enzymatic detachment agents bypasses the need of indispensible wash steps to wash away the fetal calf serum and to neutralize the enzymatic activity to decrease cell toxicity and potential antigen loss [4-9]. Bypassing washing steps not only contributes to the HT format of the protocol, but it also contributes to the cell retrieval by preventing cell loss, which is especially a problem when working with small cell numbers. Even though Kaur and Esau show their 384-well protocol is compatible with several commercially available dyes, they have not optimized the 384-well format protocol in combination with (multiplexed) antibody staining [10]. Furthermore, they show a clear need for cell line specific optimization of their protocol, limiting the throughput potential of the protocol.

Based on our data, decreasing the cell density prior to flow cytometric analysis markedly increased cell retrieval (3.8-fold). This indicates that cell density during analysis is a crucial factor in this protocol: when cell density is too high, the EDTA cannot avoid the tendency of cells to clump, thereby affecting (reproducibility of) cell retrieval. This also explains the reduction in reproducibility of the protocol when exceeding a seeding density of 5,000 cells/well. The fact that cell density rather than other cellular parameters is so critical in this protocol also emphasizes the universal potential of this protocol.

Analysis of the very slow growing and clumping HepG2 cell line with our protocol showed decreased cell retrieval when compared to the other cell lines. We believe this can be explained by the extreme adherent nature of the cells, as well as by the slow growth rate. This was further confirmed by an ~1.5-fold increase in average cell retrieval (average single-cell count = 1,115 (± SD = 236) (n = 9)), without a marked increase in variability between wells when increasing the plating density to 5,000 cells/well. Even though the unmodified protocol still gave sufficient cell retrieval, these results indicate that the protocol might benefit from cell plating density titration when analyzing slow-growing cell lines. However, the extreme clumping nature of the HepG2 line makes its suitability questionable for flow cytometry analysis in general, and alternative hepatocyte cell lines may be preferred.

It has been reported that EDTA could have a significant impact on antibody binding capacity [22], especially when the structure of the epitope depends on ions, such as calcium. It is therefore of importance to compare conventional and high-throughput staining protocols for every newly utilized antibody. Furthermore, more general, we recommend to include appropriate controls for every utilized antibody on every HTS plate to be able to monitor basal protein expression and antibody staining efficiency.

To the best of our knowledge, we are the first to report a universal "no-touch" HTFC antibody staining protocol for adherent cell lines in 384-well microplate format. We show that our protocol allows for multiplexing antibody staining and addition of reporter gene analysis, thereby improving the output of cell-based screening of drug libraries in a cost-efficient manner.

## REFERENCES

1. An WF, Tolliday N. Cell-Based Assays for High-Throughput Screening. *Mol. Biol.* **2010**; 45;180-186, doi:10.1007/s12033-010-9251-z.
2. Picot J, Guerin CL, Kim CLV, Boulanger CM. Flow Cytometry: retrospective, fundamentals and recent instrumentation. *Cytotechnology* **2012**;64(2);109-130, doi:10.1007/s10616-011-9415-0.
3. Black CB, Duensing TD, Trinkle LS, Dunlay RT. Cell-Based Screening Using High-Throughput Flow Cytometry. *Technol. Rev.* **2011**;9(1);13-20, doi:10.1089/adt.2010.0308.
4. Haynes MK, Strouse JJ, Waller A, Leitao A, Curpan RF, Bologa C, Oprea TI, Prossnitz ER, Edwards BS, Sklar LA et al. Detection of Intracellular Granularity Induction in Prostate Cancer Cell Lines by Small Molecules Using the HyperCyt® High- Throughput Flow Cytometry System. *J. Biomed. Screen.* **2009**;14;596-609, doi:10.1177/1087057109335671.
5. Young SM, Bologa CM, Fara D, Bryant BK, Strouse JJ, Arterburn JB, Ye RD, Oprea TI, Prossnitz ER, Sklar LA et al. Duplex High Throughput Flow Cytometry Screen Identifies Two Novel Formylpeptide Receptor Family Probes. *Cytometry* **2009**;75;253-263, doi: 10.1002/cyto.a.20645.
6. Glazer ES, Massey KL, Curley SA. A protocol to effectively create single cell suspensions of adherent cells for multiparameter high-throughput flow cytometry. *In Vitro Cell. Dev. Biol.* **2010**;46(2);97-101, doi:10.1007/s11626-009-9256-8.
7. Martinez EM, Klebanoff SD, Secrest S, Romain G, Haile ST, Emtage PCR, Gilbert AE. High-Throughput Flow Cytometric Method for the Simultaneous Measurement of CAR-T Cell Characterization and Cytotoxicity against Solid Tumor Cell Lines. *SLAS Discov.* **2018**;23(7); 603-612, doi:10.1177/2472555218768745.
8. Tsuji K, Ojima M, Otabe K, Ho rie M, Koga H, Sekiya I, Menuta T. Effects of Different Cell-Detaching Methods on the Viability and Cell Surface Antigen Expression of Synovial Mesenchymal Stem Cells. *Cell Transplant* **2017**;26(6);1089-1102, doi: 10.3727/096368917X694831.
9. Huang HL, Hsing HW, Lai TC, Chen YW, Lee TR, Chan HT, Lyu PC, Wu CL, Lu YC, Lin ST et al. Trypsin-induced proteome alteration during cell subculture in mammalian cells. *J. Biomed. Sci.* **2010**;17(1);36, doi:10.1186/1423-0127-17-36.
10. Kaur M, Esau L. Two-step protocol for preparing adherent cells for high-throughput flow cytometry. *Biotechniques* **2015**;59;119-126, doi:10.2144/000114325.
11. Spel L, Nieuwenhuis J, Haarsma R, Stickel E, Bleijerveld OB, Altelaar M, Boelens JJ, Brummelkamp TR, Nierkens S, Boes M. Nedd4 Binding Protein 1 (N4BP1) and TNFAIP3 Interacting Protein 1 (TNIP1) control MHC-1 display in neuroblastoma. *Cancer Res.* **2018**; epub ahead of print, doi:10.1158/0008-5472.CAN-18-0545.
12. Maecker HT, Frey T, Nomura LE, Trotter J. Selecting fluorochrome conjugates for maximum sensitivity. *Cytometry A* **2004**; 62(2);169-173, doi:10.1002/cyto.a.20092.
13. Chang YJ, Holtzman MJ, Chen CC. Interferon-γ-induced Epithelial ICAM-1 Expression and Monocyte Adhesion. *J. Biol. Chem.* **2002**;277(9);7118-7126, doi:10.1074/jbc.M109924200.
14. Ren G, Zhao X, Zhang L, Zhang J, L'Huillier A, Ling W, Roberts AI, Le AD, Shi S, Shao C et al. Inflammatory Cytokine-Induced Intercellular Adhesion Molecule-1 and Vascular Cell Adhesion Molecule-1 in Mesenchymal Stem Cells Are Critical for Immunosuppression. *J. Immunol.* **2010**;184;2321-2328, doi:10.4049/jimmunol.0902023.

15. Dondero A, Pastorino F, Della Chiesa M, Corrias MV, Morandi F, Pistoia V, Olive D, Bellora F, Locatelli F, Castellano A et al. PD-L1 expression in metastatic neuroblastoma as an additional mechanism for limiting immune surveillance. *Oncoimmunology* **2016**;5(1);e1064578, doi: 10.1080/2162402X.2015.1064578.
16. Hino R, Kabashima K, Kato Y, Yagi H, Nakamura M, Honjo T, Okazaki T et al. Tumor cell expression of programmed cell death-1 ligand 1 is a prognostic factor for malignant melanoma. *Cancer* **2010**;116(7);1757-1766, doi:10.1002/cncr.24899
17. Taube JM, Klein A, Brahmer JR, Xu H, Pan X, Kim JH, Chen L. Association of PD-1, PD-1 ligands, and other features of the tumor immune microenvironment with response to anti-PD-1 therapy. *Clin. Cancer Res.* **2014**; 20(19);5064-5074, doi:10.1158/1078-0432.CCR-13-3271
18. Pistillo MP, Tazzari PL, Palmisano GL, Pierri I, Bolognesi A, Ferlito F, Capanni P et al. CTLA-4 is not restricted to the lymphoid cell lineage and can function as a target molecule for apoptosis induction of leukemic cells. *Blood* **2003**;101(1);202-209, doi:10.1182/blood-2002-06-1668
19. Paulsen EE, Thomas KK, Rakaee M, Richardsen E, Hald SM, Andersen, S, Busund LT et al. CTLA-4 expression in the non-small cell lung cancer patient tumor microenvironment: diverging prognostic impact in primary tumors and lymph node metastases. *Cancer Immunol. Immunother.* **2017**;66(11);1449-1461, doi: 10.1007/s00262-017-2039-2
20. Zaretsky JM, Garcia-Diaz A, Shin DS, Escuin-Ordinas H, Hugo W, Hu-Lieskovan S, Torrejon DY et al. Mutations Associated with Acquired Resistance to PD-1 Blockade in Melanoma. *N. Engl. J. Med.* **2016**;375(9);819-829, doi: 10.1056/NEJMoa1604958
21. Pfirschke C, Engblom C, Rickelt S, Cortez-Retamozo V, Garris C, Pucci F, Yamazaki T et al. Immunogenic chemotherapy sensitizes tumors to checkpoint blockade therapy. *Immunity* **2016**;44(2);343-354, doi:10.1016/j.immuni.2015.11.024
22. Giroux M & Denis F. Influence of Calcium Ions in the Flow Cytometric Analysis of Human CD8-Positive Cells. *Cytometry* **2004**;62;61-64, doi:10.1002/cyto.a.20084

## SUPPLEMENTARY MATERIAL

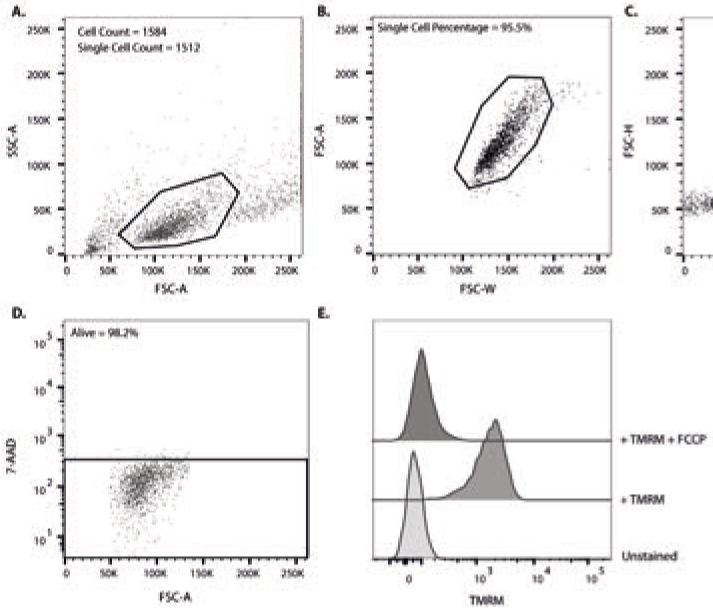

**Figure S1.** Flow cytometric characteristics of GIMEN cells after protocol optimization.
***(A)*** *FSC/SSC after optimization, gate reflects the non-debris population (total cell retrieval = 1,584, single cell retrieval = 1,512);* ***(B)*** *FSC-W/FSC-A graph of the non-debris population. Gate contains the single cell population (95.5% of non-debris population is single cell).* ***(C)*** *FSC-H/time were plotted against each other to detect potential drifts. Flow rate is constant.* ***(D)*** *7-AAD staining of single cell population. The gate contains the alive cell population (98.2% of the single cells are alive).* ***(E)*** *TMRM staining of single cell population. TMRM staining intensity in unstained cells (bottom), TMRM-stained cells (middle), and TMRM stained cells to which the mitochondrial oxidative phosphorylation uncoupler FCCP is added (top). Data shown are from a typical experiment using the HTFC protocol on GIMEN neuroblastoma cells and is representative of at least six independent experiments.*

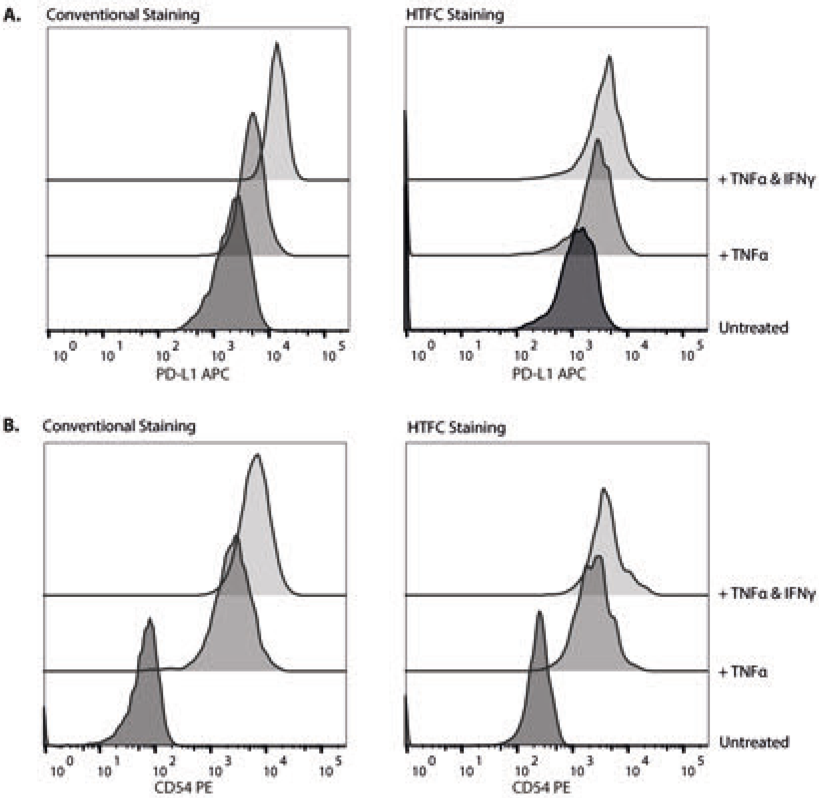

**Figure S2.** Flow cytometric characteristics of GIMEN cells after protocol optimization.
**(A**) *FSC/SSC after optimization, gate reflects the non-debris population (total cell retrieval = 1,584, single cell retrieval = 1,512);* ***(B)*** *FSC-W/FSC-A graph of the non-debris population. Gate contains the single cell population (95.5% of non-debris population is single cell).* ***(C)*** *FSC-H/time were plotted against each other to detect potential drifts. Flow rate is constant.* ***(D)*** *7-AAD staining of single cell population. The gate contains the alive cell population (98.2% of the single cells are alive).* ***(E)*** *TMRM staining of single cell population. TMRM staining intensity in unstained cells (bottom), TMRM-stained cells (middle), and TMRM stained cells to which the mitochondrial oxidative phosphorylation uncoupler FCCP is added (top). Data shown are from a typical experiment using the HTFC protocol on GIMEN neuroblastoma cells and is representative of at least six independent experiments.*

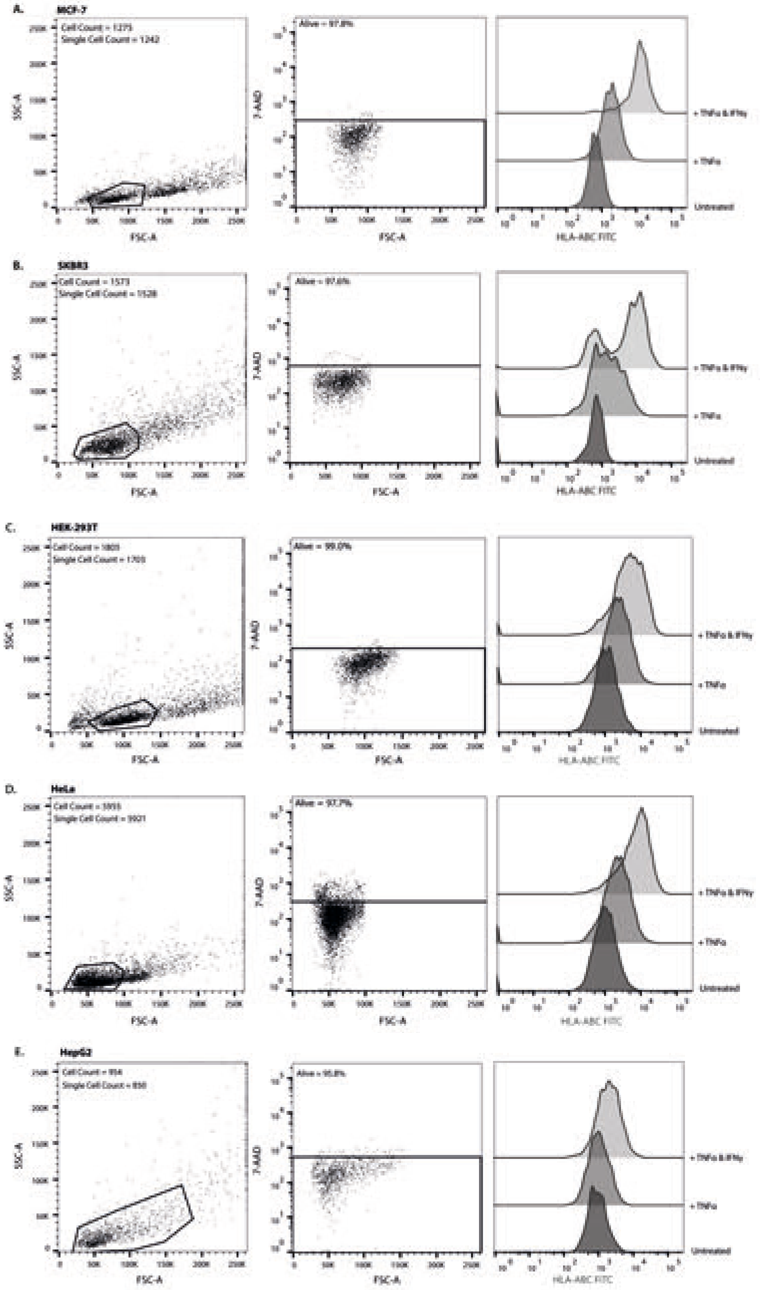

**Figure S3.** Cell retrieval and HLA-ABC antibody staining of additional analyzed cell lines analyzed with the unmodified HTFC staining protocol.

*Left: FSC/SSC of MCF-7* ***(A)****, SKBR3* ***(B)****, HEK-293 T* ***(C)****, HeLa* ***(D)****, and HepG2* ***(E)*** *cell lines, gate reflects the non-debris population. Single cell retrieval is based on exclusion via FSC-W/FSC-A characteristics (data not shown). Cells outside the non-debris gate are confirmed to be doublets. Middle: Viability of MCF-7* ***(A)****, SKBR3* ***(B)****, HEK-293 T* ***(C)****, and HeLa* ***(D)****, and HepG2* ***(E)*** *cell lines. Gating is based on unstained controls of the respective cell lines. Right: HLA-ABC staining intensity in untreated controls (bottom), TNF-α (middle) or TNF-α + IFN-γ (top) treated MCF-7* ***(A)****, SKBR3* ***(B)****, HEK-293 T* ***(C)****, HeLa* ***(D)****, and HepG2* ***(E)*** *cell lines. Data shown are from a representative experiment using the HTFC protocol on the respective cell line.*

# Chapter 7

## An efficient lentiviral transduction method to gene modify cord blood CD8+ T-cells for cancer therapy applications

Vania Lo Presti[1,2], Annelisa M. Cornel[1,2,*], Maud Plantinga[1,2,*], Ester Dünnebach[1,2], Jurgen Kuball[1,6], Jaap J. Boelens[1,6], Stefan Nierkens[1,2,*], Niek P. van Til[1,4,5,7]

*[1] Center for Translational Immunology, University Medical Center Utrecht, Utrecht University, The Netherlands*
*[2] Princess Máxima Center for Pediatric Oncology, Utrecht University, 3584 CS Utrecht, The Netherlands*
*[3] Stem Cell Transplant and Cellular Therapies, MSK Kids, Memorial Sloan Kettering Cancer Center, New York, USA*
*[4] AVROBIO, Inc., Cambridge, USA*
*[5] Child Neurology, Emma Children's Hospital, Amsterdam University Medical Centers, Vrije Universiteit and Amsterdam Neuroscience, Amsterdam, the Netherlands*
*[6] Department of Hematology, UMC Utrecht, Utrecht, the Netherlands*

** These authors contributed equally to this work*

*Adapted version*
*Molecular Therapy: Methods & Clinical Development 2021 Jun 11; 21, 357-368*

## ABSTRACT

Adoptive T-cell therapy utilizing tumor-specific autologous T-cells has shown promising results for cancer treatment. However, the limited number of autologous tumor-associated antigen (TAA)-specific T-cells and the functional aberrancies, due to disease progression or treatment, remain factors that may significantly limit the success of the therapy. The use of allogeneic T-cells, such as umbilical cord blood (CB) derived T-cells, overcomes these issues but requires gene modification to induce a robust and specific anti-tumor effect. CB T-cells are readily available in CB banks and show low toxicity, high proliferation rates, and increased anti-leukemic effect upon transfer. However, the combination of anti-tumor gene modification and preservation of advantageous immunological traits of CB T-cells represent major challenges for the harmonized production of T-cell therapy products. In this manuscript, we optimized a protocol for expansion and lentiviral vector (LV) transduction of CB CD8+ T-cells, achieving a transduction efficiency up to 83%. Timing of LV treatment, selection of culture media, and the use of different promoters were optimized in the transduction protocol. LentiBOOST was confirmed as a non-toxic transduction enhancer of CB CD8+ T-cells, with minor effects on the proliferation capacity and cell viability of the T-cells. Moreover, the use of LentiBOOST does not affect the functionality of the cells in the context of tumor cell recognition. Finally, CB CD8+ T-cells were more amenable to LV transduction than peripheral blood (PB) CD8+ T-cells and maintained a more naive phenotype. In conclusion, we show an efficient method to genetically modify CB CD8+ T-cells using LV, which is especially useful for the generation of off-the-shelf adoptive cell therapy products for cancer treatment. In the research described in this thesis, this protocol is exploited to generate TAA-specific (NK)T-cells to study effects on *in vitro* immunogenicity of Neuroblastoma.

## VISUAL ABSTRACT

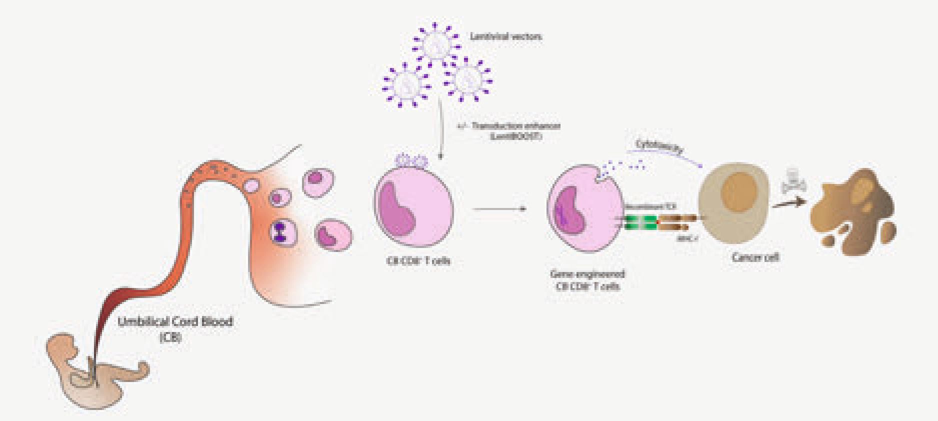
Lentiviral vectors
+/- Transduction enhancer (LentiBOOST)
Cytotoxicity
Recombinant TCR
MHC-I
CB CD8+ T cells
Gene engineered CB CD8+ T cells
Cancer cell
Umbilical Cord Blood (CB)

## INTRODUCTION

Adoptive T-cell therapy has developed into a promising treatment option for cancer patients in the last decade. The rationale towards efficient T-cell therapies is to redirect the patients' T-cells to tumor antigens, either by selection and ex vivo expansion of tumor-infiltrating lymphocytes (TILs) [1] or by genetic modification of lymphocytes. TIL therapy [1], combined with interleukin-2 (IL-2), has shown encouraging results in the treatment of metastatic melanoma patients, with a remission rate up to 72% [2,3]. Treatment with gene-modified T-cell products [4], such as chimeric antigen receptor (CAR) T-cells [5], has shown very promising results in several clinical trials [6], and Kymriah became the first approved cell therapy by the US Food and Drug Administration (FDA) and European Medicines Agency (EMA) for B-cell acute lymphoblastic leukemia (ALL) patients [7,8]. An alternative gene-modification strategy for the generation of a T-cell product is the transfer of a transgenic tumor-associated antigen (TAA)-specific T-cell receptor (TCR) recognizing a specific peptide in the context of major histocompatibility complexes (MHC). This strategy has been explored in several early-phase clinical trials, predominantly in melanoma, gastrointestinal cancer, and leukemia [9]. MART1-TCR-engineered T-cells persisted for at least 2 months after infusion in peripheral blood (PB) of 15 melanoma patients. Two patients showed high sustained levels of circulating MART1-specific T-cells and regression of metastatic melanoma lesions one year after infusion [10]. NY-ESO-TCR-engineered T-cells were well tolerated and exhibited an encouraging clinical response in multiple myeloma [11]. Post-transplantation transfer of Wilm's tumor 1 (WT1)-TCR-engineered T-cells prevented relapse in all acute myeloid leukemia (AML)-treated patients after a median of 44 months post-infusion [12]. These recent results indicate the potential of TCR engineering therapy, even when the tumor mutational burden is low, as, for example, in many childhood cancers [13].

A commonly used method for gene-modifying T-cells is the use of lentiviral vectors (LVs), which are highly efficient in transducing many cell types [14], including quiescent cells, to express a gene of interest. More specifically, the transduction efficiency in T-cells is not only dependent on the proliferation status but also on the activation status. The presence of sufficient numbers of functional patient-derived cells with adequate activation potential might be hampered by disease biology, disease progression, and/or previous therapies applied (such as chemotherapy) [15]. It has been reported that during chemotherapy cycles, T-cells drastically decrease in number [16]; show signs of senescence, low proliferation capacity and apoptotic pathway activation [17]; and require several months to return to physiological levels [18-20]. Together, the decline in numbers of naive T (Tn) cells and stem central memory T (Tscm) cells, as well as the reduced proliferation and stimulation, potentially limits the use of autologous T-cells for harmonized production of autologous T-cell therapy products.

A solution to overcome this problem is to utilize a patient-unrelated cell source, such as T-cells derived from healthy donors. Umbilical cord blood (CB)-derived T-cells are of particular interest, as they show a naive phenotype with elevated proliferation potential and low expression of exhaustion markers compared to PB-derived T-cells [21,22]. Additionally, Hiwarkar *et al.* [23] showed that CB CD8+ T-cells have an increased cytotoxic effect on human leukocyte antigen (HLA)-mismatched Epstein-Barr virus (EBV)-driven tumor cells compared to other sources. The use of CB-derived cells has been mostly limited to CD34+ hematopoietic stem cell (HSC) and progenitor cells, which are amenable to high lentiviral transduction rates [24-27]. The feasibility of the approach to introduce CARs [28-30] or recombinant TCRs (rTCRs) [31] into CB-derived T-cells has been shown mostly using non-viral gene transfer methods or retroviral vectors (RVs). However, as shown by Cieri *et al.* [32], the use of LV is superior to RV, especially for the transduction of Tn and central memory T (Tcm) cells. To date and to the best of our knowledge, the use of LV to gene modify CB-derived T-cells is very scarce but showed promising results [33].

In the present study, we developed an efficient method, using a serum-free transduction system, to transduce CB CD8+ T-cells with LV with limited effect on their naive immunophenotype. With the use of this protocol, CB CD8+ T-cells are more susceptible to LV transduction compared to PB CD8+ T-cells. In addition, we demonstrate how to further increase the transduction efficiency using the transduction enhancer LentiBOOST (LB) without altering CB CD8+ T-cells' functionality and maintaining the ability to expand *in vitro*, especially when using a low multiplicity of infection (MOI). Altogether, these results show efficient gene modification of CB CD8+ T-cells using LV to potentially generate off-the-shelf T-cell therapy products for cancer treatment.

## METHODS

### Lentiviral vector production and titration

HIV-derived, self-inactivating, third-generation LVs were constructed using the cytomegalovirus (CMV) promoter driving the expression of the viral transcript (pCCL plasmid backbone). Additionally to the packaging signal (ψ), the REV responsive element (RRE), and the central polypurine tract (cPPT), the transfer vector plasmid contains a modified Woodchuck post-translational regulatory element (bPRE4) [57,58]. Lentiviral particles coding for eGFP were produced by transient cotransfection of the lentiviral transfer vector plasmid (LV.eGFP) and the respective packaging plasmids (pRSV-Rev, pMDLg/pRRE, and pMD2-VSV-G) to HEK293T cells (ATCC CRL-3216) using the CalPhos Mammalian Transfection Kit (Clontech Laboratories), as previously described [59]. Viral supernatants were filtered through 0.45 µm low-protein-binding filters, concentrated by ultracentrifugation at 20,000 × g for 2 h, resuspended in StemMACS (Miltenyi Biotec), and stored at −80°C. We generated two LVs expressing promoter PGK.eGFP60 or a synthetic promoter MND.eGFP [61,62]. Additionally, two extra LVs were generated expressing a codon-optimized human TCR alpha- and beta-chain sequence, bridged by a T2A self-cleaving, recognizing pWT1-126 antigen [63,64] under the control of the MND promoter (MND.WT1-TCR) (**Figure 1**) and a CAR19 under the control of the PGK promoter (PGK.CAR19) (**Figure S2B**). VSV-G protein-pseudotyped lentiviral particles were titrated by serial dilution on Jurkat cells (clone E6-1; ATCC TIB-152). At 72 h post-transduction, cells were harvested and analyzed by flow cytometry for GFP expression, and viral titer was calculated.

### CD8+ T-cell isolation and expansion

Fresh CB or PB was collected after informed consent was obtained according to the Declaration of Helsinki. The collection protocol was approved by the Ethical Committee of the University Medical Center (UMC) Utrecht. CB or PB was processed to isolate CD8+ T-cells using Ficoll (GE Healthcare Bio-Sciences AB) separation and CD8-positive magnetic bead separation according to the manufacturer's protocol (Miltenyi Biotec). CD8+ T-cells were subsequently cultured in RPMI (Fisher Scientific), supplemented with 10% human serum; 1% penicillin/streptomycin (P/S) (cytotoxic T lymphocyte media [CTL media]), with aCD3/CD28 Dynabeads (Gibco; Thermo Fisher Scientific) in a 1:3 ratio (beads:T-cells); 50 U of IL-2/mL (UMC-Pharmacy); 5 ng/mL IL-7; and 5 ng/mL IL-15 (Miltenyi Biotec). CD8+ T-cells were kept in culture for 3 days, resulting in an average 4.5-fold expansion rate.

### T-cell transduction

Expanded and stimulated CD8+ T-cells were transduced at MOI 1 and 10 with two different methods: spinoculation and overnight incubation. For the spinoculation, T-cells were mixed and incubated with the LV for 30 min at room temperature and centrifuged for 30 min at 800 × g at 32°C. After the centrifugation step, transduction media were replaced with complete CTL media. For the overnight transduction, T-cells were mixed and incubated with the LV for 14–16 h, after which, transduction media were replaced with complete CTL media. We used two different transduction media: X-Vivo15 (Lonza) and StemMACS (Miltenyi Biotec), supplemented with 1% P/S, with or without supplementation of the transduction enhancer LB (1:100 of the total volume; SIRION Biotech).

## Vector Copy Number Determination

Genomic DNA was isolated from transduced cells using a Genomic DNA Purification kit (QIAGEN). qRT-PCR was performed with SYBR Green PCR Master Mix (Thermo Fisher Scientific) and primers targeting the U3 region (FW: 5'-CTGGAAGGGCTAATTCACTC-3') and Psi (RV: 5'-GGTTTCCCTTTCGCTTTCAA-3'). Amplification of the β-actin gene was used as a reference gene (FW primer: 5'-AGCGGGAAATCGTGCGTGAC-3'; R primer: 5'-CAATGGTGATGACCTGGCCGT-3'). Serial dilutions of a standard DNA plasmid containing one integrated copy of the LV sequence were used to plot a standard curve. Samples and standard serial dilutions were run in duplicate.

## CD8+ T-cell proliferation assay

Untransduced and transduced CD8+ T-cells were washed with PBS to remove serum that affects staining. Then, cells were suspended in PBS at a concentration of $2.4 \times 10^6$ cells/mL and labeled with the CTV Proliferation Kit (5 mM; Thermo Fisher Scientific) at 37°C for 20 min. Subsequently, cells were washed with warm fetal calf serum and resuspended in CTL media. After 24 h, cells were analyzed with flow cytometry to confirm CTV staining. Cells were stimulated with aCD3/CD28 Dynabeads in a ratio 1:8 (beads:T-cells) or with a tetramer molecule loaded with pWT1-126. After 4 and 7 days, T-cells were stained with Fixable Viability Dye and analyzed with flow cytometry to detect a decrease of CTV signal.

## Tetramer staining

A tetramer molecule was generated according to an established protocol [65], consisting of pWT1-126 stained with fluorescent-labeled streptavidin (phycoerythrin [PE] and PE-Cy7). Untransduced and transduced CD8+ T-cells were treated with dasatinib (VWR International) at a final concentration of 50 nM. Cells were incubated at 37°C for 30 min to allow stabilization of the TCR on the cell surface. Cells were subsequently washed once with fluorescence-activated cell sorting (FACS) buffer, after which the tetramer staining was initiated by adding approximately 0.1 µg per peptide:MHC complex and incubated 15 min at 37°C. Without washing, an antibody mix was added to the cells: CD8-APC (clone RPA-T8, ref. 555369; BD Pharmingen); CD3-Pacific Blue (clone UCHT1, ref. 558117; Becton Dickinson [BD]); Fixable Viability Dye eFluor 780 (ref. 65-0865-14; Thermo Fisher Scientific); and TCR Vβ21.3 (lone IG125, ref. PN IM1483; Beckman Coulter). Cells were incubated with the antibodies mix for 15 min at 4°C, washed, and analyzed on a BD Fortessa using FACSDiva.

## Killing assay and cytokine analysis

T2 cells (ATCC CRL-1992), were stained with CTV (following the method explained in CD8+ T-cell proliferation assay above) and subsequently pulsed with 1 µg/mL of pWT1-

126. T2 cells were co-cultured overnight with untransduced or transduced CB-CD8+ T-cells in a 1:1 or a 1:10 effector-to-target ratio (E:T). After 14–16 h, cells were stained with 7-AAD (BD Pharmingen), after which flow cytometry analysis was performed on a BD LSRFortessa using FACSDiva, with acquisition of a fixed amount of total volume for each sample. Cytokines in supernatants were measured using the LEGENDplex assay (BioLegend). Flow cytometry analysis was performed on a BD LSRFortessa using FACSDiva, and post-acquisition analysis was performed with LEGENDplex Data Analysis Software.

### Flow cytometry analysis

Transduced CD8+ T-cells were stained for 15 min at 4°C with fluorescently labeled antibodies against CD3-Pacific Blue (clone UCHT1, ref. 558117; BD) and CD8-PE (clone RPA-T8, ref. 301008; BioLegend); Fixable Viability Dye eFluor 780 (ref. 65-0865-14; Thermo Fisher Scientific) was used to evaluate transduction efficiency. Fresh, expanded, and transduced cells were stained with Fixable Viability Dye eFluor 780 (ref. 65-0865-14; Thermo Fisher Scientific), CD62L-BV650 (clone DREG-56, ref. 2124160; Sony Biotechnology), CD25-PerCP Cy5.5 (clone BC96, ref. 2113130; Sony Biotechnology), TIM3-APC (clone 34482, ref. FAB2365A; R&D Systems [R&D]), CD3-AF700 (clone UCHT1, ref. 300424; Sony Biotechnology), CD45RA-BV421 (clone HI100, ref. 304118; BioLegend), CD45RO-BV711 (clone UCHL1, ref. 304236; BioLegend), LAG3-PE (ref. FAB2319P; R&D), CD8-PE-Cy7 (clone SK1, ref. 335822; BD), TCR Vβ21.3 (clone IG125, ref. PN IM1483; Beckman Coulter), and CD19 CAR detection reagent (ref. AB_2811310; Miltenyi Biotec). Flow cytometry analysis was performed on a BD LSRFortessa using FACSDiva, with acquisition of a fixed number of cells for each experiment. FACS data analysis was performed using FlowJo version (v.)10 . Data are presented as percent of cells and as MFI.

### Statistical analysis

Statistical analyses were performed using GraphPad Prism v.6.00 for Windows (GraphPad Software, La Jolla, CA, USA). Due to the small number of samples, normality was assessed using QQ-plot visualization. One-way analysis of variance and Student's t test were used to determine differences between groups. The results are presented as average ± standard deviation (SD). p values are considered statistically significant when $*p \leq 0.05$.

## RESULTS

### Method optimization for efficient lentiviral transduction of CB CD8+ T-cells

Two different methods were compared for transduction efficiency: spinoculation and overnight incubation. 3 days after expansion, CB CD8+ T-cells were transduced with either enhanced green fluorescent protein (eGFP) under the control of the phosphoglycerate kinase (PGK.eGFP) promoter or a synthetic promoter that contains the U3 region of a modified Moloney murine leukemic virus (MoMuLV) long terminal repeat (LTR) with myeloproliferative sarcoma virus enhancer (MND.eGFP) at a MOI of 10 using X-Vivo15 media (**Figure 1**). With the use of spinoculation, 6 days after transduction, 24% ± 5% of CD8+ T-cells were GFP+ with the PGK.eGFP vector and 31% ± 9% with the MND.eGFP vector, whereas overnight incubation showed 48% ± 11% GFP+ cells for PGK.eGFP and 68% ± 8% for MND.eGFP (**Figure 2A**). Additionally, the use of two different types of media during the transduction strongly influenced the efficiency of transduction of CD8+ T-cells. Overnight culture in StemMACS HSC Expansion Media XF (StemMACS) showed a significant increase in the percentage of transduced cells up to 78% ± 7.7% for PGK.eGFP and 83% ± 8.8% for MND.eGFP in contrast to X-Vivo15 (**Figure 2B+C**). Hence, overnight incubation in StemMACS medium was used for further experiments (from hereafter referred to as STND protocol). No significant differences were observed in the percentage of transduced cells if the eGFP was under the control of the MND or the PGK promoter; however, the protein expression, calculated as median fluorescence intensity (MFI), increased significantly using the MND promoter. GFP-positive CB CD8+ T-cells showed a 3-fold increase in MFI compared to the CB CD8+ T-cells transduced with PGK.eGFP (**Figure 2D**), also when normalized for vector copy number (VCN) (**Figure 2E**).

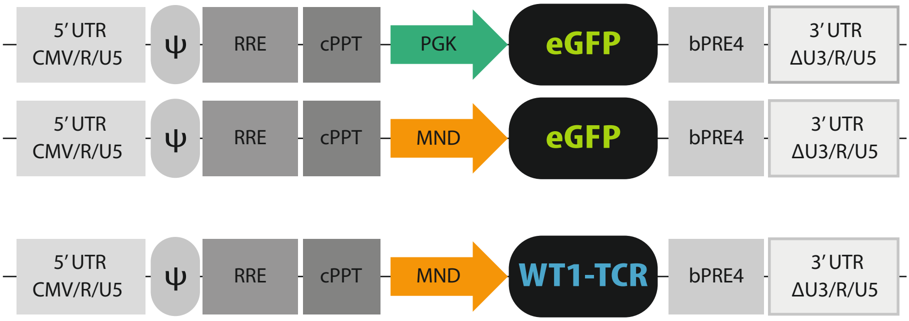

**Figure 1.** Schematic overview of lentiviral transfer vector plasmid maps.
*Third-generation self-inactivating (SIN) lentiviral vectors (LVs) were constructed using the CMV promoter driving the expression of the viral transcript (pCCL). The transfer vector contains the packaging signal (ψ), the REV responsive element (RRE), central polypurine tract (cPPT), and a modified Woodchuck post-translational regulatory element (bPRE4). Expression of the reporter gene eGFP was under the control of either the PGK or MND promoter (arrows). The WT1-TCR was under the control of the MND promoter.*

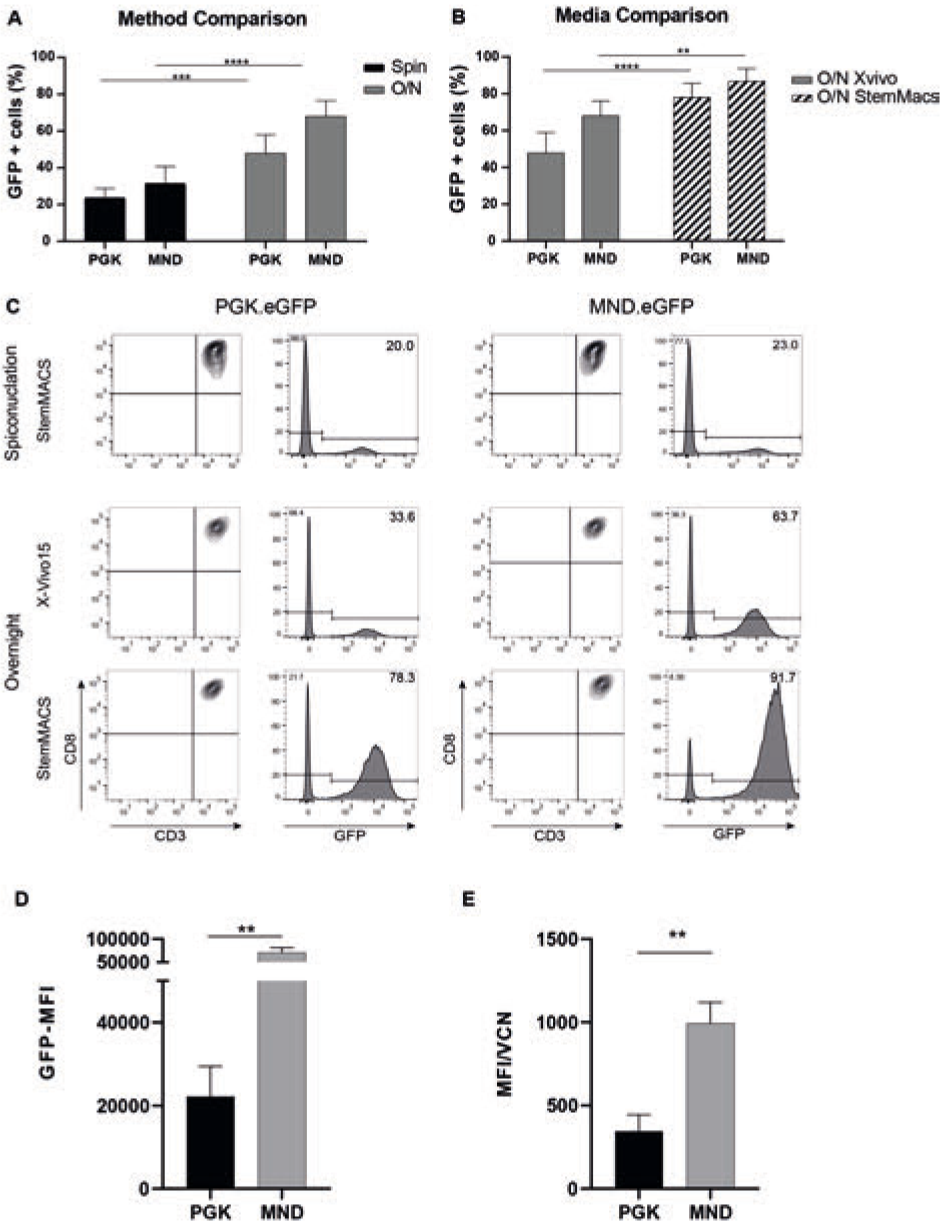

**Figure 2.** Optimization of the lentiviral transduction method for CB CD8+ T-cells.
***(A)** Transduction efficiency, presented as percentage of GFP+ cells, comparing two methods for T-cell transduction: spinoculation (black) and overnight incubation (gray). **(B)** Transduction efficiency, presented as percentage of GFP+ cells, comparing the use of different culture media during overnight transduction: X-Vivo15 (gray) and StemMACS media (stripes). **(C)** Representative flow cytometry plots of methods and media tested using both transduction with PGK.eGFP and MND.eGFP. The density plots are showing the measured CD3 and CD8 expression (on the left) and GFP expression in CD3+ CD8+ T-cells (on the right) in the left (PGK.eGFP) and right (MND.eGFP) panels. **(D)** Protein expression, presented as MFI of eGFP signal, is statistically increased using the MND promoter. **(E)** qPCR analysis of the VCN-positive correlates with the MFI results. The data correspond to ≥3 independent experiments and are shown as average ± standard deviation; $*p \leq 0.05$; $**p \leq 0.01$; $***p \leq 0.001$; $****p \leq 0.0001$.*

### CB CD8+ T-cells are more efficiently transduced than PB CD8+ T-cells with LV.MND.eGFP

Autologous PB T-cells are often the main cell source for adoptive cell therapy to treat cancer. Here, we developed a method to transduce allogeneic CB CD8+ T-cells, and hence, we compared the two T-cell sources for efficient transduction by LVs. PB CD8+ T-cells were isolated from healthy donors, expanded, and transduced following the same method developed for CB CD8+ T-cells. As shown in **Figures 3A+B**, this method transduces CB CD8+ T-cells more efficiently than PB CD8+ T-cells, which was observed using MND.eGFP.

The immunophenotype, based on markers for Tn cells (CD45RO, CD62L, CD45RA), of freshly isolated (day 0; fresh) T-cells substantially differs between CB CD8+ T-cells and PB CD8+ T-cells. As shown in **Figures 3C+D**, fresh CB CD8+ T-cells are characterized by a homogeneous population expressing classic Tn cell markers (CD45RO− CD62L+ CD45RA+), whereas fresh PB CD8+ T-cells consist of a more heterogeneous population containing Tn, effector memory [Tem] (CD45RO+CD62L-), and central memory [Tcm] (CD45RO+CD62L+) T-cells. During the expansion phase, characterized by the presence of cytokines and anti-CD3/CD28 (aCD3/CD28) beads, a shift occurs towards a Tcm phenotype in both CB and PB CD8+ T-cells, resulting in a similar phenotype in cells from both sources (**Figures 3C–3E**). Moreover, both CB and PB CD8+ T-cells showed similarly high levels of the IL-2 receptor (CD25), indicating an activated state at the moment of transduction (**Figure S1A**). Interestingly, 6 days after transduction (day 10; transduced), CB CD8+ T-cells reverted to a more Tn phenotype, with a specific loss of expression of CD45RO and increased expression of CD45RA, which did not occur in PB CD8+ T-cells (**Figure 3E**). Moreover, CB and PB CD8+ T-cells showed differential expression of the co-inhibitory receptor (TIM3 and LAG3) during all experimental steps (**Figures 3F and S1B**).

### The transduction enhancer LB increases transduction efficiency and maintains proliferation capacity of CB CD8+ T-cells in vitro

To further improve the transduction efficiency, we tested whether the addition of the non-ionic, amphiphilic Poloxamer Synperonic F108 (LB) [25,34] could further enhance the GFP expression in CB CD8+ T-cells, while limiting its effect on viability and proliferation capacity of the CB CD8+ T-cells. MOIs in the range of MOI 1–20 were used, as these are commonly MOIs to transduce PB T-cells [35-37]. As shown in **Figures 4A+B**, the use of LB increased both the percentage of transduced T-cells and the MFI of the signal. With the use of an MOI 10 to transduce CB CD8+ T-cells, the LB resulted in 15% more GFP+ T-cells. With a lower MOI (MOI 1), the increase in the percentage of GFP+ T-cells was even more pronounced, with an average increase of 25% compared to the STND protocol. Lentiviral VCN analysis by qPCR confirmed that in both cases (MOI 10 and MOI 1), the use of LB significantly increased the VCN (**Figure 4C**). The use of LB increased the transduction efficiency also when using an LV.rTCR (next paragraph) and an LV.CAR against CD19 (CAR19) (**Figure S2**). 6 days post-transduction, CB CD8+ T-cells were stained with CellTrace Violet (CTV) and followed over 4 days to determine the proliferation capacity. CB CD8+ T-cells transduced with an MOI 10, in the presence of LB, maintained their proliferation capacity after a strong stimulation with aCD3/CD28 beads, but this was reduced compared to untransduced cells (**Figure 4D**). To determine the direct influence of the LB on proliferation, untransduced cells were cultured overnight in the presence of LB. LB alone did not show any effect on the proliferation rate of untransduced CB CD8+ T-cells (**Figure 4E**). FlowJo analysis using the proliferation tool additionally showed a trend of impaired proliferation, division, and expansion rate in CB CD8+ T-cells transduced in the presence of LB but not a significant difference (**Figure 4F**). In contrast, CB CD8+ T-cells transduced with an MOI 1, in the presence of LB, did not show lower proliferation capacity (**Figure S3A**). The use of LB only slightly and not significantly decreased viability when compared to transduced T-cells in the absence of LB (**Figure 4G and Figure S3B**).

### CB CD8+ T-cells transduced with a TAA-specific TCR, in the presence or absence of LB, show comparable and efficient antigen recognition, proliferation, and killing capacity

To further test the effect of LB on CB CD8+ T-cell proliferation and functionality *in vitro*, CB CD8+ T-cells transduced with a LV expressing a WT1-specific TCR in the presence of LB were tested for antigen recognition, antigen-specific proliferation, and killing capacity. To test antigen recognition, transduced CB CD8+ T-cells were incubated with fluorophore-coupled tetramer molecules pulsed with the target WT1-derived peptide (pWT1-126). As shown in **Figures 5A+B**, both T-cells, transduced in the presence or absence of LB, showed recognition of pWT1-126, with a percentage similar to the transduction efficiency, with an MOI 1 (STND: 8.9% ± 2.3%; STND + LB: 18.4% ± 2.2%) and an MOI 10 (STND: 60.5% ± 10%; STDN + LB: 80% ± 7.3%). qPCR analysis of VCN shows a higher number of integration, both when using an MOI 10 and an MOI 1, in the presence of LB (**Figure 5C**). 6 days after transduction, CB CD8+ T-cells were stained with CTV and followed over the course of 7 days in the presence of pWT1-126 tetramer stimulation. WT1-TCR CB CD8+ T-cells, transduced in the presence or absence of LB, showed a similar proliferation capacity (**Figure 5D**). These cells were subsequently co-cultured overnight with T2 cells that were loaded with pWT1-126 at an E:T ratio of 1:1. WT1-TCR-engineered cells, both in the absence or presence of LB, targeted T2 cells to a similar extend (81% and 90% targeting of T2 cells, respectively) (**Figures 5E and 5G**). Cytotoxic cytokine levels (interferon [IFN]-γ, tumor necrosis factor [TNF]-α,

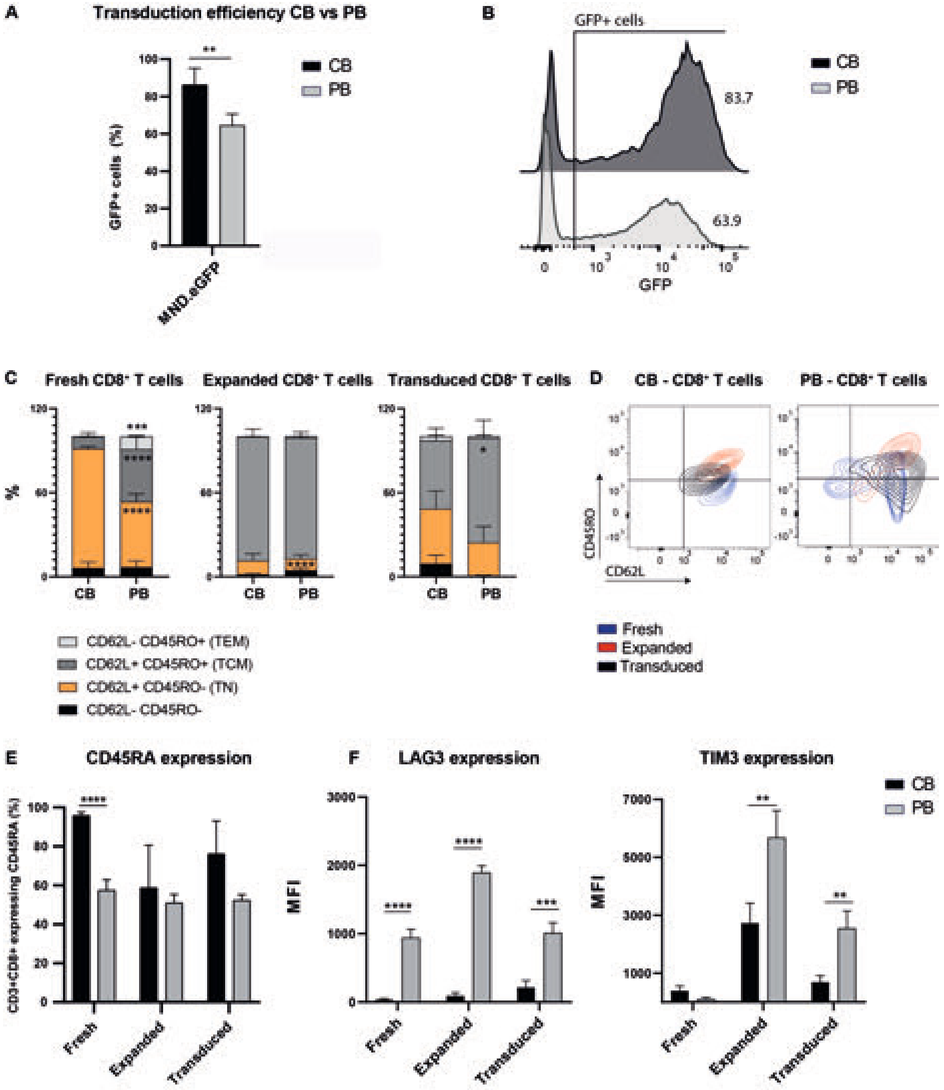

**Figure 3.** CB and PB CD8+ T-cells show different immune phenotype and transduction efficiency. ***(A)*** *Transduction efficiency, as percentage of GFP+ cells in CB CD8+ T-cells (black) compared to PB CD8+ T-cells (gray) using MND.eGFP.* ***(B)*** *Representative flow cytometry plot of CB and PB CD8+ T-cells transduced with MND. eGFP.* ***(C)*** *Proportion of naive T (Tn) cells, effector memory T (Tem) cells, and central memory T (Tcm) cells based on the expression of CD45RO and CD62L, in both CB and PB in CD8+ fresh, expanded, and transduced T-cells.* ***(D)*** *Representative flow cytometry plot of CD45RO-CD62L-expressing cells during the three selected time points (i.e., fresh, expanded, transduced).* ***(E)*** *CD45RA expression in CB (black) and PB (gray) CD8+ fresh, expanded, and transduced T-cells.* ***(F)*** *Co-inhibitory receptor expression in CB (black) and PB (gray) CD8+ fresh, expanded, and transduced T-cells. The data correspond to ≥3 independent experiments and are shown as average ± standard deviation; ∗$p \leq 0.05$; ∗∗$p \leq 0.01$; ∗∗∗$p \leq 0.001$; ∗∗∗∗$p \leq 0.0001$.*

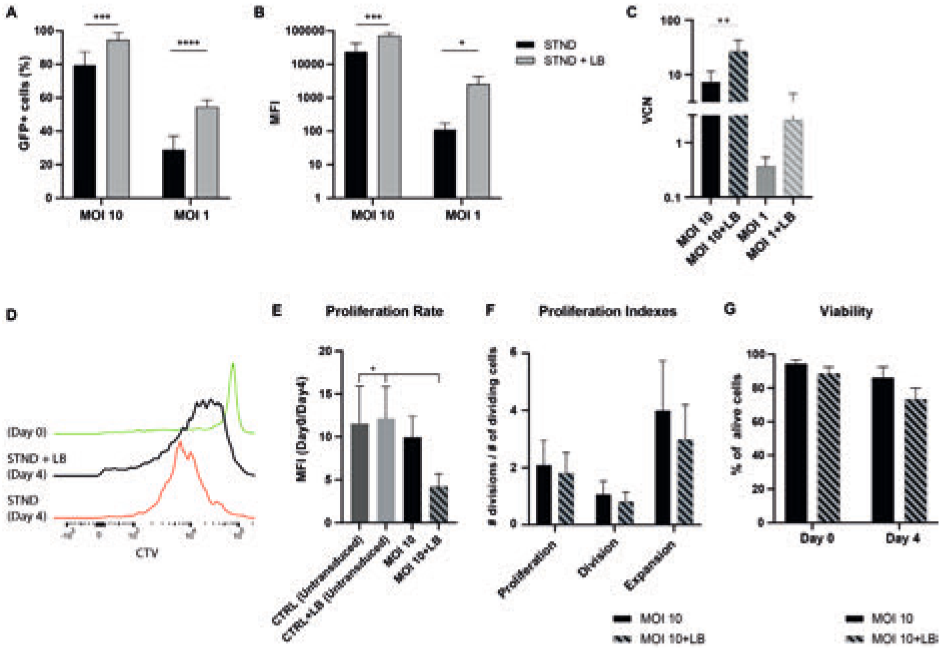

**Figure 4.** LentiBOOST (LB) increases transduction efficiency of CB CD8+-transduced T-cells and maintains proliferation *in vitro*.
*(**A**) Transduction efficiency, presented as percentage of GFP+ cells, is improved by the use of LB together with LV at MOI 10 (left) and MOI 1 (right). (**B**) Protein expression, calculated as MFI of eGFP signal, is increased by the use of LB together with both LV at MOI 10 (left) and MOI 1 (right). (**C**) qPCR analysis of the VCN in CB CD8+ T-cells transduced with an MOI 10 in the absence (black) or presence (black stripes) of LB or transduced with an MOI 1 in the absence (gray) or presence (gray stripes) of LB. (**D**) Representative flow cytometry plot of proliferation analysis using CellTrace Violet (CTV) on CB CD8+ T-cells transduced with the STND method or with STND+LB. (**E**) Proliferation rate (as CTV-MFI of day 0/day 4) in CB CD8+ T-cells untransduced and transduced in the presence or absence of LB. (**F**) Proliferation indexes (calculated using proliferation model of FlowJo v.10) define proliferation, division, and expansion rate of CB CD8+ T-cells transduced in the presence of LB (black stripes) compared to STND protocol (black). Proliferation index: total number of divisions divided by the number of cells that went into division, division index: average number of cell divisions per cell in original population, expansion index: fold-expansion of the overall culture. (**G**) Cell viability, respectively, at day 0 and day 4 of a proliferation assay in CB CD8+ T-cells transduced in the presence of LB (black stripes) compared to STND protocol (black). The data correspond to ≥3 independent experiments and are shown as average ± standard deviation; ∗p ≤ 0.05; ∗∗p ≤ 0.01; ∗∗∗p ≤ 0.001; ∗∗∗∗p ≤ 0.0001.*

granzyme A, granzyme B, and perforin) were analyzed in the supernatant of the killing assays. WT1-TCR-transduced cells produced a higher amount of cytotoxic cytokines compared to untransduced cells, statistically significant for IFN-γ and granzyme B (p value: <0.0001), whereas there were no differences between transduced T-cells in the presence or absence of LB (**Figure 5F**). To support our findings, additional experiments were performed with a more limiting E:T ratio of 1:10, which showed a slightly increased killing capacity of WT1-TCR-transduced CB CD8+ T-cells in the presence of LB, likely due to the presence of a larger proportion of WT1-TCR-transduced T-cells (**Figure S4**).

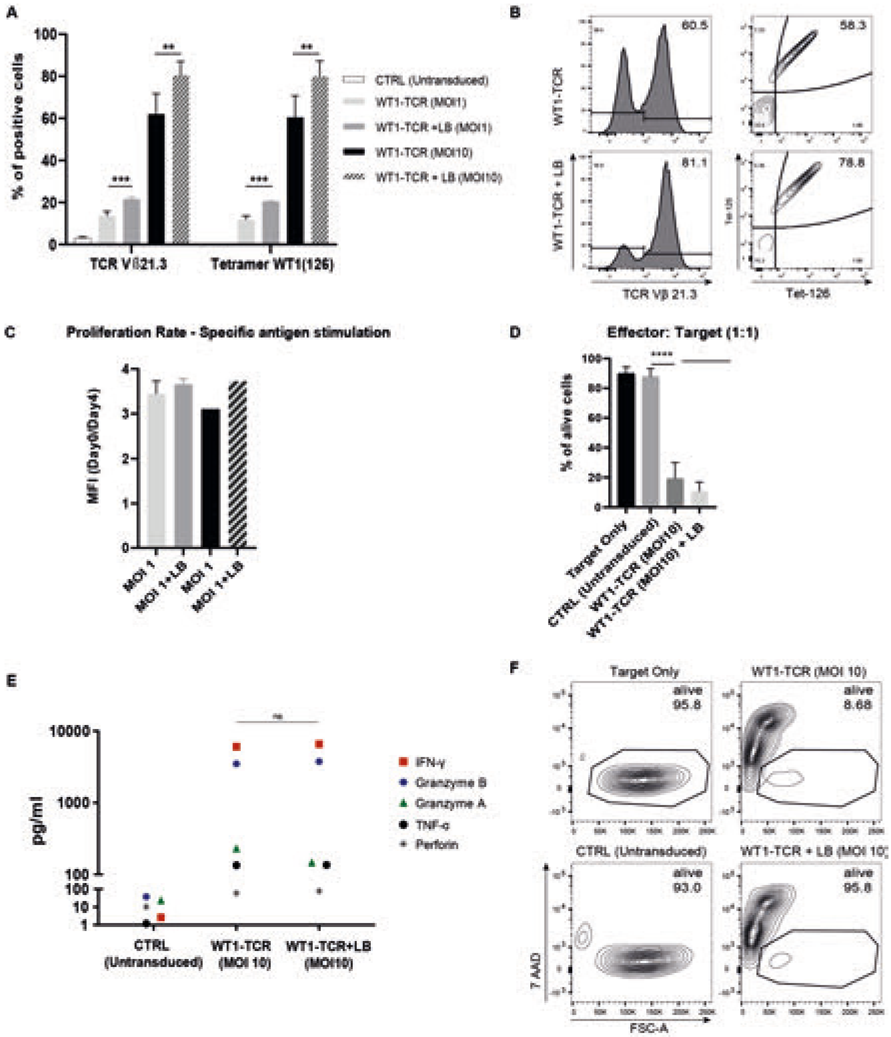

**Figure 5.** LB does not affect functionality of WT1-TCR-transduced CB CD8+ T-cells.

***(A)*** *Transduction efficiency and antigen recognition, presented as percentage of TCR Vß 21.3+ T-cells (left) and tetramer+ cells (right), improved by the use of LB at MOI 1 and MOI 10 compared to STND method.* ***(B)*** *Representative flow cytometry plot of CB CD8+ T-cell transduction efficiency and pWT1-126 tetramer staining.* ***(C)*** *qPCR analysis of the VCN in CB CD8+ T-cells transduced with an MOI 10 in the absence (black) or presence (black stripes) of LB or transduced with an MOI 1 in the absence (gray) or presence (gray stripes) of LB.* ***(D)*** *Proliferation rate (as CTV-MFI of day 0/day 7) of CB CD8+ T-cells untransduced and transduced with WT1-TCR (MOI 10) in the presence or absence of LB and stimulated with tetramer loaded with pWT1-126.* ***(E)*** *Killing capacity of WT1-TCR CB CD8+ T-cells transduced in the presence or absence of LB, depicted as percentage of alive target cells in a co-culture experiment with target cells loaded with pWT1-126.* ***(F)*** *Levels of cytotoxic cytokines in the supernatant of co-culture experiments produced by WT1-TCR-transduced CB CD8+ T-cells in the presence or absence of LB compared to untransduced cells.* ***(G)*** *Representative flow cytometry plot of percentage of alive target cells after overnight co-culture with WT1-TCR-transduced CB CD8+ T-cells. Co-culture experiments were performed at an effector-to-target ratio of 1:1. The data correspond to ≥3 independent experiments and are shown as average ± standard deviation;* $*p \leq 0.05$*;* $**p \leq 0.01$*;* $***p \leq 0.001$*;* $****p \leq 0.0001$*.*

## DISCUSSION

The possibility to gene modify immune cells has opened a broad range of cell therapy applications for difficult-to-treat tumor types. However, it remains challenging to obtain enough functionally proficient autologous T-cells from cancer patients and to efficiently gene modify immune cells. In this manuscript, we studied the use of allogeneic CB cells as a rich source to obtain CD8+ T-cells that are amenable for lentiviral transduction. The use of CB-derived cells is well established in clinical applications, such as hematopoietic cell transplantation (HCT) [38-40]. CB T-cell cultures can result in more than 100-fold magnitude of expansion, enabling feasible upscaling processes to generate sufficient cell numbers for therapeutic purposes [41,42]. Furthermore, CB lymphocytes are associated with favorable graft versus tumor effects, reaching sufficient numbers, and efficiency for donor lymphocyte infusion post-HCT [43,44]. Several clinical trials are testing the safety and the potential benefit of infusing CB-derived, naturally occurring lymphocytes [45,46], including T-cells, natural killer (NK) cells, and cytokine-induced killer cells (CIK), to avoid relapse (ClinicalTrials.gov: NCT01630564) or viral reactivation (Clinical Trials.gov: NCT03594981) after HCT. Although the results of CB-derived T-cell infusions are promising, the generation of specific, gene-modified CB T-cells for therapeutic approaches is still in its infancy compared to using PB T-cells. In this manuscript, we present an optimized method to obtain highly efficient lentiviral transduction of CB CD8+ T-cells, which could potentially be translated for use in clinical settings. In fact, the use of serum-free StemMACS medium showed a transduction efficiency of more than 80% of CB CD8+ T-cells, using a relatively low MOI, favorable for future good manufacturing practice (GMP) production and safety concerns (**Figure 2**). This method also confirmed the enhanced expression achieved with the use of a viral-derived promoter (MND) compared to the constitutively expressed promoters (PGK).

With the use of this protocol, the total fraction of CB CD8+ T-cells was more amenable to transduction compared to the total fraction of PB CD8+ T-cells. We speculate that this protocol may be beneficial by exploiting the naive characteristics of CB CD8+ T-cells, in accordance to previous studies that showed an increased transduction efficiency in PB-derived Tn cells and Tscm cells [32,47]. Nevertheless, we may expect an increased potency of CB CD8+ T-cells due to the differences in immune phenotype between the two cell sources [48,49]. Pre-clinical and clinical studies have shown the short persistence and low proliferation properties of engineered T-cells derived from PB of adult patients [50]. Moreover, *in vivo* studies have shown the superiority of Tn over Tm cells in adoptive immunotherapeutic applications [51,52]. The proposed method combines high transduction efficiency with a global maintenance of the least differentiated Tscm or Tn phenotype of the CB CD8+ T-cells, confirmed by the downregulation of CD45RO and the upregulation of CD45RA (**Figure 3**). This method increases the feasibility to use CB CD8+ T-cells in clinical applications; however, its clinical significance will rely on the activation, proliferation, and long-term survival of genetically modified cells *in vivo*. The naive phenotype, together with the intermediate to low expression of inhibitory receptors (TIM3, LAG3), which were maintained low in the current protocol, could be a valuable feature for improving proliferation, persistence, and efficacy in future pre-clinical and clinical studies. The difference in transduction efficiency between the cell sources may also be influenced by the expression levels of the cognate glycoprotein receptors on the target cells, defining the probability of binding between viral particle and cell membrane [53]. This effect was previously shown by substituting the envelope from vesicular stomatitis virus G protein (VSV-G) to measles virus (MV)37 or baboon retroviral envelope (BaEV) [53], which increased the transduction efficiency of the LV, a strategy that can be further explored.

Further improvements in the transduction efficiency was achieved using the transduction enhancer LB. The active component of LB is Poloxamer 338/Pluronic F108 and belongs to the class of A-B-A-type tri-block copolymers composed of hydrophilic ethyleneoxide and hydrophobic propyleneoxide. This structure confers a capability of interacting with hydrophobic particles and biological membranes. The advantage of using this enhancer and alternative poloxamers (Poloxamer 407) has already been proven in HSCs and mouse-derived T-cells [25,34,54], and its GMP-grade formula has already been used in clinical trials. The use of LB clearly increased the transduction efficiency also in CB CD8+ T-cells using different LV constructs (LV.eGFP, LV.WT1-TCR, and LV.CAR19), especially interesting for applications requiring low MOI or when vector titers are limited. As previously shown [34,55], the use of LB very minimally affects T-cell viability, as shown also by using our optimized protocol (**Figure 4G**). With the use of a tracer molecule, we observed that LB affected the proliferation rate of CB CD8+ T-cells transduced with an MOI 10, after providing both the primary and co-stimulatory signals that are required for activation and expansion of T-cells via aCD3/CD28 beads. The reduced proliferation rate was visible only when using LV.eGFP and an MOI 10, whereas untransduced cells treated with the LB molecule (**Figure 4E**) and cells transduced with an MOI 1 (**Figure S3**) did not show impaired proliferation upon aCD3/CD28 stimulation (**Figure S4**). The effect on proliferation coincided with an increase in VCN in the transduced T-cells in the presence of LB, possibly caused by genotoxic stress in the CB CD8+ T-cells, supported by the observation that CB CD8+ T-cells transduced at an MOI 1 did not show a decreased proliferation rate. As previously reported, self-inactivating LVs have the tendency to integrate into transcriptionally active genes in T-cells [56], potentially causing genotoxic effects at higher VCNs. Interestingly, the decrease in proliferation was not visible when CB CD8+ T-cells were transduced with a

TAA-specific TCR in the presence of LB and stimulated with antigen-specific tetramers. Moreover, WT1-TCR CB CD8+ T-cells, transduced in the presence of LB, did not show any impairment in terms of functionality, as assessed by killing capacity and cytotoxic cytokines produced (**Figures 5E–5G**).

In conclusion, we present an efficient expansion and transduction method for CB CD8+ T-cells using LVs that is GMP compliant. Furthermore, this method shows better transduction of the total fraction of CB CD8+ T-cells compared to the total fraction of PB CD8+ T-cells, while preserving the CB naive phenotypic markers, increasing the chance to generate a cellular product that will persist and proliferate *in vivo*. Additionally, we confirmed the use of the LB as a valid transduction enhancer for CB CD8+ T-cells in the field of gene and cell therapy. Overall, these results underlie the possibilities and advantages of using gene-modified CB CD8+ T-cells as a source for future application in cancer cell therapy. In the research described in this thesis, this protocol is exploited to generate TAA-specific (NK)T-cells to study effects on *in vitro* immunogenicity of Neuroblastoma.

## ACKNOWLEDGMENTS

The authors thank the staff of the Flow Core Facility (Center for Translational Immunology, UMC Utrecht [UMCU], the Netherlands), especially Jeroen van Velzen, for the support and help in the sample analysis. The authors also thank the women for donating the CB and the nurses (Wilhelmina's Children Hospital, UMCU, the Netherlands) for collecting it.

## REFERENCES

1. Dudley M.E., Wunderlich J.R., Shelton T.E., Even J., Rosenberg S.A. Generation of tumor-infiltrating lymphocyte cultures for use in adoptive transfer therapy for melanoma patients. *J. Immunother.* **2003**;26:332–342, doi:10.1097/00002371-200307000-00005.
2. Rosenberg S.A., Yang J.C., Sherry R.M., Kammula U.S., Hughes M.S., Phan G.Q., Citrin D.E., Restifo N.P., Robbins P.F., Wunderlich J.R. Durable complete responses in heavily pretreated patients with metastatic melanoma using T-cell transfer immunotherapy. *Clin. Cancer Res.* **2011**;17:4550–4557, doi: 10.1158/1078-0432.CCR-11-0116.
3. Dudley M.E., Yang J.C., Sherry R., Hughes M.S., Royal R., Kammula U., Robbins P.F., Huang J., Citrin D.E., Leitman S.F. Adoptive cell therapy for patients with metastatic melanoma: evaluation of intensive myeloablative chemoradiation preparative regimens. *J. Clin. Oncol.* **2008**;26:5233–5239, doi:10.1200/JCO.2008.16.5449.
4. Lim W.A., June C.H. The Principles of Engineering Immune Cells to Treat Cancer. *Cell.* **2017**;168:724–740, doi:10.1016/j.cell.2017.01.016.
5. June C.H., Sadelain M. Chimeric Antigen Receptor Therapy. *N. Engl. J. Med.* **2018**;379: 64–73, doi:10.1056/NEJMra1706169.
6. Grigor E.J.M., Fergusson D., Kekre N., Montroy J., Atkins H., Seftel M.D., Daugaard M., Presseau J., Thavorn K., Hutton B. Risks and Benefits of Chimeric Antigen Receptor T-Cell (CAR-T) Therapy in Cancer: A Systematic Review and Meta-Analysis. *Transfus. Med. Rev.* **2019**;33:98–110, doi:10.1016/j.tmrv.2019.01.005.
7. European Medicines Agency: Committee for Medicinal Products for Human Use (CHMP) **2018**. Assessment Report - Kymriah. https://www.ema.europa.eu/en/medicines/human/EPAR/kymriah
8. Leary M.O., Przepiorka D., George B., Theoret M. **2017**. BLA Clinical Review Memorandum. https://www.fda.gov/media/107973/download
9. Zhang J., Wang L. The emerging world of TCR-T cell trials against cancer: A systematic review. *Technol. Cancer Res. Treat.* **2019**;18,1533033819831068 doi: 10.1177/1533033819831068.
10. Morgan R.A., Dudley M.E., Wunderlich J.R., Hughes M.S., Yang J.C., Sherry R.M., Royal R.E., Topalian S.L., Kammula U.S., Restifo N.P. Cancer regression in patients after transfer of genetically engineered lymphocytes. *Science.* **2006**;314:126–129, doi:10.1126/science.1129003.
11. Rapoport A.P., Stadtmauer E.A., Binder-Scholl G.K., Goloubeva O., Vogl D.T., Lacey S.F., Badros A.Z., Garfall A., Weiss B., Finklestein J. NY-ESO-1-specific TCR-engineered T cells mediate sustained antigen-specific antitumor effects in myeloma. *Nat. Med.* **2015**;21:914–921, doi:10.1038/nm.3910.
12. Chapuis A.G., Egan D.N., Bar M., Schmitt T.M., McAfee M.S., Paulson K.G., Voillet V., Gottardo R., Ragnarsson G.B., Bleakley M. T cell receptor gene therapy targeting WT1 prevents acute myeloid leukemia relapse post-transplant. *Nat. Med.* **2019**;25:1064–1072, doi:10.1038/s41591-019-0472-9.
13. Gröbner S.N., Worst B.C., Weischenfeldt J., Buchhalter I., Kleinheinz K., Rudneva V.A., Johann P.D., Balasubramanian G.P., Segura-Wang M., Brabetz S., ICGC PedBrain-Seq Project. ICGC MMML-Seq Project The landscape of genomic alterations across childhood cancers. *Nature.* **2018**;555:321–327, doi:10.1038/nature25480.
14. Zufferey R., Dull T., Mandel R.J., Bukovsky A., Quiroz D., Naldini L., Trono D. Self-inactivating lentivirus vector for safe and efficient in vivo gene delivery. *J. Virol.* **1998**;72:9873–9880, doi:10.1128/JVI.72.12.9873-9880, doi:10.1128/JVI.72.12.9873-9880.1998.
15. Graham C., Jozwik A., Pepper A., Benjamin R. Allogeneic CAR-T Cells: More than Ease of Access? *Cells.* **2018**;7:1–11, doi:10.3390/cells7100155.

**16.** Mackall C.L., Fleisher T.A., Brown M.R., Magrath I.T., Shad A.T., Horowitz M.E., Wexler L.H., Adde M.A., McClure L.L., Gress R.E. Lymphocyte depletion during treatment with intensive chemotherapy for cancer. *Blood*. **1994**;84:2221–2228.

**17.** Stahnke K., Fulda S., Friesen C., Strauss G., Debatin K.M. Activation of apoptosis pathways in peripheral blood lymphocytes by in vivo chemotherapy. *Blood*. **2001**;98:3066–3073, doi:10.1182/blood.v98.10.3066.

**18.** Mackall C.L., Fleisher T.A., Brown M.R., Andrich M.P., Chen C.C., Feuerstein I.M., Magrath I.T., Wexler L.H., Dimitrov D.S., Gress R.E. Distinctions between CD8+ and CD4+ T-cell regenerative pathways result in prolonged T-cell subset imbalance after intensive chemotherapy. *Blood*. **1997**;89:3700–3707.

**19.** Fagnoni F.F., Lozza L., Zibera C., Zambelli A., Gibelli N., Ponchio L., Oliviero B., Pavesi L., Gennari R., Vescovini R. T-cell dynamics after high-dose chemotherapy in adults : elucidation of the elusive CD8 + subset reveals multiple homeostatic T-cell compartments with distinct implications for immune competence. *Immunology*. **2002**;106:27–37, doi:10.1046/j.1365-2567.2002.01400.x.

**20.** Onyema O.O., Decoster L., Njemini R., Forti L.N., Bautmans I., De Waele M., Mets T. Chemotherapy-induced changes and immunosenescence of CD8+ T-cells in patients with breast cancer. *Anticancer Res*. **2015**;35: 1481–1489.

**21.** Paloczi K. Immunophenotypic and functional characterization of human umbilical cord blood mononuclear cells. *Leukemia*. **1999**;13(Suppl 1):S87–S89, doi:10.1038/sj.leu.2401318.

**22.** Lo Presti V., Nierkens S., Boelens J.J., van Til N.P. Use of cord blood derived T-cells in cancer immunotherapy: milestones achieved and future perspectives. *Expert Rev. Hematol*. **2018**;11:209–218, doi: 10.1080/17474086.2018.1431119.

**23.** Hiwarkar P., Qasim W., Ricciardelli I., Gilmour K., Quezada S., Saudemont A., Amrolia P., Veys P. Cord blood T cells mediate enhanced antitumor effects compared with adult peripheral blood T cells. *Blood*. **2015**;126: 2882–2891, doi:10.1182/blood-2015-06-654780.

**24.** Oki M., Ando K., Hagihara M., Miyatake H., Shimizu T., Miyoshi H., Nakamura Y., Matsuzawa H., Sato T., Ueda Y. Efficient lentiviral transduction of human cord blood CD34(+) cells followed by their expansion and differentiation into dendritic cells. *Exp. Hematol*. **2001**;29:1210–1217, doi:10.1016/s0301-472x(01)00695-6.

**25.** Hauber I., Beschorner N., Schrödel S., Chemnitz J., Kröger N., Hauber J., Thirion C. Improving Lentiviral Transduction of CD34+ Hematopoietic Stem and Progenitor Cells. *Hum. Gene Ther. Methods*. **2018**;29:104–113, doi:10.1089/hgtb.2017.085.

**26.** Liu Y., Hangoc G., Campbell T.B., Goodman M., Tao W., Pollok K., Srour E.F., Broxmeyer H.E. Identification of parameters required for efficient lentiviral vector transduction and engraftment of human cord blood CD34(+) NOD/SCID-repopulating cells. *Exp. Hematol*. **2008**;36:947–956, doi:10.1016/j.exphem.2008.06.005.

**27.** Evans J.T., Kelly P.F., O'Neill E., Garcia J.V. Human cord blood CD34+CD38- cell transduction via lentivirus-based gene transfer vectors. *Hum. Gene Ther*. **1999**;10:1479–1489, doi:10.1089/10430349950017815.

**28.** Serrano L.M., Pfeiffer T., Olivares S., Numbenjapon T., Bennitt J., Kim D., Smith D., McNamara G., Al-Kadhimi Z., Rosenthal J. Differentiation of naive cord-blood T cells into CD19-specific cytolytic effectors for posttransplantation adoptive immunotherapy. *Blood*. **2006**;107:2643–2652, doi:10.1182/blood-2005-09-3904.

**29.** Micklethwaite K.P., Savoldo B., Hanley P.J., Leen A.M., Demmler-Harrison G.J., Cooper L.J.N., Liu H., Gee A.P., Shpall E.J., Rooney C.M. Derivation of human T lymphocytes from cord blood and peripheral blood with antiviral and antileukemic specificity from a single culture as protection against infection and relapse after stem cell transplantation. *Blood.* **2010**;115:2695–2703, doi:10.1182/blood-2009-09-242263.

**30.** Pegram H.J., Purdon T.J., van Leeuwen D.G., Curran K.J., Giralt S.A., Barker J.N., Brentjens R.J. IL-12-secreting CD19-targeted cord blood-derived T cells for the immunotherapy of B-cell acute lymphoblastic leukemia. *Leukemia.* **2015**;29:415–422, doi:10.1038/leu.2014.215.

**31.** Frumento G., Zheng Y., Aubert G., Raeiszadeh M., Lansdorp P.M., Moss P., Lee S.P., Chen F.E. Cord blood T cells retain early differentiation phenotype suitable for immunotherapy after TCR gene transfer to confer EBV specificity. *Am. J. Transplant.* **2013**;13:45–55, doi:10.1111/j.1600-6143.2012.04286.x.

**32.** Cieri N., Camisa B., Cocchiarella F., Forcato M., Oliveira G., Provasi E., Bondanza A., Bordignon C., Peccatori J., Ciceri F. IL-7 and IL-15 instruct the generation of human memory stem T cells from naive precursors. *Blood.* **2013**;121:573–584, doi:10.1182/blood-2012-05-431718.

**33.** Tammana S., Huang X., Wong M., Milone M.C., Ma L., Levine B.L., June C.H., Wagner J.E., Blazar B.R., Zhou X. 4-1BB and CD28 signaling plays a synergistic role in redirecting umbilical cord blood T cells against B-cell malignancies. *Hum. Gene Ther.* **2010**;21:75–86, doi:10.1089/hum.2009.122.

**34.** Delville M., Soheili T., Bellier F., Durand A., Denis A., Lagresle-Peyrou C., Cavazzana M., Andre-Schmutz I., Six E. A Nontoxic Transduction Enhancer Enables Highly Efficient Lentiviral Transduction of Primary Murine T Cells and Hematopoietic Stem Cells. *Mol. Ther. Methods Clin. Dev.* **2018**;10:341–347, doi:10.1016/j.omtm.2018.08.002.

**35.** Cavalieri S., Cazzaniga S., Geuna M., Magnani Z., Bordignon C., Naldini L., Bonini C. Human T lymphocytes transduced by lentiviral vectors in the absence of TCR activation maintain an intact immune competence. *Blood.* **2003**;102:497–505, doi:10.1182/blood-2003-01-0297.

**36.** Jones S., Peng P.D., Yang S., Hsu C., Cohen C.J., Zhao Y., Abad J., Zheng Z., Rosenberg S.A., Morgan R.A. Lentiviral vector design for optimal T cell receptor gene expression in the transduction of peripheral blood lymphocytes and tumor-infiltrating lymphocytes. *Hum. Gene Ther.* **2009**;20:630–640, doi:10.1089/hum.2008.048.

**37.** Frecha C., Costa C., Nègre D., Gauthier E., Russell S.J., Cosset F.L., Verhoeyen E. Stable transduction of quiescent T cells without induction of cycle progression by a novel lentiviral vector pseudotyped with measles virus glycoproteins. *Blood.* **2008**;112:4843–4852, doi:10.1182/blood-2008-05-155945.

**38.** Ballen K.K., Gluckman E., Broxmeyer H.E. Umbilical cord blood transplantation: the first 25 years and beyond. *Blood.* **2013**;122:491–498, doi:10.1182/blood-2013-02-453175.

**39.** Boelens J.J. The power of cord blood cells. Blood. **2016**;127:3302–3303, doi:10.1182/blood-2016-04-713065.

**40.** Barker J.N., Davies S.M., DeFor T., Ramsay N.K.C., Weisdorf D.J., Wagner J.E. Survival after transplantation of unrelated donor umbilical cord blood is comparable to that of human leukocyte antigen-matched unrelated donor bone marrow: results of a matched-pair analysis. *Blood.* **2001**;97:2957–2961, doi:10.1182/blood.v97.10.2957.

**41.** Azuma H., Yamada Y., Shibuya-Fujiwara N., Yamaguchi M., Murahashi H., Fujihara M., Sato N., Fukazawa K., Ikebuchi K., Ikeda H. Functional evaluation of ex vivo expanded cord blood lymphocytes: possible use for adoptive cellular immunotherapy. *Exp. Hematol.* **2002**;30:346–351, doi:10.1016/s0301-472x(02)00776-2.

**42.** Okas M., Gertow J., Uzunel M., Karlsson H., Westgren M., Kärre K., Ringden O., Mattsson J., Uhlin M. Clinical expansion of cord blood-derived T cells for use as donor lymphocyte infusion after cord blood transplantation. *J. Immunother.* **2010**;33:96–105, doi:10.1097/CJI.0b013e3181b291a4.

**43.** Parmar S., Robinson S.N., Komanduri K., St John L., Decker W., Xing D., Yang H., McMannis J., Champlin R., de Lima M. Ex vivo expanded umbilical cord blood T cells maintain naive phenotype and TCR diversity. *Cytotherapy*. **2006**;8:149–157, doi: 10.1080/14653240600620812.

**44.** Kwoczek J., Riese S.B., Tischer S., Bak S., Lahrberg J., Oelke M., Maul H., Blasczyk R., Sauer M., Eiz-Vesper B. Cord blood-derived T cells allow the generation of a more naïve tumor-reactive cytotoxic T-cell phenotype. *Transfusion*. **2018**;58:88–99, doi:10.1111/trf.14365.

**45.** Berglund S., Gertow J., Uhlin M., Mattsson J. Expanded umbilical cord blood T cells used as donor lymphocyte infusions after umbilical cord blood transplantation. *Cytotherapy*. **2014**;16:1528–1536, doi:10.1016/j.jcyt.2014.08.001.

**46.** Balassa K., Rocha V. Anticancer cellular immunotherapies derived from umbilical cord blood. *Expert Opin. Biol. Ther.* **2018**;18:121–134, doi:10.1080/14712598.2018.1402002.

**47.** Sabatino M., Hu J., Sommariva M., Gautam S., Fellowes V., Hocker J.D., Dougherty S., Qin H., Klebanoff C.A., Fry T.J. Generation of clinical-grade CD19-specific CAR-modified CD8+ memory stem cells for the treatment of human B-cell malignancies. *Blood*. **2016**;128:519–528, doi:10.1182/blood-2015-11-683847.

**48.** Gattinoni L., Klebanoff C.A., Palmer D.C., Wrzesinski C., Kerstann K., Yu Z., Finkelstein S.E., Theoret M.R., Rosenberg S.A., Restifo N.P. Acquisition of full effector function in vitro paradoxically impairs the in vivo antitumor efficacy of adoptively transferred CD8+ T cells. *J. Clin. Invest*. **2005**;115:1616–1626, doi:10.1172/JCI24480.

**49.** Klebanoff C.A., Gattinoni L., Torabi-Parizi P., Kerstann K., Cardones A.R., Finkelstein S.E., Palmer D.C., Antony P.A., Hwang S.T., Rosenberg S.A. Central memory self/tumor-reactive CD8+ T cells confer superior antitumor immunity compared with effector memory T cells. *Proc. Natl. Acad. Sci. USA*. **2005**;102:9571–9576, doi:10.1073/pnas.0503726102.

**50.** Robbins P.F., Dudley M.E., Wunderlich J., El-Gamil M., Li Y.F., Zhou J., Huang J., Powell D.J., Jr., Rosenberg S.A. Cutting edge: persistence of transferred lymphocyte clonotypes correlates with cancer regression in patients receiving cell transfer therapy. *J. Immunol*. **2004**;173:7125–7130, doi:10.4049/jimmunol.173.12.7125.

**51.** Hinrichs C.S., Borman Z.A., Gattinoni L., Yu Z., Burns W.R., Huang J., Klebanoff C.A., Johnson L.A., Kerkar S.P., Yang S. Human effector CD8+ T cells derived from naive rather than memory subsets possess superior traits for adoptive immunotherapy. *Blood*. **2011**;117:808–814, doi:10.1182/blood-2010-05-286286.

**52.** Sommermeyer D., Hudecek M., Kosasih P.L., Gogishvili T., Maloney D.G., Turtle C.J., Riddell S.R. Chimeric antigen receptor-modified T cells derived from defined CD8+ and CD4+ subsets confer superior antitumor reactivity in vivo. *Leukemia*. **2016**;30:492–500, doi:10.1038/leu.2015.247.

**53.** Costa C., Hypolite G., Bernadin O., Lévy C., Cosset F.-L., Asnafi V., Macintyre E., Verhoeyen E., Tesio M. Baboon envelope pseudotyped lentiviral vectors: a highly efficient new tool to genetically manipulate T-cell acute lymphoblastic leukaemia-initiating cells. *Leukemia*. **2017**;31:977–980, doi:10.1038/leu.2016.372.

**54.** Uchida N., Nassehi T., Drysdale C.M., Gamer J., Yapundich M., Demirci S., Haro-Mora J.J., Leonard A., Hsieh M.M., Tisdale J.F. High-Efficiency Lentiviral Transduction of Human CD34+ Cells in High-Density Culture with Poloxamer and Prostaglandin E2. *Mol. Ther. Methods Clin. Dev*. **2019**;13:187–196, doi:10.1016/j.omtm.2019.01.005.

**55.** Simon B., Harrer D.C., Thirion C., Schuler-Thurner B., Schuler G., Uslu U. Enhancing lentiviral transduction to generate melanoma-specific human T cells for cancer immunotherapy. *J. Immunol. Methods*. **2019**;472:55–64, doi:10.1016/j.jim.2019.06.015.

**56.** Field A.C., Vink C., Gabriel R., Al-Subki R., Schmidt M., Goulden N., Stauss H., Thrasher A., Morris E., Qasim W. Comparison of lentiviral and sleeping beauty mediated αβ T cell receptor gene transfer. *PLoS ONE*. **2013**;8: e68201, doi:10.1371/journal.pone.0068201.

**57.** Schambach A., Bohne J., Baum C., Hermann F.G., Egerer L., von Laer D., Giroglou T. Woodchuck hepatitis virus post-transcriptional regulatory element deleted from X protein and promoter sequences enhances retroviral vector titer and expression. *Gene Ther*. **2006**; 13:641–645, doi:10.1038/sj.gt.3302698.

**58.** van Til N.P., Sarwari R., Visser T.P., Hauer J., Lagresle-Peyrou C., van der Velden G., Malshetty V., Cortes P., Jollet A., Danos O. Recombination-activating gene 1 (Rag1)-deficient mice with severe combined immunodeficiency treated with lentiviral gene therapy demonstrate autoimmune Omenn-like syndrome. *J. Allergy Clin. Immunol*. **2014**;133: 1116–1123, doi:10.1016/j.jaci.2013.10.009.

**59.** Tiscornia G., Singer O., Verma I.M. Production and purification of lentiviral vectors. *Nat. Protoc*. **2006**;1:241–245, doi:10.1038/nprot.2006.37.

**60.** Singer-Sam J., Keith D.H., Tani K., Simmer R.L., Shively L., Lindsay S., Yoshida A., Riggs A.D. Sequence of the promoter region of the gene for human X-linked 3-phosphoglycerate kinase. *Gene*. **1984**;32:409–417, doi:10.1016/0378-1119(84)90016-7.

**61.** Li H., Ginzburg Y.Z. Crosstalk between Iron Metabolism and Erythropoiesis. *Adv. Hematol*. **2010**;2010:605435, doi:10.1155/2010/605435

**62.** Logan A.C., Nightingale S.J., Haas D.L., Cho G.J., Pepper K.A., Kohn D.B. Factors influencing the titer and infectivity of lentiviral vectors. *Hum. Gene Ther*. **2004**;15:976–988, doi:10.1089/hum.2004.15.976.

**63.** Wolfl M., Kuball J., Ho W.Y., Nguyen H., Manley T.J., Bleakley M., Greenberg P.D. Activation-induced expression of CD137 permits detection, isolation, and expansion of the full repertoire of CD8+ T cells responding to antigen without requiring knowledge of epitope specificities. *Blood*. **2007**;110:201–210, doi: 10.1182/blood-2006-11-056168.

**64.** Kuball J., Dossett M.L., Wolfl M., Ho W.Y., Voss R.H., Fowler C., Greenberg P.D. Facilitating matched pairing and expression of TCR chains introduced into human T cells. *Blood*. **2007**; 109:2331–2338, doi:10.1182/blood-2006-05-023069

**65.** Rodenko B., Toebes M., Hadrup S.R., van Esch W.J.E., Molenaar A.M., Schumacher T.N.M., Ovaa H. Generation of peptide-MHC class I complexes through UV-mediated ligand exchange. *Nat. Protoc*. **2006**;1:1120–1132, doi:10.1038/nprot.2006.121.

## SUPPLEMENTARY MATERIAL

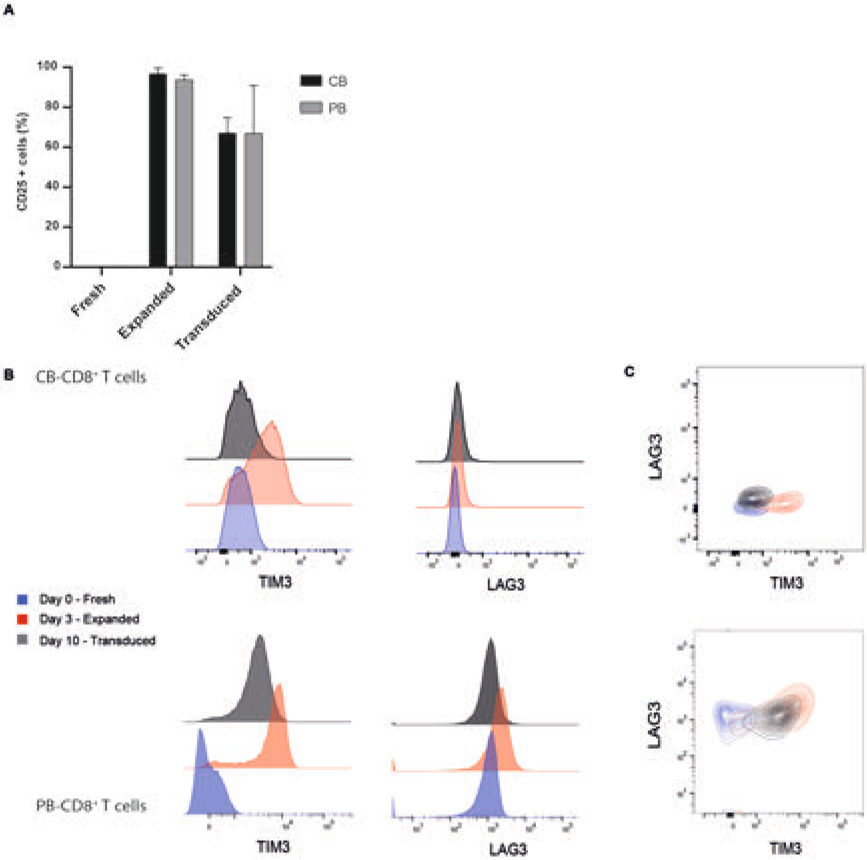

**Figure S1.** Expression of CD25, TIM3 and LAG3 in CB and PB CD8+ T-cells
*(**A**) CD25 expression in CB (black) and PB (gray). (**B**) TIM3 and LAG3 expression histograms in both CB (top) and PB (bottom) CD3+CD8+ T-cells, in the three different time points: Day 0 – Fresh (blue), Day 3 - Expanded (red), Day 10 – Transduced (black). (**C**) Co-staining of TIM-3 and LAG-3 representative plots for both CB and PB CD3+CD8+ T-cells. The data corresponds to ≥ 3 independent experiments and are shown as average ± standard deviation.*

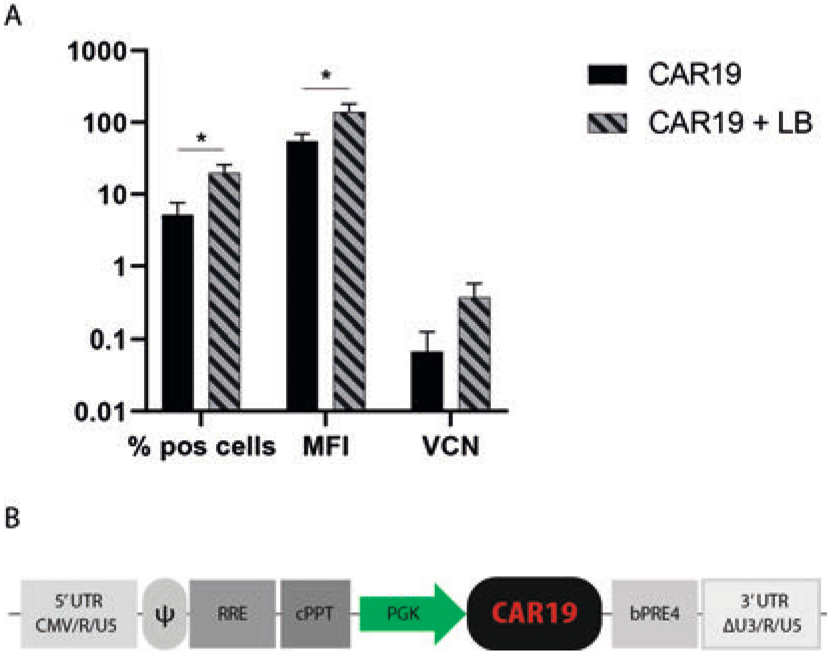

**Figure S2.** LB also increases transduction efficiency with the LV.CAR19 construct
*__(A)__ CB CD8+ T-cells transduced with LV.CAR19 (MOI1) showed 5.2% ± 2.5 transduction efficiency (black), while the use of LB increased the % of transduced cells to 19.9 ± 5.9 (black stripes). The same trend is also visible for the MFI and the VCN. __(B)__ Schematic representation of plasmid LV.CAR19 vector design. The data corresponds to ≥ 3 independent experiments and are shown as average ± standard deviation; $p \leq 0.05$ (*); $p \leq 0.01$ (**) ; $p \leq 0.001$ (***); $p \leq 0.0001$ (****).*

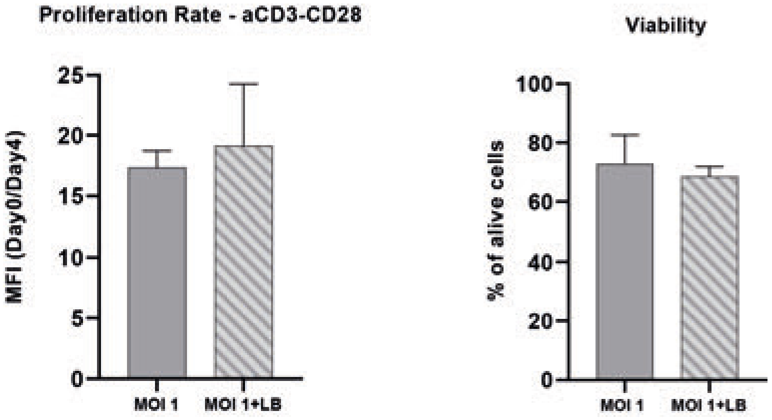

**Figure S3.** LB effect on proliferation and cell viability on CB CD8+ T-cells transduced with an MOI 1
***(A)*** *Proliferation rate after 4 days of aCD3/CD28 beads stimulation in CB CD8+ T-cells transduced with and MOI 1 in the presence of LB (gray stripes) compared to STND method (gray).* ***(B)*** *Cell viability analysis, 4 days after aCD3/CD28 beads stimulation, of CB CD8+ T-cells transduced with and MOI 1 in the presence of LB (gray stripes) compared to STND method (gray). The data corresponds to ≥ 3 independent experiments and are shown as average ± standard deviation; p ≤ 0.05 (*); p ≤ 0.01 (**) ; p ≤ 0.001 (***); p ≤ 0.0001 (****).*

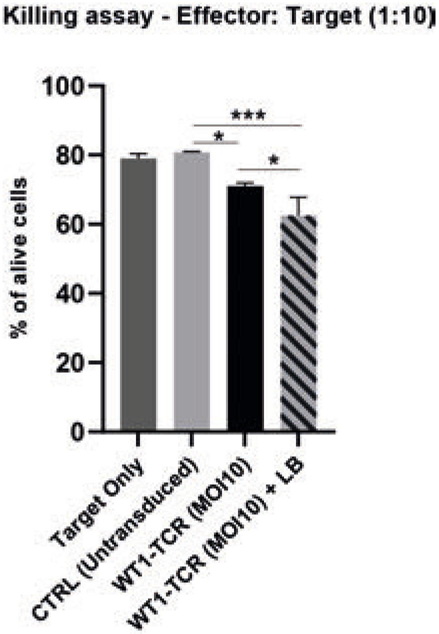

**Figure S4.** Killing capacity of WT1-TCR CB CD8+ T-cells transduced, in the presence or absence of LB, depicted as % of alive cells in a co-culture experiment with target cells loaded with pWT1-126.
*Co-culture experiments were performed at an effector-to-target ratio of 1:10. The data corresponds to ≥ 3 independent experiments and are shown as average ± standard deviation; p ≤ 0.05 (*); p ≤ 0.01 (**); p≤ 0.001 (***); p ≤ 0.0001 (****).*

# Chapter 8

## Epigenetic modulation of neuroblastoma enhances T- and NK-cell immunogenicity by inducing a tumor cell lineage switch

Cornel A.M.[1,2], Dunnebach E.[1,2], Hofman D.A.[1], Das S.[3,4], Sengupta S.[3,4], van den Ham F.[1,], Wienke J.[1], Strijker J.G.M.[1], van den Beemt D.A.M.H.[1,2], Essing A.H.W.[1] , Koopmans B.[1], Engels S.A.G.[1] , Lo Presti V.[1,2], Szanto C.S.[1], George R.E.[3,4], Molenaar J.J.[1], van Heesch S.[1], Dierselhuis M.P.[1], Nierkens S.[1,2,*]

[1] *Princess Máxima Center for Pediatric Oncology, Utrecht, The Netherlands*
[2] *Center for Translational Immunology, University Medical Center Utrecht, Utrecht, The Netherlands*
[3] *Department of Pediatric Oncology, Dana-Farber Cancer Institute, Boston, MA, USA*
[4] *Department of Pediatrics, Harvard Medical School, Boston, MA, USA*

*Journal for Immunotherapy of Cancer 2022 Dec 15;10(12), e005002*

## ABSTRACT

### Background

Immunotherapy in high-risk neuroblastoma (HR-NBL) does not live up to its full potential due to inadequate (adaptive) immune engagement caused by the extensive immunomodulatory capacity of HR-NBL. We aimed to tackle one of the most notable immunomodulatory processes in NBL, absence of MHC-I surface expression, a process greatly limiting cytotoxic T-cell engagement. We and others have previously shown that MHC-I expression can be induced by cytokine-driven immune modulation. Here, we aimed to identify tolerable pharmacological repurposing strategies to upregulate MHC-I expression, and therewith enhance T-cell immunogenicity in NBL.

### Methods

Drug repurposing libraries were screened to identify compounds enhancing MHC-I surface expression in NBL cells using high-throughput flow cytometry analyses optimized for adherent cells. The effect of positive hits was confirmed in a panel of NBL cell lines and patient-derived organoids. Compound-treated NBL cell lines and organoids were co-cultured with PRAME reactive tumor-specific T-cells and healthy-donor NK-cells to determine the *in vitro* effect on T- and NK-cell cytotoxicity. Additional immunomodulatory effects of histone deacetylase inhibitors (HDACi) were identified by transcriptome and translatome analysis of treated organoids.

### Results

Drug library screening revealed MHC-I upregulation by inhibitor of apoptosis inhibitor (IAPi)- and histone deacetylase inhibitor (HDACi) drug classes. The effect of IAPi was limited due to repression of NFκB pathway activity in NBL, while the MHC-I modulating effect of HDACi was widely translatable to a panel of NBL cell lines and patient-derived organoids. Pre-treatment of NBL cells with the HDACi Entinostat enhanced the cytotoxic capacity of tumor-specific T-cells against NBL *in vitro*, which coincided with increased expression of additional players regulating T-cell cytotoxicity (e.g. TAP1/2 and immunoproteasome subunits). Moreover, MICA and MICB, important in NK-cell cytotoxicity, were also increased by Entinostat exposure. Intriguingly, this increase in immunogenicity was accompanied by a shift towards a more mesenchymal NBL cell lineage.

### Conclusions

This study indicates the potential of combining (immuno)therapy with HDACi to enhance both T- and NK-cell-driven immune response in patients with HR-NBL.

## INTRODUCTION

Immune surveillance by the immune system is essential to prevent the development and progression of neoplastic cells into cancer. Various innate and adaptive players are involved in this process, of which cytotoxic T-cells are particularly well equipped [1]. Cytotoxic T-cells recognize their target in major histocompatibility complex class I (MHC-I), a protein expressed on all post-embryonic nucleated cells. This way, cytotoxic T-cells sense and act upon intracellular changes, for example caused by viral infection or malignant transformation. However, tumor cells can escape recognition by- and cytotoxicity of T-cells via a range of mechanisms.

One well-known T-cell escape mechanism of cancer cells is the dysregulation of surface expression of MHC-I, a process described in 40-90% of human tumors and often correlated with poor prognosis [2]. Lack of MHC-I expression can either result from MHC-I downregulation, which occurs through a survival advantage of cells lacking MHC-I, or an intrinsic lack of MHC-I expression due to tumor origin. MHC-I downregulation can often be found in adult tumors and can be caused by irreversible, genetic aberrations as well as by reversible, (post)transcriptional modifications [2]. Intrinsic lack of MHC-I expression is often observed in pediatric tumors that arise from embryonic tissues lacking immunological features, of which neuroblastoma (NBL) is a well-known example [3]. Intrinsic lack of MHC-I expression is mostly reversible and results from epigenetic and/or (post)transcriptional processes. The intrinsic reversible nature provides an opportunity to restore MHC-I expression and facilitate anti-tumor T-cell cytotoxicity against NBL [4,5].

NBL is an embryonal tumor derived from the sympathoadrenal progenitor cells of the developing sympathetic nervous system. It is the most common pediatric extracranial solid tumor and accounts for ~15% of all worldwide pediatric oncology deaths [6]. NBL cells can either be of the mesenchymal cell lineage (defined by lineage markers including PRRX1, FOSL1, and FOSL2) or the adrenergic cell lineage (defined by lineage markers including PHOX2B, DBH, and TH) [7,8]. It was recently shown that mesenchymal cells show more immunogenic features [9]. Despite intense multi-modal therapy, including maintenance immunotherapy consisting of anti-GD2 monoclonal antibody and isotretinoin, 5-year event-free survival of high-risk NBL (HR-NBL) patients is still ~50% [6,10]. The additive effect of the immunotherapy regimen [11,12], despite the low immunogenicity of HR-NBL [13], however, shows the potential of immunotherapy in NBL.

We hypothesize that the clue to further enhance (immuno)therapy efficacy in HR-NBL is to effectively engage T-cells, thereby enhancing anti-tumor cytotoxicity and creating immunological memory to prevent future relapse. MHC-I unrestricted T-cell engaging strategies, like CAR T-cell therapy, are tested in NBL to bypass the need for tumoral MHC-I expression, however, the current observed clinical benefit is limited [13]. We have previously shown that MHC-I expression on NBL cells can be readily upregulated by cytokine-driven immune modulation, thereby directing T-cell cytotoxicity to NBL [4,5,14]. Nonetheless, even though results from a pilot clinical trial administering IFNγ to HR-NBL patients were encouraging [14,15], the broad range of biological activities of these cytokines limits their therapeutic applicability due to severe toxicities [2]. Therefore, we here aimed to identify pharmacological repurposing strategies to upregulate MHC-I expression, and therewith enhance T-cell immunogenicity in NBL.

## MATERIALS & METHODS

### Cell culture

LAN5, SHEP21N, SK-N-SH, and IMR32 were obtained from the Princess Maxima Centre for Pediatric Oncology, GIMEN via the Academic Medical Center of Amsterdam. GIMEN NFκB reporter cells and N4BP1 knockout SK-N-SH were generated as described previously [17]. GIMEN and IMR32 were maintained in DMEM, LAN5 and SHEP21N in RPMI, both supplemented with Glutamax, 10% FCS (Sigma-Aldrich), 1% penicillin/streptomycin (P/S) (50 units/ml), and 2% non-essential amino acids (NEAA) (both Life Technologies). LAN5, SK-N-SH, and IMR32 were previously identified as adrenergic, GIMEN and SHEP21N are from the mesenchymal cell lineage [9].

**Table 1** – Genetic characteristics of the patient-derived organoids

| **Aberrations** | **Patient-derived organoids** | | | | |
|---|---|---|---|---|---|
| | *691b* | *039* | *753T* | *059* | *772T2* |
| *MYCN Amp.* | X | X | | | |
| *ALK* | | | | | |
| *CDKN2A Del.* | | | | | |
| *TERT Act.* | | | X | X | |
| *ATRX* | | | | | Homdel |
| *1p loss* | X | X | X | | |
| *11q loss* | | X | X | X | X |
| *17q gain* | X | X | X | X | X |
| *2p gain* | X | X | | | |
| *3p loss* | | X | | | |
| *6q loss* | | X | | | |

*Abbreviations: Amp. = Amplified; Del. = Deletion, Homdel = homologous deletion, Act.: activation via enhancer hijacking*

Patient-derived NBL organoids were established as described previously [49]. Organoids were maintained in DMEM low glucose, Glutamax supplemented medium, supplemented with 25% HAM's F-12 Nutrient Mix, 2% B-27 supplement minus vitamin A, 1% N-2 Supplement, 1% P/S (all Life Technologies), 20 ng/mL Animal-Free Recombinant Human-EGF, 40 ng/mL FGF-basic, 200 ng/mL IGF-I, 10 ng/mL PDGF-AA, and 10 ng/mL PDGF-BB (all Peprotech). Once a week, spheres were disrupted using Accutase (Sigma Aldrich) and pipetting and subcultured to avoid overcrowding and necrosis in the organoid cores. A half media change was performed biweekly. An overview of organoid characteristics can be found in **Table 1**, all organoids reflect a more adrenergic cell lineage (**Figure S9**).

### Drug repurposing library screening

Two repurposing libraries were screened on their effect on MHC-I surface expression in NBL: the Center for Drug Design & Discovery (CD3) Repurposing Library, containing 3700 mainly FDA-approved drugs, and our Pediatric Cancer Library, comprising 194 drugs with implications in pediatric cancer treatment. The CD3 library is stored at -20 °C in 384LDV plates (Labcyte), the pediatric cancer library in 384-well plates (Corning) at room temperature under N2 pressure.

Drug screening was performed using a GIMEN NFκB reporter line, utilizing a previously established high-throughput flow cytometry-based screening workflow [16]. The Pediatric Cancer Library was screened at a concentration range between 0.01 and 10 μM, the CD3 Repurposing Library at 300 nM and 3 μM. The Pediatric Cancer Library was added 4 hours after cell seeding using the Biomek i7 Hybrid (Beckman Coulter) and incubated for 48 hours before MHC-I expression analysis. The CD3 repurposing library was pre-spotted in empty 384-well plates using ECHO 520 acoustic droplet ejection (Labcyte). Reporter cells were added to these wells and incubated for 48 hours before MHC-I expression analysis. Vehicle-treated cells (DMSO) were used as a negative control, two cytokines with a known effect on MHC-I expression, IFNγ (R&D, 1000 U/mL) and TNFα (Miltenyi Biotec, 50 ng/uL), were used as positive controls. Conditions were omitted from analysis when single cell count was <500 to avoid false positivity due to toxicity. Unstained control cells of hits were analyzed to rule out false positivity due to autofluorescence. An incubation period of 48 hours was chosen based on experience of CD3, kinetics were later validated for positive hits (**Figure S10**). Cells were incubated for 48 hours with indicated drug concentrations, after which media was refreshed. MHC-I expression was determined at indicated time points.

### Validation of hits and determination of surface protein expression

Hits from the initial screen were diluted in DMSO (Sigma Aldrich) at a concentration of 10 mM and stored in aliquots at -80 °C to avoid freeze-thaw cycles (all SelleckChem). Respective cells and organoids were cultured for 48h with indicated concentrations of the drugs, upon which cell-surface expression of proteins of interest were determined by flow cytometry. Decreased expansion of cells was observed when cultured with Entinostat, viability was not significantly affected. Assembled MHC-I complexes were determined with the pan HLA-ABC AF647/FITC antibody (W6/32), other utilized antibodies include anti-MICA/MICB PE/Cy7 (6D4), HLA-E APC (3D12), HLA-DP/DQ/DR FITC (Tu39), PVR PE (SKII.4) (all Biolegend), PD-L1 BV650 (MIH1, BD Biosciences), B7H3 PerCP/eFluor710 (7-517, Life Technologies), Nectin-2 APC (R2.525, Ebioscience). Antibody panels were combined with 7-AAD (BD Biosciences) or the Fixable Viability eFluor 780 Dye (eBioscience) to select viable cells. Analysis was performed on a BD FACSCanto or LSRFortessa (BD Biosciences) .

CS&T beads (BD Biosciences) were used to check the performance and verify the optical path and stream flow of the utilized flow cytometers. This procedure enables controlled standardized results and allows the determination of long-term drifts and incidental changes within the flow cytometer. No changes were observed which could affect the results.

### Generation of $\text{PRAME}_{\text{SLLQHLIGL}}$-directed T-cells

The HLA-A2 restricted PRAME HSS1 T-cell clone (specific against SLLQHLIGL) was described previously [18], the TCR sequence was derived from patent US20160263155A1. A furin cleavage site was inserted upstream of the T2A sequence linking the TCR beta and alpha chains. The gene was synthesized (Genscript) and cloned into the pCCL-cPPT-hPGK-ORF-bPRE4-SIN lentiviral transfer vector [50]. Lentiviral particles were produced using standard calcium phosphate transfection (Clontech) of HEK-293T-cells with the pMDL-g/pRRE, pMD2-VSVg, and pRSV-Rev plasmids [51,52]. Transducing units per mL of concentrated vector batches were determined using serial dilution on Jurkat cells followed by flow cytometric analysis of Vβ1 expression (anti-Vβ1 FITC (REA662, Miltenyi)).

CD8+ T-cells were separated from peripheral blood of healthy donors, stimulated, and transduced at a multiplicity of infection (MOI) of 10 according to a previously described protocol [50]. Following transduction, cells were FACS-sorted on Vβ1 expression (BD FACSAria II) after which they are stimulated once every other week using a rapid expansion protocol (REP) in CTL medium [53].

### T-cell activation assay

HLA-A2 haplotype confirmed NBL cells, GIMEN and 691b, were incubated for 48h with the indicated concentrations of compounds, upon which cells were washed and co-cultured with NBL-specific T-cells. $\text{PRAME}_{\text{SLLQHLIGL}}$-directed T-cells were co-cultured with NBL cells overnight at an effector-to-target ratio (E:T) of 1:1 to determine the effect of pre-incubation with compounds of interest on T-cell activation. After overnight incubation, cells were spun down and supernatants were collected to determine cytokine levels (TNFα and IFNγ) using ELISA according to manufacturer's instructions (Life Technologies). T-cells were subsequently stained with Fixable Viability Dye eFluor™ 780 (Life Technologies), anti-CD3 BV510 (OKT3, Biolegend), anti-CD8 FITC (G42-8, BD Biosciences), and anti-CD137 PE (4B4-1, Biolegend) as a marker for antigen-specific T-cell activation. Flow cytometry analysis was performed on the BD Fortessa (BD Biosciences).

### T- and NK-cell cytotoxicity assay

GIMEN cells were transduced with a lentiviral construct encoding for GFP and luciferase (pSLuc2-GFP), upon which they were single cell sorted based on GFP expression. Luciferase-expressing 691b organoids were generated previously [54]. Luciferase expressing targets were seeded in organoid medium and incubated for 48h with indicated compound concentrations. $\text{PRAME}_{\text{SLLQHLIGL}}$-directed T-cells were added to the target cells (CTL medium:organoid medium ratio of 1:1) and are incubated overnight at an E:T of 1:1 to determine the effect of pre-incubation with compounds of interest on the cytotoxic capacity of T-cells. 150 ug/mL D-Luciferin Firefly (Biosynth) was added to the co-cultures and incubated for 10 minutes at 37 °C after which luminescence was measured using the Spectramax M3 (Life Technologies). Cytotoxicity was calculated by comparing luminescence of co-cultured cells with target only, treatment-matched controls. MHC-I dependence was studied by incubation with 10 ug/mL of HLA-ABC antibody (W6/32, Biotechne) for an hour prior to co-culture, IgG isotype (Invitrogen) was used as a control [55].

The cytotoxicity protocol was adjusted to be able to also address NK-cell cytotoxicity. Healthy-donor NK-cells were pre-stimulated overnight with 1000 U/mL IL-2 and 50 ng/mL IL-15, after which 691b cells were co-cultured for 5h with healthy-donor NK-cells at an E:T of 1:1.

### T-cell proliferation assay

Healthy-donor CD3+ T-cells were pre-treated overnight with 2.5 μM Entinostat + 50 U/mL IL-2, controls were treated with 50 U/mL IL-2 only. Cells were subsequently labeled with CellTrace™ Violet (CTV) and stimulated with 2.5 mg/mL PHA (or left unstimulated). After 72h, proliferative capacity was determined by measuring CTV dilution using flow cytometry and additional staining with anti-CD3 AF700 (UCHT1, Sony), anti-CD4 PE (RPA-T4, BD Biosciences), and anti-CD8 (SK1, BD Biosciences) on the LSRFortessa.

## RNA isolation and sequencing

691b organoids were treated for 48h with 2.5 μM Entinostat. Cells were harvested and snap frozen in liquid nitrogen. Total RNA was isolated from cell lysates using the TRIzol LS reagent (Life Technologies). RNA was then purified using the RNA Clean and Concentrator-5 kit (Zymo Research) and treated with DNAse I. RNA concentrations were measured on a NanoDrop One spectrophotometer (Life Technologies). RIN values were determined on a BioAnalyzer 2100 using the RNA 6000 Nano kit (Agilent), with values ranging between 9.4 and 10.0. TruSeq mRNA-seq library preparation (Illumina) and strand-specific mRNA-sequencing were performed by Genewiz. Briefly, mature mRNA was selected through PolyA enrichment, and RNA sequencing was performed using the Illumina NovaSeq 6000 platform in a 2x150bp configuration. Samples were sequenced to an average depth of 136 million reads. Adapter sequences were trimmed and low-quality reads were filtered using Trimgalore v0.6.651, which invoked Cutadapt v3.452 and FastQC v0.11.953. Next, reads were aligned to the human transcriptome (hg38/GRCh38.p13; Ensembl release 102 provided in GTF format55) using STAR v2.7.8a54 in the 2-pass mapping mode. We used the default STAR settings together with the following modified parameters: --outFilterType BySJout, --outSAMunmapped Within, --outSAMattributes NH HI AS nM NM MD jM jI MC ch XS, --outSAMtype BAM SortedByCoordinate, --outFilterMismatchNmax 6, --alignSJoverhangMin 10, --outFilterMultimapNmax 10, --outFilterScoreMinOverLread 0.75. Reads were quantified using featureCounts from the Subread v2.0.256. software package, provided with default settings and Ensembl release 102 annotation information for gene-level read count summarization. DESeq2 v1.32.057 was used for read count normalization.

## Derivation of gene signature scores

Based on the immune pathway signature genes [9,56,57], immune activation (IA) scores for all replicates were determined. All immune signature genes were ranked based on their expression levels in each replicate. The ranking order was subsequently established for each gene and the percentiles were derived for each gene on the entire list of genes. All the IA signature genes in a sample were averaged to determine the IA score for each sample. Similarly, adrenergic (A) and mesenchymal (M) scores were calculated for each sample based on the gene signatures outlined by van Groningen and colleagues [7]. In total, 6 IA genes were removed from the 485-gene mesenchymal signature genes in order to ensure that IA signature genes did not overlap with predefined adrenergic and mesenchymal signatures. To further identify a sample as either adrenergic or mesenchymal, the A-score was deducted from the M-score (M-A score). Samples with low M-A scores were considered more adrenergic, whereas high M-A were considered mesenchymal. In addition, IFN-response signatures specific to HR-NBL were determined using the SEQC-498 tumor cohort and cell lines including SH-SY5Y, LDK-resistant SH-SY5Y, and SH-EP cells, as described by Sengupta *et al.* [9].

### Quantitative real-time PCR analysis

To confirm the findings observed with RNA-seq, qPCR analysis was performed. GIMEN and 691b cells were treated for 48h with 5 μM and 2.5 μM Entinostat respectively. Cells were pelleted, RNA was extracted with the RNeasy mini extraction kit (Qiagen), and cDNA was synthesized using the RevertAid H Minus First Strand cDNA Synthesis Kit with random hexamer primers (Life Technologies). mRNA expression was subsequently quantified using the TaqMan™ Human Antigen Processing and Presentation by MHCs Gene Expression Array on a ViiA7 RT-PCR system (Both Life Technologies). All kits were used according manufacturer's instructions.

### Data Analysis and statistics

Flow cytometry data analysis was performed with FlowJo V10.7.1, flow cytometry data are presented as % of cells, mean fluorescent intensity (MFI), or fold-change in MFI. ELISA data were analyzed using MicroPlate Manager 6 (BioRad). Graphs for flow cytometry, ELISA, and luminescence data were generated and statistics were performed using Graphpad Prism 8.3. Heatmaps were generated using the ComplexHeatmap v2.8.0 and the ggplot2 package from RStudio (v3.3.3) [58,59].

Fold-changes, reflecting differences in protein expression and qPCR analysis, were logarithmically transformed, after which a one-sample T-test was performed. Differences in MFI; reflecting protein surface expression, T-cell activation, cytokine secretion levels, cytotoxic capacity of cells, and differences in expression of immune signature genes were analyzed with the non-parametric Mann-Whitney U test between separate groups. Values of $p<0.05$ were considered significant.

## RESULTS

### Screening drug repurposing libraries for their effect on MHC-I expression

Drug repurposing libraries, containing ~3800 unique compounds, were tested for their ability to upregulate surface display of MHC-I in the GIMEN NBL cell line containing an NFκB reporter. The effect of compounds on MHC-I expression was evaluated after 48h of incubation using high throughput flow cytometry [16] (exemplary gating strategy in **Figure S1**). MHC-I expression of screened drugs standardized to untreated control cells is shown in **Figure 1A**. Two groups of drugs, those inhibiting inhibitor of apoptosis (IAPi) and histone deacetylase inhibitors (HDACi) were selected for further evaluation, as 16/29 HDACi (**Table S1**) and 6/6 screened IAPi (**Table S2**) increased MHC-I expression in our GIMEN NFκB reporter system.

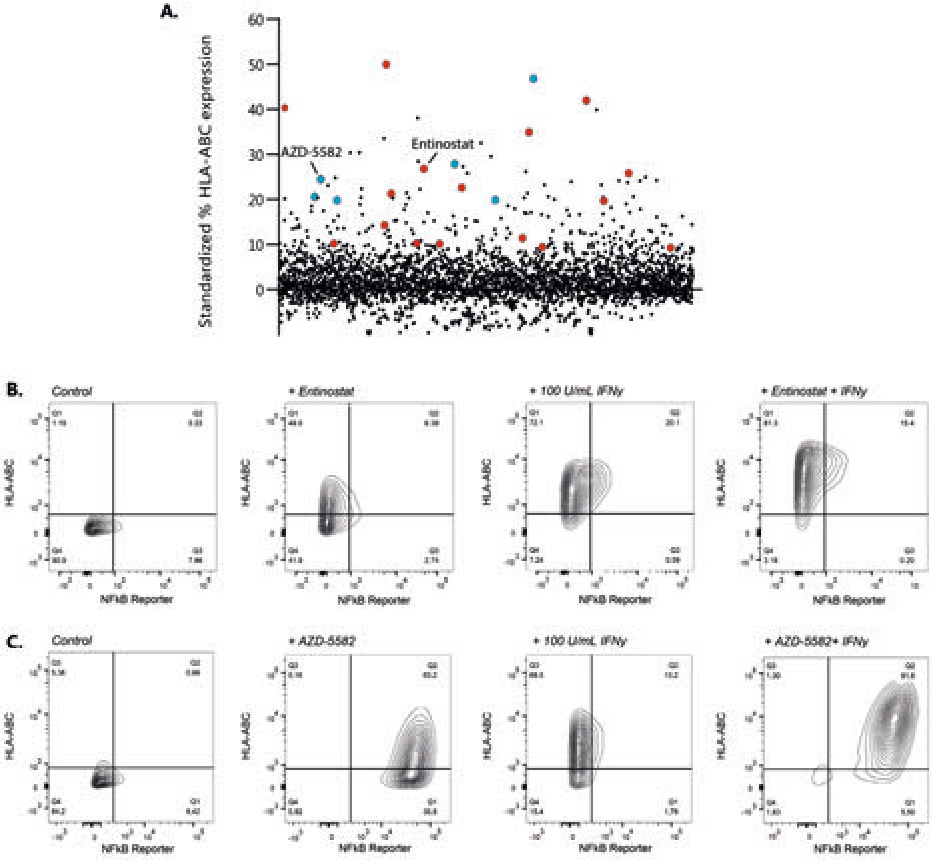

**Figure 1.** Identification of MHC-I expression enhancing compounds in NBL.
***(A)*** *Screening results of 3800 compounds are shown as standardized % of HLA-ABC expression compared to untreated control GIMEN NFκB reporter cells. Compounds marked in red are histone deacetylase inhibitors (HDACi), compounds marked in blue reflect the inhibitor of apoptosis inhibitors (IAPi).* ***(B)*** *MHC-I expression in GIMEN reporter cells treated with Entinostat (5 μM) or IFNγ (100 U/mL) as single agents, and in combination (Entinostat + IFNγ). Control indicates untreated cells.* ***(C)*** *MHC-I expression in GIMEN reporter cells treated with AZD-5582 (250 nM) or IFNγ (100 U/mL) as single agents, and in combination (AZD-5582 + IFNγ). Control indicates untreated cells.*

The data shown in this paper focuses on, but are not limited to (supplementary material), the HDACi Entinostat, currently tested in children with relapsed or refractory malignancies in combination with checkpoint inhibition (NCT03838042), and the IAPi AZD-5582. MHC-I upregulation by Entinostat was not mediated by NFκB reporter activation (**Figure 1B**), whereas the effect of AZD-5582 was mediated by induction of NFκB expression (**Figure 1C**). Further increase in MHC-I expression was observed when the cells were co-treated with IFNγ (**Figure 1B+C, right panels**).

## NFκB pathway repression inhibits the effect of IAPi on MHC-I expression in the majority of neuroblastoma models

GIMEN cells were co-cultured with T-cells directed against the NBL-specific PRAME antigen ($PRAME_{SLLQHLIGL}$) to address the effect of AZD-5582-induced MHC-I on T-cell activation and cytotoxicity. GIMEN were pre-incubated for 48h with AZD-5582, the MHC-I enhancing cytokines IFNα and/or IFNγ acted as positive controls. Determination of CD137 expression, as a surrogate marker for antigen-specific T-cell activation, and the cytotoxic capacity after subsequent overnight co-culture with T-cells revealed enhanced activation and cytotoxicity of T-cells, to a similar extent as cytokine pre-treated controls (**Figure 2A**).

We subsequently assessed the effect of AZD-5582 (**Figure 2B**) and two other IAPi, Birinapant and Xevinapant (**Figure S2)**, on a panel of NBL cell lines and patient-derived organoids. The significant induction of MHC-I expression in the GIMEN line could, however, only be translated to the MHC-I expressing SHEP21N line, and was not observed in other NBL cell lines and patient-derived organoids. We noticed that all adrenergic models (all except GIMEN and SHEP21N), insensitive to TNFα-mediated MHC-I induction, did not respond to IAPi (**Figure S3**). We therefore hypothesized that IAPi target upstream of previously identified key negative regulators of NFκB signaling in NBL, N4BP1 and TNIP1 [17]. To test this hypothesis, we determined the effect of AZD-5582 on the adrenergic N4BP1 knock-out (KO) SK-N-SH cell line [9,17]. KO of N4BP1 by itself already increased MHC-I levels (**Figure 2C**). Nevertheless, we did observe a further increase in MHC-I expression upon AZD-5582 pretreatment in N4BP1 KO in SK-N-SH cells. In addition, this effect was amplified by co-incubation with IFNγ (**Figure 2C, lower panel**). These data indicate that IAPi enhance NFκB expression, and therewith MHC-I expression, upstream of these key negative regulators of NFκB signaling in NBL.

8

## Entinostat increases MHC-I expression in a panel of in vitro neuroblastoma models

The lack of NFκB reporter activity in Entinostat-treated GIMEN (**Figure 1A**) suggests that the repressed NFκB pathway activity in many NBL models does not limit MHC-I upregulation by HDACi via Entinostat. To this end, we determined the effect of HDACi in a panel of NBL cell lines as well as in patient-derived organoids representing the diverse spectrum of genomic aberrations associated with NBL (i.e. MYCN amplification, TERT activation, ATRX inactivation, loss of 1p/11q/17q/3p/6q, and 17q gain) (**Table 1**). Indeed, we observed increases in MHC-I expression in all screened NBL lines **(Figure 3A**), and all but one of the patient-derived organoids (**Figure 3B**). Interestingly, a marked upregulation was observed even in the MHC-I+ SHEP21N cell line, indicating that the effect of HDAC inhibition is not limited to NBL models lacking MHC-I expression.

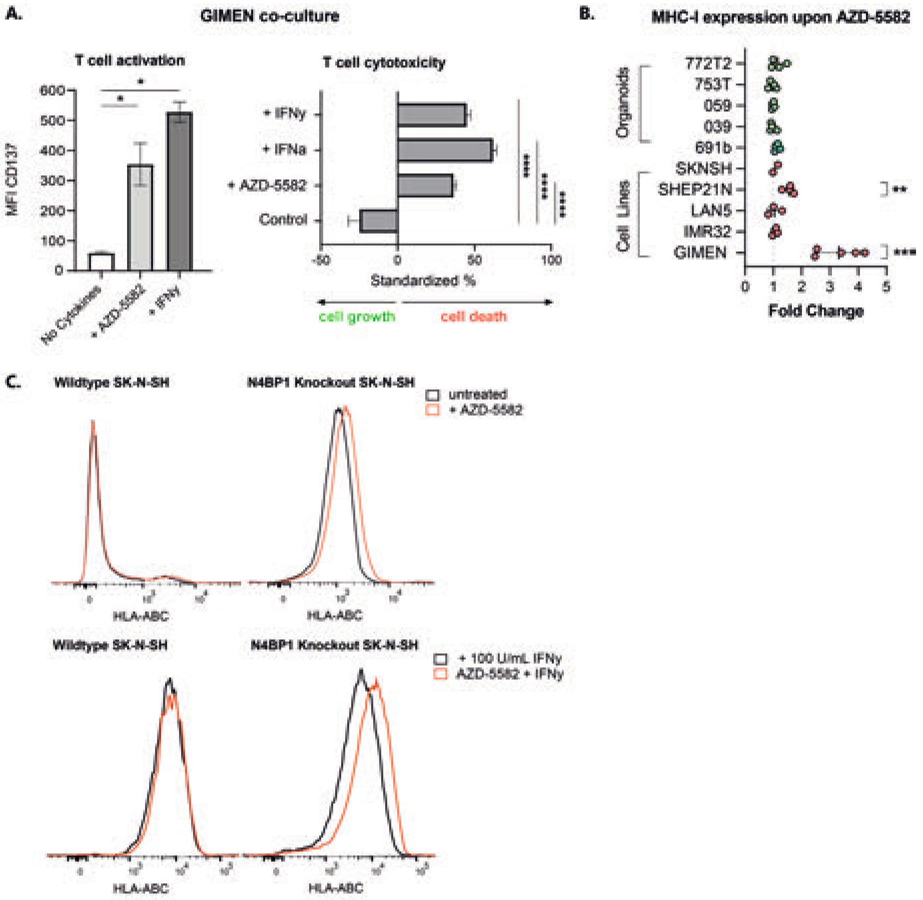

**Figure 2.** Key regulators of NFκB signaling in NBL inhibit effect of IAPi in majority of cell lines and patient-derived organoids.

***(A)*** *CD137 expression-based activation (left) and cytotoxic capacity (right) of PRAME*$_{SLLQHLIGL}$*-directed T-cells after co-culture with GIMEN cells pre-incubated with 125 nM AZD-5582 for 48h (or respective controls, 100 U/mL IFNγ or 1000 U/mL IFNα). T-cell activation and cytotoxicity were assessed upon overnight co-culture at an effector-to-target ratio (E:T) of 1:1. Cytotoxicity was standardized to target only, treatment matched controls, n=4. Data presented as mean ± SEM.* ***(B)*** *Fold-change in MHC-I expression on a panel of NBL cell lines and organoids after 48 incubation with 125 nM AZD-5582. Fold-change reflects increases in HLA-ABC MFI relative to untreated control cells. Data presented as mean ± SD. LAN5: n=3, GIMEN: n=5, rest: n=4, Statistical differences between log(fold-changes) were calculated using a one-sample T-test, **p<0.01, ***p<0.001.* ***(C)*** *Histograms reflecting MHC-I expression on wildtype SK-N-SH (left) and SK-N-SH in which the NFκB pathway regulator N4BP1 is knocked out (right) upon 48h incubation with 125 nM AZD-5582. Control histograms are shown in black, histograms of AZD-5582 treated cells are shown in red. The top panel reflects cells without co-incubation with MHC-I enhancing cytokines, the lower panel shows expression of cells pre-treated with 100 U/mL IFNγ. Statistical differences were calculated using the Mann Whitney U test, *p<0.05, **** p<0.0001.*

Moreover, co-incubation of Entinostat with cytokines known to affect MHC-I expression, IFNα and IFNγ, further augments this upregulation (**Figure 3C**). Together, these findings demonstrate that Entinostat induces expression of the main prerequisite for cytotoxic T-cell recognition of neuroblastoma cells: surface expression of MHC-I. Not only

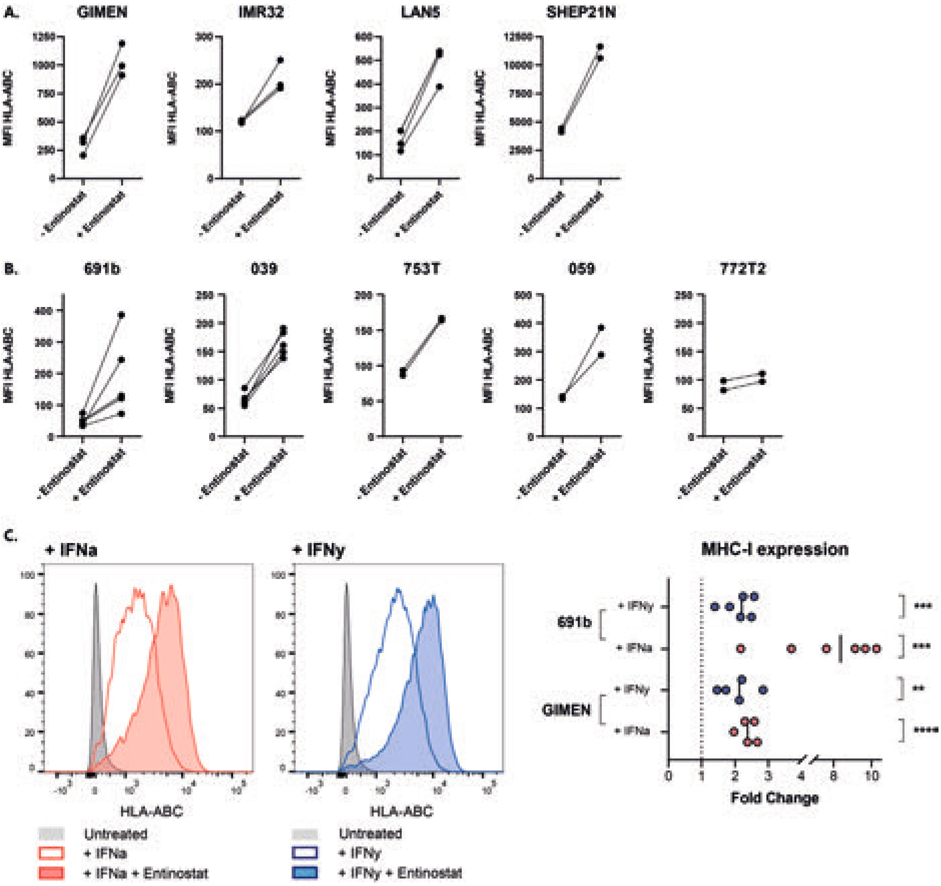

**Figure 3.** Entinostat increases MHC-I expression in a panel of NBL cell lines and patient-derived organoids. *(**A+B**) MHC-I expression after 48h of incubation with Entinostat with cell lines (**A**) or patient-derived organoids (**B**). Entinostat concentrations: GIMEN & LAN5, 039, 772T2 : 5 µM (n=3, n=3, n=5, and n=2, respectively), 691b: 2.5 µM (n=5), IMR32, SHEP21N, 753T & 059: 1.25 µM (IMR32 n=3, rest n=2). Untreated cells (- Entinostat in graph) served as control. Paired data of separate experiments are shown. (**C**) MHC-I expression after 48h of incubation with Entinostat, combined with the MHC-I enhancing cytokine 1000 U/mL IFNα or 100 U/mL IFNγ. Left: flow cytometry histograms of GIMEN cells, right: fold-changes of Entinostat + cytokine treated cells compared to cytokine treated controls. Statistical differences between log(fold-changes) were calculated using a one-sample t-test.*

Entinostat, but also two other screened HDACi, Tucidinostat and Fimepinostat, showed similar effects on MHC-I upregulation in a panel of NBL lines (**Figure S4**).

## Entinostat sensitizes neuroblastoma cells to T-cell-mediated cytotoxicity

Next, we determined whether Entinostat-induced MHC-I upregulation results in enhanced activation and cytotoxicity of $\text{PRAME}_{\text{SLLQHLIGL}}$-directed T-cells [18]. GIMEN and patient-derived 691b organoid cells, both MHC-I negative, were selected for these assays based on the presence of both the HLA-A2 haplotype as well as endogenous PRAME expression. Activation and cytotoxic capacity of T-cells were assessed by

CD137 expression on T-cells, TNFα and IFNγ secretion by T-cells, and cytotoxicity in an overnight assay.

CD137 expression significantly increased upon pre-treatment of target cells with Entinostat, which was magnified by co-treatment with MHC-I enhancing cytokines IFNα and IFNγ (**Figure 4A**). Analysis of the supernatants of these cultures for the presence of T-cell activation-related cytokines IFNγ and TNFα revealed that the increase in CD137 expression conjointly resulted in a significant increase in secretion of these cytokines (**Figure 4B**). This suggests a self-perpetuating positive feedback loop once T-cells become activated as a result of Entinostat-mediated immunogenicity of NBL cells.

Finally, the cytotoxic capacity of the T-cells was determined in an overnight luminescence-based cytotoxicity assay with luciferase transduced 691b cells. Entinostat pre-treatment resulted in a similar increase in cytotoxic capacity of T-cells as pre-treatment with MHC-I enhancing cytokines (**Figure 4C**). MHC-I dependence was confirmed by MHC-I blocking experiments (**Figure S5**). The co-culture experiment was performed in the presence of Entinostat, indicating that Entinostat did not affect the cytotoxic capacity of the T-cells. T-cell functionality in presence of Entinostat was further confirmed in a proliferation assay with Entinostat pre-treated healthy-donor CD3+ T-cells (**Figure S6**). Collectively, these data indicate that Entinostat increases T-cell immunogenicity of NBL cells via upregulation of MHC-I antigen presentation.

### The immunogenic effect of Entinostat reaches beyond MHC-I antigen presentation

HDACs are important transcriptional regulators with a broad mechanism of action. So far, we focused on MHC class I mediated antigen presentation. Nevertheless, the degree of immune engagement depends on the balance between a wide variety of inhibitory and stimulatory signals to immune cells [13]. Therefore, RNA-seq was performed to compare expression of these molecules between untreated and Entinostat-treated 691b organoids.

Unsupervised clustering of replicates resulted in complete separation between untreated and Entinostat-treated organoid replicates (**Figure 5A**). Based on the relative expression of a curated set of 41 genes known to have major roles in tumor cell-intrinsic immune functions [9], an immune activation (IA) score was calculated for untreated and Entinostat-treated 691b organoids, which revealed a significant increase in IA-score upon Entinostat treatment (**Figure 5B**). Besides significant increases in expression of genes involved in MHC-I antigen presentation (i.e. *HLA-A/B/C, TAP1/2, ERAP2, B2M*), we

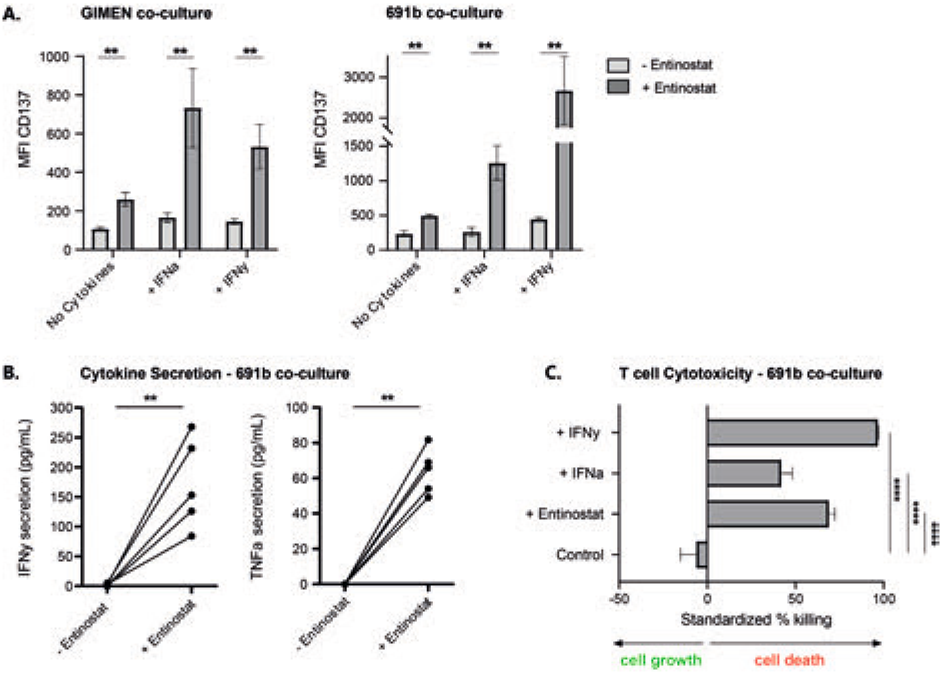

**Figure 4.** Entinostat treatment increases the activation and cytotoxic capacity of antigen-specific T-cells. ***(A)*** *CD137 expression based activation of NBL-specific PRAME$_{SLLQHLIGL}$-directed T-cells after 48h pre-incubation of GIMEN cells (left) or the patient-derived organoid 691b (right) ± Entinostat upon overnight co-culture at an E:T of 1:1. Entinostat concentration in GIMEN and no cytokine 691b condition was 5 µM, concentration in remaining 691b conditions was 2.5 µM. 100 U/mL IFNγ or 1000 U/mL IFNα was added to the indicated conditions. Data are shown from five replicates of three individual experiments.* ***(B)*** *IFNγ (left) and TNFα (right) secretion in pg/mL in the supernatants of the overnight co-culture between 691b organoids and PRAME$_{SLLQHLIGL}$-directed T-cells from (A), determined by ELISA. 5 replicates are shown from three individual experiments.* ***(C)*** *Luminescence-based cytotoxicity against luciferase-transduced 691b organoids after 48h pre-incubation with 2.5 µM Entinostat, 1000 U/mL IFNα, or 100 U/mL IFNγ. Cells were co-cultured overnight at an E:T of 1:1. Data are shown from three individual experiments. Data are shown as mean ± SEM. Statistical differences were calculated using the Mann Whitney U test, **p<0.01, **** p<0.0001.*

also noted significant upregulation of expression of genes encoding NK-related receptor ligands (i.e. *HLA-E/F, MICA/B, ULBP2/3*) and immunoproteasome (IP) subunits (*PSMB8/9*). These increases were confirmed with qPCR analysis of GIMEN and 691b organoids (**Figure S7**). Additionally, RNA-seq revealed a significant increase in the expression of transcripts encoding the immune checkpoint ligands CD274 (PD-L1) and NECTIN2. Nevertheless, subsequent flow cytometric analysis did not reveal any differences in cell surface protein expression of these checkpoint receptor ligands (**Figure 5C**).

The enhanced levels of NK-cell stimulatory (i.e. MICA/B, ULBP2/3) and inhibitory ligands (HLA-A/B/C/E/F) prompted the question whether the effect of Entinostat would tip the balance towards a pro- or anti-immunogenic effect on NK-cells. First, we determined whether the observed increase in transcript levels could be translated to cell surface protein expression. Indeed, besides the known increase in surface display in HLA-A/B/C, we observe a significant Entinostat-induced increase in cell surface expression of HLA-E and MICA/MICB (**Figure 5D**). The cytotoxic capacity of NK-cells was subsequently determined in a 5h luminescence-based cytotoxicity assay with luciferase transduced 691b. Entinostat pre-treatment of 691b, but not pre-treatment with MHC-I enhancing cytokines IFNα and IFNγ, resulted in a significant increase in cytotoxic capacity of healthy-donor NK-cells (**Figure 5E**). Together, these data show that the Entinostat-mediated increase in immunogenicity of NBL tumors is not limited to increased immunogenicity of cytotoxic T-cells, but also to other immune subsets like NK-cells.

### Entinostat-induced immunogenicity is accompanied by a neuroblastoma tumor cell lineage switch

It was recently shown that NBL tumor cell lineage, defined by a well-established 485-gene mesenchymal signature [7], is linked to the propensity of eliciting an immune response [9]. Plasticity between the less immunogenic, adrenergic and immunogenic, mesenchymal cell lineages was shown, which was demonstrated to be regulated by epigenetic imprinting [9,19]. Based on these data, we investigated whether the observed Entinostat-induced immunogenicity is accompanied by a switch towards a more immunogenic, mesenchymal cell lineage phenotype. Indeed, transcriptome analysis revealed that Entinostat treatment of 691b organoids induced an adrenergic to mesenchymal cell lineage switch (**Figure 6A+B, Figure S8A**). This cell lineage switch was accompanied by increase in IA-score (**Figure 6C**) and IFN-response signature (**Figure S8B**). Taken together, this suggests that Entinostat-mediated epigenetic modulation results in a tumor cell lineage switch that is accompanied by increased immunogenic properties of NBL tumors.

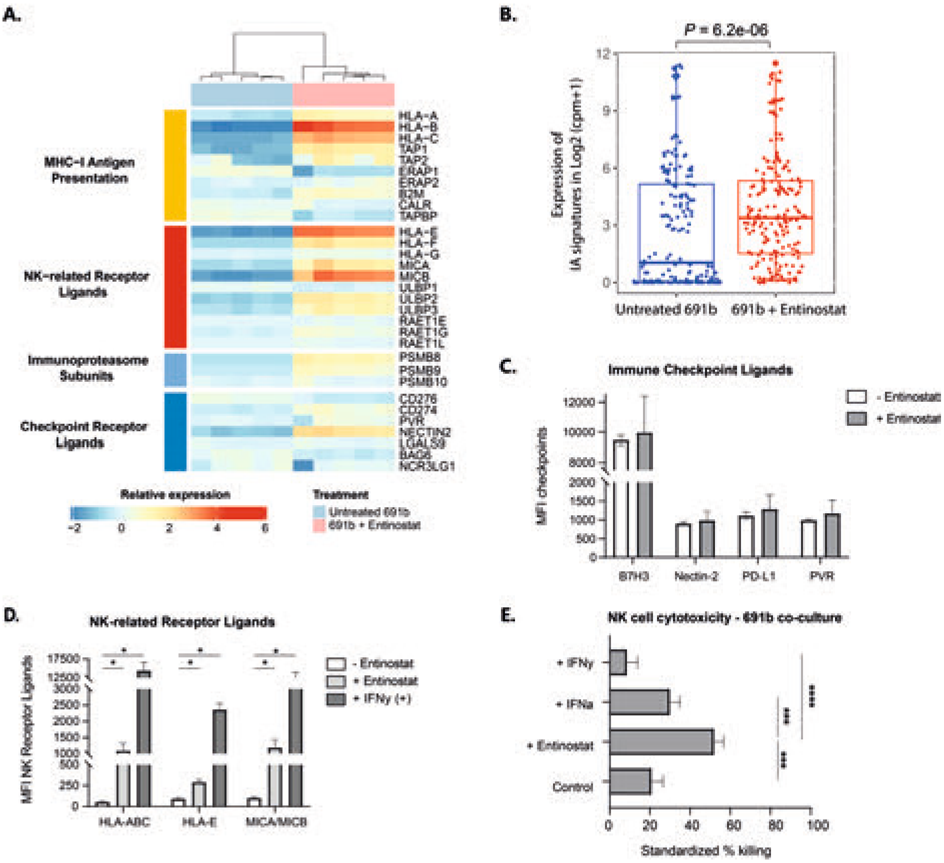

**Figure 5.** The pro-immunogenic effect of Entinostat goes beyond MHC-I antigen presentation.
***(A)*** *Unsupervised clustering of RNA-seq data of untreated 691b organoids (blue) and Entinostat-treated organoids (pink). Data are depicted as log2(fold-change).* ***(B)*** *Immune activation signature (IA-score) based on relative expression of 41 genes with major roles in tumor-cell intrinsic immune functions, such as regulation of MHC expression, antigen processing and presentation, NK-cell immunogenicity, and T- and NK-cell infiltration[9]. Score is compared between untreated (blue) and Entinostat treated (red) organoids. Expression of IA signatures in Log2 (cpm+1) is shown as median ± 25th and 75th percentiles, whiskers reflect minima and maxima. Data are normalized to cpm, Log2 value is shown. (A+B) Cells were treated for 48h with 2.5 µM Entinostat or vehicle control. Both groups: n=5* ***(C+D)*** *Flow cytometric analysis of surface expression of known immune checkpoint receptor ligands* ***(C)*** *or NK receptor ligands* ***(D)*** *after 48h of incubation with 2.5 µM Entinostat (or 1000 U/mL IFNγ as a positive control in the NK receptor ligand panel). Data are shown as mean fluorescent intensity ± SEM and reflects minimally three individual experiments. Statistical differences were calculated using the Mann Whitney U test, *p<0.05.* ***(E)*** *Luminescence-based NK-cell cytotoxicity against luciferase-transduced 691b organoids after 48h pre-incubation with 2.5 µM Entinostat, 1000 U/mL IFNα, or 100 U/mL IFNγ. NK-cells were pre-activated overnight with 1000 U/mL IL-2 and 50 ng/mL IL-15. Cells were co-cultured for 5h at an E:T of 1:1. Data are shown from four individual experiments with four different donors, and are standardized to target only, treatment matched control cells. Data are shown as mean ± SEM. Statistical differences were calculated using the Mann Whitney U test, **p<0.01, ***<0.001, **** p<0.0001.*

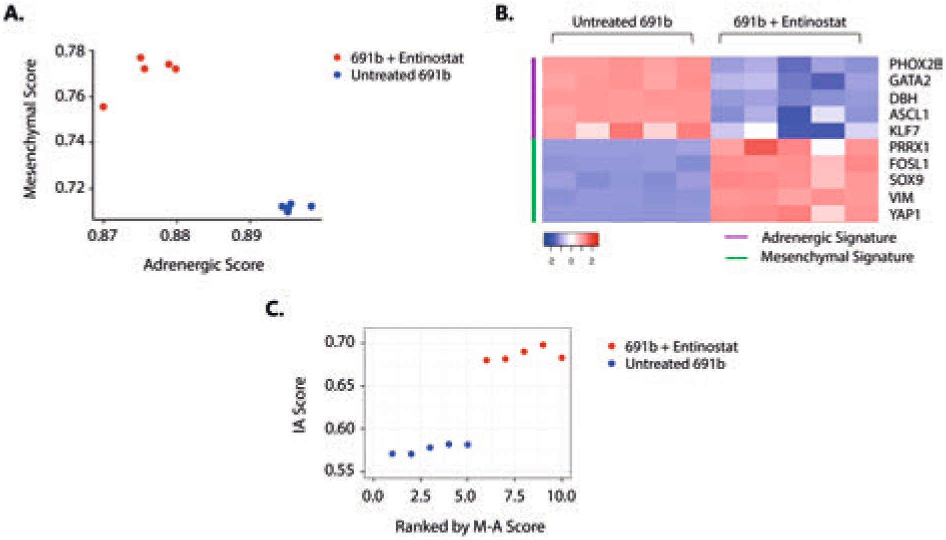

**Figure 6.** Entinostat induces an adrenergic-to-mesenchymal cell lineage shift which is accompanied by increased immunogenicity.
***(A)*** *Cell lineage score of untreated (blue) and Entinostat-treated (red) 691b organoids. Adrenergic (A) and mesenchymal (M) scores were calculated for each sample based on the gene signatures outlined by van Groningen and colleagues [7].* ***(B)*** *Expression of representative adrenergic (purple) and mesenchymal (green) signature genes in untreated and Entinostat-treated 691b organoids. Log2 gene expression values were z-score transformed for heatmap visualization.* ***(C)*** *Correlation plot between Mesenchymal minus Adrenergic Score (M-A score) and immune activation (IA) score in untreated (blue) and Entinostat-treated 691b organoids (red). X-axis denotes organoids ranked in increasing order of (M-A) score. Cells were treated for 48h with 2.5 µM Entinostat or vehicle control. Both groups: n=5.*

## DISCUSSION

Immunotherapy against NBL currently does not live up to its full potential, likely due to inadequate adaptive immune cell engagement, circumventing anti-tumor cytotoxicity and induction of immunological memory to prevent future relapse. We here show that treatment of NBL cells with the HDACi Entinostat results in induction of expression of the most important prerequisite for cytotoxic T-cell activation: surface expression of MHC-I.

MHC-I expression is controlled by multiple pathways, including the type I and II IFN pathways, as well as the (non-) canonical NFκB pathway [2]. We previously reported NFκB pathway repression in NBL, which is a result of high expression of two key negative regulators of NFκB signaling; N4BP1 and TNIP1 [17]. Targeting these regulators markedly sensitizes cells to NFκB-mediated MHC-I upregulation. Consequently, we hypothesize that compounds enhancing MHC-I expression in NBL should either enhance MHC-I expression via bypassing NFκB pathway activation, or repress or function downstream of these NFκB pathway regulators. NFκB reporter activity in our GIMEN reporter system revealed that IAPi induce MHC-I expression via NFκB pathway activation, while MHC-I expression by most HDACi is independent of NFκB pathway activation.

As the MHC-I expression enhancing effect of IAPi could not be translated to most of our *in vitro* NBL models, together with the confirmed insensitivity to NFκB-mediated MHC-I upregulation, we decided to study the effect of IAPi upon knockout/down of one of these key negative regulators, N4BP1. Indeed, N4BP1 knockout/down resulted in sensitization to MHC-I upregulation by the IAPi AZD-5582. We thus conclude that IAPi act upstream of N4BP1/TNIP1 and therefore do not induce MHC-I expression in the majority of NBL tumors, as most exert repressed NFκB pathway activity. Notwithstanding, pre-clinically, the synergistic effect of IAPi with checkpoint inhibition in glioblastoma [20] and enhanced radiation-induced immunological cell death in head and neck cancer [21] does show the potential of the immunomodulatory effect of IAPi in cancer, however, intact NFκB signaling seems to be a prerequisite for this.

During embryogenesis, neural crest cells (NCCs) gain multipotent differentiation potential to be able to differentiate into a wide variety of tissues of epithelial, mesenchymal and endothelial origin [22]. Differentiation of these NCCs is an intricate process regulated via a complex transcriptional/epigenetic regulatory scheme. Dysregulation of these regulatory schemes may result in inhibition of this maturation process, which may predispose multipotent NCCs to malignant transformation and NBL development. This is supported by studies that found increased HDAC expression in HR-NBL [23]. We show that HDACi resulted in increased expression in genes involved in antigen processing and presentation, without IFN/NFκB pathway activation, indicating that the poor immunogenic properties of NBL are indeed a derivate of a differentiational halt during embryogenesis. In other words, HDACi merely create a more accessible epigenetic landscape of loci involved in antigen presentation, thereby increasing responsiveness to IFN/NFκB pathway activation. This is underlined by the observation that MHC-I upregulation and T-cell activation is magnified when cells are co-treated with Entinostat and MHC-I enhancing cytokines. A recent study by Seier and colleagues, showing that inhibition of histone methyltransferases in NBL cell lines results in increased immunogenic properties, underlines that this effect is not restricted to epigenetic modelling by HDACi [24,25]. As other embryonal cell-derived pediatric tumors, including malignant rhabdoid tumors and medulloblastoma, also display low levels of immunogenic markers and have been shown to also result from differentiational halt during embryogenesis [26–29], we expect that the potential of HDACi to induce immunogenicity is translatable to other embryonal-cell derived tumors.

MHC-I expression is the most important, but not the only prerequisite for NBL-induced cytotoxic T-cell engagement. Pediatric tumors display a low mutational burden [13], causing a narrow repertoire of T-cells that specifically recognize and target NBL. We here observe Entinostat-mediated induction of IP subunits PSMB8 and -9. IP activation induces more efficient and differential proteasome-mediated peptide processing [30], which may result in a broader and more efficient NBL-specific T-cell response upon Entinostat treatment. In addition, clinical studies in melanoma and pre-clinical studies in bladder cancer reported induction of expression of several neoantigens upon Entinostat treatment [31,32], which is accompanied by an increase in CD8+ effector memory T-cells at the tumor site. Moreover, increased expression of known NBL-associated antigens, cancer germline genes and GD2 expression respectively, was reported upon epigenetic modulation in NBL [33–35]. These data may imply that Entinostat increases NBL T-cell immunogenicity at multiple layers. Nonetheless, systemic T-cell dysfunction [36], expression of immune checkpoint molecules, presence of immunosuppressive stromal- and myeloid cells, as well as secretion of immunoregulatory mediators by NBL are remaining factors to be tackled to maximize T-cell immunogenicity [13].

Most studies evaluate the effect of HDACi on tumor cells, but much less is known about the effect on systemic and local effect on immune cell subsets. The effect of HDACi on leukocyte function is debated in literature, as studies report both immunosuppressive [37] and immune enhancing effects [31,34,35,38–41]. It is suggested that the effect of HDACi on immune cells is highly dependent on the class(es) of targeted HDAC(s) [41]. Consequently, one should be careful translating results from one class of HDACi to the other. We studied the effect of Entinostat on T- and NK-cell cytotoxicity in the presence of Entinostat, and observed a clear enhanced cytotoxic capacity. This is underlined by the observation that T-cell proliferation was still observed in presence of a high dose of Entinostat. Two NBL mouse models showed that Vorinostat, another class I HDACi, decreased abundance and immunosuppression of myeloid-derived suppressor cells and tumor-associated macrophages, which may decrease immunoregulatory signals in the tumor microenvironment affecting T-cell engagement [34,35]. In addition, besides other studies showing Entinostat-induced upregulation of stimulatory NK-receptor ligands in other cancer types [38,39], increased expression of natural cytotoxicity receptors (i.e. NKG2D and NKp30) was reported on NK-cells themselves, suggesting that NK function might even be enhanced [39,40].

Several pre-clinical studies have shown an anti-tumor effect of HDACi in HR-NBL, generally highlighting their potency to inhibit cell proliferation, promoting cell cycle arrest, differentiation, and apoptosis, as reviewed by Phimmachanh and colleagues [42]. Nonetheless, the increase in immunogenicity accompanying this HDACi-induced differentiation of NBL tumors we observe in our study is largely unreported. Several clinical trials are being conducted to investigate the potential of HDACi in NBL [42]. Three of these trials (NCT02559778, NCT03332667, and NCT03838042) combine HDACi with immunotherapy (with Dinutuximab/GM-CSF/IL-2 and isotretinoin, MIBG/Dinutuximab/Vorinostat, and checkpoint inhibition, respectively), studying the synergistic potential of these combinations.

Two clinical studies in various advanced adult cancers report improved outcome when combining immunotherapy with Entinostat [43,44]. Pre-clinical studies have revealed that this is a result of increased adaptive immune engagement, of which reversion of MHC-I expression is one of the described mechanisms [41,45–48]. Nevertheless, one should be careful translating immunogenic effects of drugs in adult tumors to pediatric tumors, and even more so to embryonal cell derived pediatric tumors, as the essential difference in tumorigenesis should be taken into account.

Taken together, this study shows that epigenetic modulation by Entinostat results in a tumor cell lineage switch which is accompanied by increased T- and NK-cell immunogenicity against NBL via expression induction of several antigen-presenting machinery players, including MHC-I, MICA/B, and IP subunits. These results substantiate the combination of (immuno)therapy with HDACi as a potential strategy to enhance T-cell engagement and therewith immunogenicity to improve outcome for children suffering from HR-NBL.

## Acknowledgements

The pSLuc-GFP plasmid was kindly provided by Dr. Christian Buchholz (Paul-Ehrlich-Institut, Langen, Germany). The authors thank the Center for Drug Design & Discovery (CD3) for providing the CD3 repurposing library. This work was supported by the Villa Joep Foundation [IWOV-Actief.51391.180034].

## REFERENCES

1. Töpfer, K.; Kempe, S.; Müller, N.; Schmitz, M.; Bachmann, M.; Cartellieri, M.; Schackert, G.; Temme, A. Tumor Evasion from T Cell Surveillance. *J. Biomed. Biotechnol.* **2011**, doi:10.1155/2011/918471.
2. Cornel, A.M.; Mimpen, I.L.; Nierkens, S. MHC Class I Downregulation in Cancer: Underlying Mechanisms and Potential Targets for Cancer Immunotherapy. *Cancers (Basel).* **2020**, *12*, 1–33, doi:10.3390/cancers12071760.
3. Spel, L.; Schiepers, A.; Boes, M. NFκB and MHC-1 Interplay in Neuroblastoma and Immunotherapy. *Trends in Cancer* **2018**, *4*, 715–717.
4. Spel, L.; Boelens, J.J.; Van Der Steen, D.M.; Blokland, N.J.G.; van Noesel, M.M.; Molenaar, J.J.; Heemskerk, M.H.M.; Boes, M.; Nierkens, S. Natural Killer Cells Facilitate PRAME-Specific T-Cell Reactivity against Neuroblastoma. *Oncotarget* **2015**, *6*, 35770–35781, doi: 10.18632/oncotarget.5657.
5. Lorenzi, S.; Forloni, M.; Cifaldi, L.; Antonucci, C.; Citti, A.; Boldrini, R.; Pezzullo, M.; Castellano, A.; Russo, V.; van der Bruggen, P.; et al. IRF1 and NF-KB Restore MHC Class I-Restricted Tumor Antigen Processing and Presentation to Cytotoxic T Cells in Aggressive Neuroblastoma. *PLoS One* **2012**, *7*, 1–8, doi: 10.1371/journal.pone.0046928.
6. Park, J.R.; Bagatell, R.; London, W.B.; Maris, J.M.; Cohn, S.L.; Mattay, K.M.; Hogarty, M. Children's Oncology Group's 2013 Blueprint for Research: Neuroblastoma. *Pediatr. Blood Cancer* **2013**.
7. Van Groningen, T.; Koster, J.; Valentijn, L.J.; Zwijnenburg, D.A.; Akogul, N.; Hasselt, N.E.; Broekmans, M.; Haneveld, F.; Nowakowska, N.E.; Bras, J.; et al. Neuroblastoma Is Composed of Two Super-Enhancer-Associated Differentiation States. *Nat. Genet.* **2017**, *49*, 1261–1266, doi:10.1038/ng.3899.
8. van Groningen, T.; Akogul, N.; Westerhout, E.M.; Chan, A.; Hasselt, N.E.; Zwijnenburg, D.A.; Broekmans, M.; Stroeken, P.; Haneveld, F.; Hooijer, G.K.J.; et al. A NOTCH Feed-Forward Loop Drives Reprogramming from Adrenergic to Mesenchymal State in Neuroblastoma. *Nat. Commun.* **2019**, *10*, 1–11, doi:10.1038/s41467-019-09470-w.
9. Sengupta, S.; Das, S.; Crespo, A.C.; Cornel, A.M.; Patel, A.G.; Mahadevan, N.R.; Campisi, M.; Ali, A.K.; Sharma, B.; Rowe, J.H.; Huang, H.; Debruyne, D.N.; Cerda, E.D.; Krajewska, M.; Dries, R.; Chen, M.; Zhang, S.; Soriano, L.; Cohen, M.A.; Versteeg, R.; Jaenisch, R.; Spranger, S.; Romee, R.; Miller, B.C.; Barbie, D.A.; Nierkens, S.; Dyer, M.A.; Lieberman, J.; George, R.E. Mesenchymal and adrenergic cell lineage states in neuroblastoma possess distinct immunogenic phenotypes. *Nat. Cancer* **2022**, doi:10.1038/s43018-022-00427-5
10. Pinto, N.R.; Applebaum, M.A.; Volchenboum, S.L.; Matthay, K.K.; London, W.B.; Ambros, P.F.; Nakagawara, A.; Berthold, F.; Schleiermacher, G.; Park, J.R.; et al. Advances in Risk Classification and Treatment Strategies for Neuroblastoma. *J. Clin. Oncol.* **2015**, *33*, 3008–3017, doi:10.1200/JCO.2014.59.4648.
11. Yu, A.L.; Gilman, A.L.; Ozkaynak, M.F.; London, W.B.; Kreissman, S.G.; Chen, H.X.; Smith, M.; Anderson, B.; Villablanca, J.G.; Matthay, K.K.; et al. Anti-GD2 Antibody with GM-CSF, Interleukin-2, and Isotretinoin for Neuroblastoma. *N. Engl. J. Med.* **2010**, *363*, 1324–1334, doi:10.1056/nejmoa0911123.
12. Yu, A.L.; Gilman, A.L.; Ozkaynak, M.F.; Naranjo, A.; Diccianni, M.B.; Gan, J.; Hank, J.A.; Batova, A.; London, W.B.; Tenney, S.C.; et al. Long-Term Follow-up of a Phase III Study of Ch14.18 (Dinutuximab) + Cytokine Immunotherapy in Children with High-Risk Neuroblastoma: COG Study ANBL0032. *Clin. Cancer Res.* **2021**, *18*, clincanres.3909.2020, doi:10.1158/1078-0432.ccr-20-3909.

**13.** Wienke, J.; Dierselhuis, M.P.; Tytgat, G.A.M.; Künkele, A.; Nierkens, S.; Molenaar, J.J. The Immune Landscape of Neuroblastoma: Challenges and Opportunities for Novel Therapeutic Strategies in Pediatric Oncology. *Eur. J. Cancer* **2021**, *144*, 123–150, doi: 10.1016/j.ejca.2020.11.014.

**14.** Reid, G.S.D.; Shan, X.; Coughlin, C.M.; Lassoued, W.; Pawel, B.R.; Wexler, L.H.; Thiele, C.J.; Tsokos, M.; Pinkus, J.L.; Pinkus, G.S.; et al. Interferon-γ-Dependent Infiltration of Human T Cells into Neuroblastoma Tumors in Vivo. *Clin. Cancer Res.* **2009**, *15*, 6602–6608, doi: 10.1158/1078-0432.CCR-09-0829.

**15.** Yang, X.; Merchant, M.S.; Romero, M.E.; Tsokos, M.; Wexler, L.H.; Kontny, U.; Mackall, C.L.; Thiele, C.J. Induction of Caspase 8 by Interferon γ Renders Some Neuroblastoma (NB) Cells Sensitive to Tumor Necrosis Factor-Related Apoptosis-Inducing Ligand (TRAIL) but Reveals That a Lack of Membrane TR1/TR2 Also Contributes to TRAIL Resistance in NB. *Cancer Res.* **2003**, *63*, 1122–1129.

**16.** Cornel, A.M.; Szanto, C.L.; van Til, N.P.; van Velzen, J.F.; Boelens, J.J.; Nierkens, S. A “No-Touch” Antibody-Staining Method of Adherent Cells for High-Throughput Flow Cytometry in 384-Well Microplate Format for Cell-Based Drug Library Screening. *Cytom. Part A* **2020**, *97*, 845–851, doi:10.1002/cyto.a.23956.

**17.** Spel, L.; Nieuwenhuis, J.; Haarsma, R.; Stickel, E.; Bleijerveld, O.B.; Altelaar, M.; Boelens, J.J.; Brummelkamp, T.R.; Nierkens, S.; Boes, M. Nedd4-Binding Protein 1 and TNFAIP3-Interacting Protein 1 Control MHC-1 Display in Neuroblastoma. *Cancer Res.* **2018**, *78*, 6621–6631, doi:10.1158/0008-5472.CAN-18-0545.

**18.** Amir, A.L.; Van Der Steen, D.M.; Van Loenen, M.M.; Hagedoorn, R.S.; De Boer, R.; Kester, M.D.G.; De Ru, A.H.; Lugthart, G.J.; Van Kooten, C.; Hiemstra, P.S.; et al. PRAME-Specific Allo-HLA-Restricted T Cells with Potent Antitumor Reactivity Useful for Therapeutic T-Cell Receptor Gene Transfer. *Clin. Cancer Res.* **2011**, *17*, 5615–5625, doi:10.1158/1078-0432.CCR-11-1066.

**19.** Wolpaw, A.J.; Grossmann, L.D.; Dessau, J.L.; Dong, M.M.; Aaron, B.J. Epigenetic State Determines in Fl Ammatory Sensing in Neuroblastoma. *Proc Natl Acad Sci U S A* **2022**, *119*, doi:10.1073/pnas.2102358119/-/DCSupplemental.Published.

**20.** Beug, S.T.; Beauregard, C.E.; Healy, C.; Sanda, T.; St-Jean, M.; Chabot, J.; Walker, D.E.; Mohan, A.; Earl, N.; Lun, X.; et al. Smac Mimetics Synergize with Immune Checkpoint Inhibitors to Promote Tumour Immunity against Glioblastoma. *Nat. Commun.* **2017**, *8*, 1–15, doi:10.1038/ncomms14278.

**21.** Ye, W.; Gunti, S.; Allen, C.T.; Hong, Y.; Clavijo, P.E.; Van Waes, C.; Schmitt, N.C. ASTX660, an Antagonist of CIAP1/2 and XIAP, Increases Antigen Processing Machinery and Can Enhance Radiation-Induced Immunogenic Cell Death in Preclinical Models of Head and Neck Cancer. *Oncoimmunology* **2020**, *9*, doi: 10.1080/2162402X.2019.1710398.

**22.** Louis, C.U.; Shohet, J.M. Neuroblastoma: Molecular Pathogenesis and Therapy. *Annu. Rev. Med.* **2015**, *66*, 49–63, doi:10.1146/annurev-med-011514-023121.

**23.** Jubierre, L.; Jiménez, C.; Rovira, E.; Soriano, A.; Sábado, C.; Gros, L.; Llort, A.; Hladun, R.; Roma, J.; Toledo, J.S. de; et al. Targeting of Epigenetic Regulators in Neuroblastoma. *Exp. Mol. Med.* **2018**, *50*, doi:10.1038/s12276-018-0077-2.

**24.** Seier, J.A.; Reinhardt, J.; Saraf, K.; Ng, S.S.; Layer, J.P.; Corvino, D.; Althoff, K.; Giordano, F.A.; Schramm, A.; Fischer, M.; et al. Druggable Epigenetic Suppression of Interferon-Induced Chemokine Expression Linked to MYCN Amplification in Neuroblastoma . *J. Immunother. Cancer* **2021**, *9*, e001335, doi: 10.1136/jitc-2020-001335.

**25.** Burr, M.L.; Sparbier, C.E.; Chan, K.L.; Chan, Y.C.; Kersbergen, A.; Lam, E.Y.N.; Azidis-Yates, E.; Vassiliadis, D.; Bell, C.C.; Gilan, O.; et al. An Evolutionarily Conserved Function of Polycomb Silences the MHC Class I Antigen Presentation Pathway and Enables Immune Evasion in Cancer. *Cancer Cell* **2019**, *36*, 385-401.e8, doi:10.1016/j.ccell.2019.08.008.

26. Custers, L.; Khabirova, E.; Coorens, T.H.H.; Oliver, T.R.W.; Calandrini, C.; Young, M.D.; Vieira Braga, F.A.; Ellis, P.; Mamanova, L.; Segers, H.; et al. Somatic Mutations and Single-Cell Transcriptomes Reveal the Root of Malignant Rhabdoid Tumours. *Nat. Commun.* **2021**, *12*, 1–11, doi:10.1038/s41467-021-21675-6.
27. Yarmarkovich, M.; Maris, J.M. When Cold Is Hot: Immune Checkpoint Inhibition Therapy for Rhabdoid Tumors. *Cancer Cell* **2019**, *36*, 575–576, doi:10.1016/j.ccell.2019.11.006.
28. Garancher, A.; Suzuki, H.; Haricharan, S.; Chau, L.Q.; Masihi, M.B.; Rusert, J.M.; Norris, P.S.; Carrette, F.; Romero, M.M.; Morrissy, S.A.; et al. Tumor Necrosis Factor Overcomes Immune Evasion in P53-Mutant Medulloblastoma. *Nat. Neurosci.* **2020**, *23*, 842–853, doi:10.1038/s41593-020-0628-4.
29. Marquardt, V.; Theruvath, J.; Pauck, D.; Picard, D.; Reifenberger, G.; Borkhardt, A.; Cheshier, S.; Kurz, T.; Remke, M.; Mitra, S. IMMU-19. HDAC INHIBITORS SENSITIZE MYC-AMPLIFIED MEDULLOBLASTOMA TO IMMUNOTHERAPY BY ACTIVATING THE NF-KB PATHWAYS. *Neuro. Oncol.* **2020**, *22*, doi:10.1093/neuonc/noaa222.375.
30. Tripathi, S.C.; Peters, H.L.; Taguchi, A.; Katayama, H.; Wang, H.; Momin, A.; Jolly, M.K.; Celiktas, M.; Rodriguez-Canales, J.; Liu, H.; et al. Immunoproteasome Deficiency Is a Feature of Non-Small Cell Lung Cancer with a Mesenchymal Phenotype and Is Associated with a Poor Outcome. *Proc. Natl. Acad. Sci. U. S. A.* **2016**, *113*, E1555–E1564, doi:10.1073/pnas.1521812113.
31. Truong, A.S.; Zhou, M.; Krishnan, B.; Utsumi, T.; Manocha, U.; Stewart, K.G.; Beck, W.; Rose, T.L.; Milowsky, M.I.; He, X.; et al. Entinostat Induces Antitumor Immune Responses through Immune Editing of Tumor Neoantigens. *J. Clin. Invest.* **2021**, *131*, doi:10.1172/JCI138560.
32. Lauss, M.; Donia, M.; Harbst, K.; Andersen, R.; Mitra, S.; Rosengren, F.; Salim, M.; Vallon-Christersson, J.; Törngren, T.; Kvist, A.; et al. Mutational and Putative Neoantigen Load Predict Clinical Benefit of Adoptive T Cell Therapy in Melanoma. *Nat. Commun.* **2017**, *8*, 1–11, doi:10.1038/s41467-017-01460-0.
33. Krishnadas, D.K.; Shusterman, S.; Bai, F.; Diller, L.; Sullivan, J.E.; Cheerva, A.C.; George, R.E.; Lucas, K.G. A Phase I Trial Combining Decitabine/Dendritic Cell Vaccine Targeting MAGE-A1, MAGE-A3 and NY-ESO-1 for Children with Relapsed or Therapy-Refractory Neuroblastoma and Sarcoma. *Cancer Immunol. Immunother.* **2015**, *64*, 1251–1260, doi:10.1007/s00262-015-1731-3.
34. Kroesen, M.; Büll, C.; Gielen, P.R.; Brok, I.C.; Armandari, I.; Wassink, M.; Looman, M.W.G.; Boon, L.; den Brok, M.H.; Hoogerbrugge, P.M.; et al. Anti-GD2 MAb and Vorinostat Synergize in the Treatment of Neuroblastoma. *Oncoimmunology* **2016**, *5*, 1–12, doi:10.1080/2162402X.2016.1164919.
35. van den Bijgaart, R.J.E.; Kroesen, M.; Brok, I.C.; Reijnen, D.; Wassink, M.; Boon, L.; Hoogerbrugge, P.M.; Adema, G.J. Anti-GD2 Antibody and Vorinostat Immunocombination Therapy Is Highly Effective in an Aggressive Orthotopic Neuroblastoma Model. *Oncoimmunology* **2020**, *9*, doi:10.1080/2162402X.2020.1817653.
36. Szanto, C.L.; Cornel, A.M.; Tamminga, S.M.; Delemarre, E.M.; de Koning, C.C.H.; van den Beemt, D.A.M.H.; Dunnebach, E.; Tas, M.L.; Dierselhuis, M.P.; Tytgat, L.G.A.M.; et al. Immune Monitoring during Therapy Reveals Activitory and Regulatory Immune Responses in High-Risk Neuroblastoma. *Cancers (Basel).* **2021**, *13*, 1–18, doi:10.3390/cancers13092096.
37. Akimova, T.; Ge, G.; Golovina, T.; Mikheeva, T.; Wang, L.; Riley, J.L.; Hancock, W.W. Histone/Protein Deacetylase Inhibitors Increase Suppressive Functions of Human FOXP3+ Tregs. *Clin. Immunol.* **2010**, *136*, 348–363, doi:10.1016/j.clim.2010.04.018.
38. Kiany, S.; Huang, G.; Kleinerman, E.S. Effect of Entinostat on NK Cell-Mediated Cytotoxicity against Osteosarcoma Cells and Osteosarcoma Lung Metastasis. *Oncoimmunology* **2017**, *6*, 1–13, doi:10.1080/2162402X.2017.1333214.

**39.** Zhu, S.; Denman, C.J.; Cobanoglu, Z.S.; Kiany, S.; Lau, C.C.; Gottschalk, S.M.; Hughes, D.P.M.; Kleinerman, E.S.; Lee, D.A. The Narrow-Spectrum HDAC Inhibitor Entinostat Enhances NKG2D Expression without NK Cell Toxicity, Leading to Enhanced Recognition of Cancer Cells. *Pharm. Res.* **2015**, *32*, 779–792, doi:10.1007/s11095-013-1231-0.

**40.** Idso, J.M.; Lao, S.; Schloemer, N.J.; Knipstein, J.; Burns, R.; Thakar, M.S.; Malarkannan, S. Entinostat Augments NK Cell Functions via Epigenetic Upregulation of IFIT1-STING-STAT4 Pathway. *Oncotarget* **2020**, *11*, 1799–1815, doi:10.18632/oncotarget.27546.

**41.** Briere, D.; Sudhakar, N.; Woods, D.M.; Hallin, J.; Engstrom, L.D.; Aranda, R.; Chiang, H.; Sodré, A.L.; Olson, P.; Weber, J.S.; et al. The Class I/IV HDAC Inhibitor Mocetinostat Increases Tumor Antigen Presentation, Decreases Immune Suppressive Cell Types and Augments Checkpoint Inhibitor Therapy. *Cancer Immunol. Immunother.* **2018**, *67*, 381–392, doi:10.1007/s00262-017-2091-y.

**42.** Phimmachanh, M.; Han, J.Z.R.; O'Donnell, Y.E.I.; Latham, S.L.; Croucher, D.R. Histone Deacetylases and Histone Deacetylase Inhibitors in Neuroblastoma. *Front. Cell Dev. Biol.* **2020**, *8*, 1–14, doi:10.3389/fcell.2020.578770.

**43.** Roussos Torres, E.T.; Rafie, C.; Wang, C.; Lim, D.; Brufsky, A.; LoRusso, P.; Eder, J.P.; Chung, V.; Downs, M.; Geare, M.; et al. Phase I Study of Entinostat and Nivolumab with or without Ipilimumab in Advanced Solid Tumors (ETCTN-9844). *Clin. Cancer Res.* **2021**, *27*, 5828–5837, doi:10.1158/1078-0432.ccr-20-5017.

**44.** Ny, L.; Jespersen, H.; Karlsson, J.; Alsén, S.; Filges, S.; All-Eriksson, C.; Andersson, B.; Carneiro, A.; Helgadottir, H.; Levin, M.; et al. The PEMDAC Phase 2 Study of Pembrolizumab and Entinostat in Patients with Metastatic Uveal Melanoma. *Nat. Commun.* **2021**, *12*, 1–10, doi:10.1038/s41467-021-25332-w.

**45.** Souri, Z.; Jochemsen, A.G.; Versluis, M.; Wierenga, A.P.A.; Nemati, F.; van der Velden, P.A.; Kroes, W.G.M.; Verdijk, R.M.; Luyten, G.P.M.; Jager, M.J. HDAC Inhibition Increases HLA Class I Expression in Uveal Melanoma. *Cancers (Basel).* **2020**, *12*, 1–14, doi:10.3390/cancers12123690.

**46.** Smith, H.J.; McCaw, T.R.; Londono, A.I.; Katre, A.A.; Meza-Perez, S.; Yang, E.S.; Forero, A.; Buchsbaum, D.J.; Randall, T.D.; Straughn, J.M.; et al. The Antitumor Effects of Entinostat in Ovarian Cancer Require Adaptive Immunity. *Cancer* **2018**, *124*, 4657–4666, doi:10.1002/cncr.31761.

**47.** Ritter, C.; Fan, K.; Paschen, A.; Reker Hardrup, S.; Ferrone, S.; Nghiem, P.; Ugurel, S.; Schrama, D.; Becker, J.C. Epigenetic Priming Restores the HLA Class-I Antigen Processing Machinery Expression in Merkel Cell Carcinoma. *Sci. Rep.* **2017**, *7*, 1–11, doi:10.1038/s41598-017-02608-0.

**48.** Blaszczak, W.; Liu, G.; Zhu, H.; Barczak, W.; Shrestha, A.; Albayrak, G.; Zheng, S.; Kerr, D.; Samsonova, A.; La Thangue, N.B. Immune Modulation Underpins the Anti-Cancer Activity of HDAC Inhibitors. *Mol. Oncol.* **2021**, *15*, 3280–3298, doi:10.1002/1878-0261.12953.

**49.** Bate-Eya, L.T.; Ebus, M.E.; Koster, J.; Den Hartog, I.J.M.; Zwijnenburg, D.A.; Schild, L.; Van Der Ploeg, I.; Dolman, M.E.M.; Caron, H.N.; Versteeg, R.; et al. Newly-Derived Neuroblastoma Cell Lines Propagated in Serum-Free Media Recapitulate the Genotype and Phenotype of Primary Neuroblastoma Tumours. *Eur. J. Cancer* **2014**, *50*, 628–637, doi:10.1016/j.ejca.2013.11.015.

**50.** Lo Presti, V.; Cornel, A.M.; Plantinga, M.; Dünnebach, E.; Kuball, J.; Boelens, J.J.; Nierkens, S.; van Til, N.P. Efficient Lentiviral Transduction Method to Gene Modify Cord Blood CD8+ T Cells for Cancer Therapy Applications. *Mol. Ther. - Methods Clin. Dev.* **2021**, *21*, 357–368, doi:10.1016/j.omtm.2021.03.015.

51. Zufferey, R.; Dull, T.; Mandel, R.J.; Bukovsky, A.; Quiroz, D.; Naldini, L.; Trono, D. Self-Inactivating Lentivirus Vector for Safe and Efficient In Vivo Gene Delivery. *J. Virol.* **1998**, *72*, 9873–9880, doi:10.1128/jvi.72.12.9873-9880.1998.

52. Dull, T.; Zufferey, R.; Kelly, M.; Mandel, R.J.; Nguyen, M.; Trono, D.; Naldini, L. A Third-Generation Lentivirus Vector with a Conditional Packaging System. *J. Virol.* **1998**, *72*, 8463–8471, doi:10.1128/jvi.72.11.8463-8471.1998.

53. Marcu-Malina, V.; Heijhuurs, S.; Van Buuren, M.; Hartkamp, L.; Strand, S.; Sebestyen, Z.; Scholten, K.; Martens, A.; Kuball, J. Redirecting AβT Cells against Cancer Cells by Transfer of a Broadly Tumor-Reactive ΓδT-Cell Receptor. *Blood* **2011**, *118*, 50–59, doi:10.1182/blood-2010-12-325993.

54. Kholosy, W.M.; Derieppe, M.; van den Ham, F.; Ober, K.; Su, Y.; Custers, L.; Schild, L.; van Zogchel, L.M.J.; Wellens, L.M.; Ariese, H.R.; et al. Neuroblastoma and DIPG Organoid Coculture System for Personalized Assessment of Novel Anticancer Immunotherapies. *J. Pers. Med.* **2021**, *11*, doi: 10.3390/jpm11090869.

55. Strijker, J.G.M.; Pscheid, R.; Drent, E.; van der Hoek, J.J.F.; Koopmans, B.; Ober, K.; van Hooff, S.R.; Kholosy, W.M.; Cornel, A.M.; Coomans, C.; et al. Aβ-T Cells Engineered to Express Γδ-T Cell Receptors Can Kill Neuroblastoma Organoids Independent of MHC-I Expression. *J. Pers. Med.* **2021**, *11*, doi:10.3390/jpm11090923.

56. Bindea, G.; Mlecnik, B.; Tosolini, M.; Kirilovsky, A.; Waldner, M.; Obenauf, A.C.; Angell, H.; Fredriksen, T.; Lafontaine, L.; Berger, A.; et al. Spatiotemporal Dynamics of Intratumoral Immune Cells Reveal the Immune Landscape in Human Cancer. *Immunity* **2013**, *39*, 782–795, doi:10.1016/j.immuni.2013.10.003.

57. Cursons, J.; Souza-Fonseca-Guimaraes, F.; Foroutan, M.; Anderson, A.; Hollande, F.; Hediyeh-Zadeh, S.; Behren, A.; Huntington, N.D.; Davis, M.J. A Gene Signature Predicting Natural Killer Cell Infiltration and Improved Survival in Melanoma Patients. *Cancer Immunol. Res.* **2019**, *7*, 1162–1174, doi: 10.1158/2326-6066.CIR-18-0500.

58. Gu, Z.; Eils, R.; Schlesner, M. Complex Heatmaps Reveal Patterns and Correlations in Multidimensional Genomic Data. *Bioinformatics* **2016**, *32*, 2847–2849, doi: 10.1093/bioinformatics/btw313.

59. Warnes GJ, Bolker B, Bonebakker L, Gentleman G, Liaw WHA, Lumley T, Maechler M, Magnusson A, Moeller S, Schwartz M, V.B. Gplots: Various R Programming Tools for Plotting Data. R Package Version 3.0.1.1. 2019.

## SUPPLEMENTARY MATERIAL

**Table S1** – List of HDAC inhibitors upregulating MHC-I expression in GIMEN reporter cells.

| Compound | Alternative Names | Target | % HLA-ABC expression |
|---|---|---|---|
| Citarinostat | ACY-241, HDAC-IN-2 | HDAC3/6 | 10.2% |
| Fimepinostat | CUDC-907 | PI3K, & HDAC1/2/3/10 | 49.9% |
| Pracinostat | SB939 | panHDAC | 41.9% |
| Abexinostat | PCI-24781, CRA-024781 | panHDAC, most potent against HDAC1 | 40.3% |
| Mocetinostat | MGCD0103, MG0103 | HDAC 1/2/3/11 | 34.9% |
| Entinostat | MS-275, SNDX-275 | HDAC1/3 | 26.8% |
| Sodium Phenylbutyrate | 4-BPA, 4-phenylbutyric acid | HDAC1/2a | 25.7% |
| Tucidinostat | Chidamide, HBI-8000, CS-055 | HDAC1/2/3/10 | 22.8% |
| Dacinostat | LAQ824, NVP-LAQ824 | panHDAC | 21.2% |
| Resminostat | RAS2410 | HDAC1/3/6 | 19.7% |
| CUDC-101 | - | HDAC1/2, EGFR, HER2 | 14.1% |
| LMK-235 | - | HDAC4/5 | 10.7% |
| Citarinostat | ACY-241, HDAC-IN-2 | HDAC3/6 | 10.2% |
| Droxinostat | NS41080 | HDAC3/6/8 | 9.9% |
| Tubastatin A | - | panHDAC, most potent against HDAC6 | 9.9% |
| RGFP96 | - | panHDAC, most potent against 3 | 9.4% |

*HDAC = Histon Deacetylase, % HLA-ABC expression standardized to untreated control cells*

**Table S2** – List of IAPi upregulating MHC-I expression in GIMEN reporter cells.

| Compound | Alternative Names | Target | % HLA-ABC expression |
|---|---|---|---|
| MX69 | | MDM2, XIAP | 46.8% |
| GDC-0152 | | cIAP1+2, XIAP, ML-IAP | 27.8% |
| AZD-5582 | | cIAP1+2, XIAP | 24.4% |
| Xevinapant | AT-406 | cIAP1+2, XIAP | 20.5% |
| Birinapant | TL32711 | cIAP1 mostly, less potent against XIAP | 20.0% |
| LCL-161 | | cIAP1+2, XIAP | 19.8% |

*IAP = inhibitor of apoptosis, % HLA-ABC expression standardized to untreated control cells*

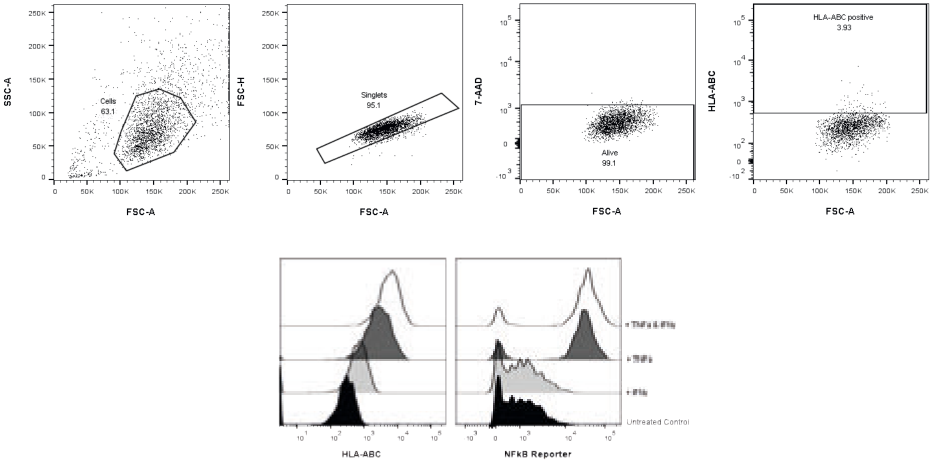

**Figure S1.** Drug library screen gating strategy & representative controls.
*Upper Panel: Gating strategy to identify HLA-ABC expressing cells. Lower Panel: MHC-I (left) and NFκB Reporter (right) induction upon cytokine incubation. Untreated cells were used as negative controls. Cells treated with 1000 U/mL IFNγ, and/or 50 ng/mL TNFα were used as a positive control for MHC-I expression (HLA-ABC AF647) or NFκB Reporter (GFP) induction.*

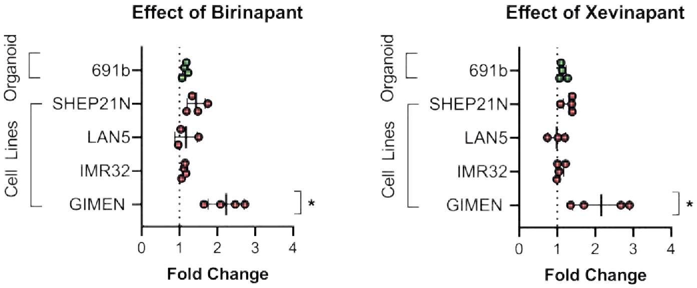

**Figure S2** – Effect of two other IAPi across a panel of NBL lines.
*Fold Induction of MHC-I expression relative to untreated control cells after 48h of incubation with 250 nM Birinapant or 500 nM Xevinapant. Data depicted as mean ± SD. LAN5: n=3, rest: n=4, statistical differences between MFIs were calculated with the Mann Whitney U test, *p<0.05.*

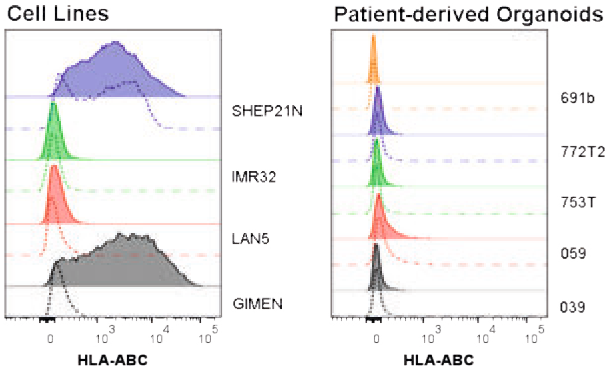

**Figure S3** – Sensitivity of NBL models to TNFα-mediated NFκB pathway activation. *Dotted lines reflect unstimulated cells, filled histograms are stimulated with TNFα (0.5 ng/mL).*

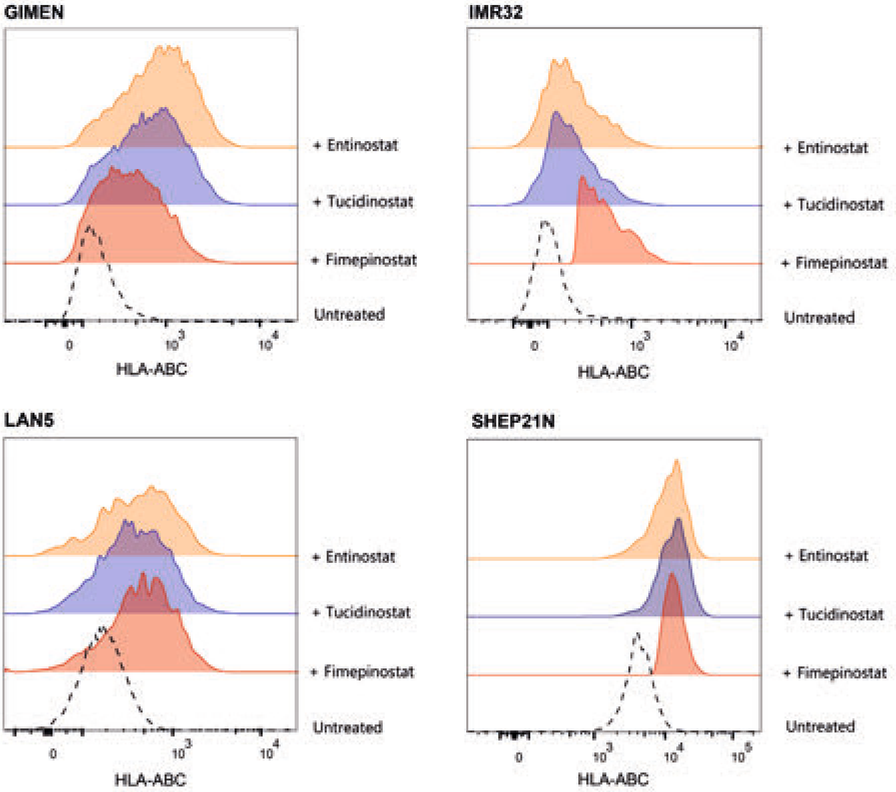

**Figure S4** – Effect of two other HDACi, tucidinostat and fimepinostat, across a panel of NBL lines. *MHC-I upregulation after 48h treatment with Tucidinostat (GIMEN & LAN5: 5 uM, SHEP21N: 2.5 uM, IMR32 1.25 uM) or Fimepinostat (GIMEN: 100 nM, LAN5 & SHEP21N: 25 nM, IMR32: 12.5 nM). Dotted line reflects untreated control cells.*

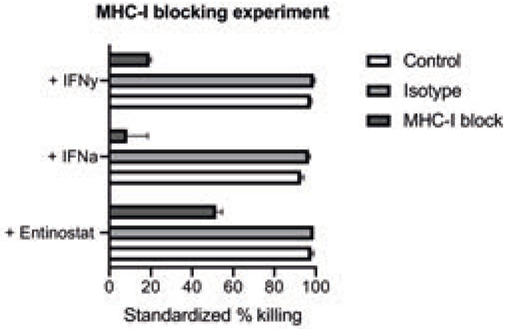

**Figure S5** – Entinostat-induced T-cell cytotoxicity is MHC-I dependent.
*Luminescence-based cytotoxicity against luciferase-transduced 691b organoids after 48h pre-incubation with 2.5 µM Entinostat, 1000 U/mL IFNα, or 100 U/mL IFNγ. Co-cultures were performed either without presence of blocking antibody, with an isotype control, and with an MHC-I blocking antibody. Cells were co-cultured overnight at an E:T of 1:1. Data are shown as mean ± SEM.*

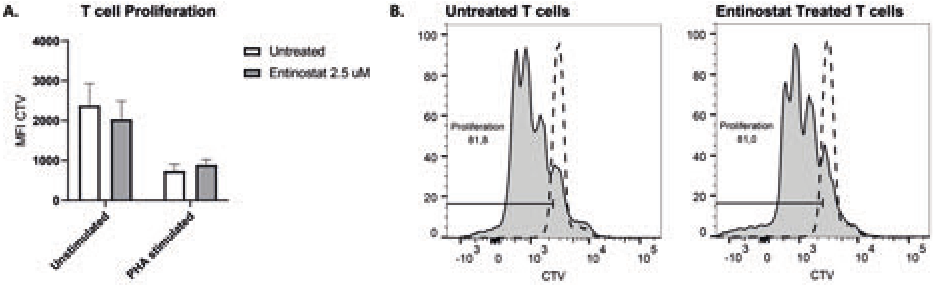

**Figure S6** – Intact proliferative capacity of Entinostat pre-treated healthy-donor T-cells.
*Proliferative capacity of T-cells based on CTV-dilution.* ***(A)*** *Shows the MFI in CTV in untreated and 2.5 µM Entinostat pre-treated healthy-donor CD3+ T-cells. Data is shown from four donors, no significant differences based on the Mann Whitney U test.* ***(B)*** *Shows the CTV division pattern in untreated (left) and entinostat pre-treated T-cells (right).*

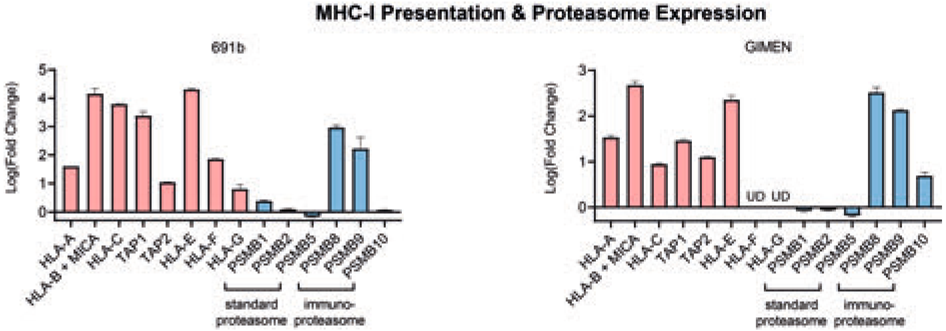

**Figure S7** – qPCR validation of increases in transcript abundance observed with RNAseq.
*Data is depicted as log(fold change) between untreated and entinostat-treated 691b organoids (left) or GIMEN (right). Data relative to GAPDH. 691b: All log(fold changes) are significant, except HLA-G and PSMB9 (p=0.09 and 0.08, respectively). GIMEN: all log(fold changes) are significant, except PSMB1/2/5. UD = undetected. Duplos are shown as mean ± SD. Statistical differences between log(fold changes) were calculated with a one sample T test.*

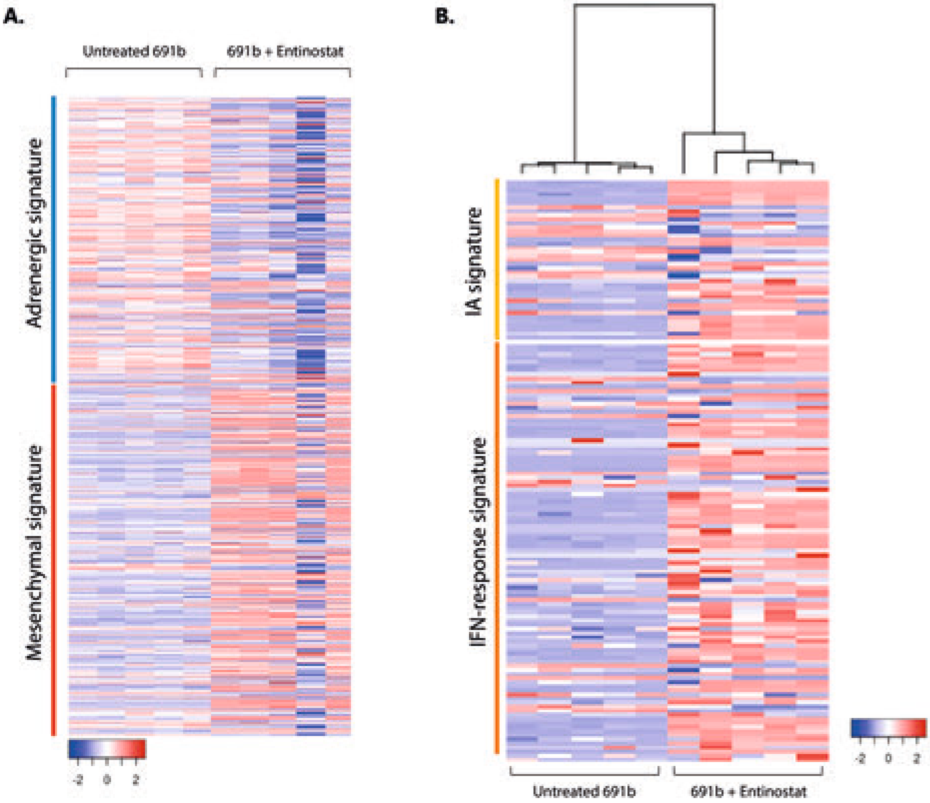

**Figure S8** – Increased mesenchymal-, immune activation-, and IFN-response signature upon Entinostat treatment of 691b organoids.
*Heatmap showing individual signature components of cell lineage* ***(A)*** *and immune activation (IA) / IFN-response* ***(B)*** *in untreated and 691b Entinostat-treated organoids (48h, 2.5 uM Entinostat). Log2 gene expression values were z-score transformed for heatmap visualization.*

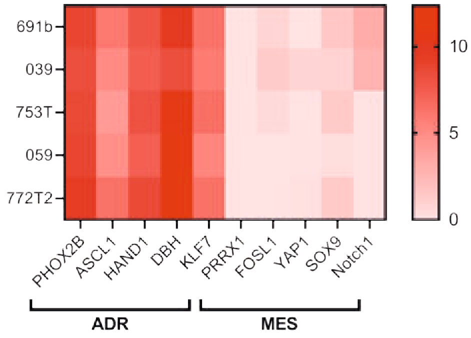

**Figure S9** – Neuroblastoma cell lineage markers in utilized patient-derived organoid models.
*ADR = adrenergic, MES = mesenchymal.*

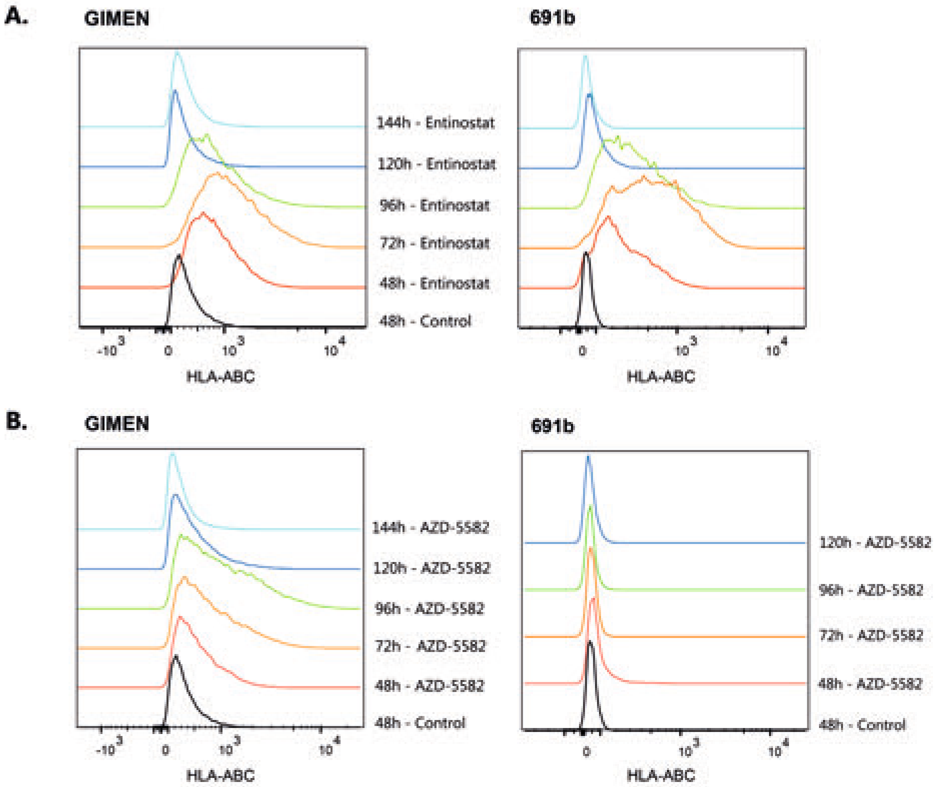

**Figure S10** – MHC-I upregulation kinetics after drug incubation.
*GIMEN (left) and 691b (right) were incubated with 2.5 µM entinostat **(A)** or 62.5 nM AZD-5582 **(B)** for 48h, after which media was refreshed. Effect on MHC-I expression was determined at indicated timepoints. HLA-ABC expression in controls remained unchanged overtime, expression after 48h is shown as an example of baseline expression.*

# Part III

## Cell Therapy Strategies to Enhance Adaptive Immune Engagement in Neuroblastoma

# Chapter 9

## Best of two worlds: Engineering NKT-cells to generate an alternative adaptive cell therapy strategy against neuroblastoma

Annelisa M. Cornel[1,2], Caitlyn L. Forbes[1,2], Ester Dünnebach[1,2],
Miranda P. van Dierselhuis, Stefan Nierkens[1,2]

*[1] Princess Máxima Center for Pediatric Oncology, Utrecht University, 3584 CS Utrecht, The Netherlands*
*[2] Center for Translational Immunology, University Medical Center Utrecht, Utrecht University, The Netherlands*

*Manuscript in preparation*

## ABSTRACT

Despite intensive, multi-modal treatment, survival changes of high-risk neuroblastoma (HR-NBL) patients are still ~50%. The lack of immunogenicity of the tumor, due to its embryonal origin, is an important limiting factor in HR-NBL therapy efficacy. One of the most notable immunomodulatory processes is the absence of major histocompatibility complex I (MHC-I) surface display in NBL, which greatly limits cytotoxic T-cell engagement. We and others have previously shown that MHC-I expression can be induced by cytokine-driven immune modulation upon natural killer (NK)-cell activation. It is suggested that the high degree of plasticity in MHC-I expression in NBL allows alternate evasion of both cytotoxic T- and NK-cells. To avoid MHC-I plasticity-mediated immune evasion of NBL, we combined NK-cell mediated cytotoxicity mechanisms with MHC-I restricted cytotoxicity by NBL-specific T-cell receptor (TCR) introduction in naturally occurring CD3+CD56+ natural killer T (NKT)-cells. Phenotypical analysis of the total CD3+CD56+ NKT-cell fraction revealed NKG2D expression on all NKT-cells, and NKp46 and KIR2D expression on a subset of NKT-cells. In this manuscript, we show that NKT-cells, like NK-cells, can engage in NK-cell mechanism dependent cytotoxicity, recognize and kill a panel of NBL cells, and induce MHC-I expression on surviving NBL cells. The NBL-specific PRAME HSS1 TCR was subsequently effectively introduced in NKT-cells, after which peptide recognition and antigen-dependent cytotoxicity was confirmed. Finally, we observed a superior cytotoxic capacity of PRAME TCR engineered NKT-cells compared to wildtype NKT-cells as well as to PRAME TCR engineered T-cells. This pilot study shows the potential of the use of TCR-engineered NKT-cells as a cellular therapy source to improve outcome for children with HR-NBL.

## INTRODUCTION

The absence of MHC-I surface display in high-risk neuroblastoma (HR-NBL) is one of the main limiting factors in generation of T-cell immunogenicity and subsequent formation of immunological memory to prevent future relapse. The previous observation that MHC-I surface display on NBL cells is inducible [1,2] brings an opportunity to induce T-cell engagement against HR-NBL. Nonetheless, plasticity in MHC-I expression is thought to alternately cause evasion of both cytotoxic T- and NK-cells, thereby hampering their cytotoxic potential. We hypothesize that engineering of a cell that can both engage in NK-cell mediated cytotoxicity, for example via missing-self recognition, as well as in recognition of malignant transformation in MHC-I context will result in the generation of a cell type that can no longer be evaded by MHC-I plasticity.

These properties may be intrinsic to natural killer T (NKT) cells, a CD3+CD56+ subset of T-cells that express receptors typically associated with NK-cells [3]. NKT-cells are a poorly understood, heterogeneous population of cells comprising up to 20% of the lymphocyte population in human peripheral blood [4–7]. Due to the expression of both NK- and T-cell markers, these cells are able to exert major histocompatibility complex (MHC)-unrestricted and MHC-restricted cytotoxicity [3,6,7,9]. Furthermore, like NK-cells, NKT-cells are also capable of producing large amounts of IFNγ following activation [3,7,10]. Nomenclature remains controversial, for example, many studies reporting on NKT-cells study a small subpopulation of NKT-cells, the invariant NKT (iNKT) fraction. This is a rare CD1d restricted subset of NKT-cells, often constituting less than 0.1% of peripheral blood lymphocytes, expressing a semi-invariant Vα24Jα18 TCR [3,4,8]. The vast majority of cells in the NKT-cell population, the NKT-like cells, however, are MHC-I rather than CD1d restricted, feature a variable αβ TCR, and comprise the majority of the NKT-cell fraction [6,7].

Although NKT-like cells have been described as potent anti-tumor effector cells [7,9,10], they have not been extensively investigated and therefore their presence and function, particularly in the context of cancer, is poorly described. However, the dual NK- and T-cell functionality of these cells makes them an interesting option for a novel cell therapy in NBL. This is underlined by a study by Hurtado and colleagues [11], who found enrichment of the CD3+CD56+ cell population in NBL tumor-infiltrating lymphocytes (TILs) compared to blood (n=31). The fact that only 0.9% of these CD3+CD56+ cells were classified as iNKT-cells underlines the potential of the full CD3+CD56+ NKT-cell fraction in NBL cell therapy strategies.

This study investigates the cytotoxic activity of CD3+CD56+ NKT-cells against HR-NBL, as well as their capacity to upregulate MHC-I expression on the surface of NBL cells. Furthermore, we introduced an NBL-directed TCR on the surface of NKT-cells and compared the capacity of TCR engineered NKT-cells to target NBL cells with that of conventional T-cells. These pilot data show feasibility and potential of engineering CD3+CD56+ NKT-cells to target MHC-I plasticity in HR-NBL.

## MATERIALS & METHODS

### Cells lines and reagents

K562 (ATCC® CCL-243) and T2 cells (ATCC® CRL-1992) were used as missing-self and antigen-specific model readout system, respectively. The cytotoxic capacity against several NBL cell lines (GIMEN, CHP-212, IMR32, NLF) was assessed to determine the cytotoxic capacity against NBL. GIMEN cells were obtained via the Academic Medical Centre of Amsterdam, CHP-212 and NLF via the Dana Farber Cancer Institute, and IMR32 via the Princess Máxima Center for Pediatric Oncology. GIMEN and IMR32 were maintained in DMEM, whilst CHP-212 and NLF were maintained in RMPI, all supplemented with Glutamax, 10% FCS (Sigma-Aldrich), 1% penicillin/streptomycin (P/S) (50 units/mL) (Life Technologies), and 2% non-essential amino acids (NEAA) (Life Technologies). All were cultured under standard culturing conditions (37°C, 5% CO2) and split biweekly.

The NBL patient-derived organoid, 691b, was established as previously described [12]. Organoids were maintained in DMEM low glucose, Glutamax supplemented medium, supplemented with 25% HAM's F-12 Nutrient Mix, 2% B-27 supplement minus vitamin A, 1% N-2 supplement, 1% P/S (all Life Technologies), 20ng/mL Animal-Free Recombinant Human-EGF, 40ng/mL FGF-basic, 200ng/mL IGF-I, 10ng/mL PDGF-AA, and 10ng/mL PDGF-BB (all Peprotech). Medium was stored at -20°C, and stored for a maximum of one week at 4°C after thawing. Organoids were grown under standard culturing conditions (37°C, 5% CO2), with a half media change performed twice per week. Once per week, spheres were disrupted using Accutase (Sigma-Aldrich) and pipetting, then subcultured to avoid overcrowding/necrosis in organoid cores.

### Primary cell isolation and expansion

Peripheral blood (PB) from healthy donors was collected under informed consent in accordance with the Declaration of Helsinki, and collection protocol approved by the Ethical Committee of the University Medical Center (UMC) Utrecht. PB mononuclear cells (PBMCs) were isolated through Ficoll-Paque PLUS separation (GE Healthcare Biosciences AB).

In the experiments in which unedited NK- (CD56+CD3-), NKT- (CD3+CD56+) and T-cells (CD56-CD3+) were compared directly (based on phenotyping and cytotoxic capacity against K562), CD45+ cells were isolated using magnetic bead separation according to manufacturer's instructions (Miltenyi Biotec). Cells were subsequently stained with antibodies against CD56 PE-Cy7 (NCAM16.2) (BD Biosciences), CD3 AF700 (UCHT1) (Sony Biotechnology), and CD16 BV510 (3G8) (eBiosciences), and FACS-sorted based on CD3 and CD56 expression using a BD FACSAria (BD Biosciences). In this set of experiments, phenotyping and functional assays were performed using freshly isolated cells.

In all other experiments, CD3+CD56+ NKT-cells and CD3+ T-cells were isolated using magnetic bead separation according to the manufacturer's recommendations (CD3+CD56+ NKT-Cell Isolation Kit and CD3 human Microbeads, respectively) (Miltenyi Biotec). When collected from the same donor, CD3+ T-cells were obtained from the negative fraction following NKT-cell isolation. All (NK)T-cells were expanded using a previously adopted rapid expansion protocol (REP) [13] and **Chapter 8**. Briefly, (NK) T-cells were co-cultured with irradiated LCL-TM (80 Gy) and donor-pooled PBMCs (35 Gy) in human RPMI (huRPMI), consisting of Glutamax supplemented RPMI with 5% human serum and 1% P/S. Cultures were supplemented with 1 ug/mL PHA-L (Oxoid BV) and 50 U/mL IL-2 (Novartis). In addition, 5 ng/mL IL-15 (Miltenyi Biotec) was added to the NKT-cell cultures. Media and cytokines were refreshed biweekly. After a REP cycle, cells were either used for functional assays, transferred to a new REP, or cryopreserved for later use.

### Lentiviral TCR introduction in (NK)T-cells

(NK)T-cells were transduced with lentiviral particles encoding the HLA-A2 restricted PRAME HSS1 TCR (recognizing the SLLQHLIGL peptide) [14] that were generated previously (**Chapter 8**). Transduction was performed according to the protocol optimized in **Chapter 7** [15]. In short, healthy donor-matched CD3+CD56+ NKT- and CD3+ T-cells were isolated as indicated above, after which they were stimulated at a concentration of $5x10^5$ cells/mL in huRPMI supplemented with CD3/CD28 microbeads (bead:cell ratio of 1:3) (Invitrogen), 50 U/mL IL-2, 5 ng/mL IL-7 (Miltenyi Biotec), and 5 ng/mL IL-15 for 3 days. Beads were removed, after which cells were resuspended in StemMacs medium (Miltenyi Biotec) at a concentration of $2.5x10^6$ cells/mL. Cells were transduced at an MOI of 10 with the LentiBoost transduction enhancer (SIRION Biotech) and incubated overnight under standard culturing conditions. Remaining lentivirus was subsequently washed away and (NK)T-cells were put in culture at a density of $5x10^5$ in huRPMI supplemented with 50 U/mL IL-2, 5 ng/mL IL-7 (Miltenyi Biotec), and 5 ng/mL IL-15.

Transduction efficacy was determined 5 days post-transduction by evaluating variable bèta chain 1 (Vβ1) expression with the transduction efficacy panel indicated below. Transduced cells were sorted by magnetic bead separation. First, cells were stained with anti-Vβ1 FITC (REA662, Miltenyi Biotec). Cells were subsequently incubated with anti-FITC microbeads and sorted based on manufacturer's recommendations (Miltenyi Biotec).

## Cell phenotyping & flow cytometry analysis

Phenotyping of NK-, T- and NKT-cells was performed using a panel containing antibodies against CD56 PE/Cy7, CD3 AF700, CD16 BV510, KIR2D PE (NKVSF1) (Miltenyi Biotech), NKG2D PE/Dazzle495 (1D11), CD62L BV421 (DREG-56), NKp46 BV711 (9E2), CD8 PerCP-Cy5.5 (RPA-T8), CD4 APC (RPA-T4) (All Biolegend), and Fixable Viability Dye eFluor780 (Life Technologies). When specifically determining KIR2DL2/3 expression, KIR2D PE was replaced by anti-CD158b PE (CH-L) (BD Biosciences).

Transduction efficacy upon lentiviral introduction of the PRAME HSS1 TCR to NK(T) cells was determined 5 days post-transduction. Cells were stained with antibodies against CD3 BV510 (OKT3) (Biolegend), CD56 PE/Cy7, CD8 APC (RPA-T8) (eBiosciences), Vβ1 FITC, and 7-AAD (BD Biosciences).

Flow cytometry analysis was performed on a BD LSRFortessa (BD Biosciences), all data was analyzed using FACSDiva V8.0.1 and FlowJo V10.7.1 (all BD Biosciences). Data is shown from alive singlets and presented as dot plots or mean ± standard deviation (SD).

## Functional assays

### *Cytotoxicity assay*

The cytotoxic capacity of cells was assessed using a flow-based or luminescence-based cytotoxicity assay. Effector cells were either pre-stimulated overnight with indicated stimulation protocols (i.e. 1000 U/mL IL-2 + 50 ng/mL IL-15, or 5 ng/mL IL-12 + 20 ng/mL IL-15 + 50 ng/mL IL-18) or left unstimulated.

Target cells (K562 and T2 cytotoxicity assays) or effector cells (NBL-specific cytotoxicity assays) were labeled with Cell-Tracer Violet (CTV) (Life Technologies) according to manufacturer's instructions to allow discrimination between effectors and targets. Cells were co-cultured at indicated effector-to-target ratio (E:T) for indicated durations. Cells were spun down, supernatants were harvested for cytokine determination, and 7-AAD was added to discriminate dead cells. Samples were acquired on a BD FACSCanto, analyzed using FACSDiva V8.0.1 and FlowJo V10.7.1, and visualized using

Graphpad Prism 8.3. Data is standardized to target only controls and presented as mean ± SD. Statistical analysis was performed using the non-parametric Mann-Whitney U test between separate groups. Supernatants were analyzed to determine secretion of cytokines and other molecules of cells by ELISA (Life Technologies) or Legendplex (Biolegend) according to manufacturer's instructions. Data is presented as mean ± SD.

Luciferase-expressing GIMEN and patient-derived 691b were generated as described in **Chapter 8**. Cells were co-cultured at indicated E:T for indicated durations. 150 ug/mL D-Luciferin Firefly (Biosynth) was added to the co-cultures and incubated for 10 minutes at 37 °C after which luminescence was measured using the Spectramax M3 (Life Technologies). Cytotoxicity was calculated by comparing luminescence of co-cultured cells with target only conditions.

The flow-based cytotoxicity assay was performed to answer multiple research questions. First, the NK-receptor mediated killing capacity of cells was assessed in a co-culture with the NK-sensitive K562 cell line. Secondly, the capacity of wildtype effector cells to target a panel of NBL cells was determined. Thirdly, antigen-specific cytotoxicity, via the PRAME HSS1 TCR in TCR-transduced cells, was evaluated by overnight co-culture of PRAME HSS1 TCR expressing cells with the antigen-presenting T2 model cell line, which was pre-incubated for 1h with 1 µg/mL of SLLQHLIGL peptide (Think Peptides). Lastly, we determined the additive value of TCR introduction in cultures with NLF cells. The luminescence-based cytotoxicity assay was performed to determine the additive value of TCR introduction in cultures with GIMEN and patient-derived 691b organoids.

### *Co-culture induced MHC-I surface display determination*

To determine whether co-culture with the respective effector cell populations results in induction of MHC-I surface display on NBL cells, we assessed MHC-I expression based on HLA-ABC antibody staining (W6/32, Biolegend) on the live (7-AAD-) cell populations at indicated incubation times and E:T ratios. Effector cells were either pre-stimulated overnight with indicated stimulation protocols (i.e. 1000 U/mL IL-2 + 50 ng/mL IL-15, or 5 ng/mL IL-12 + 20 ng/mL IL-15 + 50 ng/mL IL-18) or left unstimulated. Samples were measured on a BD FACSCanto and data are presented as histograms, median fluorescent intensity (MFI) or % of HLA-ABC expressing cells.

## RESULTS

### NKT-cells express KIRs and other NK-cell associated receptors

The observation of inducible MHC-I expression by NBL cells highlights the opportunity to induce a T-cell mediated immune response to fight HR-NBL [1,2]. We previously showed that pre-stimulated NK-cells upregulate MHC-I expression on NBL cells via IFNγ secretion, which caused susceptibility to NBL-specific T-cell mediated cytotoxicity [2]. We questioned whether NK- and T-cell mediated cytotoxicity can be combined in a CD3+CD56+ NKT-cell product to decrease immune escape of NBL via plasticity in MHC-I expression.

We first investigated how NKT-cells phenotypically relate to NK- and T-cells. NK- (CD56+CD3-), T- (CD56-CD3+) and NKT-cells (CD3+CD56+) cells were sorted (**Figure 1A**) and phenotyped for presence of NK-markers. Expression of Killer Ig-like Receptors (KIRs), known to be involved in missing-self cytotoxicity [16], was identified with the anti-KIR2D antibody, which is a pan-KIR antibody against all KIRs with two Ig domains. When comparing cells from the same donor, we observed 78.6% KIR2D expression in NK-cells, 35.7% in NKT-cells, and 0.81% of T-cells (**Figure 1B**). CD158b, an inhibitory KIR in the KIR2D fraction (KIR2DL2/3) accounted for about one third of the expressed KIR2D molecules in both NK- and NKT-cells (**Figure S1**). When data from three donors is combined, we observe 20.4% (±13.9%) KIR2D expression in NKT-cells, 54.8% (±27.3%) in NK-cells, and 0.96% (±0.27%) in T-cells (**Figure 1C**). These data indicate that, like NK-cells, at least a subset of NKT-cells can engage in missing-self recognition.

Two well-known stimulatory NK-cell receptors, NKG2D and NKp46, were expressed in respectively 84.0 (±7.3%) and 56.1% (±16.8%) of NKT-cells, 82.5 (±8.1%) and 78.6% (±18.3%) of NK-cells, and 16.2 (±11.6) and 22.8% (±17.9%) of T-cells (**Figure 1C and Figure S1**). These results indicate that the majority of NKT-cells express stimulatory NK-cell receptors which could induce antigen-independent cytotoxicity against NBL cells.

### NKT-cells functionally resemble NK-cells and induce MHC-I upregulation on NBL cells

We next explored how NKT-cells functionally relate to NK- and T-cells. Sorted cells were pre-stimulated overnight, after which they were co-cultured for 5 hours with the NK-sensitive K562 cell line to determine their NK-cell mechanism-mediated cytotoxic potential. While only background levels of cytotoxicity were detected in T-cells in increasing E:T ratio, a clear ratio dependent increase in cytotoxicity was observed in co-cultures with both NK- and NKT-cell (**Figure 2A**). At a 10:1 ratio, 56.2% (±10.6%) of K562 are killed in NKT-cell cultures, 73.6% (±2.9%) in NK-cell cultures, and 20.9% (±5.9) in T-cell cultures. This demonstrates that at least a fraction of NKT-cells is able to exert cytotoxicity via NK-cell cytotoxicity mediated mechanisms.

These pre-stimulated, donor-matched NK-, T-, and NKT-cells were subsequently co-cultured overnight with the GIMEN NBL cell line and the patient-derived 691b organoid to determine their effect on MHC-I surface display on NBL cells. Co-culture with pre-stimulated NK- and NKT-cells did result in major induction of MHC-I expression when compared to pre-stimulated T-cell co-cultures (**Figure 2B**). Mean Fluorescent Intensity (MFI) of T-cell co-cultures was 1,113 ± 2 (GIMEN) and 846 ± 285 (691b), MFI of NKT-cell co-cultures was 5,678 ± 719 (GIMEN) and 15,395 ± 2,338 (691b), and MFI of NK-cell co-cultures was 13,919 ± 1,185 (GIMEN) and 14,522 ± 2,870 (691b). These data reveal that, like NK-cells [2], activation of NKT-cells results in upregulation of MHC-I expression on NBL cells.

We then explored the cytotoxic capacity of non-engineered NKT-cells towards a panel of NBL cells. We assessed the overnight cytotoxic capacity of unstimulated NKT-cells, maintained with IL-15, and pre-stimulated NKT-cells (overnight with IL-12, IL-15, and IL-18). Cells were pre-stimulated with IL-12, IL-15, and IL-18, as this cytokine combination was shown to induce a more cytokine-releasing NK-cell phenotype compared to IL-2/IL-15 pre-stimulated cells [17,18] and **Chapter 10**. All three assessed cell lines (GIMEN, CHP-212, and IMR-32) are targeted by pre-stimulated NKT-cells (**Figure 2C**). Interestingly, we also observed cytotoxicity in unstimulated NKT-cell co-cultures, in particular in the 10:1 E:T conditions. Cytotoxicity was accompanied by cytokine secretion (**Figure 2D**), of which IFNγ, in concordance to NK-cell data [18], seems to be most prominently secreted.

These data show that NKT-cells are able to recognize and kill NBL cells via NK-cell mediated cytotoxicity mechanisms. In addition, MHC-I expression induction upon NKT-cell activation may hamper cytotoxicity and explain incomplete cytotoxicity observed even after overnight co-culture at a 10:1 E:T ratio.

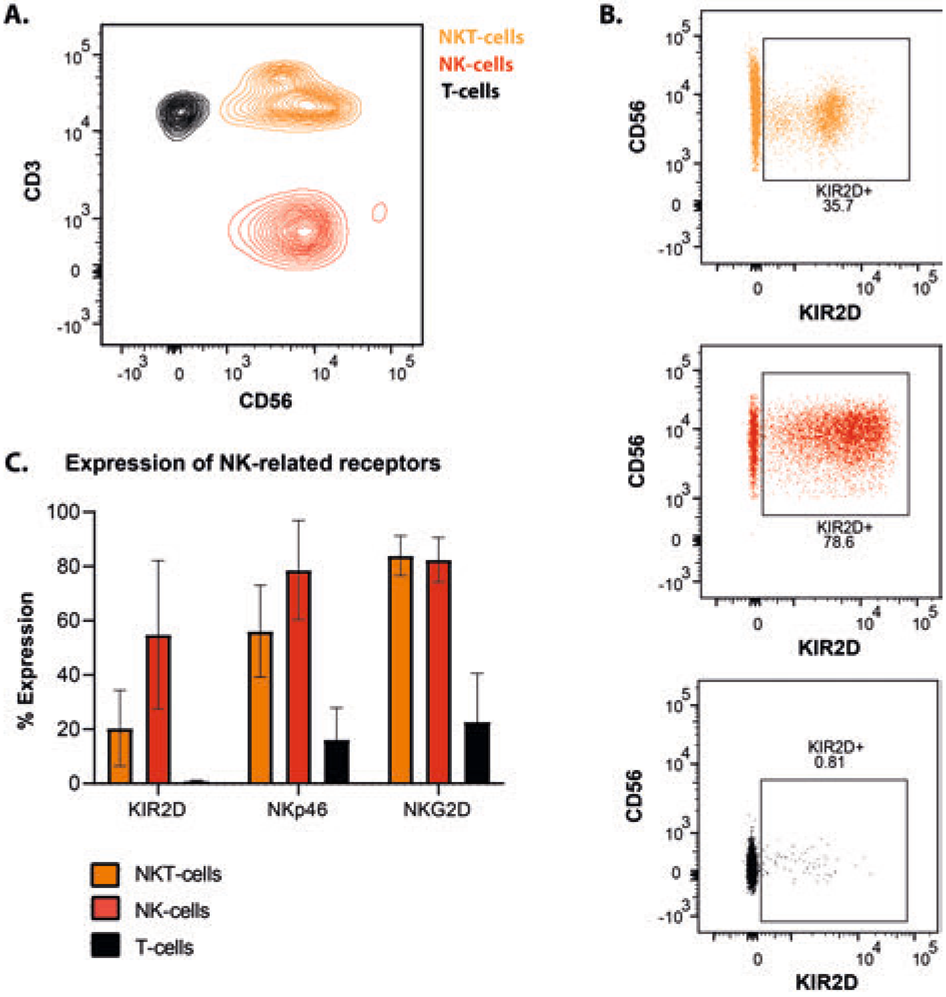

**Figure 1.** Expression of NK-related receptors in CD3$^+$CD56$^+$ NKT-cell fraction.
*(A) Representative example of NK- (red), T- (black), and NKT-cells (orange) cell populations sorted based on CD3 and CD56 expression. (B) KIR2D expression in NKT- (top), NK- (middle) or T-cells (bottom). (C) Quantification of fraction of NK- (red), NKT- (orange) and T-cells (black) expressing NK-related receptors KIR2D, NKp46 and NKG2D. KIR2D: data reflects sorted cells from 3 healthy donors, NKp46 and NKG2D: data reflects sorted cells from 6 healthy donors. Data is based on the alive, single cell population.*

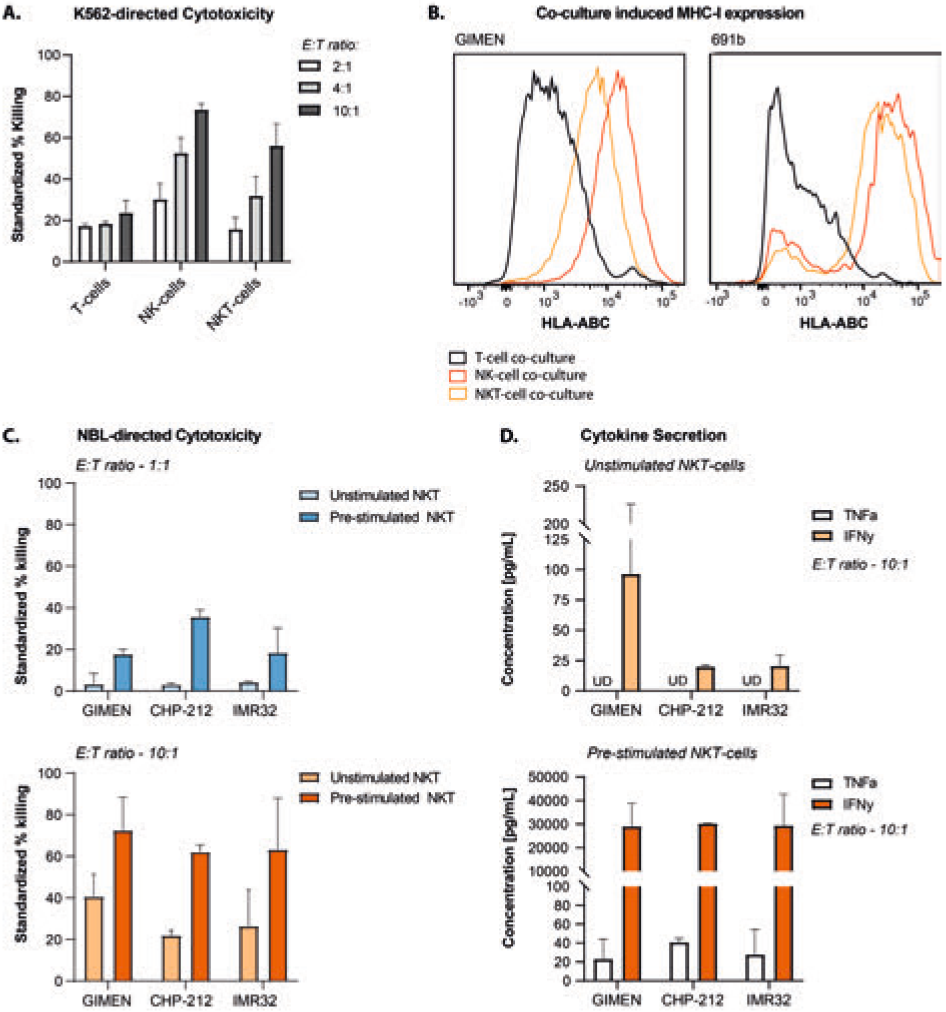

**Figure 2.** NKT-cells modify MHC-I expression and exert cytotoxicity towards NBL.
***(A)*** *% of standardized killing of the NK-sensitive K562 cell line after 5h of co-culture of donor-matched, pre-stimulated T-, NK- or NKT-cells at indicated E:T ratios. Killing was standardized to target only controls. Graphs reflect data from three individual donors, data shown as mean ± SD* ***(B)*** *MHC-I expression on live cells after overnight co-culture of GIMEN (left) or patient-derived 691b (right) with pre-stimulated T-, NK-, or NKT-cells at an E:T of 1:1. (A+B) Cells were freshly isolated and pre-stimulated overnight with 1000 U/mL IL-2 and 50 ng/mL IL-15.* ***(C)*** *% of standardized killing by NKT-cells against the GIMEN, CHP-212, and IMR32 NBL lines after overnight co-culture at an E:T of 1:1 (top) or 10:1 (bottom). Killing was standardized to respective target only controls.* ***(D)*** *IFNγ and TNFα secretion in pg/mL in NKT-NBL co-cultures from (C) after overnight incubation at an E:T of 10:1. Secretion was based on ELISA analysis. UD = undetectable (C+D) Expanded NKT-cells were rested, after which they have been left unstimulated (maintenance-dose of IL-15) or were pre-stimulated with IL-12, IL-15, and IL-18. Graphs reflect data from three individual donors, data shown as mean ± SD.*

## Understanding the kinetics of MHC-I upregulation during NKT-cell co-culture

To study the dynamics of MHC-I upregulation during co-culture with NKT-cells, we co-cultured GIMEN with NKT-cells for 2 to 72 hours, after which paired MHC-I expression and IFNγ secretion was measured. NKT-cells were either left unstimulated (with a maintenance dose of IL-15), or pre-stimulated overnight with different cytokine combinations.

Based on the MFI of panHLA-ABC staining, we observed that upregulation of MHC-I expression started between 8 and 24h after co-culture initiation (**Figure 3A**). Even though more dramatic at an E:T of 1:1 (left), kinetics were similar at a lower E:T (1:10, right). Interestingly, when assessing percentage of MHC-I expressing cells instead of MFI, we could already detect increases in percentage of MHC-I expressing cells as early as after 6 hours (**Figure 3B**). IFNγ secretion was induced rapidly and peaked around 7 hours after initiation of co-culture in all conditions (**Figure 3C)**.

When assessing the different types of pre-stimulation, we observed that IFNγ concentration was already high in IL-12+IL-15+IL-18 (triple) pre-stimulated conditions 2 hours after co-culture initiation, indicating these cells already produce IFNγ independent of NBL cell encounter **(Figure 3C**) [18]. IFNγ secretion in IL-12+IL-18 pre-stimulated cells was less pronounced than in the triple stimulated conditions, but still superior to unstimulated cells. Interestingly, even though expression was highest in triple stimulated conditions, the low levels of IFNγ secreted during co-culture with unstimulated NKT-cells were sufficient to induce MHC-I expression at both E:T (**Figure 3A**).

These data indicate that pre-stimulation of NKT-cells cells may not be required for IFNγ-release and MHC-I upregulation during co-culture. In addition, as MHC-I expression would be required to provide a window for NKT-cells engineered to express a NBL-specific TCR, we conclude that a culture duration of at least 24 hours, but preferably around 48 hours, is required.

## PRAME HSS1 TCR introduction results in the generation of antigen-specific NKT-cells

To determine the potential of introducing a NBL-specific TCR in NKT-cells, NKT- and T-cells were isolated from the same donor and transduced with a lentiviral vector encoding the PRAME HSS1 TCR [14,15]. Five days after transduction, 24% (±10.8%) of the NKT-cells and 50.5% (±8.7%) of the T-cells expressed the PRAME TCR (**Figure 4A**). Cell sorting of PRAME HSS1 TCR+ cells resulted in the generation of a TCR-enriched NKT- (93.6%) and T-cell (97.6%) population (**Figure 4B**). In line with the significantly lower transduction efficacy in NKT-cells, we observed a decreased MFI of PRAME TCR expression in NKT-cells compared to T-cells (1764 in NKT- versus 7852 in T-cells). No significant difference in targeting capacity of PRAME HSS1 TCR+ T- and NKT-cells was observed when cells were co-cultured overnight with the antigen-presenting T2 model cell line loaded with PRAME SLLQHLIGL peptide (**Figure 4C**). All in all, even though transduction efficacy in NKT-cells is lower compared to T-cells, it is feasible to generate functional PRAME-directed NKT-cells.

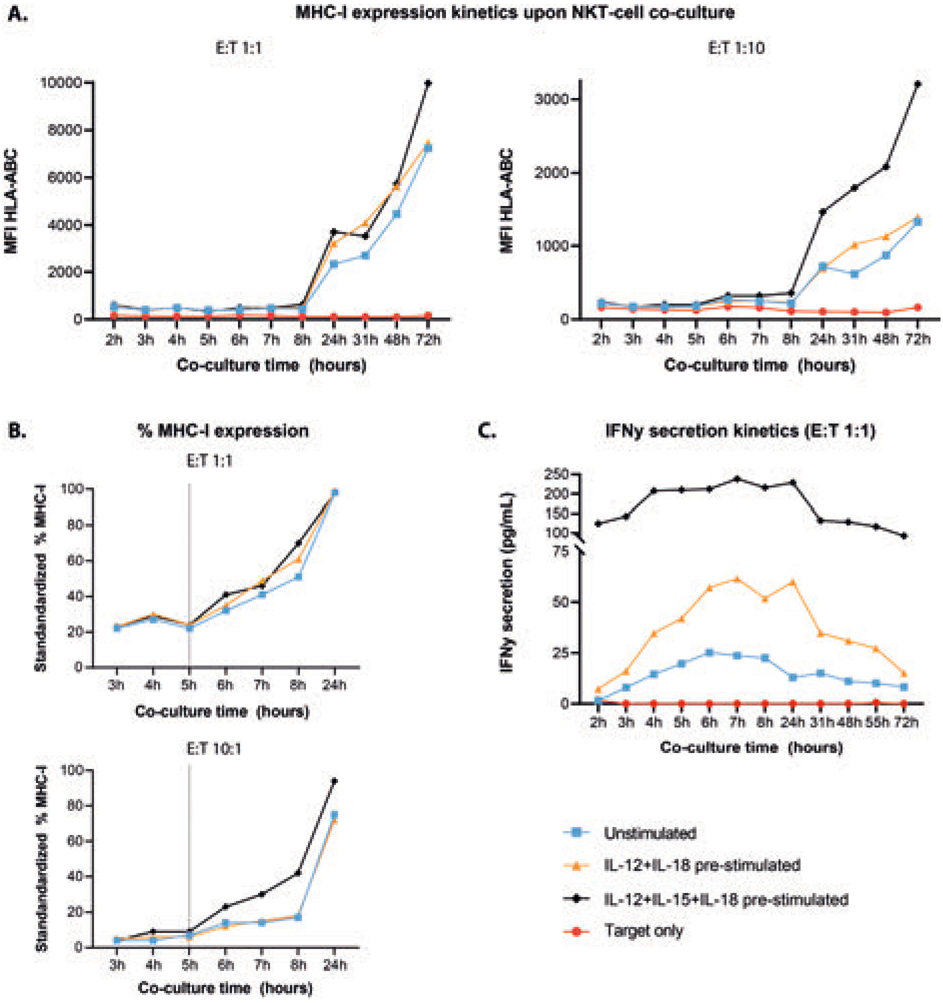

**Figure 3.** MHC-I surface display and IFNγ secretion kinetics in GIMEN during co-culture with NKT-cells. ***(A)*** *MHC-I expression kinetics in GIMEN cells based on MFI of HLA-ABC after indicated hours of co-culture with NKT-cells. MFI of HLA-ABC of the live, NKT-cell excluded fraction is shown.* ***(B)*** *% MHC-I expressing cells, standardized to target only controls, after indicated hours of co-culture. The % MHC-I expressing cells is based on the live, NKT-cell excluded fraction.* ***(C)*** *IFNγ secretion kinetics during co-culture of NKT-cells and GIMEN cells after indicated hours of co-culture. Data are based on co-cultures with one donor.*

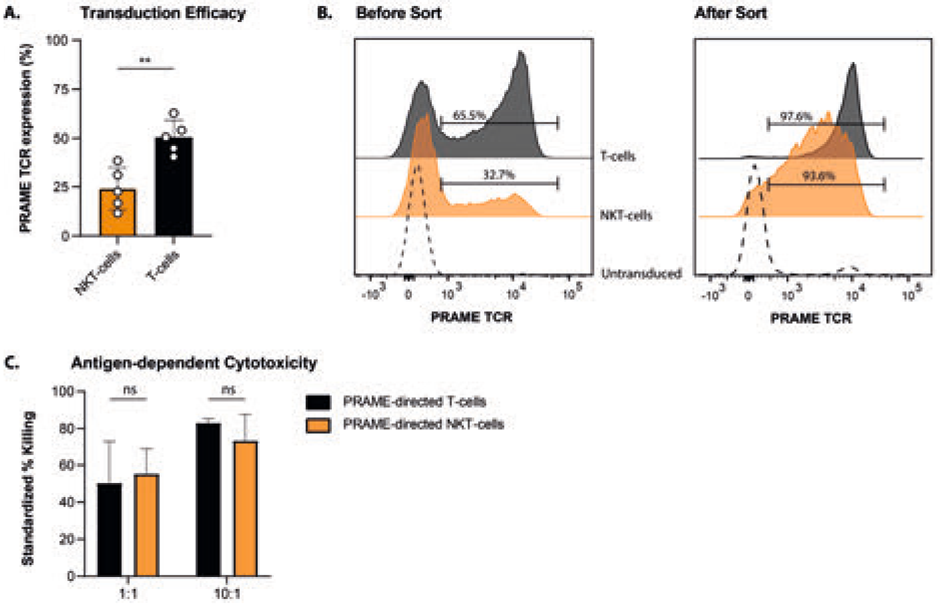

**Figure 4.** PRAME HSS1 TCR introduction in donor-matched T- and NKT-cells.
***(A)*** *Transduction efficacy, defined as the difference in percentage of $V\beta1$ expression of the $CD3^+CD56^+$ (NKT) or $CD3^+CD56^-$ (T) cells between transduced and untransduced cells, 5 days after transduction. n=5.* ***(B)*** *Transduction efficacy based on $V\beta1$ expression before (left) and after sort (right) in donor-matched $CD3^+CD56^+$ NKT- and $CD3^+CD56^-$ T-cells. Gating based on untransduced control cells, a representative histogram from one of the five donors is shown.* ***(C)*** *Antigen-dependent cytotoxicity assay against the antigen-presenting T2 model cell line loaded with PRAME SLLQHLIGL peptide. Standardized % killing compared to T2 only conditions is shown after overnight incubation at indicated E:T, data standardized to unpulsed T2 controls, n=3. Statistical differences were calculated using the Mann Whitney U test, **p<0.01, ns= non-significant*

## PRAME HSS1 TCR+ NKT-cells show a superior cytotoxic capacity against NBL cells

To examine the additive effect of PRAME HSS1 TCR introduction in NKT-cells, matched untransduced (wildtype) and PRAME HSS1 TCR+ (PRAME-directed) NKT-cells were co-cultured with the $HLA\text{-}A2^+PRAME^+$ GIMEN cell line (**Figure 5A**). Regardless of the nature of pre-stimulation of NKT-cells, we observe superior killing of GIMEN by PRAME-directed NKT-cells compared to wildtype counterparts. After 48h of co-culture, an average additive effect of PRAME HSS1 TCR introduction of 17.6% (± 7.2%) was observed in co-cultures with unstimulated NKT-cells, 28.3% (± 2.6%) in IL-12 + IL-18 pre-stimulated NKT-cell co-cultures, and 10.2 (± 10.6%) in IL-12 + IL-15 + IL-18 pre-stimulated NKT-cell co-cultures. This additive effect was unique to NKT-cells and was not observed in matched T-cells. The additive effect of PRAME HSS1 TCR introduction in NKT-cells was also observed in co-cultures of pre-stimulated NKT-cells with NLF (63.1% ± 17.9%) and patient-derived 691b organoids (90.7% ± 3.0%) (**Figure 5B**). Thus, co-culture with both unstimulated and pre-stimulated NKT-cells resulted in an enhanced cytotoxic capacity of PRAME HSS1 TCR+ NKT-cells compared to untransduced counterparts, which increased over time.

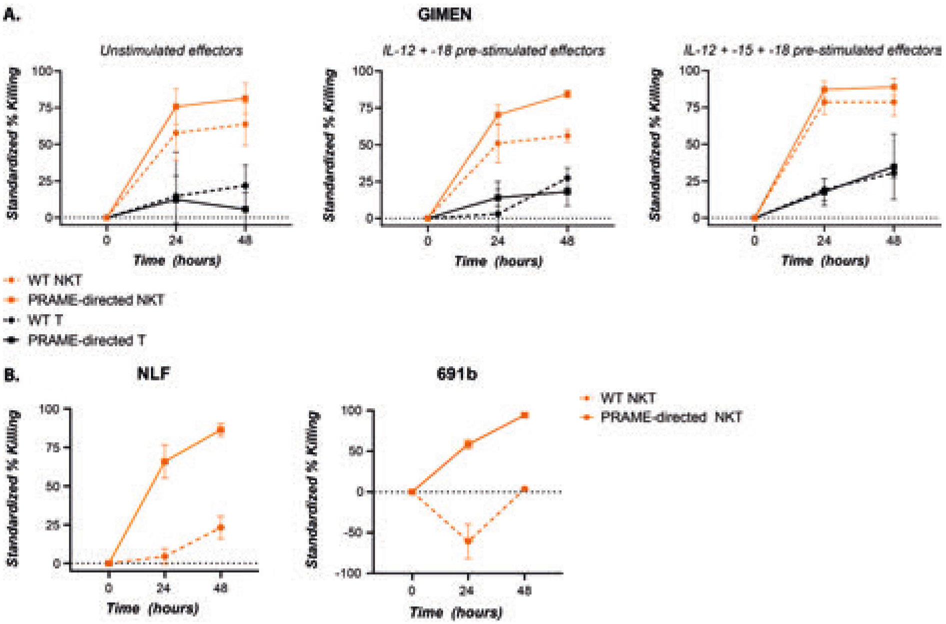

**Figure 5.** The additive effect of TCR introduction to the cytotoxic capacity of NKT-cells against NBL cells. *Killing % standardized to target only conditions after co-culture of NBL cells with effector cells ± PRAME-directed TCR introduction after indicated hours of co-culture.* ***(A)*** *Co-culture of GIMEN with NKT- and T-cell effectors ± TCR introduction after overnight pre-stimulation of effectors with maintenance dose IL-15 (left), IL-12 + IL-18 (middle) or IL-12+ IL-15 + IL-18 (right). Orange: NKT-cells, black: T-cells* ***(B)*** *Co-culture of NLF (left) or patient-derived 691b organoids (right) with NKT-cells ± TCR introduction after overnight pre-stimulation of effectors with IL-12 + IL-15 + IL-18. Data shown as mean ± SEM, GIMEN + NLF: n=3 from one donor, 691b: triplo from single experiment.*

## DISCUSSION

Most studies into the therapeutic potential of NKT-cells are referring to iNKT-cells. Even though these efforts are promising and proceeded to clinical trials [19], these cells comprise <5% of the total CD3+CD56+ and <1% of the total lymphocyte fraction. Consequently, massive *ex vivo* expansion is required to generate sufficient cell numbers for (re-)infusion. The current study, together with the observation by Hurtado and colleagues [11] who found that >99% of the CD3+CD56+ TILs in NBL tumors were non-iNKT cells, underlines the potential of utilization of the full CD3+CD56+ NKT-cell fraction in NBL cell therapy strategies. In addition, the here reported superior cytotoxic capacity of TCR-engineered NKT-cells over T-cells shows the potential of combining NK-cell mediated and antigen-specific cytotoxicity to overcome immune evasion caused by MHC-I plasticity in NBL cells.

Recently, Romero-Olmedo *et al.* used a panel of 41 antibodies to comprehensively phenotype the human CD3+CD56+ NKT-cell fraction by mass cytometry [5]. They observed that NKT-cells did not form a separate cluster in the t-SNE projection of total PBMCs, but constituted parts of the CD4+, CD8+, DN, TCRγδ+, MAIT cell subsets. FlowSOM analysis revealed the presence of a total of 19 separate clusters in the NKT-cell fraction. This study demonstrates the heterogeneity of the NKT-cell population, and shows that the historical subdivision into CD1d-restricted (type I & type II NKT) and CD1d-unrestricted (NKT-like) cells [3,5,20] is oversimplified and may confound results. Future research will focus on the repertoire of isolated NKT-cells, how abundance of these subsets changes during *in vitro* culture, and which subset(s) exert the most promising effector function (*in vitro* and *in vivo*).

Terminally differentiated CD45RA+ T-cells (TEMRA) are effector T-cells with complete competence, which upregulate NK-cell receptors, including CD56 [21]. The TEMRA fraction of T-cells increases with age, resulting in increased abundance of the CD3+CD56+ NKT-cell fraction with age [3]. However, studies into cell therapy products show that therapy persistence and efficacy is enhanced in less differentiated, naïve (Tn), stem-cell memory (Tscm) and central memory T-cells (Tcm) compared to effector(memory) T-cells and TEMRA [22]. Romero-Olmedo and colleagues showed that identified cell clusters could be subdivided in two groups of cells based on CCR7, CD27, CD28, CD127, CD161, CD45RA and GZMB expression, which was hypothesized to be indicative for less and more differentiated cells [5]. This finding again stresses the importance of culture characterization and studies into NKT-cell subsets and their efficacy and persistence *in vitro* as well as *in vivo*.

When NK-cells are separated from the PBMC fraction, pre-stimulation is required to induce NK-cell cytotoxicity *in vitro*, to mimic *in vivo* activation by T-cells and antigen-presenting cells [18,23]. We show that stimulation with IL-2+IL-15 as well as with IL-12+IL-15+IL-18 induced increased cytotoxic capacity of NKT-cells against NBL. In addition, IL-12+IL-15+IL-18 stimulation induces an increase in cytokine-secretion capacity of cells. Pre-stimulation with cytokines, however, is artificial and does not completely reflect the *in vivo* situation. For future experiments, we could irradiate the NK-depleted cell fraction and co-culture with these autologous cells to provide the needed stimulation [23]. In addition, we should further study the cytokine-induced IFNγ secretion of NK-cells in absence of tumor cells, to conclude whether IFNγ secretion actually further enhances after tumor cell recognition [2]. *In vivo* murine studies in humanized, immunocompetent mouse, for example the MISTRG model[24], will be most illustrative to study the potency of TCR-engineered NKT-cells in a more physiological setting.

We show that PRAME HSS1 engineered NKT-cells can be generated upon transduction with a VSVg envelope-based lentiviral vector [15 and **Chapter 8**], although a significantly lower transduction efficacy of NKT-cells was observed compared to T-cells. This was accompanied with a lower MFI in TCR expression in transduced, sorted cells, which probably corresponds to a lower integrated number of vector copies in the NKT-cell genome. This is in line with what is observed in NK-cells (unpublished data and [25]). The TCR-dependent cytotoxic capacity, however, was similar between PRAME HSS1 TCR+ T- and NKT-cells. The decreased transduction efficacy most probably is a consequence of differential upregulation of the major entry receptor of VSVg envelope-based lentiviral vectors, the LDL-receptor [26], upon T- and NKT-cell activation. This could be caused by suboptimal activation of NKT-cells in our current T-cell activation and expansion protocol optimized for $CD8^+$ T-cell transduction [15]. Besides adjusting the VSVg-transduction based protocol to NKT-cells, we could also use a baboon enveloped pseudotyped lentiviral vector instead, as these have been described to more efficiently transduce NK-cells [25]. Another promising strategy would be do design single-chain variable fragment based entry-proteins [27], for example against NKG2D or NKp46, to induce specific transduction of NKT-cells. This is a promising approach, as this does not require prior stimulation and expansion to increase entry receptor expression. In addition, such a strategy in theory allows modification to specifically target any (NKT) cell subset of interest. Despite the fact that transduction efficacy of NKT-cells with the present protocol was suboptimal, we do show that TCR introduction in NKT-cells is feasible and results in the generation of NBL-specific NKT-cells.

Collectively, this pilot study shows the potential and provides groundwork for further investigation of the use of NKT-cells as a cell therapy source to improve outcome for children suffering from HR-NBL. This study supports our hypothesis that combining NK receptor-mediated cytotoxicity with MHC-I restricted targeting is a promising strategy to overcome MHC-I plasticity-related immune evasion by NBL.

## REFERENCES

1. Lorenzi, S.; Forloni, M.; Cifaldi, L.; Antonucci, C.; Citti, A.; Boldrini, R.; Pezzullo, M.; Castellano, A.; Russo, V.; van der Bruggen, P.; et al. IRF1 and NF-KB Restore MHC Class I-Restricted Tumor Antigen Processing and Presentation to Cytotoxic T Cells in Aggressive Neuroblastoma. *PLoS One* **2012**, *7*, 1–8, doi: 10.1371/journal.pone.0046928.
2. Spel, L.; Boelens, J.J.; Van Der Steen, D.M.; Blokland, N.J.G.; van Noesel, M.M.; Molenaar, J.J.; Heemskerk, M.H.M.; Boes, M.; Nierkens, S. Natural Killer Cells Facilitate PRAME-Specific T-Cell Reactivity against Neuroblastoma. *Oncotarget* **2015**, *6*, 35770–35781, doi: 10.18632/oncotarget.5657.
3. Peralbo, E.; Alonso, C.; Solana, R. Invariant NKT and NKT-like Lymphocytes: Two Different T Cell Subsets That Are Differentially Affected by Ageing. *Exp. Gerontol.* **2007**, *42*, 703–708, doi:10.1016/j.exger.2007.05.002.
4. Exley, M.A.; Hou, R.; Shaulov, A.; Tonti, E.; Dellabona, P.; Casorati, G.; Akbari, O.; Akman, H.O.; Greenfield, E.A.; Gumperz, J.E.; et al. Selective Activation, Expansion, and Monitoring of Human INKT Cells with a Monoclonal Antibody Specific for the TCR α-Chain CDR3 Loop. *Eur. J. Immunol.* **2008**, *38*, 1756–1766, doi:10.1002/eji.200737389.
5. Romero-Olmedo, A.J.; Schulz, A.R.; Huber, M.; Brehm, C.U.; Chang, H.D.; Chiarolla, C.M.; Bopp, T.; Skevaki, C.; Berberich-Siebelt, F.; Radbruch, A.; et al. Deep Phenotypical Characterization of Human CD3+CD56+ T Cells by Mass Cytometry. *Eur. J. Immunol.* **2021**, *51*, 672–681, doi:10.1002/eji.202048941.
6. Kaszubowska, L.; Foerster, J.; Kwiatkowski, P.; Schetz, D. NKT-like Cells Reveal Higher than T Lymphocytes Expression of Cellular Protective Proteins HSP70 and SOD2 and Comparably Increased Expression of SIRT1 in the Oldest Seniors. *Folia Histochem. Cytobiol.* **2018**, *56*, 231–240, doi:10.5603/FHC.A2018.0025.
7. Almeida, J.S.; Couceiro, P.; López-Sejas, N.; Alves, V.; Růžičková, L.; Tarazona, R.; Solana, R.; Freitas-Tavares, P.; Santos-Rosa, M.; Rodrigues-Santos, P. Nkt-like (Cd3+cd56+) Cells in Chronic Myeloid Leukemia Patients Treated with Tyrosine Kinase Inhibitors. *Front. Immunol.* **2019**, *10*, 1–14, doi:10.3389/fimmu.2019.02493.
8. Schmid, H.; Schneidawind, C.; Jahnke, S.; Kettemann, F.; Secker, K.A.; Duerr-Stoerzer, S.; Keppeler, H.; Kanz, L.; Savage, P.B.; Schneidawind, D. Culture-Expanded Human Invariant Natural Killer T Cells Suppress T-Cell Alloreactivity and Eradicate Leukemia. *Front. Immunol.* **2018**, *9*, 1–10, doi:10.3389/fimmu.2018.01817.
9. Wang, H.; Yang, D.; Xu, W.; Wang, Y.; Ruan, Z.; Zhao, T.; Han, J.; Wu, Y. Tumor-Derived Soluble MICs Impair CD3+CD56+ NKT-like Cell Cytotoxicity in Cancer Patients. *Immunol. Lett.* **2008**, *120*, 65–71, doi:10.1016/j.imlet.2008.07.001.
10. Bojarska-Junak, A.; Hus, I.; Sieklucka, M.; Wasik-Szczepanek, E.; Mazurkiewicz, T.; Polak, P.; Dmoszynska, A.; Rolinski, J. Natural Killer-like T CD3+/CD16+CD56+ Cells in Chronic Lymphocytic Leukemia: Intracellular Cytokine Expression and Relationship with Clinical Outcome. *Oncol. Rep.* **2010**, *24*, 803–810, doi:10.3892/or.
11. Hurtado, M.O.; Wolbert, J.; Fisher, J.; Flutter, B.; Stafford, S.; Barton, J.; Jain, N.; Barone, G.; Majani, Y.; Anderson, J. Tumor Infiltrating Lymphocytes Expanded from Pediatric Neuroblastoma Display Heterogeneity of Phenotype and Function. *PLoS One* **2019**, *14*, 1–18, doi:10.1371/journal.pone.0216373.
12. Bate-Eya, L.T.; Ebus, M.E.; Koster, J.; Den Hartog, I.J.M.; Zwijnenburg, D.A.; Schild, L.; Van Der Ploeg, I.; Dolman, M.E.M.; Caron, H.N.; Versteeg, R.; et al. Newly-Derived Neuroblastoma Cell Lines Propagated in Serum-Free Media Recapitulate the Genotype and Phenotype of Primary Neuroblastoma Tumours. *Eur. J. Cancer* **2014**, *50*, 628–637, doi:10.1016/j.ejca.2013.11.015.

13. Marcu-Malina, V.; Heijhuurs, S.; Van Buuren, M.; Hartkamp, L.; Strand, S.; Sebestyen, Z.; Scholten, K.; Martens, A.; Kuball, J. Redirecting AβT Cells against Cancer Cells by Transfer of a Broadly Tumor-Reactive ΓδT-Cell Receptor. *Blood* **2011**, *118*, 50–59, doi:10.1182/blood-2010-12-325993.

14. Amir, A.L.; Van Der Steen, D.M.; Van Loenen, M.M.; Hagedoorn, R.S.; De Boer, R.; Kester, M.D.G.; De Ru, A.H.; Lugthart, G.J.; Van Kooten, C.; Hiemstra, P.S.; et al. PRAME-Specific Allo-HLA-Restricted T Cells with Potent Antitumor Reactivity Useful for Therapeutic T-Cell Receptor Gene Transfer. *Clin. Cancer Res.* **2011**, *17*, 5615–5625, doi:10.1158/1078-0432.CCR-11-1066.

15. Lo Presti, V.; Cornel, A.M.; Plantinga, M.; Dünnebach, E.; Kuball, J.; Boelens, J.J.; Nierkens, S.; van Til, N.P. Efficient Lentiviral Transduction Method to Gene Modify Cord Blood CD8+ T Cells for Cancer Therapy Applications. *Mol. Ther. - Methods Clin. Dev.* **2021**, *21*, 357–368, doi:10.1016/j.omtm.2021.03.015.

16. Pende, D.; Falco, M.; Vitale, M.; Cantoni, C.; Vitale, C.; Munari, E.; Bertaina, A.; Moretta, F.; Del Zotto, G.; Pietra, G.; et al. Killer Ig-like Receptors (KIRs): Their Role in NK Cell Modulation and Developments Leading to Their Clinical Exploitation. *Front. Immunol.* **2019**, *10*, doi:10.3389/fimmu.2019.01179.

17. Cheng, M.; Chen, Y.; Xiao, W.; Sun, R.; Tian, Z. NK Cell-Based Immunotherapy for Malignant Diseases. *Cell. Mol. Immunol.* **2013**, *10*, 230–252, doi:10.1038/cmi.2013.10.

18. Lusty, E.; Poznanski, S.M.; Kwofie, K.; Mandur, T.S.; Lee, D.A.; Ashkar, A.A. IL-18/IL-15/IL-12 Synergy Induces Elevated and Prolonged IFN-γ Production by Ex Vivo Expanded NK Cells Which Is Not Due to Enhanced STAT4 Activation. *Mol. Immunol.* **2017**, *88*, 138–147, doi:10.1016/j.molimm.2017.06.025.

19. Exley, M.A.; Dellabona, P.; Casorati, G. Exploiting CD1-Restricted T Cells for Clinical Benefit. *Mol. Immunol.* **2021**, *132*, 126–131, doi:10.1016/j.molimm.2020.12.015.

20. Kato, S.; Berzofsky, J.A.; Terabe, M. Possible Therapeutic Application of Targeting Type II Natural Killer T Cell-Mediated Suppression of Tumor Immunity. *Front. Immunol.* **2018**, *9*, doi:10.3389/fimmu.2018.00314.

21. Van Acker, H.H.; Capsomidis, A.; Smits, E.L.; Van Tendeloo, V.F. CD56 in the Immune System: More than a Marker for Cytotoxicity? *Front. Immunol.* **2017**, *8*, 1–9, doi:10.3389/fimmu.2017.00892.

22. Ren, H.; Cao, K.; Wang, M. A Correlation Between Differentiation Phenotypes of Infused T Cells and Anti-Cancer Immunotherapy. *Front. Immunol.* **2021**, *12*, 1–11, doi:10.3389/fimmu.2021.745109.

23. Peighambarzadeh, F.; Najafalizadeh, A.; Esmaeil, N.; Rezaei, A.; Ashrafı, F.; Hakemi, M.G. Optimization of in Vitro Expansion and Activation of Human Natural Killer Cells against Breast Cancer Cell Line. *Avicenna J. Med. Biotechnol.* **2020**, *12*, 17–23.

24. Rongvaux, A.; Willinger, T.; Martinek, J.; Strowig, T.; Gearty, S. V.; Teichmann, L.L.; Saito, Y.; Marches, F.; Halene, S.; Palucka, A.K.; et al. Development and Function of Human Innate Immune Cells in a Humanized Mouse Model. *Nat. Biotechnol.* **2014**, *32*, 364–372, doi:10.1038/nbt.2858.

25. Colamartino, A.B.L.; Lemieux, W.; Bifsha, P.; Nicoletti, S.; Chakravarti, N.; Sanz, J.; Roméro, H.; Selleri, S.; Béland, K.; Guiot, M.; et al. Efficient and Robust NK-Cell Transduction With Baboon Envelope Pseudotyped Lentivector. *Front. Immunol.* **2019**, *10*, 1–7, doi:10.3389/fimmu.2019.02873.

26. Amirache, F.; Lévy, C.; Costa, C.; Mangeot, P.-E.; Torbett, B.; Wang, C.; Nègre, D.; Cosset, F.-L.; Verhoeyen, E. Mystery Solved: VSV-G-LVs Do Not Allow Efficient Gene Transfer into Unstimulated T Cells, B Cells, and HSCs Because They Lack the LDL Receptor. *Blood* **2014**, *123*, 1422–1424, doi:10.1071/MU931254.

**27.** Frank, A.M.; Braun, A.H.; Scheib, L.; Agarwal, S.; Schneider, I.C.; Fusil, F.; Perian, S.; Sahin, U.; Thalheimer, F.B.; Verhoeyen, E.; et al. Combining T-Cell-Specific Activation and in Vivo Gene Delivery through CD3-Targeted Lentiviral Vectors. *Blood Adv.* **2020**, *4*, 5702–5715, doi:10.1182/bloodadvances.2020002229.

# SUPPLEMENTARY MATERIAL

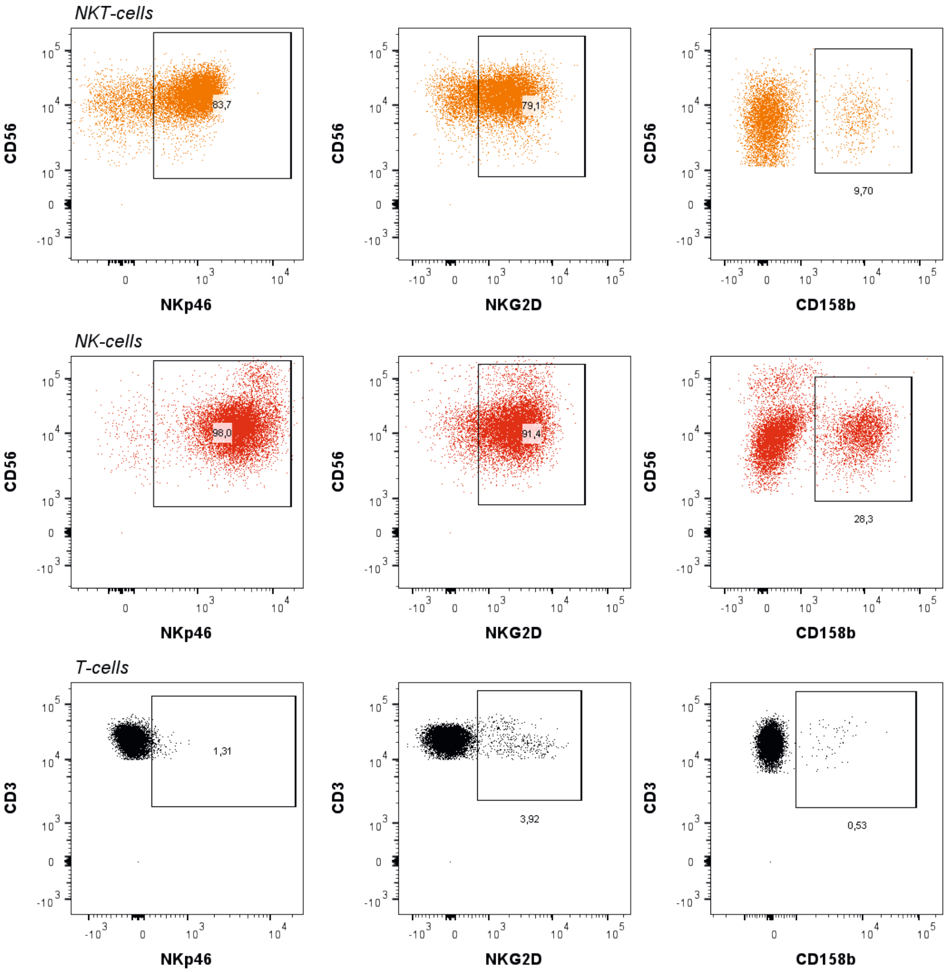

**Figure S1.** Expression of NK-related receptors in NK-, T- and NKT-cells.
*Expression of NKp46, NKG2D (middle) and an inhibitory KIR (CD158b) (right) in NKT-cells (orange), NK-cells (red) & T-cells (black). Representative data of one donor is shown. CD158b is assessed in a different panel than NKp46 and NKG2D, explaining the differences in CD56 intensity in the different graphs. Data shown are representative examples of three donors.*

# Chapter 10

## Ex Vivo generated CD34+ stem cell-derived thymic NK-cells as a cellular therapy source in Neuroblastoma

Annelisa M. Cornel[1,2], Diana P. Petcu[2,*], Ester Dünnebach[1,2.,*], Caitlyn L. Forbes[1,2], Vania lo Presti[1,2], Coco de Koning[1,2], Miranda P. Dierselhuis[1], Stefan Nierkens[1,,2]

*[1] Princess Máxima Center for Pediatric Oncology, Utrecht University, 3584 CS Utrecht, The Netherlands*
*[2] Center for Translational Immunology, University Medical Center Utrecht, Utrecht University, The Netherlands*

** Authors Contributed Equally*

*Manuscript in preparation*

## ABSTRACT

The significant but incomplete survival benefit of high-risk neuroblastoma (HR-NBL) patients upon immunotherapy addition to the treatment regimen shows both the potential and a window of improvement of immune interference in HR-NBL. NK-cells have been shown to be particularly important in targeting NBL. They target tumor cells via missing-self cytotoxicity, as HR-NBL cells often lack MHC class I (MHC-I) expression, and are important effector cells during dinutuximab-based immunotherapy. Cytotoxicity of NK-cells is, however, majorly decreased at NBL diagnosis as well as during therapy, indicating the potential to boost NK-cell cytotoxicity to increase immunotherapy efficacy. Moreover, it is suggested that the high degree of plasticity in MHC-I expression in NBL allows alternate evasion of both cytotoxic T- and NK-cell recognition. We hypothesize that introduction of a NBL-specific T-cell receptor (TCR) in NK-cells may provide a solution for MHC-I plasticity-mediated immune evasion of NBL. We implemented an ex vivo OP9/DL1 co-culture protocol in which CD34+ stem cells can be differentiated into NK-cells. This four week co-culture produces CD56bright intracellular CD3e+ (cyCD3e+) NK-cells expressing similar levels of natural cytotoxicity receptors, superior granzymes levels, similar cytotoxicity against the MHC-I- K562 line, and at least similar cytotoxic capacity against NBL lines compared to healthy-donor peripheral blood NK-cells. The high cytotoxic capacity and CD56brightcyCD3e+ phenotype of these cells is consistent with a thymic NK-cell phenotype. Interestingly, the endogenous intracellular CD3 expression allowed surface translocation of a TCR without the need to co-introduce CD3 subunits and resulted in generation of CD56bright TCR+ NK-cells with both intact NK receptor-mediated and TCR-dependent cytotoxicity. PRAME HSS1 TCR+ NK-cells show superior cytotoxicity to various HLA-A2+PRAME+ NBL cell lines compared to TCR counterparts. This study shows the potential of both non-engineered and TCR-engineered CD34+ stem cell-derived NK-cells as a cell therapy-based immune boosting strategy to improve immune engagement to treat HR-NBL. In the context of NBL treatment, autologous CD34+ stem cell harvest to rescue hematopoiesis after high-dose chemotherapy provides a unique opportunity for additional cell therapy-based immune boosting strategies.

## INTRODUCTION

Neuroblastoma (NBL) is an embryonal, sympathoadrenal progenitor-derived, tumor accounting for about 15% of all pediatric cancer deaths [1,2]. Multimodal treatment of high-risk NBL (HR-NBL) patients entails induction- and high-dose chemotherapy followed by an autologous stem-cell rescue, tumor resection, local irradiation, and anti-GD2 based immunotherapy as consolidation therapy [3–5]. Despite extensive multimodal treatment, 5-year event-free survival is still <60% [5]. Nonetheless, regardless of the immunosuppressive environment of NBL, a significant, though incomplete, increase in survival was observed upon immunotherapy addition to the treatment regimen, indicating the potential of immune interference in NBL. Increasing immune engagement is key to further improve outcome of patients suffering from HR-NBL.

It is suggested that the poor immunogenic properties of NBL are the result of a combination of a low mutational burden [6], a derivate of the lack of immunogenic features of the embryonal cell of origin [7; **Chapter 8**], and the immunomodulatory effect of NBL on the cytotoxic capacity of immune subsets [8]. One of the most important immunogenic features absent on the surface of embryonal neural crest cells is MHC class I (MHC-I), a peptide-presenting molecule necessary for cytotoxic T-cells to sense and activate upon recognition of malignant transformation, which causes evasion of T-cell cytotoxicity [9,10, **Chapter 8]**. Nevertheless, lack of MHC-I expression on cells should trigger activation and cytotoxicity of natural killer (NK) cells via missing-self recognition [10].

NK-cells are an immune subset of particular importance in NBL, as they are reported to target NBL cells via missing-self cytotoxicity, have been shown to be able to recognize NBL via several natural cytotoxicity receptors (NCRs) [11], and are important effector cells during anti-GD2 (dinutuximab)-based immunotherapy. Nonetheless, NK-cell cytotoxicity is shown to be majorly decreased at NBL diagnosis as well as during therapy [8], indicating the potential to boost NK-cell cytotoxicity to increase immunotherapy efficacy.

Absence of MHC-I on NBL cells should trigger missing-self recognition of NBL by NK-cells. We have previously shown, however, that secretion of IFNγ by NK-cells upon NBL cell recognition results in induction of expression of MHC-I on NBL cells, thereby resulting in evasion of missing-self mediated cytotoxicity by NK-cells [9]. This suggests that the high degree of plasticity in MHC-I expression may allow alternate evasion of both cytotoxic T- and NK-cells. As illustrated in **Chapter 9**, we hypothesize that the generation of a cell that can both engage in NK-cell mediated cytotoxicity, for example via missing-self recognition, as well as in recognition of malignant transformation in MHC-I context will result in the generation of a cell type that can no longer be evaded by MHC-I plasticity.

Autologous CD34+ stem cell harvest to rescue hematopoiesis after high-dose chemotherapy in HR-NBL patients provides a unique opportunity for additional cell therapy-based immune boosting strategies. Several groups have succeeded in generating mature and functional T-cells from CD34+ stem cells by co-culture with a bone marrow-derived stromal OP9 cell line transduced with Notch Ligand (DL1) [12–15]. De Smedt and colleagues have adapted this protocol to generate NK-cells instead [16]. Interestingly, they show that Notch signaling, necessary for commitment to the T- but not the NK-cell lineage [16,17], during NK-cell development results in the generation of a thymic NK-cell (tNK) population that can be identified by intracellular CD3e expression (cyCD3) without presence of a fully rearranged TCR [16]. We hypothesize that introduction of a NBL-specific T-cell receptor (TCR) in these cyCD3+ NK-cells may provide a cell type both engaging in missing-self and MHC-I mediated cytotoxicity.

In this pilot study, we implemented the ex vivo OP9/DL1 co-culture protocol in which CD34+ stem cells are differentiated into tNK-cells [16] and studied the feasibility to introduce an NBL-specific TCR in these cells. The effect of TCR introduction in CD34+ stem cells on co-culture derived NK-cell (CC NK-cell) development, phenotype and (NBL-directed) functionality was studied. These pilot data show feasibility and potential of engineered OP9/DL1 CC NK-cells to target MHC-I plasticity in HR-NBL.

## MATERIALS & METHODS

### Primary Cell Isolation

Fresh umbilical cord blood (CB) and peripheral blood (PB) was collected after informed consent was obtained in accordance to the Declaration of Helsinki. The collection protocol was approved by the Ethical Committee of the University Medical Center (UMC) Utrecht. CB or PB mononuclear cells (C/PBMC) were isolated by means of Ficoll-Paque PLUS separation (GE Healthcare Bio-Sciences AB). CD34$^+$ stem cells were isolated from CB, NK-cells or CD8$^+$ T-cells from PB using magnetic bead separation according manufacturer’s instructions (Miltenyi Biotec). Cells were cryopreserved at -80 °C until use.

### Cell Lines and Reagents

The Murine, bone marrow-derived OP9 stromal cell line overexpressing DL1 were kindly provided by the University of Toronto. K562 (ATCC® CCL-243) and T2 cells

(ATCC® CRL-1992) were used as a missing-self and antigen-specific model readout system, respectively. Wildtype GIMEN were obtained via the Academic Medical Center of Amsterdam, eGFP-luciferase transduced GIMEN were generated as described previously (**Chapter 8**). IMR32 were obtained via the Princess Maxima Center for Pediatric Oncology, CHP212 and NLF were provided by the Dana Faber Cancer Institute. OP9/DL1 cells were cultured in alpha MEM medium (Life Technologies) supplemented with 10% heat-inactivated fetal calf serum (FCS) (Sigma-Aldrich) and 1% penicillin/streptomycin (p/s) (50 units/mL) (Life Technologies). K562 and T2 were maintained in Glutamax™ supplemented RPMI (Life Technologies) with 10% FCS and 1% p/s, GIMEN and IMR32 in Glutamax™ supplemented DMEM with 10% FCS, 1% p/s, and 2% non-essential amino acids (Life Technologies). All cells were cultured under standard culturing conditions and split biweekly.

CD137L overexpressing K562 feeder cells were generated by lentiviral introduction of CD137L. The CD137L sequence was codon optimized and synthesized by Genscript, cloned into our pCCL-cPPT-hPGK-GFP-bPRE4-SIN lentiviral transfer vector in place of the GFP sequence, and viral particles were generated according to a previously established protocol (**Chapter 8**). Cells were transduced at a multiplicity of infection (MOI) of 1 and sorted based on CD137L expression (BD FACS Aria).

### OP9/DL1-CD34+ Stem Cell Co-culture

Following thawing, $CD34^+$ stem cells were resuspended in NK co-culture medium comprising alpha-MEM medium, supplemented with 2.2 g/L sodium bicarbonate (Sigma-Aldrich), 5% FCS , 1% p/s, 50 µg/ml phosphor-ascorbic acid (Sigma-Aldrich), IL-7 (5 ng/ml), FLT3 ligand (5 ng/ml), SCF (50 ng/ml), and IL-15 (20 ng/ml) and put on an 80% confluent layer of OP9/DL1 cells. Medium was replenished biweekly, progenitor cells were transferred to a new OP9/DL1 layer weekly. Developing progenitors were harvested from the monolayer via forceful pipetting and filtering using a 40 um nylon cell strainer (Sigma-Aldrich). Cells were resuspended at a concentration between $5x10^5$ and $1x10^6$ cells/mL and added to a new monolayer of OP9/DL1 stromal cells. Cells were co-cultured with stromal cells for a total duration of four weeks.

### Transduction of CD34+ Stem Cells

CD34+ stem cells were transduced with lentiviral particles encoding the HLA-A2 restricted PRAME HSS1 TCR (specific against SLLQHLIGL) [18] that were generated previously (**Chapter 8**). CD34+ cells were thawed and resuspended at a concentration of 2.5x10^6 cells/mL in StemMacs medium (Miltenyi Biotec) supplemented with FLT3 ligand (100 ng/ml) (Miltenyi), SCF (100 ng/ml) (Miltenyi) and TPO (20 ng/ml) (Miltenyi). Cells were transduced at an MOI of 10 and incubated overnight under standard culturing conditions, after which remaining lentivirus was washed away and the NK co-culture was initiated as indicated above.

### Cell Phenotyping

Cell differentiation during co-culture was monitored weekly using a flow cytometry panel containing antibodies against CD7 PE (MT701), CD56 PE-Cy7 (NCAM16.2), CD16 BV510 (3G8), CD158b FITC (CH-L) (all BD Biosciences), CD25 PerCP-Cy5.5 (BC96), CD3 AF700 (UCHT1), CD34 BV605 (581) (all Sony Biotechnology), NKp46 BV711 (CD28.2), CD62L BV421 (DREG-56), pan abTCR BV685 (IP26), NKG2D PE/Dazzle495 (1D11) (all Biolegend), CD5 (L17F12) APC, and Fixable Viability Dye eFluor780 (both Life Technologies).

After 4 weeks of co-culture, cells were harvested and cultured using several culture protocols (see below) and checked regularly for maturity using a flow cytometry panel containing antibodies against CD56 PE/Cy7, NKG2D PE/Dazzle495, CD3 AF700, CD62L BV421, NKp46 BV711, KIR2D PE (NKVFS1) (Miltenyi Biotech), CD8 PerCP-Cy5.5 (RPA-T8), CD4 APC (RPA-T4) (Both Biolegend), CD16 BV510 (eBiosciences) and Fixable Viability Dye eFluor780.

Transduction efficiency was determined one week post-transduction. As these progenitors do not express CD3 yet, this was done by intracellular staining using the Fixation/Permeabilization Solution of BD according manufacturer's instructions (BD Biosciences). Cells were stained extracellularly with antibodies against CD5 APC, CD16 BV510, CD34 BV605, CD7 PE, CD56 PE-Cy7, and Fixable Viability Dye eFluor780, fixed and permeabilized, after which they were stained intracellularly for CD3 AF700 and the Vβ1 chain present in the PRAME HSS1 TCR (REA662) (Miltenyi Biotec).

Flow cytometry analysis for all indicated panels was performed on a BD LSRFortessa, data were analyzed using FACSDiva V8.0.1 and FlowJo V10.7.1 (all BD Biosciences). Data from these panels are depicted as raw flow cytometry plots, % of cells, fold changes, or mean fluorescent intensity (MFI).

### CD34+ Stem Cell Derived NK Maturation Protocols

After four weeks of co-culture, cells were harvested from the stromal cell layer and split to test the effect of different culture protocols on NK-cell phenotype/maturation. Cells were resuspended at $5x10^5$ cells/mL in Glutamax supplemented RPMI with 10% human serum and 1% p/s (huRPMI). Cells were cultured in the presence of IL-15 only (20 ng/ml), or IL-15 combined with either IL-2 (50 U/mL), a short pulse of IL-21 (20 ng/mL) on day 7), IL-12 (5 ng/mL), IL-12 and IL-18 (2 ng/mL), or irradiated feeders (50 Gy, feeder:NK ratio of 2:1) (IBL437) for ten days. Cytokines and media was replenished and cell density was adjusted biweekly. Cells were immunophenotyped after 10 days with the flow cytometric panel described above.

Transduced cells were taken off the stromal cell layer after four weeks and cultured for 10 days with either IL-15 only (20 ng/mL), or with a rapid expansion protocol (REP) adopted in our lab for T-cell expansion [19]. This REP protocol consists of co-culture of the transduced cells with irradiated LCL-TM (80 Gy) and donor-pooled PBMCs (35 Gy) in huRPMI, together with PHA-L (1 µg/mL (Oxoid BV), IL-15 (20 ng/mL) (Miltenyi Biotec), and IL-2 (50 U/mL) (Novartis).

### Functional Assays

Cytotoxic capacity of CC NK-cells was assessed using a flow-based cytotoxicity assay. NK-cells were either pre-stimulated overnight with 1000 U/mL IL-2 and 50 ng/mL IL-15 or left unstimulated. Indicated target cells were labeled with Cell-Tracer Violet (CTV) (Life Technologies) according to manufacturer's instructions. Cells were co-cultured at indicated effector to target ratios (E:T) for indicated durations (5h or overnight). Cells were spun down, supernatants were harvested for cytokine determination, and 7-AAD (BD Biosciences) was added to evaluate cytotoxicity. Supernatants were analyzed to determine secretion of cytokines and other molecules of cells by Legendplex (Biolegend) according to manufacturer's instructions.

The protocol above was modified to determine the antigen-specific cytotoxic capacity of PRAME HSS1 TCR transduced NK-cells. Transduced CC NK-cells were cultured overnight with the antigen-presenting T2 model cell line, which was pre-incubated for 1h with 1 µg/mL of SLLQHLIGL peptide (Think Peptides).

Healthy-donor PB NK-cells served as controls. Previously generated PRAME HSS1 TCR transduced CD8+ T-cells (**Chapter 8**) served as controls in the antigen-specific T2 cytotoxicity assay. Samples were measured on a BD FACSCanto, analyzed using FACSDiva V8.0.1 and FlowJo V10.7.1, and visualized using Graphpad Prism 8.3. Data are presented as mean ± standard deviation (SD).

### Transcriptome Analysis

Cryopreserved CC NK-cells were thawed and stained for CD7 PE, CD5 APC, CD56 PE-Cy7, CD3 BV510 (OKT3) (Biolegend). CD7+CD5-CD3-CD56bright cells were sorted using a BD FACSAria (BD Biosciences). To generate controls, two buffy coats were ordered from Sanquin and PBMCs were isolated using Ficoll-Paque PLUS separation. CD45+ cells were isolated using magnetic bead separation according manufacturer's instructions (Miltenyi Biotec). Cells were stained for CD45 PE/Cy7 (HI30) (BD Biosciences), CD3 BV510, CD56 FITC (NCAM16.2) (BD Biosciences), and CD16 APC (CB16). CD45+CD3+CD56- T-cells and CD45+CD3-CD56+CD16+ NK-cells were sorted using a BD FACSAria (BD Biosciences). RNA was extracted using the RNeasy mini kit (QIAGEN) following the manufacturer's instructions. Sequencing libraries were generated using a modified CELseq2 protocol [20] with a sequence depth of 10 million. Sequencing and analysis was performed by Single Cell Discoveries (Utrecht, the Netherlands). Data are visualized using Graphpad Prism 8.3.

## RESULTS

### CD34+ stem cells differentiate into cells with an NK-like phenotype upon OP9/DL1 co-culture

We adjusted a previously established OP9/DL1 – CD34+ cell co-culture to generate mature T-cells [12]. De Smedt and colleagues reported that addition of IL-15 to the co-culture skewed the differentiation of stem cells towards tNK-cells development [16]. Indeed, longitudinal phenotyping revealed a decrease in CD34+ cells over time, which coincides with an increase in CD5-CD7+CD56+ cells (**Figure 1A**). We observed that NK-cells develop exclusively from the CD5-CD7+ cell fraction (**Figure 1B**), unlike T-cells, known to develop from CD5+CD7+ cells [21,22]. The CD56+ cell fraction gained expression of NK-cell markers NKp46, NKG2D, and CD16 along the course of the co-culture (**Figure 1C**). After four weeks of co-culture, NKG2D and NKp46 was present on the majority of CD56+ cells (92.2% and 75.6% respectively), whereas CD16 expression was detected on 24.3% of the cells. Of note, in the example of Figure 1B, 52.3% of the generated cells have committed to the CD5+CD7+ T lymphoid lineage, and 51% of the CD5-CD7+ fraction expressed CD56 and other NK-related factors, indicating that about 20% (ranging between 9.0 and 27.1%) of all generated cells represent the NK-like fraction of interest.

After 4 weeks of co-culture, cells were harvested from the OP9/DL1 layer and cultured in the presence of IL-15 for a week to allow further maturation. The fraction of CD56+ cells increased in this week from 18.6% to 90.3% (**Figure 1D**), which is thought to be a result of death by neglect of T-cell progenitors. Comparison of the transcriptome of sorted co-culture-derived CD56+ cells with PB NK- and T-cells from two healthy donors confirmed the generation of cells with an NK-like phenotype (**Figure S1**).

Unlike PB NK-cells, CC NK-cells were CD56bright, corresponding to an immature, cytokine-releasing NK-cell phenotype (**Figure 2B**). Interestingly, cell surface expression of the activating NK-cell receptors NKp46 and NKG2D was similar between PB NK and CC

NK-cells (**Figure 2C**), which corresponds to a cytotoxic NK-cell phenotype. Transcriptome analysis confirmed the CD56brightCD16- phenotype of CC NK-cells (**Figure 2D**). Analysis of additional markers reported to be correlated with cytotoxic CD56dimCD16+ and cytokine-releasing CD56brightCD16- cells further pointed towards a shared phenotype between the two in CC NK-cells. Some cytotoxic markers (e.g. Granzyme-H, -B, -M, CD69, CX3CR1) were expressed to a lower extent, whereas others were expressed similarly or higher (e.g. Granzyme –A,-K, Perforin, IL2Ra). High expression of CD56, KIT and IL2RB in turn pointed towards a cytokine-releasing phenotype, however, low expression of IL7R, CCR7, and L-selectin argues against that. [23,24]

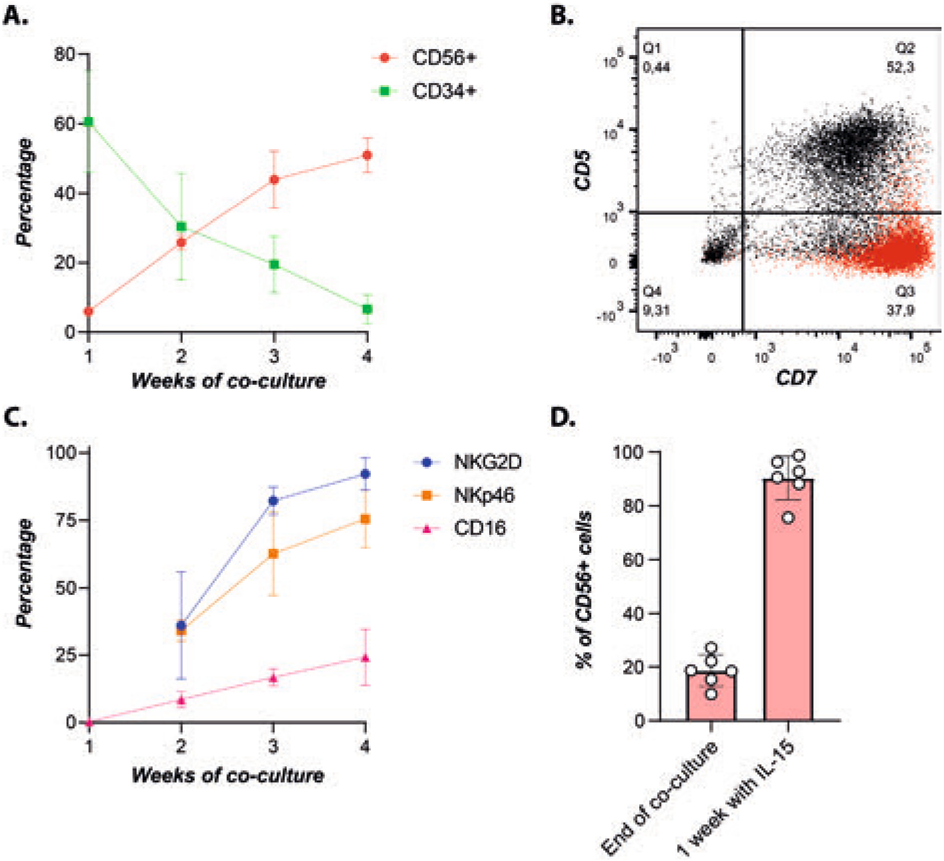

**Figure 1.** Differentiation of CD34+ stem cells into cells with an NK-like phenotype during OP9/DL1 co-culture. ***(A)*** *CD34 (green) and CD56 (red) expression over time during OP9/DL1 CD34+ stem cell co-culture. CD34 expression is determined in the total, alive population. CD56 expression reflects the % of CD34-CD5-CD7+ cells expressing CD56. Every time point reflects at least 4 donors.* ***(B)*** *CD5 and CD7 expression in CD34- cells after 4 weeks of co-culture. Red population reflects the CD56+ cell population.* ***(C)*** *Expression of NKG2D (blue), NKp46 (orange), and CD16 (pink) in CD34-CD5-CD7+CD56+ cell fraction over time during OP9/DL1 co-culture. Data are shown from at least 3 donors.* ***(D)*** *% of CD56 expressing cells at the end of OP9/DL1 co-culture (left) and after 1 week of culture in huRPMI supplemented with 20 ng/mL IL-15. Data reflect 6 donors. (A+C+D) Data are shown as mean ± SD.*

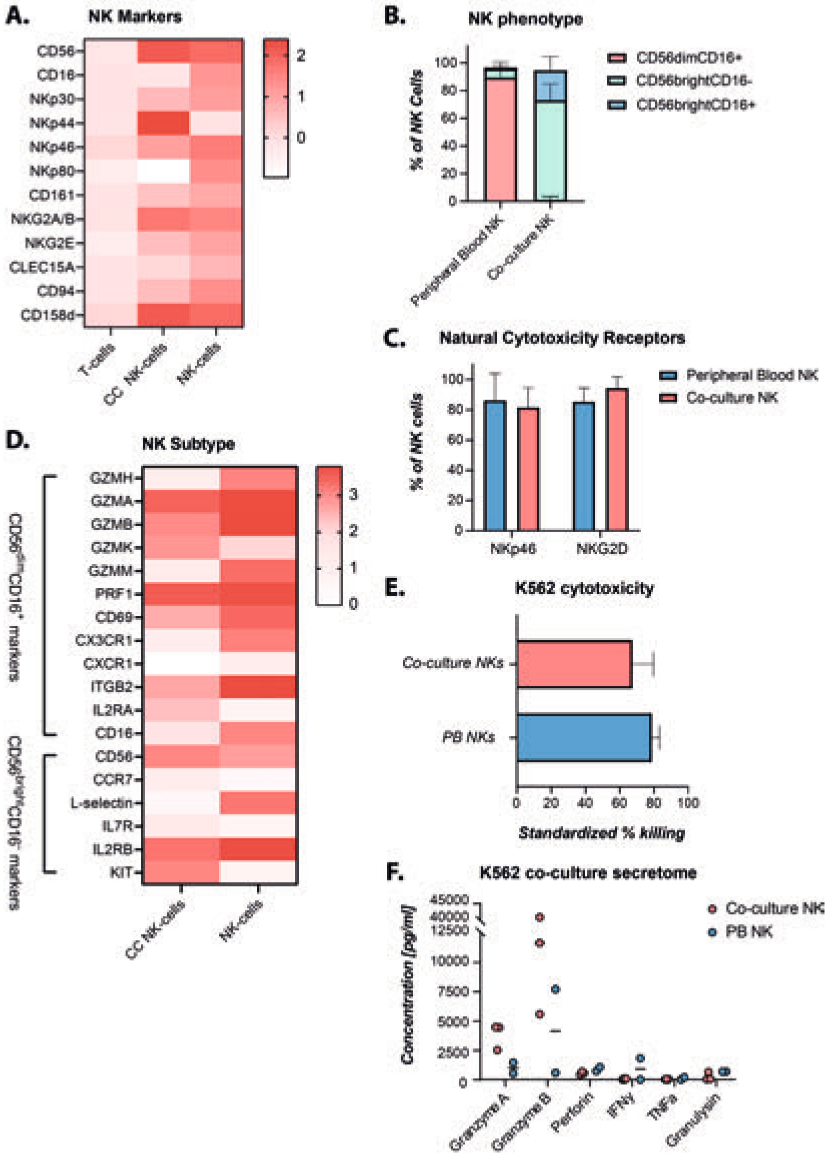

**Figure 2.** Co-culture derived NK-cells are CD56$^{bright}$, but show a high cytotoxic capacity.
*(A) Comparing RNAseq expression data of CC NK-cells to healthy-donor PB T- and NK-cells. Technical duplicates are averaged, expression of CC NK-cells from one donor is shown, average expression of T- and NK-cells from two healthy-donors is shown. Expression levels are depicted relative to T-cells (log2(fold-change)). **(B)** NK-cell phenotype of CC and PB NK-cells based on CD56 and CD16 expression. PB NK: n=8, CC NK: n=4. **(C)** Expression of NKG2D and NKp46 in CC and PB NK-cells. PB+CC NK: n=3. **(D)** Comparing RNAseq expression data of NK-cell subset markers of CC NK-cells to healthy-donor PB NK-cells. Technical duplicates are averaged, expression of CC NK-cells from one donor is shown, average expression of NK-cells from two healthy-donors is shown. Expression is depicted as log2(normalized counts). **(E)** % of standardized killing after 5h of co-culture of NK-cells with K562 cells (E:T = 10:1) to assess the cytotoxic capacity of NK-cells. PB+CC NK: n=2. **(F)** Cytokine production and expression of other molecules by PB or CC NK-cells upon overnight co-culture with K562 target cells (E:T = 10:1), n=3. (E+F) Cells were pre-stimulated overnight with 1000 U/mL IL-2 and 50 ng/mL IL-15. Data shown as mean ± SD*

To determine whether these phenotypic features correlate to the cytotoxic- and cytokine-releasing capacity of cells, NK-cells were co-cultured with the NK sensitive K562 cell line. In contrast to the CD56bright phenotype, but in line with the other phenotypical features, we observed that CC NK-cells targeted K562 to the same extent as PB NK-cells (**Figure 2E**). Analysis of supernatants of these co-culture assays revealed low cytokine releasing capacity (TNFα and IFNγ), but superior levels of granzymes (GZM) A+B (3.8 and 4.7x higher, respectively) of CC NK-cells when compared to PB NK-cells (**Figure 2F**). These data indicate the potent cytotoxic capacity of generated CC NK-cells.

### Co-culture derived NK-cells elicit a potent anti-neuroblastoma reponse

To investigate their capacity to recognize and target NBL cells, NK-cells were either left unstimulated or pre-stimulated overnight with IL-2 and IL-15, after which they were co-cultured for 5 hours (**Figure 3A**) or overnight (only unstimulated) (**Figure 3B**) with the GIMEN and IMR32 NBL cell lines. Short- and long-term cytotoxic efficacy of GIMEN and IMR32 similar between PB and CC NK-cells. In line with the K562 cytotoxicity assay, secretome analysis after overnight co-culture with GIMEN revealed a low cytokine releasing capacity (TNFα and IFNγ) and superior levels of GZM A+B (6.6 and 3.1-fold higher, respectively) of CC NK-cells compared to PB NK-cells (**Figure 3C**). A trend to lower levels of secreted granulysin and perforin was observed in CC NK- compared to PB NK-cell co-cultures.

### Skewing co-culture NK phenotype and functionality by different cytokine combinations

To investigate whether phenotype, cytokine secretion capacity, and/or cytotoxicity can be affected by the culture protocol after co-culture, we studied the effect of different cytokine combinations on CC NK phenotype and function upon removal from the co-culture. These cytokines were selected based on their described effects in NK-cell maturation [25].

A week of culture with the different cytokine combinations did not result in major differences in NK phenotype, based on CD56 and CD16 expression (**Figure 4A**). An overall increase in CD56dim cells was observed compared to the cells that were taken from the stromal cell layer, however, the majority of the cells remain CD56bright and CD16- in all conditions. We next performed a preliminary experiment, with CC NK-cells from one donor, in which we determined the cytotoxicity of cells cultured with different cytokine combinations towards the GIMEN NBL cell line. We observed similar cytotoxic capacity in all but the IL-15 + IL-12 + IL-18 conditions (**Figure 4B**). Supernatant analysis did not reveal any clear differences in secreted cytolytic factors (**Figure S2**). Strikingly, we did observe a major increase in secreted cytokines (mostly IFNγ, but also TNFα) in the IL-15 + IL-12 + IL-18 culture condition (respectively 13.1 and 2.3-fold higher than IL-15 cultured cells), and to a lesser extent also in the IL-15 + IL-12 condition (4.8 and 1.4-fold increase compared to IL-15 cultured cells) (**Figure 4C**). MHC-I expression on the live cell fraction after overnight co-culture was increased in all co-cultures, but this increase was most prominent in both conditions in which cytokine secretion was enhanced (16.3-fold increase in IL-15 + IL-12 + IL18 condition, 7.5-fold increase in IL-12 + IL-18) (**Figure 4D**). These results have to be validated before hard conclusions can be drawn, but do stress the importance to consider which cytokines are used to expand and culture cells based on downstream applications.

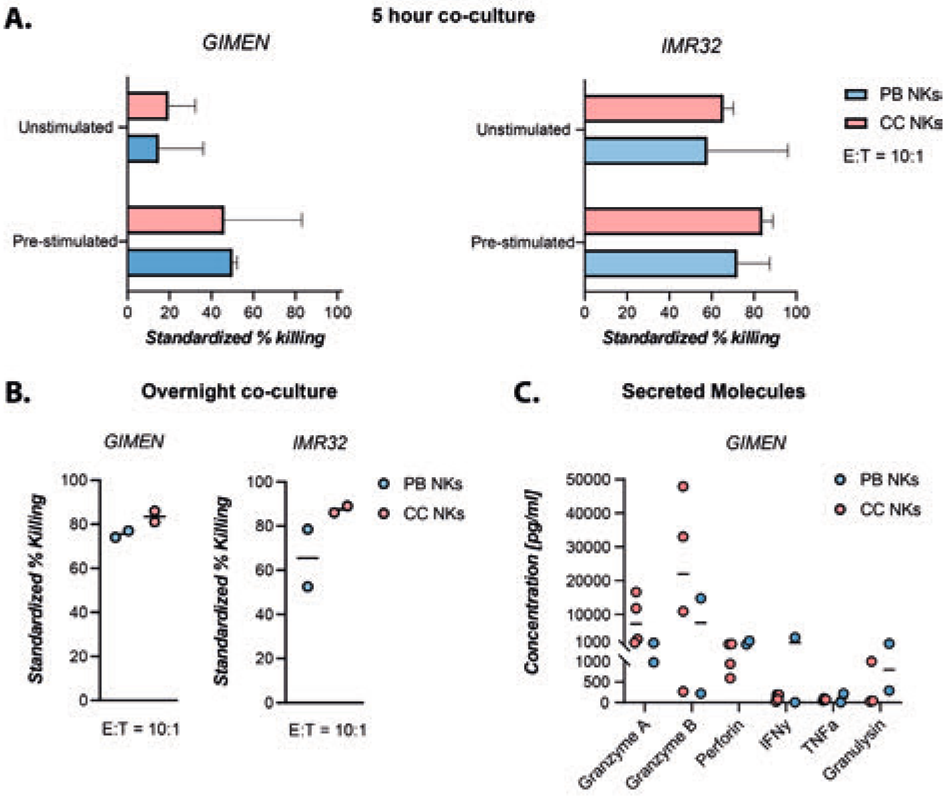

**Figure 3.** Co-culture derived NK-cells elicit cytotoxicity towards NBL cell lines.
*5 hour* ***(A)*** *or overnight* ***(B)*** *cytotoxicity assay with GIMEN (left) or IMR32 (right) NBL cells at an E:T of 10:1. NK-cells were either pre-stimulated with 1000 U/mL IL-2 + 50 µg/mL IL-15 or left unstimulated in the 5h assay (A), NK-cells were left unstimulated in the overnight assay (B), 5h PB NK & CC NK IMR32: n=2, CC NK GIMEN: n=3, 24h: n=2.* ***(C)*** *Cytokine production and expression of other molecules by pre-stimulated PB or CC NK-cells upon overnight co-culture with GIMEN target cells (E:T = 10:1), CC NK: n=4, PB NK: n=2. Data are shown as mean ± SD.*

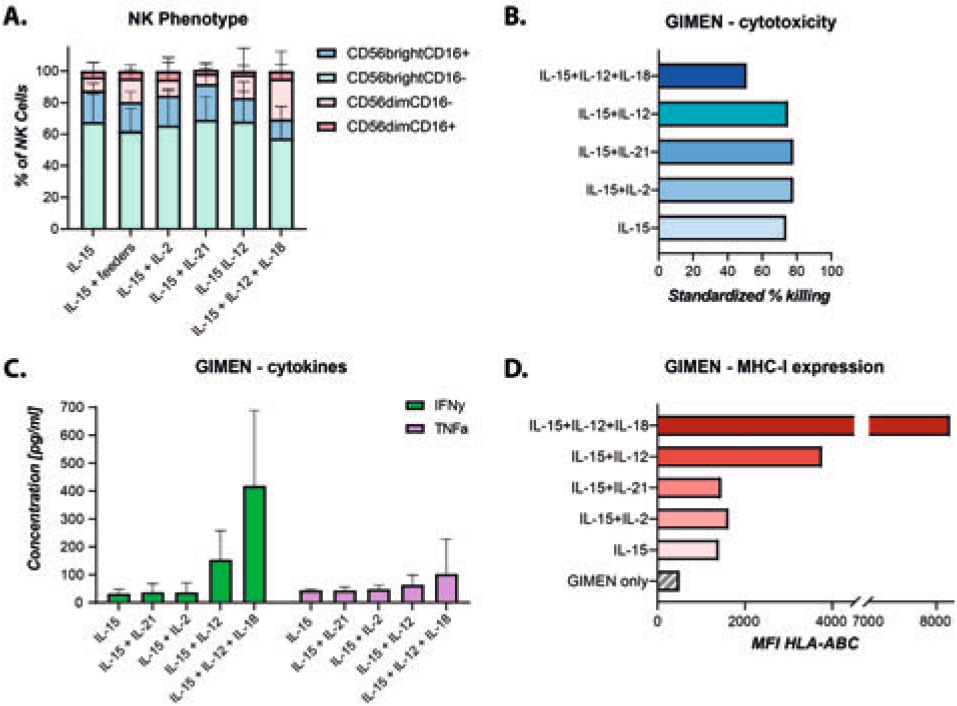

**Figure 4.** Phenotype and functionality after NK-cell culture with NK maturation-associated cytokine combinations.

*(A) NK-cell phenotype of CC NK-cells cultured with different cytokine combinations based on CD56 and CD16 expression. n=4 per group (IL-15+feeders: n=3). (B-D) Overnight co-culture of CC NK-cells with the GIMEN NBL line cultured with different cytokine combinations. Cytotoxicity (E:T 5:1) (n=1 per group) (B), cytokine secretion (E:T 10:1) (n=3 per group) (C), and MHC-I expression (E:T 5:1) (n=1 per group) after co-culture on live target cells (D) are shown. MHC-I expression is based on panHLA-ABC staining and shown as mean fluorescent intensity (MFI). Data are shown as mean (± SD).*

## TCR introduction in CD34+ stem cells results in the generation of antigen-specific NK-cells

A unique feature of these CC NK-cells is their Notch-signaling induced cyCD3e expression, without the presence of a fully rearranged TCR [16] (**Figure 5A**). This provides the opportunity to introduce a recombinant TCR in these NK-cells, without the need to co-introduce CD3 subunits to allow for surface translocation. In the final part of this project, we sought to exploit cyCD3e expression of these CC NK-cells to generate TCR expressing NK-cells. This way, we aim to generate a cell type that can both engage in NK receptor mediated cytotoxicity as well as in antigen-specific cytotoxicity to maximize the anti-NBL effect of the cell product.

CD34+ stem cells were transduced overnight with a lentiviral vector expressing the PRAME$_{SLLQHLIGL}$-specific HSS1 TCR, after which cells were co-cultured using the established OP9/DL1 protocol to generate CC NK-cells. After 1 week of co-culture, we observed HSS1 TCR expression in 40.4% of the culture (**Figure 5B**, left). In mature CC NK-cells, we observed that all HSS1 TCR+ cells show coinciding CD3 surface expression, indicating that the CD3-TCR complex is translocated to the cell surface (**Figure 5B**, right).

TCR+ CC NK-cells were subsequently co-cultured with K562 cells and peptide-pulsed antigen presenting T2 cells to determine NK-specific and antigen-specific cytotoxic capacity. Targeting of MHC-negative K562 cells revealed undisturbed NK receptor mediated cytotoxicity upon TCR introduction (**Figure 5C**). Furthermore, co-culture with peptide-pulsed T2 cells revealed efficient antigen-specific targeting, similar to HSS1 expressing T-cells, whereas unpulsed T2 cells were left undisturbed (**Figure 5D**).

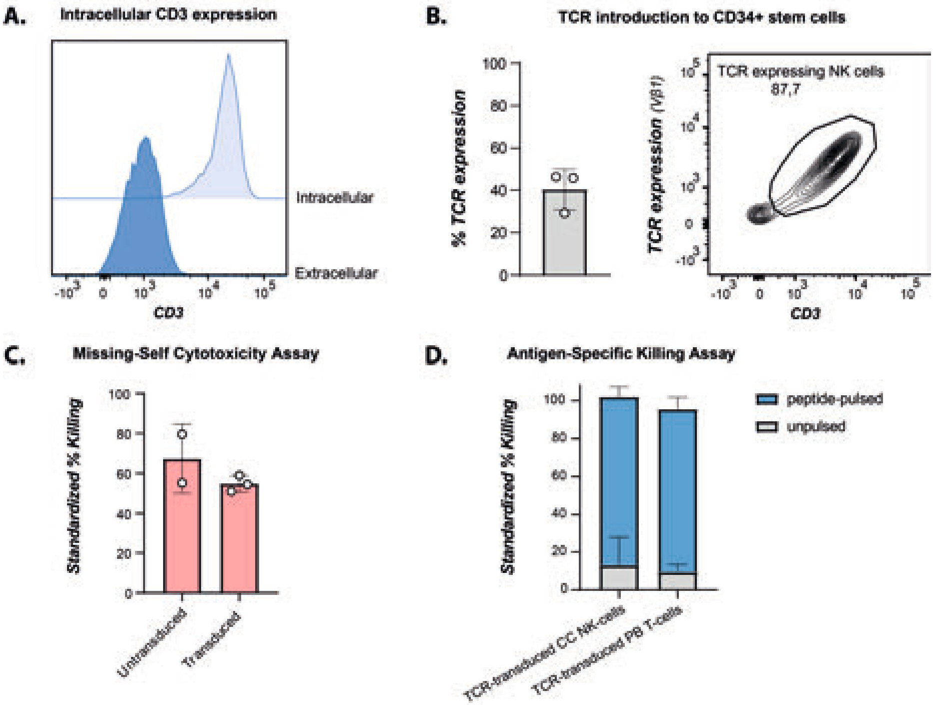

**Figure 5.** Transduction efficiency and functionality of TCR transduced CC NK-cells.
*(**A**) Evaluation of extra- and intracellular CD3 expression. (**B**) Left: Evaluation of intracellular Vβ1 expression after 1 week of co-culture to evaluate transduction efficiency, n=3. Right: Evaluation of HSS1 TCR and CD3 surface expression in mature CC NK-cells. (**C**) % of standardized killing after 5h of co-culture of CC NK-cells with K562 cells (E:T = 10:1) in TCR- and TCR+ NK-cells. NK-cells were pre-stimulated with 1000 U/mL IL-2 and 50 ng/mL IL-15 overnight before co-culture with K562 cells. TCR-: n=2. TCR+: n=3. (**D**) % of standardized killing after overnight co-culture of TCR+ CC NK-cells with unpulsed or PRAME HSS1 SLLQHLIGL peptide-pulsed T2 cells (E:T = 10:1). The cytotoxic capacity was compared to HSS1 TCR+ CD8+ T-cells, n=3. Data are shown as mean ± SD.*

## Pure, mature TCR+ co-culture NK-cells population generation, despite initial disturbances of culture dynamics upon TCR introduction

As we hypothesized that TCR introduction in the stem cell phase might skew towards commitment to the T lymphoid lineage, the effect of TCR introduction to CD34+ stem cells on the co-culture dynamics was studied in more detail. Even though no obvious differences were observed in the percentage of CD5-CD7+ cells, from which CC NK-cells arise, we did observe an increase in T lymphoid lineage commitment, as the abundance of CD5+CD7+ cells increased (**Figure 6A**). Delay of the time point of TCR introduction did increase the percentage of CD56+ cells expressing a TCR, with a maximal transduction efficacy of 83.5% when transduction was delayed to day 14 of co-culture (**Figure S3A**). However, we observed an even more dramatic increase in cells committing to the T lymphoid lineage (CD5+CD7+), coinciding with decreased abundance of CD5-CD7+ cells (**Figure S3B**). Consequently, we conclude that delaying TCR introduction does not result in restoration of culture dynamics and will not aid in maximizing the yield of TCR+ CC NK-cells.

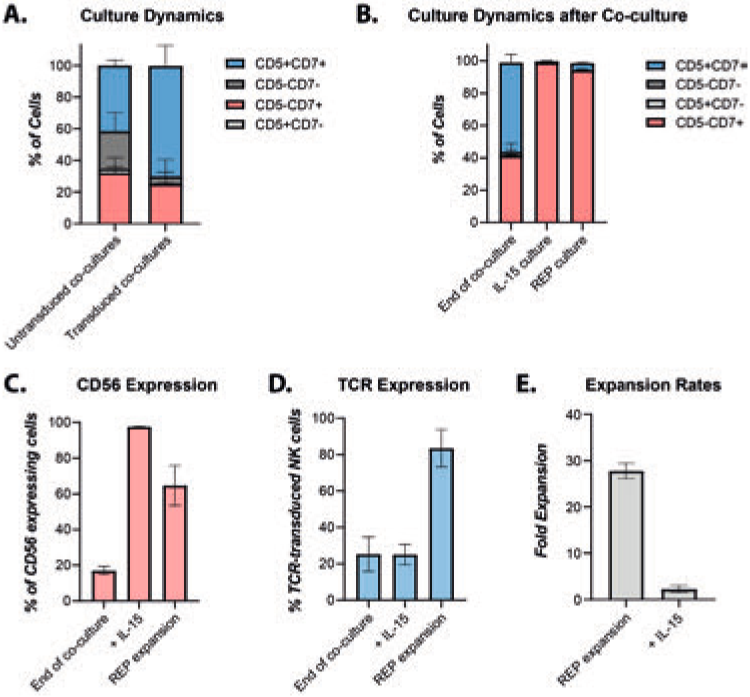

**Figure 6.** Culture dynamics after TCR introduction in co-culture NK-cells.
***(A)*** *Culture dynamics in TCR- and TCR+ NK co-cultures based on CD5 and CD7 expression at the end of OP9/DL1 co-culture, TCR-: n=3, TCR+: n=5.* ***(B-D)*** *TCR+ culture dynamics based on CD5 and CD7 expression (**B**), expression of CD56 **(C)**, and percentage of TCR+ NK-cells **(D)** at the end of co-culture or after 10 days of culture with either 20 ng/mL of IL-15 or according to a REP protocol developed for T-cells (with pooled irradiated feeders, 1 µg/mL PHA, 50 U/mL IL-2, and 5 ng/mL IL-15). n=2 per group.* ***(E)*** *Fold expansion between day 1 and day 10 of culture with the respective culture strategies, n=2 per group. Data are shown as mean ± SD.*

At the end of the co-culture stage, the majority of transduced cells (69.8%) were CD5+CD7+. Cells were subsequently cultured for 10 days with either IL-15 or on a REP culture protocol developed for T-cell expansion (irradiated feeder cells, PHA-L, IL-2, and IL-15). Interestingly, the CD5+CD7+ population almost completely disappeared from the culture (**Figure 6B**). Furthermore, a simultaneous increase of CD56+ cells in the culture was shown, indicating that NK-cells overtook the culture (**Figure 6C**). When comparing the percentage of TCR+ NK-cells between IL-15 and REP culture conditions, we observed a marked expansion benefit of TCR+ NK-cells during REP expansion but not during culture with IL-15 (**Figure 6D**). This increase coincided with massive expansion rates during REP culture (**Figure 6E**). These results indicate that T-cell progenitors die when taken off the co-culture layer, whereas NK-cells remain viable. In addition, the REP culture protocol seems to specifically activate and expand TCR+ NK-cells, which is underlined by the observation that untransduced CC NK-cells did not expand during REP culture (data not shown). Altogether, these data show that, despite initial disturbance of the co-culture dynamics upon TCR introduction, we are able to generate high numbers and good purity of TCR+ CC NK-cells.

## Superior cytotoxic capacity in TCR+ co-culture NK-cells

As TCR+ CC NK-cells are able to elicit both NK-cell mediated as well as antigen-mediated cytotoxicity, we co-cultured donor-matched TCR- and TCR+ CC NK-cells overnight with three HLA-A2+PRAME+ cell lines (GIMEN, CHP212, NLF) to study the effect of TCR introduction on the cytotoxic capacity against NBL cells. The extent of targeting of cell lines by TCR- CC NK-cells varied; cytotoxic capacity against GIMEN was 11.5%, CHP212 36.5%, and NLF 52.2% (**Figure 7**). In all cell lines, a clear increase was observed in overnight cytotoxicity of TCR$^{+}$ CC NK-cells, ranging from 27% in NLF, 27.8% in GIMEN, to 29.5% in CHP212. These results have to be validated with additional donors, but show the potential to combine NK- and T-cell mediated cytotoxicity to enhance targeting of NBL cells.

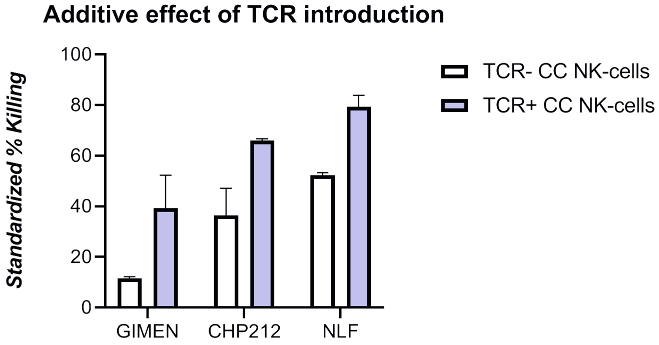

**Figure 7.** Effect of TCR introduction in CC NK-cells on cytotoxic capacity of cells.
*% of standardized killing after overnight co-culture of TCR- and PRAME HSS1 TCR+ CC NK-cells with HLA-A2+PRAME+ GIMEN, CHP212, and NLF. Cells were not pre-stimulated and co-cultured overnight at an E:T of 1:1. Data reflect duplos from two donors. Data are shown as mean ± SD.*

## DISCUSSION

NK-cells have been shown to be a particularly important immune subset in anti-NBL immune responses, as they can recognize NBL cells via missing-self cytotoxicity, expression of other NK-receptor ligands, and are important mediators during dinutuximab-based immunotherapy. Nonetheless, the cytotoxic NK-cell ratio is shown to be majorly decreased at NBL diagnosis as well as during therapy, indicating the need to boost NK-cell cytotoxicity to maximize their NBL-specific cytotoxic capacity. We here report effective ex vivo generation of tNK-cells from CB-derived CD34+ stem cells. TCR-introduction in the CD34+ stem cells results in the generation of functional TCR+ tNK-cells that can engage in NBL cytotoxicity via NK ligand cytotoxicity as well as via TCR antigen-specific cytotoxicity.

Phenotypic and functional analysis of the generated CC NK-cells did show a discrepancy between NK phenotype and functionality. CC NK-cells were CD56brightCD16dim/-, which corresponds to an immature, cytokine-releasing phenotype. In contrast to this, functional assays and supernatant analysis revealed a cytotoxic capacity similar to PB NK-cells, pointing towards a mature, cytotoxic NK-cell phenotype. This was underlined by transcriptome analysis, in which we observed mixed expression of markers ascribed to the two NK-cell subsets. As tissue-resident NK-cells have been described to differ in phenotype from peripheral NK-cells, we studied literature to learn more about tNK-cells. Even though literature in human is scarce, tNK-cells are indeed suggested to be part of the CD56brightCD16dim/- NK-cell fraction [26,27]. Their function is largely unknown, but they are suggested to be important in circumventing uncontrolled proliferation of thymocytes and regulation of T-cell selection, which explains their cytolytic potential. Besides that, tNK-cells in mice are actively transported from the thymus to the periphery, suggesting roles intrathymically as well as in the periphery [26]. The combined cytokine-releasing and cytotoxic capacity of these CC NK-cells makes them an interesting candidate as a cell source for cell therapy strategies in NBL.

NK-cells are not only important in endogenous tumor cell lysis, but are also important effector cells during dinutuximab-based immunotherapy [28]. GD2-bound dinutuximab can be recognized by NK-cells via binding to CD16, resulting in antibody-mediated cytotoxicity (ADCC). As expression of CD16 in CC NK-cells is low, these NK-cells may not be the best candidate to directly boost dinutuximab efficacy. Nonetheless, the capacity of CC NK-cells to engage in ADCC should be functionally examined *in vitro* before hard conclusions can be drawn. When aiming to maximize dinutuximab-mediated cytotoxicity, one could decide to co-culture CD34+ stem cells with OP9 cells that do not express Notch ligand instead, as this has been shown to cause generation of conventional NK-cells [16].

We hypothesize, however, that the high degree of plasticity in MHC-I surface display in NBL is an important mechanism by which NBL tumors bypass targeting by both cytotoxic T- and NK-cells. Combining NK receptor-mediated cytotoxicity with recognition of malignant transformation in MHC-I context in one engineered cell product may result in a cell type that can no longer be evaded by MHC-I plasticity. We here show that TCR introduction in CC NK-cells is feasible and results in cell surface expression and functionality of the TCR. Even though currently only studied in two donors, we show a clear enhanced cytotoxic capacity of PRAME HSS1 TCR$^+$ CC NK-cells to three NBL cell lines. These data indicate the feasibility and potential to use TCR$^+$ CC NK-cells to overcome MHC-I plasticity-mediated immune escape by NBL.

We show that culture of CC NK-cells with different cytokine combinations may affect its functionality. Even though results are preliminary, we observe that the combination of IL-15, IL-12, and IL-18, and to a lesser extent also IL-15 and IL-12, results in a major increase in cytokine-releasing capacity of NK-cells, which goes hand-in-hand with an increase in MHC-I expression of GIMEN target cells. This stresses the importance to consider different NK-cell culture protocols based on downstream applications. Interestingly, we observe that "standard" culturing with IL-15, and the relatively modest release of IFNγ and TNFα and MHC-I expression accompanied with this, is sufficient to induce superior cytotoxicity of TCR+ CC NK-cells.

The main limitation of this protocol is that currently, after four weeks of OP9/DL1 co-culture, only 20% of the generated cells are NK-cells, which is in line with previous findings of de Smedt and colleagues [16]. In TCR-transduced cultures, this yield is even lower. The majority of cells is CD7+CD5+, which corresponds to a T-cell progenitor phenotype [29]. The generated mixed phenotype is not surprising, as T- and tNK-cells are thought to have a common thymic progenitor [30–32]. An interesting clue to increase culture efficacy might be the difference in Notch-dependency between T-cells and tNK-cells [16,33]. While T-cells require high levels of Notch signaling during the whole developmental phase [33], four days of Notch-signaling was sufficient to generate cyCD3+ NK-cells [16]. In follow-up experiments, we will culture CD34+ stem cells with OP9/DL1 for a short period, after which we will switch to wildtype OP9 to investigate whether this may increase culture efficacy.

A striking observation was that the impure population of cells after OP9/DL1 co-culture turned into a pure NK-cell population after a week of culture in absence of OP9/DL1 cells.

We hypothesize that the T-cell progenitors either do not have a fully rearranged TCR yet, or if they do, they died by neglect due to lack of positive selection. This hypothesis is underlined by two studies in which T-cells are generated in the OP9/DL1 system that show the need for agonistic peptide stimulation at the end of co-culture to generate mature T-cells [12,21]. In addition, culture of transduced cells using a T-cell specific REP-protocol induced selection of TCR+ CC NK-cells. This indicates that, while most T-cell progenitors still died due to lack of positive selection, TCR- CC NK-cells are not activated by the PHA- and feeder based rapid expansion protocol, while TCR+ CC NK-cells are. These findings are remarkable, as Luhm *et al*. show massive expansion when using a similar PHA- and irradiated PBMC feeder based protocol [34]. Nonetheless, PHA-concentration in their protocol was 100-fold higher than in our culture protocol, which may explain this discrepancy. One hypothesis is that TCR-mediated signaling due to HLA-mismatch against the donor-pooled PBMC fraction may result in overgrowing of the TCR+ NK-cell population. Despite the fact that we are already able to generate a pure TCR+/- CC NK-cell population, optimization of the OP9 co-culture protocol is required to decrease the degree of expansion of mature NK-cells required to generate sufficient cell numbers for a potential cell therapy product.

We here show one strategy in which NK receptor-mediated cytotoxicity is combined with MHC-I restricted targeting of tumor cells. Other strategies might involve TCR introduction in NKT-like cells, NK receptor expressing γδ T-cell fraction, or conventional NK-cells. A clear disadvantage of all three strategies over the use of CC NK-cells is that these cells have to be expanded in mature states to reach sufficient numbers for cell therapy product generation, which may decrease *in vivo* persistence. In addition, the absence of an endogenous TCR in the CC NK-cells avoids the risk of mispairing of recombinant and endogenous TCR chains. The use of conventional NK-cells requires additional co-transduction with CD3 subunits [35–37], which decreases efficacy and increases complexity of engineering. An advantage of T-cell based strategies is their ability to create immunological memory to prevent future relapse. Notwithstanding, it is now recognized that NK-cells are also able to generate a memory-like phenotype [38,39]. Studies into *in vivo* persistence of these CC NK-cells are required to appreciate their potential.

In follow-up experiments, we aim to determine whether this protocol can be applied to generate CC NK-cells from CD34+ cells from apheresis material of HR-NBL patients. This is important, as HR-NBL often disseminates to the bone marrow [40,41], which may affect fitness of NBL patient-derived CD34+ stem cells. In addition, future work will involve mouse studies to test *in vivo* efficacy of the generated CC NK-cells, for example using the immunocompetent humanized MISTRG mouse model [42]. Finally, efforts should be made to change the protocol to meet good manufacturing process (GMP) compliance, as the current protocol utilizes multiple types of non GMP-compliant feeder cells. GMP-compliant engineered K562 are generated and used to expand NK-cells for clinical trials [43]. The OP9/DL1 stromal cells can be replaced by either coating of the culture vessel with Notch ligand [12] or by beads expressing Notch ligand [44]. Lastly, pooled irradiated PBMC feeders for T-cell expansion can potentially be replaced by either aCD3/CD28 antibodies, beads, or other GMP-compliant engineered feeders [45].

Altogether, this study provides foundation for further investigation of the potential to use ex vivo generated cyCD3+ NK-cells from CD34+ stem cells as a cell therapy source to increase therapy efficacy in children with HR-NBL. In addition, in concordance with the engineered NKT-cells in **Chapter 9**, this study further supports our hypothesis that generating a cell product combining NK receptor-mediated cytotoxicity with MHC-I restricted targeting is a promising strategy to overcome MHC-I plasticity-related immune evasion by NBL.

## REFERENCES

1. Howlader N, Noone A, K.M. SEER Cancer Statistics Review, 1975-2016; **2019**
2. Park, J.R.; Bagatell, R.; London, W.B.; Maris, J.M.; Cohn, S.L.; Mattay, K.M.; Hogarty, M. Children's Oncology Group's 2013 Blueprint for Research: Neuroblastoma. Pediatr. Blood Cancer **2013**.
3. Yu, A.L.; Gilman, A.L.; Ozkaynak, M.F.; London, W.B.; Kreissman, S.G.; Chen, H.X.; Smith, M.; Anderson, B.; Villablanca, J.G.; Matthay, K.K.; et al. Anti-GD2 Antibody with GM-CSF, Interleukin-2, and Isotretinoin for Neuroblastoma. N. Engl. J. Med. **2010**, 363, 1324–1334, doi:10.1056/NEJMoa0911123.
4. Ladenstein, R.; Pötschger, U.; Valteau-Couanet, D.; Luksch, R.; Castel, V.; Yaniv, I.; Laureys, G.; Brock, P.; Michon, J.M.; Owens, C.; et al. Interleukin 2 with Anti-GD2 Antibody Ch14.18/CHO (Dinutuximab Beta) in Patients with High-Risk Neuroblastoma (HR-NBL1/SIOPEN): A Multicentre, Randomised, Phase 3 Trial. Lancet Oncol. **2018**, 19, 1617–1629, doi:10.1016/S1470-2045(18)30578-3.
5. Yu, A.L.; Gilman, A.L.; Ozkaynak, M.F.; Naranjo, A.; Diccianni, M.B.; Gan, J.; Hank, J.A.; Batova, A.; London, W.B.; Tenney, S.C.; et al. Long-Term Follow-up of a Phase III Study of Ch14.18 (Dinutuximab) + Cytokine Immunotherapy in Children with High-Risk Neuroblastoma: COG Study ANBL0032. Clin. Cancer Res. **2021**, 18, clincanres.3909.2020, doi:10.1158/1078-0432.ccr-20-3909.
6. Wienke, J.; Dierselhuis, M.P.; Tytgat, G.A.M.; Künkele, A.; Nierkens, S.; Molenaar, J.J. The Immune Landscape of Neuroblastoma: Challenges and Opportunities for Novel Therapeutic Strategies in Pediatric Oncology. Eur. J. Cancer **2021**, 144, 123–150, doi:10.1016/j.ejca.2020.11.014.
7. Spel, L.; Schiepers, A.; Boes, M. NFκB and MHC-1 Interplay in Neuroblastoma and Immunotherapy. Trends in Cancer **2018**, 4, 715–717.
8. Szanto, C.L.; Cornel, A.M.; Tamminga, S.M.; Delemarre, E.M.; de Koning, C.C.H.; van den Beemt, D.A.M.H.; Dunnebach, E.; Tas, M.L.; Dierselhuis, M.P.; Tytgat, L.G.A.M.; et al. Immune Monitoring during Therapy Reveals Activitory and Regulatory Immune Responses in High-Risk Neuroblastoma. Cancers (Basel). **2021**, 13, 1–18, doi:10.3390/cancers13092096.
9. Spel, L.; Boelens, J.J.; Van Der Steen, D.M.; Blokland, N.J.G.; van Noesel, M.M.; Molenaar, J.J.; Heemskerk, M.H.M.; Boes, M.; Nierkens, S. Natural Killer Cells Facilitate PRAME-Specific T-Cell Reactivity against Neuroblastoma. Oncotarget **2015**, 6, 35770–35781, doi:10.18632/oncotarget.5657.
10. Cornel, A.M.; Mimpen, I.L.; Nierkens, S. MHC Class I Downregulation in Cancer: Underlying Mechanisms and Potential Targets for Cancer Immunotherapy. Cancers (Basel). **2020**, 12, 1–33, doi:10.3390/cancers12071760.
11. Sivori, S.; Parolini, S.; Marcenaro, E.; Castriconi, R.; Pende, D.; Millo, R.; Moretta, A. Involvement of Natural Cytotoxicity Receptors in Human Natural Killer Cell-Mediated Lysis of Neuroblastoma and Glioblastoma Cell Lines. J. Neuroimmunol. **2000**, 107, 220–225, doi:10.1016/S0165-5728(00)00221-6.
12. Fernandez, I.; Ooi, T.; Krishnendu, R. Generation of Functional Antigen-Specific CD8 Human T Cells from Cord Blood Stem Cells.Stem Cells **2014**, 32, 93–103, doi:10.1002/stem.1512.
13. La Motte-Mohs, R.N.; Herer, E.; Zúñiga-Pflücker, J.C. Induction of T-Cell Development from Human Cord Blood Hematopoietic Stem Cells by Delta-like 1 in Vitro. Blood **2005**, 105, 1431–1439, doi:10.1182/blood-2004-04-1293.
14. Awong, G.; Herer, E.; La Motte-Mohs, R.N.; Zúñiga-Pflücker, J.C. Human CD8 T Cells Generated in Vitro from Hematopoietic Stem Cells Are Functionally Mature. BMC Immunol. **2011**, 12, doi:10.1186/1471-2172-12-22.

15. Holmes, R.; Zuñiga-Pflücker, J.C. The OP9-DL1 System: Generation of T-Lymphocytes from Embryonic or Hematopoietic Stem Cells in Vitro. Cold Spring Harb. Protoc. **2009**, 4, 1–13, doi:10.1101/pdb.prot5156.
16. De Smedt, M.; Taghon, T.; Van De Walle, I.; De Smet, G.; Leclercq, G.; Plum, J. Notch Signaling Induces Cytoplasmic CD3ε Expression in Human Differentiating NK Cells. Blood **2007**, 110, 2696–2703, doi:10.1182/blood-2007-03-082206.
17. Deftos, M.L.; Bevan, M.J. Notch Signaling in T Cell Development. Curr. Opin. Immunol. **2000**, 12, 166–172, doi:10.1016/j.coi.2008.03.004.
18. Amir, A.L.; Van Der Steen, D.M.; Van Loenen, M.M.; Hagedoorn, R.S.; De Boer, R.; Kester, M.D.G.; De Ru, A.H.; Lugthart, G.J.; Van Kooten, C.; Hiemstra, P.S.; et al. PRAME-Specific Allo-HLA-Restricted T Cells with Potent Antitumor Reactivity Useful for Therapeutic T-Cell Receptor Gene Transfer. Clin. Cancer Res. **2011**, 17, 5615–5625, doi:10.1158/1078-0432.CCR-11-1066.
19. Marcu-Malina, V.; Heijhuurs, S.; Van Buuren, M.; Hartkamp, L.; Strand, S.; Sebestyen, Z.; Scholten, K.; Martens, A.; Kuball, J. Redirecting AβT Cells against Cancer Cells by Transfer of a Broadly Tumor-Reactive ΓδT-Cell Receptor. Blood **2011**, 118, 50–59, doi:10.1182/blood-2010-12-325993.
20. Hashimshony, T.; Senderovich, N.; Avital, G.; Klochendler, A.; de Leeuw, Y.; Anavy, L.; Gennert, D.; Li, S.; Livak, K.J.; Rozenblatt-Rosen, O.; et al. CEL-Seq2: Sensitive Highly-Multiplexed Single-Cell RNA-Seq. Genome Biol. **2016**, 17, 1–7, doi:10.1186/s13059-016-0938-8.
21. Bonte, S.; De Munter, S.; Goetgeluk, G.; Ingels, J.; Pille, M.; Billiet, L.; Taghon, T.; Leclercq, G.; Vandekerckhove, B.; Kerre, T. T-Cells with a Single Tumor Antigen-Specific T-Cell Receptor Can Be Generated in Vitro from Clinically Relevant Stem Cell Sources. Oncoimmunology **2020**, 9, 1–12, doi:10.1080/2162402X.2020.1727078.
22. Snauwaert, S.; Verstichel, G.; Bonte, S.; Goetgeluk, G.; Vanhee, S.; Van Caeneghem, Y.; De Mulder, K.; Heirman, C.; Stauss, H.; Heemskerk, M.H.M.; et al. In Vitro Generation of Mature, Naive Antigen-Specific CD8 + T Cells with a Single T-Cell Receptor by Agonist Selection. Leukemia **2014**, 28, 830–841, doi: 10.1038/leu.2013.285.
23. Cooper, M.A.; Fehniger, T.A.; Caligiuri, M.A. The Biology of Human Natural Killer-Cell Subsets. Trends Immunol. **2001**, 22, 633–640, doi:10.1016/S1471-4906(01)02060-9.
24. Montaldo, E.; Del Zotto, G.; Della Chiesa, M.; Mingari, M.C.; Moretta, A.; Maria, A. De; Moretta, L. Human NK Cell Receptors/Markers: A Tool to Analyze NK Cell Development, Subsets and Function. Cytom. Part A **2013**, 83, 702–713, doi:10.1002/cyto.a.22302.
25. Cheng, M.; Chen, Y.; Xiao, W.; Sun, R.; Tian, Z. NK Cell-Based Immunotherapy for Malignant Diseases. Cell. Mol. Immunol. **2013**, 10, 230–252, doi:10.1038/cmi.2013.10.
26. Di Santo, J.P.; Vosshenrich, C.A.J. Bone Marrow versus Thymic Pathways of Natural Killer Cell Development. Immunol. Rev. **2006**, 214, 35–46, doi:10.1111/j.1600-065X.2006.00461.x.
27. Vosshenrich, C.A.J.; García-Ojeda, M.E.; Samson-Villéger, S.I.; Pasqualetto, V.; Enault, L.; Goff, O.R. Le; Corcuff, E.; Guy-Grand, D.; Rocha, B.; Cumano, A.; et al. A Thymic Pathway of Mouse Natural Killer Cell Development Characterized by Expression of GATA-3 and CD127. Nat. Immunol. **2006**, 7, 1217–1224, doi:10.1038/ni1395.
28. Tarek, N.; Luduec, J.B. Le; Gallagher, M.M.; Zheng, J.; Venstrom, J.M.; Chamberlain, E.; Modak, S.; Heller, G.; Dupont, B.; Cheung, N.K. V.; et al. Unlicensed NK Cells Target Neuroblastoma Following Anti-GD2 Antibody Treatment. J. Clin. Invest. **2012**, 122, 3260–3270, doi:10.1172/JCI62749.
29. Azzam, B.H.S.; Grinberg, A.; Lui, K.; Shen, H.; Shores, E.W.; Love, P.E. Receptor ( TCR ) Signals and TCR Avidity. J. Exp. Med. **1998**, 188.

**30.** Sánchez, M.J.; Spits, H.; Lanier, L.L.; Phillips, J.H. Human Natural Killer Cell Committed Thymocytes and Their Relation to the T Cell Lineage. J. Exp. Med. **1993**, 178, 1857–1866, doi:10.1084/jem.178.6.1857.

**31.** Veinotte, L.L.; Greenwood, C.P.; Mohammadi, N.; Parachoniak, C.A.; Takei, F. Expression of Rearranged TCRγ Genes in Natural Killer Cells Suggests a Minor Thymus-Dependent Pathway of Lineage Commitment. Blood **2006**, 107, 2673–2679, doi:10.1182/blood-2005-07-2797.

**32.** Charoudeh, H.N.; Tang, Y.; Cheng, M.; Cilio, C.M.; Jacobsen, S.E.W.; Sitnicka, E. Identification of an NK/T Cell-Restricted Progenitor in Adult Bone Marrow Contributing to Bone Marrow- and Thymic-Dependent NK Cells. Blood **2010**, 116, 183–192, doi:10.1182/blood-2009-10-247130.

**33.** De Smedt, M.; Hoebeke, I.; Reynvoet, K.; Leclercq, G.; Plum, J. Different Thresholds of Notch Signaling Bias Human Precursor Cells toward B-, NK-, Monocytic/Dendritic-, or T-Cell Lineage in Thymus Microenvironment. Blood **2005**, 106, 3498–3506, doi:10.1182/blood-2005-02-0496.

**34.** Luhm, J.; Brand, J.M.; Koritke, P.; Höppner, M.; Kirchner, H.; Frohn, C. Large-Scale Generation of Natural Killer Lymphocytes for Clinical Application. J. Hematotherapy Stem Cell Res. **2002**, 11, 651–657, doi:10.1089/15258160260194794.

**35.** Parlar, A.; Sayitoglu, E.C.; Ozkazanc, D.; Georgoudaki, A.M.; Pamukcu, C.; Aras, M.; Josey, B.J.; Chrobok, M.; Branecki, S.; Zahedimaram, P.; et al. Engineering Antigen-Specific NK Cell Lines against the Melanoma-Associated Antigen Tyrosinase via TCR Gene Transfer. Eur. J. Immunol. **2019**, 49, 1278–1290, doi:10.1002/eji.201948140.

**36.** Morton, L.T.; Wachsmann, T.L.A.; Meeuwsen, M.H.; Wouters, A.K.; Remst, D.F.G.; van Loenen, M.M.; Falkenburg, J.H.F.; Heemskerk, M.H.M. T Cell Receptor Engineering of Primary NK Cells to Therapeutically Target Tumors and Tumor Immune Evasion. J. Immunother. Cancer **2022**, 10, 1–14, doi:10.1136/jitc-2021-003715.

**37.** Sheikhi, A.; Saadati, K.; Salmani, R.; Yahaghi, N.; Sheikhi, A.; Siemens, D.R. In Vitro Modulation of Natural Killer Activity of Human Peripheral Blood Mononuclear Cells against Prostate Tumor Cell Line. Immunopharmacol. Immunotoxicol. **2011**, 33, 700–708, doi:10.3109/08923973.2011.561437.

**38.** Fehniger, T.A.; Cooper, M.A. Harnessing NK Cell Memory for Cancer Immunotherapy. Trends Immunol. **2016**, 37, 877–888, doi:10.1016/j.it.2016.09.005.

**39.** von Andrian, U.H. NK Cell Memory: Discovery of a Mystery. Nat. Immunol. **2021**, 22, 669–671, doi:10.1038/s41590-021-00890-9.

**40.** Tamura, A.; Inoue, S.; Mori, T.; Noguchi, J.; Nakamura, S.; Saito, A.; Kozaki, A.; Ishida, T.; Sadaoka, K.; Hasegawa, D.; et al. Low Multiplication Value of Absolute Monocyte Count and Absolute Lymphocyte Count at Diagnosis May Predict Poor Prognosis in Neuroblastoma. Front. Oncol. **2020**, 10, 1–9, doi:10.3389/fonc.2020.572413.

**41.** Chung, H.S.; Higgins, G.R.; Siegel, S.E.; Seeger, R.C. Abnormalities of the Immune System in Children with Neuroblastoma Related to the Neoplasm and Chemotherapy. J. Pediatr. **1977**, 90, 548–554, doi:10.1016/S0022-3476(77)80364-8.

**42.** Rongvaux, A.; Willinger, T.; Martinek, J.; Strowig, T.; Gearty, S. V.; Teichmann, L.L.; Saito, Y.; Marches, F.; Halene, S.; Palucka, A.K.; et al. Development and Function of Human Innate Immune Cells in a Humanized Mouse Model. Nat. Biotechnol. **2014**, 32, 364–372, doi:10.1038/nbt.2858.

**43.** Liu, E.; Ang, S.O.T.; Kerbauy, L.; Basar, R.; Kaur, I.; Kaplan, M.; Li, L.; Tong, Y.; Daher, M.; Ensley, E.L.; et al. GMP-Compliant Universal Antigen Presenting Cells (UAPC) Promote the Metabolic Fitness and Antitumor Activity of Armored Cord Blood CAR-NK Cells. Front. Immunol. **2021**, 12, 1–14, doi:10.3389/fimmu.2021.626098.

44. Trotman-Grant, A.C.; Mohtashami, M.; De Sousa Casal, J.; Martinez, E.C.; Lee, D.; Teichman, S.; Brauer, P.M.; Han, J.; Anderson, M.K.; Zúñiga-Pflücker, J.C. DL4-Mbeads Induce T Cell Lineage Differentiation from Stem Cells in a Stromal Cell-Free System. Nat. Commun. **2021**, 12, 1–11, doi:10.1038/s41467-021-25245-8.
45. Butler, M.O. Human Cell-Based Artificial Antigen-Presenting Cells for Cancer Immunotherapy. **2014**, 257, 191–209, doi:10.1111/imr.12129

.

## SUPPLEMENTARY MATERIAL

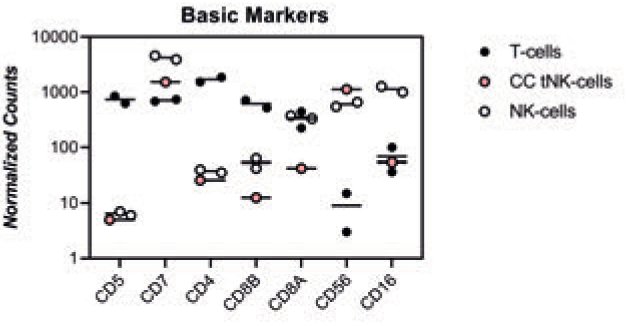

**Figure S1** – Transcriptome analysis of NK- and T-cell markers.
*Comparing RNAseq expression data of CC NK-cells to healthy-donor PB T- and NK-cells. Technical duplicates are averaged, expression of CC NK-cells from one donor is shown, expression of T- and NK-cells from two healthy-donors is shown. Expression levels are depicted as normalized counts.*

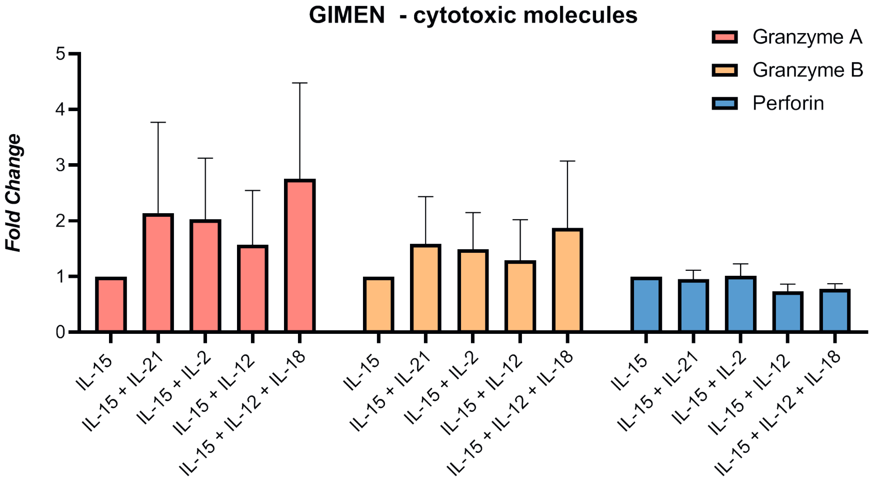

**Figure S2** – Secreted cytolytic markers after overnight co-culture with GIMEN NBL cells.
*Co-culture of the GIMEN NBL line with CC NK-cells cultured with different cytokine combinations (E:T = 10:1). Cytolytic markers were analyzed in the supernatant. Data shown as fold change compared to IL-15 condition (mean ± SD), n=3 per group.*

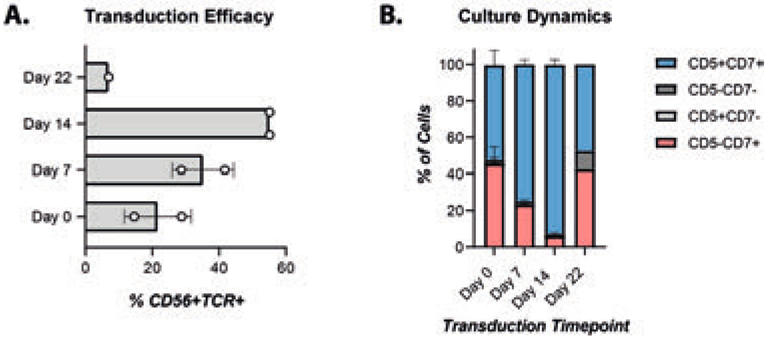

**Figure S3** – Delayed TCR introduction increases NK-transduction efficacy, but skews the culture towards T-cell progenitor development.

*(**A**) % of TCR+ CD56 cells at the end of co-culture after transduction at different timepoints during co-culture, all n=2, except day 22 (n=1). % of TCR+ NK-cells was shown, n=2 per group, except day 22 (n=1). (**B**) NK co-culture dynamics based on CD5 and CD7 expression at the end of OP9/DL1 co-culture after TCR introduction at different timepoints. N=2 per group, except for day 22 (n=1). Data shown as mean ± SD.*

# Chapter 11

## Immunogenicity of Neuroblastoma: Summary, Conclusions, and Perspectives

Over the past decades, impressive progress has been made in the treatment of high-risk neuroblastoma (HR-NBL). In 1990, children with HR-NBL had a 19% 5-year survival rate in the Netherlands, this increased to 43% in 2014 [1]. Treatment is, however, extremely aggressive and elaborate, combining (high-dose) chemotherapy, surgery, radiation, and immunotherapy. Long-term toxicity in survivors is observed in up to 95% of the patients and include ototoxicity, endocrinopathies, pulmonary-, cardiac and renal dysfunction, and increased risk of secondary malignant neoplasms [2]. Besides this, still about 50% of the children dies, despite the intensive treatment regimen. Consequently, there is a desperate need for more effective, but also more targeted, less toxic, therapeutic strategies.

Immunotherapy has now established itself as a novel treatment pillar and has brought significant improvement for patients in terms of survival as well as quality of life [3]. Immunotherapeutic strategies generally aim to emphasize differences between tumor and healthy tissue, thereby inducing tumor immunogenicity. This can be achieved with so-called active strategies, in which agents are administered to induce endogenous immune activation (e.g. vaccination, immune checkpoint inhibition, and administration of immunogenic (chemo)therapy). Alternatively, passive strategies involve administration of active immune system components (e.g. adoptive cell therapy (like CAR T-cell strategies) and antibody therapy).

Unlike adult tumors, pediatric tumors are characterized by a scarcity of targetable molecules due to their low mutational burden. This significantly decreases recognition by the immune system. In addition, a subset of pediatric tumors, such as NBL, arise from embryonic tissues that intrinsically lack immunological features. This majorly limits immunotherapy efficacy in HR-NBL and other embryonal tumors. Nonetheless, the potential of immunotherapeutic interference is underlined by the success of addition of the NBL-antigen GD2 directed monoclonal antibody dinutuximab to the treatment regimen, which resulted in a 20% 2-year and 10% 5-year increase in event-free survival in patients suffering from HR-NBL [4,5].

We hypothesize that the observed relapse in about half of the patients, together with the decrease in event-free survival over-time, is a result of inadequate adaptive immune activation. This thesis postulates that the clue to further enhance (immuno) therapy efficacy in HR-NBL is to effectively engage T-cells, thereby enhancing anti-tumor cytotoxicity and creating immunological memory to prevent future relapse. The research described in this thesis focused on strategies to establish enhanced T-cell immunogenicity of HR-NBL to improve outcome of children suffering from HR-NBL.

## PART I - IMMUNE RESPONSES DURING NEUROBLASTOMA THERAPY

The first section of this thesis revolves around immune monitoring in HR-NBL patients at diagnosis and during therapy. **Chapter 2** summarizes studies into the (implications of) presence of immune subsets in NBL, **Chapter 3** proposes a strategy to synchronize flow cytometers between centers to avoid inconsistencies in interpretation of results. **Chapter 4** reports findings from our first prospective, in-depth longitudinal pilot study into immune dynamics along the HR-NBL treatment course. A visual summary of our pilot data can be found in **Figure 1**.

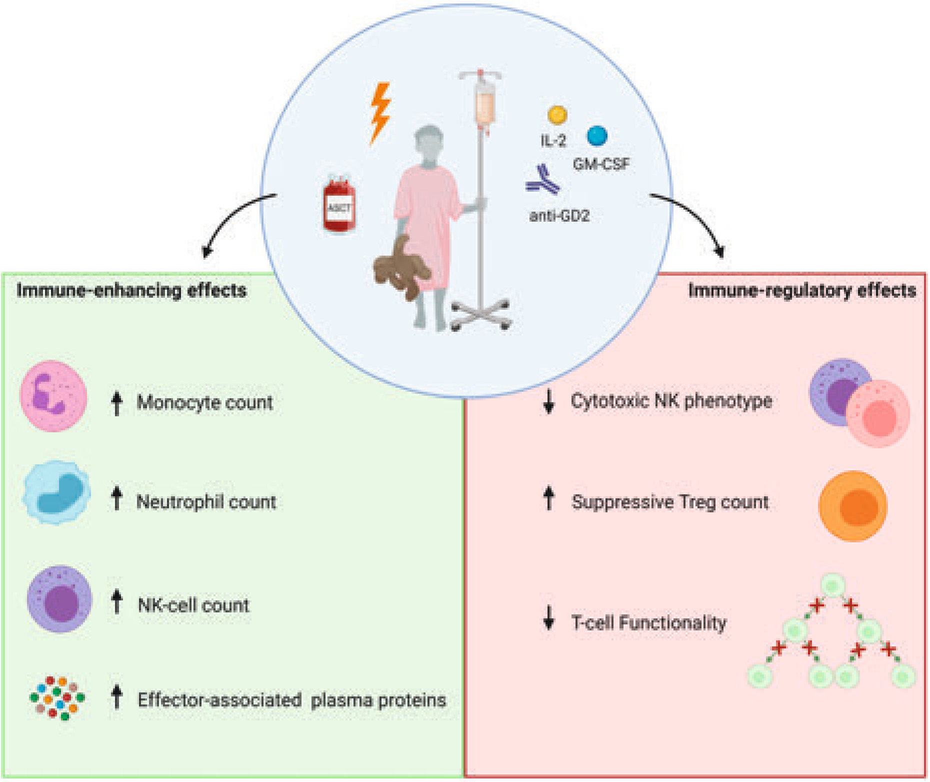
ASCT
IL-2
GM-CSF
anti-GD2
Immune-enhancing effects
↑ Monocyte count
↑ Neutrophil count
↑ NK-cell count
↑ Effector-associated plasma proteins
Immune-regulatory effects
↓ Cytotoxic NK phenotype
↑ Suppressive Treg count
↓ T-cell Functionality

**Figure 1.** Immune-enhancing and immune-regulatory effects observed in peripheral blood immune subsets during the multimodal NBL treatment regimen consisting of (high-dose) chemotherapy followed by autologous stem cell rescue, surgery, radiation, and immunotherapy. *Created with BioRender.com*

To me, summarization of studies into the (implications of) presence of immune subsets in NBL, together with our preliminary pilot data provided valuable lessons for future study design and direction of thinking for therapeutic interference:

### Immune infiltration in NBL: a strong prognostic factor?

The importance of considering immune infiltration in NBL is stressed by Mina and colleagues, who found that the prognostic value of the amount of infiltrating T-cells at diagnosis is higher than the criteria currently used to stage NBL [6]. This is what we, tumor immunologists, anticipate on in our studies, but quite some skepticism remains on feasibility of inducing immune infiltration in solid tumor masses. In my opinion, studies like this set the stage for extension of immune interfering strategies to increase outcome of patients with HR-NBL.

### Predicting local responses in the periphery: the importance of paired monitoring

Most research so far has focused on analysis of tumor-infiltrating lymphocytes (TILs) after biopsy or debulking surgery. However, this is not an option when you are interested in monitoring immune dynamics *during* therapy. Monitoring cell subsets and soluble molecules in peripheral blood (PB) is easily accessible and not very invasive, to me making PB the preferred source for monitoring. Nonetheless, paired monitoring studies between PB and cells from the tumor microenvironment (TME) are currently largely lacking. As the immune system is a multifaceted system, it is important to study how findings in the circulation can be related to the TME. To get better insight into this, we will collect blood samples in our upcoming longitudinal immune monitoring protocol (the DINO study) at the timepoint of biopsy/debulking surgery and compare this to matched biopsy/tumor samples.

### Drawing conclusions based on total immune cell subsets: tempting but risky

We noticed that in-depth immunophenotyping in HR-NBL is largely lacking, or only performed in small cohorts with inconsistency between studies in included markers. In my opinion, one should be careful drawing conclusions on total subsets of cells. A first example of this is the presence and abundance of Tregs in the total CD3+ fraction, which may be a major confounding factor in correlation with prognosis. Another example is the early NK-cell recovery-based timing of immunotherapy after autologous stem cell rescue. Based on our pilot data, NK-cells (CD56+CD3-) indeed recover early after transplant. If we, however, zoom in on the subsets of NK-cells, we observe that they are mainly of the more “immature” (CD56brightCD16-) rather than the cytotoxic (CD56dimCD16+) phenotype necessary for effective dinutuximab-based cytotoxicity [7]. Availability of these data back when immunotherapy was embedded in the treatment protocol might have resulted in different positioning. This demonstrates the necessity to standardly embed immunophenotyping in clinical trials to retrospectively study immune dynamics and correlation with clinical response.

The lack of in-depth phenotyping is most probably mainly due to lack of knowledge on clinical relevance, together with limited accessibility of material in pediatric patient cohorts. Evolving technologies, like spectral flow cytometry and CyTOF, will be a main gamechanger here, as a lot more markers can be measured simultaneously, increasing the amount of information that can be subtracted from a sample.

### Functional immune monitoring: it's what's inside that matters

Even though flow-based immunophenotyping is instrumental, it does not provide information on the functionality of cells. The failure of T-cells from HR-NBL patients to proliferate and produce cytokines upon stimulation with aCD3 to me was one of the most important findings from our pilot study. This dysfunction is already present at diagnosis and can therefore not fully be attributed to the intensive treatment. We speculate that tumor deposition and/or tumor-related suppressive factors present in the bone marrow niche may cause the observed dysfunction. Remarkably, repressive capacity of Tregs seemed to be intact. To this end, it is important to study functionality of other immune cell types, like NK-cells and neutrophils, as, if the tumor deposition hypothesis holds true, one might expect similar issues in these cell subsets.

To study the cause behind the observed T-cell dysfunction, single cell transcriptomics could potentially provide insights into pathway disturbances in cells. Nonetheless, single-cell proteomics would be even more instrumental to learn more about activation status of pathways. The Isoplexis Isolight can analyze the single cell intracellular proteome of T-cells upon stimulation, which can in the near future even be coupled to transcriptomics. Ideally, a genome-wide CRISPR screen (or knock-in screen) on patient-derived T-cells would be very interesting to study key regulators involved in the inhibition of proliferation [8]. Such an experiment would, however, not be feasible in such a pediatric cohort as required cell numbers will not be met. Alternatively, one could go for a more targeted approach, in which the proteomics data will guide to pathways or proteins which could be studied in more detail with knock-in/out experiments.

### Immune stimulation strategies during dinutuximab-based immunotherapy: don't ditch it, replace it

Ladenstein and colleagues concluded from a phase III clinical trial that there was no benefit of IL-2 administration during the dinutuximab-based immunotherapy phase [9]. This study, together with the fact that GM-CSF is no longer available in large parts of Europe, resulted in omission of the immunostimulatory cytokines from the current immunotherapy protocol.

Although I understand the current decision from a clinical perspective, the data from our pilot study clearly show the immunostimulatory effects of these cytokines. IL-2 cycles markedly induced NK-cell expansion, maturation state, and NK-cell activation-associated protein markers. GM-CSF cycles induced expansion and increase in activation-associated plasma proteins of neutrophils, monocytes, and eosinophils. I think that these positive effects are counteracted by the dramatic expansion of Tregs, both in IL-2 and GM-CSF containing immunotherapy cycles. A bell started ringing, as I learned before about efforts to administer low doses of IL-2 to autoimmune patients to induce Treg expansion. Indeed, similar IL-2 doses are used in these patient cohorts, causing preferential Treg expansion [10]. Our pilot supports the hypothesis that *selective* stimulation of cell types involved in dinutuximab-based cytotoxicity may enhance immunotherapy efficacy and increase survival in HR-NBL patients.

When I started studying NK-cells, I quickly became puzzled about the selection of IL-2 as an NK-stimulatory cytokine, and not a more restricted cytokine, like IL-15. Now I understand IL-2 was selected as an immunostimulatory cytokine based on *in vitro* studies and, most importantly, availability in clinical grade setting. Instead of omitting, I suggest searching for better immunostimulatory strategies. Interesting efforts are made in the field to more specifically stimulate NK-cells, for example by IL-15 [11,12], the anti-KIR antibody Lirilumab (NCT02813135), and the CD122-biased cytokine agonist NKTR-214 [13,14]. Efforts like these are important, as, even though we see an about 10% increase in 5-year survival upon immunotherapy addition to the treatment protocol, relapse is still observed in about half of the HR-NBL patients. Nonetheless, monitoring during the new, cytokine lacking immunotherapy phase will provide more insight into whether the observed immunostimulatory effects can be ascribed to the presence of immunostimulatory cytokines.

### Alone we can do so little; together we can do so much ~ Helen Keller

Quite some inconsistencies were observed between markers included in monitoring studies summarized in **Chapter 2**, making it difficult to compare studies and draw conclusions on discrepancies. Standardization of panels across centers is very important, not only because NBL is a rare disease, but also because a lot of different treatment arms are present in the current treatment protocols. As different drugs may have different effects on (subsets of) immune cells, it is important to discriminate between treatment regimens. With only 10-14 HR-NBL patients diagnosed in the Netherlands annually [1], it will take years before we reach enough patients per treatment arm to draw firm conclusions. I would advocate for standardized, harmonized, immune monitoring, either in all centers treating patients according the the Society of pediatric oncology Europe NBL group SIOPEN HR2 (or later) treatment protocol or in a centralized laboratory to maximize the knowledge we will gain from these trials.

All in all, my conclusion from this thesis section is that, even though standard in-depth immune monitoring is largely lacking, efforts that have been made show its potential to guide and modulate immune responses, predict treatment responses, and steer clinical decision making in the future. I strongly envision that monitoring will allow evidence-based rather than empirical positioning and development of (additional) immunotherapy strategies, something required to make the most out of immunotherapeutic interventions to increase survival chances of children with HR-NBL. Our upcoming, in-depth, longitudinal immune monitoring initiative (the DINO study) will hopefully lay the groundwork for many more immune monitoring initiatives, in NBL, but also in other (pediatric) cancers.

## Part II & III – Improving Neuroblastoma Immunogenicity via Pharmacological- and Cell-based Therapy Strategies

In the first section of this thesis, the presence of immune cells and their capacity to elicit an immune response against NBL have been discussed. However, the immune system can be as potent as it can be, but if the tumor fails to express ligands and other markers needed to be recognized by the immune system, a strong anti-tumor response will be avoided. Section II & III of this thesis focuses on strategies to enhance adaptive immune engagement in NBL to increase anti-tumor cytotoxicity and create immunological memory to prevent future relapse. **Section II** focuses on pharmacological strategies; **section III** explores cell therapy-based strategies.

Section II revolves around pharmacological induction of expression of major histocompatibility complex class I (MHC-I) on tumor cells, a main prerequisite for immunogenicity to CD8$^+$ T-cells. **Chapter 5** summarizes literature on MHC-I dysregulation in cancer and provides an overview of MHC-I upregulatory strategies described in literature. We took an unbiased approach, in which drug repurposing libraries were screened for their effect on MHC-I surface display. To this end, a high-throughput flow cytometry protocol was developed to assess MHC-I surface display (**Chapter 6**). In addition, we developed a protocol to engineer T-cells to express a tumor-specific T-cell receptor (TCR) (**Chapter 7**), with which we engineered T-cells expressing a TCR against the NBL-antigen PRAME, which could be used in subsequent T-cell cytotoxicity assays. **Chapter 8** summarizes the findings from the drug repurposing screens, identifying histone deacetylase inhibitors (HDACi) as an MHC-I surface display inducing drug class. A visual summary from our main findings is presented in **Figure 2**.

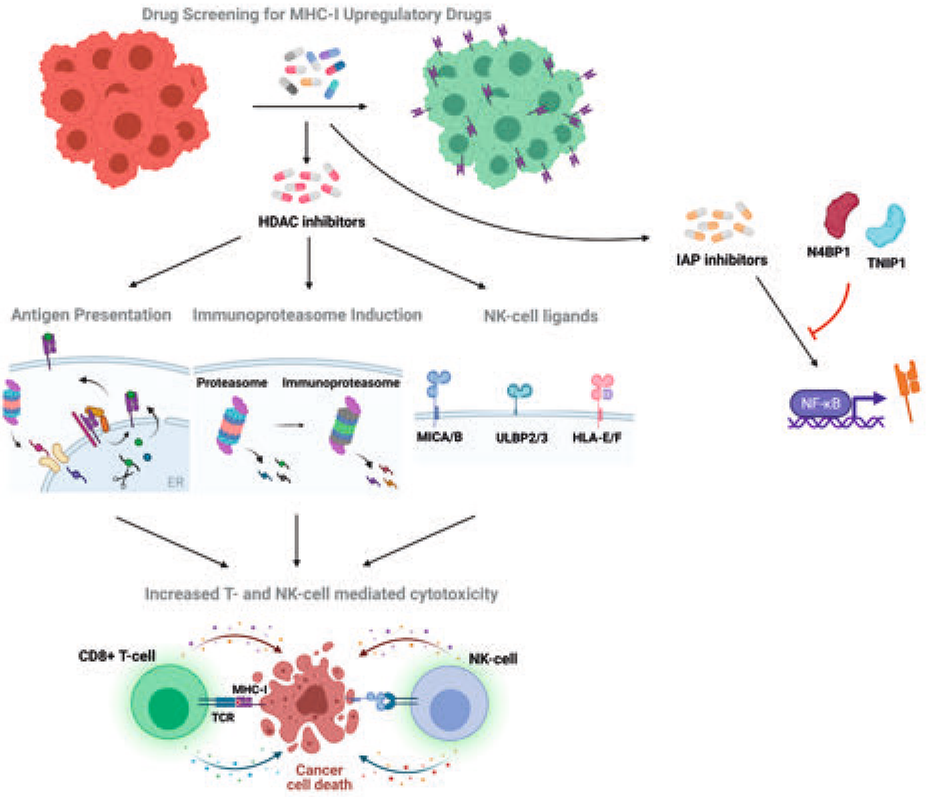
Drug Screening for MHC-I Upregulatory Drugs
HDAC inhibitors
IAP inhibitors
N4BP1
TNIP1
NF-κB
Antigen Presentation
Immunoproteasome Induction
NK-cell ligands
ER
Proteasome
Immunoproteasome
MICA/B
ULBP2/3
HLA-E/F
Increased T- and NK-cell mediated cytotoxicity
CD8+ T-cell
NK-cell
MHC-I
TCR
Cancer cell death

**Figure 2.** Drug repurposing screening revealed HDAC inhibition as a promising strategy to increase immunogenicity of NBL.
*HDAC inhibition enhances antigen presentation, immunoproteasome induction, and NK-cell ligand expression, thereby increasing NBL immunogenicity. IAP inhibition required intact NFκB signaling, limiting its application in HR-NBL. Created with BioRender.com*

Section III explores cell-therapy based strategies to target and induce immunogenicity of NBL. The projects discussed in this section arose around our hypothesis about MHC-I plasticity-mediated evasion of both T- and NK-cells. We hypothesize that generation of a cell product that can both engage in missing-self cytotoxicity as well as in recognition of malignant transformation in MHC-I context will result in an effector cell that cannot be evaded by MHC-I plasticity. This thesis section explores different immune cell sources to engineer such a cell product. **Chapter 9** reports the potential to use $CD3^{+}CD56^{+}$ NKT-like cells, **Chapter 10** describes an OP9/DL1 co-culture system to differentiate genetically engineered CD34+ stem cells into TCR+ thymic NK-cells. A visual summary of explored strategies is displayed in **Figure 3**.

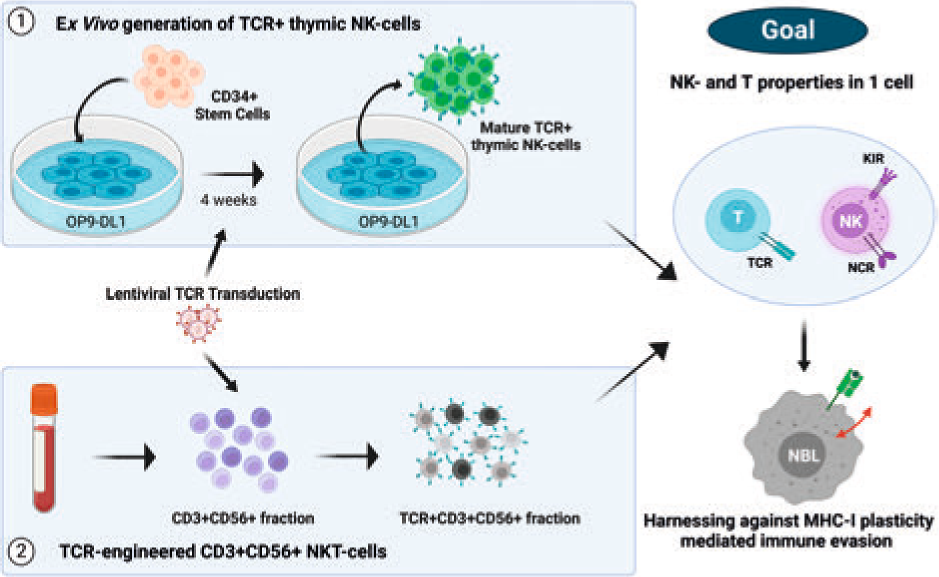
① Ex Vivo generation of TCR+ thymic NK-cells
CD34+ Stem Cells
OP9-DL1
4 weeks
OP9-DL1
Mature TCR+ thymic NK-cells
Lentiviral TCR Transduction
CD3+CD56+ fraction
TCR+CD3+CD56+ fraction
② TCR-engineered CD3+CD56+ NKT-cells
Goal
NK- and T properties in 1 cell
KIR
T
NK
TCR
NCR
NBL
Harnessing against MHC-I plasticity mediated immune evasion

**Figure 3.** Explored strategies to harness immune cells against MHC-I plasticity-mediated immune evasion. *NCR = natural cytotoxicity receptor. Created with BioRender.com*

### Embryonal tumors from an immunological perspective: a separate class of tumors?

Even though all are classified as "cancer", it is now widely accepted that the pathobiology of pediatric tumors deviates from adult tumors [15]. From an immunological perspective and based on the data in this thesis, I think we can even take this one step further, and state that pediatric tumors should be further subdivided into embryonal (e.g. malignant rhabdoid tumors, medulloblastoma, and NBL) and non-embryonal tumors (e.g. hematological tumors and gliomas). Where non-embryonal cell-derived tumors immunologically tend to behave more like adult tumors (except for the lack of targetable molecules due to the lower mutational burden), embryonal tumors intrinsically seem to lack immunological features due to their origin. To me, this is one of the main take-home messages from the research described in this thesis section: in embryonal tumors, like NBL, we should not be talking about MHC-I downregulation, but about *lack of MHC-I upregulation*.

Why do I think this is so important? Differentiation of the NBL cell of origin, a neural crest cell stage, into differentiated parental cells is regulated by a complex regulatory scheme of transcriptional and epigenetic modifications [16]. Treatment with HDACi seems to trigger the NBL cells to change their epigenetic landscape, thereby inducing a cell lineage switch which goes hand-in-hand with induction of tumor immunogenicity.

So, unlike non-embryonal tumors, I believe that embryonal tumors do not escape immune clearance. Instead, they simply are non-immunogenic in the first place. This makes these types of tumors of particular interest to me for immunomodulatory therapy strategies, for example with HDACi [17,18]. For future research, I would like to study the possibility to find embryonal tumor overarching pharmacological and/or cell therapy-based strategies to induce immunogenicity.

### The more mature, the better in hide and seek: A plot twist!

It has been shown that the more NBL cells differentiate, the less aggressive the tumor becomes, and the better it responds to chemotherapeutic strategies [19,20]. It is hypothesized that differentiation goes hand in hand with increased overall immunogenicity, thereby subjecting these cells to immunotherapeutic strategies. This is substantiated by the observation that low-risk tumors have a higher degree of differentiation, which is accompanied with more detected TILs in the TME [6]. These findings underlie the rationale for administration of the retinoic acid isoform isotretinoin during the consolidation phase of the current therapy regimen to force differentiation of remaining tumor cells, which is combined with the anti-GD2 antibody dinutuximab.

This all sounds very sound: the closer the cells come to a mature, differentiated phenotype, the more they present to the immune system, resulting in immunogenicity. Surprisingly, a collaborative study with the George lab from Harvard revealed the contrary [21]. NBL tumors contain a mixed population of both undifferentiated, mesenchymal (MES) cells and committed adrenergic (ADR) cells, which can interconvert [22,23]. In our collaborative study, correlation between the NBL cell lineage and immunogenicity was examined more closely [21]. A dataset of 498 primary NBL tumors revealed that more undifferentiated tumors with a higher MES-score had significant higher expression of markers related to innate and adaptive immunogenicity signatures [21]. In line with this, we observed a cell lineage switch to a MES phenotype upon treatment with the HDACi Entinostat, which was accompanied by increased innate and adaptive immunogenicity signatures (**Chapter 8**). **Figure 4** provides a revised schematic on how NBL immunogenicity is related to cell lineage and differentiation state.

If these findings hold true, this will have major implications for the way we look at (immuno)therapy strategies in NBL. First, it has been reported that MES cells are more resistant to chemotherapy, skewing treated NBL tumors to a more MES phenotype [22]. This would then provide a window for immunotherapeutic strategies to eliminate the remaining chemo-resistant tumor cells. Second, and maybe even more urgent, these data would directly argue against combining isotretinoin with immunotherapy, as isotretinoin is administered to induce differentiation and rewire ADR signaling in remaining NBL cells [24].

As the current immunotherapy regimen is directed to GD2, it is also important to consider GD2 expression in the different cell lineages. One study in TH-MYCN mice reports that GD2 expression is lost with the conversion from the ADR to MES lineage [25]. In contrast, no difference in expression of GD2 synthase was observed between human ADR and MES cell lines and patient-derived organoids [26]. In addition, mouse studies with Vorinostat, another type I HDACi, even reported an increase in GD2 and GD2 synthase expression [27]. Future experiments should be performed to conclude whether this is also observed upon Entinostat treatment. Moreover, studies in human setting are required to conclude whether GD2 expression is correlated with NBL cell lineages.

The seemingly positive correlation between tumor aggression and immunotherapy efficacy complicates the timing of therapy components. On the one hand, we would like to skew the tumor to a more committed ADR cell lineage, as these more differentiated cells are reported to have a less aggressive phenotype. On the other hand, immunotherapy, and subsequent generation of immunological memory, may be most effective when tumors display a more aggressive MES phenotype. Hypothetically, as MES resistance to chemotherapy skews cells towards a more MES phenotype, timing of immunotherapy after chemotherapy would be ideal. Nonetheless, the immune status after chemotherapy is often disturbed and might require passive immunotherapy strategies, like adoptive T-cell therapy, to ensure efficacy.

Besides this, the isotretinoin issue remains, as consolidation with isotretinoin may decrease the likelihood of activation of immunological memory upon tumor rechallenge. As MES cells have been reported to be largely resistant to differentiation induced by retinoic acid (and might even aid proliferation and migration of cells) [22], one might hypothesize that isotretinoin administration *before* or *during* chemotherapy might be an interesting strategy. These hypotheses, however, are all based on indirect observations in other research and should be studied in more detail to be able to conclude the benefit of isotretinoin in any therapy stage.

Altogether, this shows that the tumor cell status is extremely important in immune recognition and immunotherapy efficacy. The observed tumor cell plasticity shows that not only the (immuno)therapy strategy itself, but also the timing is extremely important and may make or break a therapeutic strategy. More in-depth knowledge on these processes and implications for therapy efficacy are required to be able to make educated decisions. Nevertheless, I hope this section aids to the notion that empirical decision making is tempting (and sometimes required), but risky.

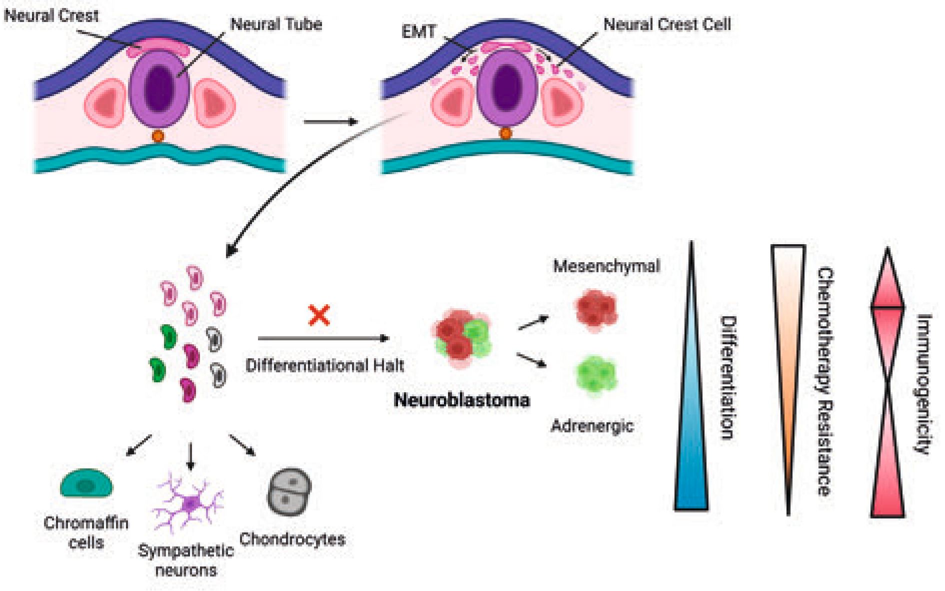
Neural Crest
Neural Tube
EMT
Neural Crest Cell
Differentiational Halt
Neuroblastoma
Mesenchymal
Adrenergic
Differentiation
Chemotherapy Resistance
Immunogenicity
Chromaffin cells
Sympathetic neurons
Chondrocytes

**Figure 4.** NBL immunogenicity in relation to cell lineage.
*Undifferentiated, mesenchymal NBL cells are more immunogenic, but also more aggressive and less sensitive to chemotherapy. Committed, adrenergic NBL cells are less immunogenic, but more sensitive to chemotherapy. Created with BioRender.com*

## Entinostat treatment to increase NBL immunogenicity: steps from bench to bedside

Combining HDACi with immunotherapy to maximize immunotherapy efficacy is increasingly studied in both pediatric and adult cancer cohorts [28–30]. Our *in vitro* study showed a multimodal effect of Entinostat on tumor cells, positively affecting both T- and NK-cell immunogenicity. In addition, previous studies using an NBL mouse model showed that Vorinostat, another class I HDACi, decreased abundance and immunosuppression of myeloid-derived suppressor cells (MDSCs) and tumor-associated macrophages (TAMs), which may further increase immunogenicity [27,31]. The effect of HDACi on lymphocyte subsets is more debated and seems to be HDACi class dependent. We did observe intact T-cell proliferation in the presence of a high-dose of Entinostat. In addition, others have reported increased expression of natural-cytotoxicity receptors on NK-cells, suggesting that NK-cell function may even be enhanced [32,33]. Immunocompetent NBL mouse models would aid in understanding the net effect of multi-modal immune editing by Entinostat. An orthotopic, competent mouse model would be fit to study this effect [27]. Alternatively, and probably more translatable to the human situation, a humanized, competent mouse-model could be used, for example MISTRG mice repopulated with a human immune system [34]. Co-administration of PRAME HSS1 TCR expressing T-cells is possible in this model, thereby enabling control of the presence of tumor-specific T-cells.

The second hurdle that has to be overcome is the minimum age required to receive Entinostat. The current multi-center INFORM2 trial (NCT03838042), which is also conducted in our center, studies the effect of Nivolumab and Entinostat in children and adolescents with high-risk refractory malignancies. Even though refractory or relapsed NBL patients could be eligible for this study, the minimum age for inclusion is 6 years. This age restriction is due to the currently available formulation [35], requiring patients to be able to swallow tablets and have a minimum body surface area of 0.9 $m^2$, and not due to toxicity issues. A change in formulation is required to solve this issue and make Entinostat available for the majority of NBL patients.

The last major hurdle remaining is that of positioning of Entinostat in the multimodal treatment regimen. Current trials in NBL position HDACi prior to (Vorinostat, NCT02559778) or during (Vorinostat, NCT03332667) immunotherapy, or in refractory/relapsed disease (Entinostat, INFORM2). Considering the observed switch to a more mesenchymal tumor lineage, which is correlated with resistance to chemotherapy, I think positioning Entinostat after chemotherapy but prior to or during immunotherapy would be ideal to most effectively target the remaining tumor cells after initial chemotherapy. *In vivo* mouse studies in which the HR-NBL therapy regimen is mimicked could aid in evaluation of most effective positioning.

### Never bet on one horse: future directions to determine the potential of other drug hits

Besides inhibitor of apoptosis inhibitors (IAPi) and HDACi, we found four other drug categories that upregulate MHC-I expression on NBL cells: topoisomerase inhibitors (TIi), tyrosine kinase inhibitors (TKi), proteasome inhibitors, and antimalarials. Validation in other *in vitro* NBL models is required to verify results.

Studies into the immunomodulatory capacity of TIi and TKi would be of particular interest in NBL. The TIi topotecan is currently administered to refractory/relapsed HR-NBL patients included in the VERITAS study. In addition, a wide range of TKis affected MHC-I expression during our drug screen. Especially TKis targeting the ALK pathway are of interest, as both ALK and downstream RAS-MAPK kinases are frequently mutated in HR-NBL [36], and several clinical trials are evaluating the anti-tumor effect of TKis targeting these pathways in refractory/relapsed HR-NBL. An immunomodulatory effect of these drugs, besides the anticipated antineoplastic effect, might make them an even more interesting candidate to improve treatment for HR-NBL patients. As reviewed in **Chapter 5**, a similar effect on MHC-I expression was reported upon repression of tyrosine kinase pathways as well as by TIis in various pre-clinical adult cancer models.

We initially started this pharmacological screening project to find compounds re-sensitizing NBL cells to NFκB pathway activation, as we previously found high expression of two key regulators of NFκB signaling; N4BP1 and TNIP1 [37]. Unfortunately, such a drug was not identified during this project. Literature describes two interesting compounds we could aim future research at. The first ones are the Cyanopyrrolidine derivates (WO2017109488), which have been patented to specifically targeting one of the key downstream factors of N4BP1: Cezanne1. The second one is Clomipramine, which negatively regulates another downstream factor, Itch. Another strategy would be to screen libraries of small molecules that specifically target Cezanne1, a strategy described for other deubiquitinase inhibitors [38].

### Cytokine-induced MHC-I expression in a clinical setting: is there a potential?

MHC-I expression-enhancing cytokines, although encouraging in a pilot clinical trial in HR-NBL [39,40], have limited systemic therapeutic applicability due to severe toxicities resulting from their broad range of biological activities [41]. Finding better tolerable compounds that increase MHC-I expression on tumor cells is one strategy, but another strategy would be a targeted delivery strategy of cytokines, for example by immune cells.

One elegant way is the gene-therapy-mediated delivery of cytokines, in which hematopoietic stem cells are transduced with a vector expressing IFNγ/TNFα/IFNα controlled by the pro-tumoral macrophage-specific Tie2 promotor [42,43]. This way, expression of the cytokines is targeted to the tumor site. Based on current data, IFNα seems to be the most promising candidate for delivery, as they have been shown to repolarize MDSCs and TAMs to a less pro-tumorigenic phenotype [44].

The autologous transplant after high-dose chemotherapy during NBL treatment would provide an excellent opportunity for this gene-therapy based strategy. However, we have to be cautious with these type of strategies, as lentiviral integration of the Tie2-regulated transgenes will be random, which is in my opinion a particularly critical point in multipotent hematopoietic stem cells. In addition, I believe that virtually every endogenous promotor will be activated during some type of physiological process, as it is an endogenous promotor for a reason. Tie2, for example, seems to have an effect in the maintenance of adult vasculature [45]. Nonetheless, the approach will always be a lot more targeted than systemic delivery. More studies should be performed to determine safety and tolerability. It would be interesting to see if we would be able to introduce one of these cytokines in a T-cell therapy product, under expression of promotors particularly activated in T-cells in the TME, for example a promotor important in dampening T-cell activation in the tumor.

Another strategy would be to use the endogenous capability of cells to produce cytokines upon activation. Two of these strategies are explored in this thesis: the use of tumor-specific TCR transduced co-culture derived thymic NK-cells (**Chapter 10**) or CD3+CD56+ NKT-cells (**Chapter 11**). Both strategies result in the generation of a functional cell product, which can recognize in both TCR-dependent and a more NK-like, TCR-independent manner. Theoretically, recognition of missing-self or natural cytotoxicity receptor (NCR) engagement results in NK-cell activation, which in turn causes release of IFNγ. IFNγ induces MHC-I expression, thereby sensitizing the tumor cells to TCR-mediated cytotoxicity. But which strategy is the way to go?

The big advantage of the use of co-culture derived thymic NK-cells is that they do not have to be majorly expanded once mature, thereby potentially increasing their persistence compared to products produced from mature NK-cells [46]. The disadvantage, on the other hand, is that they are NK-cells, hitting hard and fast, but not necessary displaying longevity and memory formation. Notwithstanding, NK-cells are now recognized to also be able to generate a memory-like phenotype [47,48]. The question remains, however, if the thymic NK-cells we generate *in vitro* can generate such a memory response.

CD3+CD56+ cells, on the other hand, are a relatively abundant lymphocyte subset (1-11%), can be easily expanded with conventional T-cell expansion protocols, and are capable to generate immunological memory [49]. The observed T-cell dysfunction in HR-NBL patients discussed in the first part of this thesis, however, might complicate the expansion and potency of generated autologous cell products. Nonetheless, several autologous cell engineering strategies are studied in clinical trials, indicating that the observed dysfunction can be overcome ex vivo. Besides this, the total CD3+CD56+ cell fraction is heterogeneous and includes both pro- and anti-tumorigenic cell subsets [50]. Where CD1d-restricted type I NKT (invariant NKT) and CD1d-unrestricted NKT-like cells have been described to promote tumor immunity, CD1d-restricted type II NKT-cells are reported to suppress tumor immunity [50]. Recently, FlowSOM analysis of deep phenotypical characterization of the full CD3+CD56+ cell fraction of healthy donors revealed even more complexity, as 19 individual subsets were identified by clustering [49]. Future experiments should focus on the difference in anti-tumor capacity of heterogeneous and more homogenous cell products, the potential skewing of populations due to permissiveness to lentiviral transduction, and discrimination of the most promising cell fractions within the heterogeneous CD3+CD56+ cell fraction.

### Focus on MHC-I expression to increase T-cell engagement: Old-fashioned or is there something to it?

One might wonder, a whole thesis section on inducing MHC-I expression to increase T-cell immunogenicity, is this not a bit old-fashioned? Chimeric Antigen Receptor (CAR) T-cells are already around for years and unconventional, MHC-I unrestricted T-cells, like iNKT-cells, γδ T-cells, and MAIT-cells are increasingly acknowledged for their anti-tumor capacity. Moreover, the MHC-I locus is highly polymorphic, complicating the generation of cell therapy products to individuals with designated HLA-A/B/C polymorphisms.

Many CART engineering strategies are currently in pre-clinical and clinical development in NBL [51]. Two of the main studied targets are GD2 and B7H3. Even though CART initially showed limited success in NBL (and solid tumors in general), many strategies are in development to boost efficacy. Preferential use of specific T-cell subsets, inclusion of IL-15 (or other cytokines) into the vector design to boost a stem-cell memory phenotype [52,53], studies into the optimal CAR design (e.g. length of spacer, type of signaling domain, origin of the scFv domain) [54], CART targeting the suppressive TME [55], and use of alternative cell types (e.g. NK- or iNKT-cells) are all promising strategies to improve efficacy [56]. The main advantage of CART is that they are unrestricted of antigen-presentation and MHC-I expression, which makes that one CAR receptor design can be used as a backbone for every CART-product. This in contrast to MHC-I targeting strategies, in which different TCRs have to be identified in different HLA contexts to be able to treat all. The main disadvantage of CART is that they can only target surface proteins, which represents only a fraction of all proteins expressed. This is especially problematic in pediatric cancer, as the mutational burden is low, and the list of promising targets is already limited. Besides this, the “unnatural” CART structure subjects it to potential immunogenicity against the CAR, causing less CART persistence [57]. In addition, it is increasingly recognized that the persistence of CART-cells is further affected by the harsh, “unnatural” way of stimulation [58]. I think both MHC-I-restricted and CART strategies have their advantages and disadvantages, and the future will tell which strategy will be most effective.

Then on to native MHC-I unrestricted T-cells. Based on this thesis and literature, I believe that the lack of immunogenicity of NBL is not restricted to MHC-I restricted T-cells. In a collaborative study we observed that, even though all tested NBL organoids express CD277 (the protein recognized by γδ T-cells), co-culturing these organoids with endogenous γδ T-cells did not result in cytotoxicity [59]. When αβ T-cells were engineered to express a γδ TCR (a cell product named TEG002), we observed cytotoxicity in half of the tested organoids, but *only* when cells were pre-treated with pamidronate [59]. γδ T-cells namely recognize elevated levels of phosphoantigens in stressed cells, which can be induced by treatment with pamidronate, but also with chemo(immuno)therapy strategies with temozolomide [60]. In addition, in an ongoing research effort (unpublished), we observed that T-cells expressing a recently identified "pan-cancer" TCR, against the monomorphic MHC-I related protein 1 (MR1) [61], are also not able to target most NBL cells.

CD1d, the MHC-I like molecule recognized by iNKT-cells, is hardly expressed on NBL cells (own unpublished data and [62]), limiting their contribution in cytotoxicity of NBL. An interesting observation, which gives food for thought, is that TAMs in the TME, however, are subjected to CD1d-mediated cytotoxicity by iNKTs, resulting in the generation of a more permissive tumor environment, indirectly increasing immunogenicity of tumor cells [63]. This again is an example to advocate for the use of immunocompetent models with presence of all sorts of immune cells to be able to study the net anti-tumor effect of cell therapy strategies.

And finally, last but not least, another bold thought. CD4+ T-cells have been treated as bystanders in tumor elimination for years, but are increasingly recognized in their importance in long-term remission [64-66]**.** This makes me wonder, besides introduction of MHC-I restricted TCRs in CD4+ T-cells, is there also a potential for MHC-II restricted T-cell strategies? Several cancer types have been reported to express MHC-II [67], and our transcriptome data indicates induction of expression of MHC-II expression in NBL cells upon Entinostat treatment (unpublished data). These data have to be confirmed on a protein level, but could provide a rationale for MHC-II restricted adoptive TCR therapy strategies. In addition, even though MDSCs and TAMs in the TME express low levels of MHC-II, class I HDACs are reported to enhance MHC-II presentation, which may provide another interesting immune modulating option of MHC-II restricted adoptive T-cell therapy [27,31].

To conclude, the potential of many MHC-I unrestricted T-cells are evaluated in NBL. I believe that the embryonal origin of NBL cells causes an overall lack of immunological features, not restricted to MHC-I and conventional T-cells. Consequently, immunogenicity enhancing strategies are also required to utilize their potential. These non-conventional T-cells do have the advantage of recognizing molecules which are non-polymorphic in the population, which would decrease the complexity of generation of a cell product to treat NBL patients regardless of HLA background. Nonetheless, the broad repertoire of presented peptides in MHC-I, the native signaling cascades in

T-cells, and the abundance of MHC-I restricted T-cells compared to MHC-I unrestricted T-cells to me makes that there is definitely something to MHC-I restricted T-cell therapy strategies.

## Let’s mention the elephant in the room: it’s not just MHC-I presentation

Lack of MHC-I expression on tumor cells might be one of the main, most basal limiting factors in cytotoxic T-cell activation, but many additional immunomodulatory processes in the TME limit T-cell engagement in NBL. Consequently, expression of checkpoint ligands, secretion of all sorts of immunomodulatory proteins, presence of suppressive cell populations (e.g. TAMs, MDSCs, and Tregs), and impaired T-cell functionality are all additional factors that have to be tackled to maximize cytotoxic anti-tumor capacity of cytotoxic T-cells.

I think a multi-faceted therapy approach is required to beat the immunomodulatory capacity of the tumor and its environment to be able to truly master this game of hide and seek. Unraveling the ideal regimen and timing, however, is easier said than done. We first need to better understand the dynamics and implications of the individual immunomodulatory processes and the total impact of (timing of) manipulations in fully immunocompetent settings. It is quite important to not only study interventions on their own, but also complete treatment regimens, as I think every component of a regimen may affect subsequent treatments. A lot can be learned from humanized, immunocompetent mouse models, like the MISTRG model [34], but of course findings have to be related to the human situation. To that end, studying biopsies/debulking material at diagnosis, after induction chemotherapy, and in case of relapse could aid in relating findings between mouse and human setting.

Even if we manage to make the tumor immunogenic and the immune system functional, tumor cells look a lot like their healthy counterparts, resulting in no, or a very narrow, immune response against tumor cells. To this end, pipelines are needed to find tumor-specific or treatment-induced changes that could be picked up by immunotherapeutic strategies. Cell surface proteomics and transcriptome analysis could aid in identification of these differences. One promising technique is ribosome profiling (RiboSeq), a technique the van Heesch lab recently introduced in the Princess Máxima Center. As a pilot, we performed RiboSeq on a patient-derived NBL organoid before and after Entinostat treatment. Interestingly, we identified new, previously unannotated, treatment-induced neo-antigens (unpublished data), which shows the potential of such a technique. The question, however, remains if these treatment-induced effects are tumor-specific, or whether they can also be found in treated healthy tissues. In addition, it remains to be observed if neo-antigen expression is shared in patient populations.

Besides this, studying tumor-specific antigens in untreated NBL is a challenge, as it remains questionable which tissue should be used to compare to. In a collaborative project, we will try to tackle these questions in the coming years and optimize the pipeline to identify new general tumor-specific or treatment-induced neo-antigens to increase immunogenicity of NBL and other pediatric tumors.

All in all, my conclusion from the second and third section of this thesis is that there are many unknowns and many possibilities and efforts to increase NBL immunogenicity. My biggest eye-opener is that NBL immunogenicity is not positively correlated to differentiation status of cells. The observation that more committed ADR cell lineages seem to be better targeted by chemotherapy, and undifferentiated MES cell lineages by immunotherapy, tells me that combining the two in one regimen is even more promising as I previously already recognized. The plasticity in cell lineage may have huge implications on therapy efficacy and timing of individual therapy components in the treatment regimen may make or break therapy strategies.

## CONCLUDING REMARKS

The research described in this thesis focuses on strategies to enhance NBL immunogenicity to improve outcome of children suffering from HR-NBL. The main objective was to find pharmacological and cell-based strategies to induce one of the most important prerequisites for cytotoxic T-cell engagement: cell surface display of MHC-I. The ultimate goal is to effectively engage T-cells, thereby enhancing anti-tumor cytotoxicity and creating immunological memory to prevent future relapse.

To improve the current therapy regimen, we need to understand why the current strategy fails. The pilot data of the functional, longitudinal immune monitoring strategy we developed shows clues for therapy improvement and emphasizes the potential of such a monitoring strategy to study therapy responses in patients. However, we can show the potential, but we do need collaborative approaches within the European association involved with neuroblastoma research (SIOPEN) to gain enough power to be able to draw firm conclusions in such a rare disease treated with many different treatment arms.

We identified HDAC inhibition as a promising approach to induce surface display of MHC-I expression on NBL cells, thereby causing *in vitro* susceptibility to NBL-specific T-cell cytotoxicity. The HDACi Entinostat induces a general increase in factors important in both innate and adaptive immunogenicity, which, to our surprise, was accompanied by a switch towards a more undifferentiated, MES NBL cell lineage. This implies that chemo-resistant NBL cells are more sensitive to immunotherapy, and vice versa. These new insights in cell lineage plasticity in response to chemo- and immunotherapy stresses the importance of considering therapy timing to reach maximum therapy efficacy.

Immune monitoring during therapy revealed that, besides the low immunogenicity of NBL cells in general, immune cells themselves may be dysfunctional, which further complicates the generation of NBL-specific immune responses. Adoptive cell therapy strategies may therefore be required complementary to immunogenicity-enhancing strategies to maximize anti-tumor responses. This thesis hints to the potential of cell therapy strategies which combine natural NK-cell cytotoxicity with TCR-mediated cytotoxicity of T-cells in one cell to overcome MHC-I plasticity-related immune evasion.

Altogether, understanding of the impact of (timing of) individual components of the HR-NBL treatment regimen on tumor destruction, tumor phenotype, immunogenicity, and immune cell function is key to further improve efficacy of the treatment regimen. This thesis identifies and shows the potential of strategies to increase NBL immunogenicity to, among others, T-cells, to induce an NBL-specific immune response and generate immunological memory to prevent future relapse. This is a start, but translating our findings to a fully immunocompetent setting, together with investigation of other immunogenicity-restricting processes, is needed to bring mastering of this game of hide and seek to the next level.

## REFERENCES

1. Tas, M.L.; Reedijk, A.M.J.; Karim-Kos, H.E.; Kremer, L.C.M.; van de Ven, C.P.; Dierselhuis, M.P.; van Eijkelenburg, N.K.A.; van Grotel, M.; Kraal, K.C.J.M.; Peek, A.M.L.; et al. Neuroblastoma between 1990 and 2014 in the Netherlands: Increased Incidence and Improved Survival of High-Risk Neuroblastoma. *Eur. J. Cancer* **2020**, *124*, 47–55, doi:10.1016/j.ejca.2019.09.025.
2. Friedman, D.N.; Henderson, T.O. Late Effects and Survivorship Issues in Patients with Neuroblastoma. *Children* **2018**, *5*, 1–15, doi: 10.3390/children5080107.
3. Esfahani, K.; Roudaia, L.; Buhlaiga, N.; Del Rincon, S. V.; Papneja, N.; Miller, W.H. A Review of Cancer Immunotherapy: From the Past, to the Present, to the Future. *Curr. Oncol.* **2020**, *27*, 87–97, doi:10.3747/co.27.5223.
4. Yu, A.L.; Gilman, A.L.; Ozkaynak, M.F.; London, W.B.; Kreissman, S.G.; Chen, H.X.; Smith, M.; Anderson, B.; Villablanca, J.G.; Matthay, K.K.; et al. Anti-GD2 Antibody with GM-CSF, Interleukin-2, and Isotretinoin for Neuroblastoma. *N. Engl. J. Med.* **2010**, *363*, 1324–1334, doi:10.1056/NEJMoa0911123.
5. Yu, A.L.; Gilman, A.L.; Ozkaynak, M.F.; Naranjo, A.; Diccianni, M.B.; Gan, J.; Hank, J.A.; Batova, A.; London, W.B.; Tenney, S.C.; et al. Long-Term Follow-up of a Phase III Study of Ch14.18 (Dinutuximab) + Cytokine Immunotherapy in Children with High-Risk Neuroblastoma: COG Study ANBL0032. *Clin. Cancer Res.* **2021**, *18*, clincanres.3909.2020, doi:10.1158/1078-0432.ccr-20-3909.
6. Mina, M.; Boldrini, R.; Citti, A.; Romania, P.; D'Alicandro, V.; Ioris, M. De; Castellano, A.; Furlanello, C.; Locatelli, F.; Fruci, D. Tumor-Infiltrating T Lymphocytes Improve Clinical Outcome of Therapy-Resistant Neuroblastoma. *Oncoimmunology* **2015**, *4*, 1–14, doi:10.1080/2162402X.2015.1019981.
7. Nassin, M.L.; Nicolaou, E.; Gurbuxani, S.; Cohn, S.L.; Cunningham, J.M.; LaBelle, J.L. Immune Reconstitution Following Autologous Stem Cell Transplantation in Patients with High-Risk Neuroblastoma at the Time of Immunotherapy. *Biol. Blood Marrow Transplant.* **2018**, *24*, 452–459, doi:10.1016/j.bbmt.2017.11.012.
8. Shifrut, E.; Carnevale, J.; Tobin, V.; Roth, T.L.; Woo, J.M.; Bui, C.T.; Li, P.J.; Diolaiti, M.E.; Ashworth, A.; Marson, A. Genome-Wide CRISPR Screens in Primary Human T Cells Reveal Key Regulators of Immune Function. *Cell* **2018**, *175*, 1958-1971.e15, doi:10.1016/j.cell.2018.10.024.
9. Ladenstein, R.; Pötschger, U.; Valteau-Couanet, D.; Luksch, R.; Castel, V.; Yaniv, I.; Laureys, G.; Brock, P.; Michon, J.M.; Owens, C.; et al. Interleukin 2 with Anti-GD2 Antibody Ch14.18/CHO (Dinutuximab Beta) in Patients with High-Risk Neuroblastoma (HR-NBL1/SIOPEN): A Multicentre, Randomised, Phase 3 Trial. *Lancet Oncol.* **2018**, *19*, 1617–1629, doi: 10.1016/S1470-2045(18)30578-3.
10. Ye, C.; Brand, D.; Zheng, S.G. Targeting IL-2: An Unexpected Effect in Treating Immunological Diseases. *Signal Transduct. Target. Ther.* **2018**, *3*, 1–10, doi:10.1038/s41392-017-0002-5.
11. Isvoranu, G.; Surcel, M.; Munteanu, A.; Bratu, O.; Ionita-Radu, F.; Neagu, M.; Chiritoiu-Butnaru, M. Therapeutic Potential of Interleukin-15 in Cancer (Review). *Exp. Ther. Med.* **2021**, *22*, 1–6, doi:10.3892/etm.2021.10107.
12. Waldmann, T.A.; Dubois, S.; Miljkovic, M.D.; Conlon, K.C. IL-15 in the Combination Immunotherapy of Cancer. *Front. Immunol.* **2020**, *11*, doi:10.3389/fimmu.2020.00868.
13. Charych, D.H.; Hoch, U.; Langowski, J.L.; Lee, S.R.; Addepalli, M.K.; Kirk, P.B.; Sheng, D.; Liu, X.; Sims, P.W.; VanderVeen, L.A.; et al. NKTR-214, an Engineered Cytokine with Biased IL2 Receptor Binding, Increased Tumor Exposure, and Marked Efficacy in Mouse Tumor Models. *Clin. Cancer Res.* **2016**, *22*, 680–690, doi: 10.1158/1078-0432.CCR-15-1631.

**14.** Diab, A.; Tannir, N.M.; Bentebibel, S.E.; Hwu, P.; Papadimitrakopoulou, V.; Haymaker, C.; Kluger, H.M.; Gettinger, S.N.; Sznol, M.; Tykodi, S.S.; et al. Bempegaldesleukin (NKTR-214) plus Nivolumab in Patients with Advanced Solid Tumors: Phase I Dose-Escalation Study of Safety, Efficacy, and Immune Activation (PIVOT-02). *Cancer Discov.* **2020**, *10*, 1158–1173, doi:10.1158/2159-8290.CD-19-1510.

**15.** Kattner, P.; Strobel, H.; Khoshnevis, N.; Grunert, M.; Bartholomae, S.; Pruss, M.; Fitzel, R.; Halatsch, M.E.; Schilberg, K.; Siegelin, M.D.; et al. Compare and Contrast: Pediatric Cancer versus Adult Malignancies. *Cancer Metastasis Rev.* **2019**, *38*, 673–682, doi:10.1007/s10555-019-09836-y.

**16.** Louis, C.U.; Shohet, J.M. Neuroblastoma: Molecular Pathogenesis and Therapy. *Annu. Rev. Med.* **2015**, *66*, 49–63, doi:10.1146/annurev-med-011514-023121.

**17.** Custers, L.; Khabirova, E.; Coorens, T.H.H.; Oliver, T.R.W.; Calandrini, C.; Young, M.D.; Vieira Braga, F.A.; Ellis, P.; Mamanova, L.; Segers, H.; et al. Somatic Mutations and Single-Cell Transcriptomes Reveal the Root of Malignant Rhabdoid Tumours. *Nat. Commun.* **2021**, *12*, 1–11, doi:10.1038/s41467-021-21675-6.

**18.** Marquardt, V.; Theruvath, J.; Pauck, D.; Picard, D.; Reifenberger, G.; Borkhardt, A.; Cheshier, S.; Kurz, T.; Remke, M.; Mitra, S. IMMU-19. HDAC INHIBITORS SENSITIZE MYC-AMPLIFIED MEDULLOBLASTOMA TO IMMUNOTHERAPY BY ACTIVATING THE NF-KB PATHWAYS. *Neuro. Oncol.* **2020**, *22*.

**19.** Jansky, S.; Sharma, A.K.; Körber, V.; Quintero, A.; Toprak, U.H.; Wecht, E.M.; Gartlgruber, M.; Greco, A.; Chomsky, E.; Grünewald, T.G.P.; et al. Single-Cell Transcriptomic Analyses Provide Insights into the Developmental Origins of Neuroblastoma. *Nat. Genet.* **2021**, *53*, 683–693, doi:10.1038/s41588-021-00806-1.

**20.** Reynolds, C.P.; Matthay, K.K.; Villablanca, J.G.; Maurer, B.J. Retinoid Therapy of High-Risk Neuroblastoma. *Cancer Lett.* **2003**, *197*, 185–192, doi:10.1016/S0304-3835(03)00108-3.

**21.** Sengupta, S.; Das, S.; Crespo, A.C.; Cornel, A.M.; Patel, A.G.; Mahadevan, N.R.; Campisi, M.; Ali, A.K.; Sharma, B.; Rowe, J.H.; Huang, H.; Debruyne, D.N.; Cerda, E.D.; Krajewska, M.; Dries, R.; Chen, M.; Zhang, S.; Soriano, L.; Cohen, M.A.; Versteeg, R.; Jaenisch, R.; Spranger, S.; Romee, R.; Miller, B.C.; Barbie, D.A.; Nierkens, S.; Dyer, M.A.; Lieberman, J.; George, R.E. Mesenchymal and adrenergic cell lineage states in neuroblastoma possess distinct immunogenic phenotypes. *Nat Cancer* **2022**, 3, 1228-1246, doi:10.1038/s43018-022-00427-5

**22.** Van Groningen, T.; Koster, J.; Valentijn, L.J.; Zwijnenburg, D.A.; Akogul, N.; Hasselt, N.E.; Broekmans, M.; Haneveld, F.; Nowakowska, N.E.; Bras, J.; et al. Neuroblastoma Is Composed of Two Super-Enhancer-Associated Differentiation States. *Nat. Genet.* **2017**, *49*, 1261–1266, doi:10.1038/ng.3899.

**23.** van Groningen, T.; Akogul, N.; Westerhout, E.M.; Chan, A.; Hasselt, N.E.; Zwijnenburg, D.A.; Broekmans, M.; Stroeken, P.; Haneveld, F.; Hooijer, G.K.J.; et al. A NOTCH Feed-Forward Loop Drives Reprogramming from Adrenergic to Mesenchymal State in Neuroblastoma. *Nat. Commun.* **2019**, *10*, 1–11, doi:10.1038/s41467-019-09470-w.

**24.** Zimmerman, M.W.; Durbin, A.D.; He, S.; Oppel, F.; Shi, H.; Tao, T.; Li, Z.; Berezovskaya, A.; Liu, Y.; Zhang, J.; et al. *Retinoic Acid Rewires the Adrenergic Core Regulatory Circuitry of Childhood Neuroblastoma*; **2021**; *7*, eabe0834, doi:10.1126/sciadv.abe0834

**25.** McNerney, K.; Karageorgos, S.; Ferry, G.; Wolpaw, A.; Burudpakdee, C.; Khurana, P.; Toland, C.; Vemu, R.; Vu, A.; Hogarty, M.; et al. TH-MYCN Tumors, but Not Tumor-Derived Cell Lines, Are Adrenergic Lineage, GD2+, and Responsive to Anti-GD2 Antibody Therapy . *Oncoimmunology* **2022**, *11*, doi: 10.1080/2162402x.2022.2075204.

**26.** Van Wezel, E.M.; Lieke, ; Van Zogchel, M.J.; Van Wijk, J.; Timmerman, I.; Vo, N.-K.; Zappeij-Kannegieter, L.; Boris, ; Simon, T.; Van Noesel, M.M.; et al. Mesenchymal Neuroblastoma Cells Are Undetected by Current MRNA Marker Panels: The Development of a Specific Neuroblastoma Mesenchymal Minimal Residual Disease Panel. **2019**, doi:10.1200/PO.18.

**27.** Kroesen, M.; Büll, C.; Gielen, P.R.; Brok, I.C.; Armandari, I.; Wassink, M.; Looman, M.W.G.; Boon, L.; den Brok, M.H.; Hoogerbrugge, P.M.; et al. Anti-GD2 MAb and Vorinostat Synergize in the Treatment of Neuroblastoma. *Oncoimmunology* **2016**, *5*, 1–12, doi:10.1080/2162402X.2016.1164919.

**28.** Phimmachanh, M.; Han, J.Z.R.; O'Donnell, Y.E.I.; Latham, S.L.; Croucher, D.R. Histone Deacetylases and Histone Deacetylase Inhibitors in Neuroblastoma. *Front. Cell Dev. Biol.* **2020**, *8*, 1–14, doi:10.3389/fcell.2020.578770.

**29.** Roussos Torres, E.T.; Rafie, C.; Wang, C.; Lim, D.; Brufsky, A.; LoRusso, P.; Eder, J.P.; Chung, V.; Downs, M.; Geare, M.; et al. Phase I Study of Entinostat and Nivolumab with or without Ipilimumab in Advanced Solid Tumors (ETCTN-9844). *Clin. Cancer Res.* **2021**, *27*, 5828–5837, doi:10.1158/1078-0432.ccr-20-5017.

**30.** Ny, L.; Jespersen, H.; Karlsson, J.; Alsén, S.; Filges, S.; All-Eriksson, C.; Andersson, B.; Carneiro, A.; Helgadottir, H.; Levin, M.; et al. The PEMDAC Phase 2 Study of Pembrolizumab and Entinostat in Patients with Metastatic Uveal Melanoma. *Nat. Commun.* **2021**, *12*, 1–10, doi:10.1038/s41467-021-25332-w.

**31.** van den Bijgaart, R.J.E.; Kroesen, M.; Brok, I.C.; Reijnen, D.; Wassink, M.; Boon, L.; Hoogerbrugge, P.M.; Adema, G.J. Anti-GD2 Antibody and Vorinostat Immunocombination Therapy Is Highly Effective in an Aggressive Orthotopic Neuroblastoma Model. *Oncoimmunology* **2020**, *9*, doi:10.1080/2162402X.2020.1817653.

**32.** Zhu, S.; Denman, C.J.; Cobanoglu, Z.S.; Kiany, S.; Lau, C.C.; Gottschalk, S.M.; Hughes, D.P.M.; Kleinerman, E.S.; Lee, D.A. The Narrow-Spectrum HDAC Inhibitor Entinostat Enhances NKG2D Expression without NK Cell Toxicity, Leading to Enhanced Recognition of Cancer Cells. *Pharm. Res.* **2015**, *32*, 779–792, doi:10.1007/s11095-013-1231-0.

**33.** Idso, J.M.; Lao, S.; Schloemer, N.J.; Knipstein, J.; Burns, R.; Thakar, M.S.; Malarkannan, S. Entinostat Augments NK Cell Functions via Epigenetic Upregulation of IFIT1-STING-STAT4 Pathway. *Oncotarget* **2020**, *11*, 1799–1815, doi:10.18632/oncotarget.27546.

**34.** Rongvaux, A.; Willinger, T.; Martinek, J.; Strowig, T.; Gearty, S. V.; Teichmann, L.L.; Saito, Y.; Marches, F.; Halene, S.; Palucka, A.K.; et al. Development and Function of Human Innate Immune Cells in a Humanized Mouse Model. *Nat. Biotechnol.* **2014**, *32*, 364–372, doi:10.1038/nbt.2858.

**35.** Bukowinski, A.; Chang, B.; Reid, J.M.; Liu, X.; Minard, C.G.; Trepel, J.B.; Lee, M.J.; Fox, E.; Weigel, B.J. A Phase 1 Study of Entinostat in Children and Adolescents with Recurrent or Refractory Solid Tumors, Including CNS Tumors: Trial ADVL1513, Pediatric Early Phase-Clinical Trial Network (PEP-CTN). *Pediatr. Blood Cancer* **2021**, *68*, 1–7, doi:10.1002/pbc.28892.

**36.** Eleveld, T.F.; Oldridge, D.A.; Bernard, V.; Koster, J.; Daage, L.C.; Diskin, S.J.; Schild, L.; Bentahar, N.B.; Bellini, A.; Chicard, M.; et al. Relapsed Neuroblastomas Show Frequent RAS-MAPK Pathway Mutations. *Nat. Genet.* **2015**, *47*, 864–871, doi:10.1038/ng.3333.

**37.** Spel, L.; Nieuwenhuis, J.; Haarsma, R.; Stickel, E.; Bleijerveld, O.B.; Altelaar, M.; Boelens, J.J.; Brummelkamp, T.R.; Nierkens, S.; Boes, M. Nedd4-Binding Protein 1 and TNFAIP3-Interacting Protein 1 Control MHC-1 Display in Neuroblastoma. *Cancer Res.* **2018**, *78*, 6621–6631, doi:10.1158/0008-5472.CAN-18-0545.

**38.** Varca, A.C.; Casalena, D.; Chan, W.C.; Hu, B.; Magin, R.S.; Roberts, R.M.; Liu, X.; Zhu, H.; Seo, H.S.; Dhe-Paganon, S.; et al. Identification and Validation of Selective Deubiquitinase Inhibitors. *Cell Chem. Biol.* **2021**, *28*, 1758-1771.e13, doi:10.1016/j.chembiol.2021.05.012.

**39.** Reid, G.S.D.; Shan, X.; Coughlin, C.M.; Lassoued, W.; Pawel, B.R.; Wexler, L.H.; Thiele, C.J.; Tsokos, M.; Pinkus, J.L.; Pinkus, G.S.; et al. Interferon-γ-Dependent Infiltration of Human T Cells into Neuroblastoma Tumors in Vivo. *Clin. Cancer Res.* **2009**, *15*, 6602–6608, doi: 10.1158/1078-0432.CCR-09-0829.

**40.** Yang, X.; Merchant, M.S.; Romero, M.E.; Tsokos, M.; Wexler, L.H.; Kontny, U.; Mackall, C.L.; Thiele, C.J. Induction of Caspase 8 by Interferon γ Renders Some Neuroblastoma (NB) Cells Sensitive to Tumor Necrosis Factor-Related Apoptosis-Inducing Ligand (TRAIL) but Reveals That a Lack of Membrane TR1/TR2 Also Contributes to TRAIL Resistance in NB. *Cancer Res.* **2003**, *63*, 1122–1129.

**41.** Cornel, A.M.; Mimpen, I.L.; Nierkens, S. MHC Class I Downregulation in Cancer: Underlying Mechanisms and Potential Targets for Cancer Immunotherapy. *Cancers (Basel).* **2020**, *12*, 1–33, doi:10.3390/cancers12071760.

**42.** Mucci, A.; Antonarelli, G.; Caserta, C.; Vittoria, F.M.; Desantis, G.; Pagani, R.; Greco, B.; Casucci, M.; Escobar, G.; Passerini, L.; et al. Myeloid Cell-based Delivery of IFN-γ Reprograms the Leukemia Microenvironment and Induces Anti-tumoral Immune Responses. *EMBO Mol. Med.* **2021**, *13*, 1–18, doi:10.15252/emmm.202013598.

**43.** De Palma, M.; Mazzieri, R.; Politi, L.S.; Pucci, F.; Zonari, E.; Sitia, G.; Mazzoleni, S.; Moi, D.; Venneri, M.A.; Indraccolo, S.; et al. Tumor-Targeted Interferon-α Delivery by Tie2-Expressing Monocytes Inhibits Tumor Growth and Metastasis. *Cancer Cell* **2008**, *14*, 299–311, doi:10.1016/j.ccr.2008.09.004.

**44.** Birocchi, F.; Cusimano, M.; Rossari, F.; Beretta, S.; Rancoita, P.M. V; Ranghetti, A.; Colombo, S.; Costa, B.; Angel, P.; Sanvito, F.; et al. Targeted Inducible Delivery of Immunoactivating Cytokines Reprograms Glioblastoma Microenvironment and Inhibits Growth in Mouse Models. *Sci. Transl. Med.* **2022**, *14*, eabl4106, doi:10.1126/scitranslmed.abl4106.

**45.** Peters, K.G.; Kontos, C.D.; Lin, P.C.; Wong, A.L.; Rao, P.; Huang, L.; Dewhirst, M.W.; Sankar, S. Functional Significance of Tie2 Signaling in the Adult Vasculature. *Recent Prog. Horm. Res.* **2004**, *59*, 51–71, doi:10.1210/rp.59.1.51.

**46.** Morton, L.T.; Wachsmann, T.L.A.; Meeuwsen, M.H.; Wouters, A.K.; Remst, D.F.G.; van Loenen, M.M.; Falkenburg, J.H.F.; Heemskerk, M.H.M. T Cell Receptor Engineering of Primary NK Cells to Therapeutically Target Tumors and Tumor Immune Evasion. *J. Immunother. Cancer* **2022**, *10*, 1–14, doi:10.1136/jitc-2021-003715.

**47.** Fehniger, T.A.; Cooper, M.A. Harnessing NK Cell Memory for Cancer Immunotherapy. *Trends Immunol.* **2016**, *37*, 877–888, doi:10.1016/j.it.2016.09.005.

**48.** von Andrian, U.H. NK Cell Memory: Discovery of a Mystery. *Nat. Immunol.* **2021**, *22*, 669–671, doi:10.1038/s41590-021-00890-9.

**49.** Romero-Olmedo, A.J.; Schulz, A.R.; Huber, M.; Brehm, C.U.; Chang, H.D.; Chiarolla, C.M.; Bopp, T.; Skevaki, C.; Berberich-Siebelt, F.; Radbruch, A.; et al. Deep Phenotypical Characterization of Human CD3+CD56+ T Cells by Mass Cytometry. *Eur. J. Immunol.* **2021**, *51*, 672–681, doi:10.1002/eji.202048941.

**50.** Kato, S.; Berzofsky, J.A.; Terabe, M. Possible Therapeutic Application of Targeting Type II Natural Killer T Cell-Mediated Suppression of Tumor Immunity. *Front. Immunol.* **2018**, *9*, doi:10.3389/fimmu.2018.00314.

**51.** Morandi, F.; Sabatini, F.; Podestà, M.; Airoldi, I. Immunotherapeutic Strategies for Neuroblastoma: Present, Past and Future. *Vaccines* **2021**, *9*, 1–23, doi:10.3390/vaccines9010043.

52. Hurton, L. V.; Singh, H.; Najjar, A.M.; Switzer, K.C.; Mi, T.; Maiti, S.; Olivares, S.; Rabinovich, B.; Huls, H.; Forget, M.A.; et al. Tethered IL-15 Augments Antitumor Activity and Promotes a Stem-Cell Memory Subset in Tumor-Specific T Cells. *Proc. Natl. Acad. Sci. U. S. A.* **2016**, *113*, E7788–E7797, doi:10.1073/pnas.1610544113.

53. Lanitis, E.; Rota, G.; Kosti, P.; Ronet, C.; Spill, A.; Seijo, B.; Romero, P.; Dangaj, D.; Coukos, G.; Irving, M. Optimized Gene Engineering of Murine CAR-T Cells Reveals the Beneficial Effects of IL-15 Coexpression. *J. Exp. Med.* **2021**, *218*, e20192203, doi:10.1084/jem.20192203.

54. Kyte, J.A. Strategies for Improving the Efficacy of CAR T Cells in Solid Cancers. *Cancers (Basel).* **2022**, *14*, doi:10.3390/cancers14030571.

55. Rodriguez-Garcia, A.; Palazon, A.; Noguera-Ortega, E.; Powell, D.J.; Guedan, S. CAR-T Cells Hit the Tumor Microenvironment: Strategies to Overcome Tumor Escape. *Front. Immunol.* **2020**, *11*, 1–17, doi:10.3389/fimmu.2020.01109.

56. Cortés-Selva, D.; Dasgupta, B.; Singh, S.; Grewal, I.S. Innate and Innate-Like Cells: The Future of Chimeric Antigen Receptor (CAR) Cell Therapy. *Trends Pharmacol. Sci.* **2021**, *42*, 45–59, doi:10.1016/j.tips.2020.11.004.

57. Gorovits, B.; Koren, E. Immunogenicity of Chimeric Antigen Receptor T-Cell Therapeutics. *BioDrugs* **2019**, *33*, 275–284, doi:10.1007/s40259-019-00354-5.

58. Mansilla-Soto, J.; Eyquem, J.; Haubner, S.; Hamieh, M.; Feucht, J.; Paillon, N.; Zucchetti, A.E.; Li, Z.; Sjöstrand, M.; Lindenbergh, P.L.; et al. HLA-Independent T Cell Receptors for Targeting Tumors with Low Antigen Density. *Nat. Med.* **2022**, *28*, 345–352, doi:10.1038/s41591-021-01621-1.

59. Strijker, J.G.M.; Pscheid, R.; Drent, E.; van der Hoek, J.J.F.; Koopmans, B.; Ober, K.; van Hooff, S.R.; Kholosy, W.M.; Cornel, A.M.; Coomans, C.; et al. Αβ-T Cells Engineered to Express Γδ-T Cell Receptors Can Kill Neuroblastoma Organoids Independent of MHC-I Expression. *J. Pers. Med.* **2021**, *11*, doi:10.3390/jpm11090923.

60. Jonus, H.C.; Burnham, R.E.; Ho, A.; Pilgrim, A.A.; Shim, J.; Doering, C.B.; Spencer, H.T.; Goldsmith, K.C. Dissecting the Cellular Components of Ex Vivo Γδ T Cell Expansions to Optimize Selection of Potent Cell Therapy Donors for Neuroblastoma Immunotherapy Trials . *Oncoimmunology* **2022**, *11*, 1–16, doi: 10.1080/2162402x.2022.2057012.

61. Crowther, M.D.; Dolton, G.; Legut, M.; Caillaud, M.E.; Lloyd, A.; Attaf, M.; Galloway, S.A.E.; Rius, C.; Farrell, C.P.; Szomolay, B.; et al. Genome-Wide CRISPR–Cas9 Screening Reveals Ubiquitous T Cell Cancer Targeting via the Monomorphic MHC Class I-Related Protein MR1. *Nat. Immunol.* **2020**, *21*, 178–185, doi: 10.1038/s41590-019-0578-8.

62. Mise, N.; Takami, M.; Suzuki, A.; Kamata, T.; Harada, K.; Hishiki, T.; Saito, T.; Terui, K.; Mitsunaga, T.; Nakata, M.; et al. Antibody-Dependent Cellular Cytotoxicity toward Neuroblastoma Enhanced by Activated Invariant Natural Killer T Cells. *Cancer Sci.* **2016**, *107*, 233–241, doi:10.1111/cas.12882.

63. Song, L.; Asgharzadeh, S.; Salo, J.; Engell, K.; Wu, H.W.; Sposto, R.; Ara, T.; Silverman, A.M.; DeClerck, Y.A.; Seeger, R.C.; et al. Vα24-Invariant NKT Cells Mediate Antitumor Activity via Killing of Tumor-Associated Macrophages. *J. Clin. Invest.* **2009**, *119*, 1524–1536, doi: 10.1172/JCI37869.

64. Melenhorst, J.J.; Chen, G.M.; Wang, M.; Porter, D.L.; Chen, C.; Collins, M.K.A.; Gao, P.; Bandyopadhyay, S.; Sun, H.; Zhao, Z.; et al. Decade-Long Leukaemia Remissions with Persistence of CD4+ CAR T Cells. *Nature* **2022**, *602*, 503–509, doi:10.1038/s41586-021-04390-6.

65. Oh, D.Y.; Fong, L. Cytotoxic CD4+ T Cells in Cancer: Expanding the Immune Effector Toolbox. *Immunity* **2021**, *54*, 2701–2711, doi: 10.1016/j.immuni.2021.11.015.

66. Inderberg, E.M.; Wälchli, S. Long-Term Surviving Cancer Patients as a Source of Therapeutic TCR. *Cancer Immunol. Immunother.* **2020**, *69*, 859–865, doi:10.1007/s00262-019-02468-9.

**67.** Axelrod, M.L.; Cook, R.S.; Johnson, D.B.; Balko, J.M. Biological Consequences of MHC-II Expression by Tumor Cells in Cancer. *Clin. Cancer Res.* **2019**, *25*, 2392–2402, doi: 10.1158/1078-0432.CCR-18-3200.

# Chapter 12

## Nederlandse Samenvatting

Neuroblastoom is een zeldzame vorm van kinderkanker. Het is een tumor die ontstaat uit embryonale voorlopercellen, genaamd blasten (vandaar "blastoom"), die in gezonde situatie uitrijpen tot allerlei componenten van het sympathische zenuwstelsel (vandaar "neuro"), waaronder het bijniermerg en andere delen van het sympathische zenuwstelsel. Primaire tumormassa's presenteren zich daarom vaak op deze locaties in het lichaam. De gemiddelde leeftijd bij diagnose is 18 maanden en de overlevingskans van patiënten is enorm afhankelijk van het stadium van de ziekte. Kinderen met laag-risico neuroblastoom hoeven vaak niet behandeld te worden en overleven in meer dan 90% van de gevallen, terwijl kinderen met hoog-risico (HR) neuroblastoom op dit moment slechts in de helft van de gevallen meer dan 5 jaar na diagnose nog in leven zijn. Het risico wordt onder andere hoger met leeftijd, genetische afwijkingen in de tumor en mate van uitzaaiing door het lichaam.

Met 10-14 diagnoses per jaar in Nederland wordt HR-neuroblastoom geclassificeerd als een zeer zeldzame ziekte. Door de agressiviteit van deze tumor is neuroblastoom echter wel de oorzaak van 15% van de wereldwijde aan kinderkanker toe te schrijven doden. Deze cijfers benadrukken de noodzaak van ontwikkeling van betere behandelstrategieën ter genezing van kinderen met HR-neuroblastoom.

Kinderen met HR-neuroblastoom worden behandeld met een intensief behandelregime, bestaande uit chemotherapie, bestraling, chirurgische resectie van de tumor en immuuntherapie. Immuuntherapie wordt gegeven in de vorm van het anti-GD2 antilichaam dinutuximab dat tumorcellen beter zichtbaar maakt voor het immuunsysteem. Toevoeging van immuuntherapie aan het behandelregime heeft gezorgd voor toename in overlevingskansen van kinderen met hoog risicoziekte. Na twee jaar werd een 20% toename in eventvrije overleving gezien, na vijf jaar was deze toename nog 10%. Dit laat het potentieel zien van immuuntherapeutische interventie ter verbetering van de behandeling van neuroblastoom.

Ook al zien we deze toegevoegde waarde van immuuntherapie, de realiteit is dat nog steeds ongeveer de helft van de kinderen een recidief krijgt. Daarnaast neemt de toegevoegde waarde van de immuuntherapie over de jaren af. Wij denken dat dit komt omdat het huidige antilichaam-gebaseerde immuuntherapieregime vooral gericht is op activatie van het aangeboren immuunsysteem, getraind om hard en snel te handelen, maar het aangeleerde immuunsysteem onvoldoende activeert. Activatie van het aangeleerde immuunsysteem is van belang om immunologisch geheugen te bewerkstelligen om een recidief te voorkomen. Onze hypothese is dan ook dat het verhogen van T-cel herkenning cruciaal is om de effectiviteit van immuuntherapeutische interventies tegen neuroblastoom te maximaliseren.

Dit proefschrift richt zich op strategieën om herkenning van neuroblastoom door T-cellen te verhogen en draagt bij aan identificatie van nieuwe (additionele) immuuntherapeutische interventies om overlevingskansen van kinderen met neuroblastoom te verbeteren. Dit proefschrift is onderverdeeld in drie delen. **Deel 1** van dit proefschrift onderzoekt het potentieel van het monitoren van immuunreacties tijdens de behandeling van kinderen met neuroblastoom. Immuunmonitoren zou bijvoorbeeld ingezet kunnen worden als tool om nieuwe potentiële therapeutische strategieën en biologische markers voor het al dan niet aanslaan van behandelingen te identificeren. **Deel 2** beschrijft de identificatie van medicijnen die T-cel herkenning van neuroblastoom verhogen. **Deel 3** van dit proefschrift onderzoekt de potentie van celtherapeutische strategieën om herkenning van neuroblastoom door het immuunsysteem te verbeteren.

## DEEL 1 – IMMUUNREACTIES TIJDENS HET BEHANDELREGIME VAN HR-NEUROBLASTOOM

Met slechts 10-14 Nederlandse hoog-risico patiënten per jaar zijn patiëntgroepen vaak te klein om behandelprotocollen goed te kunnen optimaliseren en vergelijken. Dit wordt onderschreven door het feit dat de dosis, timing en combinatie van immuuntherapeutische componenten momenteel vooral gekozen zijn op basis van ervaring. Zo worden bijvoorbeeld de status van het immuunsysteem van patiënten en individuele effecten van behandelcomponenten nog weinig in acht genomen bij het opstellen van behandelprotocollen. Twee recente studies, een naar het individuele effect van IL-2 in een eerder behandelregime, de ander naar het effect van de snelheid van infusie van de antilichaamtherapie, laten het belang en potentieel zien van dit soort studies om de slagingskans van behandelingen te maximaliseren. Diepgaand monitoren van het immuunsysteem tijdens behandeling wordt momenteel echter nog weinig uitgevoerd.

**Hoofdstuk 2** vat de huidige literatuur over de status van het immuunsysteem van kinderen met neuroblastoom bij diagnose en tijdens therapie samen. Individuele studies laten veelbelovende aanwijzingen zien over waarom het effect van immuuntherapie niet maximaal is. Observaties hinten naar nieuwe interessante (additionele) immuuntherapeutische strategieën. Wat ook opviel is de inconsistentie tussen wat en de manier waarop er gemonitord wordt in individuele studies. De kleine patiëntgroepen per centrum zorgen er daardoor vaak voor dat het onmogelijk is om harde conclusies te trekken op basis van verkregen data. Wij pleiten voor gestandaardiseerde monitoring van het immuunsysteem in alle kinderen die behandeld worden volgens het huidige Europese behandelprotocol. Op deze manier kan maximale kennis worden opgedaan om het behandelregime in de toekomst verder te verbeteren. In **Hoofdstuk 3** beschrijven we een strategie waarmee flowcytometers met verschillende complexiteit op elkaar afgestemd kunnen worden om inconsistentie van interpretatie van resultaten tussen centra te voorkomen. In **Hoofdstuk 4** beschrijven we de resultaten van onze eerste pilot studie waarin we de dynamiek van het immuunsysteem tijdens het behandelregime bestudeerd hebben in 25 patiënten met HR-neuroblastoom. Buiten het feit dat deze pilot interessante aanwijzingen verschaft voor het verbeteren van de timing van (individuele componenten van) het immuuntherapieregime is voor mij een misschien nog wel belangrijkere conclusie: beoordeel nooit een boek naar zijn kaft. We zien dat (subsets van) immuuncellen op het eerste gezicht aanwezig zijn, maar als we vervolgens de functionaliteit van bepaalde celtypes bepalen, zijn deze disfunctioneel. Het is dus van belang om niet alleen aanwezigheid, maar ook functionaliteit van immuuncellen te monitoren om betrouwbare conclusies te kunnen trekken. De afgelopen jaren hebben wij gewerkt aan het opstellen van een gestandaardiseerd protocol om het immuunsysteem tijdens het behandelregime te monitoren. Op het moment van schrijven kan deze studie, bekend als de DINO studie, ieder moment van start gaan in het Prinses Máxima Centrum. Ons ultieme doel is om dit monitoring protocol in samenwerking met andere Europese instituten uiteindelijk te implementeren voor alle kinderen behandeld met het Europese HR-neuroblastoom behandelprotocol.

## DEEL 2 – VERBETEREN VAN T-CEL HERKENNING VAN NEUROBLASTOOM VIA FARMACOLOGISCHE VERHOGING VAN MHC-I

In het eerste deel van dit proefschrift hebben we gekeken naar de aanwezigheid en capaciteit van immuuncellen om HR-neuroblastoom te herkennen. Een complicerende factor in herkenning van neuroblastoom door het immuunsysteem is echter dat de cellen grotendeels onzichtbaar zijn voor het immuunsysteem, omdat de voorloper cellen waaruit de tumor ontstaat normaal alleen tijdens de embryonale fase, maar niet in een volgroeid kindje, aanwezig zijn. We kunnen dus strategieën ontwikkelen om het immuunsysteem maximaal potent te maken, maar zolang de tumor geen moleculen op het oppervlak toont die immuuncellen nodig hebben voor herkenning, zal het immuunsysteem de tumor niet elimineren. Een molecuul noodzakelijk voor herkenning door killer T-cellen is MHC klasse I (MHC-I).

**Hoofdstuk 5** geeft een overzicht van de onderliggende mechanismen van disregulatie in MHC-I expressie in allerlei soorten kanker en beschrijft strategieën die geïdentificeerd zijn om MHC-I expressie in verschillende tumorsoorten te bewerkstelligen. Een belangrijke conclusie van dit hoofdstuk is dat het van belang is onderscheid te maken tussen tumoren met irreversibele verandering in MHC-I expressie, veroorzaakt door onomkeerbare aanpassingen in het DNA, en reversibele MHC-I disregulatie, veroorzaakt door omkeerbare disregulatie in cellulaire processen. Afwezigheid van MHC-I in HR-neuroblastoom wordt veroorzaakt door een reversibele disregulatie, wat perspectief biedt voor het verhogen van MHC-I expressie (en dus T-cel herkenning) met geneesmiddelen. Verschillende cytokines (moleculen die een belangrijke rol spelen in de afweer) met een bekend effect op MHC-I expressie verhogen MHC-I expressie in neuroblastoom. Cytokines hebben echter een hele brede biologische activiteit, waardoor het gebruik als medicijn leidt tot veel bijwerkingen. Daarom hebben we ons in dit deel van het proefschrift gericht op de identificatie van farmacologische strategieën om MHC-I expressie in neuroblastoom te induceren. **Hoofdstuk 6** beschrijft de ontwikkeling van een “high-throughput” screening methode waarmee we, onder andere, MHC-I expressie verhogende medicijnen kunnen identificeren met behulp van flowcytometrie. In **Hoofdstuk 7** wordt de ontwikkeling van een protocol besproken waarmee we T-cellen van navelstrengbloed en gezonde donoren genetisch kunnen modificeren om herkenning van specifieke tumoren, zoals neuroblastoom, te kunnen bewerkstelligen. Dit protocol kan vervolgens gebruikt worden om tumor-specifieke T-cel herkenning in het lab te bestuderen. **Hoofdstuk 8** laat de resultaten zien van het screenen van het effect van ~3800 medicijnen op MHC-I expressie in neuroblastoom. Hier identificeren we Entinostat, een zogenoemde histon deacetylase remmer, als een veelbelovend medicijn om T-cel herkenning van neuroblastomen te verbeteren, onder andere via inductie van MHC-I expressie. We zien dat tumorcellen zich na behandeling met Entinostat compleet anders gaan gedragen, waarbij ze switchen van een zogenoemd “adrenerg” naar een meer “mesenchymaal” type. Dit gaat hand-in-hand met een verhoging van allerlei factoren belangrijk in immuunherkenning van de tumor, niet beperkt tot herkenning van T-cellen alleen. Dit is een opvallende observatie, omdat dit de tot voor kort geldende hypothese dat meer uitgerijpte neuroblastomen beter door het immuunsysteem kunnen worden herkend, tegenspreekt. Deze observatie wordt ondersteund met data uit een samenwerking met het George lab van het Dana Farber instituut in Boston. Deze bevindingen vragen naar mijn mening om herziening van de hypotheses waarop (de timing van) behandelcomponenten, zoals het combineren van immuuntherapie met isotretinoïne, gebaseerd zijn.

## DEEL 3 – CELTHERAPEUTISCHE STRATEGIEËN TER VERBETERING VAN NEUROBLASTOOM HERKENNING DOOR IMMUUNCELLEN

Ons immuunsysteem heeft een veiligheidsmechanisme ingebouwd waardoor cellen die zichzelf niet meer laten zien aan het immuunsysteem herkend en geëlimineerd worden. Afwezigheid van MHC-I expressie op het oppervlak van cellen induceert bijvoorbeeld activatie van natural killer cellen (NK-cellen), die MHC-I negatieve cellen vervolgens elimineren. Echter, activatie van NK-cellen gaat samen met uitscheiden van cytokines waarvan we weten dat ze MHC-I expressie op neuroblastoom cellen kunnen verhogen. Het gevolg is dat de MHC-I expressie tijdelijk omhooggaat waardoor die tumorcellen niet geëlimineerd worden door NK-cellen, maar ook weer afneemt zodra er geen geactiveerde cellen meer in de omgeving van de tumor zijn. We hypothetiseren dat deze zogenoemde plasticiteit in MHC-I expressie zorgt voor het ontwijken van eliminatie van neuroblastoom door zowel T- als NK-cellen.

De studies in dit deel van het proefschrift zijn ontstaan rond de hypothese dat neuroblastomen eliminatie door het immuunsysteem niet langer kunnen ontwijken via MHC-I plasticiteit wanneer een celtherapie product tumoren kan elimineren in zowel aan- als afwezigheid van MHC-I expressie. We onderzoeken het gebruik van twee verschillende bronnen van immuuncellen om een dergelijk product te genereren. In **Hoofdstuk 9** worden cellen die van nature in bloed voorkomen, NKT-cellen, uit bloed geïsoleerd en genetisch gemanipuleerd met een neuroblastoom-specifieke T-cel receptor (TCR) zodat tumorcellen met MHC-I op het oppervlak herkend worden. In **Hoofdstuk 10** beschrijven we een kweeksysteem waarmee we van navelstrengbloed verkregen stamcellen genetisch manipuleren met dezelfde neuroblastoom-specifieke TCR en vervolgens laten uitrijpen tot NK-cellen. Deze cellen worden in zowel aan- als afwezigheid van MHC-I expressie geactiveerd. In beide gevallen zien we dat de celproducten met een neuroblastoom-specifieke TCR tumorcellen beter elimineren dan niet gemanipuleerde cellen. Vervolgonderzoek, zowel in het lab als in muizen, zal moeten uitwijzen wat de meest veelbelovende strategie is om een dergelijk celtherapie strategie te ontwikkelen.

Tot slot worden in **Hoofdstuk 11** van dit proefschrift de belangrijkste conclusies getrokken en worden resultaten in perspectief gezet. Al met al kunnen we concluderen dat het begrijpen van de impact van de (timing van) verschillende onderdelen van het behandelregime op de eliminatie, immuunherkenning en fitheid van het immuunsysteem zelf de sleutel is tot verbetering van de behandeling. Dit proefschrift identificeert en laat de potentie zien van strategieën om immuunherkenning van neuroblastoom, onder andere door T-cellen, te verhogen. Dit onderzoek legt de basis voor het effectief inzetten van T-cellen in de bestrijding van HR-neuroblastoom, om immunologisch geheugen te genereren en recidieven te voorkomen. Vervolgonderzoek in muis en mens is nodig om geïdentificeerde strategieën verder te onderzoeken om de komende jaren nóg beter te worden in verstoppertje en neuroblastoom niet langer een kans te bieden om onvindbaar te blijven.

# Chapter 13

## Appendices

**Curiculum Vitae**
**List of Publications**
**Dankwoord**

## CURRICULUM VITAE

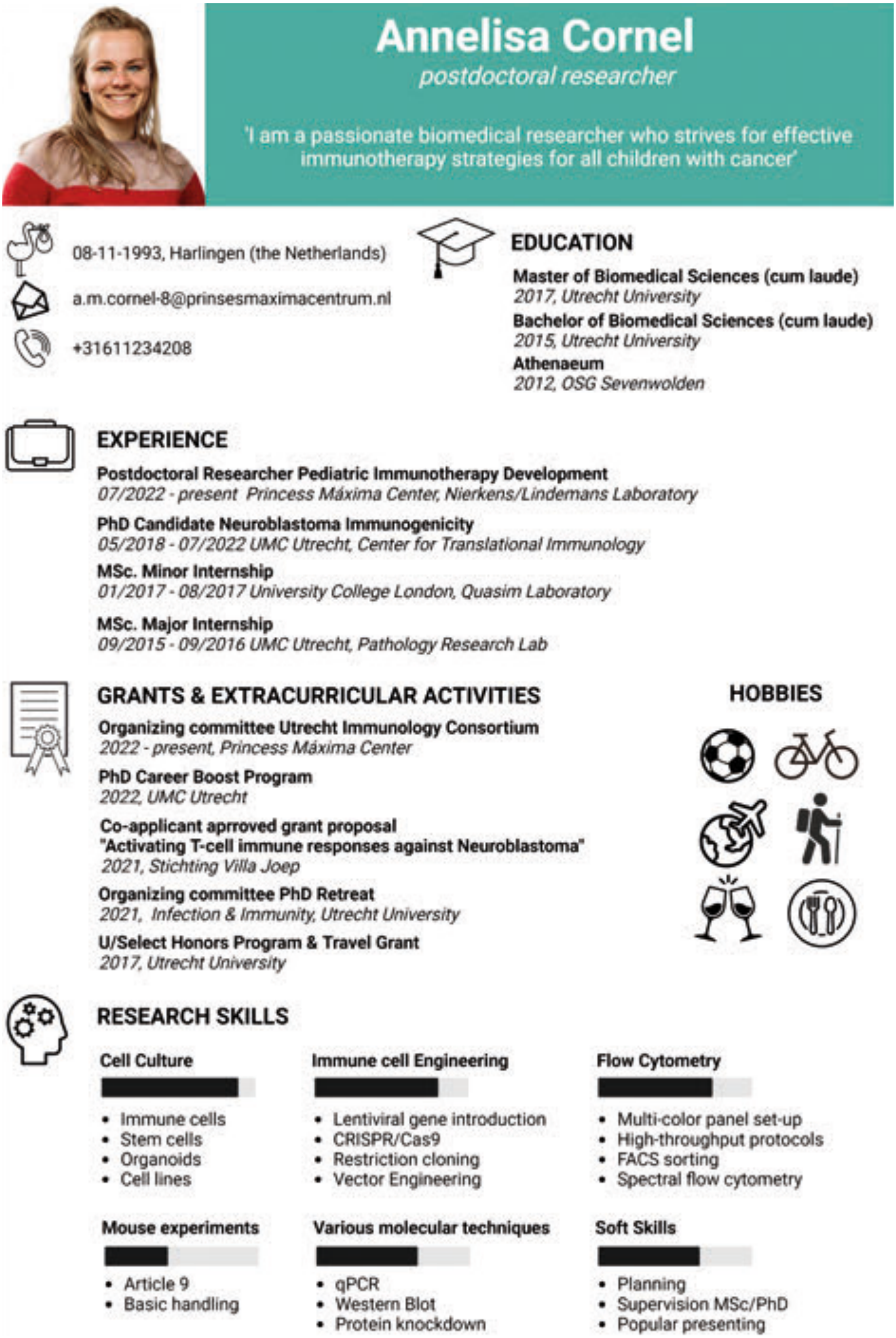

# Annelisa Cornel

*postdoctoral researcher*

'I am a passionate biomedical researcher who strives for effective immunotherapy strategies for all children with cancer'

08-11-1993, Harlingen (the Netherlands)

a.m.cornel-8@prinsesmaximacentrum.nl

+31611234208

### EDUCATION

**Master of Biomedical Sciences (cum laude)**
*2017, Utrecht University*
**Bachelor of Biomedical Sciences (cum laude)**
*2015, Utrecht University*
**Athenaeum**
*2012, OSG Sevenwolden*

### EXPERIENCE

**Postdoctoral Researcher Pediatric Immunotherapy Development**
*07/2022 - present Princess Máxima Center, Nierkens/Lindemans Laboratory*

**PhD Candidate Neuroblastoma Immunogenicity**
*05/2018 - 07/2022 UMC Utrecht, Center for Translational Immunology*

**MSc. Minor Internship**
*01/2017 - 08/2017 University College London, Quasim Laboratory*

**MSc. Major Internship**
*09/2015 - 09/2016 UMC Utrecht, Pathology Research Lab*

### GRANTS & EXTRACURRICULAR ACTIVITIES

**Organizing committee Utrecht Immunology Consortium**
*2022 - present, Princess Máxima Center*

**PhD Career Boost Program**
*2022, UMC Utrecht*

**Co-applicant aprroved grant proposal**
**"Activating T-cell immune responses against Neuroblastoma"**
*2021, Stichting Villa Joep*

**Organizing committee PhD Retreat**
*2021, Infection & Immunity, Utrecht University*

**U/Select Honors Program & Travel Grant**
*2017, Utrecht University*

### HOBBIES

### RESEARCH SKILLS

**Cell Culture**

- Immune cells
- Stem cells
- Organoids
- Cell lines

**Immune cell Engineering**

- Lentiviral gene introduction
- CRISPR/Cas9
- Restriction cloning
- Vector Engineering

**Flow Cytometry**

- Multi-color panel set-up
- High-throughput protocols
- FACS sorting
- Spectral flow cytometry

**Mouse experiments**

- Article 9
- Basic handling

**Various molecular techniques**

- qPCR
- Western Blot
- Protein knockdown

**Soft Skills**

- Planning
- Supervision MSc/PhD
- Popular presenting

# LIST OF PUBLICATIONS

## This thesis:

**Cornel AM**, Szanto CL, van Til NP, van Velzen JF, Boelens J, Nierkens S, A “No-Touch” Antibody-Staining Method of Adherent Cells for High-Throughput Flow Cytometry in 384-Well Microplate Format for Cell-Based Drug Library Screening. *Cytometry A* **2020**;98:845-851.

**Cornel AM***, Szanto CL*, Vijver SV, Nierkens S, Monitoring Immune Responses in Neuroblastoma Patients during Therapy. *Cancers* **2020**;12:516.

**Cornel AM**, Mimpen IL, Nierkens S, MHC Class I Downregulation in Cancer: Underlying Mechanisms and Potential Targets for Cancer Immunotherapy. *Cancers* **2020**;12:1760.

**Cornel AM**, van der Burght CAJ, Nierkens S, van Velzen JF, FACSCanto II and LSRFortessa flow cytometer instruments can be synchronized utilizing single-fluorochrome-conjugated surface-dyed beads for standardized immunophenotyping. *J Clin Lab Anal*. **2020**;34:e23361.

**Cornel AM***, Szanto CL*, Tammings SM, Delemarre EM, de Koning CCH, van den Beemt DAMH, Dunnebach E, Tas ML, Dierselhuis MP, Tytgat LGAM, van Noesel MM, Kraal KCJM, Boelens J, Huitema ADR, Nierkens S, Immune Monitoring during Therapy Reveals Activitory and Regulatory Immune Responses in High-Risk Neuroblastoma. *Cancers* **2021**;13:2096.

Lo Presti V, **Cornel AM**, Plantinga M, Dunnebach E, Kuball J, Boelens J, Nierkens S, van Til NP, Efficient lentiviral transduction method to gene modify cord blood CD8 + T cells for cancer therapy applications. *Mol Ther Methods Clin Dev*. **2021**;21:357-368.

**Cornel AM**, Dunnebach E, Hofman DA, Das S, Sengupta S, van den Ham F, Wienke J, Strijker JGM, van den Beemt DAMH, Essing AHW, Koopmans B, Engels SAG, Lo Presti V, Szanto CS, George RE, Molenaar JJ, van Heesch S, Dierselhuis MP, Nierkens S, Epigenetic modulation of neuroblastoma enhances T- and NK-cell immunogenicity by inducing a tumor cell lineage switch. *J Immunother Cancer* **2022;**10:e005002

## Other:

**Cornel AM**, van Til NP, Boelens J, Nierkens S, Strategies to Genetically Modulate Dendritic Cells to Potentiate Anti-Tumor Responses in Hematologic Malignancies. *Frontiers in Immunol*. **2018**;9:982.

Strijker JGM, Pscheid R, Drent E, van der Hoek JJF, Koopmans B, Ober K, van Hooff SR, Kholosy WM, **Cornel AM**, Coomans C, Bisso A, van Loenen MM, Molenaar JJ, Wienke J, αβ-T Cells Engineered to Express γδ-T Cell Receptors Can Kill Neuroblastoma Organoids Independent of MHC-I Expression. *J Pers Med* **2021**;11:923.

Lo Presti V, Cutilli A, Dogariu Y, Müskens KF, Dünnebach E, van den Beemt DAMH, **Cornel AM**, Plantinga M, Nierkens S, Gene Editing of Checkpoint Molecules in Cord Blood-Derived Dendritic Cells and CD8 + T Cells Using CRISPR-Cas9. *CRISPR J* **2022**;5:435-444.

Dekkers JF, Alieva M, Cleven A, Keramati F, Wezenaar AKL, van Vliet EJ, Puschhof J, Brazda P, Johanna I, Meringa AD, Rebel HG, Buchholz M, Barrera Román M, Zeeman AL, de Blank S, Fasci D, Geurts MH, **Cornel AM**, Driehuis E, Millen R, Straetemans T, Nicolasen MJT, Aarts-Riemans T, Ariese HCR, Johnson HR, van Ineveld RL, Karaiskaki F, Kopper O, Bar-Ephraim Y, Kretzschmar K, Eggermont AMM, Nierkens S, Wehrens EJ, Stunnenberg HG, Clevers H, Kuball J, Sebestyen Z, Rios AC, Uncovering the mode of action of engineered T cells in patient cancer organoids. *Nat Biotechnol* **2022,** online ahead of print.

Sengupta S, Das S, Crespo AC, **Cornel AM**, Patel AG, mahadevan NR, Campisi M, Ali AK, Sharma B, Rowe JH, Huang H, Debruyne DN, Cerda ED, Krajewska M, Dries R, Chen M, Zhang S, Soriano L, Cohen MA, Versteeg R, Jaenisch R, Spranger S, Romee R, Miller BC, Barbie DA, Nierkens S, Dyer MA, Lieberman J, George RE, Mesenchymal and adrenergic cell lineage states in neuroblastoma possess distinct immunogenic phenotypes. *Nat Cancer* **2022**;3:1228-1246.

## DANKWOORD

Een PhD haal je niet in je eentje. Er zijn zoveel mensen die er de afgelopen jaren voor me zijn geweest, wetenschappelijk maar juist ook op persoonlijk vlak. Jullie zijn zo belangrijk voor mij, dus daarom heb ik besloten om mijn lengte van stof (weer eens) de vrije loop te laten, hier komt ie.

**Jolet** & **Lisa**, we go many years back. Jol, vanaf de basisschool al vriendinnetjes en met z'n tweeën gaan studeren en samenwonen in Utrecht. Wat was het fijn om elkaar altijd dichtbij te hebben toen we samen vanuit het Friese land naar Utrecht verhuisden. Ik ben zo trots op alles wat je bereikt hebt de afgelopen jaren, en zo leuk dat we uiteindelijk allebei medisch onderzoek zijn gaan doen! Ook al woon je al jaren aan de overkant van de plas, ik heb nog steeds het gevoel dat we elkaar in twee woorden begrijpen. Lies, wat een geluk dat jullie een jaar in Nederland kwamen wonen en dat we toen bij elkaar in het voetbalteam en op school terecht kwamen. En nog meer geluk dat je Nederland, en sinds 2.5 jaar zelfs Utrecht, zo leuk vond dat je hier bent komen wonen. Dankjewel dat je altijd voor me klaarstaat Lies, it means the world!

Samen beginnen met studeren, dat schept een band. Gezellig samen studeren en ieder feestje afgaan tijdens onze studie, wat overbleef is een hechte vriendschap. **Fabian, Noël, Kim, Annet**, dankjewel voor de oneindige gezelligheid, onze heerlijke nerdgesprekken, de eeuwige referenties naar mijn (al dan niet imponerende) lengte en niet te vergeten de tequila's 'sunder' ice (hè Noël?).

**Hercu Herman**, zaterdag is de mooiste dag van de week! Kampioen in de derde helft worden we elk jaar op afstand. Dank jullie wel voor alle gezelligheid en ontspanmomentjes op- en buiten het veld! Ik ben blij dat ik onze senior beschermer mag zijn! ;)

**Joëlle** & **Angelique**, dreamteam tijdens alle mastervakken en daarna doorgegroeid als 'mooi weer afdwingers' met jullie fantastische mannen. Dankjewel voor alle lol, cocktailfeestjes, gezelligheid en goede gesprekken. An, dankjewel voor je onvoorwaardelijke support, begrip en vertrouwen. A.A. Milne liet het mijn favoriete beer in een rood truitje heel treffend zeggen: "It makes such a difference to have someone who believes in you".

**Cathy**, dankjewel voor je supervisie tijdens de eerste stappen die ik in het lab zette. Ik heb zoveel geleerd van jouw wetenschappelijke blik, kritische houding en de vrijheid die je me gaf in het project. (Former) team Waseem, and in particular **Christos**, **Roland**,

**Annie** & **Abe**, I get a big smile on my face every time I think about my time in London. Thank you so much for making me feel at home, and for all your time and patience in teaching me all the technical and tactical aspects of lymphocyte engineering (and science in general). I have so much respect for you as scientists (Abe, in particular your ridiculously high lentiviral titers, your talent to create an amazing atmosphere, your entrepreneuring skills, and not to forget your essay about Beyonce). More importantly, thank you for the cozy dinners, karaoke- and pub nights and getting through the day after together (I'm sure you remember the particular morning I am referring to, Christos? ;)). Roland (a.k.a. professor Terminal), do you remember our bet on me writing the word 'rigmarole' somewhere in my thesis? Did you ever find it? Here it is again, in my PhD thesis. I bet I won.

**Stefan,** dankjewel voor je vertrouwen in mij. Ik herinner me nog goed ons gesprek na het inleveren van mijn masterthesis, een enorme boost voor het geloof in mezelf als wetenschapper. De afgelopen vier jaar gaf je me ruimte om mezelf te ontwikkelen, maar was je er ook altijd als ik iemand nodig had om mee te sparren. Altijd kritisch op elkaar en de bedachte theorieën, maar ook altijd tijd voor een grapje of scherpe opmerking. Ik heb veel respect voor hoe je alle ballen hoog weet te houden en bovenal een goede sfeer in de groep weet te garanderen. Ik heb heel veel zin in de komende jaren, ben benieuwd wat we voor elkaar gaan boksen! **Miranda**, ik was zo blij om je enthousiasme te zien toen ik je vroeg mijn copromotor te zijn! Dankjewel dat je me hebt geleerd om niet te vergeten om af en toe een klinische bril op te zetten.

My dear paranymphs **Brigitte**, **Ester, and Vania**. Thank you for helping me arrange this big day, and more importantly for standing by my side in the past 4.5 years. I really couldn't and didn't want to choose between you three, so I'm happy Vania set the stage with her three paranymphs, haha! Dear Vania, thank you for your positivity, your smile, the delicious cakes, the supporting messages on my desk during long days/nights at work, and most importantly: for being my friend. Lieve Ester, dankjewel voor alle gezellige dagen in het lab, de bergen met werk die je voor ons allemaal (en mij in het bijzonder) verzet en de gezellige hapjes, drankjes en borrels na het werk. Ik ben zo blij dat we de komende tijd nóg intensiever kunnen gaan samenwerken en samen allerlei mooie dingen klaar te gaan boksen! Lieve, lieve Bri, ik denk dat het feit dat jouw beste vriendinnetje binnen 10 minuten opmerkte hoeveel wij op elkaar lijken (en dan niet qua uiterlijk), genoeg zegt. Ik kijk enorm naar je op in hoe jij in het leven staat en voel me mega gezegend met wie je voor mij bent en wat je me hebt geleerd de afgelopen jaren. Ik vind het ZÓ leuk om te zien hoe geweldig goed je op je plaats zit nu bij defensie! We komen er wel ;).

Lieve BoNi's, baboons, NiLis, team Pierkens, of hoe we onszelf ook noemen, haha. **Shanice, Bas, Maud, Niek, Celina, Coco, Denise, Caro, Linde, Maike, Konradin, Joyce, Jorik, Tiago, Suze, en Leiah** (ja ook jij bent one of the team!). Dank jullie wel voor alle gezelligheid, koffietjes en wetenschappelijke discussies! Maike, ik heb zoveel respect voor je keuze om je PhD niet af te maken en ik ben zo blij om te zien hoe goed je nu op je plek zit bij CellPoint! Lieve lieve Lin, wat vind ik het moeilijk dat je je al zo'n lange tijd niet jezelf voelt. Ik vind je een fantastische wetenschapper, vrouw en vriendin, ik weet zeker dat je hier uiteindelijk sterker uitkomt. Leiah, dé enige echte uitvindster van e. colia-sparaginase. Elke vrijdag weer het zelfde grapje met Stefan, wat zijn we toch een harde werkers hé!? Wat is het heerlijk om je als appendix van de Nierkens groep te hebben: lachen is gezond hè!

**Loutje, Caitlyn, Marta, Diana, Iris, Laura, Anne,** and **Saskia**. Thank you for thrusting me as your supervisor and for teaching me an incredible lot. I enjoyed all our meetings, lab sessions, and reading the beautiful theses you produced. Iris, zó leuk dat onze wegen elkaar op zo'n grappige manier weer kruisten en wat bijzonder dat we samen een hele mooie review hebben kunnen publiceren (met práchtige figuren van je moeder!). Als er ooit nog een Bernebrêge reünie komt dan hebben wij vast het sterkste verhaal te vertellen, haha! Loutje, je hebt echt een speciaal plekje in mijn hart veroverd afgelopen jaar. Wat ben je enorm gegroeid: als wetenschapper, maar nog veel meer qua vertrouwen in jezelf! En nu gewoon begonnen aan een Master! Zó trots! Caitlyn, I'm happy I found someone who likes NK(T) cells as much as I do, haha. I am so excited to be able to continue working with you the coming years! You are going to rock that PhD, I'm sure of that!

**Mam, Marieke** en **Aline**. Dankjewel dat jullie mij gesteund hebben in mijn pad tot Doctor. Wat ik ook zou willen worden of zijn, ik heb het gevoel dat jullie me daarin altijd zouden steunen, heel erg bedankt daarvoor. Marieke, je hebt een van de leukste en schattigste wezentjes op aarde gecreëerd, ik ben trots dat ik mezelf tante mag noemen van jullie prachtige dochter Eden.

Lieve **Paul, Margreet, Tessa & Robbin**. Dankjewel voor wie jullie voor mij zijn en wat jullie allemaal voor mij doen. Ik weet dat ik maar hoef te bellen en jullie op de stoep staan als ik jullie nodig heb. **Paul**, dankjewel voor alle verhuizingen en hulp met klusjes in mijn huis. Gelukkig heb ik nu je oude boormachine, dan hoef ik je niet overal meer voor te vragen, haha! Dank jullie wel voor jullie steun in, en het af en toe even in perspectief zetten van, de lange weg tot Doctor. Wat zou pap onze sterke band bijzonder hebben gevonden.

Lieve **Guus**¸ je zult het de afgelopen 1.5 jaar af en toe vast zwaar hebben gehad met het aanhoren van mijn eeuwige verhalen over werk, mijn thesis en de wetenschap. Dankjewel voor de knuffels, de nodige boosts in mijn zelfvertrouwen en al je wijze raad (waar ik niet altijd genoeg mee doe). Ik heb zóveel zin in onze avonturen samen, ik hou van jou!

En dan wil ik eindigen met jou **Pap**, aan wie ik elke letter van deze thesis opdraag. Wat is het verdrietig dat je mij niet hebt kunnen zien ontwikkelen tot de vrouw die ik nu ben. Als je één droom had voor je kinderen dan was het wel dat op het gebied van studeren ons niets tekort mocht komen. Nou pap, ik nam het vrij letterlijk en heb het studeren aan de universiteit nu toch wel ongeveer uitgespeeld! Je bent een voorbeeld voor mij geweest in hoe je met een flinke dosis enthousiasme en een ijzeren doorzettingsvermogen uiteindelijk kan komen waar je wil. Die wijze lessen hebben mij gevormd tot wie ik nu ben. Ik dacht laatst weer eens aan ‘ons’ Disney versje dat we ‘s avonds voor het slapengaan samen oplazen. Het viel me op dat er eigenlijk een prachtige analogie is met ‘mijn’ wetenschap: misschien een klein puzzelstukje van een grote puzzel, maar wel míjn puzzelstukje:

### ***Mijn eigen zee***

*Mijn zee is in het algemeen,*
*heel groot, en blauw, en plat.*
*Maar, dat zag ik al meteen,*
*voornamelijk erg nat!*

*Ík ben de baas van deze zee,*
*ik heb hem zelf gevonden!*
*Maar konijn, die schudde nee,*
*en zei toen onomwonden:*

*“De zee die is oneindig groot;*
*je kunt er varen met een boot!*
*Deze plas is véél te klein,*
*om een echte zee te zijn!“*

*Pfu, ik lachte toen en zei alleen:*
*Blijf jij maar lekker zeuren!*
*De horizon, daar ga ik heen,*
*ik ga naar haaien speuren!*

*Mijn zee is dan een regenplas,*
*maar dat kan mij níets schelen.*
*Ik hoef me sinds mijn zee er was,*
*nóóit meer te vervelen!*